Impact of alkaline activator and fly ash on strength, microstructure and durability assessment through corrosion resistance of geopolymer concrete in the presence of chloride ions

A thesis submitted in partial fulfillment of the requirements
for the award of

Doctor of PHILOSOPHY

in

Civil Engineering

By

SATHISHRAJ M.
(Roll No. 126104032)

Under the supervison of

Dr. Bulu Pradhan

Department of Civil Engineering
Indian Institute of Technology Guwahati
Guwahati 781039

August 2024

Dedicated to

All members of my Family, especially to

My Parents

(M Radha – R Mani)

&

My Wife and My Son

(S Sowmiya – S Vishnuraj)

Department of Civil Engineering

Indian Institute of Technology Guwahati

Guwahati - 781039, Assam, India

Dr. Bulu Pradhan
Professor
Email: bulu@iitg.ac.in
Phone: +91-361-258-2425

Certificate

It is certified that the work contained in the thesis entitled "**Impact of alkaline activator and fly ash on strength, microstructure and durability assessment through corrosion resistance of geopolymer concrete in the presence of chloride ions**" submitted by **Mr. Sathishraj M. (Roll No. 126104032)** to the Indian Institute of Technology Guwahati for the award of the degree of **Doctor of Philosophy** has been carried out under my supervision in the Department of Civil Engineering, Indian Institute of Technology Guwahati. This work has not been submitted elsewhere for the award of any other degree or diploma.

Place: IIT Guwahati **(Dr. Bulu Pradhan)**

ACKNOWLEDGEMENT

"A person who never made a mistake never tried anything new." – **Prof. Albert Einstein**

As I approach the conclusion of my Ph.D. journey, the enduring resonance of this quote remains constant. Nevertheless, its profound meaning has gained a new level of significance in my life as I near the completion of this academic milestone.

The completion of this thesis owes much to the invaluable support and close association with individuals who consistently stood by me when I needed them the most. I seize this moment to express my gratitude and acknowledge their contributions, without which this thesis would not have been possible. In reaching this milestone, my foremost gratitude goes to the Government of India for founding IIT Guwahati, providing a platform for the realization of technical and scientific knowledge.

I embrace the opportunity to express my deep sense of gratitude to my supervisor **Prof. Bulu Pradhan**, PG Associate Dean of Academic Affairs, Department of Civil Engineering, IIT Guwahati for his constant guidance, valuable suggestions and kind encouragement during my Ph.D. journey. His encouragement, constant support, intellectual stimulation, perceptive guidance, immensely valuable ideas, and suggestions from the initial to the final level enabled me to develop an understanding of the subject. His scholarly suggestions, prudent admonitions, immense interest, constant financial help and affectionate behavior have been a source of inspiration for me. His suggestions will remain with me as an inexhaustible source of scientific learning throughout my life. I am proud to have been the first student under his guidance, conducting research on **"Fly ash based Geopolymer Concrete"** at IIT Guwahati. This significant moment will remain etched in my memory throughout my life. Furthermore, I express sincere appreciation to **Prof. Davidovits**, the pioneer of geopolymer concrete.

I would like to express my sincere and wholehearted gratitude to my doctoral committee: **Prof. Anjan Dutta (**Chairman**)**, **Prof. Kaustubh Dasgupta**, and **Prof. Mihir Kumar Purkait**. They generously gave their time to offer me valuable comments toward improving my work. In particular, **Prof. Anjan Dutta and Prof. Kaustubh Dasgupta** showed me the advisable solution to all stages in my Ph.D. research work and thesis. In addition, **Prof. Mihir Kumar Purkait** provided needful feedback, which helped me develop a broader perspective to my Ph.D. work and thesis.

I express profound gratitude to the Head of the Department, **Prof. Sharad Gokhale** and all respected faculties of the Department of Civil Engineering. I appreciate the Dr. Arun Ch. Borsaikia (Scientific Officer), Mr. Pranab Hazarika (Technical Superintendent), Mr. Saurabh Kr. Mudoi (Junior Technician), Mrs. Juri Jyoti Hazarika (Junior Technical Superintendent) and Mr. Susanta Kumar Sarma (Junior Assistant) for generously provided the help whenever it was required. I wish to express my appreciation to Mr. Om Prakash Prasad for being there to help me during the preparation of test specimens. The outcomes presented in this thesis owe much to the collaborative efforts with these laboratories. My sincere gratitude extends to **Prof. Tharmalingam Punniyamurthy** (Department of Chemistry, IIT Guwahati), Dr. Sidananda Sarma (Scientific Officer, Department of Physics), Dr. Kula Kamal Senapati (Scientific Officer, Central Instruments Facility), Dr. Shyam Kumar Yadav, Dr. Santosh Kumar Yedla (Department of Chemical Engineering, IIT Guwahati) and Mr. Sujit Kumar Deb (Junior Technical Superintendent, Central Instruments Facility) for providing access to modern instruments.

My acknowledgment would be incomplete without a special mention of my labmates, who not only introduced me to the lab culture but also exemplified the hard realities of life. I extend my gratitude to Dr. Arya Anuj Jee and Dr. Smrati Jain for their encouragement and valuable suggestions throughout my research period. Dr. Arya Anuj Jee deserves special thanks for his motivation and unwavering support since the early days of my Ph.D. I express my heartfelt appreciation to my senior lab members, especially Dr. Fouzia Shaheen, Mr. Divyesh Sharma, and Mr. Suresh Chandra Sadangi for their constant support in various forms. In addition, I am thankful to my lab members Dr. Jyotish Kumar Das, Dr. Jnyanendra Kumar Prusty, Mr. Narendra Guru Basavaraj, Mr. Kunal Pradhan, Mr. M. Leela Sai Rangarao, Mr. Abhishek Kamishetty, Mr. Arup Kumar Mohapatra, Mr. Vijayan, Ms. T. Nicola, Ms. Shehnaazdeep Kaur, Mr. Akhil Charat, Mr. Siddharth Kashyup, Mr. Shivam Gupta, and Mr. Uday boddepalli for their all kind of support.

I consider myself fortunate to extend heartfelt appreciation to some remarkable individuals whose support has been invaluable. Words fall short in conveying my gratitude to Mr. Arjun Puthuserry, Mr. Ardendhu Sekar Choudry, Mr. Mojaidul Islam Nayyar, Dr. Shyam Kumar Yadav, Dr. Santosh Kumar Yedla, Dr. Narashima Rao, Dr. K. Dharmalingam, Dr. Geeta Kumari, Dr. Suresh Manickcam, Dr. Arunachalam, Dr. Rahul Narashiman, Dr. Abhay Tawalare, Dr. Balaji, Dr. Rakhee Das, Dr. Mithali Sahu, Dr. G. Surendhar, Dr. M. Arun, Dr. Anjali, Mr. Manoj kumar, Mr. M. Bala, Mr. Ujjwal Jyoti Dutta, Mr. C. Aswinkarthick, Mr.

S.R. Vignesh, Mr. Dinesh G, Mr. Sathishraja, Mr. R. Vishwa, Mr. Ragav, Mr. S. Jeevanandham, and Mr. Alan. Their unwavering support, generous care, and the homely atmosphere at the hostel have contributed significantly to making my stay at IIT Guwahati both enjoyable and memorable. Their presence during both joyful and challenging times provided constant motivation and encouragement.

I am also grateful for the support of the IIT Guwahati Hospital and GNRC Hospital, including the doctors, nurses, and staff, for their conscientious care of my health, particularly in addressing my asthma, migraine, covid-19, and post-traumatic stress disorder concerns during my stay at IIT Guwahati.

I express my deep gratitude to my homeland, India, as well as to my esteemed role models, **Dr. A.P.J. Abdul Kalam** and **Prof. Albert Einstein**. I am indebted to the educational institutions that shaped my academic journey, including IIT Guwahati, NIT Warangal, and Anna University (St. Peter's Engineering College, Chennai). Special thanks go to my teachers, **Prof. Bulu Pradhan** and **Dr. Mohammad Ali**, and my mentor, **Dr. Koteeswaran, and Mr. Nithyanandham**. I extend my appreciation to the schools throughout my educational journey: Fathima Higher Secondary School in Puducherry and Sri Ramakrishna BHEL Higher Secondary School in Ranipet, Tamil Nadu. My heartfelt thanks go to my grandparents, **Late Smt. Saraswathi** & **Late Shri Subramani**, and **Late Smt. Kalyani** & **Late Shri Radha Krishnan**; my parents, **Shri Mani** and **Smt. Radha**; my wife, Mrs. Sowmiya Sathishraj along with my son, Mr. Vishnuraj Sathishraj; my younger sister family, Late Shri. Dayalan, Smt. Ezhilarasi, Shri. Selvakumaran, Mrs. Eswari, Shri. Kumaran and Smt. Mala; and rest of my family members, Shri. Radhakrishnan, Smt. Selvi, Shri. Durai, Smt. Uma, Shri. Lakshmi Narayanan, Smt. Latha, Shri. Karthikeyan, Smt. Gajalakshmi, Shri. Ramalingam, Smt. Malathi, Shri. Sankar Narayanan, Smt. Indira, Shri. Ezhilmaran, Smt. Chithra, Shri. Nagaraj, Shri. Parasuram, Smt. Indirani, and Mr. Velan for their unwavering love, affection, and support throughout every moment of my life. My sincere honor to **"Ayya" Dr. S. Ramadoss** (Founder of Pattali Makkal Katchi), **"Anna" Dr. Anbumani Ramadoss** (Member of Rajyasabha) and **21 vanniyar martyrs** who struggled for right to vanniyar's education that helped myself to achieve this milestone. I acknowledge with gratitude the support from the Ministry of Education (MOE), Government of India, for providing the necessary fellowship that enabled me to pursue my research work. Finally, I attribute the completion of this work to the grace of the **Almighty God** and **Chola Emperors**.

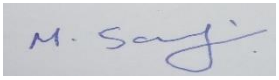

SATHISHRAJ M

ABSTRACT

To mitigate the problems related to higher energy consumption, higher CO_2 emission and disposal of industrial wastes, geopolymer binders based on these industrial waste materials are now widely considered as the promising substitute for Portland cement binders. It may be noted that the production of Portland cement accounts for higher energy consumption and higher amount of CO_2 emissions. The geopolymer binder has the potential to produce sustainable concrete. In the present research work, fly ash based geopolymer concrete (GPC) mixes were prepared with different concentrations of NaOH solution i.e., 8 M, 10 M, 12 M, 14 M and 16 M, alkaline solution contents of 190 kg/m^3 and 210 kg/m^3, sodium silicate solution to sodium hydroxide solution (SS/SH) ratios of 1.5 and 1.75, fly ash particles of different sizes i.e., passing through 150 µm sieve, and 300 µm sieve, and fly ash contents of 425 kg/m^3, and 450 kg/m^3. Sodium chloride (NaCl) of different concentrations i.e., 1.5%, 3% and 4.5% by mass of geopolymer solids were admixed in GPC mixes during the time of preparation. For compressive strength test, cube specimens of size 150 mm, and for corrosion measurement, prismatic specimens of size 72 mm × 72 mm × 300 mm with a centrally embedded steel bar were prepared from GPC mixes. Slump test on fresh GPC mixes, and compressive strength test on cube specimens at different ages were carried out. To evaluate the corrosion behaviour of rebar in the presence of chloride ions, half-cell potential measurement, and linear polarization resistance measurement for corrosion current density were carried out on prismatic specimens at different ages. The microstructure of GPC was analyzed by carrying out XRD (X-ray diffraction) analysis, FESEM (Field emission scanning electron microscope) analysis and FTIR (Fourier transform infrared) spectroscopy on geopolymer concrete powder samples obtained from cube specimens and prismatic specimens. In addition, free chloride, total chloride and bound chloride content of GPC mixes were determined from the powder samples obtained from cube and prismatic specimens.

The presence of sodium chloride in GPC mixes improved the consistency when compared with control GPC mix (without admixed NaCl). The compressive strength of GPC increased with increase in molarity of NaOH solution from 8 M to 16 M in control, and 1.5% NaCl admixed GPC mixes whereas in GPC mixes admixed NaCl concentrations of 3% and 4.5%, the compressive strength increased with molarity of NaOH solution from 8 M to 14 M followed by a decrease at NaOH solution of 16 M. Increase in alkaline solution content, and SS/SH ratio resulted an increase in compressive strength of GPC. However, opposite variation in compressive strength was observed with particle size of fly ash between GPC mixes made with

lower and higher fly ash contents. The particle size of fly ash greatly influenced the variation in compressive strength of NaCl admixed GPC with change in fly ash content. The GPC admixed with sodium chloride showed lower compressive strength as compared to control mix. Further, the compressive strength decreased with increase in NaCl concentration. The compressive strength of GPC increased with age from 7 to 28 days in control as well as in NaCl admixed GPC mixes, whereas, it mostly decreased with age from 28 to 90 days. The GPC mixes made with larger fly ash particles, and that made with higher fly ash content mostly showed higher free chloride content than that made with smaller fly ash particles, and lower fly ash content. The variation in total chloride content of GPC mixes with mix parameters was similar to that in case of free chloride content. Mostly higher chloride binding was observed at lower molarity of NaOH solution than higher molarity of NaOH solution. The formation of more amount of geopolymer gels in GPC mixes made with larger fly ash particles as indicated by higher compressive strength resulted in higher extent of physical binding of chloride ions with geopolymer gels that led to higher bound chloride content in case of larger fly ash particles than smaller fly ash particles.

From the obtained results of XRD analysis, the peak intensity of albite, anorthoclase, and nepheline in the XRD patterns mostly increased with increase in molarity of NaOH solution from 8 M to 16 M in control as well as 1.5% NaCl admixed GPC mixes at the age of 7, 28 and 90 days thereby showing more formation of geopolymer gels at higher molarity of NaOH solution. In GPC mixes admixed with NaCl concentrations of 3% and 4.5%, the peak intensity of the compounds related to geopolymer gels in the XRD patterns mostly increased with increase in molarity of NaOH solution from 8 M to 14 M followed by a decrease at NaOH solution of 16 M. These variations in the peak intensity of the compounds related to geopolymer gels are corroborated with the variations in the compressive strength of GPC with molarity of NaOH solution. From the XRD patterns, the variations in the peak intensity of albite, anorthoclase, nepheline, sodalite, and muscovite are mostly consistent with the variations in compressive strength of GPC with alkaline solution content, SS/SH ratio, particle size of fly ash, fly ash content, NaCl concentration and age. From the FTIR spectra, the variations in the wavenumber associated with the peak corresponding to asymmetric stretching vibration of Si–O–Si(Al) bond in the FTIR spectra that shows the presence of geopolymer gels in GPC mixes at different ages, and the formation of microstructure in GPC as observed from the FESEM images are in line with the variations in the peak intensity of the compounds related

to geopolymer gels in XRD patterns with molarity of NaOH solution, alkaline solution content, SS/SH ratio, particle size of fly ash, fly ash content, admixed NaCl concentration and age.

The extent of chloride induced corrosion increased with increase in alkaline solution content and SS/SH ratio. The obtained results indicated that both particle size of fly ash and fly ash content influenced the corrosion activity of steel reinforcement in the presence of chloride ions in GPC. At the age of 600 days, the GPC made with lower molarity of NaOH solution showed higher free chloride content near rebar level, which resulted in more negative corrosion potential and higher corrosion current density at lower molarity of NaOH solution as compared to higher molarity of NaOH solution. However, higher bound chloride content was observed at lower molarity of NaOH solution as compared to higher molarity of NaOH solution. With SS/SH ratio, there was consistent variation in the effect of chloride ions on extent of corrosion of rebar in GPC at later age for NaOH solution of 10 M whereas there was inconsistent variation at NaOH solution of 14 M. At the age of 600 days, the formation of more amount of geopolymer gels as indicated by higher peak intensity of albite, anorthoclase and nepheline in the XRD patterns of GPC near rebar level in the prismatic specimens at higher molarity of NaOH solution resulted in denser microstructure that led to lower free chloride content near rebar level thereby resulting in lower corrosion activity in GPC made with higher molarity of NaOH solution than lower molarity of NaOH solution. The formation of more amount of geopolymer gels in GPC mixes at lower alkaline solution content, and lower SS/SH ratio as indicated by higher peak intensity of the compounds related to geopolymer gels in XRD patterns led to comparatively higher extent of physical binding of chloride ions with geopolymer gels than higher alkaline solution content, and higher SS/SH ratio. The formation of more amount of geopolymer gels in GPC as indicated by higher peak intensity of the compounds related to geopolymer gels in XRD patterns in case of larger fly ash particles resulted in lower free chloride content near rebar level at the later age of 600 days when compared with smaller fly ash particles. From the FTIR spectra of GPC near steel reinforcement at the later age, the variation in the wavenumber associated with the peak corresponding to asymmetric stretching vibration of Si–O–Si(Al) bond was not significant with molarity of NaOH solution, alkaline solution content, SS/SH ratio, particle size of fly ash, fly ash content, and admixed NaCl concentration. Further, from FESEM images, the variations in the formation of microstructure with mix parameters are supported by the variations in the peak intensity of the compounds related to geopolymer gels in XRD patterns of GPC near steel reinforcement in prismatic specimens at later age.

TABLE OF CONTENTS

CHAPTER 3: Experimental Program

CHAPTER 4: Influence of Mix Parameters on Consistency, Compressive Strength and Chloride Content of Fly ash based Geopolymer Concrete

CHAPTER 7: Conclusions and Suggestions for Future Work

LIST OF FIGURES

LIST OF TABLES

LIST OF SYMBOLS AND ABBREVIATIONS

Å	Angstrom
°C	Degree Celsius
µm	Micrometer
µA	Microampere
θ	Diffraction angle of X-rays
λ	Wavelength of X-ray
I_{corr}	Corrosion current density
Rp	Polarization resistance of steel reinforcement
C_f	Free chloride content
C_b	Bound chloride content
C_t	Total chloride content
A	Albite
AL	Alkaline liquid content or alkaline solution content
Al-O	Aluminum-oxygen
Al-Si	Aluminosilicate
ASTM	American society for testing and materials
Ano	Anorthoclase
CO_2	Carbon dioxide
C-S-H	Calcium silicate hydrate
C-A-S-H	Calcium aluminosilicate hydrate
EJ	Exajoules
FA	Fly ash
FTIR-ATR	Fourier transform infrared spectroscopy – Attenuated total reflectance
FESEM	Field emission scanning electron microscope

GGBS	Ground granulated blast furnace slag
GPC	Geopolymer concrete
H	Halite
ICDD	International center for diffraction data
IS	Indian standards
LPR	Linear polarization resistance
KOH	Potassium hydroxide
K_2SiO_3	Potassium silicate
kW	Kilowatt
mV	millivolt
MSA	Maximum size of aggregate
Mu	Muscovite
N	Nepheline
NH	Sodium hydroxide
NS	Sodium silicate
N-A-S-H	Sodium aluminosilicate hydrate
NaCl	Sodium chloride
NC	Sodium chloride
OPC	Ordinary Portland cement
PC	Portland cement
PDF	Powder diffraction file
Q	Quartz
R	Ratio of alkaline solution
S	Sodalite
SCE	Saturated calomel electrode

SCM	Supplementary cementitious material
SH	Sodium hydroxide
Si-O	Silicon-oxygen
SS	Sodium silicate
TMT	Thermomechanically treated
XRF	X-ray fluorescence
XRD	X-ray diffraction

Chapter 1

Introduction

1.1 General

Concrete made from ordinary Portland cement (OPC) is the second most widely used material of any type behind water as it is the most common building material used in construction for over 175 years [1,2]. However, the use of OPC as a major building material has raised concerns about whether it is an eco-friendly material in real-world applications over the previous few decades [3]. Because of the large quantities of Portland cement (PC) produced, it consumes 10-11 EJ of energy each year, accounting for about 2-3 percent of primary energy use worldwide [2]. Furthermore, being the world's third-largest industrial sector, the building materials industry contributes to CO_2 emissions significantly, accounting for roughly 10% of total man-made CO_2 emissions, almost all of which is attributed to concrete manufacturing. Cement production accounts for around 85% of CO_2 emissions, with the majority of CO_2 emitted during production (about 95%) and 5% released during transportation (which requires ingredients for manufacture and finished goods) [4]. Sustainability in construction is the drive, which is shaping our attitudes toward alternatives to Portland cement (PC). Despite the fact that the building materials industry is essentially sustainable in terms of raw material supply and concrete production, which emits significantly less CO_2 per unit volume than most competitive construction materials, the current focus on climate change has led to serious concerns about cement industry-generated CO_2 emissions [5]. As a result, the cement industry is under increasing pressure to reduce both energy usage and its carbon footprint, and it is actively seeking new alternatives to ensure human future sustainability [2,4]. Through the re-use of waste materials from other industries, the construction materials industry aims for substantial low-CO_2 and low-energy consumption binders. Portland cement concrete is adapting to a wide range of industrial waste materials as secondary cementing materials such as fly ash, ground granulated blast furnace slag (GGBS), silica fume, rice husk ash etc., in order to reduce CO_2 emissions and energy consumption. These supplementary cementing materials are being used to replace a portion of Portland cement, which typically ranges from 10% to 50%, although sometimes greater replacements levels are also used [2].

In the context of sustainability, many studies are now focused on searching alternative binders associated with lesser energy consumption and low CO_2 emission [2]. The disposal of industrial wastes has become a huge problem [6], due to rapid industrialization. To reduce the

problems of higher energy consumption, higher CO_2 emission and disposal of industrial wastes, the waste materials can be used in the production of useful products such as geopolymer binders. Among various alternatives, geopolymer binders are widely considered as the promising substitute for Portland cement binders [7]. The geopolymer is a high-potential binder with the ability to produce sustainable concrete [8]. The term "Geopolymer" was coined by Prof. J. Davidovits in the year 1978 [9]. The concept behind geopolymer is the polymerization of Si-O-Al-O bond that occurs when the aluminosilicate (Al-Si) source material reacts with alkaline activators [9]. In the production of geopolymer concrete, the aluminosilicate (Al-Si) source materials such as fly ash, slag, and metakaolin; and alkaline activators such as sodium hydroxide (NaOH) solution, potassium hydroxide (KOH) solution, mixture of NaOH and sodium silicate (Na_2SiO_3) solution, or mixture of KOH and potassium silicate (K_2SiO_3) solution are used [10,11]. Metakaolin in geopolymers results an increase in CO_2 emissions per tonne of product. Furthermore, due to high cost of metakaolin, and higher water demand of metakaolin based geopolymer, it is not considered as a viable option for production of geopolymer in large scale in civil infrastructure applications [11]. On the other hand, from sustainability viewpoint, the geopolymers based on fly ash and slag are more suitable binders. Additionally, using fly ash and slag in geopolymer concrete has environmental benefits by reducing landfill disposal and converting a greater proportion of waste into building materials. Further, using fly ash in geopolymer concrete requires less water demand due to its spherical shape particles. In the geopolymerization process, the reaction of Al-Si source material like fly ash with the alkaline activator produces sodium aluminosilicate hydrate (N-A-S-H) gel, which is responsible for the strength development of geopolymer concrete (GPC) [11,12]. The properties of alumino-silicate source materials such as Si/Al ratio, calcium content, Si and Al speciation, presence of impurities, and particle size distribution; curing temperature and period; and type, proportion, and quantity of alkaline solution are the factors that influence the geopolymerization process [13].

1.2 Geopolymer reaction mechanism

A geopolymer is a three-dimensional zeolite-like network structure made up of tetrahedral silicon-oxygen (Si-O) and aluminum-oxygen (Al-O) ions [14,15]. The geopolymerization process occurs through the dissolution of silicon and aluminum components in a highly alkaline environment [16]. The geopolymer reaction mechanism is influenced by the method of synthesis, chemical composition and physical characteristics of the aluminosilicate source materials, and amount and type of alkali activator used [17]. The geological polymerization

reactions are more complex than OPC hydration [18]. According to Davidovits, the structure of a geopolymer is as follows [15,19,20]:

$$M_n [– (SiO_2)_Z – AlO_2]_n . wH_2O \quad (1.1)$$

Where, M is an alkali metal cation; n is the degree of polycondensation; w is the number of chemically bound water molecules; and Z is the silicon-to-aluminum ratio (Si/Al), which is either 1, 2, or 3. According to the Z value, the geopolymer structures are classified as single silicon-aluminum (Gel 1, Si/Al = 1), i.e., poly(sialate) (-Si-O-Al-O-), double silicon-aluminum (Gel 2, Si/Al = 2) i.e., poly(sialate-siloxo) (-Si-O-Al-O-Si-O-), and triple silicon-aluminum (Gel 3, Si/Al = 3) i.e., poly(sialate-disiloxo) (-Si-O-Al-O-Si-O-Si-O-) [15,19,20]. These structures are depicted in Fig. 1. The poly (sialates) are the chain and ring polymers with Si^{4+} and Al^{3+} in IV-fold coordination with oxygen, and range from amorphous to semi-crystalline [15].

The hardening of geopolymer materials is accomplished by breaking and recombining the Si-O and Al-O bonds in the presence of an alkaline activator. The four steps that comprise the reaction process are as follows; (i) dissolution: under the influence of an alkali activator, the Si-O and Al-O bonds in aluminosilicate materials are broken, releasing Si-O and Al-O tetrahedral monomers, (ii) diffusion: in the reaction system, the dissolved Si-O and Al-O tetrahedral monomers diffuse. According to chemical equilibrium, the concentrations of silicon and aluminium on the particle surface drop due to diffusion, and the dissolution process continues, (iii) polycondensation: polymerization of Si-O and Al-O tetrahedra results in formation of amorphous -Si-O-Al-O- structures or zeolite crystals, and (iv) hardening: as a result of the dehydration reaction, a hardened geopolymer with greater mechanical strength is formed. The polymerization mechanisms in geopolymer materials made from different raw materials are not identical, however, they generally follow the aforementioned reaction process.

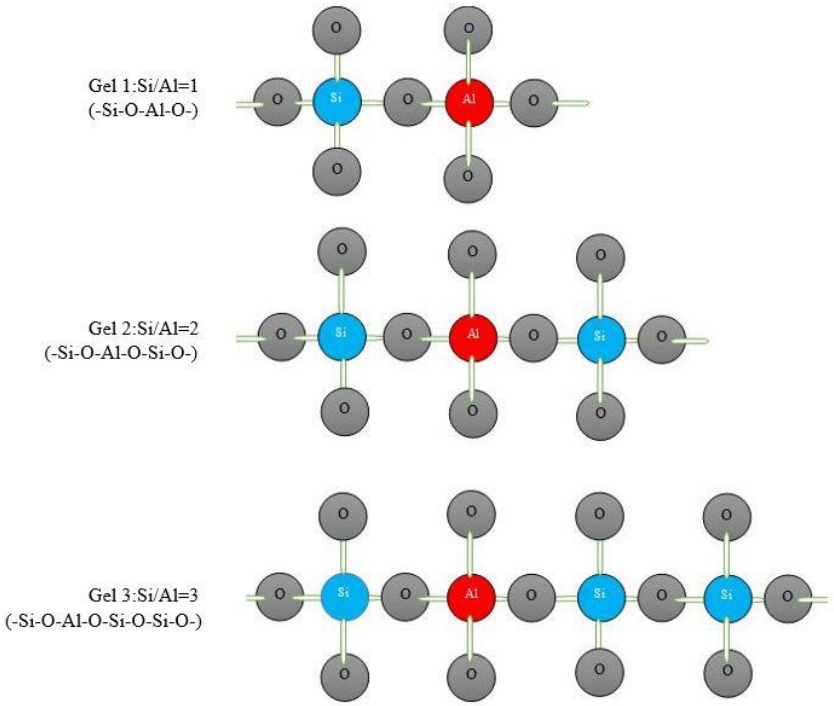

Fig. 1.1: Geopolymer structures according to Davidovits model [19]

According to the model developed by Glukhovsky [19,21], the alkali activation process comprises of deconstruction, gel formation, polycondensation, and crystallization.

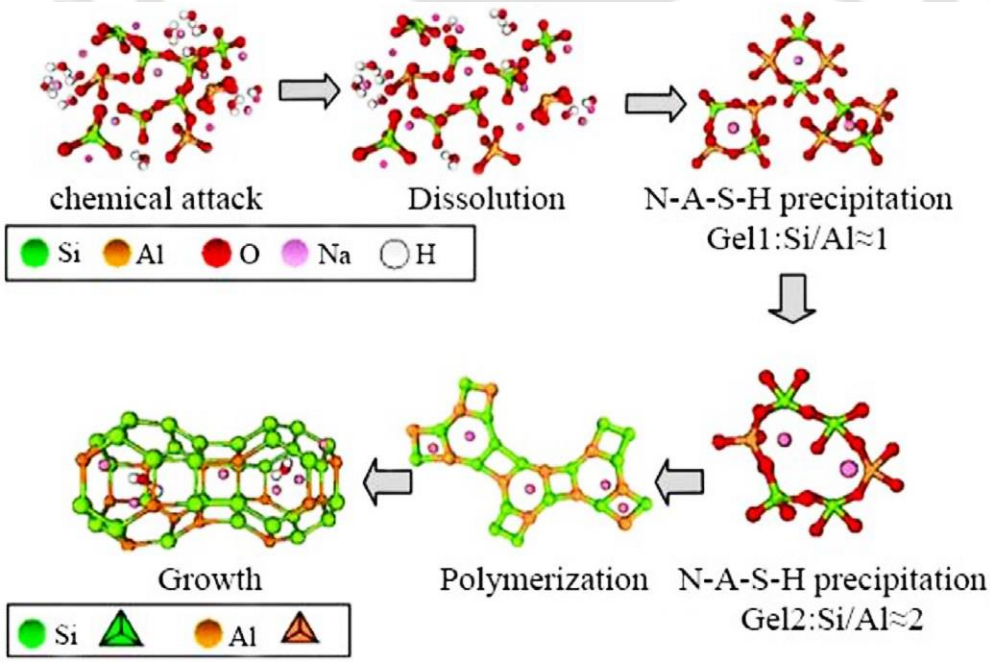

Fig. 1.2: Glukhovsky conceptual model for geopolymerization [19,21]

As depicted in Fig. 1.2, there are five reaction processes that occur during geopolymerization in the Glukhovsky model. In contrast to the Davidovits model, the polycondensation process is divided into two processes i.e., gelation and reconstitution in Glukhovsky model. The

gelation involves dehydration to form oligomeric gel when the aluminosilicate is in saturated state, and the reconstitution involves rearrangement of the oligomeric gels. The gels are dehydrated and condensed, thereby gradually forming a three-dimensional network structure of the geopolymer.

1.3 Geopolymer concrete

Geopolymer concrete has the potential to replace the conventional Portland cement concrete due its enhanced mechanical and durability properties while also being environmentally friendly and low-cost alternative [22,23]. The two major components used to manufacture geopolymer concrete are aluminosilicate source materials and alkaline solutions [24]. As stated earlier, the industrial wastes such as fly ash, slag, rice husk ash etc., and metakaolin from geological resources are used as aluminosilicate precursor materials. The alkaline solutions often used are sodium hydroxide or potassium hydroxide solutions in combination with sodium silicate or potassium silicate solutions. The geopolymer concrete is made by combining a source material or a combination of source materials with an alkaline solution, and binding it with aggregates to produce a homogeneous mix, which can be handled and cast in the same way as the conventional Portland cement concrete [24].

1.4 Fly ash based geopolymer concrete

The fly ash based geopolymer concrete has gained significant consideration in the last two decades as an alternative to Portland cement concrete for the production of structural/non-structural elements because of reduction in CO_2 emission, and lower energy consumption [25]. However, fly ash is not a standard product as its physical and chemical properties considerably change not only from source to source but also change from the same thermal power plant over a period of time [26]. The varying chemical composition of fly ash can influence the geopolymer product [27]. Thus, variable characteristics of fly ash pose difficulties for its use in geopolymer production [28]. In fly ash based geopolymer, the geopolymerization mechanisms responsible for the formation of geopolymer gel are complex and still not fully understood [26].

Different types of fly ash namely class F and class C are used in the production of geopolymer concrete. The chemical composition of fly ash varies greatly depending on the source of coal used in coal-fired power plants. The oxide composition of fly ash comprises mainly of SiO_2, Al_2O_3, CaO, and Fe_2O_3, which exist in amorphous and crystalline form [29]. As per ASTM C618 [30], the fly ash is classified as class F when the content of $SiO_2 + Al_2O_3 + Fe_2O_3$ is

minimum 50%, and the content of CaO is up to 18%. Similarly, the fly ash is classified as class C when the content of SiO_2 + Al_2O_3 + Fe_2O_3 is minimum 50%, and the content of CaO is greater than 18%. During geopolymerization, the type and concentration of alkaline solution have an impact on the release of silica and alumina from fly ash. A high concentration alkaline solution is often advantageous for achieving high compressive strength. Among different alkaline solutions used, the combination of NaOH and Na_2SiO_3 solution is commonly used in the production of geopolymer binders. The aggregates i.e., fine aggregate (sand) and coarse aggregate (gravel, crushed aggregates) used in the production of conventional Portland cement concrete are suitable for geopolymer concrete. Although, the aggregates are considered as inert in concrete, however, their physical, thermal and sometimes chemical properties can influence the behaviour of concrete [31]. From the economic viewpoint, it is beneficial to use a concrete mix with as much aggregate content and as lesser binder content as possible, however, the associated cost benefit needs to be balanced against the desired fresh, mechanical and durability properties of concrete [31].

1.5 Behaviour of fly ash based geopolymer concrete

The degree of compaction significantly influences the properties of concrete in hardened state such as volume stability, mechanical properties and durability. Thus, the workability of fresh concrete mix should be such that it can be easily transported, placed, and adequately compacted followed by finishing without segregation [31]. Similar to conventional Portland cement concrete, the workability of geopolymer concrete (GPC) should be such that the fresh concreting operations including adequate compaction can be accomplished easily. The workability of fly ash based GPC is influenced by various factors such as concentration of alkaline solution, alkaline solution-to-fly ash (aluminosilicate source material) ratio, fineness and amount of fly ash, and ratio of Na_2SiO_3 to NaOH solution [32]. The strength properties of concrete are considered to be important and they provide an overall picture of the quality of concrete as they are related to the structure of the hydrated cement paste in case of conventional concrete [31]. Further, properties related to durability such as watertightness or impermeability, and resistance to aggressive weathering agents are considered to be dependent on the strength of concrete. The compressive strength of concrete is several times higher than other types of strength. Thus, majority of the concrete elements are designed to exploit the higher compressive strength of concrete. The 28-day uniaxial compressive strength of concrete is universally accepted as a general index of concrete strength [33]. Since in practice, concrete is subjected mostly to combination of compressive, shearing, and tensile stresses, the

relationships between uniaxial compressive strength and other strength properties such as tensile, flexural, shear and biaxial strength are established.

Similar to the conventional concrete, the strength properties of geopolymer concrete indicate its quality, which influence the performance in the given exposure environment. The variations in strength of fly ash based geopolymer concrete depend on the extent of formation of geopolymer gels, which in turn is influenced by different parameters such as composition of alkaline solution, molarity of NaOH solution, alkaline solution-to-fly ash ratio, fineness and content of fly ash, and curing condition. The variations in compressive strength of geopolymer concrete with changes in above parameters are of significant interest and these variations need to be correlated with the changes in the microstructure of geopolymer concrete to understand its behaviour. In addition, the variations in strength of geopolymer concrete with changes in mix parameters when subjected to different exposure environment also need to be established and correlated with the microstructural variations. In addition to the strength, the durability characteristics of geopolymer concrete against different exposure environment need to be studied. The different durability problems encountered in reinforced concrete structures are sulfate attack, acid attack, attack by seawater, corrosion of steel reinforcement etc. Among these problems, corrosion of steel reinforcement is the most serious durability problem that occurs in reinforced concrete structures. The performance of fly ash based geopolymer concrete needs to be evaluated to understand its behaviour against different durability problems in general and against corrosion of steel reinforcement in particular.

1.6 Corrosion of steel reinforcement

Reinforcing steel corrosion in concrete is an electrochemical process. The differences in the electrochemical potential on the surface of steel reinforcement form anodic and cathodic regions, which are connected by the electrolyte in the form of concrete pore solution [31]. In the electrochemical process, at the anodic region, the positively charged ferrous ions Fe^{++} pass into the solution, whereas the negatively charged free electrons e^{-} pass along the steel into the cathodic region, where they are absorbed by the electrolyte constituents and combine with water and oxygen to form hydroxyl ions $(OH)^{-}$. The hydroxyl ions combine with ferrous ions to form ferrous hydroxide, which is on further reaction with oxygen and water forms ferric hydroxide that constitutes hydrated red rust. The electrochemical corrosion process proceeds only when water and oxygen are available.

As stated earlier, steel reinforcement corrosion is one of the most serious durability issues that can degrade the reinforced concrete structures during the service life. Corrosion of steel reinforcement in reinforced concrete results in high repair and maintenance costs [34]. The formation of a thin protective film of iron oxide over the surface of steel reinforcement due to highly alkaline nature of concrete (pH of about 13) prevents the corrosion of steel reinforcement. However, corrosion can occur, if the carbonation front reaches the vicinity of steel reinforcement or the chloride ions penetrate into concrete and reach near the rebar level, and water and oxygen are present [31]. Between the two causes of corrosion i.e., chloride ions, and carbonation, chloride ions are considered as the primary cause of rebar corrosion in concrete. In case of marine environment, and in the areas where the soil and groundwater are contaminated, the process of deterioration in reinforced concrete structures primarily occurs due to chloride induced rebar corrosion [35]. The ingress of chloride ions in concrete occurs as a result of combination of several mechanisms, which includes penetration, absorption (or capillary suction), and diffusion [35]. The chloride ions may enter into the concrete form the external exposure environment as well as internally through its ingredients. The penetration of chloride ions into geopolymer composites from the external environment depends mainly on the resistance of the binder to the transport of chloride ions, and the binding capacity of binder on producing specific reaction products [36]. In case of internal chloride, the chloride ions may be introduced into the concrete through its ingredients such as chloride contaminated mixing water, aggregates, and chloride containing admixtures. In geopolymer concrete, the sources of internal chloride can be the water, which is used in the preparation of alkaline solutions, may be contaminated with chloride ions, use of extra mixing water (may also be contaminated) and contaminated aggregates.

The chloride ions exist as free chloride and bound chloride in concrete. The presence of free chloride in the concrete pore solution is mainly responsible for inducing corrosion of steel reinforcement. The amount of free chloride in the concrete pore solution, as well as the presence of oxygen and water, as stated earlier are the critical factors for the initiation and propagation of chloride induced corrosion in reinforced concrete structures [37]. The chloride binding capacity of concrete is an important factor while predicting the service life of reinforced concrete structures as it controls the amount of free chloride ions available in the vicinity of steel reinforcement. The mechanism of chloride binding in geopolymer concrete, which is made using aluminosilicate source materials and alkaline activators is not well understood. The relationship between free and bound chloride in geopolymer concrete is still

unknown. Due to variations in the interaction of chloride ions with the geopolymer gels and that in the pore solution chemistry, the chloride binding capacity in geopolymer concrete is expected to be different from Portland cement concrete [37]. In Portland cement concrete, the chloride ions are physically adsorbed on C-S-H gel as well as bound chemically with calcium aluminate hydrates. In geopolymer concrete, the chloride ions are adsorbed physically on geopolymer gels i.e., sodium aluminosilicate hydrate (N-A-S-H) gel and calcium aluminosilicate hydrate (C-A-S-H) gel to certain extent while the mechanism of chemical binding of chloride ions with aluminosilicate gels is not clearly known. The chlorides are physically adsorbed on C-A-S-H gel without altering the mineral structure, whereas a porous N-A-S-H gel adsorbs chlorides on its surface by hosting a high-chloride pore solution, resulting in NaCl precipitates upon evaporation. The addition of fly ash to geopolymer results in stronger physical adsorption of chlorides onto the N-A-S-H gel due to its larger surface area. It is reported that the N-A-S-H gel has a higher chloride binding capacity than C-A-S-H gel [38]. Different research investigations have found formation of chloride-bearing zeolites in geopolymers [39]. On the contrary, other researchers have observed that N-A-S-H gel has higher chloride binding capacity due to its higher physical chloride adsorption capability [39].

1.7 Challenges in fly ash based geopolymer concrete

As stated earlier, the physical and chemical properties of fly ash vary considerably from one source to another as well as vary from the same thermal power plant over a period of time. These variable characteristics of fly ash affect different properties of geopolymer and pose challenges for the production of geopolymer concrete (GPC). The curing temperature as well as curing period play a significant role in the strength development of fly ash based geopolymer concrete [26]. Although, GPC can set at ambient temperature [40], the extent of reaction of fly ash in the geopolymerization process is low. However, the rate of geopolymeric reaction increases with an increase in the temperature of curing medium. The fly ash based geopolymer concrete can achieve higher strength at temperatures between 60 °C and 100 °C for a curing period ranging from about 24 to 48 hours in contrast to Portland cement concrete, which generally requires room temperature curing [41–43]. The application of high temperature curing in the development of fly ash based geopolymer concrete poses difficulty in its widespread field application, however, prefabricated concrete members can easily be produced with the application of adequate temperature curing. The lapsed time between end of casting of geopolymer concrete, and the start of the heat curing is referred to as the rest period. The start of high temperature curing may be delayed for several days without adversely affecting

the properties of geopolymer concrete. In fact, an increase in the rest period significantly increases the strength of the geopolymeric product [40]. Keeping in view the above points, there is a need to understand the influence of variable characteristics of fly ash, mix parameters related to fly ash and alkaline solution, and curing condition on different properties of fly ash based geopolymer concrete.

1.8 Significance of present research work

One of the major barriers to the widespread use of fly ash based geopolymer concrete in industrial applications is attributed to the lack of comprehensive understanding of its behavior with regard to strength development, variations in microstructure and resistance to different durability problems. Different researchers have studied the fresh, mechanical, and microstructure of fly ash based geopolymer concrete. However, a very few studies have been carried out to evaluate the long term durability property of fly ash based geopolymer concrete in general, and chloride induced corrosion of steel reinforcement in particular. In these limited studies, the influence of different mix parameters related to aluminosilicate source material, and alkaline solution on chloride induced corrosion of steel reinforcement in fly ash based geopolymer concrete has not been investigated comprehensively. Thus, there is a need to study the long term chloride induced corrosion of steel reinforcement in fly ash based geopolymer concrete, and evaluate the effect of different mix parameters on corrosion behavior of steel reinforcement. Further, it is essential to understand the variations in the microstructure of fly ash based geopolymer concrete in the presence of chloride ions. Keeping the above aspects in view, the objectives of the present research work have formulated to investigate the influence of mix parameters such as particle size and quantity of fly ash, molarity of NaOH solution, alkaline solution content, and ratio of alkaline solution on workability, compressive strength development, variation in microstructure, and corrosion of steel reinforcement in fly ash based geopolymer concrete (GPC) in the presence of internal chloride.

1.9 Thesis organization

The research work carried out in the present study has been organized in seven chapters, which are presented below.

- **Chapter 1** introduces the background, and significance of the present research work. The organization of the thesis is also presented in this chapter.

- **Chapter 2** presents the review of literature on fresh, hardened, microstructure and durability properties of fly ash based geopolymer paste, mortar, and concrete. The objectives of the present research work are also mentioned in this chapter.
- **Chapter 3** presents the details about the materials used, test specimens, and different tests conducted to evaluate the workability, compressive strength, chloride content, microstructure, and corrosion behaviour of steel reinforcement in fly ash based geopolymer concrete.
- **Chapter 4** describes the results, and discussions on the effects of molarity of NaOH solution, alkaline solution content, ratio of alkaline solution, particle size of fly ash, and fly ash content on variations in workability, and compressive strength of control and NaCl admixed fly ash based geopolymer concrete (GPC). In addition, the obtained results of free chloride and total chloride contents of NaCl admixed fly ash based GPC mixes are discussed in this chapter.
- **Chapter 5** presents the results obtained from the microstructure analysis of fly ash based geopolymer concrete. The variations in microstructure of control and NaCl admixed GPC mixes with molarity of NaOH solution, alkaline solution content, ratio of alkaline solution, particle size of fly ash, and fly ash content are discussed in this chapter.
- **Chapter 6** presents the results, and discussions on corrosion behaviour of steel reinforcement in fly ash based geopolymer concrete in the presence of internal chloride. Further, the variations in obtained free chloride and total chloride contents of fly ash based GPC at rebar level in prismatic specimens are discussed in this chapter. In addition, the obtained results of microstructure analysis of geopolymer concrete at rebar level in prismatic specimens are also discussed in this chapter.
- **Chapter 7** provides the conclusions obtained from the present research work. In addition, the suggestions for future research work are also mentioned in this chapter.

Chapter 2

Review of Literature

2.1 General

The fresh, mechanical, microstructure, and durability properties of fly ash based geopolymer paste, mortar, and concrete were covered in detail in this chapter. The effect of various mix factors such as NaOH concentration, fly ash content, particle size of fly ash, alkaline solution content, and ratio of alkaline solution are studied, particularly from the standpoint of fresh and hardened properties of fly ash based geopolymer concrete. The most relevant parts of a literature review on microstructure and chloride-induced steel reinforcement corrosion of geopolymer concrete made with fly ash are presented. This chapter concludes with a discussion of the research gaps identified in the literature and the objectives of the present research study.

2.2 Fresh and hardened properties of fly ash based geopolymer paste, mortar and concrete

2.2.1 Effect of alkaline solution on fresh and hardened properties

Chindaprasirt et al. [44] have investigated the workability and compressive strength of high calcium fly ash based geopolymer mortar. Sodium hydroxide (NaOH) and sodium silicate (Na_2SiO_3) solution were used in the preparation of geopolymer mortar. In this study, different molarity of NaOH solution i.e., 10 M, 15 M and 20 M and sodium silicate to sodium hydroxide ratios of 0.67, 1, 1.5 and 3 were used. Extra water or superplasticizer was used to obtain the mixes with similar flow patterns. The mixing of geopolymer mortar was performed in an air-conditioned room at temperature of about 25° C. After mixing, the flow of fresh geopolymer mortar was determined as per ASTM C124. Subsequently, the mortar was placed in 50 mm size of cube moulds. Further, the specimens were placed in oven curing at temperatures of 30 °C, 45 °C, 60 °C, 75 °C and 90 °C after the predetermined delay time. After temperature curing, the specimens were kept in the laboratory condition to cool down and demoulded after 24 hours and were kept at room temperature of 25 °C to 28 °C till the age of testing. In accordance with ASTM C109, the compressive strength test was carried out on the cube specimens at the age of 7 days. From the obtained test results, the authors reported that workable flow of the geopolymer mortar mixes was in the range of 110 ± 5% to 135 ± 5%. An increase in concentration of NaOH solution and the amount of sodium silicate solution decreased the workability of the mortar mixes and improvement in the workability could be

achieved with the addition of extra water or superplasticizer. The test results revealed that the higher strength was achieved in the geopolymer mortar at optimum sodium silicate to sodium hydroxide ratios of 0.67–1. The effect of variation in molarity of NaOH solution between 10 M and 20 M on strength of geopolymer mortar was small. The delay time before heat curing had no adverse effect on compressive strength of geopolymer mortar. Higher strength was achieved in the geopolymer mortar prepared with delay time (after demoulding and before subjecting to heat curing) of 1 hour and heat curing in oven at temperature of 75 °C for a period of not less than 48 hours.

Kaur et al. [45] had studied the variation in compressive strength of fly ash based geopolymer mortar by varying the molarity of sodium hydroxide (NaOH) solution and accompanied with sodium silicate (Na_2SiO_3) solution at same molarity. The source material for geopolymer mortar in this investigation was low calcium (Class F) fly ash. The experimental study used locally available river sand as fine aggregate. Total six mixtures were prepared in this study. NaOH solution was used as the alkaline activator solution for three mixtures. The combination of NaOH solution and Na_2SiO_3 solution was used as the alkaline activator solution for remaining three mixtures. Three different molarity of NaOH solution i.e., 12 M, 14 M, and 16 M were used in this study. The alkaline activator solution to fly ash ratio, and the sodium silicate to sodium hydroxide solution ratio were set at 0.45 and 2.0 respectively for all geopolymer mortar mixtures. The geopolymer mortar mixtures were cast into mortar cube specimens of size 70.6 mm to measure the compressive strength. After 3 hours of casting, the geopolymer mortar cubes along with the moulds were placed in an oven at temperature of 80 °C for 24 hours. After 24 hours of temperature curing, the cubes with moulds were removed from oven and demoulded. Further, the cubes were maintained at room temperature for ambient curing until the day of testing. The compressive strength of all geopolymer mortar specimens was measured at the age of 3, 7, 14 and 28 days after casting. From the obtained results, the authors reported that the compressive strength of fly ash based geopolymer mortar increased with increase in the molar concentration of NaOH solution, and curing age. The fly ash based geopolymer mortar mixes activated using a combination of sodium hydroxide and sodium silicate solutions exhibited higher compressive strength than the mixes activated with sodium hydroxide solution alone.

Rattanasak and Chindaprasirt [46] have investigated the influence of NaOH solution and ratio of alkaline solution on compressive strength of fly ash based geopolymer mortar. In this study, high calcium (Class C) fly ash was used as the source material for making of geopolymer

mortar. River sand was used as fine aggregate in the preparation of geopolymer mortar. Three different molarity (5 M, 10 M, and 15 M) of NaOH solution was used in this study. The alkaline solution was prepared by mixing of NaOH (NH) solution with Na_2SiO_3 (NS) solution. The ratio of NS to NH solution were 0.5, 1, 1.5, and 2 for all the mixes. Two types of mixing were adopted in this study, namely, separate mixing and normal mixing. For separate mixing, NaOH solution (5 M, 10 M, and 15 M) was mixed with fly ash for the first 10 minutes and subsequently sodium silicate solution was added to the mixture. For normal mixing, fly ash, NaOH solution (10 M) and sodium silicate solution were incorporated and mixed at the same time. The geopolymer mortar cube specimens of size 50 mm were prepared. The cube specimens were wrapped with clingfilm to avoid evaporation of moisture during heat curing. The cube specimens were oven cured at the temperature of 65 °C for 48 hours. Subsequently, the specimens were cooled down to the room temperature and subjected to compressive strength test as per ASTM C109. The obtained experiment results indicated that the compressive strength increased with increase in molarity of NaOH solution and ratio of NS/NH solution from 0.5 to 1 in case of separate mixing. However, there was no systematic variation in compressive strength with molarity of NaOH solution for NS/NH solution ratios of 1.5 and 2. For normal mixing, the compressive strength obtained from10 M NaOH solution increased with increase in ratio of NS/NH solution from 0.5 to 1.5. However, the compressive strength declined at NS/NH solution ratio of 2. The compressive strength obtained at 10 M NaOH solution was higher in case of separate mixing than normal mixing at NS/NH solution ratios of 0.5 and 1, whereas normal mixing was more effective than separate mixing at NS/NH solution ratios of 1.5 and 2.

Topark-Ngarm et al. [47] have investigated the fresh and mechanical properties of high calcium fly ash based geopolymer concrete. The source material for geopolymer concrete in this study was high calcium (Class C) fly ash. For the preparation of fly ash based geopolymer concrete mixes, 20 mm maximum size of aggregate (MSA) and river sand were used as coarse aggregate and fine aggregate respectively. The alkaline solution to fly ash ratio by weight was 0.5 for all the mixes. The NaOH solution concentrations of 10 M, 15 M and 20 M, and the Na_2SiO_3 (NS)/NaOH (NH) solution ratio by weight of 1.0 and 2.0 were used. The mixing of geopolymer concrete was done at controlled temperature of 23 ± 2 °C. The slump flow test was carried out on a plastic sheet placed on flat wooden board within 5 minutes after mixing. The setting time of geopolymer concrete was measured as per ASTM C807 by using mortar sample collected from fresh concrete mix. The geopolymer concrete was cast into different

cylindrical steel moulds of size 100 mm × 200 mm for compressive strength and splitting tensile strength tests, 150 mm × 300 mm for modulus of elasticity, and 100 mm × 150 mm for pullout bond test at the respective ages of 7 and 28 days. Two methods of curing condition were adopted. The first method was oven curing at temperature of 60 ± 2°C for 24 hours after the delay period of 2 hours. For the second curing method, the specimens were kept at controlled room temperature of 23 ± 2 °C. After 24 hours of curing, all the concrete cylinders were removed from the mould and wrapped with vinyl sheet, and cured at controlled room temperature of 23 ± 2 °C until the age of testing. The test results indicated that the flow values and setting time of high calcium fly ash based geopolymer concrete mixes decreased with increase in molarity of NaOH solution. The compressive strength and splitting tensile strength of geopolymer concrete mixes were higher in oven curing condition than room temperature curing at both the ages. The compressive strength and splitting tensile strength of geopolymer concrete mixes increased with increase in molarity of NaOH solution from 10 M to 15 M when room temperature curing was used for both the ages. However, for both ages, the compressive strength and splitting tensile strength increased with increase in molarity of NaOH solution from 10 M to 20 M when oven temperature curing was used. Further, the compressive strength and splitting tensile strength were higher at both ages when higher ratio of sodium silicate solution to sodium hydroxide ratio was used in case of room temperature curing. However, the compressive strength and splitting tensile strength were higher at both the ages when lower ratio of sodium silicate solution to sodium hydroxide ratio was used in case of oven curing. The splitting tensile strength, elastic modulus, and bond strength were correlated with the compressive strength. The bond strength between high calcium fly ash based geopolymer concrete and rebar was significantly higher when compared with normal Portland cement concrete as given by ACI 318 design code.

Aliabdo et al. [9] have studied the influence of alkaline solution, additional water and water reducing admixture on different properties of fly ash based geopolymer concrete (GPC). Class F fly ash was used as the source material for the preparation of geopolymer concrete. In this study, pink limestone of nominal maximum size 9.5 mm was used as the coarse aggregate and natural siliceous sand was used as fine aggregate. The alkaline solution was prepared by adding different molarity (12 M, 16 M and 18 M) of NaOH solution and Na_2SiO_3 solution. The alkaline solution to fly ash ratios were 0.3, 0.35, 0.4 and 0.45. The NaOH solution to Na_2SiO_3 solution ratios of 0.30, 0.40 and 0.50 were used in the GPC mixes. The fly ash content was 400 kg/m^3. The alkaline solution contents of 120 kg/m^3, 140 kg/m^3, 160 kg/m^3, and 180 kg/m^3, and

extra water contents of 10, 20, 30 and 35 kg/m^3 were used in the preparation of GPC mixes. The high range water reducing admixture (ASTM Type F) was used to improve the workability of GPC and the quantities used were 2.5, 5, 7.5 and 10.5 kg/m^3 of concrete. The fly ash based geopolymer concrete mixtures were cast into the moulds for different test specimens. The moulds with the specimens were kept at room temperature of 20 - 23 °C leaving the top surface exposed to air. The specimens were demoulded after 24 hours of casting and then subjected to hot air oven curing for 48 hours at temperature of 50 °C, and subsequently, kept at ambient temperature till the day of testing. Different tests were performed to determine the workability, compressive strength, tensile strength, modulus of elasticity, water absorption and porosity of fly ash based geopolymer concrete. From the obtained test results, the authors reported that increase in additional water content and dosage of high range water reducing admixture resulted an increase in slump value of GPC, however, the mechanical properties i.e., compressive strength (at 7 and 28 days), tensile strength (at 28 days) and static modulus of elasticity (at 28 days) of GPC decreased with increase in additional water content and dosage of high range water reducing admixture. Further, the water absorption (at 28 days) and porosity (at 28 days) of GPC increased with increase in additional water content and dosage of high range water reducing admixture. The increase in molarity of NaOH solution decreased the workability of GPC whereas increase in alkaline solution to fly ash ratio resulted an increase in the workability of GPC mixes. Further, the increase in molarity of NaOH solution from 12 M to 16 M, and that in alkaline solution to fly ash ratio from 0.30 to 0.40 decreased the mechanical properties and increased the water absorption and porosity of GPC followed by the opposite variation at NaOH solution of 18 M and alkaline solution to fly ash ratio of 0.45. The authors observed that the workability of GPC increased with increase in NaOH to Na_2SiO_3 solution ratio. Further, the compressive strength, tensile strength and static modulus of elasticity decreased whereas, the water absorption and porosity of GPC increased with increase in NaOH to Na_2SiO_3 solution ratio.

Gorhan and Kurklu [48] have determined the effect of sodium hydroxide (NaOH) concentration on physical and mechanical properties of Class F fly ash based geopolymer mortar under different curing temperatures. Three different molarity of NaOH solution i.e., 3 M, 6 M and 9 M, and sodium silicate (Na_2SiO_3) solution to sodium hydroxide (NaOH) solution ratio of 2 were used in the preparation of geopolymer mortar. The ratio of alkaline solution to fly ash were 0.97, 1.00, and 1.04. The mortar mixes were cast in moulds of size 40 mm × 40 mm × 160 mm. The specimens were cured in oven at temperature of 65 °C and

85 °C for curing period of 2 hours, 5 hours and 24 hours. At the end of curing process, the specimens were stored at room temperature till the physical and mechanical tests were carried out. The physical properties such as water absorption, porosity, bulk density and apparent density, and mechanical properties such as compressive strength and flexural strength were determined. The obtained results indicated that the geopolymer mortar prepared with 6 M NaOH solution achieved the optimum condition and the highest compressive strength when cured at temperature of 85 °C. It was observed that an increase in curing temperature increased the compressive strength and flexural strength of geopolymer mortar while having no influence on the physical properties. Further, the flexural strength of geopolymer mortar was not affected by the molarity of NaOH solution.

Joseph and Mathew [49] have carried out a study on the influence of total aggregate content, ratio of fine aggregate to total aggregate, curing temperature, curing period, molarity of sodium hydroxide solution, ratio of alkaline solution, and ratio of water to geopolymer solids on compressive strength of fly ash based geopolymer concrete mixes. The low calcium fly ash was used as the aluminosilicate source material in the study. The crushed granite rock of nominal size 20 mm and natural river sand of nominal size 4.5 mm were used as coarse aggregate and fine aggregate respectively. Total aggregate content ranged from 60% to 75% of volume of concrete. For each total aggregate content, the fine aggregate-to-total aggregate mass ratio was changed from 0.2 to 0.4. Combination of NaOH solution and Na_2SiO_3 solution was used as the alkaline solution. Different molarity of NaOH solution i.e., 8 M, 10 M, 12 M, 14 M and 16 M were used in the preparation of geopolymer concrete. The ratios of water to geopolymer solids, and alkali liquid to fly ash varied from 0.20 to 0.32, and 0.35 to 0.65, respectively. The naphthalene-based water reducing admixture was used to improve the workability of GPC mixtures. The ratio of sodium silicate solution to sodium hydroxide solution (ratio of alkaline solution) were 1.5, 2.0, 2.5, 3.0 and 3.5. Cube specimens of size 150 mm were cast. After casting, the specimens were maintained at room temperature for 60 minutes before being thermally cured. Then, the specimens along with the moulds and cover plates were subjected to oven curing at various curing temperatures of 60–120 °C and curing period of 6–72 hours. The specimens were removed from the moulds at the end of the curing period and stored at room temperature under laboratory condition until the age of testing. The compressive strength of geopolymer concrete cube specimens was determined at the age of 7 days. The obtained test results indicated that the compressive strength increased with increase in total aggregate content (of volume of concrete) from 60% to 70% followed by a decrease at

75% for all ratios of fine aggregate to total aggregate content. Further, it was observed that the compressive strength increased with increase in fine aggregate to total aggregate mass ratio from 0.2 to 0.35 followed by a decrease at 0.40 for all total aggregate contents. This indicates variations in the extent of binding of aggregates by geopolymer gel with changes in proportion of fine and coarse aggregates. The compressive strength increased with increase in alkaline solution ratio, and alkaline solution to fly ash ratio from 1.5 to 2.5, and 0.35 to 0.55 respectively followed by a decrease thereafter. The compressive strength of geopolymer concrete increased with increase in curing period, and with increase in curing temperature from 30 to 100 °C followed by a decrease at 120 °C. The reduction in compressive strength beyond curing temperature of 100 °C was attributed to the loss of moisture from the geopolymer concrete. It was observed that the compressive strength increased with increase in molarity of NaOH solution from 8 M to 10 M followed by a decrease thereafter till 16 M. The decrease in compressive strength at higher molarity of NaOH solution was attributed to the fact that excess alkali content hinders the condensation of silicate species. Further, the compressive strength decreased with increase in ratio of water to geopolymer solids for all ratios of alkali solution to fly ash. From the study of other mechanical properties, the geopolymer concrete made with total aggregate content of 70% (of volume of concrete), ratio of fine aggregate to total aggregate of 0.35, NaOH solution molarity of 10 M, alkaline solution ratio of 2.5, and alkaline solution to fly ash ratio of 0.55, when cured for 24 hours at 100 °C that had a compressive strength of 52 N/mm^2 exhibited higher value of poisson's ratio and modulus of elasticity when compared with ordinary cement concrete with almost same compressive strength.

Hadi et al. [28] have examined the compressive strength of fly ash based geopolymer mortar prepared from five different sources of fly ash. Class F- fly ash was used as the source material in this study. The different sources of fly ash used in this investigation were designated as ER, MP, BW, GL and CL corresponding to the fly ashes Eraring, Mt-Piper, Bayswater, Gladstone and Collie, respectively. The median particle size of fly ashes ER, MP, BW, GL and CL were 24.8 µm, 20.5 µm, 17.0 µm, 3.5 µm, and 9.0 µm, respectively and their corresponding amorphous contents were 72.19%, 84.13%, 78.75%, 75.72% and 76.30%. In this study, the median particle size of the fly ash was used to express its particle size distribution. The alkaline solution was prepared by mixing of NaOH solution (12 M, 14 M and 16 M) and Na_2SiO_3 solution. The alkaline solution was blended with fly ash into four weight ratios of (AL/FA), which were 0.4, 0.5, 0.6 and 0.7. The Na_2SiO_3 solution was blended with NaOH solution into three weight ratios, which were 1.5, 2 and 2.5. The alkaline solution contents used were

207 kg/m^3, 208 kg/m^3, 259 kg/m^3, 260 kg/m^3, 300 kg/m^3, 302 kg/m^3, 362 kg/m^3, and 364 kg/m^3. The fly ash contents used were 500 kg/m^3, 503.3 kg/m^3, 517.14 kg/m^3, 517.5 kg/m^3, 518 kg/m^3, and 520 kg/m^3. A total of 180 numbers of fly ash based geopolymer mortar mixes were prepared and tested for compressive strength at the age of 7 days. The results indicated that compressive strength of fly ash based geopolymer mortar was in the range of 7 MPa to 67 MPa. Fly ashes with a high content of amorphous components (SiO_2, Al_2O_3, CaO and Fe_2O_3) and a low median particle size (< 17 μm) required a low dosage of alkaline activator in terms AL/FA, Na_2SiO_3/NaOH ratio and concentration of NaOH solution to achieve the optimum compressive strength. In contrast, the optimum compressive strength of the fly ash based geopolymer mortar that used fly ash with a low content of amorphous components and high median particle size (> 17 μm) required a higher dosage of alkaline activator. The particle size distribution of fly ash affected the extent of compressive strength development for the fly ashes with similar chemical composition.

Abdulrahman et al. [50] have investigated the mechanical properties and bond stress-slip performance of fly ash based geopolymer concrete. The class C fly ash was used as the source material. The combination of 14 M NaOH (SH) solution, and sodium silicate (SS) solution was used as alkaline solution. The proportion of the total fine and coarse aggregates was maintained between 65% and 70% of the total weight, and the ratio of SS/SH was fixed at 1.5 by weight. The fly ash content was the primary variable among these mixes, with alkaline activator to fly ash (AA/FA) ratios between 0.30 and 0.40. To ensure adequate workability, extra water was added to the fresh concrete to make it workable. Furthermore, a small quantity of borax (0.5% of fly ash content) was added to the mixes to prolong the setting time of fly ash based geopolymer concrete. The standard slump test was conducted immediately after mixing to evaluate the workability of fresh concrete. The fly ash based geopolymer concrete mixes were cast in the standard cube moulds of size 100 mm to determine the compressive strength at the age of 7 days, 28 days and 180 days. Similarly, the geopolymer concrete mixes were cast in the standard cylindrical moulds of size 150 mm × 300 mm to determine the splitting tensile strength at the age of 180 days. In addition, the bond stress was determined from the pullout cube specimens with dimension of 100 mm with single deformed steel bar of diameter either 10 mm, 12 mm and 16 mm. In this study, only ambient curing regime was used for all types of specimens. After casting, the GPC specimens were stored in ambient condition for 24 hours before being demoulded, after which the specimens were again stored in ambient laboratory condition until testing. The obtained test results indicated that the slump values increased with

increase in ratio of alkaline activator to binder. However, the compressive strength and splitting tensile strength increased with decrease in ratio of alkaline activator to binder. The higher compressive strength and splitting tensile strength at lower ratio of alkaline activator to binder was due to the effect of adequate amount of source material that supported the polymerization process. When the compressive strength increased, both critical and maximum bond strengths increased, which was attributed to the enhanced interfacial transition zone (ITZ) between fly ash based geopolymer paste with aggregates that led to increase in splitting, bearing, cohesion, and friction strengths of concrete.

Deb et al. [51] have evaluated the effect of different proportions of ground granulated blast-furnace slag (GGBFS) and activator content on workability and strength properties of fly ash based geopolymer concrete. In this study, class F fly ash was used as the main geopolymer binder and GGBFS was used as a partial replacement of fly ash. The combination of 14 M NaOH solution and Na_2SiO_3 solution was used as alkaline activator. The crushed granite and sand were used as coarse aggregate and fine aggregate respectively. The two-test series were performed, which includes first test series of geopolymer concrete mixes made with different GGBFS replacement levels (10% and 20%), alkaline activator content of 160 kg/m^3, activator to binder ratio of 0.40, and SS/SH ratios of 2.5 and 1.5. The second test series of geopolymer concrete mixes were made with different GGBFS replacement levels (0%, 10% and 20%), alkaline activator content of 140 kg/m^3, activator to binder ratio of 0.35, and SS/SH ratios of 2.5 and 1.5. The third test series of OPC based concrete mixes was for reference purpose. The extra water and superplasticiser were added to improve the workability of some of geopolymer concrete mixtures. The GPC and OPC based concrete cylinder specimens were cast in the mould size of 100 × 200 mm. These specimens were used for compressive strength test at the age of 7, 28, 56, 90, 180 days. The cylinder specimens of size of 150 × 300 mm were cast for the splitting tensile strength test at the age of 7, 28, 90 days. The workability of GPC was determined immediately after mixing of the concrete by slump test. The GPC specimens were cured in ambient condition at 20 ± 2 °C and 70 ± 10% relative humidity, and the OPC based concrete specimens were cured in water at the same temperature. From the test results, the authors reported that the slump values of GPC mixes decreased with increase in GGBFS replacement level. In addition, the slump of GPC mixes decreased with decrease in activator to binder ratio whereas it increased with increase in SS/SH ratio. Besides, the slump value of GPC mixes was higher than OPC based concrete mixes. The compressive strength and split-tensile strength of GPC mixes mostly increased with increase in GGBFS replacement level and

curing age for both activator to binder ratio, and SS/SH ratio. However, both the compressive strength and split-tensile strength of GPC mixes increased with decrease in SS/SH ratio whereas these increased with increase in activator to binder ratio. Further, the compressive strength and split-tensile strength of GPC mixes were comparable with those of OPC based concrete mixes.

Saha and Rajasekaran [52] have studied the properties of fly ash based geopolymer paste with the incorporation of GGBFS at various percentage levels, and different concentrations of sodium hydroxide solution. In this study, class F fly ash and ground granulated blast furnace slag (GGBFS) were used as binder for making of fly ash based geopolymer paste and fly ash-GGBFS based geopolymer paste. The GGBFS contents were 10%, 20%, 30%, 40% and 50% for making of fly ash-GGBFS based geopolymer paste. The combination of NaOH solution and Na_2SiO_3 solution was used as alkaline solution. In this study, different molarity of NaOH solution were used such as 6 M, 8 M, 10 M, 12 M, 14 M and 16 M. The setting time of fresh geopolymer paste was determined immediately after mixing. The fresh geopolymer paste was poured into cube moulds of size 50 mm. After casting, the cube specimens were demoulded and kept in the room temperature for ambient curing till the age of testing. The compressive strength of geopolymer paste specimens were tested at the age of 7, 28 and 56 days. From the test results, the authors reported that the setting time of fresh fly ash-GGBFS based geopolymer paste mixes decreased with increase in GGBFS content. The setting time of fresh fly ash-GGBFS based geopolymer paste mixes at higher dosages of GGBFS were decreased due to high CaO content in GGBFS, which may help to form C-S-H gel along with the 3D stable silico-aluminate structure by the geopolymeric reaction at the early age. In addition, the setting time of fresh fly ash based geopolymer paste mixes were higher as compared to fly ash-GGBFS based geopolymer paste mixes. However, there was unsystematic variation in setting time of both fly ash and fly ash-GGBFS based geopolymer paste mixes with molarity of NaOH solution. The compressive strength of both fly ash and fly ash-GGBFS based geopolymer paste mixes increased with increase in molarity of NaOH solution as well as increase in GGBFS content (in case of fly ash-GGBFS based geopolymer paste). Further, the compressive strength of fly ash-GGBFS based geopolymer paste mixes were higher as compared to fly ash based geopolymer paste mixes. Besides, the compressive strength of both fly ash and fly ash-GGBFS based geopolymer paste mixes increased with increase in curing age. From the SEM analysis, the formation of dense microstructure was confirmed from the morphology of fly ash-GGBFS

based geopolymer paste made with higher GGBFS content as compared to fly ash based geopolymer paste mixes.

2.2.2 Effect of fly ash on fresh and hardened properties of fly ash based geopolymer paste, mortar and concrete

Aliabdo et al. [22] have evaluated the influence of fly ash content, additional Portland cement content, alkaline solution resting time, curing temperature and curing period on properties of fly ash based geopolymer concrete (GPC). The source material for the geopolymer binder was Class F fly ash. Type I Ordinary Portland cement was used to evaluate the effect of additional Portland cement content on fly ash based geopolymer concrete. The crushed pink limestone and natural siliceous sand were used as coarse aggregate and fine aggregate respectively. The activator solution was made by mixing 16 M NaOH solution and Na_2SiO_3 solution. The fly ash contents of 350 kg/m^3, 400 kg/m^3, and 450 kg/m^3, and cement contents of 20 kg/m^3, 40 kg/m^3 and 60 kg/m^3 were used in the study. Two durations of alkaline solution resting time were considered: 30 minutes and 24 hours. The extra water and superplasticizer content were 35 kg/m^3 and 10.5 kg/m^3 respectively for all GPC mixes. The different curing temperatures used were 28 °C, 50 °C, 70 °C, and 90 °C, and the curing periods were 24 hours, 48 hours, and 72 hours. The fly ash based geopolymer concrete mixes were cast into different moulds of size 100 mm × 100 mm × 100 mm, 75 mm × 150 mm, 100 mm × 200 mm, and 70 mm × 70 mm × 70 mm for determining compressive strength (at the age of 7 and 28 days), tensile strength (at the age of 28 days), modulus of elasticity (at the age of 28 days), and absorption (at the age of 28 days) respectively. The moulds were kept in the storage room at temperature of 20 - 23 °C (without being wrapped) with the top surface exposed to air. The specimens were demoulded after 24 hours of casting and then cured in a hot air oven for certain curing period and temperature, and were kept at room temperature till the age of testing. The thermogravimetric analysis was performed to determine the weight loss rate of fly ash based geopolymer concrete at the age of 28 days. From the test results, the authors reported that the slump value, compressive strength, tensile strength, and modulus of elasticity increased with increase in fly ash content. Similarly, compressive strength, tensile strength and modulus of elasticity increased with increase in curing period. In addition, water absorption and porosity reduced with increase in fly ash content, additional Portland cement content and curing period. The additional Portland cement content resulted in reduced slump value but it improved the compressive strength, tensile strength and modulus of elasticity. However, the water absorption and porosity increased with increase in alkaline solution resting time whereas the

slump value, compressive strength, tensile strength and modulus of elasticity increased with decrease in alkaline solution resting time. Further, compressive strength, tensile strength and modulus of elasticity increased with increase in curing temperature from 28 °C to 70 °C and then it decreased at 90 °C whereas water absorption and porosity reduced with increase in curing temperature from 28 °C to 70 °C and then it increased at 90 °C. Further, the TGA analysis indicated that the weight loss rate decreased with decrease in alkaline solution resting time whereas it increased by adding Portland cement content.

Shehab et al. [53] have investigated the mechanical properties of geopolymer concrete made with partial and complete replacement of cement. In this investigation, ordinary Portland cement type (I) with high grade 52.5N and low calcium fly ash were used as cementitious materials. A mixture of 10 M NaOH solution, and Na_2SiO_3 solution was used as alkali liquid solution. The cement replacement ratios of 0%, 25%, 50%, 75% and 100% were considered in this study. The binder content of 300 kg/m^3 and 350 kg/m^3 were chosen for alkali liquid solution to binder ratio of 0.55 and 0.45. The extra water content used were 50.76 kg/m^3, 68.81 kg/m^3, 59.23 kg/m^3 and 80.28 kg/m^3. The geopolymer concrete specimens were left for 24 hours before demoulding and placed in an oven at 100 °C for 24 hours before being taken out of the oven to be air cured for 5-6 hours at room temperature before storing in temperature controlled water (40 °C) until the day of testing. The fly ash based geopolymer concrete mixes were prepared and cast into different moulds of size 100 mm × 100 mm × 100 mm, 100 mm × 100 mm × 500 mm, 100 mm × 200 mm, and 100 mm × 200 mm to perform compression test (at the age of 7 and 28 days), flexural strength test (at the age of 28 days), split-tension test (at the age of 28 days) and pull out test (at the age of 28 days) respectively. From the test results, the authors reported that the compressive strength, flexural strength, tensile strength and bond strength increased with increase in cement replacement ratio from 0% to 50% and then it decreased. However, the compressive strength, flexural strength, tensile strength and bond strength increased with increase in binder content for all cement replacement ratios and alkali liquid solution to binder ratios. In addition, all the above strengths increased with increase in alkali liquid solution to binder ratio. Further, the compressive strength, flexural strength, tensile strength and bond strength of geopolymer concrete mixes made with 25% to 100% cement replacement ratios were higher as compared to the mixes made with 0% cement replacement ratio.

Nguyen et al. [23] have evaluated the mechanical properties of fly ash based geopolymer concrete. Class F- fly ash was used as the source material in this study. The alkaline liquid was prepared by mixing of NaOH solution (8 M) and Na_2SiO_3 solution at three weight ratios (Na_2SiO_3 solution/NaOH solution) of 1, 2 and 2.5. The alkaline liquid to fly ash-weight ratios were 0.4, 0.5, and 0.6. The coarse aggregate and fine aggregate were used for the preparation of fly ash based geopolymer concrete mixes. The fly ash contents and alkaline liquid contents used were 418 kg/m^3, 431 kg/m^3, and 445 kg/m^3, and 178 kg/m^3, 216 kg/m^3, and 251 kg/m^3 respectively. Three different curing temperatures i.e., 60 °C, 90 °C and 120 °C were applied to the cylindrical geopolymer concrete specimens. The fly ash based geopolymer concrete cylindrical specimens of size 150 mm × 300 mm were prepared for compressive strength, modulus of elasticity and splitting tensile strength test at the age of 7 days. Beam specimens of size 100 mm × 200 mm × 2000 mm were prepared from geopolymer concrete for flexural strength. The test results indicated that the measured values of modulus of elasticity of heat-cured low-calcium fly ash based geopolymer concrete with compressive strength in the range 45-58 MPa were different from that of conventional concrete. These measured values were lower than the values calculated using the current standards AS 3600 and ACI 363. The Poisson's ratio of fly ash based geopolymer concrete with compressive strength in the range of 45-58 MPa was from 0.16 to 0.21. These values were similar to that of conventional concrete. The stress-strain relations of heat-cured fly ash based geopolymer concrete in compression matched well with the formulation designed for Portland cement concrete. The measured indirect tensile strength of fly ash based geopolymer concrete was greater than that calculated using an expression designed for Portland cement concrete. The deflections at mid-span and crack patterns of geopolymer concrete beam obtained from finite element model matched well with the experimental results than with the results obtained from elastic theory.

Chindaprasirt et al. [54] have studied the effect of fineness of fly ash on setting time of geopolymer pastes, workability and compressive strength of geopolymer mortars made from classified fine high calcium fly ash. In this study, coarse original fly ash, medium-fineness fly ash, and fine fly ash were used. Coarse fly ash (CFA) was the as received fly ash. Medium fineness fly ash (MFA) was used as 40% fine portion of the as received fly ash with 60% coarse portion discarded, and fine fly ash (FFA) was used as 10% portion of as received fly ash with 90% coarse portion discarded. 10 M NaOH solution and sodium silicate solution was used as alkaline activator in this study. In addition, base water was used to improve the workability of geopolymer mortar. Locally available river sand was used to prepare geopolymer mortar.

Sodium silicate solution to NaOH solution of mass ratio 1:1, and a water to geopolymer solids mass ratio of 0.2 were used to prepare geopolymer paste for determining setting time. The delay periods of 0, 1, 2, 3, 6, and 24 hours before heat curing were used to investigate the effect of different delay periods on compressive strength of geopolymer mortar. After the delay period, the specimens were kept in oven at the temperature of 75°C for 48 hours. For investigating the effect of heat curing temperature, different curing temperatures of 30 °C, 45 °C, 60 °C, 75 °C, and 90 °C were used. Similarly, different periods of heat curing i.e., 1, 2, 3, 4, and 5 days at temperature of 75°C with the delay period of 1 h were used to investigate the effect of period of heat curing. The flow value was determined immediately after the completion of mixing of fresh geopolymer mortar. After obtaining flow value, the fresh geopolymer mortar was placed in cube moulds of size 50 mm. The compressive strength test was carried out at the age of 7, 28, and 91 days. From the obtained results, both initial and final setting time of geopolymer paste decreased with increase in fineness of fly ash whereas flow of mortar increased with increase in fly ash fineness. The compressive strength of fly ash based geopolymer mortar increased with increase in curing age. For all ages, highest compressive strength was achieved at the delay periods of 3 hours, 2 hours and 1 hours for CFA, MFA, and FFA respectively. In addition, geopolymer mortar made from fine fly ash (FFA) exhibited higher compressive strength as compared to other classified fly ash (MFA and CFA). For all ages, compressive strength of geopolymer mortar increased with increase in curing temperature from 30 °C to 75 °C and then it declined at 90 °C. In addition, geopolymer mortar made from fine fly ash (FFA) exhibited higher compressive strength as compared to other classified fly ash (MFA and CFA) at the temperature of 75 °C. Further, compressive strength of geopolymer mortar increased with increase in heat curing period from 1 to 3 days followed by a decrease thereafter.

Guades [55] has evaluated the effect of sand to fly ash ratio on compressive strength and tensile strength of geopolymer mortar mixes. In this study, class F fly ash was used as source material for making of geopolymer binder. The combination of 14 M NaOH solution and Na_2SiO_3 solution was used as alkaline activator. The clean dry river sand was used as fine aggregate. The alkaline activator to fly ash ratio, and Na_2SiO_3/NaOH ratio were kept at 0.30 and 1.0, respectively. The sand to fly ash ratio used in fly ash based geopolymer mortar mixes was in the range of 0.3–6.0. The fly ash based geopolymer paste, and cement-based mortar were used for reference purpose. The geopolymer mortar and paste mixes were cast into cylindrical moulds size of 50 mm × 100 mm. After casting, all the specimens were kept in the

moulds for a rest period of at least 48 hours and then demoulded. Further, the specimens were kept under ambient condition till the age of testing. The compressive strength and tensile strength tests were conducted at the age of 7, 14, and 28 days. From the test results, the author reported that compressive strength and tensile strength of fly ash based geopolymer mortar mixes increased with decrease in sand to fly ash ratio. The compressive strength and tensile strength of fly ash based geopolymer paste mixes were higher as compared to fly ash based geopolymer mortar mixes. In addition, the compressive strength of fly ash based geopolymer paste and mortar mixes were higher than cement-based mortar mixes. Further, the compressive strength and tensile strength of fly ash based geopolymer paste and mortar mixes increased with increase in curing age.

2.3 Microstructural properties of fly ash based geopolymer paste, mortar and concrete

The various studies were reported on microstructure of fly ash based geopolymer paste, mortar and concrete. The following review of microstructure of fly ash based geopolymer paste, mortar and concrete are discussed below in this section.

Lokuge et al. [56] have developed fly ash based geopolymer concrete using mix design method based on Multivariate Adaptive Regression Spline (MARS) model incorporating key parameters namely water/geopolymer solids ratio, alkaline activator/fly ash ratio, Na_2SiO_3 solution/NaOH solution ratio, and NaOH solution molarity. In this study, low calcium fly ash, and alkaline activator (mixture of both 10 M NaOH solution and Na_2SiO_3 solution) were used for preparing different geopolymer concrete mixes i.e., M30, M40, M50 and M55. The alkaline activator to fly ash ratios of 0.45, 0.50, 0.45 and 0.50, Na_2SiO_3 to NaOH solution ratios of 1.75, 3.0, 3.50, and 4.00, and water to geopolymer solids ratios of 0.40, 0.25, 0.25 and 0.25 were used that correspond to geopolymer concrete mixes M30, M40, M50 and M55 respectively. The fly ash content was 410 kg/m^3 for all GPC mixes. In addition, extra water was also added to the GPC mixes. The geopolymer concrete cube specimens of size of 100 mm were prepared where the specimens were heat cured in an oven for 24 hours at 80 °C temperature followed by allowing them to cool to laboratory temperature before demoulding, and subsequently keeping the specimens in the laboratory condition until testing. The compressive strength test was conducted at the age of 7 and 28 days. Scanning Electron Microscopy (SEM) was used to examine the microstructure of fly ash based geopolymer concrete at the age of 28 days. From the test results, the authors reported that M55 mixes exhibited higher compressive strength than other mixes i.e., M30, M40 and M50 at both the ages. The targeted compressive strength ranging from 30 MPa to 55 MPa at the age of 28 days

was achieved with the laboratory experiments using the proposed MARS mix design methodology. The SEM analysis revealed that the geopolymer concrete mixes M40, M50 and M55 had fewer unreacted/partially reacted fly ash particles at the age of 28 days than M30 concrete mix, indicating higher extent of geopolymerization reaction and gel formation in these mixes. The M30 and M40 geopolymer concrete mixes contained micro-cracks, but M30 had more and a wider crack width. The SEM images showed the geopolymer gel diffused through the surface, covering and coalescing the partially reacted fly ash particles. The M50 and M55 geopolymer concrete mixes showed the gel being filled in interior gaps, forming a semi-homogeneous, and highly compacted denser microstructure.

Mehta and Siddique [42] have investigated the strength, permeability and microstructural characteristics of fly ash based geopolymer concrete. The fly ash was partially replaced with 0%, 10%, 20%, and 30% of ordinary Portland cement (OPC). Class C fly ash and 43 grade ordinary Portland cement (OPC) were used in the study. Crushed stone aggregates and natural river sand were used as coarse aggregate and fine aggregate respectively. The sodium hydroxide (NaOH) solution with a molarity of 10 M and sodium silicate (Na_2SiO_3) solution was used as alkali solution. Naphthalene based admixture at 2% dosage by total weight of fly ash and OPC was added to the alkali solution before mixing them to the dry mixture. After mixing, the concrete specimens were cast in moulds of different sizes such as 150 mm cubical moulds for compressive strength test, 100 × 200 mm cylindrical moulds for split tensile strength, and 150 × 300 mm cylindrical moulds for rapid chloride permeability test (RCPT). Slump test and compaction factor test were used to evaluate the workability of mixes. Compressive strength, split tensile strength, and rapid chloride permeability (RCPT) tests were carried out at the age of 28 days. For microstructure study, SEM, EDS, and XRD analyses were performed at the age of 28 days. From the obtained results, the authors reported that both slump and compaction factor values decreased with increase in OPC dosage. The compressive strength and split tensile strength mostly increased with increase in percentage of OPC from 0% to 20% and then it declined at all ages. The compressive strength at 20% OPC was higher due to the formation of C-S-H gel in addition to C-A-S-H and N-A-S-H gels. In addition, the permeation properties decreased with increase in percentage of OPC from 0% to 20% and then it increased. The chloride resistance increased with increase in dosage of OPC from 0% to 20%, which indicated very low chloride permeability. The addition of OPC exhibited dense and compact microstructure with lesser voids, which was observed from the microstructural analysis.

Mehta and Siddique [57] have investigated the compressive strength and permeation properties of fly ash based geopolymer concrete. Class F Fly ash was replaced in part by 0%, 10%, 20%, and 30% ordinary Portland cement (OPC). A 10 M NaOH solution mixed with sodium silicate (Na_2SiO_3) solution was used as alkaline activating solution. The cube specimens of size 150 mm were cast and oven cured for 24 hours at 80 °C. The GPC mixes were tested for compressive strength at the age of 3, 7, 28, 90, and 365 days. The microstructural characteristics of GPC powder samples were investigated by various techniques such as SEM, EDS, and XRD analyses. Water absorption, rate of sorptivity, rapid chloride permeability and porosity tests were also performed on geopolymer concrete specimens at the age of 28, 90, and 365 days. From the obtained results, the authors reported that with the addition of OPC as a fly ash replacement, the compressive strength of low-calcium fly ash based geopolymer concrete increased by up to 20% at all ages. The increase in strength was due to the formation of additional calcium-based products by hydration mechanism, which coexisted with the alumina-silicate polymeric products. The permeation properties such as sorptivity, porosity, and water absorption were reduced when up to 20% of fly ash was replaced with OPC. The strength and permeation properties at OPC beyond 20% replacement was decreased due to the formation of relatively lower geopolymeric binders than hydrated calcium-based binders. The formation of additional calcium-based products by the hydration mechanism that coexisted with the alumina-silicate polymeric products, and dense microstructure with the addition of OPC were observed from XRD and SEM-EDS analyses respectively. The resistance to penetration of chloride ions was found to be moderate in geopolymer concrete specimens, but with the addition of OPC, even at 10%, the resistance to penetration of chloride ions improved significantly with a very low permeability range at all ages. The specimens with 20% OPC exhibited superior performance in terms of total charge passed.

Nagalia et al. [58] have examined the role of alkali hydroxide and its concentration on the compressive strength and microstructure of fly ash based geopolymer concrete. In this study, source material based on CaO content of fly ash (Class F and Class C), alkali hydroxide, water and superplasticizer were used to prepare the geopolymer concrete mixes. The NaOH, KOH, $Ba(OH)_2$ and LiOH based solutions were used as different types of alkali hydroxide solutions. The combinations of these alkali hydroxide solutions, and sodium silicate solution were also used. Different Molarity of NaOH solution i.e., 8 M, 12 M and 14 M and Na_2SiO_3 (NS)/NaOH (NH) solution ratio by mass of 2 were used. The activator solution to fly ash ratio was 0.31.

Different curing methods were adopted for the GPC specimens, which included oven curing at temperatures of 55 °C and 70 °C, and steam curing at temperature of 46 °C and 100% humidity. To study the effect of curing time, the mixes were cured for 24 hours and 48 hours in oven at the temperature of 55 °C. Cylindrical specimens of size 100 mm × 200 mm were prepared from geopolymer concrete mixes to determine the compressive strength at the age of 1, 3, 7 and 28 days. The microstructure was investigated through XRD and SEM-EDS analyses. The obtained results indicated that using any alkali hydroxide solution other than NaOH solution reduced the compressive strength significantly. With respect to type of fly ash, class C fly obtained higher strength as compared to Class F fly ash. The higher amount of class C fly ash was able to react with higher molarity of NaOH solution and resulted in strength increment. The compressive strength increased with increase in curing temperature. Maximum compressive strength was achieved at oven temperature curing as compared to steam curing. The geopolymer concrete mix, which was cured for 48 hours exhibited higher compressive strength as compared to that cured for 24 hours. The XRD analysis showed higher peak intensity of a sodium alumina silicate complex such as $NaAlSi_3O_8$ (albite) with increase molarity of NaOH solution and curing time. The SEM images showed large number of pores and hollow spheres in case of geopolymer concrete made with 8 M NaOH solution as compared to that made with 14 M NaOH solution, which may be ascribed to insufficient extent of geopolymerization process at 8 M NaOH solution.

Chindaprasirt et al. [59] have carried out a study on compressive strength and microstructural characteristics of fly ash geopolymer (FAG) and bottom ash geopolymer (BAG) composites. Sodium hydroxide (NaOH) solution at 5 M, 10 M, and 15 M concentration and sodium silicate (Na_2SiO_3) solution were used to make fly ash based geopolymer paste and mortar. The Na_2SiO_3/NaOH mass ratio of 1.5 was used to make paste specimens (25 mm diameter × 25 mm height) and mortar specimens (50 mm × 50 mm × 50 mm). The geopolymer mortar was poured into 50 mm cube moulds and wrapped with cling film to prevent moisture evaporation during heat curing. Following that, the mortar specimens were cured for 48 hours at temperature of 65 °C. The specimens were then cooled to room temperature. Compressive strength test was carried out on mortar specimens. The geopolymer paste specimens were cured for 48 hours at 65 °C. On the hardened sample, FT-IR, DSC (Differential Scanning Calorimetry), XRD, and SEM-EDX analyses of geopolymer paste were performed. From the test results, the authors reported that the fly ash based geopolymer mortar made with 10 M NaOH solution exhibited optimum compressive strength as compared to 5 M and 15 M NaOH

solution. However, the compressive strength of bottom ash geopolymer mortar increased with increase in molarity of NaOH solution. Overall, fly ash based geopolymer mortar achieved higher compressive strength than bottom ash geopolymer mortar for all molarity of NaOH solution. The fly ash based geopolymer mortar achieved the compressive strength of 35 MPa, which was significantly higher than that of bottom ash geopolymer mortar i.e., 18 MPa. From the microstructural analysis, the SEM images indicated unreacted and/or partially reacted fly ash particles and a continuous mass of alumino-silicate in fly ash based geopolymer paste. The larger fly ash particles were mostly partially reacted and still the matrix was observed with continuous and relatively dense structure with voids and cracks. In case of bottom ash geopolymer paste, a continuous mass of alumino-silicate with unreacted and/or partially reacted irregular coal ash particles was observed in SEM images, which led to more porous structure and resulted in lower compressive strength. The results of the EDX analyses of the fly ash and bottom ash based geopolymer pastes showed that the major elements were Si and Al along with the presence of Na and Ca. The ratio of Si/Al for the fly ash based geopolymer paste was 3.0 whereas that for bottom ash based geopolymer paste was 6.0. The higher ratio of Si/Al resulted in lower compressive strength in case of bottom ash. Similarly, DSC analysis of bottom ash geopolymer paste exhibited low degree of geopolymerization as compared to fly ash based geopolymer paste. Further, FT-IR analysis indicated lower frequency of Si-O-Si vibration that showed higher degree of geopolymerization, which was observed in fly ash based geopolymer paste as compared to bottom ash based geopolymer paste. In addition, asymmetric stretching vibration of Si-O-Si bond shifted toward lower frequency with increase in molarity of NaOH solution, which indicated higher degree of geopolymerization.

Ryu et al. [60] have examined the effects of chemical changes of alkaline activators on compressive strength of fly ash based geopolymer mortar and to analyse the microstructure of fly ash based geopolymer paste through SEM, EDS, XRD, FTIR and by porosity assessments. In this study, Class F Fly ash with a mean particle size of 15 μm was used as geopolymer precursor. Three studies were investigated. In the first study, the molarity of NaOH solution was varied, i.e., 6 M, 9 M and 12 M. The alkaline activator was prepared by mixing of NaOH solution and Na_2SiO_3 solution. Second study included five different mass ratios of NaOH to Na_2SiO_3, which were 0:100, 25:75, 50:50, 75:25 and 100:0 for 9 M NaOH solution. In the third study, geopolymer mortar mixes were prepared with only sodium silicate (Na_2SiO_3) solution, and with only 9 M NaOH solution. The geopolymer mortar specimens of size 50 mm were prepared. The sealed specimens were cured in oven for 24 hours at 60°C followed by air dry

curing for 24 hours at ambient condition (23 ± 2 °C, RH 50%). As per EFNARC specification, mini-cone slump test was conducted to investigate the fresh properties of geopolymer mortar mixes. As per ASTM C109, the compression test was conducted to measure the compressive strength at the age of 1, 3, 7, 14, 28, 56 and 91 days. X-ray diffraction (XRD), fourier transform infrared spectroscopy (FT-IR), and scanning electron microscopy-Energy dispersive spectroscopy (SEM-EDS) techniques were conducted to analyse the microstructural characteristics of geopolymer paste specimens at the age of 28 days. From the test results, the authors reported that the flow of fly ash based geopolymer mortar mixes decreased with increase in molarity of NaOH solution whereas the compressive strength of fly ash based geopolymer mortar mixes increased with increase in molarity of NaOH solution. In addition, the flow and compressive strength of fly ash based geopolymer mortar mixes were higher at NaOH to Na_2SiO_3 mass ratio of 50:50. Further, the fly ash based geopolymer mortar mixes made with only sodium silicate solution exhibited mostly higher compressive strength than mixes made with only 9 M NaOH solution. With respect to curing age, the compressive strength of fly ash based geopolymer mortar mixes increased with increase in curing age. The compact microstructure with the variation of Si/Al and Na/Si ratio of the fly ash based geopolymer paste made with NaOH to Na_2SiO_3 mass ratio of 50:50 was confirmed by SEM-EDS analysis. From the XRD patterns, higher peak intensity of alumino-silicate based products were observed in fly ash based geopolymer paste prepared with higher molarity of NaOH solution. From the FTIR analysis, asymmetric stretching of Si-O-Si bond shifted towards lower frequencies at higher molarity of NaOH solution, which indicated higher extent of geopolymerization process.

Hanjitsuwan et al. [61] have investigated the effect of NaOH solution concentration on setting time, compressive strength and electrical properties of high calcium fly ash based geopolymer pastes. High calcium fly ash was used as source material in this study. The alkaline solution was prepared by mixing of NaOH solution (8 M, 10 M, 12 M, 15 M and 18 M) with Na_2SiO_3 solution. The alkaline solution to fly ash ratio, and Na_2SiO_3/NaOH ratio were 0.4, and 0.67 respectively. The fresh geopolymer pastes were tested for setting time at the room temperature of 25 °C using standard vicat needle apparatus. Then, the paste was cast in the plastic moulds of size of 3 cm diameter and 6 cm height for compressive strength test at the age of 7 days. The specimens were wrapped with clingfilm to prevent loss of moisture and kept in an oven at temperature of 40 °C for 24 hours. After oven curing, the specimens were left in controlled room temperature of 25 °C for 1 hour. For dielectric measurement, discs of 19 mm diameter

and 2 mm thickness were cast and prepared in the same manner as the compressive strength specimens. The microstructure of geopolymer pastes were investigated by X-ray diffraction (XRD) and scanning electron microscopy (SEM). From the test results, the authors reported that the initial and final setting time of geopolymer pastes as well as compressive strength increased with increase in molarity of NaOH solution. The dielectric constant, dielectric loss and conductivity of geopolymer pastes were affected by the concentration of NaOH solution. At lower frequency range of 10^2 - 10^3 Hz, the geopolymer paste exhibited high dielectric constant values of 10^4 - 10^5. At the frequency of 10^3 Hz, all dielectric values of pastes were approximately the same at 10^4. At higher frequencies, the dielectric values decreased substantially and were related to NaOH concentration. The decrement was less with increase in NaOH solution concentration and compressive strength of paste. From the XRD pattern of fly ash based geopolymer paste, the peak intensity of hydrosodalite (geopolymer gel) and C-S-H gel increased with increase in molarity of NaOH solution that resulted in strength gain of paste. From the morphology of fly ash based geopolymer paste, partially reacted/unreacted fly ash grains and continuous mass of alumino-silicate were detected. With increase in NaOH solution concentration, the fly ash particles were less abundant and the matrix was denser.

Xie and Ozbakkaloglu [62] have carried out an experimental study on the behaviour of fly ash, bottom ash and blended fly ash and bottom ash based geopolymer concrete (GPC) cured at ambient temperature. The alkaline activator solution used in this study was 14 M NaOH solution and sodium silicate (Na_2SiO_3) solution. The ordinary Portland cement (OPC) was used in this investigation for reference purpose. The fly ash contents used were 400 kg/m^3 and 475 kg/m^3. The liquid to binder ratios of 0.25, 0.30, 0.35 and 0.5 for fly ash based GPC mixes, 1.1 and 0.5 for bottom ash-based GPC mixes, and 0.3 and 0.5 for blended coal ash based GPC mixes were used in the study. The coal ashes were added at different fly ash-to-bottom ash mass ratios of 50:50, and 25:75 for the GPC mixes. The mixing and casting process were conducted under ambient condition for both OPC and GPC mixes. After 24 hours of casting, hardened GPC and OPC specimens were demoulded. The GPC specimens, which were not fully cured after 24 hours, were allowed extra time for curing. The slump test was performed to measure the workability of concrete. The compressive strength, flexural strength and elastic modulus of concrete were tested at the age of 3, 7, 28, 56 and 70 days. Prior to compressive strength test, the drying shrinkage was monitored up to 70 days of concrete age through measurement of shrinkage strains and related weight loss of the specimens. From the test results, the authors reported that the workability of geopolymer concrete increased with

increase in liquid to binder ratio and fly ash to bottom ash ratio whereas workability decreased with increase in fly ash content. The geopolymer concrete mixtures exhibited higher workability as compared to OPC concrete. The compressive strength, flexural strength and elastic modulus of GPC increased with decrease in liquid to binder ratio and increase in mass ratio of fly ash to bottom ash. The OPC concrete exhibited higher compressive strength than geopolymer concrete. In comparison to OPC concrete, the GPC made from coal ash at ambient temperature showed higher drying shrinkage. It was attributed to large amount of unreacted coal ash particles in the hardened GPC structure that resulted from a lower degree of geopolymerization when coal ash based GPC is cured at ambient temperature. The SEM analysis showed denseness and homogeneous structure of geopolymer concrete, which indicated higher degree of geopolymerization at higher fly ash content and lower alkaline solution content. Further, denser microstructure was observed in OPC based concrete as compared to GPC mixes.

Jang and Lee [43] have investigated the effect of fly ash characteristics on delayed high strength development of fly ash based geopolymer paste (GP). Fly ash was used as source material in this study. The measured mean particle diameters for corresponding types of fly ashes labelled as FA1, FA2 and FA3 were 10.03, 13.13 and 16.49 μm, respectively. The labels 'GP1', 'GP2' and 'GP3' represent the geopolymer paste samples made from three types of fly ashes, 'FA1', 'FA2' and 'FA3', respectively. Sodium silicate solution and 9 M NaOH solution was used as the alkali activator. The geopolymer paste samples were cast into cubic moulds of size of 5 cm. The geopolymer paste specimens were sealed to prevent water evaporation, and cured at 60 °C for 24 h in an oven. After initial curing, all samples were kept in a chamber with relative humidity of 65% at 20 °C until the day of testing. The compressive strength of geopolymer paste samples were measured at the ages of 1, 3, 7, 28, 56 and 91 days. The SEM-EDS and FTIR analyses were conducted to analyse the microstructural characteristics of fly ash based geopolymer paste. From the test results, the compressive strength of fly ash based geopolymer paste increased with increase in particle size of fly ash at the age of 91 days. However, the compressive strength increased with decrease in particle size of fly ash at the age of 7 days. From the results of FTIR spectra, the asymmetric stretching vibration of Si-O-T bond shifted to lower frequency at initial stage that indicated Al-rich geopolymer gel whereas the Si-O-T bond shifted to higher frequency at later stage that indicated Si-rich geopolymer gel. From the morphology of GP, it indicated that the geopolymer consisted of weakly bonded matrix, which was colloidal aluminosilicate with loosely distributed, and crystalline phase was

not visible in GP1 and GP2. However, the crystalline and amorphous phase of fly ash was observed in GP3 at 3 days. At 91 days, the geopolymer matrix was densely distributed amorphous phase when compared to that at 3 days and crystalline phases were visible in all specimens. In GP3, the large amount of needle shaped crystal was observed at 91 days. From the EDS analysis, it was observed that needle shaped crystal was rich in silica and alumina but lower in sodium content. The new geopolymerization product formation, which was similar to mullite was supported by the crystal shape and its atomic ratio. The main observation of delayed compressive strength of geopolymer (GP1, GP2 and GP3) indicated later age strength development The particle size of fly ash significantly affected the strength development with increased particle size of fly ash resulted in delayed strength development.

Sajan et al. [63] have investigated the combined effect of alkaline solution concentration, curing temperature and curing period on mechanical properties of fly ash based geopolymer paste. For the geopolymer paste preparation, Class F fly ash was employed as a geopolymer binder. Sodium hydroxide (NaOH) solution and sodium silicate (Na_2SiO_3) solution was used as the activator in this study. Three different concentrations of NaOH solution were prepared i.e., 10 M, 12 M, and 14 M. The fly ash based geopolymer paste was cast in cylindrical moulds of size of 50 mm diameter and 100 mm height, and the samples were cured at temperatures of 20, 40, 60 and 80 °C and for curing periods of 3, 7 and 14 days. Then, all the cured specimens were tested for unconfined compressive strength, poisson's ratio and young's modulus of elasticity. For microstructure study, SEM analysis was carried out. From the test results, the authors reported that the uniaxial compressive strength and young's modulus of fly ash based geopolymer paste mostly increased with increase in curing temperature and curing age. It was attributed to progressive geopolymerization process at higher curing temperature and increase in curing age. However, the uniaxial compressive strength and poisson's ratio of fly ash based geopolymer paste mostly did not vary systematically with molarity of NaOH solution and curing period. Besides, poisson's ratio of fly ash based geopolymer paste mostly increased with increase in curing temperature. The SEM analysis revealed formation of less N-A-S-H crystals with higher amount of small unreacted fly ash particles due to lower geopolymerization process in fly ash based geopolymer paste samples made with lower curing temperature. However, the fly ash based geopolymer paste samples made with higher curing temperature indicated more amount of N-A-S-H crystals due to higher extent of geopolymerization process, which was mainly responsible for the strength development of fly ash based geopolymer paste.

Parveen et al. [64] have investigated the mechanical and microstructural characteristics of fly ash based geopolymer concrete (GPC) incorporating alccofine at ambient curing. This study employed low calcium class F fly ash, and alccofine 1203, which was a microfine substance made from low-calcium slag. The alkaline activators employed in this research were sodium hydroxide solution (8 M, 12 M, and 16 M) and sodium silicate solution. In this study, the fly ash content used were 350 kg/m^3, 375 kg/m^3 and 400 kg/m^3. To improve the workability of fresh geopolymer concrete mix, extra water and naphthalene sulphonate based water reducing superplasticizer were used. Nine GPC mixes with and without alccofine were prepared in the study. Compressive strength, splitting tensile strength and flexural strength tests were performed. The geopolymer concrete samples were then cured at 27 °C in ambient environment. X-ray diffraction (XRD) and scanning electron microscopy (SEM) analyses were carried out to evaluate the microstructural characteristics of geopolymer concrete samples. The test results indicated that increase in molarity of NaOH solution increased the mechanical properties of GPC, however it decreased the workability. After 28 days, the strength of the GPC mix increased at room temperature and it was attributed to hydration in addition to polymerization. Maximum compressive strength, splitting tensile strength, and flexural strength were attained at ambient temperature for NaOH solution concentration of 16 M and a fly ash content of 400 kg/m^3. In addition, the mechanical and microstructural properties of fly ash based GPC incorporating alccofine found to be improved. The SEM study confirmed the enhanced compactness of the structure of alccofine-based GPC through a denser matrix, and fewer microcracks, and pores, which resulted in higher strength.

Azevedo and Strecker [65] have investigated the behaviour of fly ash based inorganic polymers prepared using different alkali activator solutions. In this study, class F fly ash was used as source material for making geopolymer paste. Three different NaOH solution concentrations of 10 M, 12 M and 16 M were used. To activate the fly ash for making of geopolymer paste specimens, the alkaline activator solution was prepared by replacing 10, 20, and 30 wt. % of NaOH by Na_2SiO_3. The liquid to solid ratio by mass was kept constant at 0.5. Extra water was also added in the paste. The geopolymer pastes were cast into cylindrical plastic moulds with a height of 50 mm and a diameter of 25 mm. After 24 hours at room temperature, the geopolymer paste specimens were kept in the oven for curing at temperature of 65 °C for 24 hours. Then, the heat cured specimens were kept at room temperature for 1, 7, and 28 days prior to determining the physical properties (water absorption, apparent porosity and dry density), mechanical property (compressive strength) and microstructural analysis

such as XRD, FTIR and SEM-EDS. From the test results, the authors reported that fly ash based geopolymer pastes achieved higher compressive strength at 12 M NaOH solution than 10 M and 16 M. The fly ash based geopolymer pastes made from 10 M NaOH solution exhibited higher compressive strength at Na_2SiO_3 solution replacement of 10%. However, the fly ash based geopolymer pastes made from 12 M and 16 M NaOH solution exhibited mostly higher compressive strength when Na_2SiO_3 solution replacement of 30% was used. In addition, the compressive strength mostly increased with increase in curing age. The water absorption and apparent porosity of fly ash based geopolymer pastes mostly decreased with increase in molarity of NaOH solution. The dry density of fly ash based geopolymer pastes were higher at 12 M NaOH solution than 10 M and 16 M NaOH solution. The formation of higher amount of short-range ordered products, and higher degree of geopolymerization as indicated by asymmetric stretching vibration of Si-O-Si(Al) bond that shifted towards lower wavenumber were observed from the XRD and FTIR analyses of fly ash based geopolymer paste made with 12 M and 16 M NaOH solution for 30% replacement of Na_2SiO_3 solution respectively. Similarly, the fly ash based geopolymer paste made with 12 M NaOH solution for 30% replacement of Na_2SiO_3 solution showed more formation of aluminosilicate gels with a Si/Al ratio close to 3.0, and a Na/Al ratio close to 1.0 as obtained from the EDS analysis.

Nath and Kumar [66] have investigated the effect of fly ash particle size on physical, mechanical, and microstructural properties of fly ash based geopolymer paste. The class F fly ash was used at different particle sizes of coarser, medium and finer fraction. The combination of 10 M NaOH solution and Na_2SiO_3 solution was used as alkaline activator solution. After homogeneous mixing, the fly ash based geopolymer paste was cast into different moulds with sizes of 20 × 20 × 20 mm, 50 × 50 × 50 mm and 160 × 40 × 40 mm for determining the physical properties (apparent porosity and bulk density) and mechanical properties (compressive strength and flexural strength) respectively at the age of 7, 14 and 28 days. All the paste samples were heat cured at the temperature of 45 °C for 48 hours. After heat curing, the paste samples were kept in ambient condition till the age of testing. After compressive strength and flexural strength test, the crushed paste samples were used for microstructural analysis by different techniques such as TGA, XRD, FTIR, SEM-EDX and TEM. From the obtained results, the authors reported that the apparent porosity, bulk density, compressive strength and flexural strength of fly ash based geopolymer pastes mostly increased with decrease in particle size of fly ash at all ages. With size reduction, the physical properties and mechanical properties were enhanced due to formation of more hydrated products through

geopolymerization. In addition, both the compressive strength and flexural strength increased with increase in curing age. From the microstructural analysis, more amorphous gel formation was observed from lower fly ash particle size (finer fraction) of fly ash based geopolymer pastes, which enhanced the mechanical properties and it was confirmed from TGA and XRD analysis. The more amount of N-A-S-H gel with homogeneous and dense microstructure, and variations in Si/Al and Na/Al ratios were observed from SEM-EDX and TEM analysis, which correlated with better mechanical properties of fly ash based geopolymer pastes made with finer fraction of fly ash particle size.

Kumar et al. [67] have investigated the effect of different size fractions of fly ash on geopolymerization reaction of fly ash based geopolymer paste. Low calcium fly ash was used and four fly ash particle size corresponding to FA1, FA2, FA3, FA4 were 40.37, 23.64, 10.33 and 2.98 µm. The NaOH solution of 6 M was used as alkaline solution in this study. The alkaline solution to fly ash ratio was kept at 0.35. At the temperature of 27 ± 2 °C and under relative humidity of 65%, the paste samples were prepared in the cubic moulds of size of 70 mm for determining the compressive strength at the age of 3, 7, 14 and 28 days. After casting, the samples were cured at the temperature of 60 °C for 24 hours. After compressive strength test, the samples were crushed and subjected to microstructural analysis such as XRD, FTIR and SEM-EDS. The calorimetric studies were also conducted at 60 °C. From the test results, the authors reported that the compressive strength of fly ash based geopolymer pastes mostly increased with decrease in particle size of fly ash at both ambient and elevated temperatures. In addition, the compressive strength mostly increased with increase in curing age for both ambient and elevated temperatures. The XRD and SEM-EDS analyses showed more peak intensity of geopolymer reaction products and formation of more reaction products with homogeneous microstructure with gel composition variation of Si/Al and Na/Si ratios for the lower fly ash particle size (FA3 and FA4), which correlated with better mechanical properties. Further, the heat flow curve at 60 °C indicated more geopolymerization reaction occurred at lower fly ash particle size (FA4).

Al bakri et al. [68] have investigated the effect of Na_2SiO_3/NaOH ratio and NaOH molarity on compressive strength of fly ash based geopolymer paste. The low calcium fly ash was used as source material in this investigation. The combination of NaOH solution and Na_2SiO_3 solution was used as alkaline activator. Six different Na_2SiO_3/NaOH ratios (0.5, 1.0, 1.5, 2.0, 2.5, and 3.0) and six different molarity of NaOH solution (6, 8, 10, 12, 14, and 16 M) were used in this study. The geopolymer paste was placed in cube moulds of size 50 mm and cured

in oven at the temperature of 70 °C for 24 hours. After oven curing, the paste samples were kept in ambient temperature before demoulding. The compressive strength test was conducted at the age of 7 days. The XRD and SEM analyses were carried out to analyse the microstructure of fly ash based geopolymer paste. From the obtained results, the compressive strength of fly ash based geopolymer paste increased with increase in Na_2SiO_3/NaOH ratio from 0.5 to 2.5 and then it declined. This could be due to the excess OH^- concentration in the mixtures. Furthermore, the excess sodium content can form sodium carbonate by atmospheric carbonation and this may disrupt the polymerization process. Similarly, the compressive strength increased with increase in molarity of NaOH solution from 6 M to 12 M and then it declined. In the microstructural analysis, the respective higher intensity of crystalline phases and more amount of alumino-silicate gels that led to dense matrix with less unreacted fly ash particles were observed from XRD patterns and SEM images of fly ash based geopolymer paste made from 12 M NaOH solution, and ratio of alkaline solution of 2.5.

Farhan et al. [69] have investigated the engineering properties of normal and high strength fly ash based geopolymer (FAGP) concrete, and alkali activated slag (AAS) based concrete and compared with ordinary Portland cement (OPC) based concrete. The combination of sodium hydroxide (NaOH) solution and sodium silicate (Na_2SiO_3) solution was used as alkaline activator. The normal strength and high strength FAGP and AAS concrete were prepared with 12 M NaOH solution and 14 M NaOH solution, respectively. For FAGP and AAS concrete, the ratio of sodium silicate (Na_2SiO_3) to sodium hydroxide (NaOH) was set at 2 and 2.5 respectively. The alkaline activator contents were chosen at 168 kg/m^3 and 184.5 kg/m^3 for making of high strength fly ash based GPC and normal strength fly ash based GPC mixes respectively. The fly ash content used were 410 kg/m^3, and 480 kg/m^3 for making of normal and high strength fly ash based GPC mixes respectively. Extra water and superplasticizer were added to improve the workability of all the mixes. From the fresh concrete mixes, the cylindrical specimens with the size of 100 mm diameter and 200 mm height were cast to test the dry density, ultrasonic pulse velocity (UPV), and compressive strength at the age of 7 and 28 days. In addition, the cylindrical specimens with the size of 150 mm diameter and 300 mm height were cast to test the indirect tensile strength and stress-strain behaviour at the age of 7 and 28 days. Further, the prismatic specimens with the size of 100 mm × 100 mm × 500 mm were cast for flexural and direct tensile strength tests at the age of 7 and 28 days. The workability of all the mixtures were determined immediately after mixing. After casting, the FAGP and AAS concrete specimens were stored in the moulds and left in

the laboratory for 24 hours at room temperature (23 ± 3 °C). The FAGP concrete samples were heat cured for 24 hours at 80 °C. Then, the specimens were removed from the moulds and stored in the laboratory till the age of testing. After 24 hours of casting, the AAS concrete specimens were removed from the moulds and stored in the laboratory at room temperature till the age of testing. The SEM analysis was performed to examine the microstructure of FAGP, AAS, and OPC concrete. From the test results, the workability of FAGP concrete mixes were higher than AAS and OPC based concrete mixes for both normal and high strength mixes. However, normal strength concrete mixes exhibited higher workability as compared to high strength concrete mixes. The FAGP, AAS, and OPC concrete mixes exhibited equivalent mechanical properties for both normal and high strength. However, higher strength concrete mixes exhibited better mechanical properties as compared to normal strength concrete mixes. The SEM analysis revealed that FAGP and AAS concrete were denser and more compact than OPC concrete at the age of 7 days whereas less homogeneous microstructure in FAGP and AAS concrete than OPC concrete at the age of 28 days.

Chithambaram et al. [70] have investigated the effect of ground granulated blast furnace slag (GGBFS) on partial replacement of fly ash (FA) in the manufacture of ambient cured geopolymer mortar (GPM). In this investigation, class F fly ash and GGBFS were used as binding materials in the preparation of fly ash based geopolymer mortar (FGPM) and fly ash-GGBFS based geopolymer mortar (FGGPM) respectively. For the preparation of FGGPM mixes, the GGBFS content was replaced with fly ash content of 10%, 20%, 30% and 40%. The combination of NaOH solution and Na_2SiO_3 solution was used as alkaline activator solution. The ratio of activator liquid to binder, and the ratio of Na_2SiO_3/NaOH were considered as 0.45 and 2.5 respectively. Four different molar concentrations of NaOH i.e., 8 M, 10 M, 12 M and 14 M were used for both FGPM and FGGPM mixes. After mixing, the setting time of both FGPM and FGGPM mixtures was determined by standard Vicat apparatus. The FGPM and FGGPM mixes were prepared and cast in cube moulds of size 70.6 mm. After casting, the FGPM specimens were cured in oven at temperature varying from 60 °C to 100 °C at 10 °C interval. After oven curing, the FGPM specimens were kept in ambient temperature curing till the age of testing. However, after casting, all the FGGPM specimens were directly kept in ambient temperature curing till the age of testing. Besides, heat cured FGPM specimens at the age of 28 days were exposed to elevated temperatures in muffle furnace ranging from 200 °C to 1000 °C at an interval of 200 °C at the rate of 4 °C/min. All the test specimens were tested for compressive strength at the age of 3, 7 and 28 days. After compressive strength test, the

specimens were crushed and ground to powder samples. All the powder samples were subjected to microstructure analysis such as XRD and SEM-EDS at the age of 28 days. From the obtained results, the setting time of GPM mixes decreased with increase in GGBFS content for all molarity of NaOH solution whereas setting time of GPM mixes increased with increase in molarity of NaOH solution. The setting time of FGPM mixes were higher as compared to the mixes made with FGGPM for all molarity of NaOH solution. The compressive strength of FGPM mixes increased with increase in curing temperature from 60 °C to 90 °C as well as molarity of NaOH solution from 8 to 12 M and then it declined. This may be attributed to the hindrance in geopolymerization process that reduced the early stage aluminosilicate gel precipitation due to the presence of surplus hydroxide ion concentration. Further, the compressive strength of GPM mixes increased with increase in GGBFS content from 0% to 30% as well as molarity of NaOH solution from 8 M to 12 M and then it declined. Similarly, the density of GPM mixes also increased with increase in GGBFS content. The FGGPM mixes exhibited higher compressive strength as compared to FGPM mixes. Besides, the compressive strength of both FGPM and FGGPM mixes increased with increase in curing age. The percentage weight loss of 28 days matured GPM specimens exposed to elevated temperatures increased with increase in temperature from 200 °C to 1000 °C irrespective of NaOH concentration. The GPM exposed to elevated temperature above 600 °C indicated a change from crystalline to amorphous phase due to slow polymerization of unreacted materials leading to marginal strength loss. From microstructure analysis, the GPM mixes made with 12 NaOH solution, 30% GGBFS content and curing temperature of 90 °C indicated higher peak intensity of geopolymer gels and dense microstructure with suitable variations of Si/Al and Ca/Si ratios as observed from XRD and SEM analyses respectively.

Elyamany et al. [71] have evaluated the setting time, compressive strength and flexural strength of geopolymer mortar. In this study, various types of binder used were class F fly ash, GGBS and silica fume. Three curing temperatures were considered such as 30°, 60° and 90° C. Different molarity of NaOH solution used were 10 M, 12 M, 14 M and 16 M. The alkaline liquid to binder ratios were maintained at 0.35, 0.40, 0.45 and 0.50. The Na_2SiO_3/NaOH solution ratio of 2, sand-to-binder ratio of 3, extra water and superplasticizer of 6% and 3% by weight of binder respectively were kept constant for all the mixes. In this study, FA correspond to the mixes that consists of 100% fly ash and FAS correspond to mixes that consists of 50% fly ash and 50% GGBS while FASS correspond to the mixes that contained 50% fly ash, 35% GGBS and 15% silica fume. The setting time was evaluated at ambient temperature. The GPC

mixes were cast into cube moulds of size 70 mm and prism moulds size of 40 × 40 × 160 mm to determine the 7-day compressive strength, and flexural strength respectively. The specimens were demoulded after 24 hrs of casting and then cured in hot air oven for 48 hrs at various curing temperatures and kept at ambient temperature (20-23 °C) until testing. The SEM analysis was performed to evaluate the microstructure of geopolymer mortar. The test results indicated that the setting time of FA based geopolymer mortar mixes decreased with increase in molarity of NaOH solution. On the contrary, the setting time of FAS and FASS based geopolymer mortar mixes increased with increase in molarity of NaOH solution. In addition, the setting time of FA based geopolymer mortar mixes increased with increase in alkaline solution to binder ratio whereas setting time of FAS and FASS based geopolymer mortar mixes decreased with increase in alkaline solution to binder ratio. The FAS based geopolymer mortar mixes exhibited lower setting time as compared to FA and FASS based geopolymer mortar mixes. The compressive strength and flexural strength of all mixes increased with increase in molarity of NaOH solution whereas decreased with increase in ratio of alkaline solution to binder. This may be because the increase in solution content leads to increase in water content, which affects compressive strength negatively at higher ratio of alkaline solution to binder. The compressive strength and flexural strength of all mixes increased with increase in curing temperature. The FASS based geopolymer mortar mixes exhibited higher compressive strength and flexural strength as compared to FA and FAS based geopolymer mortar mixes. This may be due to the presence of calcium in the binders, which contained slag that resulted in higher density due to formation of additional geopolymerization products and multiple gels (N-A-S-H, C-A-S-H) resulted from reaction FA system with Si-O-Al-O. Additionally, the addition of silica fume in FASS mixes leads to increase the reactivity of slag that resulted in higher strength. The SEM micrographs showed that FASS based geopolymer mortar mix attained dense microstructure as compared to FA and FAS based geopolymer mortar mixes.

Phoo-ngernkham et al. [72] have investigated the effect of sodium hydroxide and sodium silicate solutions on compressive strength and shear bond strength of fly ash-GGBS based geopolymer pastes. The materials used in this investigation were fly ash (FA) and ground granulated blast furnace slag (GGBS). Three types of activators used in this study were 10 M NaOH solution, Na_2SiO_3 solution, and combination of NaOH and Na_2SiO_3 solutions. Three types of geopolymer pastes prepared in this study were fly ash based geopolymer paste, fly ash blended with GGBS based geopolymer pastes and GGBS based geopolymer paste. The alkaline liquid to binder ratio was kept constant at 0.60 for all geopolymer pastes. After mixing,

the fresh geopolymer pastes were placed into cylindrical moulds of 50 mm in diameter and 100 mm in height. The geopolymer paste specimens were covered with vinyl sheet and kept in ambient temperature curing of 23 °C. The specimens were demoulded at the age of 1 day and kept in the controlled room temperature of 23 °C till the age of testing. The compressive strength and shear bond strength of specimens were tested at the ages of 7, 28, and 60 days. At the age of 28 days, the geopolymer paste specimens were crushed and ground to powder samples for microstructure analysis such as XRD and SEM analyses. From the test results, the authors reported that the geopolymer pastes made with combination of NaOH solution and Na_2SiO_3 solution exhibited higher compressive strength as compared to pastes made with Na_2SiO_3 solution, and NaOH solution alone. In addition, the GGBS based geopolymer paste mixes exhibited higher compressive strength as compared to the pastes made with fly ash blended with GGBS, and fly ash based geopolymer paste mixes. The compressive strength of all mixes increased with increase in curing age. The highest bond strength was obtained from the geopolymer paste made with fly ash blended with GGBS and combination of NaOH solution and Na_2SiO_3 solution at the age of 28 days. The XRD analysis indicated that the fly ash based geopolymer paste contained amorphous N-A-S-H gel and some crystalline phases of the remaining of fly ash. The increase in GGBS content enhanced the compressive strength and microstructure of geopolymer pastes due to formation of additional C-S-H gel. The use of NaOH solution, and combination of NaOH solution and Na_2SiO_3 solution resulted in crystalline C-S-H, and amorphous gel, whereas the use of Na_2SiO_3 solution resulted in mainly the amorphous products. The SEM analysis revealed denser and homogenous microstructure in GGBS based geopolymer paste than fly ash blended with GGBS based geopolymer paste and fly ash based geopolymer paste. Further, the geopolymer paste made with combination of NaOH solution and Na_2SiO_3 solution, and Na_2SiO_3 solution alone showed denser microstructure than that made with NaOH solution alone.

Nath and Sarkar [73] have investigated the effect of GGBFS on setting time, workability, and early age strength properties of fly ash based geopolymer composites. In this study, class F fly ash and GGBFS were used as binders for making of fly ash and fly ash-GGBFS based geopolymer composites. The GGBFS contents of 10%, 20%, and 30% were used to replace the total binder for making of fly ash-GGBFS based geopolymer composites. The combination of 14 M NaOH solution and Na_2SiO_3 solution was used as alkaline activator solution. Total eight mixtures were prepared in this investigation for paste, mortar and concrete. Mixture 1 (S00) was the control mix made with fly ash only as the total binder. Mixtures 2 (S10), 3 (S20)

and 4 (S30) were made with GGBFS as 10%, 20% and 30% of total binder respectively. The amount of alkaline activator solution in these mixtures was constant at 40% of the total binder with Na_2SiO_3/NaOH solution ratio of 2.5. The amount of alkaline activator solution was varied as 35% and 45% of total binder in the mixture 5 (A35) and 6 (A45) respectively, while having constant amount of 10% GGBFS and Na_2SiO_3/NaOH solution ratio of 2.5. Mixtures 7 (R1.5) and 8 (R2.0) were made with varying Na_2SiO_3/NaOH solution ratios of 1.5 and 2.0 respectively. Each of these mixtures had 10% GGBFS and alkaline activator solution content at 40% of the total binder. The unit weight of mortar was taken as 2200 kg/m^3. The total binder content was constant and constituted one third of the total mixture. The other mixture variables such as slag content, amount of alkaline activator solution and ratio of Na_2SiO_3/NaOH solution remained same as in case of concrete mixtures. The setting time of geopolymer mixture was tested on corresponding paste mixes. The mix proportions of the pastes were similar to those of concrete or mortar mixtures with the aggregates excluded. The fresh geopolymer mortar and concrete mixtures were poured into different moulds of size 50 mm cube and 100 × 200 mm cylinder respectively. Then, the moulds were stored in controlled temperature of 20-23 °C leaving the top surface exposed to air. After 24 hours of casting, the samples were demoulded and left in air at 20-23 °C and 65 ± 5% relative humidity until tested to ensure a consistent environment for all the samples. The control geopolymer mixture was demoulded after 3 days of casting due to slow rate of setting. In this investigation, to study the effect of curing temperature, the geopolymer mortar and concrete made with mixture 2 were cured in oven at 60 °C for 24 hours immediately after casting to compare with those cured without elevated temperature (20-23 °C). The compressive strength test was conducted at the age of 3, 7, 28 and 56 days. Further, SEM-EDX analysis was conducted to analyse the morphology with compositional variation of two geopolymer paste mixes at the age of 28 days. Two geopolymer paste mixes, which included the mixtures 2 (S10), and 4 (S30) were made with GGBFS as 10%, and 30% of total binder respectively. The amount of alkaline activator solution in these mixtures was constant at 40% of the total binder with Na_2SiO_3/NaOH solution ratio of 2.5. From the obtained results, the setting time and workability of fly ash based geopolymer paste mixes decreased with increase in GGBFS content. Similarly, the slump values of concrete and flow percentages of mortar decreased with the increase in GGBFS content. However, the workability and setting time increased when amount of alkaline activator solution was increased, with reduced compressive strength. The mixtures having amount of alkaline activator solution with Na_2SiO_3/NaOH solution ratio of 2.5 exhibited lower slump value and setting time than those made with 1.5 and 2.0. The addition of 10% GGBFS achieved higher

compressive strength of concrete and mortar at the age of 28 days. The compressive strength decreased with increase in amount of alkaline activator solution from 35% to 45% of total binder. The variation of Na_2SiO_3/NaOH ratio from 1.5 to 2.5 decreased the strength slightly over the age. The concrete and mortar samples made without heat curing achieved the strength gradually over the age whereas samples made with heat curing achieved high early strength, which increased negligibly over the age. From SEM-EDX analysis, the microscopic images of fly ash-GGBFS geopolymer paste revealed mostly amorphous and calcium-containing hydration products. The compact microstructure with geopolymer gel increased with increase in GGBFS content. In addition, suitable variations in Si/Al and Ca/Si ratios were revealed from the EDX analysis.

2.4 Durability of fly ash based geopolymer paste, mortar and concrete

Gunasekara et al. [74] have investigated the long-term permeation properties of fly ash based geopolymer concrete made from four different fly ash sources. In this study, class F fly ash from four fly ash sources namely i.e., Gladstone (FA1), Pt. Augusta (FA2), Collie (FA3) and Tarong (FA4) was used as source material. The combination of 15 M NaOH solution and Na_2SiO_3 solution was used as activator solution. Extra water was used for FA1, FA2 and FA3 mixes. Fly ash contents used were 416 kg/m^3, 416 kg/m^3, 420 kg/m^3 and 412 kg/m^3, which corresponded to fly ash sources of FA1, FA2, FA3, and FA4 with the average particle size of 24.8 µm, 30.1 µm, 26.1 µm and 22.7 µm respectively. The slump test was conducted immediately on the fresh GPC mixtures. From the fresh GPC mixes, the cube specimens with the size of 100 mm × 100 mm × 100 mm were cast to test the compressive strength and chloride diffusion at different ages. The cylindrical specimens with the size of 100 mm × 200 mm were cast to test the density and water absorption at different ages. The specimens with the size of 100 mm × 200 mm × 200 mm were cast for ultrasonic pulse velocity (UPV) and electrical resistivity tests at different ages. Further, the specimens with the size of 100 mm × 300 mm × 300 mm were cast for water permeability and air permeability tests at different ages. After casting, the specimens were kept in room temperature condition for 24 hours. After 24 hours, the specimens were heat cured at temperature of 80 °C for 24 hours with relative humidity of 95%. After heat curing, the specimens were removed from the moulds and maintained at room temperature till the age of testing. After compressive strength test, SEM analysis was performed on crushed samples. From the test results, higher slump flow, oven dry density, UPV, and compressive strength of GPC mixes were attained from Gladstone fly ash as compared to other fly ash sources. In addition, the oven dry density, UPV and compressive

strength of GPC mixes increased with increase in curing age. The higher values of water absorption, and apparent volume of permeable voids (AVPV) were obtained from GPC mixes made from Collie fly ash source as compared to other sources. The water absorption, and apparent volume of permeable voids (AVPV) of GPC mixes decreased with increase in curing age. The fly ash based geopolymer concrete mixes made from Collie fly ash source exhibited higher water permeability and air permeability than the mixes made from other fly ash sources at the age of 28 days, 90 days and 365 days. Further, the chloride diffusion coefficient was higher in the fly ash based geopolymer concrete mixes made from Collie fly ash source as compared to other fly ash sources at the age of 28 days. Lower chloride diffusion was observed in the GPC mixes made from all fly ash sources at the age of 365 days. The SEM analysis revealed that the microstructure of all GPC mixes improved with time due to continued geopolymerization process and formation of more amount of geopolymer gel, which filled the cracks and voids in the matrix that resulted in a more homogeneous and denser pore-structure with time.

Nuaklong et al. [75] have studied the effect of recycled aggregate on strength and durability of fly ash based geopolymer concrete. High calcium fly ash was used as source material in this study. Sodium hydroxide (NH) solution with molar concentrations of 8 M, 12 M and 16 M and sodium silicate (NS) solution were used as alkali activator solution. The recycled coarse aggregate (RCA), crushed limestone coarse aggregate (LCA) and river sand as fine aggregate were used in the preparation of geopolymer concrete. All mixtures had a liquid to fly ash ratio (L/A) of 0.6, and an NS to NH ratio of 1.5 by weight. After preparation, the slump flow of geopolymer concrete mixtures was measured. Cylindrical specimens of size 100 mm diameter and 200 mm height were cast for compression and splitting tensile strength as well as for chloride penetration test. Slab specimens of size 300 mm × 300 mm × 35 mm, and prisms of size 75 mm × 75 mm × 300 mm were prepared for measuring surface abrasion resistance, and flexural strength respectively. In addition, for sulfuric acid resistance test, cube specimens of size 100 mm were used. All the specimens were cast, and covered with plastic sheet and left for 1 hour before being cured at temperature of 60 °C for 2 days. Then, all the specimens were demoulded and kept at room temperature of 23 °C and humidity of 50% until the testing age of 7 days. The obtained results indicated that the slump flow decreased with increase in molarity of NaOH solution for both GPC mixes made from limestone coarse aggregate (LCA) and recycled coarse aggregate (RCA). However, the slump flow of GPC mixes made from RCA was higher than LCA. For both RCA and LCA, the GPC made from 12 M NaOH solution

achieved better mechanical properties in terms of compressive strength, splitting tensile strength, flexural strength, and surface abrasion resistance. The geopolymer concrete made with 12 M and 16 M NaOH solution resulted in better performances with respect to water absorption, volume of permeable voids, rate of sorptivity, chloride penetration depth, and weight loss from sulfuric acid solution. Further, the geopolymer concrete made with from recycled coarse aggregate exhibited lower mechanical and durability properties when compared with limestone coarse aggregate.

Olivia and Nikraz [27] have investigated the mechanical and durability properties of fly ash based geopolymer concrete mixes in comparison to OPC based concrete under sea-water environment. In this study, fly ash based geopolymer concrete was prepared by using class F fly ash and alkaline activators (sodium hydroxide solution (14 M), and sodium silicate solution). The fly ash content used were 424.6 kg/m^3, 461.5 kg/m^3 and 498.5 kg/m^3, which correspond to alkali solution contents of 127.3 kg/m^3, 138.5 kg/m^3, 149.4 kg/m^3. In this study, ordinary Portland cement (OPC) was used for reference purpose. Extra water and superplasticizer were added to the geopolymer concrete mixtures. Slump test was conducted to evaluate the workability of fresh GPC mixes. The specimens were cast in cylinders of 100 mm diameter and 200 mm length (100 × 200 mm) for measurement of compressive strength, Young's modulus of elasticity and weight change; 150 × 300 mm cylinders for splitting tensile strength test, 100 × 50 mm cylinders for water absorption, and cylinders 100 × 110 mm were used for sorptivity test. Blocks of dimension 100 × 100 × 400 mm were used for measuring flexural strength, and 25 × 25 × 250 mm blocks were used for measuring shrinkage. Lollipop specimens: 100 × 200 mm concrete cylinders with central 16 mm diameter steel bars were used for half-cell potential and accelerated corrosion tests. The specimens were air dried in a curing room at 23-25 °C after being removed from their moulds. After 24 hours of air curing, the control OPC concrete specimens were removed from their moulds and placed in water ponds for 28 days. The specimens were taken out of the water ponds and allowed to air dry in the curing chamber until the testing age. The resistance to accelerated wetting-drying cycles in 3.5% NaCl solution was evaluated for control and GPC mixes. For the test, the specimens were subjected to immersion in 3.5% NaCl solution for 24 hours followed by drying in an oven at 80 °C for 24 hours. The changes in compressive strength and weight were determined after 10 cycles for control and GPC mixes. The test results indicated that slump values of GPC mixes were higher than OPC concrete mixes. In addition, the slump values of GPC mixes increased with increase in fly ash content and alkaline solution content. The mechanical properties of

GPC mixes in terms of compressive strength, tensile strength, flexural strength, modulus of elasticity and Poisson's ratio were similar to OPC based concrete mixes at all ages. The GPC mixes had lower water absorption, AVPV, and effective porosity than OPC based concrete at the age of 28 and 91 days. The mechanical properties of GPC mixes improved with the addition of higher amount of fly ash content and alkaline solution content. However, the water absorption, AVPV, and effective porosity values were similar to all GPC mixes. The compressive strength of GPC mixes changed significantly at each wetting-drying cycle, but weight loss was higher than that of OPC concrete. The half-cell potential measurement showed that the GPC mixes were generally more prone to corrosion, although showed low-level corrosion activity, and exhibited longer time to failure than OPC based concrete.

Reddy et al. [76] have evaluated the durability properties of low calcium fly ash based geopolymer concrete (GPC) under corrosive environment. In this study, Class F- fly ash was used. Combination of NaOH solution and Na_2SiO_3 solution was used to activate the fly ash in geopolymer concrete mixes. To prepare the control mixes, ASTM type I Portland cement was used in this study. For the workability of GPC mixes, polycarboxylate based type F high-range water reducer was added to the mixes. For the preparation of GPC mixes, 8 M and 14 M NaOH solution was used. The OPC and GPC mixes were used for preparing cylindrical specimens of size 100 × 200 mm, and beam specimens of size 150 × 150 × 525 mm, which were centrally reinforced with 13-mm rebars. After casting, all the specimens were allowed to set for 4 or 5 days. Then, the specimens were removed from the moulds and subjected to heat curing in oven at the temperature of 60˚C for 24 hours. Subsequently, the specimens were cured in room temperature for 28 days. The control specimens were also cured in room temperature for 28 days, but without initial heat curing. The compression test, splitting tensile strength, and accelerated reinforcement corrosion test were conducted on cylindrical and beam specimens to evaluate the compressive strength, splitting tensile strength, and corrosion current and cracking behaviour of OPC and GPC specimens. After accelerated corrosion test, the mass loss of corroded reinforcing steel and residual ultimate flexural loads were measured. The obtained results indicated that the compressive strength, splitting tensile strength and flexural strength of GPC mixes increased with increase in molarity of NaOH solution. However, corrosion current and time of GPC mixes were similar for both molarity of NaOH solution. Further, the compressive strength, splitting tensile strength, flexural strength, corrosion based improved crack resistance and resistance against chloride penetration of GPC mixes were higher as compared to OPC based concrete mixes. The low permeability of GPC beam specimens

delayed the depassivation of reinforcing steel. The primary reason that the OPC beam specimens exhibited high mass loss may be attributed to the wide longitudinal cracks observed on the beam specimens, which enabled chloride ions to penetrate more quickly into the concrete and accelerate the corrosion rate. Besides, the compressive strength and splitting tensile strength of GPC, and OPC based concrete increased with increase in curing age.

Kupwade-Patil and Allouche [24] have investigated the durability of steel reinforced fly ash based geopolymer concrete (GPC) and ordinary Portland cement (OPC) based concrete in cyclic wet-dry chloride environment over a period of 12 months. The GPC mix was prepared by mixing of 14 M NaOH solution and Na_2SiO_3 solution, which was mixed with fly ash, fine aggregate, and coarse aggregate. Two types of fly ash (class C and class F) and two sources (DH and OH) of Class F fly ash were used in this investigation. The ordinary Portland cement (OPC) was used for comparison with GPC. As per ASTM G109, the specimens were cast using fly ash based GPC and Portland cement Type I (ASTM 2003d). The specimens were 280 mm in length, 114 mm in width, and 150 mm in height. The steel bars of diameter 10 mm, and length 381 mm were used. All the specimens were subjected to saltwater wetting and drying cycles that included 14 days of exposure to 7.5% NaCl solution (wet cycle) followed by 14 days of air exposure (dry cycle). To simulate extreme conditions and promote corrosion, a high-concentration NaCl solution was utilized. The half-cell potential measurement was carried out in accordance with ASTM C876. Linear polarization resistance (LPR) measurement was carried out to assess the corrosion current density of steel reinforcement. The measured charge density was linked to chloride ion penetrability using ASTM C1202. After one year of chloride exposure, the chloride concentration was measured using ASTM C1152. The corrosion product of steel reinforcement was determined based on the total area corrosion coverage of steel reinforcement. Mercury intrusion porosimetry (MIP) was used to characterize the porous structure. The microstructural characterization of OPC and geopolymer concrete were investigated by x-ray diffraction (XRD), scanning electron microscopy (SEM) and Fourier transform infrared spectroscopy (FTIR). From the obtained results, it was found that geopolymer concrete specimens prepared from Class F fly ash exhibited lower diffusion coefficient, chloride content, and porosity when compared with their GPC Class C fly ash and OPC counterparts. However, the compressive strength of GPC mixes made from class C fly ash were almost similar to class F fly ash. Further, only micro-level indications of corrosion products were observed at the matrix-rebar interface for some GPC specimens, whereas multiple gross corrosion products were observed among OPC based concrete specimens from

the microstructural analysis such as SEM-EDS, XRD and FTIR. The low level of chloride penetration observed in GPC specimens implied lower chloride ion concentration at the rebar/concrete interface. GPC made from Class F fly ash (DH source) provided highest level of resistance to chloride ingress and corrosion, possibly resulted from a more complete geopolymerization process, and consequently a denser matrix. This indicated that the activation of fly ash and the extent of the subsequent geopolymerization process could play a vital role in the ability of the GPC matrix to resist chloride ingress. Overall, the GPC specimens made from Class F fly ash exhibited a significantly higher resistance to chloride-induced corrosion compared with OPC specimens as well as GPC specimens made from Class C fly ash.

Chindaprasirt and Chalee [77] have carried out a study to evaluate the effect of sodium hydroxide solution concentration on compressive strength, chloride penetration, and steel reinforcement corrosion in fly ash based geopolymer concrete under marine environment. The geopolymer concrete was prepared from high calcium fly ash with the combined alkaline liquid of NaOH solution and Na_2SiO_3 solution. The concentrations of NaOH solution used were 8 M, 10 M, 12 M, 14 M and 16 M. The liquid to binder ratio was kept constant at 0.60. In this study, the fly ash content and alkaline solution content used were 390 kg/m^3 and 234 kg/m^3 respectively. For compressive strength test, concrete cylinders of size 100 mm × 200 mm were prepared. Cube specimens of size 200 mm with embedded steel bar having cover depth of 20, 50, and 75 mm were cast for chloride penetration and steel corrosion test. The geopolymer concrete specimens were exposed to two wet-dry cycles of seawater daily. After 3 years exposure, all the specimens were tested for compressive strength, chloride penetration and corrosion of embedded steel bar. From the test results, the compressive strength of GPC mixes during 3-year exposure of seawater significantly increased with increase in NaOH solution molarity whereas chloride penetration and corrosion of embedded steel bar decreased with increase in molarity of NaOH solution. The reduction in chloride penetration in geopolymer concrete made with high concentration NaOH solution could be attributed to the refinement of pore structure as a result of polycondensation reaction and filler effect. The relatively high NaOH solution concentration enabled the leaching of more Si and Al from fly ash that resulted in greater degree of polycondensation and led to decrease in porosity of geopolymer concrete. Both free and total chloride contents of GPC mixes decreased with increase in molarity of NaOH solution. Further, chloride binding capacity of geopolymer concrete mixes increased with increase in molarity of NaOH solution.

Pasupathy et al. [78] have investigated the durability of low-calcium fly ash based geopolymer concrete in saline lake environment. The geopolymer binder was prepared from low calcium fly ash activated by using activator solution (8 M NaOH solution and Na_2SiO_3 solution). In this study, the fly ash content and activator solution content used were 409 kg/m^3 and 143 kg/m^3 respectively. The concrete cylinder specimens were prepared during the preparation of geopolymer concrete culvert to check the compressive strength and permeability properties. The compressive strength and water absorption values were obtained for GPC concrete. The GPC concrete culvert was cured at 60 °C for 24 h, while the OPC concrete culvert was cured at ambient temperature. The dimensions of the concrete box culverts were 1200 mm length, 1200 mm width and 600 mm depth. The core specimens from GPC and OPC concrete culvert were subjected to in-situ carbonation, chloride and sulphate ingress, microstructural characterization such as SEM-EDX, XRD and FTIR, and porosity measurement. The obtained results showed that the salt scaling effect in GPC culvert was higher than OPC concrete culvert. The carbonation in fly ash based GPC was higher as compared to OPC in the saline lake exposure of 6 years. The obtained results of XRD and FTIR confirmed dissolution of carbonation products in fly ash based geopolymer concrete when it is exposed to field conditions. At the same time, calcium carbonate components were detected in OPC concrete specimens. In saline environment, the chloride penetration was higher in GPC. Moreover, the chloride penetration was confirmed through SEM by observation of chloride content in deposition of film layer. The GPC exhibited higher ingress of sulphate than OPC based concrete. The SEM-EDX analysis revealed higher sulphate penetration, and no formation of ettringite was observed in GPC specimens. This indicates that the mechanism of sulphate attack in GPC is different from OPC concrete. The combined effect of chloride penetration and higher carbonation increased the corrosion activity of steel bar in GPC. Though the total porosity of GPC was higher than OPC concrete, the majority of the pores are fine pores. Specifically, the GPC has more pores between 1.25 nm - 25 nm diameter, whereas most of the pores identified in OPC concrete were in the range between 25 and 50,000 nm.

Gunasekara et al. [25] have studied steel reinforcement corrosion in geopolymer concrete prepared from three different sources of low calcium fly ash namely Gladstone, Pt. Augusta and Collie. Commercially available sodium silicate solution and 15 M NaOH solution was used as alkaline activator. The crushed granite stone and natural river sand were used as coarse aggregate and fine aggregate respectively. In this study, the fly ash contents used were 417 kg/m^3 (Gladstone and Pt. Augusta) and 420 kg/m^3 (Collie). The alkaline activator contents

used were 333 kg/m^3 (Collie) and 359 kg/m^3 (Gladstone and Pt. Augusta). The Portland cement (PC) was used for reference purpose in this study. The extra water was also added to improve the workability of geopolymer concrete and PC based concrete mixes. From each concrete type, cubes of size 150 mm were cast with ribbed bars (10 mm diameter and 120 mm length). For the cast-in-chloride specimens, the percentages of admixed sodium chloride (NaCl) were 0, 0.25, 0.5, 1, 2, 3 and 5% by weight of binder. An additional set of concrete cubes of size 150 m were cast with ribbed bars (10 mm diameter and 120 mm length) without chloride addition for ponding test. All geopolymer concrete specimens were initially kept at room temperature for 24 hour and then heat cured in oven for 24 h at 80 °C temperature. The compressive strength test was performed at the age of 28 days and 540 days. The long-term corrosion behaviour of embedded rebar in fly ash geopolymer concrete was evaluated on cast-in-chloride specimens and ponded specimens. Half-cell potential and linear polarization resistance measurements were performed to measure the corrosion potential and corrosion current density up to the age of 540 days. Near the rebar level, powdered samples were taken from 540-days matured concrete specimens for chloride content, Fourier transform infrared (FT-IR) and X-ray diffraction (XRD) analyses. Scanning electron microscopy in backscattered electron (BSE) imaging mode was performed to examine the microstructure of geopolymer concrete. The obtained results indicated that both the geopolymer concrete and Portland cement concrete mixes admixed with chloride concentration showed a strength reduction between 28 and 540 days and the strength reduction increased with increase in chloride concentration. The corrosion potential became more negative and the corrosion current density values increased in case of cast-in chloride geopolymer concrete specimens. However, in case of ponded specimens, the steel reinforcement in geopolymer concrete specimens showed lower corrosion levels. In case of ponded specimens, the formation of three-dimensional N-A-S-H and C-A-S-H cross linking in the gel matrix reduced the chloride diffusion to rebar depth, thereby resulting in a lower corrosion rate in ponded geopolymer specimens. Besides, the corrosion products in the form of hematite [Fe_2O_3], akageneite [FeO(OH)] and lepidocrocite [γ-FeO(OH)] were identified.

Pasupathy et al. [79] have investigated the long-term durability of fly ash based geopolymer concrete in a severe salt lake environment with buried and fully saturated conditions during a 10-year period. In this study, class F fly ash was used as source material for making of geopolymer concrete. The combination of 8 M NaOH solution and Na_2SiO_3 solution was used as alkali solution. The ratio of Na_2SiO_3 to NaOH solution was kept at 2.5. The ordinary

Portland cement (OPC) was used for reference purpose. In this study, the fly ash content and alkali solution content used were 409 kg/m^3 and 143 kg/m^3 respectively. The extra water and superplasticizer were added to improve the workability of concrete mixes. The GPC specimens were subjected to steam curing at the temperature of 60 °C for 24 hours whereas the OPC based concrete was cured at the ambient temperature of 23 °C. The compressive strength test was conducted at the age of 90 days. The core specimens (67 mm diameter × 90 mm height) were obtained from GPC and OPC based concrete structures and tested for chloride and sulphate ingress, pH, and microstructure (SEM) analysis. From the test results, the 90 days compressive strength of GPC and OPC concrete (before exposure to aggressive environment) were 39 MPa and 43 MPa respectively. The chloride penetration in GPC mixes was higher than OPC based concrete mixes. In addition, chloride binding capacity of GPC mixes was lower as compared to OPC based concrete mixes. The precipitation of NaCl in the microstructure of GPC mixes was observed from the SEM analysis. This confirmed the physical binding of chloride ions in the GPC mixes. Similar to chloride penetration, the sulphate penetration was higher in GPC mixes than OPC based concrete. The alkalinity of GPC mixes was lower as compared to OPC based concrete mixes. The visual observation of embedded steel bar and steel/concrete interface of GPC indicated the initiation of corrosion activity.

Ojha and Aggarwal [80] have carried out a study to evaluate the durability performance of low calcium fly ash based geopolymer concrete (GPC). To compare the durability performance, OPC concrete was also prepared. The combination of 14 M NaOH solution and Na_2SiO_3 solution was used as alkaline activator solution. The ratio of sodium silicate (Na_2SiO_3) to sodium hydroxide (NaOH) solution was 2. To improve the workability of both GPC and OPC based concrete, superplasticizer was added to fresh concrete mixtures. From the fresh concrete mixtures, the cube specimens with the size of 150 mm × 150 mm × 150 mm were cast to test the water absorption, water permeability, acid resistance, and sulphate resistance at different ages. The cylindrical specimens with the size of 70 mm diameter and 30 mm thickness were cast to test the sorptivity and rapid chloride penetration to determine the durability performance of fly ash based geopolymer concrete and OPC concrete at different ages. From the obtained results, the fly ash based geopolymer concrete showed lower water absorption, permeability, and sorptivity than OPC concrete. In addition, the fly ash based geopolymer concrete exhibited less weight loss and substantial residual compressive strength as compared to OPC based concrete. From the results on sulphate attack resistance, it was observed that the average weight gain of fly ash based geopolymer concrete was significantly higher than that

of OPC concrete. However, fly ash based geopolymer concrete mostly showed higher residual compressive strength than OPC concrete. From the obtained results on rapid chloride ion penetration, the fly ash based geopolymer concrete exhibited moderate chloride ion penetrability whereas OPC concrete showed low chloride ion penetrability.

Adak and Mandal [81] have investigated the strength and durability performance of fly ash based process-modified geopolymer concrete. In this study, low calcium fly ash was used. Grade 43 OPC was used for reference purpose. The combination of 8 M NaOH solution and Na_2SiO_3 solution was used as alkaline activator liquid for both process modified fly ash based geopolymer concrete mixture and heat cured fly ash based geopolymer concrete mixture. The process modified fly ash based geopolymer concrete (GPC-1) mixture was prepared where the fly ash was mixed with desired quantity of alkaline activator liquid and placed in hot-air oven for 45 minutes at the temperature of 60 °C before casting. The desired quantities of fine and coarse aggregates were immediately mixed with the hot mixture of fly ash and alkaline activator liquid for 2 minutes and cast in the moulds. After 10-12 hours of casting, the specimens were demoulded and kept in room temperature until the age of testing. For the preparation of heat cured GPC specimens (GPC-2), the fly ash, alkaline activator liquid, coarse aggregate and fine aggregate were mixed together and cast. The specimens were kept at room temperature for 48 hours after casting. Then, the specimens were demoulded and cured at the temperature of 60 °C in the hot-air oven for 48 hours. After curing, the specimens were kept in the room temperature until the age of testing. The water cured OPC based concrete mixes were designed, and the strength was compared with the GPC mixes. The fresh properties of three mixes (GPC-1, GPC-2 and OPC) were determined by slump test and compaction factor test. The mechanical properties i.e., compressive strength, flexural strength, split-tensile strength and bond strength of the three mixes (GPC-1, GPC-2 and OPC) were determined. For durability, water absorption, acid resistance and chloride ion penetrability were evaluated. The XRD and FESEM-EDS analyses were performed to analyze the microstructure of the concrete mixes. The obtained results indicated that the fresh properties of three mixes (GPC-1, GPC-2 and OPC) were similar. The compressive strength of the mixes (GPC-1, GPC-2 and OPC) increased with increase in curing age. GPC-1 mixes exhibited better mechanical and durability properties than other mixes, especially, both the GPC mixes (GPC-1 and GPC-2) exhibited better mechanical and durability properties than OPC concrete mixes. The XRD and FESEM-EDS analyses revealed huge amount of crystalline phases converted from amorphous compounds, and stronger ITZ between aggregates and geopolymer matrix for higher Si/Al

ratio was observed in case of GPC-1 mixes, which correlated with the better mechanical and durability properties as compared to other mixes.

Noushini et al. [35] have evaluated the chloride diffusion resistance and chloride binding capacity of fly ash based geopolymer concrete. The aluminosilicate source materials for the geopolymer binder in this investigation were Eraring and Callide source of low-calcium type fly ash, and Callide source of ground granulated blast-furnace slag (GGBS). The combination of 12 M NaOH solution and sodium disilicate ($Na_2Si_2O_5$) solution was used as alkaline solution. Twelve different heat curing conditions were applied, which involved three different heat curing temperatures of 60 °C, 75 °C, and 90 °C, and four heat curing durations of 8 hours, 12 hours, 18 hours, and 24 hours as well as ambient curing was applied to geopolymer concrete specimens. After completion of heat curing period, the samples were slowly cooled down to the ambient temperature at a rate of 24 °C per hour. Then, the samples were demoulded and stored in a controlled room at a temperature of 23 ± 2 °C till the age of testing. For ambient curing, the sealed specimens were stored in the controlled room at a temperature of 23 ± 2 °C after casting till the age of testing. For mechanical properties, the tests for compressive strength and static chord modulus of elasticity of GPC were conducted. The transport properties such as apparent volume of permeable voids, sorptivity and surface resistivity of GPC were evaluated. Further, the durability properties such as chloride migration coefficient and chloride diffusion coefficient were also evaluated. The chloride binding capacity of GPC and OPC based concrete were also determined after 35 days of exposure in 16.5% aqueous NaCl solution. The microstructural characteristics of geopolymer paste samples were evaluated using microstructural analyses such as XRD, SEM, EDS and NMR. From the obtained results, the maximum compressive strength was obtained from GPC mixes heat cured of 75 °C and curing period of 18 hours or 24 hours. Further, the fly ash-GGBS based GPC mixes heat cured at 75 °C and curing periods of 18 hours or 24 hours exhibited improved transport properties in terms of apparent volume of permeable voids, sorptivity coefficient and surface resistivity as compared to the other mixes. The chloride migration and diffusion coefficient of GPC mixes reduced with increase in curing temperature and curing duration. The SEM analysis revealed that higher curing temperature and duration resulted in more homogenous microstructure that led to formation of more amount of reaction products and a higher strength. There was no systematic variation in the obtained results of EDS analysis with curing temperature and curing duration. The NMR analysis showed that extended high temperature curing enabled better dissolution of the glassy component thereby enhancing the overall geopolymerization reaction.

The XRD analysis indicated amorphous geopolymer structure, and there was no chemical reaction between the geopolymer binder and chloride ions. This indicated lower chloride diffusion resistance and chloride binding capacity of fly ash based geopolymer concrete.

2.5 Summary of literature review

From the review of literature, it is observed that different studies have been conducted by the researchers to evaluate the fresh and mechanical properties, and microstructure of fly ash based geopolymer concrete (GPC). In these studies, the researchers have evaluated the effect of mix parameters related to aluminosilicate source material, and alkaline solution on the fresh and mechanical properties. However, there are limited studies on the effect of different mix parameters on the microstructural variation in fly ash based geopolymer concrete. Further, in the literature, some studies have been carried out to evaluate different durability aspects of fly ash based geopolymer concrete. However, very few studies have been carried out to investigate the influence of different mix parameters such as molarity of NaOH solution, alkaline solution content, ratio of alkaline solution, particle size of fly ash, and fly ash content on long term durability aspects of fly ash based geopolymer concrete in general, with emphasis on chloride induced rebar corrosion. In these few studies, corrosion behaviour of steel reinforcement was investigated in fly ash based geopolymer concrete subjected to external chloride exposure. As stated in Chapter 1, among different durability problems, chloride induced corrosion of steel reinforcement is the most serious durability problem that is encountered in reinforced concrete structures. Further, the chloride ions can enter into concrete from external exposure environment, and internally through its ingredients. It is observed from the literature review that the reported research works on corrosion behaviour of steel reinforcement in fly ash based geopolymer concrete in the presence of internal chloride is very little. Further, very few research works have been conducted to evaluate the influence of internal chloride on fresh property, strength, and microstructure of fly ash based geopolymer concrete. As observed from the literature review, the influence of different mix parameters such as molarity of NaOH solution, alkaline solution content, ratio of alkaline solution, particle size of fly ash, and fly ash content on fresh and mechanical properties, microstructure, and durability assessment based on chloride induced corrosion of steel reinforcement in fly ash-based geopolymer concrete has not been investigated comprehensively. It is essential to understand the variations in the fresh and mechanical properties of fly ash based GPC with change in different mix parameters. Further, the variations in strength properties of GPC due to change in mix parameters need to be correlated with the changes in microstructure. In

addition, in case of exposure to aggressive environment, the behaviour of fly ash based geopolymer concrete needs to be evaluated by correlating the strength and durability characteristics with the microstructural variation.

Based on the research gap in the literature, the present research work was aimed to investigate the influence of molarity of NaOH solution, alkaline solution content, mass ratio of sodium silicate solution to sodium hydroxide solution (SS/SH ratio), particle size of fly ash, and fly ash content on fresh property, strength, microstructure, and durability of fly ash based geopolymer concrete in the presence of internal chloride. For this purpose, a comprehensive experimental investigation was conducted to evaluate the effect of above mix parameters on workability, compressive strength, microstructure, and corrosion of steel reinforcement in fly ash based GPC in the presence of internal chloride i.e., admixed with different concentrations of sodium chloride (NaCl). The strength development of GPC was evaluated by determining the compressive strength at different ages. The corrosion behaviour of rebar in fly ash based GPC admixed with different concentrations of NaCl was evaluated by measuring the corrosion potential, and corrosion current density at different ages. The extent of chloride binding in fly ash based geopolymer concrete was evaluated by determining the free chloride and total chloride contents at different ages, and also near rebar level at later age in GPC mixes. Further, to evaluate the microstructural variations with change in mix parameters in fly ash based geopolymer concrete at different ages and near rebar level in the presence of sodium chloride, XRD, FESEM and FTIR analyses was performed.

2.6 Objectives of present research work

Based on the research gap in the literature, the objectives of present research study are formulated as follows:

i) To investigate the effect of fly ash content and its particle size, concentration of sodium hydroxide solution, alkaline solution content, and mass ratio of sodium silicate solution to sodium hydroxide solution on workability and compressive strength of fly ash based geopolymer concrete (GPC).

ii) To evaluate the effect of above parameters on variations in microstructure of fly ash based GPC through by X-ray diffraction (XRD), Field emission scanning electron microscope (FESEM), and Attenuated total reflectance - Fourier transform infrared spectroscopy (ATR-FTIR) analysis.

iii) To evaluate the durability performance of fly ash based geopolymer concrete in the presence of internal chloride through half-cell potential and linear polarization resistance (LPR) measurements.

iv) To study the variation in chloride content, and microstructure at rebar level in fly ash based geopolymer concrete.

Chapter 3

Experimental Program

3.1 General

This chapter describes about the properties of materials, and mix proportion used to formulate the fly ash based geopolymer concrete (GPC) mixes. In addition, the preparation of test specimens, and different tests and microstructure analysis conducted on fly ash based GPC mixes are described in this chapter.

3.2 Materials used for preparation of fly ash based geopolymer concrete mixes

3.2.1 Fly ash

In this research work, low calcium (Class-F) fly ash [30] was used as the source material for preparation of geopolymer concrete (GPC) mixes. The oxide composition of fly ash was determined using X-ray Florescence (XRF) analysis and is presented in Table 3.1. The specific gravity of fly ash was 2.15. In order to investigate the effect of particle size of fly ash on properties of GPC, the same fly ash passing through 150 µm sieve, and 300 µm sieve were used separately for preparation of geopolymer concrete mixes.

Table 3.1: Oxide composition of fly ash

Oxide (weight %)	Fly ash
CaO	2.69
SiO_2	48.96
Al_2O_3	24.48
Fe_2O_3	4.59
MgO	0.81
K_2O	1.03
Na_2O	0.03
Loss on ignition	0.43

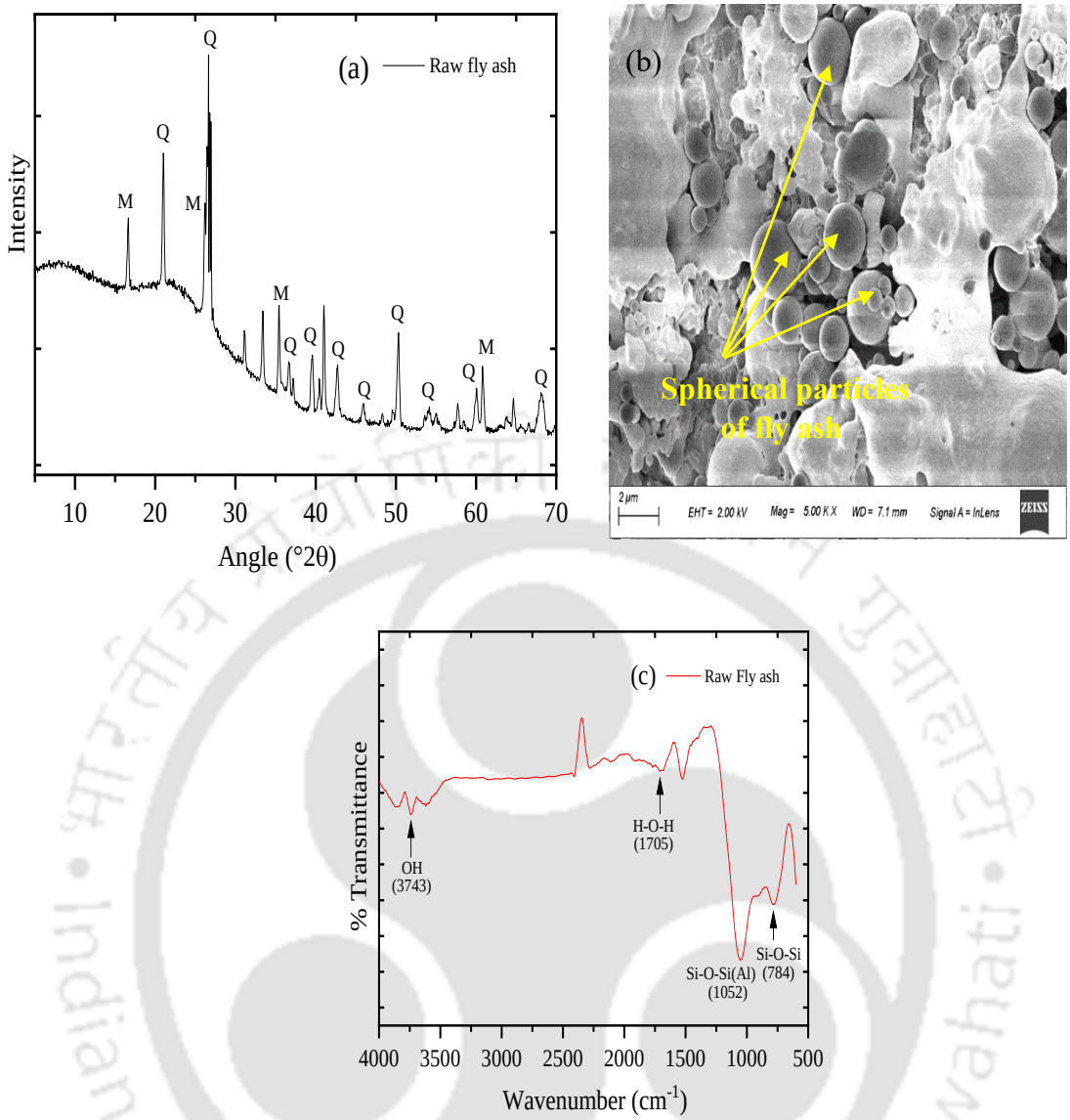

Fig. 3.1: (a) XRD pattern, (b) FESEM image and (c) FTIR spectra of raw fly ash

Note: XRD – X-ray diffraction, FESEM – Field emission scanning electron microscope and FTIR – Fourier transform infrared spectroscopy

The particle size of fly ash was determined by particle size analyser (Make: Malvern Instrument, Model: Mastersizer 2000). The measured values of particle size (d_{50}) of fly ash passing through sieve size of 150 µm and 300 µm were 23.98 µm and 32.18 µm respectively. The XRD pattern, FESEM image, and FTIR spectra of raw fly ash are shown in Fig. 3.1(a), Fig. 3.1(b) and Fig. 3.1(c) respectively. From Fig. 3.1 (a), the crystalline phases such as quartz (Q) and mullite (M) were identified in the XRD pattern of raw fly ash. The morphology of raw fly ash indicated spherical particles with smooth surface as observed from Fig. 3.1(b). The FTIR spectra shown in Fig. 3.1(c) indicated the major peak at 1052 cm^{-1}, which is associated with the asymmetric stretching vibration of Si–O–Si(Al) bond.

3.2.2 Aggregates

Locally available river sand was used as fine aggregate, and combination of coarse aggregates of size 20 mm MSA (maximum size of aggregate) and 10 mm MSA were used in the preparation of GPC mixes.

3.2.2.1 Sieve analysis, and specific gravity of aggregates

According to the guidelines given in IS: 2386-1963 (Part I) [82], the sieve analysis of fine aggregate and coarse aggregates were carried out. The particle size distribution curve of fine aggregate is shown in Fig. 3.2. The obtained cumulative percentage passing values indicated that the sand is conforming to grading zone-II as per IS: 383-2016 [83]. The obtained value of fineness modulus of sand was 2.51. The particle size distribution curves of 10 mm maximum size and 20 mm maximum size coarse aggregates are also shown in Fig. 3.2.

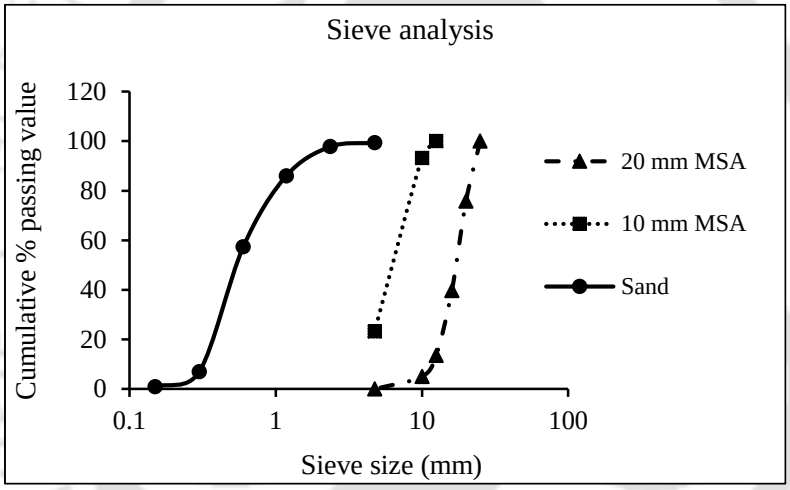

Fig. 3.2: Particle size distribution curves of fine aggregate (sand), 10 mm maximum size and 20 mm maximum size coarse aggregates

The specific gravity of sand and coarse aggregates were determined as per the guidelines of IS: 2386-1963 (Part 3) [84]. The obtained values of specific gravity of sand, 10 mm maximum size, and 20 mm maximum size coarse aggregate were 2.62, 2.66 and 2.68 respectively.

3.2.3 Alkaline solution

For the preparation of GPC mixes, combination of sodium hydroxide (NaOH) solution and sodium silicate (Na_2SiO_3) solution was used as the alkaline solution. Commercially available sodium silicate solution was used in this study. The weight percentage of different components of sodium silicate solution were Na_2O: 7.5% to 8.5% and SiO_2: 25% to 28% (as supplied by the manufacturer). The sodium hydroxide pellets and laboratory tap water were used for

preparing the sodium hydroxide (NaOH) solution of different molarity such as 8 M, 10 M, 12 M, 14 M and 16 M.

3.2.4 Admixed chloride salt

As observed from the research works reported in the literature, for chloride exposure, sodium chloride is mostly used as the source of chloride ions. In addition, sodium chloride is dominantly present in seawater as compared to other salts. Based on these points, in the present study, sodium chloride (NaCl) was used as the source of chloride ions for internal chloride exposure. In order to evaluate the effect of internal chloride on workability, compressive strength, microstructure, and corrosion of steel reinforcement, sodium chloride of different concentrations such as 0%, 1.5%, 3% and 4.5% were added to the alkaline solution at the time of preparation of GPC mixes.

3.3 Steel reinforcement

To evaluate the corrosion behaviour of rebar in geopolymer concrete (GPC), prismatic reinforced GPC specimens with a centrally embedded steel bar were prepared. For this purpose, 12 mm diameter Tempcore TMT (Thermomechanically treated) steel bar was used as the steel reinforcement.

3.4 Mix proportioning of fly ash based geopolymer concrete

In the present research work, the mix proportion of geopolymer concrete (GPC) mixes was finalized based on the results of trial tests carried out to evaluate the workability and compressive strength of GPC mixes. The fly ash contents of 425 kg/m^3 and 450 kg/m^3, and alkaline solution contents of 190 kg/m^3 and 210 kg/m^3 were used in the preparation of GPC mixes. The mass ratio of sodium silicate solution to sodium hydroxide solution of 1.5 and 1.75 were used in the GPC mixes. The proportion of 20 mm MSA and 10 mm MSA coarse aggregates was 62% and 38% respectively by mass of total coarse aggregate content. The proportion of fine aggregate was 35% by mass of total aggregate content. The detailed mix proportions of fly ash based GPC mixes are shown in Table 3.2 and Table 3.3.

Table 3.2: Mix proportion of fly ash based GPC mixes with alkaline solution content of 210 kg/m^3

Fly ash (kg/m^3)	Molarity of NaOH solution	Alkaline solution (kg/m^3)	SS*/SH** ratio	Coarse aggregate (kg/m^3)	Fine aggregate (kg/m^3)
425 (fly ash passing through 150 µm sieve)	10 M and 14 M	210	1.75	1155	622
425 (fly ash passing through 300 µm sieve)	8 M, 10 M, 12 M, 14 M and 16 M				
450 (fly ash passing through 150 µm sieve)	10 M and 14 M				
450 (fly ash passing through 300 µm sieve)	10 M and 14 M				

Note: *SS: Sodium silicate solution; **SH: Sodium hydroxide solution

Table 3.3: Mix proportion of fly ash based GPC mixes with different alkaline solution contents and SS/SH ratios

Fly ash (kg/m^3)	Molarity of NaOH solution	Alkaline solution (kg/m^3)	SS/SH ratio	Coarse aggregate (kg/m^3)	Fine aggregate (kg/m^3)
425 (fly ash passing through 150 µm sieve)	10 M and 14 M	190	1.75	1155	622
		210	1.5		

3.5 Preparation of alkaline solution for geopolymer concrete mixtures

As stated earlier, the combination of sodium hydroxide solution and sodium silicate solution was used as the alkaline solution. Sodium hydroxide pellets of required quantity were dissolved in laboratory tap water to prepare the required molar concentration of NaOH solution 48 hours prior to the casting of GPC mixes. After 24 hours of preparation of sodium hydroxide solution, sodium silicate solution was added to the sodium hydroxide solution.

3.6 Preparation of geopolymer concrete mixtures

The mixing sequence of geopolymer concrete mixture included dry mixing followed by wet mixing of the ingredients. Initially, fly ash and aggregates (fine and coarse aggregates) were dry mixed in the laboratory drum mixer for 3 minutes and then alkaline solution was introduced

into the mixer wherein the wet mixing was continued for another 4 minutes to obtain the fresh geopolymer concrete mixture. As stated earlier, sodium chloride of different concentrations such as 1.5%, 3% and 4.5% by mass of geopolymer solids (mass of fly ash plus mass of NaOH solids and Na_2SiO_3 solids) were added to the alkaline solution during the time of preparation of chloride admixed GPC mixes. The fresh GPC mixtures were prepared without using any extra water or superplasticizer. Immediately after preparation, the fresh GPC mixture was tested for slump value to check the workability. After slump test, the test specimens were prepared.

3.7 Casting of GPC test specimens

From geopolymer concrete mixtures, cube specimens of size 150 mm × 150 mm × 150 mm for compressive strength test, and prismatic specimens of size 72 mm × 72 mm × 300 mm with a centrally embedded steel bar for half-cell potential and linear polarization resistance (LPR) measurements were prepared. Tempcore TMT steel bar of size 12 mm diameter and 330 mm length was used as the steel reinforcement in prismatic specimens. Before embedding into the prismatic specimen, the steel bar was cleaned with wire brush to remove any surface scale. In order to prevent crevice corrosion, insulating tape followed by epoxy coating was applied over the reinforcing steel bar at the location where there is a discontinuity of the steel bar with surrounding concrete. The cover depth of steel bar was fixed at 30 mm both at bottom and on all sides of the prismatic reinforced specimen. The exposed length of steel bar in the prismatic specimen was 160 mm. The schematic diagram of steel bar and prismatic reinforced geopolymer concrete specimen are shown in Fig. 3.3 and Fig. 3.4 respectively. For preparation of cube specimens, freshly prepared geopolymer concrete mixture was placed into cube moulds in three layers, and each layer was subjected to 25 manual strokes by a tamping rod and then each layer was vibrated for about 15 seconds on a vibrating table. For prismatic specimens, the concrete was placed into the moulds in 2 layers and each layer was vibrated for about 15 seconds on the vibrating table. The photographs of freshly prepared cube and prismatic specimens are shown in Fig. 3.5. From each GPC mixture, three replicate cube specimens were prepared for compressive strength test at a given age. Similarly, three replicate prismatic specimens were prepared from each GPC mixture for corrosion measurement at different ages.

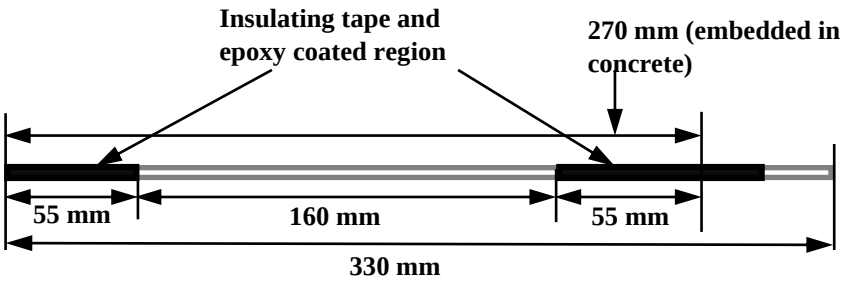

Fig. 3.3: Schematic diagram of steel bar of diameter 12 mm

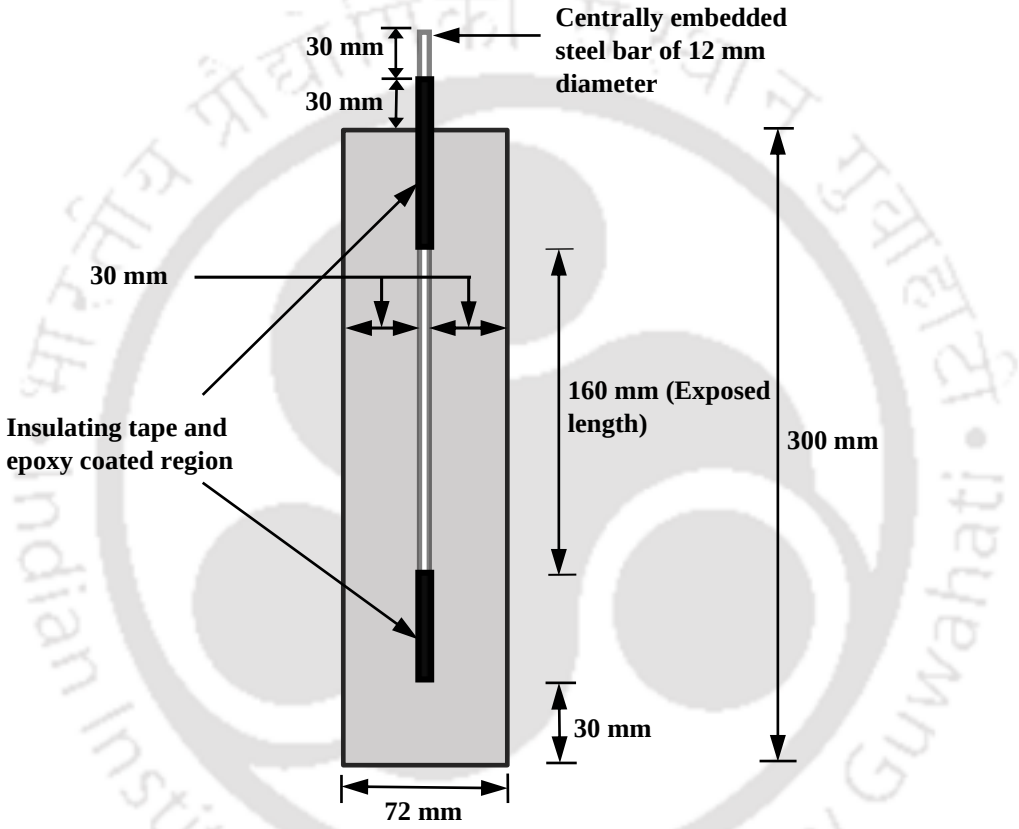

Fig. 3.4: Schematic diagram of prismatic reinforced geopolymer concrete (GPC) specimen of size 72 mm × 72 mm × 300 mm

After preparation, all the GPC cube and prismatic specimens (along with the moulds) were kept in ambient laboratory condition for 48 hours. After the rest period of 48 hours, all the specimens (inside the moulds) were heat cured in the oven at a temperature of 80 °C for another 48 hours. After oven curing, the cube and prismatic specimens were taken out from the moulds, and were kept under ambient laboratory condition till the age of testing. The photographs of hardened cube, and prismatic specimens are shown in Fig. 3.6.

(a) (b)

Fig. 3.5: Compaction of geopolymer concrete for (a) Cube specimens (b) Prismatic reinforced specimens

(a) (b)

Fig. 3.6: Hardened GPC (a) cube specimens and (b) prismatic reinforced specimens

3.8 Details of test specimens prepared from geopolymer concrete mixtures

Based on different combinations of molarity of NaOH solution, alkaline solution content, SS/SH ratio, particle size of fly ash and fly ash content, the cube and prismatic specimens were prepared from GPC mixes for different testing ages and the number of test specimens prepared are mentioned in the following tables. The influence of a mix parameter on the properties of GPC was evaluated by varying its levels at a given level of other mix parameters. i) Table 3.4: in order to evaluate the effect of molarity of NaOH solution on different properties of geopolymer concrete in the presence of chloride ions, the GPC mixes were prepared with

different molarity of NaOH solution and admixed with different concentrations of NaCl for a given alkaline solution content, SS/SH ratio, particle size of fly ash and fly ash content. Thus, variations in level of alkaline solution content, SS/SH ratio, particle size of fly ash and fly ash content were not considered. Accordingly, considering the replicates and testing age, the required number of cube and prismatic specimens were prepared from GPC mixes as shown in Table 3.4. ii) Table 3.5 and Table 3.6: for evaluating the influence of alkaline solution content on the properties of GPC, the specimens were prepared with different alkaline solution contents at a given SS/SH ratio, particle size of fly ash, fly ash content and NaCl concentration. Thus, variations in level of these parameters were not considered, although two different molarity of NaOH solution i.e., 10 M and 14 M were used in the preparation of GPC mixes as shown in Table 3.5 and Table 3.6. (iii) Table 3.6 and Table 3.7: for evaluating the effect of SS/SH ratio, the specimens were prepared with different values of SS/SH ratio for a given alkaline solution content, particle size of fly ash, fly ash content and NaCl concentration to analyse the changes in different properties of GPC mixes. iv) Table 3.4 and Table 3.6: for evaluating the effect of particle size of fly ash on properties of GPC, the cube and prismatic specimens were prepared with fly ash of different particle sizes for a given alkaline solution content, SS/SH ratio, NaCl concentration and fly ash content (425 kg/m^3). Similarly, for higher fly ash content i.e., 450 kg/m^3, the cube and prismatic specimens (Table 3.8 and Table 3.9) were prepared with fly ash of different particle sizes at a given alkaline solution content, and SS/SH ratio to evaluate the effect of particle size on the properties of GPC. Further, to analyse the effect of chloride ions on the properties of GPC, NaCl of different concentrations (shown in Table 3.8 and Table 3.9) were admixed with GPC mixes. v) similarly, to evaluate the effect of fly ash content on different properties, the GPC mixes were prepared with different fly ash contents by keeping the level of other mix parameters constant (Table 3.6 and Table 3.8; and Table 3.4 and 3.9).

Table 3.4: Number of GPC test specimens made from NaOH solution of different molarity for alkaline solution content of 210 kg/m^3, SS/SH ratio of 1.75, fly ash passing through 300 μm sieve, and fly ash content of 425 kg/m^3, and admixed with different concentrations of NaCl

Molarity of NaOH solution	Fly ash content (kg/m^3)	Admixed sodium chloride (% by mass of geopolymer solids)	Number of cube specimens	Number of prismatic specimens
8 M	425	0	9*	3**
		1.5	9	3
		3	9	3
		4.5	9	3
10 M		0	9	3
		1.5	9	3
		3	9	3
		4.5	9	3
12 M		0	9	3
		1.5	9	3
		3	9	3
		4.5	9	3
14 M		0	9	3
		1.5	9	3
		3	9	3
		4.5	9	3
16 M		0	9	3
		1.5	9	3
		3	9	3
		4.5	9	3

9*: 3 replicate cube specimens each for compressive strength at the age of 7, 28, and 90 days
3**: 3 replicate prismatic specimens for corrosion measurement at different ages

Table 3.5: Number of GPC test specimens made from alkaline solution content of 190 kg/m^3 for SS/SH ratio of 1.75, fly ash passing through 150 μm sieve and fly ash content of 425 kg/m^3 and admixed NaCl concentrations of 0% and 3%

Molarity of NaOH solution	Alkaline solution content (kg/m^3)	Admixed sodium chloride (% by mass of geopolymer solids)	Number of cube specimens	Number of prismatic specimens
10 M	190	0	6$^{\#}$	3
		3	6	3
14 M		0	6	3
		3	6	3

6$^{\#}$: 3 replicate cube specimens each for compressive strength at the age of 7, and 28 days

Table 3.6: Number of GPC test specimens made from alkaline solution content of 210 kg/m^3 for SS/SH ratio of 1.75, fly ash passing through 150 μm sieve and fly ash content of 425 kg/m^3 and admixed NaCl concentrations of 0% and 3%

Molarity of NaOH solution	Alkaline solution content (kg/m^3)	Admixed sodium chloride (% by mass of geopolymer solids)	Number of cube specimens	Number of prismatic specimens
10 M	210	0	6	3
		3	6	3
14 M		0	6	3
		3	6	3

Table 3.7: Number of GPC test specimens made from SS/SH ratio of 1.5 for alkaline solution content of 210 kg/m^3, fly ash passing through 150 μm sieve and fly ash content of 425 kg/m^3 and admixed NaCl concentrations of 0% and 3%

Molarity of NaOH solution	SS/SH ratio	Admixed sodium chloride (% by mass of geopolymer solids)	Number of cube specimens	Number of prismatic specimens
10 M	1.5	0	6	3
		3	6	3
14 M		0	6	3
		3	6	3

Table 3.8: Number of GPC test specimens made from fly ash passing through 150 μm sieve for alkaline solution content of 210 kg/m^3, SS/SH ratio of 1.75, and fly ash content of 450 kg/m^3 and admixed with different concentrations of NaCl

Molarity of NaOH solution	Fly ash passing through sieve size	Admixed sodium chloride (% by mass of geopolymer solids)	Number of cube specimens	Number of prismatic specimens
10 M	150 μm	0	9	3
		1.5	9	3
		3	9	3
		4.5	9	3
14 M		0	9	3
		1.5	9	3
		3	9	3
		4.5	9	3

Table 3.9: Number of GPC test specimens made from fly ash passing through 300 μm sieve for alkaline solution content of 210 kg/m^3, SS/SH ratio of 1.75, and fly ash content of 450 kg/m^3 and admixed with different concentrations of NaCl

Molarity of NaOH solution	Fly ash passing through sieve size	Admixed sodium chloride (% by mass of geopolymer solids)	Number of cube specimens	Number of prismatic specimens
10 M	300 μm	0	9	3
		1.5	9	3
		3	9	3
		4.5	9	3
14 M		0	9	3
		1.5	9	3
		3	9	3
		4.5	9	3

3.9 Tests for fresh and hardened properties of fly ash based GPC

3.9.1 Workability test

As mentioned earlier in Section of 3.6, the slump test was conducted to evaluate the consistency of fresh GPC mixtures immediately after its preparation. The test for measuring slump of all GPC mixtures was conducted by using slump cone with base internal diameter 200 mm, top internal diameter 100 mm and height 300 mm. The procedure mentioned in IS 1199 (Part 2): 2018 [85] was followed for conducting the slump test on fresh geopolymer concrete mixes.

3.9.2 Compressive strength test

The measurement of compressive strength of GPC cube specimens of size 150 mm was carried out at the ambient curing age of 7 days, 28 days and 90 days from the date of casting. The compressive strength measurement was performed on the cube specimens as per IS 516 (Part 1/Sec 1): 2021 [86]. The testing of GPC cube specimens at the age of 7 days for compressive strength included a rest period of 48 hours at room temperature in the laboratory after preparation of the specimens followed by heat curing at 80 °C temperature for another 48 hours, and after that keeping the specimens under room temperature in the laboratory for remaining 3 days till testing. Similarly, testing of the GPC cube specimens at the age of 28 days and 90 days for compressive strength included the same rest period and heat curing period as that for 7 days testing with the difference of keeping the specimens under room temperature in the laboratory for remaining 24 days and 86 days after heat curing respectively. The GPC cube specimens were tested in a 2000 kN capacity compression testing machine. At a given testing age, three replicate cube specimens were tested for each of the GPC mixes.

3.10 Microstructure analysis

In this research work, the microstructure of GPC mixes was analyzed by X-ray diffraction (XRD), Field emission scanning electron microscope (FESEM) and Fourier transform infrared spectroscopy - Attenuated total reflectance (FTIR-ATR) analyses. After completion of compressive strength test at different ages, the broken GPC cube specimens were further crushed in a pulverizer. The crushed material was then passed through 75 µm sieve. The powder samples passing through the sieve were stored in air tight plastic containers (Fig. 3.7).

Fig. 3.7: GPC powder samples obtained from cube specimens

Similarly, after completion of electrochemical measurements at the age of 600 days, the GPC powder samples from near the rebar level of prismatic reinforced GPC specimens were collected by drilling. To collect the GPC powder samples, the prismatic specimens were drilled on four longitudinal sides at different depth intervals i.e., 0 - 6 mm, 6 - 12 mm, 12 - 18 mm, 18 - 24 mm and 24 - 30 mm from the surface of the prismatic specimens. In order to obtain the GPC powder sample from a given depth interval, the drilled powder samples obtained from that depth interval from all the four longitudinal sides were mixed together. The powder sample obtained from the depth interval of 24 - 30 mm from the surface of the specimen represents the concrete near the steel reinforcement in the prismatic reinforced GPC specimen. The collected powder samples from near the rebar level were sieved through 75 µm sieve and the sieved powder samples were stored in air tight plastic containers (Fig. 3.8). The microstructure analysis was performed on the above obtained geopolymer concrete powder samples.

(a) (b)

Fig. 3.8: (a) Drilled prismatic reinforced GPC specimens and (b) GPC powder samples obtained from near the rebar level of prismatic specimens after drilling

3.10.1 X-ray diffraction (XRD) analysis

The phase composition of geopolymer concrete was analyzed through X-ray diffraction (XRD) analysis. The diffraction patterns of the GPC powder samples were recorded on a X-ray diffractometer (Model: Rigaku SmartLab 9 kW) with CuKα radiation (λ = 1.5405 Å). The GPC powder sample was scanned in the range of 5° to 70° 2θ with step size of 0.05° 2θ. After collection of XRD patterns, the PDF2 reference library (ICDD: International Centre for Diffraction Data) and PANalytical X'Pert HighScore Plus software were used for the phase identification analysis.

3.10.2 Field emission scanning electron microscope (FESEM) analysis

The field emission scanning electron microscope (FESEM) analysis was performed to analyze the morphology of geopolymer concrete (GPC). The analysis was performed on GPC powder samples using the FESEM instrument (make: Zeiss, model: Gemini). For the analysis, the GPC powder sample was mounted on an aluminum stub along with carbon tape, and sputtering method was used for coating it with a thin gold layer. The surface morphology of geopolymer concrete powder sample was observed using in-lens mode.

3.10.3 Fourier transform infrared (FTIR) spectroscopy - Attenuated total reflectance (ATR) analysis

Fourier transform infrared spectroscopy (FTIR) analysis was carried out to study the functional groups associated with the compounds formed in geopolymer concrete. The FTIR analysis by

attenuated total reflectance (ATR) method was performed using the FTIR instrument (make: Shimadzu, model: IRAffinity-1). The GPC powder sample was placed on the ATR crystal and the functional groups were analyzed in the wavenumber range of 4000 cm^{-1} – 600 cm^{-1} by 32 scans at a resolution of 4 cm^{-1}.

3.11 Measurement of chloride content of geopolymer concrete

The free chloride and total chloride contents of geopolymer concrete (GPC) were determined by potentiometric titration using an automatic titrator (make: Metrohm, model: 848 Titrino Plus) (Fig. 3.9).

Fig. 3.9: Test setup for potentiometric titration using automatic titrator for determination of free and total chloride content

The geopolymer concrete powder samples obtained from the cube and prismatic specimens (discussed in Section 3.10) were used for determining the free chloride and total chloride concentrations. For determining free chloride content, three grams of GPC powder sample was taken in a 100 ml beaker and 60 ml of distilled water was added to it. The powder solution was then mixed thoroughly and heated gently on a hot plate with magnetic stirrer. After that, the powder solution was cooled to room temperature and was then titrated against 0.1 M $AgNO_3$ solution in the automatic titrator. For determining total chloride content, 60 ml of concentrated nitric acid (4 N) was added with three grams of GPC powder sample in the beaker. The powder solution was then thoroughly mixed by the magnetic stirrer without heating. The total chloride

content was then determined by titrating against 0.1 M $AgNO_3$ solution in the automatic titrator. The free chloride and total chloride contents were expressed as percentage by weight of geopolymer concrete (GPC).

3.12 Electrochemical measurements

To evaluate the durability property of geopolymer concrete, half-cell potential and linear polarization resistance (LPR) measurements were carried out on the prismatic reinforced geopolymer concrete specimens at the ages of 60, 180, 360, and 600 days from the day of casting. The electrode system used in this study for electrochemical measurements consists of the embedded steel bar in the prismatic specimen as working electrode, saturated calomel electrode as reference electrode, and a pair of stainless steel plates as auxiliary electrode. The schematic diagram of test setup for half-cell potential and linear polarization resistance measurements is shown in Fig. 3.10. During corrosion test, the prismatic specimen was immersed partially in the test solution up to a height of 245 mm in the container. The test solution was prepared by adding sodium chloride in water at the same concentration (%) that was added during preparation of GPC mixes. During testing on control specimens (i.e. without NaCl), normal water was used as the test solution. The embedded steel bar (working electrode) in the prismatic specimen, a pair of stainless steel plates (auxiliary electrode), and reference electrode (saturated calomel electrode) were connected to the potentiostat (make: ACM, model: Gill AC, serial no. 1542-sequencer). The corrosion potential of steel bar embedded in the prismatic specimen was measured with reference to saturated calomel electrode (SCE). In the LPR test, the embedded steel bar was polarized to ± 20 mV from the equilibrium potential at a scan rate of 6 mV/min. The corrosion current density of steel reinforcement was calculated using the Stern-Geary equation [87], and is as follows;

$$I_{corr} = \frac{B}{R_p} \quad \text{---------- (1)}$$

Where, 'I_{corr}' is the corrosion current density, 'R_p' is the polarization resistance of steel reinforcement and 'B' is the Stern-Geary constant. The expression for Stern-Geary constant 'B' is given by:

$$B = \frac{\beta_a \times \beta_c}{2.3\,(\beta_a + \beta_c)} \quad \text{---------- (2)}$$

Where, β_a and β_c are anodic and cathodic Tafel constants respectively. Generally, the values of B equal to 52 mV for steel in passive condition and 26 mV for steel in active condition are used [88]. In this research work, the value of 'B' was taken as 26 mV, considering the

steel reinforcement in active condition [87]. The photograph of the test setup is shown in Fig. 3.11.

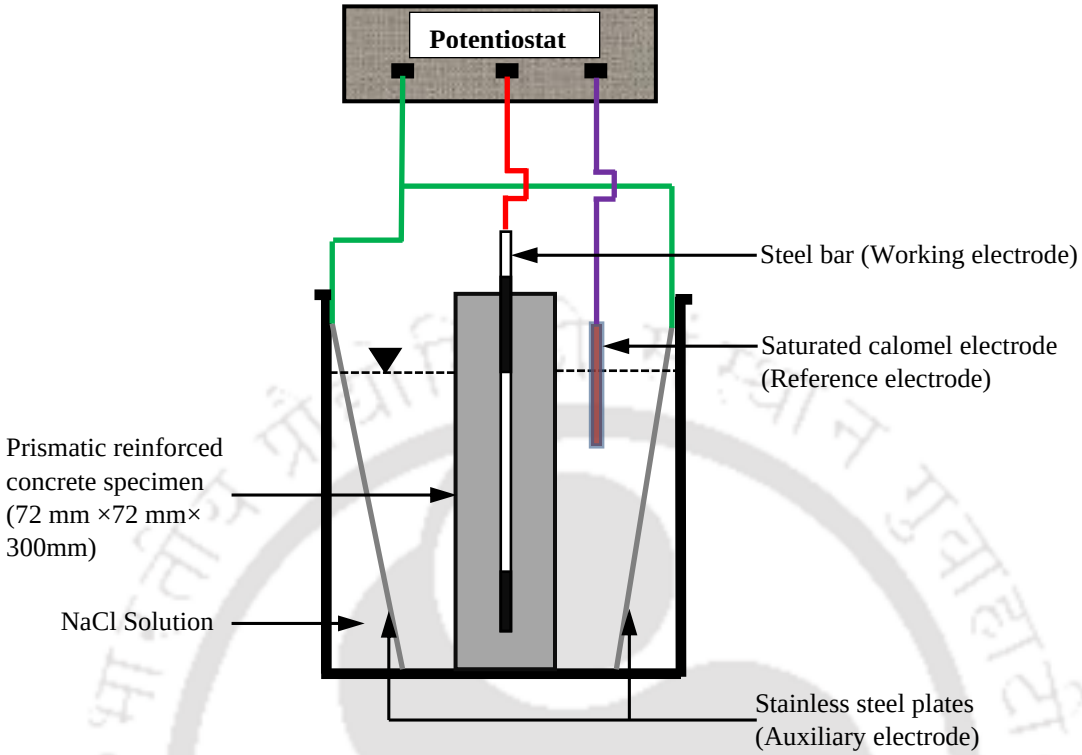

Fig. 3.10: Schematic diagram for half-cell potential and linear polarization resistance measurements

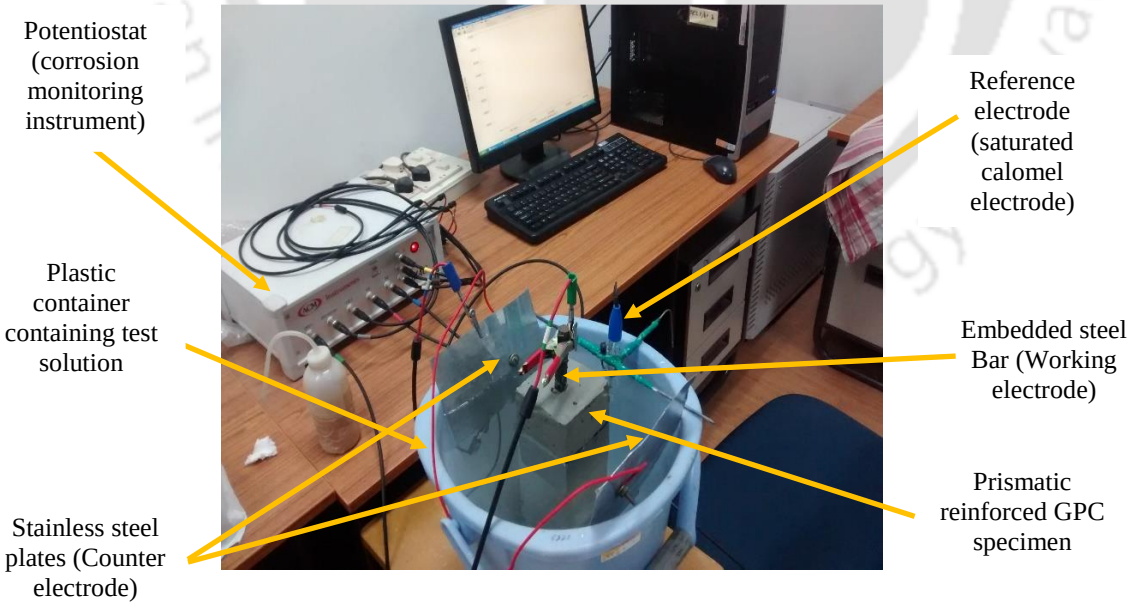

Fig. 3.11: Photograph of test setup for half-cell potential and linear polarization resistance measurements

3.13 Summary

In the present research work, the fly ash based geopolymer concrete (GPC) mixes were prepared from the combination of different mix parameters such as molarity of NaOH solution, alkaline solution content, SS/SH ratio, particle size of fly ash, and fly ash content. For internal chloride exposure, sodium chloride of different concentrations was admixed in GPC mixes during the time of preparation. Cube specimens of size 150 mm for compressive strength test, and prismatic specimens of size 72 mm × 72 mm × 300 mm with a centrally embedded reinforcing steel bar for half-cell potential and linear polarization resistance (LPR) measurements were prepared from GPC mixes with different combinations of mix parameters. Slump test on fresh GPC mixes, and compressive strength test on cube specimens were conducted at different ages. To evaluate the corrosion behaviour of rebar in the presence of chloride ions, half-cell potential measurement, and linear polarization resistance measurement for corrosion current density were performed on fly ash based GPC prismatic specimens at different ages. To examine the microstructure of GPC, XRD, FESEM and FTIR analyses were carried out on the geopolymer concrete powder samples obtained from cube specimens after completion of compressive strength test at different ages, and from prismatic specimens after completion of corrosion measurements at later age. Further, the free chloride and total chloride content of GPC mixes were determined from the powder samples obtained from cube and prismatic specimens.

Chapter 4

Influence of Mix Parameters on Consistency, Compressive Strength and Chloride Content of Fly ash based Geopolymer Concrete

4.1 General

In this chapter, the results obtained from slump test (consistency), compressive strength, and chloride content of fly ash based geopolymer concrete (GPC) are presented. The effect of molarity of sodium hydroxide (NaOH) solution, alkaline solution content, ratio of sodium silicate (Na_2SiO_3) solution to sodium hydroxide solution content, particle size of fly ash, fly ash content and admixed sodium chloride (NaCl) on variations in slump value, compressive strength, and free, total and bound chloride contents of fly ash based geopolymer concrete are analysed and discussed in this chapter.

4.2 Consistency of fly ash based geopolymer concrete

4.2.1 Effect of molarity of sodium hydroxide solution

The obtained slump values of geopolymer concrete (GPC) mixes made from sodium hydroxide (NaOH) solution of different molarity i.e., 8 M, 10 M, 12 M, 14 M, and 16 M at fly ash content of 425 kg/m^3 and admixed with different concentrations of sodium chloride (NaCl) are shown in Fig. 4.1. The slump values shown in this figure correspond to the GPC mixes made with fly ash passing through 300 μm sieve, alkaline solution content of 210 kg/m^3, and sodium silicate solution to sodium hydroxide solution ratio of 1.75.

From Fig. 4.1, it is observed that the slump value of GPC mixes decreased with increase in concentration of sodium hydroxide (NaOH) solution from 8 M to 16 M. This is attributed to the increase in solids content of NaOH solution at higher molarity for a given alkaline solution content that increased the viscosity of the alkaline solution thereby leading to decrease in consistency of the GPC mixes. However, the slump value of GPC mixes increased with increase in admixed sodium chloride (NaCl) concentration from 0% to 4.5%. The increase in consistency of GPC mixes with increase in concentration of admixed sodium chloride (NaCl) may be ascribed to the improvement in particle mobility in the mix possibly as a result of alteration in the viscosity of the GPC mix due to presence of chloride ions.

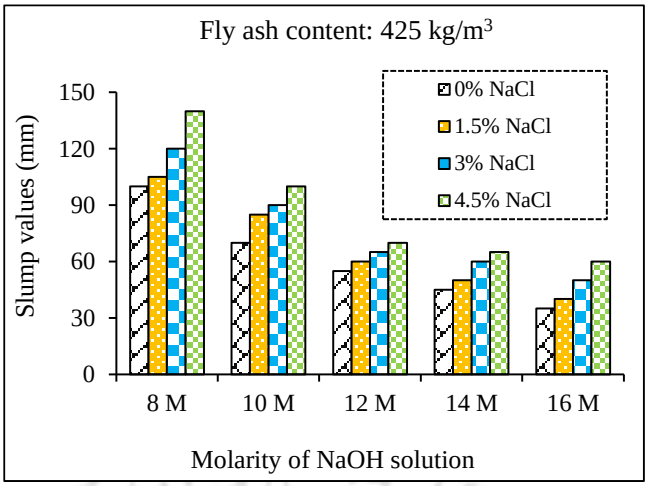

Fig. 4.1: Slump values of geopolymer concrete mixes made from NaOH solution of different molarity at fly ash content of 425 kg/m^3 and admixed with sodium chloride (NaCl) of different concentrations

4.2.2 Effect of alkaline solution content

The results of slump values of geopolymer concrete mixes made from alkaline solution of different contents i.e., 190 kg/m^3 and 210 kg/m^3 for admixed NaCl concentrations of 0% and 3% are shown in Fig. 4.2. The slump values shown in Fig. 4.2 correspond to the GPC mixes made with fly ash passing through 150 μm sieve, fly ash content of 425 kg/m^3, and sodium silicate solution to sodium hydroxide solution ratio of 1.75.

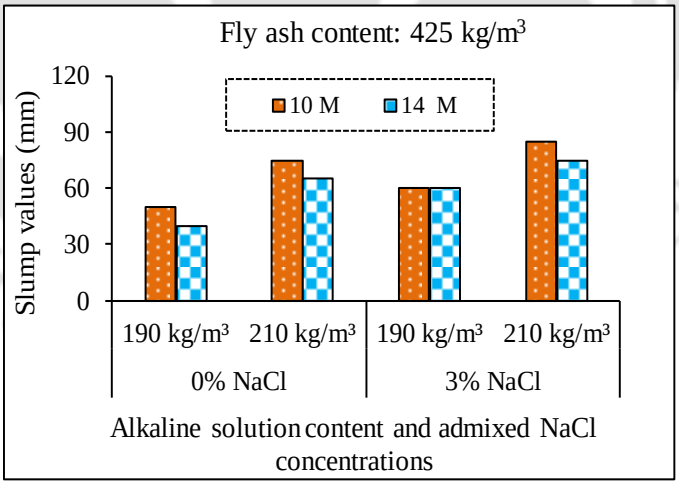

Fig. 4.2: Slump values of geopolymer concrete mixes made from alkaline solution content of 190 kg/m^3 and 210 kg/m^3

From Fig. 4.2, it is observed that the slump value of geopolymer concrete mixes increased with increase in alkaline solution content. This may be attributed to an increase in liquid content in the mix that led to higher interparticle lubrication thereby increasing the consistency of the GPC mixes. Further, the slump values of GPC mixes decreased with increase in molarity of NaOH solution and increased in the presence of chloride ions irrespective of alkaline solution

content as observed from Fig. 4.2. The reasons for the variation in the slump value of GPC mixes with molarity of NaOH solution and NaCl concentration are already stated in Section 4.2.1.

4.2.3 Effect of mass ratio of sodium silicate solution to sodium hydroxide solution

The obtained slump values of geopolymer concrete (GPC) mixes made with sodium silicate solution to sodium hydroxide solution ratio of different values i.e., 1.5 and 1.75 are shown in Fig. 4.3. The mass ratio of sodium silicate (SS) solution to sodium hydroxide (SH) solution is referred here as ratio of alkaline solution (SS/SH ratio). The slump values shown in Fig. 4.3 correspond to the GPC mixes made with fly ash content of 425 kg/m^3, fly ash passing through 150 μm sieve and alkaline solution content of 210 kg/m^3.

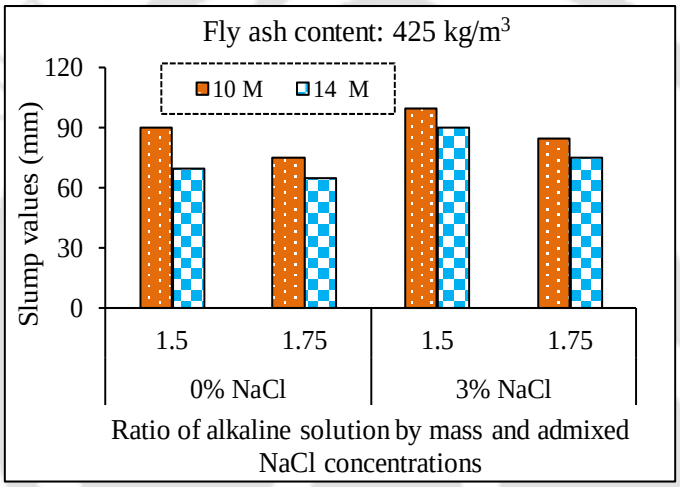

Fig. 4.3: Slump values of geopolymer concrete mixes made with ratio of alkaline solution of 1.5 and 1.75

The results shown in Fig. 4.3 indicate that the slump value of GPC mixes decreased with increase in alkaline solution ratio irrespective of molarity of NaOH solution and presence of sodium chloride in the mix. This may be attributed to the effect of more amount of sodium silicate solution at higher alkaline solution ratio for a given amount of alkaline solution that led to comparatively higher viscosity of the solution thereby decreasing the consistency of the GPC mix. In addition, the slump values of GPC mixes increased in the presence of chloride ions and decreased with increase in molarity of NaOH solution for both values of ratio of alkaline solution as observed from Fig. 4.3.

4.2.4 Effect of particle size of fly ash

The results of slump values of geopolymer concrete mixes made with fly ash passing through 150 μm sieve, and that passing through 300 μm sieve are shown in Fig. 4.4 and Fig. 4.5 for fly

ash contents of 425 kg/m^3 and 450 kg/m^3 respectively. The slump values depicted in Fig. 4.4 and Fig. 4.5 correspond to the GPC mixes made with alkaline solution content of 210 kg/m^3, and ratio of alkaline solution of 1.75.

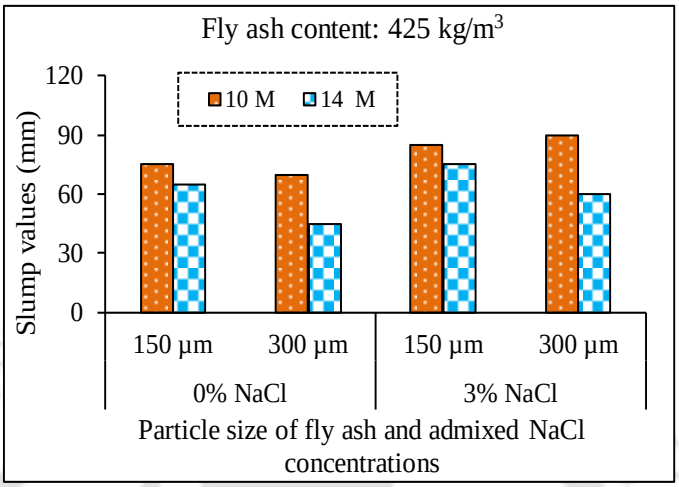

Fig. 4.4: Slump values of geopolymer concrete (GPC) mixes made with fly ash passing through 150 µm sieve, and 300 µm sieve at fly ash content of 425 kg/m^3

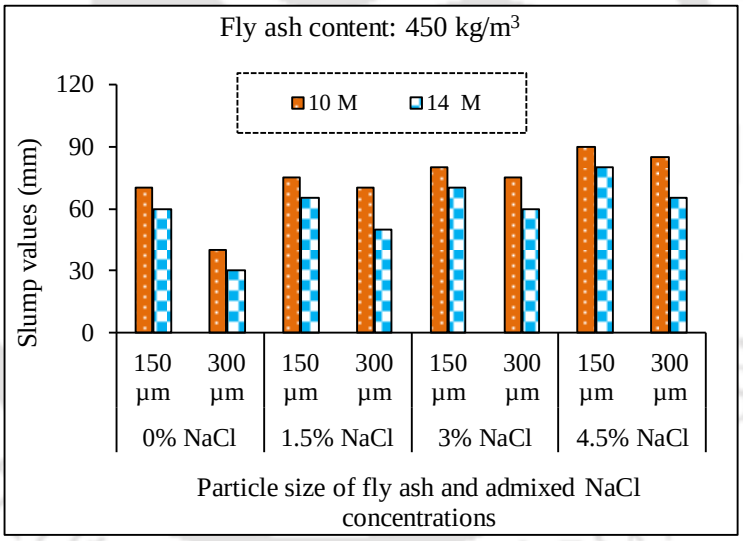

Fig. 4.5: Slump values of geopolymer concrete (GPC) mixes made with fly ash passing through 150 µm sieve, and 300 µm sieve at fly ash content of 450 kg/m^3

From Fig. 4.4 and Fig. 4.5, it is observed that the slump values of GPC mixes mostly decreased with increase in particle size of fly ash for both fly ash contents. This may be attributed to the dominant effect of lower particle mobility in case of larger fly ash particles over the effect of more specific surface area in case of smaller fly ash particles, which led to reduced consistency of GPC mix with larger fly ash particles. Further, the slump value of GPC mixes increased in the presence of NaCl and decreased with increase in molarity of NaOH solution from 10 M to 14 M for both sizes of fly ash particles as evident from Fig. 4.4 and Fig. 4.5.

4.2.5 Effect of fly ash content

The obtained slump values of geopolymer concrete mixes made from different molarity (10 M and 14 M) of NaOH solution and admixed with different dosages of sodium chloride (NaCl) for fly ash contents of 425 kg/m^3 and 450 kg/m^3 are shown in Fig. 4.6 and Fig. 4.7 for fly ash passing through 150 μm sieve, and 300 μm sieve respectively. The slump values shown in Fig. 4.6 and Fig. 4.7 correspond to the GPC mixes made with alkaline solution content of 210 kg/m^3, and ratio of alkaline solution of 1.75.

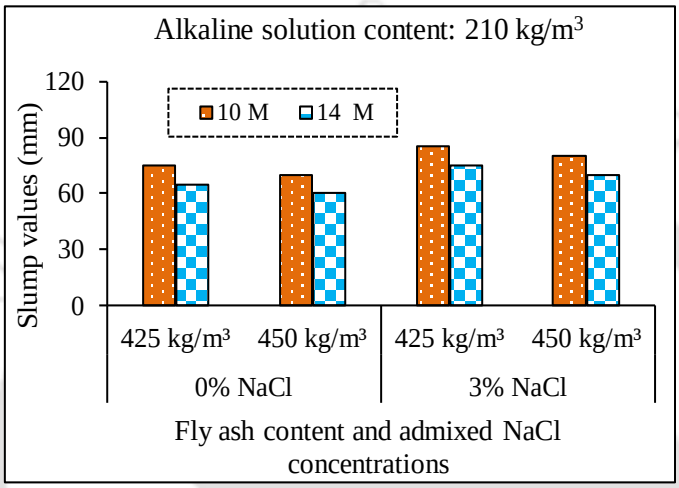

Fig. 4.6: Slump values of geopolymer concrete (GPC) mixes made with fly ash contents of 425 kg/m^3, and 450 kg/m^3 for fly ash passing through 150 μm sieve

From Fig. 4.6 and Fig. 4.7, it is noted that the slump value decreased with increase in fly ash content for both particle size of fly ash except few cases. The decrease in slump value may be ascribed to the presence of higher amount of fly ash for the same amount of alkaline liquid that reduced the consistency of GPC mix at higher fly ash content. As observed from Fig. 4.7, the slump value remained same irrespective of fly ash content in NaCl admixed GPC mixtures made from 14 M NaOH solution for fly ash passing through 300 μm sieve. This may be attributed to the dominant effect of presence of chloride ions that reduced the effect of higher fly ash content in lowering the consistency of GPC mixes made with higher molarity of NaOH solution and larger fly ash particles. Further, the slump values of GPC mixes increased with increase in dosage of admixed sodium chloride as observed in Fig. 4.6 and Fig. 4.7. In addition, the slump values of GPC mixes decreased with increase in NaOH solution concentration.

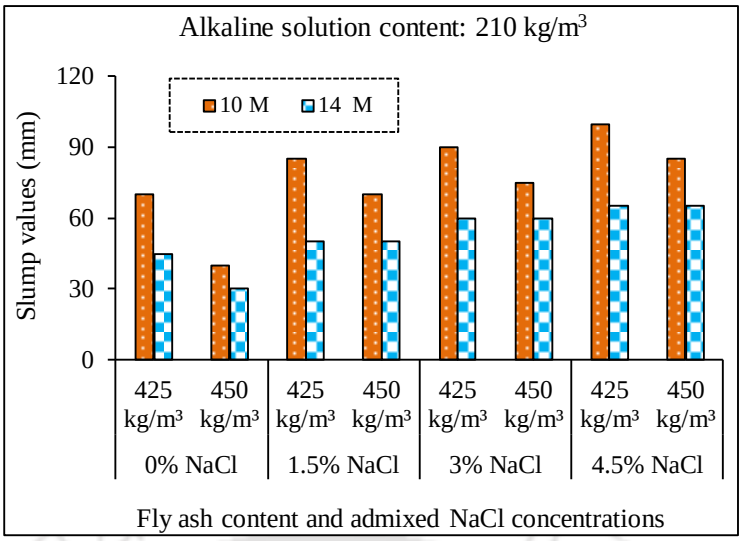

Fig. 4.7: Slump values of geopolymer concrete (GPC) mixes made with fly ash contents of 425 kg/m^3, and 450 kg/m^3 for fly ash passing through 300 μm sieve

4.3 Compressive strength of fly ash based geopolymer concrete (GPC) mixes

4.3.1 Effect of sodium hydroxide solution molarity and NaCl concentration

The obtained results of compressive strength of GPC mixes made with fly ash content of 425 kg/m^3 and admixed with NaCl of different concentrations are shown in Fig. 4.8 (a-e) for different molarity of NaOH solution. Each value of compressive strength shown in these figures is the average value of three replicate cube specimens. The results of compressive strength depicted in these figures correspond to the GPC mixes made with fly ash passing through 300 μm sieve, alkaline solution content of 210 kg/m^3, and alkaline solution ratio of 1.75.

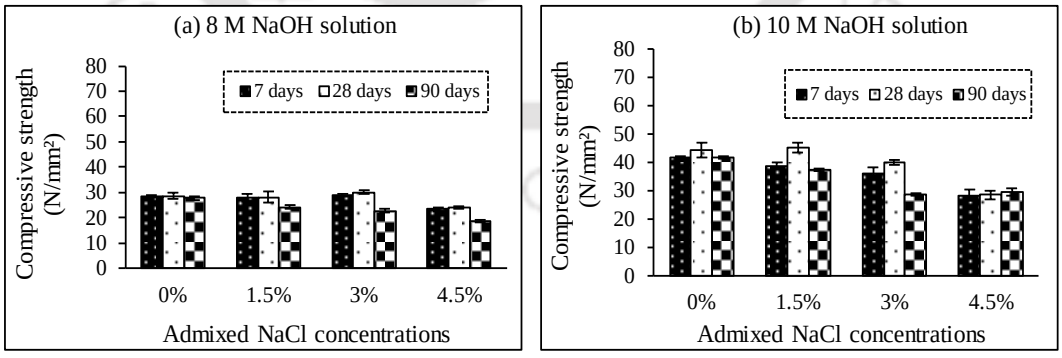

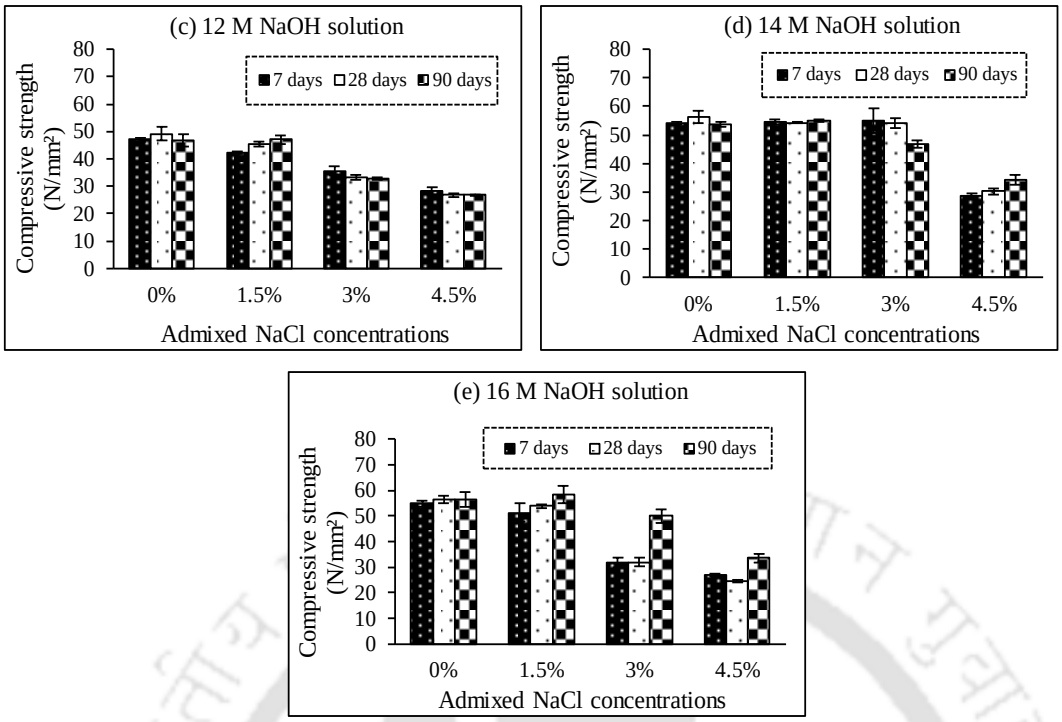

Fig. 4.8: Compressive strength of geopolymer concrete (GPC) mixes made with fly ash content of 425 kg/m^3 and admixed with different concentrations of NaCl for: (a) NaOH solution of 8 M, (b) NaOH solution of 10 M, (c) NaOH solution of 12 M, (d) NaOH solution of 14 M, and (e) NaOH solution of 16 M, at different ages

From Fig. 4.8, it is observed that the compressive strength increased with an increase in NaOH solution concentration from 8 M to 16 M for control (without NaCl) GPC mixes at all ages. The increase in compressive strength of GPC with increase in molarity of NaOH solution is attributed to the fact that higher molarity of NaOH solution resulted in more dissolution of silica and alumina from fly ash that led to improved polycondensation process thereby resulting in higher strength development. The increased dissolution of silica and alumina from fly ash due to increase in concentration of NaOH solution enhanced the formation of N-A-S-H (sodium aluminosilicate hydrate) gel [89] and resulted in formation of denser microstructure in GPC.

In case of GPC mixes admixed with NaCl concentration of 1.5%, the compressive strength mostly increased with increase in molarity of NaOH solution at all ages. For admixed NaCl concentration of 3%, the compressive strength of GPC increased with increase in molarity of NaOH solution from 8 M to 14 M followed by a decrease for NaOH solution of 16 M at the age of 7, and 28 days. However, at the age of 90 days, the compressive strength of GPC admixed with 3% NaCl increased with increase in molarity of NaOH solution from 8 M to 16 M. At NaCl concentration of 4.5%, the compressive strength increased with increase in molarity of NaOH solution from 8 M to 14 M followed by a decrease at NaOH solution of 16

M at the age of 7, and 28 days with minor difference in compressive strength between 14 M and 16 M NaOH solution at the age of 90 days i.e., slightly higher compressive strength at 14 M NaOH solution as compared to 16 M NaOH solution. The lower compressive strength at higher concentration of NaCl in case of GPC mixes made with NaOH solution of 16 M may be attributed to the effect of alteration in the extent of geopolymerization process in the presence of NaCl at higher concentration. From Fig. 4.8, it is noted that the compressive strength of NaCl admixed GPC mixes was mostly lower as compared to control GPC mixes (without NaCl) for all molarity of NaOH solution and at all ages. Further, the compressive strength mostly decreased with increase in concentration of admixed sodium chloride (NaCl) as observed from Fig. 4.8. The reduction in compressive strength of NaCl admixed GPC mixes may be attributed to the dominant effect of crystallization of sodium chloride in the pores of GPC mixes. Further, the decrease in compressive strength was comparatively more at higher concentration of admixed NaCl as evident from Fig. 4.8, which indicates crystallization of sodium chloride in the pores of GPC mixes to a comparatively greater extent at higher concentration of NaCl.

From Fig. 4.8, it is inferred that the compressive strength mostly increased with increase in age from 7 to 28 days for control as well as NaCl admixed GPC mixes for all molarity of NaOH solution except in few cases. The increase in compressive strength may be due to the effect of continued geopolymerization reaction with increase in age [90]. However, the compressive strength mostly decreased with increase in age from 28 to 90 days for control as well as chloride admixed GPC mixes for molarity of NaOH solution from 8 M to 14 M, whereas the compressive strength increased with age from 28 to 90 days at higher molarity of NaOH solution i.e., 16 M as noted from Fig. 4.8. The decrease in later age compressive strength of GPC at comparatively lower molarity of NaOH solution may be attributed to the effect of formation of shrinkage cracks as a result of loss of moisture to a comparatively higher extent from geopolymer gels in the GPC mixes at later age [91]. It may be noted that for a given amount of alkaline liquid, the lower molarity of NaOH solution has comparatively higher water content in the mix as compared to that at higher molarity of NaOH solution. At NaOH solution of 16 M, the dominant effect of comparatively higher extent of geopolymerization process contributed toward higher strength of GPC, although there may be loss of moisture to certain extent from the mix at later age.

4.3.2. Effect of quantity of alkaline solution

The obtained compressive strength of geopolymer concrete (GPC) mixes made from alkaline solution of different quantities i.e., 190 kg/m^3 and 210 kg/m^3, and admixed with and without sodium chloride (NaCl) are shown Fig. 4.9 and Fig. 4.10 for 7 days and 28 days respectively. The compressive strength values shown in Fig. 4.9 and Fig. 4.10 correspond to the GPC mixes made with fly ash passing through 150 μm sieve, fly ash content of 425 kg/m^3, sodium hydroxide solution of 10 M and 14 M, and sodium silicate solution to sodium hydroxide solution ratio of 1.75.

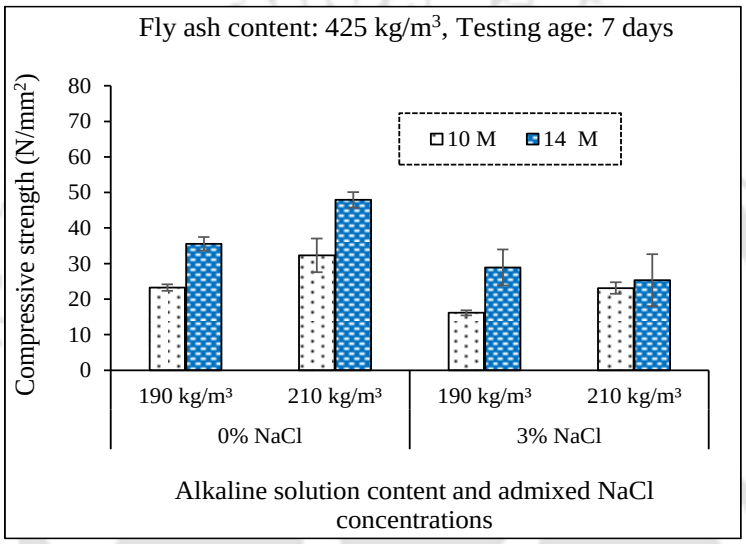

Fig. 4.9: Compressive strength of geopolymer concrete (GPC) mixes made with alkaline solution content of 190 kg/m^3 and 210 kg/m^3, at the age of 7 days

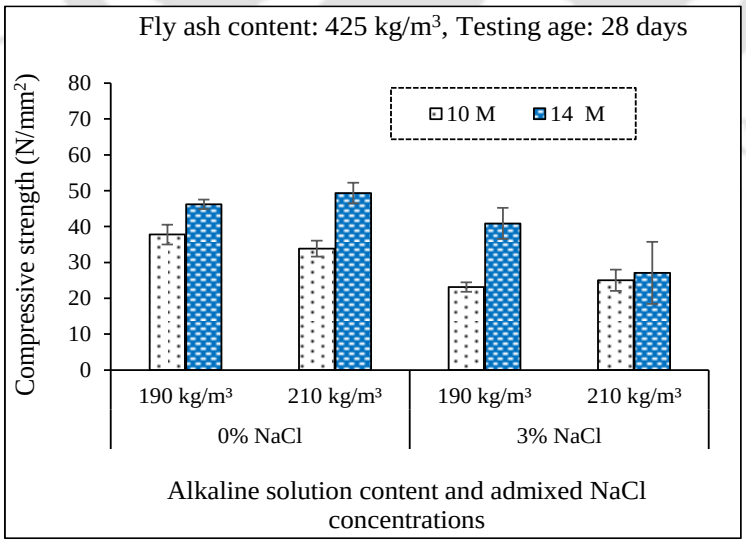

Fig. 4.10: Compressive strength of geopolymer concrete (GPC) mixes made with alkaline solution content of 190 kg/m^3 and 210 kg/m^3, at the age of 28 days

From Fig. 4.9 and Fig. 4.10, it is observed that the compressive strength of GPC mixes was mostly lower at lower alkaline solution content except few cases mostly in case of 3% NaCl admixed GPC mixes at 14 M NaOH solution. The decrease in compressive strength at lower alkaline solution content may be attributed to the effect of insufficient quantity of alkaline solution for same amount of fly ash that resulted in lower dissolution of alumina and silica from fly ash, which might have led to formation of a weaker geopolymer matrix with non-homogeneous structure [28]. Further, the lower compressive strength of 3% NaCl admixed GPC mixes at higher alkaline solution content for NaOH solution of 14 M may be ascribed to the dominant effect of alteration in the extent of dissolution of silica and alumina from fly ash in the alkaline solution in the presence of NaCl. In addition, the compressive strength increased significantly with an increase in concentration of NaOH solution from 10 M to 14 M as observed from Fig. 4.9 and Fig. 4.10 for both alkaline solution contents. Further, the compressive strength of GPC mixes decreased significantly in the presence of sodium chloride (3%) as compared to control mix, which may be attributed to the dominant effect of alteration in the extent of geopolymerization reaction as well as crystallization of sodium chloride in the pores of geopolymer matrix. In addition, the compressive strength increased from 7 to 28 days for control as well as NaCl admixed GPC mixes.

4.3.3 Effect of ratio of alkaline solution

The compressive strength of GPC mixes prepared with alkaline solution ratio (SS/SH ratio) of 1.5 and 1.75 are shown Fig. 4.11 and Fig. 4.12 for 7 days and 28 days respectively. The compressive strength values illustrated in these figures correspond to the GPC mixes made from fly ash content of 425 kg/m^3, fly ash passing through 150 μm sieve, alkaline solution content of 210 kg/m^3, and sodium hydroxide solution of 10 M and 14 M.

From Fig. 4.11 and Fig. 4.12, it is observed that the compressive strength of GPC mixes mostly increased with increase in alkaline solution ratio (SS/SH ratio), however, in few cases, lower compressive strength was observed at higher alkaline solution ratio in case of GPC mixes admixed with 3% NaCl at NaOH solution of concentration 14 M. The increase in compressive strength with increase in SS/SH ratio is attributed to the effect of improved polycondensation process due to more amount of sodium silicate in the activator solution thereby resulting in higher compressive strength of GPC. The lower compressive strength at higher SS/SH ratio in case of chloride (3% NaCl) admixed GPC mixes at higher molarity of NaOH solution (14 M) can be attributed to the alteration in the extent of dissolution of silica and alumina from fly ash in the activator solution. From Fig. 4.11 and Fig. 4.12, the compressive strength of GPC

increased with increase in concentration of NaOH solution. Further, the strength mostly decreased in the presence of admixed NaCl as observed from Fig. 4.11 and Fig. 4.12. In addition, the compressive strength increased with increase in age from 7 to 28 days for control as well as chloride admixed GPC mixes.

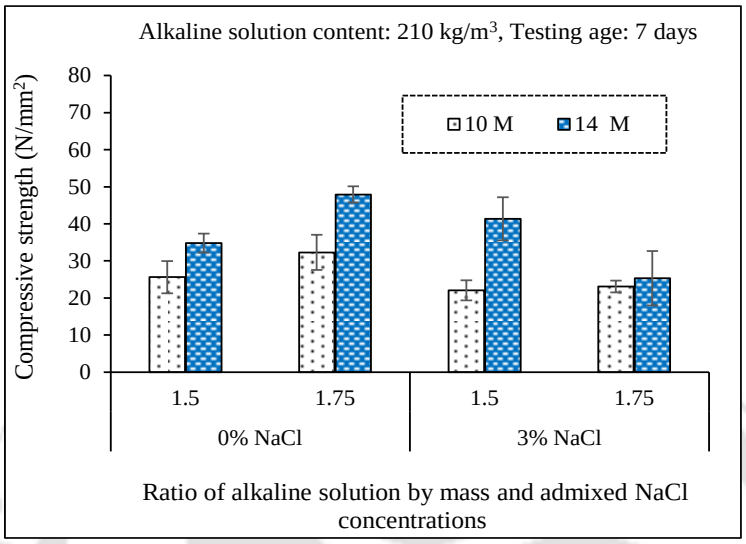

Fig. 4.11: Compressive strength of geopolymer concrete (GPC) mixes made with alkaline solution ratio (SS/SH ratio) of 1.5 and 1.75, at the age of 7 days

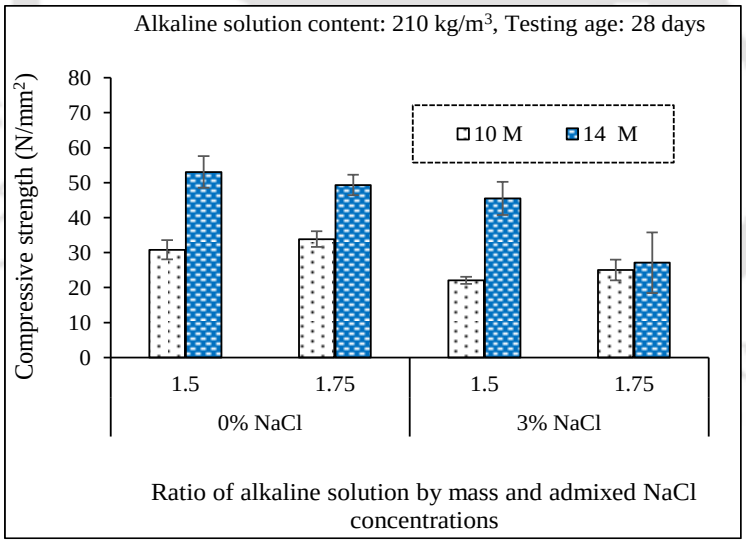

Fig. 4.12: Compressive strength of geopolymer concrete (GPC) mixes made with alkaline solution ratio (SS/SH ratio) of 1.5 and 1.75, at the age of 28 days

4.3.4 Effect of particle size of fly ash

The obtained results of compressive strength of GPC mixes made with fly ash passing through 150 μm sieve, and that passing through 300 μm sieve are shown in Fig. 4.13 and Fig. 4.14 for 7 days and 28 days respectively at fly ash content of 425 kg/m^3. The compressive strength

values depicted in these figures correspond to the GPC mixes made with alkaline solution content of 210 kg/m^3, and SS/SH ratio of 1.75.

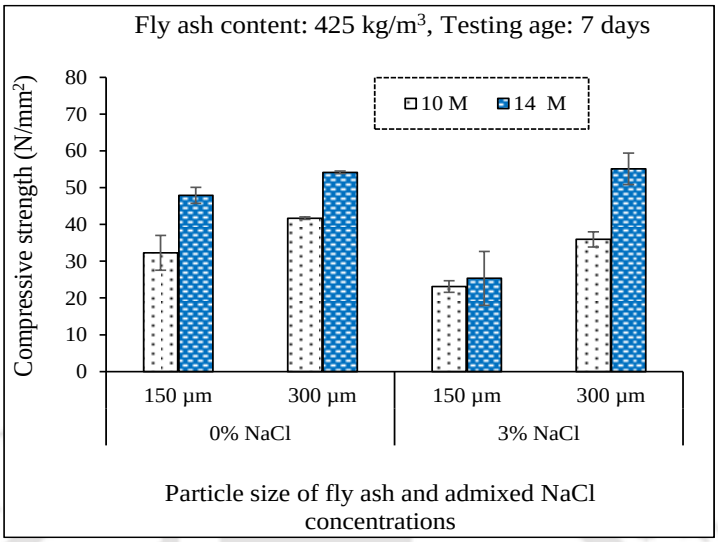

Fig. 4.13: 7-day compressive strength of geopolymer concrete (GPC) mixes made with fly ash passing through 150 µm sieve, and 300 µm sieve at fly ash content of 425 kg/m^3

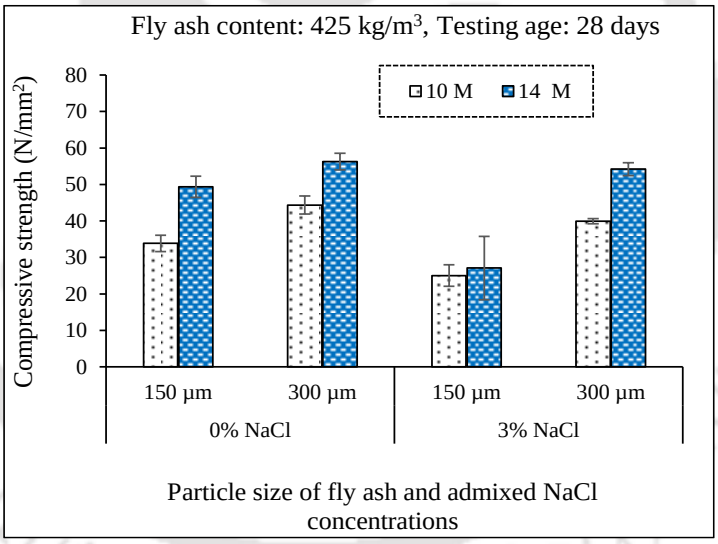

Fig. 4.14: 28-day compressive strength of geopolymer concrete (GPC) mixes made with fly ash passing through 150 µm sieve, and 300 µm sieve at fly ash content of 425 kg/m^3

From Fig. 4.13 and 4.14, it is inferred that the compressive strength was higher in the GPC mixes made with fly ash passing through 300 µm sieve as compared to that passing through 150 µm sieve. The higher compressive strength in case of larger fly ash particles may be ascribed to the combined effect of geopolymerization reaction as well as pore filling effect of unreacted/partially reacted larger fly ash particles over the effect of comparatively higher reactivity of smaller fly ash particles at comparatively lower fly ash content of 425 kg/m^3. The compressive strength of GPC mixes increased with increase in molarity NaOH solution from

10 M to 14 M as well as with increase in age from 7 to 28 days for both sizes of fly ash particles. Further, the compressive strength of chloride admixed GPC mixes was lower as compared to control (without NaCl) GPC mixes as observed from Fig. 4.13 and 4.14.

The results of compressive strength of GPC mixes made with fly ash passing through 150 μm sieve, and that passing through 300 μm sieve are shown in Fig. 4.15, Fig. 4.16, and Fig. 4.17 for 7, 28, and 90 days respectively for fly ash content of 450 kg/m^3. The compressive strength values shown in these figures correspond to the GPC mixes made with alkaline solution content of 210 kg/m^3, and SS/SH ratio of 1.75.

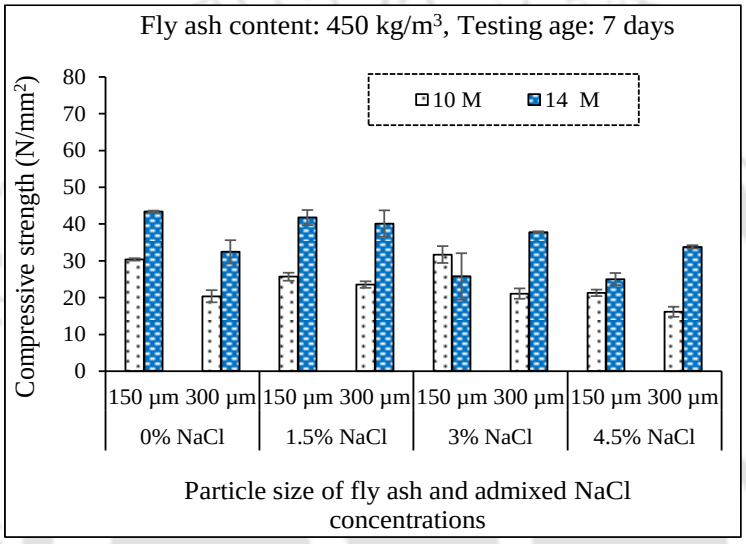

Fig. 4.15: 7-day compressive strength of geopolymer concrete (GPC) mixes made with fly ash passing through 150 μm sieve, and 300 μm sieve at fly ash content of 450 kg/m^3

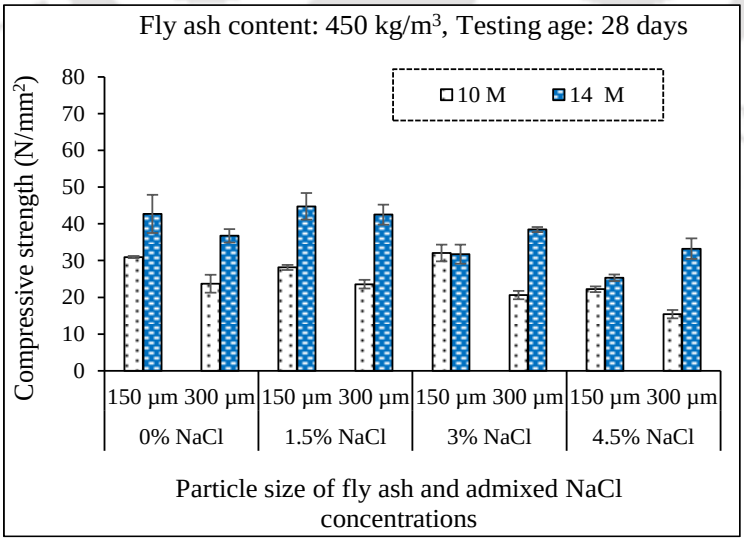

Fig. 4.16: 28-day compressive strength of geopolymer concrete (GPC) mixes made with fly ash passing through 150 μm sieve, and 300 μm sieve at fly ash content of 450 kg/m^3

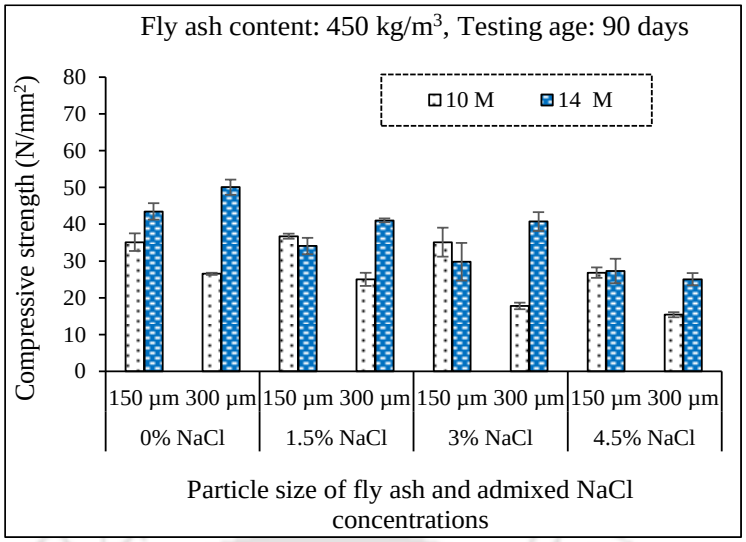

Fig. 4.17: 90-day compressive strength of geopolymer concrete (GPC) mixes made with fly ash passing through 150 µm sieve, and 300 µm sieve at fly ash content of 450 kg/m^3

From Fig. 4.15 to Fig. 4.17, it is noted that, at fly ash content of 450 kg/m^3, the compressive strength of GPC mixes made with fly ash passing through 150 µm sieve was higher as compared to that made with fly ash passing through 300 µm sieve for all cases at NaOH solution of 10 M and for some cases i.e., mostly in control mixes at NaOH solution of 14 M. The higher compressive strength of GPC mixes made with smaller fly ash particles may be attributed to the effect of higher extent of geopolymerization reaction as a result of larger specific surface of smaller fly ash particles. The larger specific surface of smaller fly ash particles leads to greater reactivity with the alkaline activator solution as result of higher dissolution of alumina and silica from fly ash during the geopolymerization process. The lower compressive strength for fly ash passing through 150 µm sieve in majority of the cases in NaCl admixed GPC mixes at 14 M NaOH solution is ascribed to the effect of NaCl, which might have inhibited the extent of polycondensation process to a certain extent at higher molarity of NaOH solution thereby resulting in lower compressive strength of GPC mixes made with smaller fly ash particles.

As observed from Fig. 4.15 to 4.17, for both sizes of fly ash particles, the compressive strength of geopolymer concrete mixes mostly increased with increase in molarity of NaOH solution from 10 M to 14 M, except few cases in NaCl admixed GPC mixes made with smaller fly ash particles. The lower compressive strength in the presence of NaCl at higher molarity of NaOH solution in these mixes may be due to the dominant effect of chloride ions that altered the geopolymerization process. Further, for both sizes of fly ash particles, the compressive strength of GPC mixes mostly increased with increase in age from 7 to 28 days, and from 28 to 90 days

except few cases mostly in GPC mixes admixed with NaCl, which can be attributed to the inhibiting effect of NaCl on geopolymerization process to certain extent thereby reducing the compressive strength of GPC in these cases. With respect to admixed chloride content, the compressive strength of GPC mixes was mostly lower in the presence of admixed NaCl when compared with control GPC mixes as observed from Fig. 4.15 to 4.17 for different molarity of NaOH solution, particle size of fly ash, and at different ages. Further, the compressive strength mostly decreased with increase in concentration of admixed NaCl as observed from Fig 4.15 to 4.17. The reason for decrease in compressive strength of GPC mixes in the presence of NaCl is already stated Section 4.3.1.

4.3.5 Effect of fly ash content

The compressive strength of GPC mixes made with fly ash contents of 425 kg/m^3 and 450 kg/m^3 are shown in Fig. 4.18 and Fig. 4.19 at 7 days and 28 days respectively for fly ash passing through 150 µm sieve. The compressive strength results illustrated in these figures correspond to the GPC mixes made with alkaline solution content of 210 kg/m^3, and SS/SH ratio of 1.75.

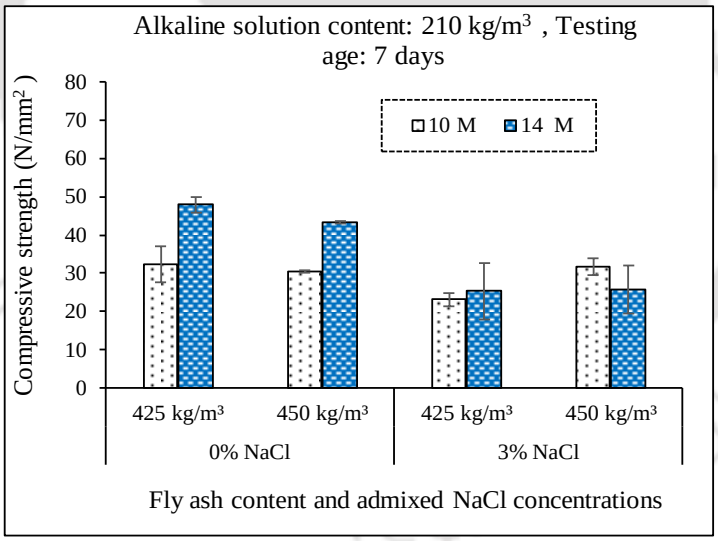

Fig. 4.18: 7-day compressive strength of geopolymer concrete (GPC) mixes made with fly ash contents of 425 kg/m^3 and 450 kg/m^3 for fly ash passing through 150 µm sieve

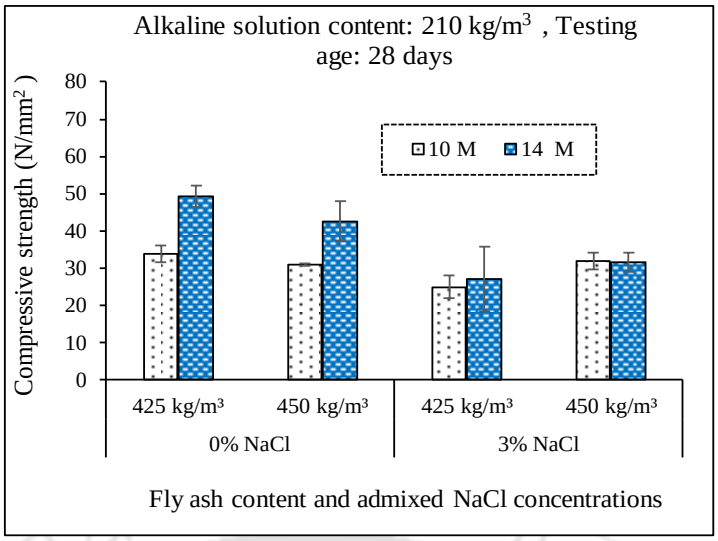

Fig. 4.19: 28-day compressive strength of geopolymer concrete (GPC) mixes made with fly ash contents of 425 kg/m^3 and 450 kg/m^3 for fly ash passing through 150 µm sieve

From Fig. 4.18 and 4.19, it is inferred that the compressive strength of control (without NaCl) GPC mixes made with higher fly ash content (450 kg/m^3) was lower as compared to that made with lower fly ash content (425 kg/m^3), which is due to the effect of insufficient amount of alkaline solution for higher content of fly ash that resulted in comparatively lower extent of geopolymerization process. However, in the presence of NaCl, the GPC mixes made with lower fly ash content showed lower compressive strength as compared to that made with higher fly ash content. This may be ascribed to the inhibiting effect of NaCl on the geopolymerization process in the GPC mix made with comparatively smaller fly ash particles to a comparatively higher extent at lower fly ash content as compared to that at higher fly ash content for the same amount of alkaline solution thereby reducing the compressive strength of GPC at lower fly ash content. As observed from Fig. 4.18 and 4.19, the compressive strength of GPC mixes mostly increased with increase in molarity of NaOH solution (except in case of 3% NaCl admixed GPC mixes at fly ash content of 450 kg/m^3), and age for both fly ash contents. Further, for both fly ash contents, the chloride admixed GPC mixes mostly showed lower compressive strength as compared to control GPC mixes as noted from Fig. 4.18 and 4.19.

Fig. 4.20, Fig. 4.21 and Fig. 4.22 illustrate the compressive strength of GPC mixes made with fly ash contents of 425 kg/m^3, and 450 kg/m^3 at 7 days, 28 days, and 90 days respectively for fly ash passing through 300 µm sieve. The compressive strength values shown in these figures correspond to the geopolymer concrete mixes made with alkaline solution content of 210 kg/m^3, and SS/SH ratio of 1.75. From Fig. 4.20 to Fig. 4.22, it is inferred that the compressive strength of GPC mixes was mostly higher at lower fly ash content (425 kg/m^3) as compared to

that at higher fly ash content (450 kg/m^3) irrespective of molarity of NaOH solution, admixed NaCl concentration, and age for fly ash passing through 300 µm sieve. As stated earlier, the lower compressive strength of GPC mixes made with higher fly ash content is ascribed to insufficient amount of alkaline solution for higher fly ash content that resulted in lower dissolution of alumina and silica from fly ash. This led to lower extent of geopolymerization process. As discussed earlier, the compressive strength was lower at lower fly ash content than that at higher fly ash content in case of NaCl admixed GPC mixes for fly ash passing through 150 µm sieve (Fig. 4.18 and Fig. 4.19). This indicates that the particle size of fly ash significantly affected the variation in compressive strength of NaCl admixed GPC mixes for different fly ash contents. The compressive strength of all the GPC mixes increased with increase in molarity of NaOH solution from 10 M to 14 M for both fly ash contents as observed from Fig. 4.20 to Fig. 4.22. This is attributed to the effect of improved polycondensation process at higher molarity of NaOH solution that resulted in higher compressive strength of GPC mixes.

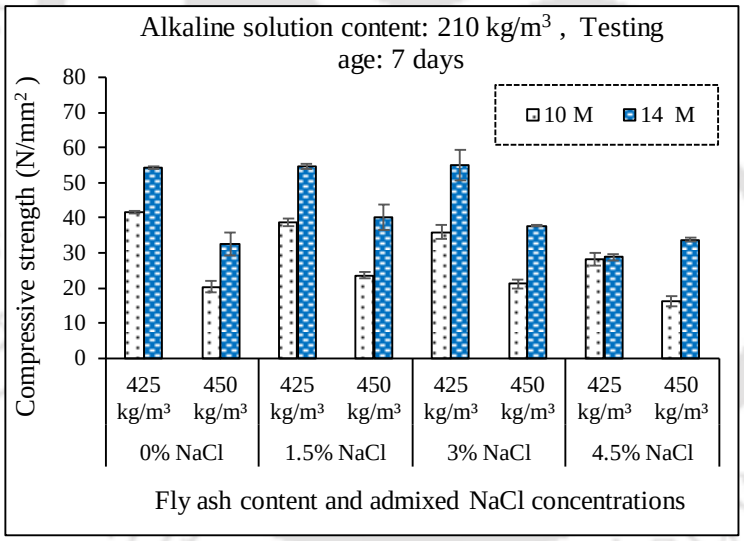

Fig. 4.20: 7-day compressive strength of geopolymer concrete (GPC) mixes made with fly ash contents of 425 kg/m^3 and 450 kg/m^3 for fly ash passing through 300 µm sieve

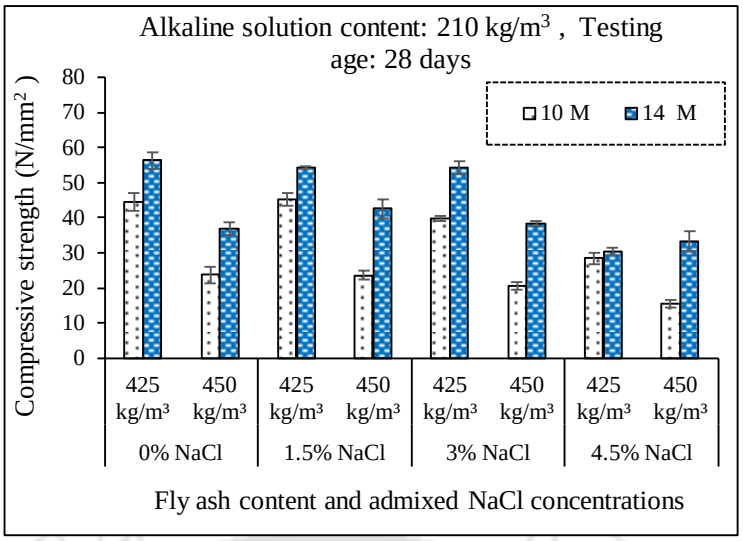

Fig. 4.21: 28-day compressive strength of geopolymer concrete (GPC) mixes made with fly ash contents of 425 kg/m^3 and 450 kg/m^3 for fly ash passing through 300 μm sieve

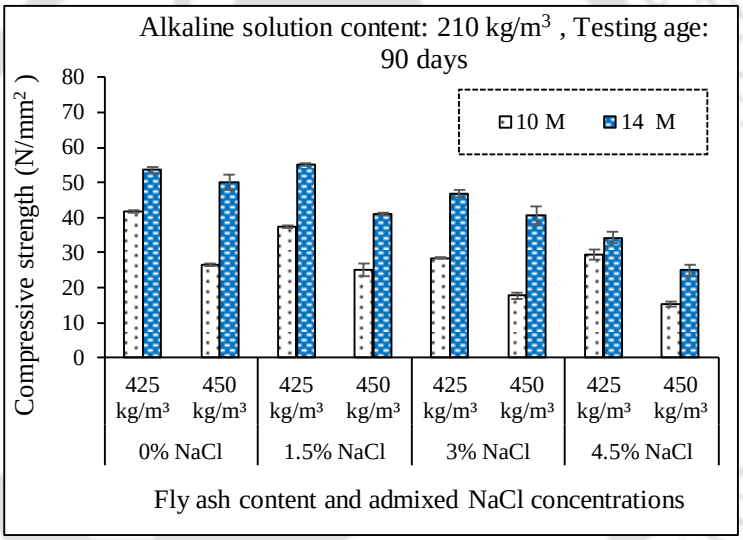

Fig. 4.22: 90-day compressive strength of geopolymer concrete (GPC) mixes made with fly ash contents of 425 kg/m^3 and 450 kg/m^3 for fly ash passing through 300 μm sieve

From Fig. 4.20 and 4.21, it is inferred that the compressive strength of control GPC mixes increased with increase in age from 7 to 28 days for both fly ash contents. However, in NaCl admixed GPC mixes, the compressive strength mostly increased with age from 7 to 28 days at lower fly ash content (425 kg/m^3) whereas mostly opposite variation in compressive strength with age from 7 to 28 days was observed at higher fly ash content (450 kg/m^3). The lower compressive strength at the age of 28 days in the NaCl admixed GPC mixes at higher fly ash content is ascribed to the combined effect of NaCl, and higher amount of fly ash at the given alkaline solution content that resulted in comparatively lower extent of geopolymerization process. From Fig. 4.21 and 4.22, the compressive strength of control GPC mixes increased with increase in age from 28 to 90 days in case of higher fly ash content (450 kg/m^3) whereas

the opposite variation was observed in case of lower fly ash content (425 kg/m^3). The lower compressive strength at the age of 90 days in control GPC mixes made with lower fly ash content may be attribuited to the effect of alteration in the extent of geopolymerization reaction in the GPC mixes made with larger fly ash particles (passing through 300 μm sieve). In NaCl admixed GPC mixes, there is no systematic varaition in compressive strength of GPC mixes with increase in age from 28 to 90 days for lower fly ash content (425 kg/m^3), whereas at higher fly ash content (450 kg/m^3), the compressive strength was mostly lower at the later age of 90 days as compared to that at 28 days. The lower compressive strength of chloride admixed GPC made with higher fly ash content at later age is ascribed to the effect of crystallization of sodium chloride in the pores to a comparatively higher extent as well as comparatively lower rate of geopolymerization reaction at later age in the presence of NaCl in the mixes made with higher fly ash content for the same alkaline solution content when compared with the GPC made with lower fly ash content. From Fig. 4.20 to 4.22, the compressive strength of control GPC mixes were mostly higher when compared with the chloride admixed GPC mixes for different molarity of NaOH solution, fly ash content, and age. In addition, mostly there was a decreasing trend of compressive strength with increase in concentration of admixed NaCl as observed from Fig 4.20 to 4.22.

4.4 Chloride content of NaCl admixed GPC mixes

As already stated in Chapter 3, the free chloride and total chloride contents of NaCl admixed GPC mixes were determined by potentiometric titration at the ages of 7, 28, and 90 days from the powder samples obtained from cube specimens. The free chloride also known as water soluble chloride is the dissolved chloride ions in the pore solution of concrete. The free chloride ions are mainly responsible for corrosion of steel reinforcement in concrete. The formation of denser microstructure in concrete reduces the chloride ion concentration in pore solution near the steel reinforcement and decreases the extent of corrosion. Chloride binding in concrete affects the availability of chloride ions in the pore solution of concrete. Higher bound chloride content results in availability of lower amount of chloride ions in the pore solution thereby reducing free chloride content, which decreases the extent of steel reinforcement corrosion in concrete. The total chloride also known as acid soluble chloride is the sum of free chloride and bound chloride contents in concrete. For a given total chloride content, higher extent of chloride binding results in lower free chloride content in concrete. The variations in free and total chloride cotents with molarity of NaOH solution, alkaline solution content, SS/SH ratio, and particle size and amount of fly ash are analyzed and discussed in the subsequent sections.

In this study, the bound chloride content was also calculated as the difference of total chloride and free chloride contents.

4.4.1 Effect of molarity of NaOH solution on chloride content of GPC

The results of free chloride and total chloride contents of geopolymer concrete (GPC) mixes made from different molarity (8 M, 10 M, 12 M, 14 M and 16 M) of NaOH solution and admixed with different concentrations of sodium chloride (NaCl) are shown in Fig. 4.23 (a, b) to Fig. 4.27 (a, b).

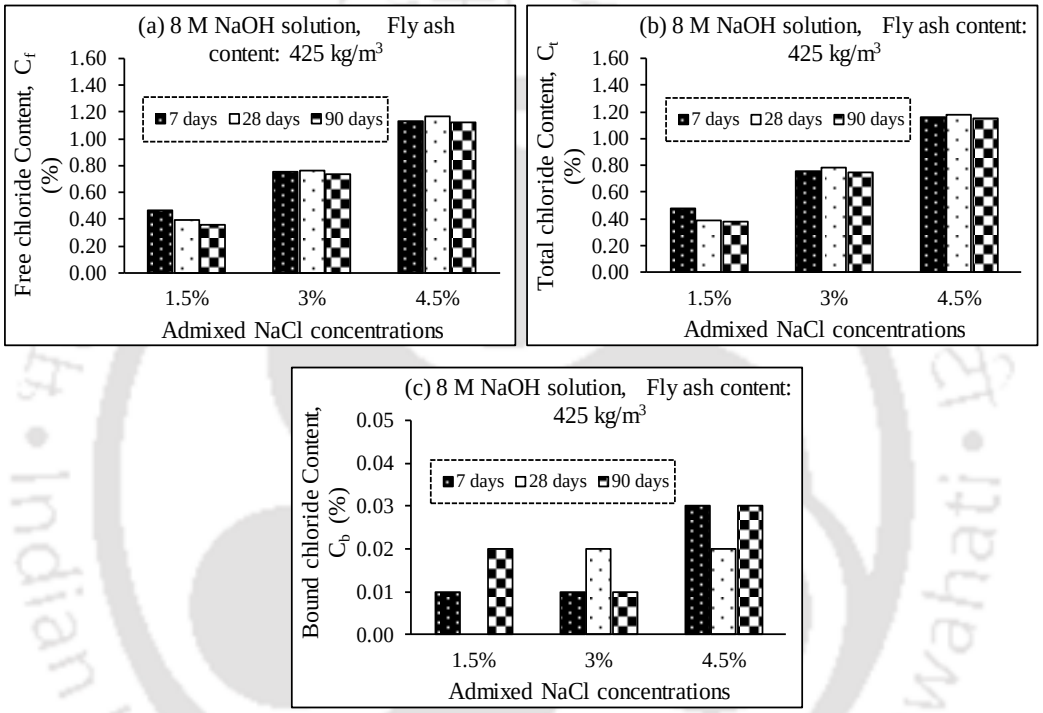

(GPC made with fly ash passing through 300 μm sieve, fly ash content of 425 kg/m³, alkaline solution content of 210 kg/m³, and SS/SH ratio of 1.75)

Fig. 4.23: (a) Free chloride content, (b) Total chloride content and (c) Bound chloride content of GPC made with 8 M NaOH solution and admixed with different concentrations of NaCl, at different ages

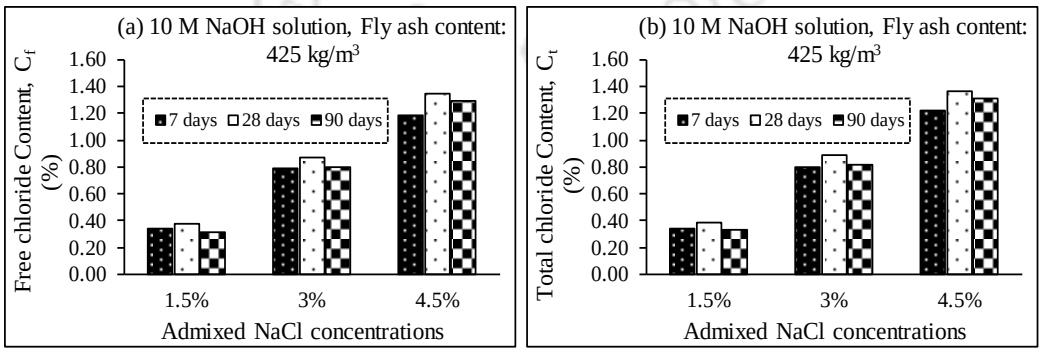

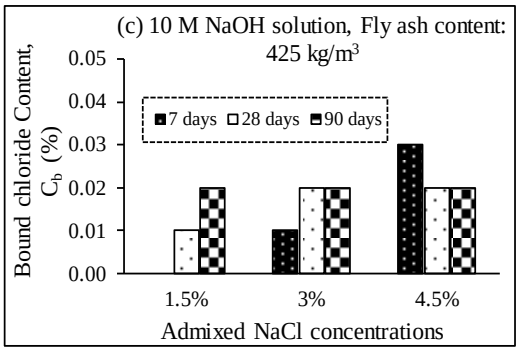

(GPC made with fly ash passing through 300 μm sieve, fly ash content of 425 kg/m^3, alkaline solution content of 210 kg/m^3, and SS/SH ratio of 1.75)

Fig. 4.24: (a) Free chloride content, (b) Total chloride content and (c) Bound chloride content of GPC made with 10 M NaOH solution and admixed with different concentrations of NaCl, at different ages

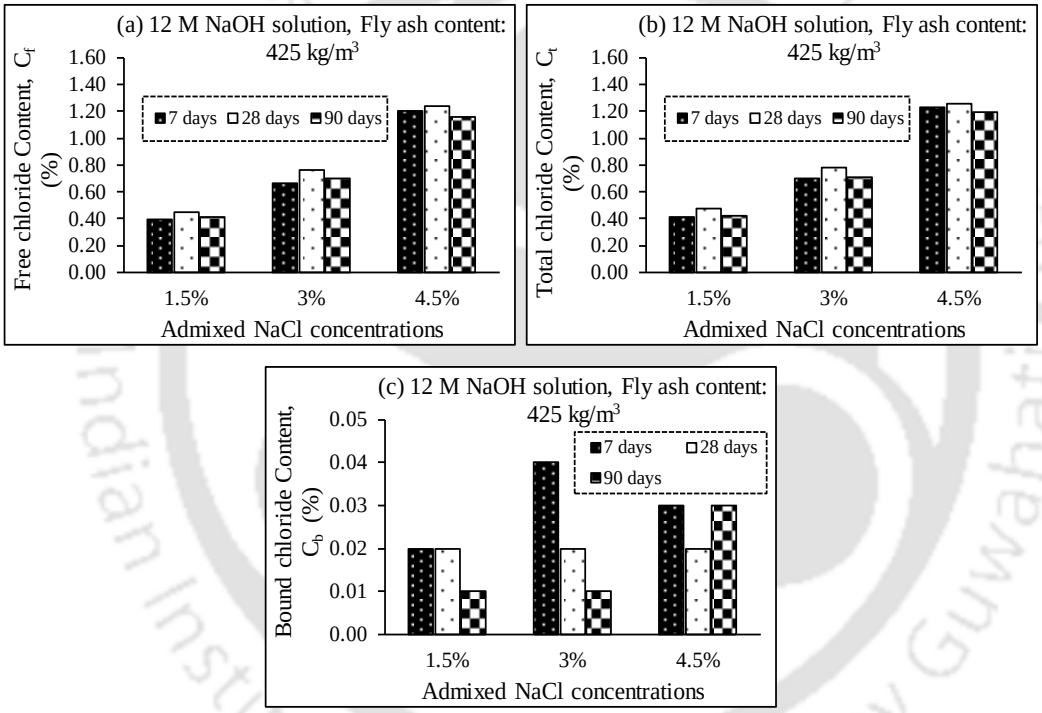

(GPC made with fly ash passing through 300 μm sieve, fly ash content of 425 kg/m^3, alkaline solution content of 210 kg/m^3, and SS/SH ratio of 1.75)

Fig. 4.25: (a) Free chloride content, (b) Total chloride content and (c) Bound chloride content of GPC made with 12 M NaOH solution and admixed with different concentrations of NaCl, at different ages

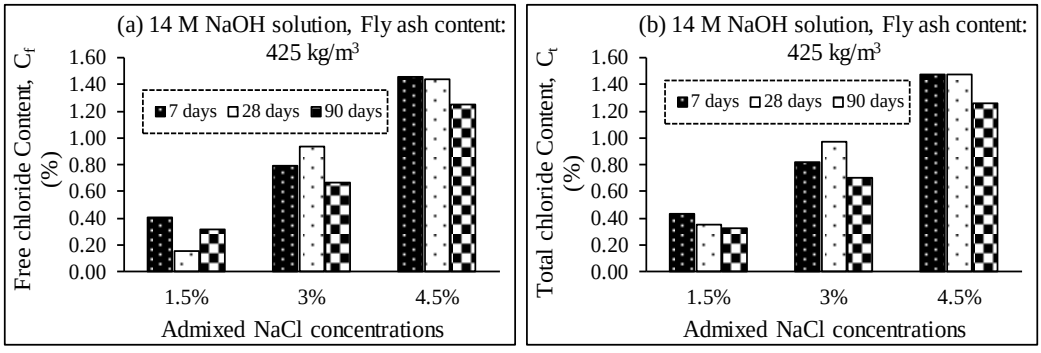

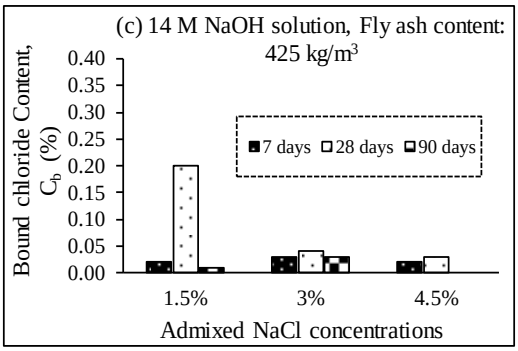

(GPC made with fly ash passing through 300 μm sieve, fly ash content of 425 kg/m^3, alkaline solution content of 210 kg/m^3, and SS/SH ratio of 1.75)

Fig. 4.26: (a) Free chloride content, (b) Total chloride content and (c) Bound chloride content of GPC made with 14 M NaOH solution and admixed with different concentrations of NaCl, at different ages

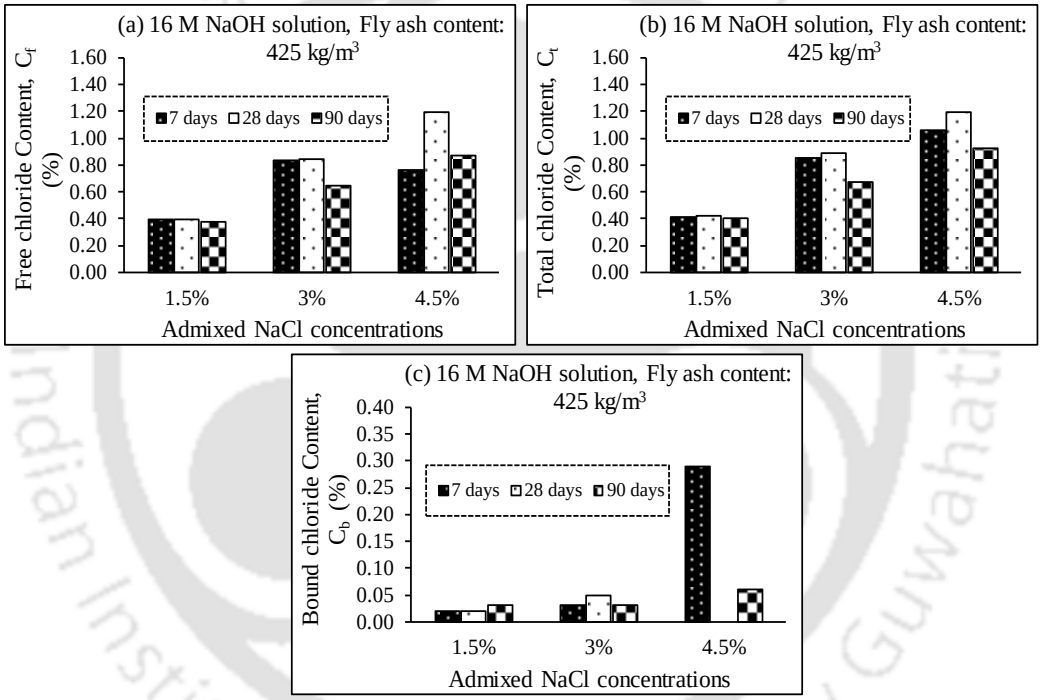

(GPC made with fly ash passing through 300 μm sieve, fly ash content of 425 kg/m^3, alkaline solution content of 210 kg/m^3, and SS/SH ratio of 1.75)

Fig. 4.27: (a) Free chloride content, (b) Total chloride content and (c) Bound chloride content of GPC made with 16 M NaOH solution and admixed with different concentrations of NaCl, at different ages

From Fig. 4.23 (a) to Fig. 4.27 (a), it is observed that the free chloride content of GPC mixes increased with increase in admixed NaCl concentration irrespective of molarity of NaOH solution and age. This may be ascribed to the effect of presence of more amount of chloride ions in the GPC mixes admixed with higher concentration of NaCl. From Fig. 4.23 (a) to Fig. 4.27 (a), it is inferred that there is no systematic variation in free chloride content of GPC mixes with molarity of NaOH solution at all ages except few cases where mostly lower free chloride content was observed for 16 M NaOH solution at the age of 90 days when compared

with lower molarity of NaOH solution. The unsystematic variation in free chloride content with molarity of NaOH solution may be due to the effect of alteration in the availability of chloride ions in the pore solution of concrete made with different molarity of NaOH solution. It may be noted that the amount of chloride ions added in the GPC mixes was more at higher molarity of NaOH solution, as the dosage of NaCl was added as percentage by mass of geopolymer solids, which includes the NaOH solids. Thus, lower free chloride content in some cases at higher molarity of NaOH solution may be attributed to the dominant effect of formation of denser microstructure that resulted in lower amount of chloride ions in the pore solution of GPC mixes. Similarly, the higher free chloride content in some cases at lower molarity of NaOH solution may be ascribed to the fact that the $(OH)^-$ ions may compete with Cl^- ions to a comparatively lower extent thereby resulting in more amount of chloride ions in the pore solution. Further, the formation of denser microstructure at higher molarity (16 M) of NaOH solution at the age of 90 days resulted in lower chloride concentration in the pore solution of GPC mixes thereby showing lower free chloride content as compared to that at lower molarity of NaOH solution.

The free chloride content mostly increased with increase in age from 7 to 28 days, whereas it mostly decreased from 28 to 90 days, except few cases, irrespective of molarity of NaOH solution and admixed NaCl dosage as evident from Fig. 4.23 (a) to 4.27 (a). The lower free chloride content at the early age i.e., 7 days may be ascribed to the dominant effect of $(OH)^-$ ions competing with Cl^- ions to a comparatively higher extent thereby resulting in less amount of chloride ions in the pore solution at the age of 7 days over the effect of denser microstructure at the age of 28 days as compared to 7 days. It may be noted that the compressive strength of GPC mixes was mostly higher at the age of 28 days than that at the age of 7 days (Fig. 4.8). The lower free chloride content of GPC mixes at the age of 90 days when compared with 28 days for NaOH solution of 16 M is ascribed to the significant effect of formation of compact microstructure that resulted in lower amount of chloride ions in the concrete pore solution. This is in line with the higher compressive strength of GPC mixes made with NaOH solution of 16 M at the age of 90 days as compared to that at 28 days (Fig. 4.8(e)). It may be noted that the compressive strength of GPC mixes was mostly lower at the age of 90 days as compared to that at 28 days for NaOH solution molarity of 8 M to 14 M (Fig. 4.8 (a-d)). Thus, the significant effect of $(OH)^-$ ions competing with Cl^- ions to a comparatively greater extent as a result of alteration in the microstructure led to lower amount of chloride ions in the pore solution of GPC mixes at the age of 90 days when compared with that at the age of 28 days for NaOH solution molarity of 8 M to 14 M.

From Fig. 4.23 (b) to 4.27 (b), it is inferred that the total chloride content increased with increase in admixed NaCl concentration regardless of NaOH solution molarity and age. Further, there was no systematic variation in total chloride content of GPC mixes with molarity of NaOH solution irrespective of age except few cases at the age of 90 days where mostly lower total chloride content was observed at 16 M NaOH solution than lower molarity of NaOH solution. This variation in total chloride content is similar to that in case of free chloride content. Further, the total chloride content mostly increased with increase in age from 7 to 28 days, whereas it mostly decreased from 28 to 90 days (Fig. 4.23 (b) to 4.27 (b)), which is similar to the variation in free chloride content with age.

The bound chloride content was calculated as the difference of total chloride and free chloride content. The obtained bound chloride contents of GPC mixes are illustrated in Fig. 4.23 (c) to 4.27 (c). From these figures, it is inferred that the bound chloride content was very less thereby indicating significantly lower chloride binding capacity of fly ash based geopolymer concrete. The chloride binding may be attributed to the physical adsorption of chloride ions on the sodium aluminosilicate hydrate (N-A-S-H) gel in the GPC mixes [39]. Although there was lower extent of chloride binding, while analyzing the variation in bound chloride content, it is inferred that mostly there is increasing trend of bound chloride content with increase in molarity of NaOH solution, which indicates comparatively greater extent of physical adsorption of chloride ions on the N-A-S-H gel at higher molarity of NaOH solution. Further, mostly there was unsystematic variation in bound chloride content with age from 7 to 28 days and that from 28 to 90 days. It may be noted that as stated earlier, both free and total chloride content increased with increase in age from 7 to 28 days whereas both decreased with age from 28 to 90 days. Thus, the unsystematic variation in bound chloride content with age may be ascribed to the inconsistent variation in both free chloride and total chloride content with increase in age at different molarity of NaOH solution. From 4.23 (c) to 4.27 (c), the bound chloride content mostly increased with increase in admixed NaCl concentration from 1.5% to 3% regardless of molarity of NaOH solution and age. This indicates comparatively higher extent of physical adsorption of chloride ions on geopolymer gels, which may be ascribed to the effect of presence of more amount of chloride ions in the GPC mixes with increase in admixed NaCl concentration from 1.5% to 3%. From Fig. 4.23 (c) to Fig. 4.27 (c), there was mostly increase in bound chloride content with increase in admixed NaCl concentration from 3% to 4.5% in majority of the cases, whereas in some cases, the opposite variation was observed mostly in case of higher molarity of NaOH solution. In these cases, the lower bound chloride content at NaCl concentration of 4.5% (although there was presence of more amount

of chloride ions in GPC mixes) indicates lower extent of physical adsorption of chloride ions, which may be due to the effect of alteration in the extent of interaction of chloride ions with geopolymer gels. In few cases, the total chloride content was equal to free chloride content in the GPC mixes. Therefore, the bound chloride content was shown as 0% for those cases (Fig. 4.23 (c), Fig. 4.24 (c), 4.26 (c), and Fig. 4.27 (c)).

4.4.2 Effect of alkaline solution content on chloride content of GPC

The obtained free, total and bound chloride content of geopolymer concrete (GPC) mixes made with alkaline solution content of 190 kg/m^3 and 210 kg/m^3 are illustrated in Fig. 4.28 (a, b, c) and Fig. 4.29 (a, b, c) respectively for 7 days and 28 days.

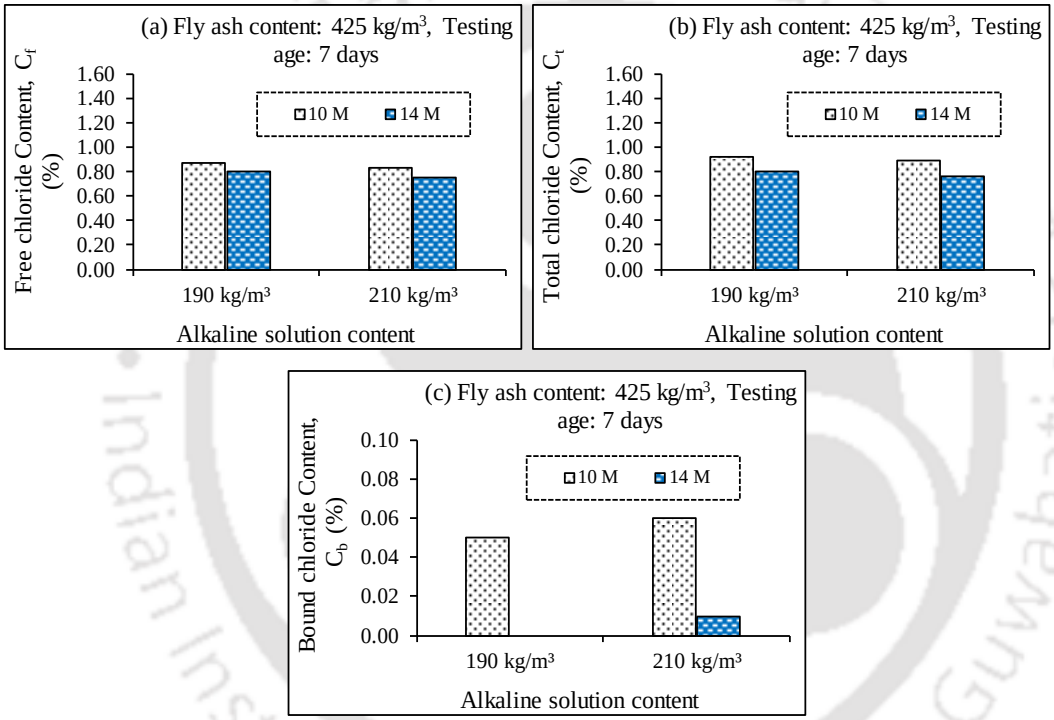

(GPC made with fly ash passing through 150 μm sieve, fly ash content of 425 kg/m^3, and SS/SH ratio of 1.75)

Fig. 4.28: GPC prepared with alkaline solution content of 190 kg/m^3 and 210 kg/m^3, and admixed with 3% NaCl: (a) Free chloride content, (b) Total chloride content and (c) Bound chloride content at the age of 7 days

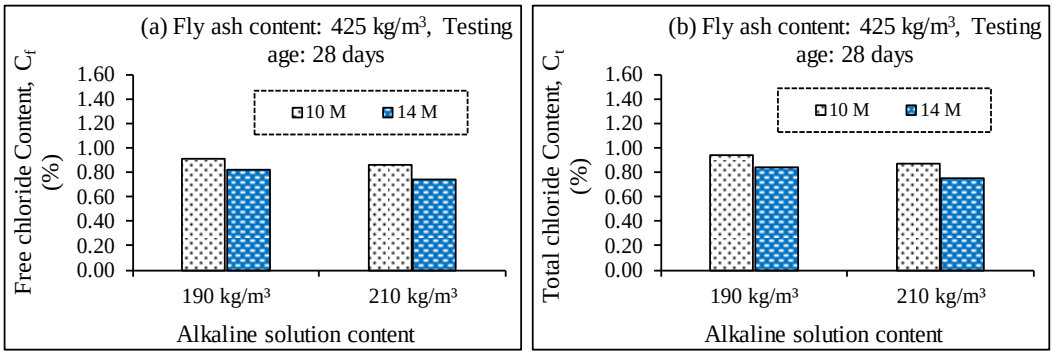

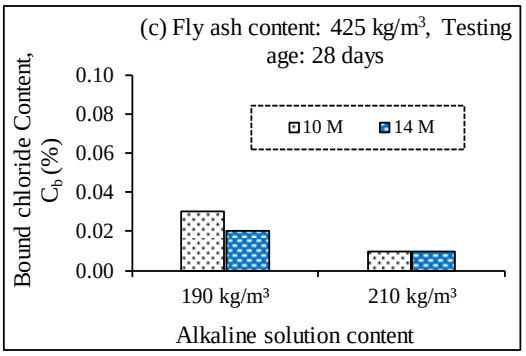

(GPC made with fly ash passing through 150 μm sieve, fly ash content of 425 kg/m^3, and SS/SH ratio of 1.75)

Fig. 4.29: GPC prepared with alkaline solution content of 190 kg/m^3 and 210 kg/m^3, and admixed with 3% NaCl: (a) Free chloride content, (b) Total chloride content and (c) Bound chloride content at the age of 28 days

From Fig. 4.28 (a) and Fig. 4.29 (a), it is noted that free chloride content decreased with increase in alkaline solution content for both molarity of NaOH solution at both 7 and 28 days. It may be noted that, as discussed earlier, the compressive strength increased with increase in alkaline solution content for 10 M NaOH solution whereas the opposite variation was observed for NaOH solution of 14 M in case of GPC mixes admixed with 3% NaCl (Fig. 4.9 and 4.10). Further, the amount of chloride ions admixed in the GPC mixes was more at higher alkaline solution content than lower alkaline solution content for both molarity of NaOH solution, as NaCl was admixed as percentage by mass of geopolymer solids, which includes the solids present in both NaOH and Na_2SiO_3 solutions. Thus, the formation of denser microstructure resulting in higher compressive strength at higher alkaline solution content contributed toward lower amount of chloride ions in the pore solution thereby showing lower free chloride content in the GPC mixes made with higher alkaline solution content for 10 M NaOH solution, although the amount of chloride ions added was more. At NaOH solution of 14 M, the denser microstructure as indicated by higher compressive strength at lower alkaline solution content did not affect the variation in chloride ion concentration in the pore solution significantly thereby leading to comparatively more free chloride content at lower alkaline solution content. From Fig. 4.28 (a) and 4.29 (a), the free chloride content was lower at higher molarity of NaOH solution (14 M) as compared to lower molarity of NaOH solution (10 M) in the GPC mixes made with fly ash passing through 150 μm sieve. The formation of denser microstructure leading to higher compressive strength at NaOH solution of 14 M as compared to NaOH solution of 10 M (Fig. 4.9 and 4.10) resulted in lower amount of chloride ions in the pore solution of GPC mix. It may be noted that there was unsystematic variation in free chloride content with molarity of NaOH solution in the GPC mixes made with fly ash passing through

300 μm sieve (Fig. 4.23 (a) to Fig. 4.27 (a)). This indicates that the particle size of fly ash affected the availability of chloride ions in the pore solution as a result of alteration in the microstructure of the GPC mixes. Further, from Fig. 4.28 (a) and Fig. 4.29 (a), the free chloride content mostly increased (although the increase was less) with age from 7 to 28 days for both alkaline solution contents and molarity of NaOH solution. It can be noted that the compressive strength of GPC increased with increase in age from 7 to 28 days (Fig. 4.9 and 4.10). Thus, availability of lower amount of Cl^- ions in the pore solution as a result of alteration in the extent of competing effect of $(OH)^-$ ions with Cl^- ions led to lower free chloride content at early age over the effect of variation in formation of microstructure with age as indicated by the compressive strength of GPC mixes.

From Fig. 4.28 (b) and Fig. 4.29 (b), it is noted that the total chloride content decreased with increase in alkaline solution content. Further, the total chloride content was higher at lower molarity of NaOH solution as compared to that at higher molarity of NaOH solution. These variations in total chloride content with alkaline solution content and molarity of NaOH solution are similar to that in case of free chloride content. Further, there was unsystematic variation in total chloride content with age as the total chloride content increased with age at lower alkaline solution content whereas it decreased with age at higher alkaline solution content. This indicates that the variation in alkaline solution content affected the chloride ion content in the GPC mixes as a result of alteration in the availability of free chloride ions in the pore solution as well as in the interaction of chloride ions with aluminosilicate network in the GPC mixes with age.

The bound chloride content shown in Fig. 4.28 (c) and Fig. 4.29 (c) indicated lower extent of chloride binding in the GPC mixes. As observed from Fig. 4.28 (c) and Fig. 4.29 (c), the bound chloride content was slightly higher at higher alkaline solution content as compared to that at lower alkaline solution content at the age of 7 days whereas, the opposite variation was observed at the age of 28 days. It may be noted that, as stated earlier, both free and total chloride content decreased with increase in alkaline solution content at both ages. Thus, the inconsistent variation in bound chloride content (although the difference was less) with alkaline solution content at different ages may be ascribed to the changes in the extent of physical adsorption of chloride ions on geopolymer gels. Further, the bound chloride content was mostly higher at lower molarity of NaOH solution than that at higher molarity of NaOH solution (Fig. 4.28 (c) and Fig. 4.29 (c)). It may be noted that there was mostly increasing trend of bound chloride content with increase in molarity of NaOH solution in case of GPC mixes made with fly ash

passing through 300 μm sieve (Fig. 4.23 (c) to Fig. 4.27 (c)). Thus, higher bound chloride content at lower molarity of NaOH solution (Fig. 4.28 (c) and Fig. 4.29 (c)) in the GPC mixes made with smaller fly ash particles (passing through 150 μm sieve) indicates changes in the extent of interaction of chloride ions with the aluminosilicate network due to combined effect of smaller fly ash particles and lower molarity of NaOH solution. Further, the bound chloride content decreased with age for NaOH solution of 10 M whereas there was no systematic variation in bound chloride content with age for NaOH solution of 14 M. It may be noted that, as stated earlier, the free chloride content mostly increased with age whereas, there was unsystematic variation in total chloride content with age for different alkaline solution contents. Thus, the aforementioned variation in bound chloride content with age for different molarity of NaOH solution may be ascribed to the changes in the extent of release of chloride ions from aluminosilicate gel with age.

4.4.3 Effect of ratio of alkaline solution (SS/SH ratio) on chloride content of GPC

The free, total and bound chloride content of GPC mixes made with alkaline solution ratios of 1.5 and 1.75 are shown Fig. 4.30 (a, b, c) and Fig. 4.31 (a, b, c) respectively for the age of 7 days and 28 days.

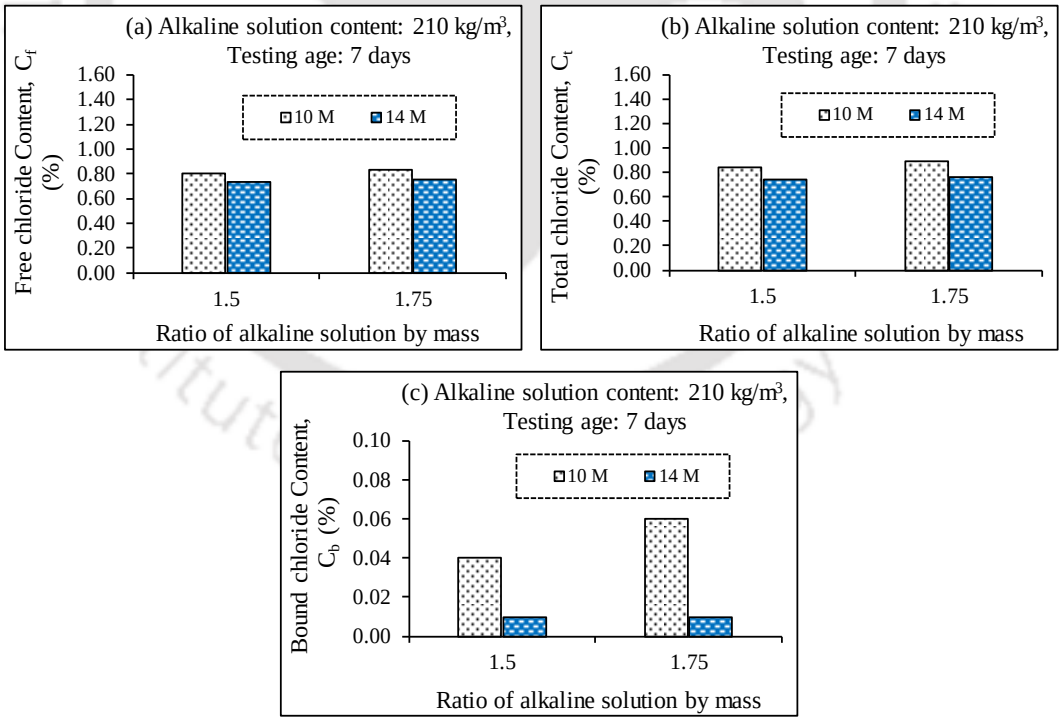

(GPC made with fly ash passing through 150 μm sieve, fly ash content of 425 kg/m³, and alkaline solution content of 210 kg/m³)

Fig. 4.30: GPC prepared with SS/SH ratio of 1.5 and 1.75, and admixed with 3% NaCl: (a) Free chloride content, (b) Total chloride content and (c) Bound chloride content at the age of 7 days

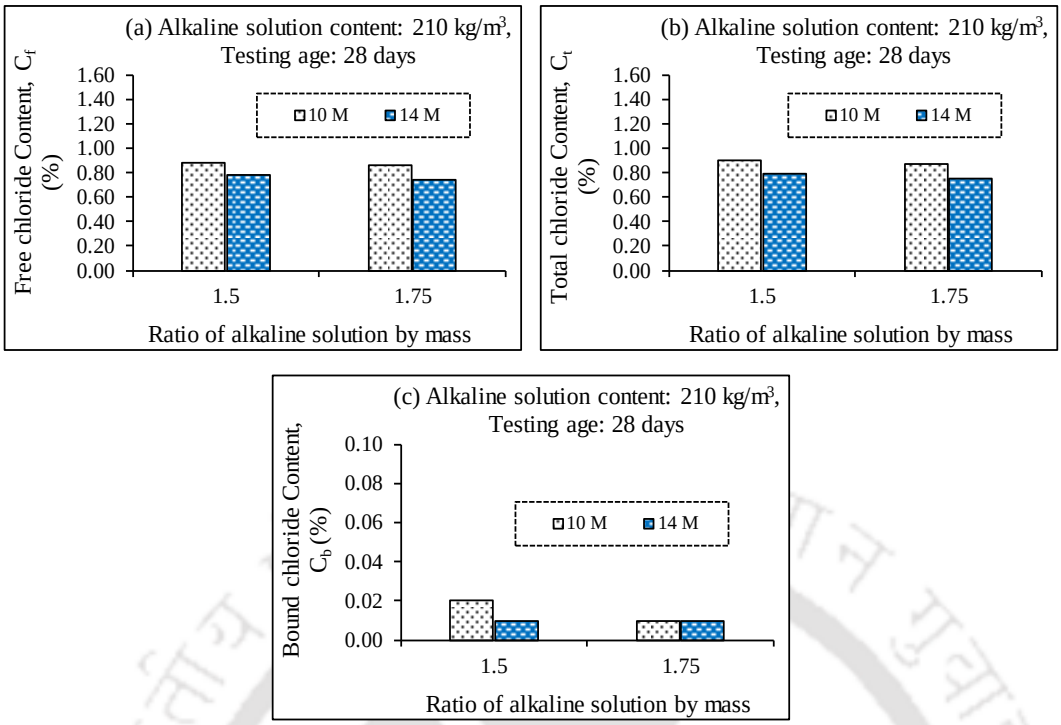

(GPC made with fly ash passing through 150 μm sieve, fly ash content of 425 kg/m³, and alkaline solution content of 210 kg/m³)

Fig. 4.31: GPC prepared with SS/SH ratio of 1.5 and 1.75, and admixed with 3% NaCl: (a) Free chloride content, (b) Total chloride content and (c) Bound chloride content at the age of 28 days

From Fig. 4.30 (a) and Fig. 4.31 (a), it is inferred that the free chloride content increased with increase in SS/SH ratio at the age of 7 days whereas the opposite variation was observed at the age of 28 days for both molarity of NaOH solution. As stated earlier (Section 4.3.3), the compressive strength of 3% NaCl admixed GPC mixes increased with increase in SS/SH ratio at NaOH solution of 10 M while the opposite variation was obtained at NaOH solution of 14 M for both ages. From these observations, mostly there is inconsistent variation in the free chloride content of GPC mixes with increase in SS/SH ratio when compared with the variations in the formation of microstructure as indicated by the compressive strength at different ages for different molarity of NaOH solution. Thus, the substantial effect of alterations in the extent of $(OH)^-$ ions competing with Cl^- ions resulted in an inconsistent variation in the availability of chloride ions in the pore solution of GPC mixes with change in SS/SH ratio. As inferred from Fig. 4.30 (a) and Fig. 4.31 (a), the free chloride content decreased with increase in molarity of NaOH solution in the GPC mixes. It may be noted that, as stated earlier, the compressive strength was higher at higher molarity of NaOH solution than that at lower molarity (Fig. 4.11 and 4.12). Thus, comparatively compact microstructure at higher molarity of NaOH solution led to lower availability of chloride ions in the pore solution of GPC mixes

thereby showing lower free chloride content. The free chloride content of GPC mixes mostly increased with increase in age from 7 to 28 days for both molarity of NaOH solution, and SS/SH ratio as inferred from Fig. 4.30 (a) and Fig. 4.31 (a). As stated earlier (Fig. 4.11 and 4.12), the compressive strength of GPC increased with age from 7 to 28 days. This indicates that the significant effect of change in the concentration of Cl^- ions in the pore solution with age due to competing effect of $(OH)^-$ ions with Cl^- ions resulted in inconsistent variation in free chloride content with increase in age when compared with the variation in compressive strength of GPC.

The total chloride content of GPC mixes increased with increase in SS/SH ratio at the early age of 7 days while at the age of 28 days, the opposite variation was observed (Fig. 4.30 (b) and Fig. 4.31 (b)), which is similar to the variation in free chloride content. In addition, the total chloride content decreased with increase in molarity of NaOH solution from 10 M to 14 M at both SS/SH ratios (similar variation as in case of free chloride content). Further, the total chloride content increased with age from 7 to 28 days at lower SS/SH ratio whereas it decreased slightly with age at higher SS/SH ratio. Thus, when compared with the variation in free chloride content with age, the inconsistent variation in total chloride content with age at different SS/SH ratios indicates variations in the extent of interaction of chloride ions with the aluminosilicate gels in the GPC mixes.

From Fig. 4.30 (c) and Fig. 4.31 (c), the bound chloride content increased slightly with increase in SS/SH ratio at the age of 7 days whereas the opposite variation was observed at the age of 28 days for NaOH solution of 10 M. However, at NaOH solution of 14 M, there was no difference in the bound chloride content with change in SS/SH ratio. Thus, insignificant extent of physical adsorption of chloride ions on aluminosilicate gels resulted in an inconsistent variation in bound chloride content with change in SS/SH ratio for different molarity of NaOH solution. Further, mostly lower bound chloride content was observed at higher molarity of NaOH solution than lower molarity of NaOH solution for both SS/SH ratios as noted from Fig. 4.30 (c) and Fig. 4.31 (c). As discussed earlier, the free chloride as well as total chloride content decreased with increase in molarity of NaOH solution for both SS/SH ratios. Thus, lower bound chloride content at higher molarity of NaOH solution indicates changes in the extent of adsorption of chloride ions on the aluminosilicate gels as there was more formation of aluminosilicate gels at higher molarity of NaOH solution than lower molarity of NaOH solution as indicated by the obtained compressive strength of GPC mixes (Fig. 4.11 and 4.12). Further, at higher molarity of NaOH solution, the excess sodium ion concentration might have

inhibited the physical adsorption of chloride ions with aluminosilicate gels to certain extent. The bound chloride content decreased with age from 7 to 28 days at NaOH solution of 10 M while there was no difference in bound chloride content with age at NaOH solution of 14 M (4.30 (c) and Fig. 4.31 (c)). As discussed earlier (Fig. 4.11 and 4.12), the compressive strength of GPC increased with age from 7 to 28 days. Although, there was increase in the formation of geopolymer gels with increase in age, the lower bound chloride content at comparatively later age of 28 days as compared to early age of 7 days for NaOH solution of 10 M may be due to the release of physically adsorbed chloride ions from the aluminosilicate gels, which is in line with higher free chloride content at the age of 28 days. Further, the same bound chloride content irrespective of age (7 and 28 days) at NaOH solution of 14 M indicates insignificant change in the extent of physical binding of chloride ions with aluminosilicate gels with age at higher molarity of NaOH solution.

4.4.4 Effect of particle size of fly ash on chloride content of GPC

The obtained free, total and bound chloride content of GPC mixes made with fly ash passing through 150 μm sieve, and 300 μm sieve are shown in 4.32 (a, b, c) and Fig. 4.33 (a, b, c) respectively for the age of 7 days and 28 days for fly ash content of 425 kg/m^3.

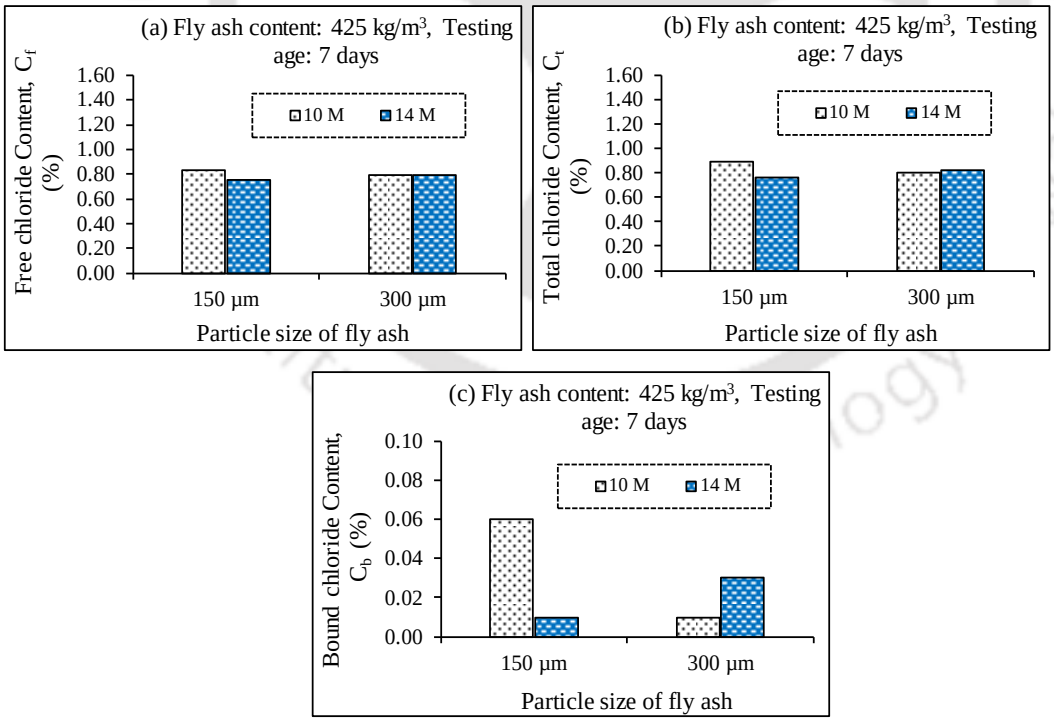

(GPC made with fly ash content of 425 kg/m^3, alkaline solution content of 210 kg/m^3 and SS/SH ratio of 1.75)

Fig. 4.32: GPC prepared with fly ash passing through 150 μm sieve, and 300 μm sieve, and admixed with 3% NaCl: (a) Free chloride content, (b) Total chloride content and (c) Bound chloride content at the age of 7 days

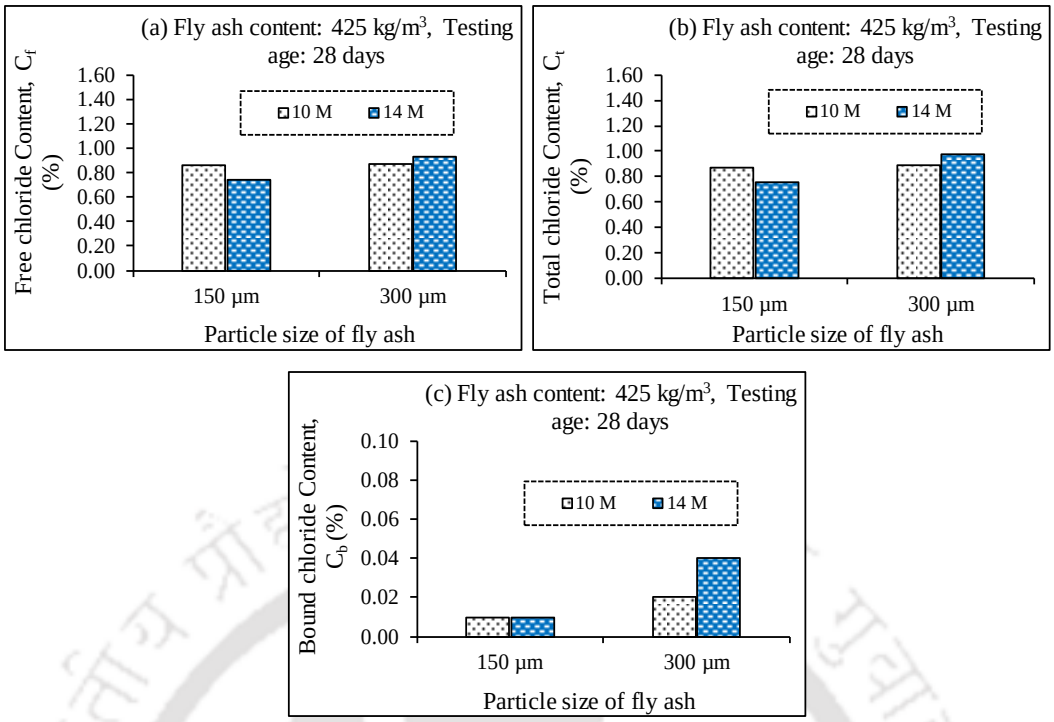

(GPC made with fly ash content of 425 kg/m^3, alkaline solution content of 210 kg/m^3 and SS/SH ratio of 1.75)

Fig. 4.33: GPC prepared with fly ash passing through 150 µm sieve, and 300 µm sieve, and admixed with 3% NaCl: (a) Free chloride content, (b) Total chloride content and (c) Bound chloride content at the age of 28 days

From Fig. 4.32 (a) and 4.33 (a), the free chloride content of GPC mixes was mostly higher in case of fly ash passing through 300 µm sieve than that passing through 150 µm sieve. As observed from the results of compressive strength (Fig. 4.13 and 4.14), the compressive strength of GPC mixes was higher for fly ash passing through 300 µm sieve as compared to that passing through 150 µm sieve at fly ash content of 425 kg/m^3. Although there was formation of compact microstructure in the GPC mixes in case of larger fly ash particles at comparatively lower fly ash content of 425 kg/m^3 as indicated by the compressive strength, the higher free chloride content in case of larger fly ash particles may be ascribed to the availability of more amount of chloride ions in the pore solution of GPC. From Fig. 4.32 (a) and 4.33 (a), the free chloride content was higher at lower molarity of NaOH solution in case of fly ash passing through 150 µm sieve whereas mostly opposite variation was observed in case of fly ash passing through 300 µm sieve. However, as discussed earlier, higher compressive strength was observed at higher molarity of NaOH solution than lower molarity for both sizes of fly ash particles (Fig. 4.13 and 4.14). Thus, the variation in the concentrations of different ionic species in pore solution i.e., Na^+ ions, K^+ ions, $(OH)^-$ ions etc., significantly influenced the availability of chloride ions at higher molarity of NaOH solution in case of larger fly ash

particles over the effect of comparatively compact microstructure of GPC at higher molarity of NaOH solution. Further, the free chloride content mostly increased with age from 7 to 28 days (Fig. 4.32 (a) and 4.33 (a)). However, there was increase in compressive strength with increase in age from 7 to 28 days (Fig. 4.13 and 4.14), which indicates inconsistent variation in free chloride content with age as compared to the variation in the formation of microstructure with age. As observed from Fig. 4.32 (b) and 4.33 (b), the variations in total chloride content with particle size of fly ash and molarity of NaOH solution were similar to that in case of free chloride content. Further, there was slightly lower total chloride content at the age of 28 days as compared to 7 days in case of fly ash passing through 150 μm sieve whereas the total chloride content increased with increase in age from 7 to 28 days for fly ash passing through 300 μm sieve. Thus, the alterations in the extent of physical adsorption of chloride ions with N-A-S-H gel contributed toward the opposite variation in total chloride content with increase in age for fly ash particles of different sizes.

From Fig. 4.32 (c) and 4.33 (c), the bound chloride content was mostly higher in the GPC mixes made with larger fly ash particles as compared to smaller fly ash particles. It may be noted that the compressive strength was higher in the GPC mixes made with larger fly ash particles as compared to smaller fly ash particles (Fig. 4.13 and 4.14). Thus, formation of more amount of geopolymer gels resulted in comparatively higher extent of adsorption of chloride ions in the GPC mixes made with larger fly ash particles. While analyzing the effect of concentration of NaOH solution, it is inferred that the bound chloride content increased with increase in molarity of NaOH solution in the GPC mixes made with larger fly ash particles (passing through 300 μm sieve). In case of GPC mixes made with smaller fly ash particles (passing through 150 μm sieve), the bound chloride content decreased with increase in molarity of NaOH solution at the age of 7 days, however, there was no difference in bound chloride content with change in molarity of NaOH solution at the age of 28 days. Thus, more bound chloride content at higher molarity of NaOH solution in the GPC mixes made with larger fly ash particles (passing through 300 μm sieve) is in line with the variation in compressive strength of GPC (Fig. 4.13 and 4.14), where more formation of aluminosilicate gels led to higher extent of physical binding of chloride ions with binding gels in the GPC mixes. Further, the bound chloride content did not change with age for 14 M NaOH solution, however it decreased with age for NaOH solution of 10 M in case of smaller fly ash particles. In case of larger fly ash particles, the bound chloride content slightly increased with age for both molarity of NaOH solution, which is consistent with the increase in formation of geopolymer gels with

increase in age as indicated by the compressive strength that resulted in comparatively more physical binding of chloride ions at later age in the GPC mixes. It may be noted that the variation in bound chloride content with age (Fig. 4.32 (c) and 4.33 (c)) is similar to that in case of total chloride content with age (Fig. 4.32 (b) and 4.33 (b)) in the GPC mixes.

The free, total and bound chloride content of GPC mixes made with fly ash passing through 150 μm sieve, and 300 μm sieve are shown in 4.34 (a, b, c), Fig. 4.35 (a, b, c), and Fig. 4.36 (a, b, c) respectively for the age of 7 days, 28 days, and 90 days for fly ash content of 450 kg/m^3.

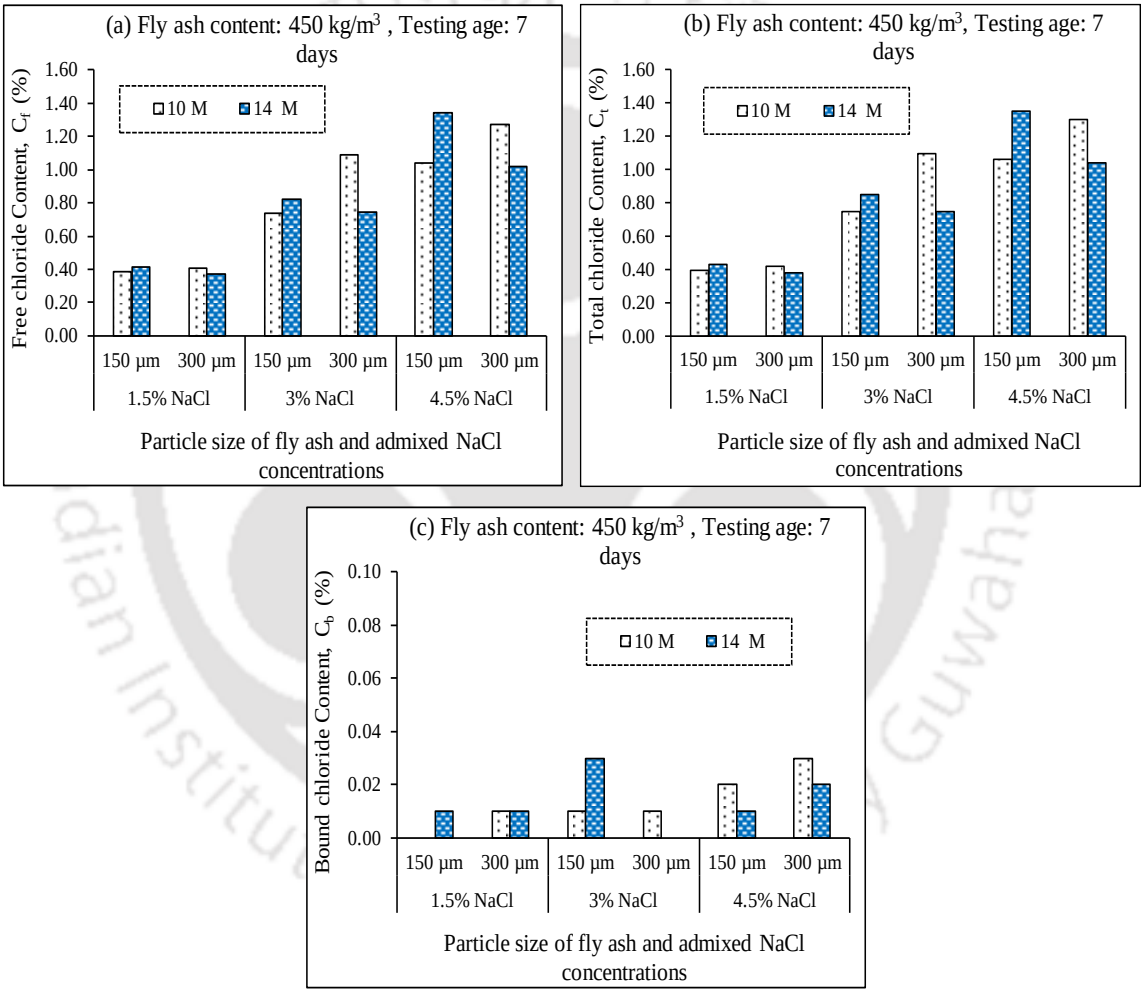

(GPC made with fly ash content of 450 kg/m^3, alkaline solution content of 210 kg/m^3 and SS/SH ratio of 1.75)

Fig. 4.34: GPC prepared with fly ash passing through 150 μm sieve, and 300 μm sieve, and admixed with different concentrations of NaCl: (a) Free chloride content, (b) Total chloride content and (c) Bound chloride content at the age of 7 days

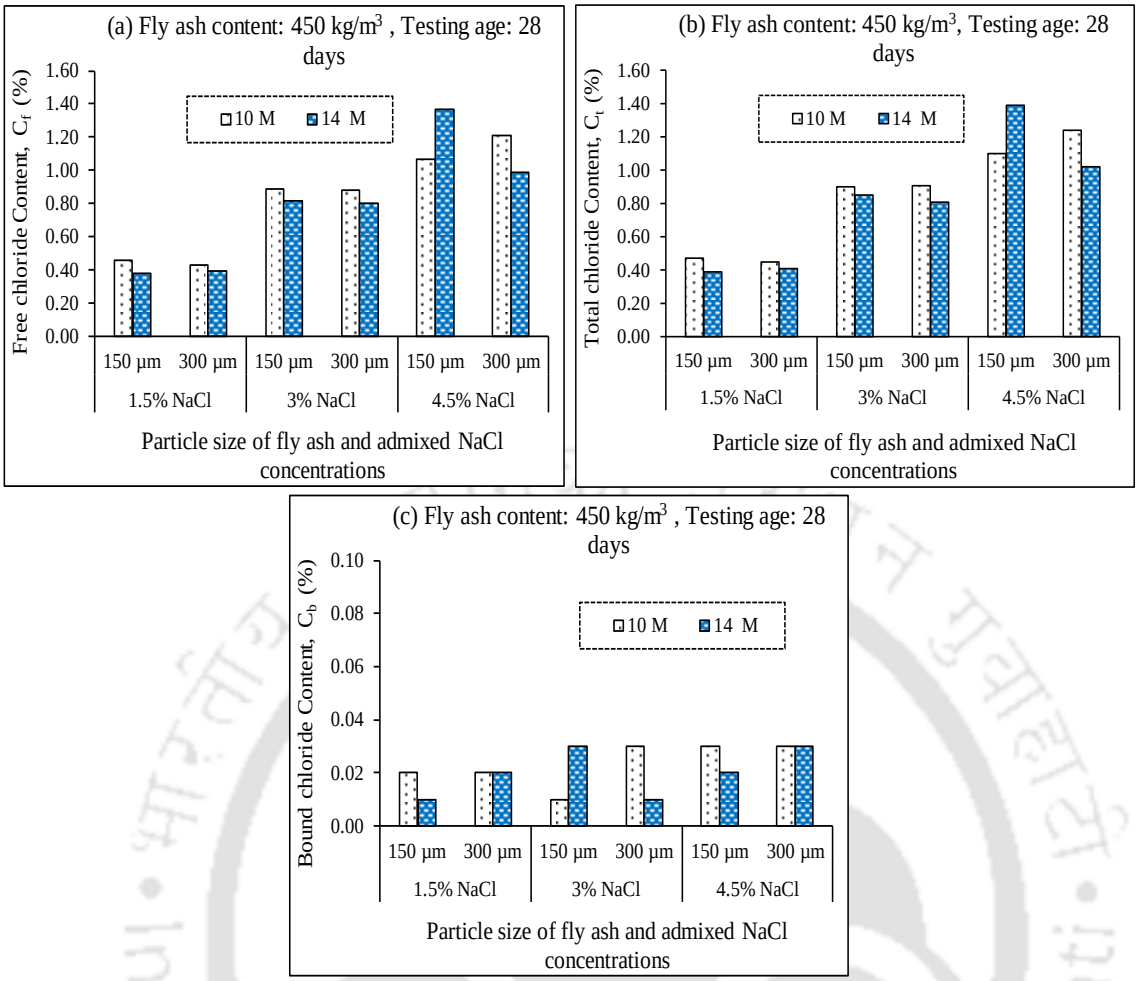

(GPC made with fly ash content of 450 kg/m³, alkaline solution content of 210 kg/m³ and SS/SH ratio of 1.75)

Fig. 4.35: GPC prepared with fly ash passing through 150 µm sieve, and 300 µm sieve, and admixed with different concentrations of NaCl: (a) Free chloride content, (b) Total chloride content and (c) Bound chloride content at the age of 28 days

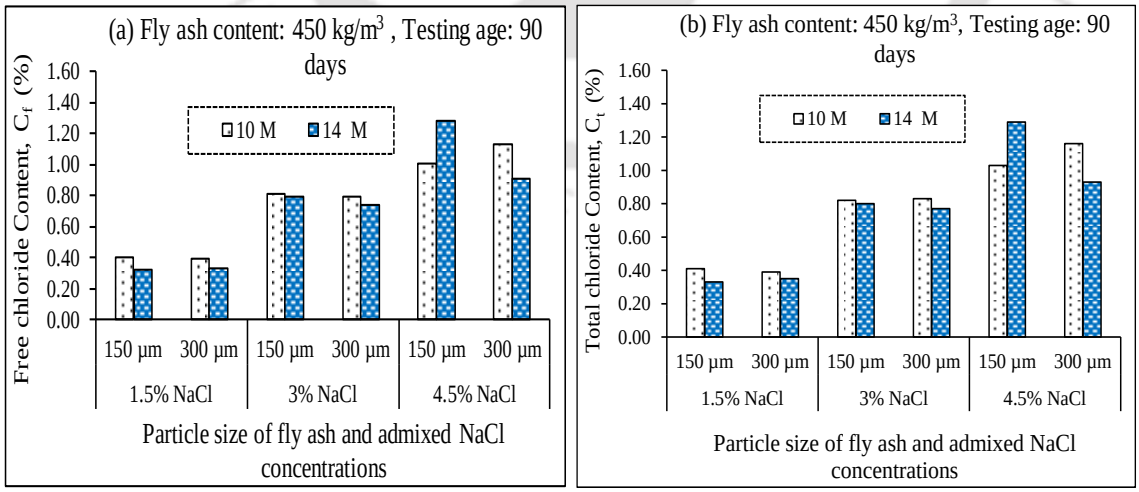

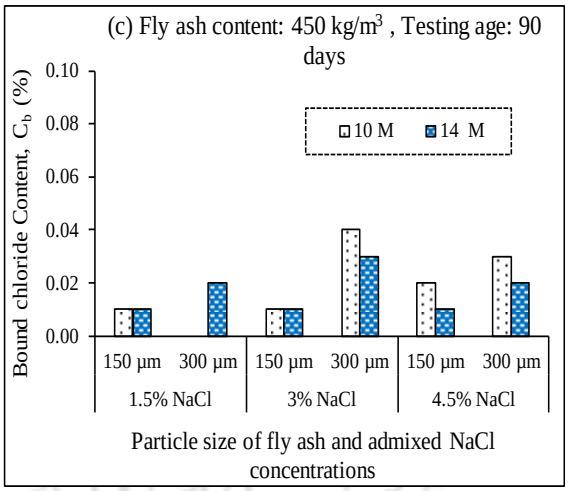

(GPC made with fly ash content of 450 kg/m^3, alkaline solution content of 210 kg/m^3 and SS/SH ratio of 1.75)

Fig. 4.36: GPC prepared with fly ash passing through 150 µm sieve, and 300 µm sieve, and admixed with different concentrations of NaCl: (a) Free chloride content, (b) Total chloride content and (c) Bound chloride content at the age of 90 days

From Fig. 4.34 (a) to 4.36 (a), it is observed that the free chloride content increased with increase in admixed NaCl concentration for both sizes of fly ash (i.e., passing through 150 µm, and 300 µm sieve) and both molarity of NaOH solution (i.e., 10 M and 14 M) at all ages (i.e., 7, 28, and 90 days). The presence of higher amount of chloride ions in the GPC mixes admixed with higher concentration of NaCl contributed toward higher free chloride content. Further, it is noted that the variation in free chloride content is mostly consistent with the variation in compressive strength of GPC mixes i.e., the free chloride content was mostly higher in the GPC mixes made with smaller fly ash particles (passing through 150 µm sieve) than larger fly ash particles (passing through 300 µm sieve) at all ages where the compressive strength was mostly lower in case of smaller fly ash particles as compared to larger fly ash particles (Fig. 4.15 to Fig. 4.17) for NaOH solution of 14 M. For NaOH solution of 10 M, the free chloride content was mostly higher in the GPC mixes made with larger fly ash particles as compared to smaller fly ash particles wherein the compressive strength was mostly lower in case of larger fly ash particles than smaller fly ash particles (Fig. 4.15 to Fig. 4.17). Thus, the variation in the formation of microstructure of GPC mixes as indicated by the compressive strength at different molarity of NaOH solution for fly ash particles of different sizes led to the above variation in the availability of chloride ions in the pore solution of GPC mixes.

From Fig. 4.34 (a) to 4.36 (a), the concrete made with higher molarity of NaOH solution (14 M) mostly exhibited lower free chloride content as compared to that made with lower molarity of NaOH solution (10 M) for both sizes of fly ash particles at different ages, which is in line with the variation in compressive strength of GPC mixes with change in molarity of NaOH

solution (Fig. 4.15 to Fig. 4.17). This indicates that the formation of improved microstructure at higher molarity of NaOH solution resulted in lower availability of chloride ions in the pore solution of GPC mixes. With increase in age, the free chloride content mostly increased from 7 to 28 days whereas it decreased from 28 to 90 days as observed from Fig. 4.34 (a) to 4.36 (a). This indicates mostly inconsistent variation in free chloride content with formation of microstructure as indicated by compressive strength of GPC with increase in age from 7 to 28 days whereas there was mostly consistent variation in free chloride content with compressive strength with increase in age from 28 to 90 days. It may be noted that the compressive strength of GPC mostly increased with increase in age from 7 to 28 days and that from 28 to 90 days (Fig. 4.15 to Fig. 4.17). From Fig. 4.34 (b) to 4.36 (b), it is observed that the total chloride content increased with increase in admixed NaCl concentration for both sizes of fly ash particles i.e., passing through 150 μm, and 300 μm sieve, irrespective of molarity of NaOH solution and age. Further, there is no systematic variation in total chloride content between both sizes of fly ash particles for both molarity of NaOH solution at different ages. This may be ascribed to the combined effect of alterations in the availability of chloride ions in the pore solution, and the extent of physical adsorption of chloride ions on geopolymer gels for fly ash particles of different sizes. As inferred from Fig. 4.34 (b) to 4.36 (b), the variations in total chloride content with increase in molarity of NaOH solution and age are similar to that in case of free chloride content for both sizes of fly ash particles.

From Fig. 4.34 (c) to 4.36 (c), the bound chloride content was slightly higher in most of the cases for fly ash passing through 300 μm sieve as compared to that passing through 150 μm sieve for both molarity of NaOH solution at different ages. As discussed earlier (Section 4.3.4), the compressive strength of GPC mixes was higher in case of fly ash passing through 150 μm sieve as compared to that passing through 300 μm sieve for NaOH solution of 10 M whereas mostly higher compressive strength was observed in case of fly ash passing through 300 μm sieve than that passing through 150 μm sieve for NaOH solution of 14 M (Fig. 4.15 to Fig. 4.17). Thus, formation of comparatively more amount of aluminosilicate gels in GPC mixes made with larger fly ash particles (passing through 300 μm sieve) at NaOH solution of 14 M as indicated by higher compressive strength led to comparatively more extent of physical adsorption of chloride ions on the aluminosilicate gels thereby showing higher bound chloride content. It may be noted that, as discussed earlier, the free chloride content was mostly lower in GPC mixes made with larger fly ash particles for NaOH solution of 14 M (Fig. 4.34 (a) to 4.36 (a)). At NaOH solution of 10 M, the lower bound chloride content in the GPC mixes made

with smaller fly ash particles (passing through 150 μm sieve), although the compressive strength was higher, may be ascribed to the effect of release of physically adsorbed chloride ions from the geopolymer gels. The release of chloride ions from the geopolymer gels led to comparatively higher free chloride content in the GPC mixes made with smaller fly ash particles for NaOH solution of 10 M (Fig. 4.34 (a) to 4.36 (a), discussed earlier). As observed from Fig. 4.34 (c) to 4.36 (c), the bound chloride content was slightly lower in majority of the cases for GPC mixes made with higher molarity of NaOH solution as compared to lower molarity of NaOH solution for both sizes of fly ash particles, which is in opposite variation with the compressive strength of GPC mixes as mostly higher compressive strength was observed at higher molarity of NaOH solution than lower molarity of NaOH solution (Fig. 4.15 to Fig. 4.17). This may be ascribed to the fact that the excess sodium ion concentration at higher molarity of NaOH solution might have hindered the physical adsorption of chloride ions with aluminosilicate gels to a certain degree. Further, the variations in bound chloride content with age from 7 to 28 days and that from 28 days to 90 days are similar to that in case of both free and total chloride contents (Fig. 4.34 (c) to 4.36 (c)). From 4.34 (c) to 4.36 (c), it is observed that the bound chloride content mostly increased with increase in admixed NaCl concentration from 1.5% to 3% irrespective of particle size of fly ash, molarity of NaOH solution and age, which shows higher extent of physical adsorption of chloride ions on N-A-S-H gel with increase in admixed NaCl concentration in GPC mixes from 1.5% to 3%. Between 3% and 4.5%, although there was more bound chloride content at NaCl concentration of 4.5% than that at 3% in majority of the cases, the opposite variation was observed in some cases, mostly at later age of 90 days. This may be ascribed to the effect of release of physically adsorbed chloride ions from the aluminosilicate gels to certain extent at later age in GPC mixes admixed with NaCl concentration of 4.5%.

4.4.5 Effect of fly ash content on chloride content of GPC

The free, total and bound chloride content of GPC mixes made with fly ash contents of 425 kg/m^3 and 450 kg/m^3 are shown in 4.37 (a, b, c), and Fig. 4.38 (a, b, c) respectively for the age of 7 days and 28 days for fly ash passing through 150 μm sieve.

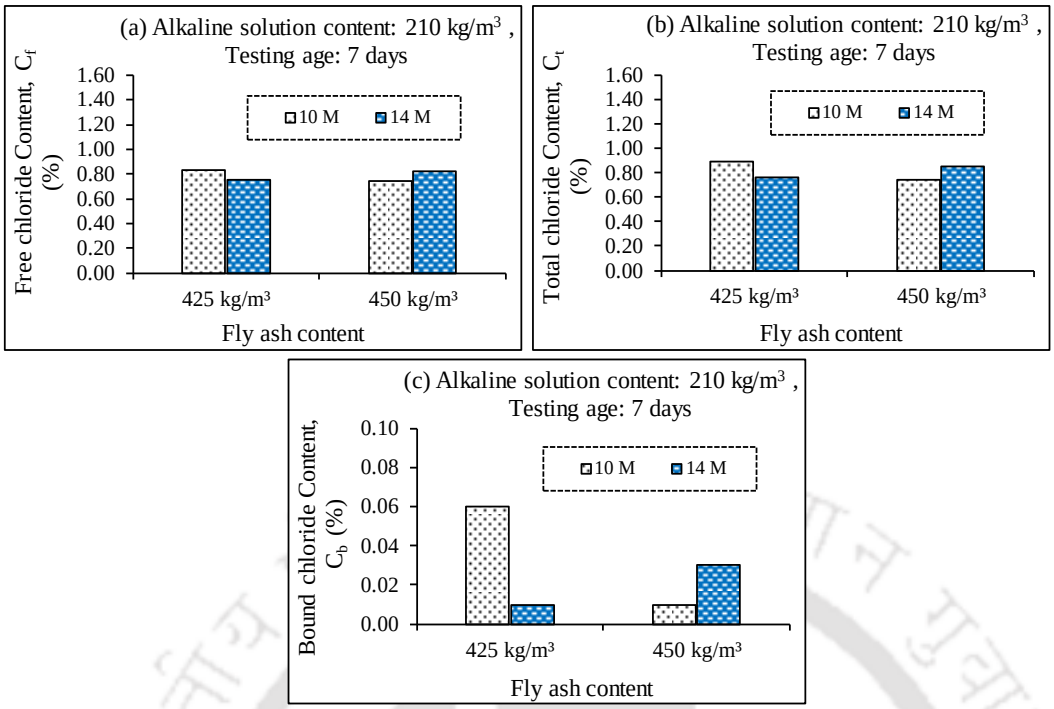

(GPC made with fly ash passing through 150 μm sieve, alkaline solution content of 210 kg/m³ and SS/SH ratio of 1.75)

Fig. 4.37: GPC prepared with fly ash content of 425 kg/m^3, and 450 kg/m^3, and admixed with 3% NaCl: (a) Free chloride content, (b) Total chloride content and (c) Bound chloride content at the age of 7 days

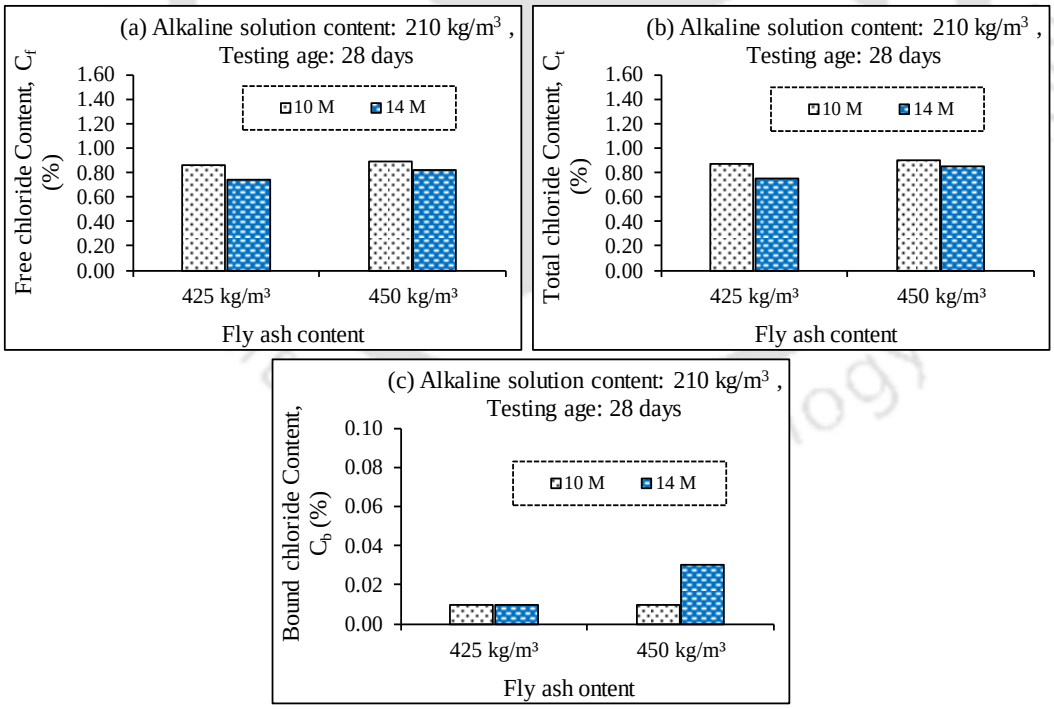

(GPC made with fly ash passing through 150 μm sieve, alkaline solution content of 210 kg/m³ and SS/SH ratio of 1.75)

Fig. 4.38: GPC prepared with fly ash content of 425 kg/m^3, and 450 kg/m^3, and admixed with 3% NaCl: (a) Free chloride content, (b) Total chloride content and (c) Bound chloride content at the age of 28 days

From Fig. 4.37 (a) and Fig. 4.38 (a), it is inferred that the GPC mixes made with higher fly ash content (450 kg/m^3) mostly exhibited higher free chloride content as compared to that made with lower fly ash content (425 kg/m^3). It may be noted that the amount of chloride ions added in the GPC mixes was more at higher fly ash content, as the dosage of NaCl was added as percentage by mass of geopolymer solids that includes fly ash content. Further, higher compressive strength indicating formation of denser microstructure was observed in case of fly ash content of 450 kg/m^3 as compared to fly ash content of 425 kg/m^3 (Fig. 4.18 and Fig. 4.19). Thus, the effect of addition of more amount of chloride ions in GPC mixes at higher fly ash content might have resulted in more free chloride content over the effect of formation of denser microstructure as indicated by higher compressive strength in case of fly ash content of 450 kg/m^3 as compared to fly ash content of 425 kg/m^3 (Fig. 4.18 and Fig. 4.19). While comparing the effect of molarity of NaOH solution, it is noted that the free chloride content was lower in case of higher molarity of NaOH solution (14 M) than lower molarity of NaOH solution (10 M) for fly ash content of 425 kg/m^3. The improved microstructure at higher molarity of NaOH solution for fly ash content of 425 kg/m^3 (as indicated by higher compressive strength, Fig. 4.18 and Fig. 4.19) resulted in lower amount of chloride ions in the GPC pore solution. However, there was unsystematic variation in free chloride content with molarity of NaOH solution for fly ash content of 450 kg/m^3. It may be noted that compressive strength was higher at lower molarity of NaOH solution than higher molarity of NaOH solution for fly ash content of 450 kg/m^3 in the presence of chloride ions (Fig. 4.18 and Fig. 4.19). Thus, the changes in the extent of formation of microstructure in the presence of chloride ions led to unsystematic variation in free chloride content with molarity of NaOH solution for higher fly ash content. Further, the free chloride content increased with age from 7 to 28 days for NaOH solution of 10 M whereas it mostly decreased slightly with age for NaOH solution of 14 M as inferred from Fig. 4.37 (a) and Fig. 4.38 (a). It may be noted that the compressive strength of GPC increased with age for both molarity of NaOH solution. The unsystematic variation in free chloride content with age between different molarity of NaOH solution may be ascribed to the effect of variations in the concentrations of different ionic species in the pore solution with age that led to changes in the availability of chloride ions in the pore solution of GPC.

The variations in total chloride content of GPC with fly ash content and NaOH solution molarity are similar to that of free chloirde conent as observed from Fig. 4.37 (b) and Fig. 4.38 (b). Further, the total chloride content decreased slightly with increase in age from 7 to 28 days for NaOH solution of 14 M whereas there was no systematic variation in total chloride content

with age for NaOH solution of 10 M. From Fig. 4.37 (c) and Fig. 4.38 (c), it is inferred that the GPC mixes made with higher fly ash content (450 kg/m^3) showed more bound chloride content than that made with lower fly ash content (425 kg/m^3) for NaOH solution of 14 M whereas for NaOH solution of 10 M, the bound chloride content was mostly lower at higher fly ash content as compared to lower fly ash content. The comparatively more extent of physical adsorption of chloride ions on binding gels resulted in higher bound chloride content as there was more formation of geopolymer gels in GPC mixes made with higher fly ash content at higher molarity of NaOH solution as indicated by the results of compressive strength (Fig. 4.18 and Fig. 4.19). It may be noted that the free chloride content was also higher at higher fly ash content (450 kg/m^3) than that at lower fly ash content (425 kg/m^3) for NaOH solution of 14 M. However, at NaOH solution of 10 M, mostly lower bound chloride content at higher fly ash content, although there was more formation of geopolymer gels as indicated by the compressive strength, may be attributed to the inadequate physical binding of chloride ions at lower molarity of NaOH solution, which resulted in higher free chloride content at higher fly ash content as compared to that at lower fly ash content for NaOH solution of 10 M. Further, the GPC mixes made with higher molarity of NaOH solution resulted in more bound chloride content than that made with lower molarity of NaOH solution at higher fly ash content whereas mostly opposite variation was observed at lower fly ash content (Fig. 4.37 (c) and Fig. 4.38 (c)). However, the variation in compressive strength (Fig. 4.18 and Fig. 4.19) with molarity of NaOH solution for different fly ash contents is opposite to the variation in bound chloride content. Thus, lower bound chloride content at higher molarity of NaOH solution (14 M) for lower fly ash content (425 kg/m^3) may be due to the effect of excess sodium ion concentration at higher molarity of NaOH solution that might have reduced the physical adsorption of chloride ions with aluminosilicate gels. Further, the lower bound chloride content at lower molarity of NaOH solution ((10 M) for higher fly ash content (450 kg/m^3) may be ascribed to the effect of more release of physically adsorbed chloride ions from the binding gels. From Fig. 4.37 (c) and Fig. 4.38 (c), the bound chloride content values indicated mostly insignificant binding of chloride ions with aluminosilicate gels with increase in age from 7 to 28 days.

The free, total and bound chloride content of GPC mixes made with fly ash content of 425 kg/m^3 and 450 kg/m^3 are illustrated in 4.39 (a, b, c), Fig. 4.40 (a, b, c), and Fig. 4.41 (a, b, c) for the age of 7 days, 28 days and 90 days respectively for fly ash passing through 300 μm sieve.

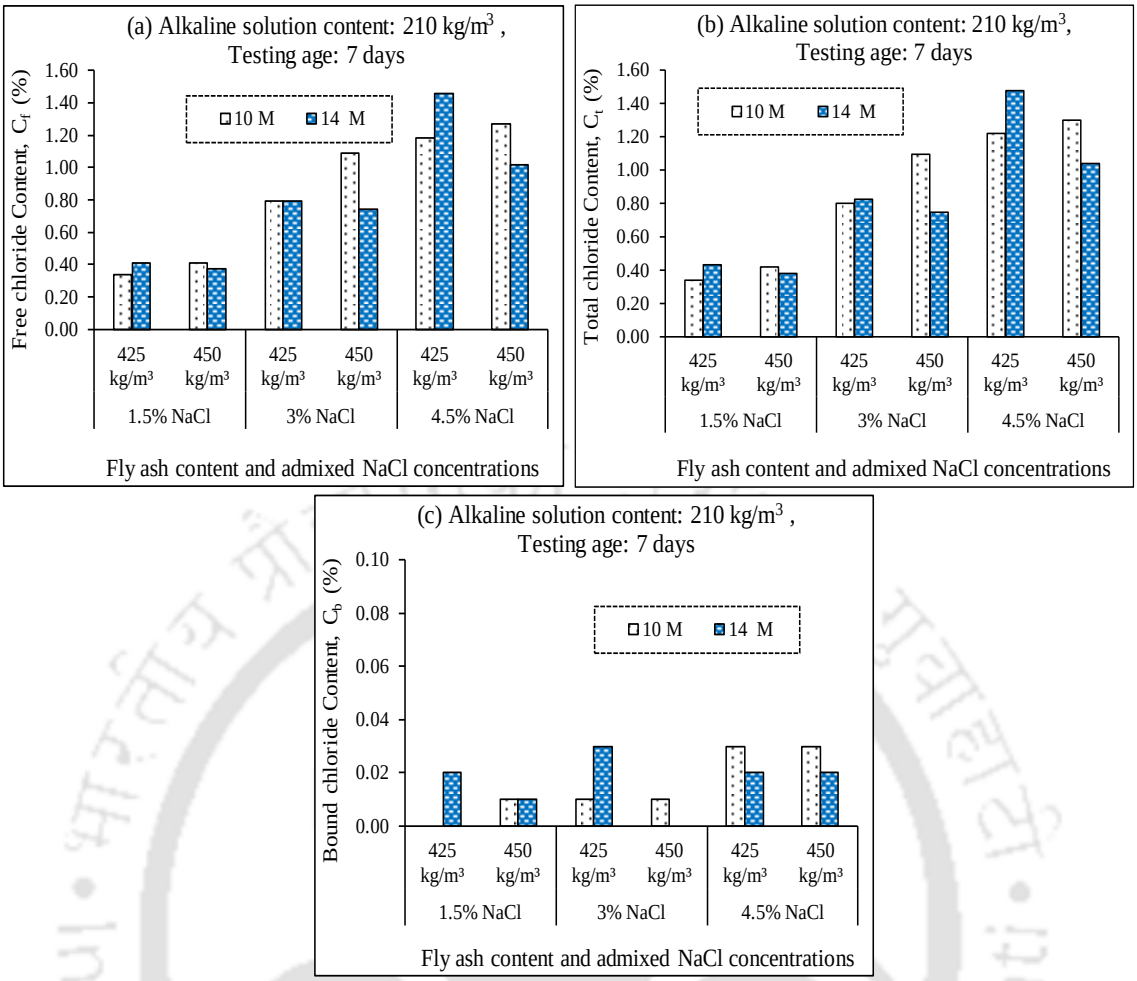

(GPC made with fly ash passing through 300 μm sieve, alkaline solution content of 210 kg/m^3 and SS/SH ratio of 1.75)

Fig. 4.39: GPC prepared with fly ash content of 425 kg/m^3, and 450 kg/m^3, and admixed with different concentrations of NaCl: (a) Free chloride content, (b) Total chloride content and (c) Bound chloride content at the age of 7 days

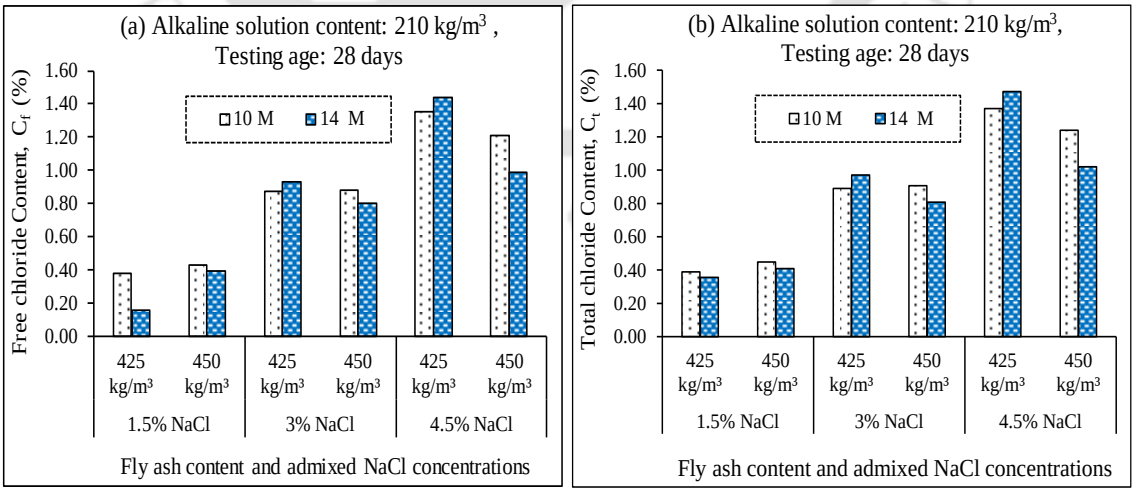

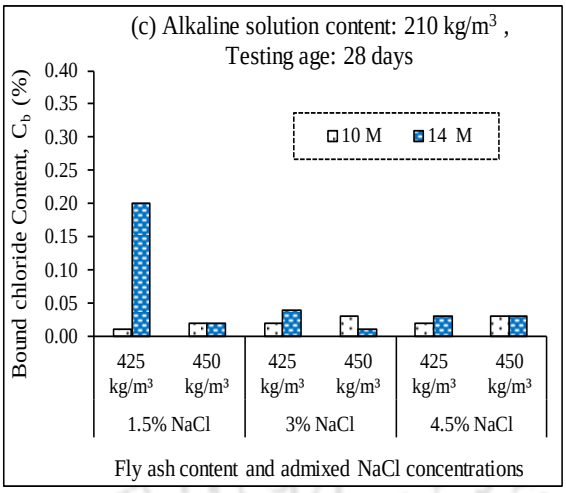

(GPC made with fly ash passing through 300 μm sieve, alkaline solution content of 210 kg/m^3 and SS/SH ratio of 1.75)

Fig. 4.40: GPC prepared with fly ash content of 425 kg/m^3, and 450 kg/m^3, and admixed with different concentrations of NaCl: (a) Free chloride content, (b) Total chloride content and (c) Bound chloride content at the age of 28 days

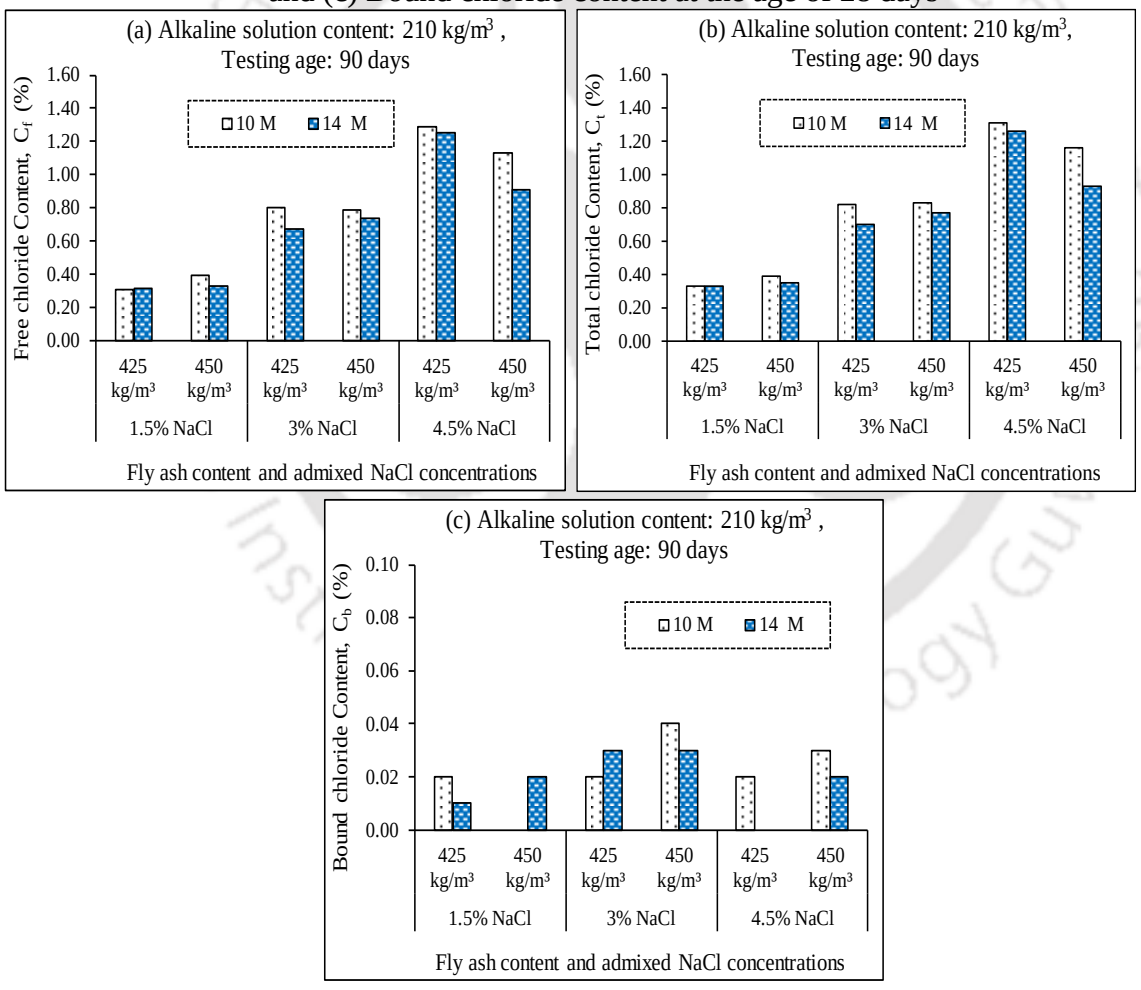

(GPC made with fly ash passing through 300 μm sieve, alkaline solution content of 210 kg/m^3 and SS/SH ratio of 1.75)

Fig. 4.41: GPC prepared with fly ash content of 425 kg/m^3, and 450 kg/m^3, and admixed with different concentrations of NaCl: (a) Free chloride content, (b) Total chloride content and (c) Bound chloride content at the age of 90 days

From Fig. 4.39 (a), Fig. 4.40 (a), and Fig. 4.41 (a), it is noted that the free chloride content of GPC mixes increased with increase in admixed NaCl concentration regardless of fly ash content, molarity of NaOH solution and age. It is observed that the free chloride content was mostly higher at higher fly ash content (450 kg/m^3) than that at lower fly ash content (425 kg/m^3) for NaOH solution of 10 M whereas, mostly opposite variation was observed in free chloride content with fly ash content for NaOH solution of 14 M (Fig. 4.39 (a), Fig. 4.40 (a), and Fig. 4.41 (a)). As stated earlier, the amount of chloride ions added in the GPC mixes was more at higher fly ash content than that at lower fly ash content, as NaCl was admixed as percentage by mass of geopolymer solids, which includes fly ash content. It may be noted that the GPC mixes made with lower fly ash content mostly exhibited higher compressive strength as compared to that made with higher fly ash content for both molarity of NaOH solution (Fig. 4.20, Fig. 4.21 and Fig. 4.22). Thus, the formation of comparatively denser microstructure at lower fly ash content for NaOH solution of 10 M as indicated by higher compressive strength as well as addition of comparatively lower amount of chloride ions in the GPC mixes at less fly ash content resulted in availability of lower amount of chloride ions in the pore solution of GPC. However, for NaOH solution of 14 M, although there was formation of denser microstructure at lower fly ash content as indicated by higher compressive strength, the higher free chloride content at lower fly ash content (though the amount of chloride added was less) may be ascribed to the effect of changes in the pore solution of GPC as a result of competing effect of chloride ions with other anions such as $(OH)^-$ ions in the pore solution.

With change in molarity of NaOH solution, it is inferred that the free chloride content was higher at lower molarity of NaOH solution (10 M) as compared to higher molarity of NaOH solution (14 M) for fly ash content of 450 kg/m^3 and fly ash passing through 300 µm sieve (Fig. 4.39 (a), Fig. 4.40 (a), and Fig. 4.41 (a)). This indicates presence of higher amount of chloride ions in GPC pore solution at lower molarity of NaOH solution, which is in line with the variation in formation of microstructure of GPC as indicated by lower compressive strength at lower molarity of NaOH solution (Fig. 4.20, Fig. 4.21 and Fig. 4.22). However, for fly ash content of 425 kg/m^3 and fly ash passing through 300 µm sieve, mostly there was higher free chloride content at higher molarity of NaOH solution than lower molarity of NaOH solution, although there was higher compressive strength at higher molarity of NaOH solution indicating formation of denser microstructure. This indicates inconsistent variation between the extent of formation of microstructure, and the availability of chloride ions in the pore solution with change in molarity of NaOH solution at lower fly ash content and larger size of fly ash particles,

which may be ascribed to the competing effect of chloride ions with $(OH)^-$ ions in the pore solution to a comparatively higher extent at lower fly ash content (425 kg/m^3) that led to more amount of chloride ions in the pore solution at higher molarity of NaOH solution. From Fig. 4.39 (a) to 4.41 (a), mostly there was increase in free chloride content with increase in age from 7 to 28 days while it decreased with age from 28 to 90 days for fly ash content of 425 kg/m^3. For fly ash content of 450 kg/m^3, there was no systematic variation in free chloride content with increase in age from 7 to 28 days whereas the free chloride content decreased with increase in age from 28 to 90 days. While comparing the variation in compressive strength of GPC mixes (Fig. 4.20 to Fig. 4.22) with the variation in free chloride content with age, it is observed that mostly there is inconsistent variation between the extent of formation of microstructure as indicated by the compressive strength, and the availability of chloride ions in pore solution, which can be attributed to the effect of alterations in the extent of geopolymerization reaction with age in chloride admixed GPC mixes for different fly ash contents.

While analyzing the total chloride content, it is inferred that the GPC mixes admixed with higher concentration of NaCl showed more total chloride content than those admixed with lower concentration of NaCl as observed from Fig. 4.39 (b) to 4.41 (b). Further, the variations in total chloride content of GPC mixes with fly ash content, molarity of NaOH solution and age are similar to that in case of free chloride content as evident from Fig. 4.39 (b) to 4.41 (b). From Fig. 4.39 (c) to 4.41 (c), it is noted that the bound chloride content was mostly lower at lower fly ash content (425 kg/m^3) as compared to that at higher fly ash content (450 kg/m^3) for NaOH solution of 10 M whereas for NaOH solution of 14 M, mostly opposite variation was observed. At lower fly ash content, the insufficient physical binding of chloride ions with the aluminosilicate gels resulted in comparatively lower bound chloride content at lower molarity of NaOH solution. Further, at higher molarity of NaOH solution, mostly higher bound chloride content at lower fly ash content thereby indicating comparatively higher extent of physical adsorption of chloride ions on binding gels is in line with the extent of formation of geopolymer gels in the GPC mixes. As discussed earlier, for both molarity of NaOH solution, the compressive strength of GPC mixes was mostly higher at lower fly ash content than that at higher fly ash content (Fig. 4.20, Fig. 4.21 and Fig. 4.22).

With molarity of NaOH solution, the bound chloride content was mostly higher at higher molarity of NaOH solution (14 M) when compared with lower molarity of NaOH solution (10 M) for lower fly ash content. However, mostly opposite variation was observed for higher fly

ash content i.e., the bound chloride content was mostly higher at lower molarity of NaOH solution as compared to higher molarity of NaOH solution (Fig. 4.39 (c) to 4.41 (c)). As discussed earlier, for both fly ash contents, the compressive strength was higher at higher molarity of NaOH solution than lower molarity of NaOH solution (Fig. 4.20, Fig. 4.21 and Fig. 4.22). Thus, at lower fly ash content, the greater extent of physical binding of chloride ions with geopolymer gels led to more bound chloride content at higher molarity of NaOH solution due to more formation of geopolymer gels. It may be noted that the free chloride content was also mostly higher at higher molarity of NaOH solution as compared to that at lower molarity of NaOH solution for lower fly ash content (425 kg/m^3). At higher fly ash content, the higher bound chloride content at lower molarity of NaOH solution (10 M) may be ascribed to the effect of release of physically adsorbed chloride ions to a lower extent as compared to that at higher molarity of NaOH solution. Further, at higher molarity of NaOH solution, the excess sodium ion concentration might have hindered the physical adsorption of chloride ions with geopolymer gels in case of higher fly ash content (450 kg/m^3) and larger fly ash particles (fly ash passing through 300 µm sieve). As stated earlier, the free chloride content was also higher at lower molarity of NaOH solution (10 M) than higher molarity of NaOH solution (14 M) for higher fly ash content (450 kg/m^3).

From Fig. 4.39 (c) and Fig. 4.40 (c), the bound chloride content mostly increased with increase in age from 7 to 28 days for both fly ash contents. This indicates increase in the extent of chloride binding with increase in age from 7 to 28 days, which is in line with the variation in the formation of microstructure with age as indicated by the compressive strength (Fig. 4.20 and Fig. 4.21) of GPC mixes made lower fly ash content. However, at higher fly ash content, the inadequate binding of chloride ions with geopolymer gels at the early age of 7 days resulted in lower amount of bound chloride. Further, the bound chloride content mostly decreased with increase in age from 28 to 90 days for lower fly ash content whereas there was unsystematic variation in bound chloride content with increase in age from 28 to 90 days for higher fly ash content. The comparison of these observations of bound chloride content with the variations in the extent of formation of microstructure as indicated by the compressive strength (Fig. 4.21 and Fig. 4.22) for different fly ash contents indicates varying extent of physical binding of chloride ions with the aluminosilicate gels in the GPC mixes with increase in age from 28 to 90 days. From 4.39 (c) to 4.41 (c), the bound chloride content mostly increased with increase in admixed NaCl concentration from 1.5% to 3% regardless of fly ash content, molarity of

NaOH solution and age. Between NaCl concentrations of 3% and 4.5%, there was mostly unsystematic variation in bound chloride content.

4.5 Summary

The results obtained from the experimental investigation showed that the mix parameters influenced the consistency of geopolymer concrete (GPC) mixes as indicated by the slump value. The consistency of GPC mixes decreased with increase in molarity of NaOH solution from 8 M to 16 M. The consistency of GPC mixes improved with increase in alkaline solution content, however opposite variation in consistency of GPC was observed with increase in alkaline solution ratio (SS/SH ratio). There was reduced consistency of GPC made with larger fly ash particles than that made with smaller fly ash particles irrespective of fly ash content. Further, higher fly ash content decreased the consistency of GPC when compared with lower fly ash content irrespective of particle size of fly ash. The presence of sodium chloride in GPC mixes resulted in higher consistency than control GPC mix, and the consistency of GPC mixes further increased with increase in admixed NaCl concentration. The obtained results indicated that the compressive strength increased with increase in molarity of NaOH solution from 8 M to 16 M in case of control, and 1.5% NaCl admixed GPC mixes. In GPC mixes admixed NaCl concentrations of 3% and 4.5%, the compressive strength increased with molarity of NaOH solution from 8 M to 14 M, however, it decreased at NaOH solution of 16 M, which is ascribed to the hindering effect of NaCl at higher concentration in the geopolymerization process in GPC mixes. Increase in alkaline solution content, and SS/SH ratio showed an increase in compressive strength of GPC. Opposite variation in compressive strength of GPC was observed with particle size of fly ash between lower and higher fly ash contents. The particle size of fly ash had significant influence on the variation in compressive strength of NaCl admixed GPC with change in fly ash content. The presence of sodium chloride reduced the compressive strength of GPC when compared with control mix, and the compressive strength decreased with increase in NaCl concentration. Although, the compressive strength mostly increased with age from 7 to 28 days in control as well as in NaCl admixed GPC mixes, however, it mostly decreased with age from 28 to 90 days.

From the obtained results of chloride content, the particle size of fly ash affected the chloride ion concentration in the pore solution due to alteration in the microstructure of GPC with change in molarity of NaOH solution thereby showing variation in free chloride content with molarity of NaOH solution. There was decrease in free chloride content of GPC with increase

in alkaline solution content. When compared with the variations in the formation of microstructure as indicated by the compressive strength, there was mostly inconsistent variation in free chloride content with SS/SH ratio for different ages. The GPC mixes made with larger fly ash particles, and that made with higher fly ash content mostly exhibited higher free chloride content as compared to that made with smaller fly ash particles, and lower fly ash content respectively. The free chloride content mostly increased with increase in age from 7 to 28 days whereas it mostly decreased with age from 28 days to 90 days irrespective of molarity of NaOH solution, alkaline solution content, SS/SH ratio, particle size of fly ash, fly ash content, and admixed NaCl dosage. The variation in total chloride content of GPC mixes was mostly similar to that in case of free chloride content. As indicated by obtained bound chloride content, lower extent of chloride binding was observed in fly ash based geopolymer concrete. The chloride binding was mostly higher at lower molarity of NaOH solution than higher molarity of NaOH solution. However, the variation in chloride binding was not systematic with alkaline solution content, and SS/SH ratio. The more formation of geopolymer gels in GPC mixes made with larger fly ash particles as indicated by higher compressive strength led to comparatively higher extent of physical adsorption of chloride ions on sodium aluminosilicate hydrate gels that resulted in higher bound chloride content in case of larger fly ash particles than smaller fly ash particles. The bound chloride content in GPC varied with fly ash content for different molarity of NaOH solution and particle size of fly ash. Further, there was unsystematic variation in bound chloride content of GPC with age. In case of admixed NaCl, the free chloride, total chloride and bound chloride content increased with increase in NaCl concentration in GPC mixes.

Chapter 5

Effect of Mix Parameters and Admixed Chloride on Microstructure of Fly ash based Geopolymer Concrete

5.1 General

In this chapter, the changes in microstructure of geopolymer concrete (GPC) with mix parameters i.e., molarity of NaOH solution, alkaline solution content, SS/SH ratio, particle size of fly ash and fly ash content at different ages are analysed and discussed through the results of X-ray diffraction (XRD), Fourier transform infrared (FTIR) spectroscopy and Field emission scanning electron microscope (FESEM) analyses. Further, the changes in microstructure of GPC with admixed NaCl concentration are also analysed and discussed in this chapter.

5.2 Microstructure analysis of fly ash based geopolymer concrete (GPC)

5.2.1 Effect of molarity of NaOH solution on microstructure of GPC

Typical plots of obtained XRD patterns of GPC mixes made from different molarity of NaOH solution (8 M, 12 M and 16 M) are shown in Fig. 5.1 to Fig. 5.4 for different concentrations of admixed NaCl (0%, 1.5%, 3% and 4.5%) and for different ages (7 days, 28 days and 90 days). The remaining plots of XRD patterns are presented in Appendix (Fig. A1 to Fig. A4). In control and chloride admixed GPC mixes, the peaks related to quartz (Q: SiO_2 at 20.86° 2θ, 26.64° 2θ, 36.54° 2θ, 39.47° 2θ, 42.45° 2θ, 45.79° 2θ, 50.14° 2θ, 54.88° 2θ, 59.96° 2θ and 68.14° 2θ), mullite (M: $Al_{2.3}Si_{0.7}O_{4.85}$ at 16.45° 2θ, 26.28° 2θ, 31.02° 2θ, 33.25° 2θ, 35.28° 2θ, 55.28° 2θ and 60.73° 2θ), muscovite (Mu: $KAl_3Si_3O_{10}(OH)_2$ at 8.85° 2θ), albite (A: $NaAlSi_3O_8$ at 13.85° 2θ, 22.05° 2θ, 27.95° 2θ, 28° 2θ and 28.10° 2θ), nepheline (N: $NaAlSiO_4$ at 23.10° 2θ, 27.10° 2θ, 38.80° 2θ and 50.60° 2θ), anorthoclase (Ano: $(Na_{0.75}K_{0.25})(AlSi_3O_8)$ at 27.45° 2θ, 27.50° 2θ and 27.60° 2θ) and sodalite (S: $Na_8Al_6Si_6O_{24}(OH)_2(H_2O)_2$ at 14.05° 2θ and 24.50° 2θ) were identified in the XRD patterns shown in Fig. 5.1 to Fig. 5.4 [58,90,92,93]. In addition, less intense peaks related to halite (H: NaCl) were identified at 31.75° 2θ, 45.45° 2θ and 66.35° 2θ in the XRD patterns of GPC mixes admixed with different concentrations of NaCl i.e., 1.5%, 3% and 4.5% [90,94,95]. The microstructure of geopolymer concrete is affected by the variations in the formation of compounds related to geopolymer gels. Thus, the formation of geopolymeric compounds i.e., albite, anorthoclase, nepheline, sodalite, and muscovite in

geopolymer concrete as identified from the XRD patterns is analyzed to evaluate the variations in microstructure of geopolymer concrete.

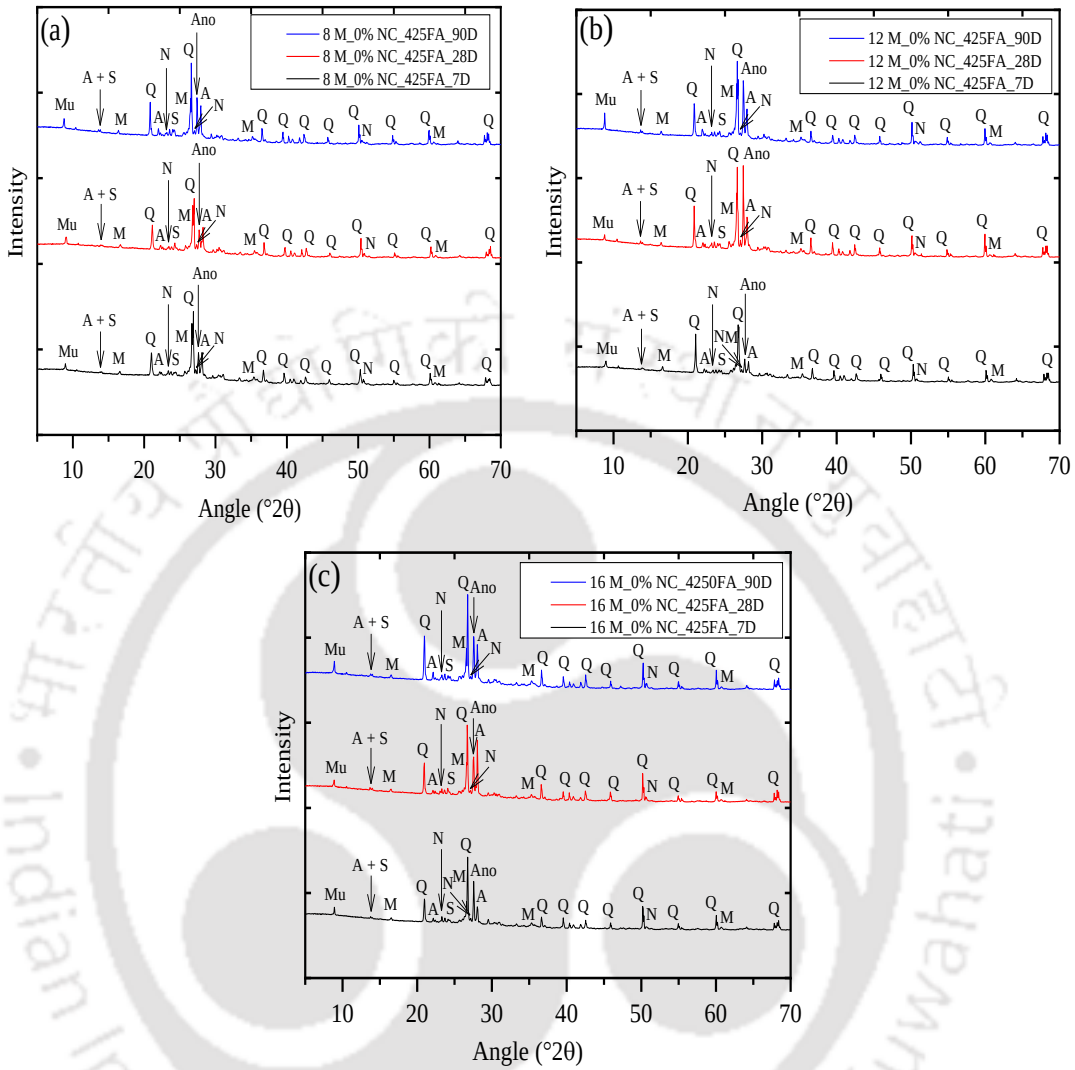

(GPC made with fly ash passing through 300 μm sieve, fly ash content of 425 kg/m^3, alkaline solution content of 210 kg/m^3, and SS/SH ratio of 1.75)

Fig. 5.1: XRD patterns of control GPC mixes at different ages: a) NaOH solution of 8 M, b) NaOH solution of 12 M, and c) NaOH solution of 16 M

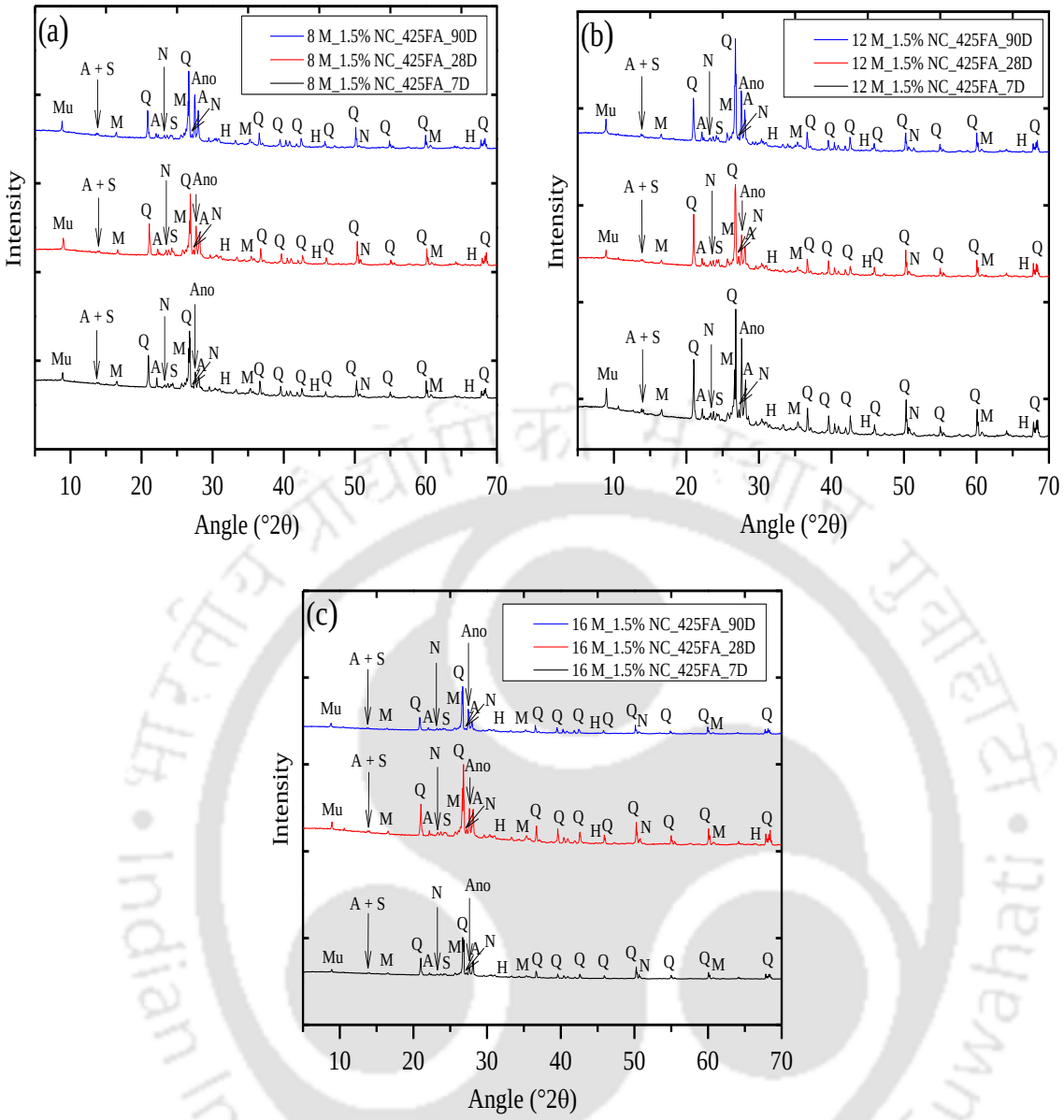

(GPC made with fly ash passing through 300 μm sieve, fly ash content of 425 kg/m^3, alkaline solution content of 210 kg/m^3, and SS/SH ratio of 1.75)

Fig. 5.2: XRD patterns of GPC mixes at different ages: a) NaOH solution of 8 M, b) NaOH solution of 12 M, and c) NaOH solution of 16 M for admixed NaCl concentration of 1.5%

From Fig. 5.1 and Fig. A1 (Appendix), the peak intensity of the compounds related to sodium aluminosilicate hydrate (N-A-S-H) gel i.e., albite, anorthoclase, and nepheline in the XRD patterns mostly increased with increase in molarity of NaOH solution in control GPC mixes at the age of 7 and 28 days. In addition, the peak intensity of sodalite and muscovite also mostly increased with increase in concentration of NaOH solution in control GPC mixes as observed from Fig. 5.1 and Fig. A1 (Appendix). The formation of more amount of geopolymer gels with increase in molarity of NaOH solution as indicated by the peak intensity of compounds related to geopolymer gel in control GPC mixes led to higher compressive strength at higher molarity

of NaOH solution at the age of 7 and 28 days as observed from the results of compressive strength shown in Fig. 4.8 (discussed in Chapter 4). From Fig. 5.1 and Fig. A1 (Appendix)), at the age of 90 days, there was unsystematic variation in the peak intensity of anorthoclase, nepheline, sodalite, and muscovite with molarity of NaOH solution, however, the peak intensity of albite mostly increased with increase in molarity of NaOH solution. Thus, the dominant effect of formation of more amount of albite as indicated by the results of XRD analysis led to higher compressive strength with increase in molarity of NaOH solution in control GPC mixes at the age of 90 days (Fig. 4.8).

From Fig. 5.2 and Fig. A2 (Appendix), the peak intensity of albite, anorthoclase, nepheline, sodalite, and muscovite in the XRD patterns mostly increased with increase in concentration of NaOH solution in 1.5% NaCl admixed GPC mixes at all ages i.e., 7, 28 and 90 days thereby indicating more formation of geopolymer gels at higher molarity of NaOH solution. This is in line with the variation in compressive strength as there was mostly increase in compressive strength of GPC mixes with increase in molarity of NaOH solution at all ages in 1.5% NaCl admixed GPC mixes (Fig. 4.8, Chapter 4).

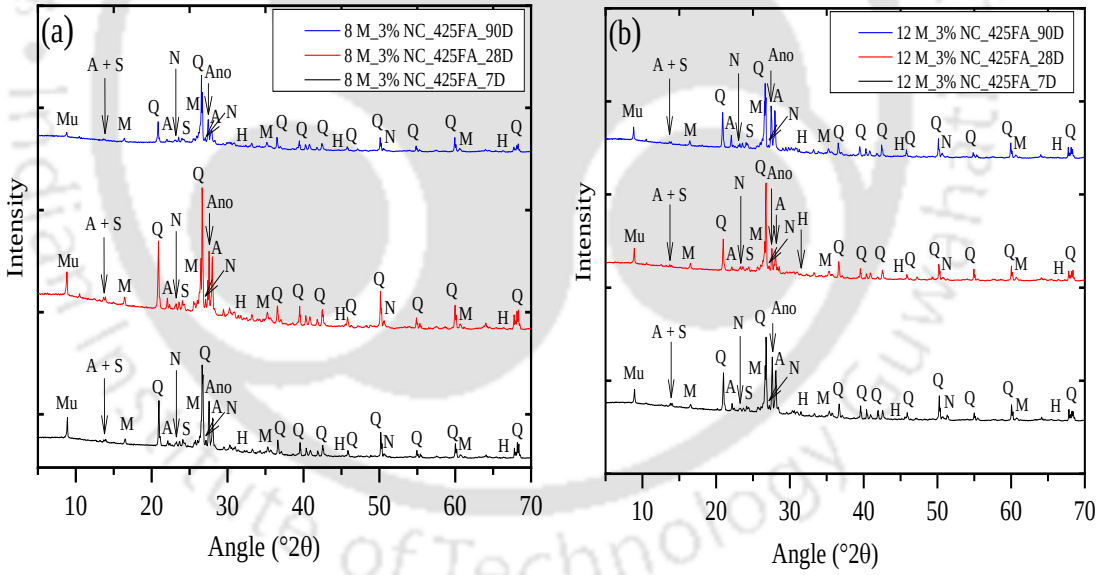

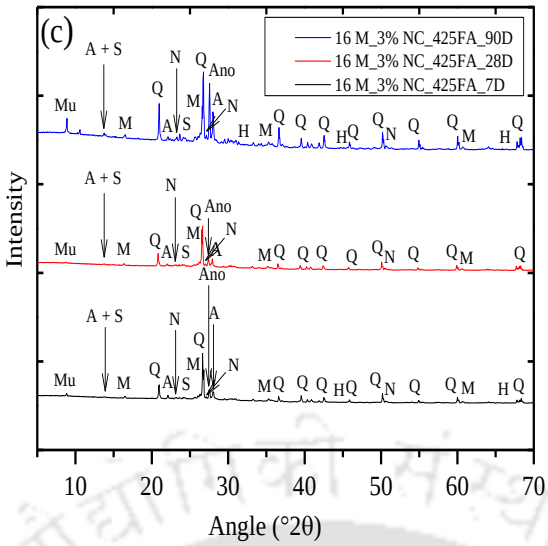

(GPC made with fly ash passing through 300 μm sieve, fly ash content of 425 kg/m^3, alkaline solution content of 210 kg/m^3, and SS/SH ratio of 1.75)

Fig. 5.3: XRD patterns of GPC mixes at different ages: a) NaOH solution of 8 M, b) NaOH solution of 12 M, and c) NaOH solution of 16 M for admixed NaCl concentration of 3%

From Fig. 5.3 and Fig. A3 (Appendix), the peak intensity of the geopolymeric compounds mostly increased with increase in molarity of NaOH solution from 8 M to 14 M in 3% NaCl admixed GPC mixes at the age of 7 and 28 days whereas the peak intensity of these compounds were higher at NaOH solution of 14 M as compared to NaOH solution of 16 M. The variations in the formation of geopolymer gels with molarity of NaOH solution as indicated by the above variations in the peak intensity of the geopolymeric compounds are comparable with the variations in compressive strength of 3% NaCl admixed GPC mixes at the age of 7 and 28 days. It may be noted that there was increase in compressive strength of GPC with increase in molarity of NaOH solution from 8 M to 14 M followed by a decrease at NaOH solution of 16 M (Fig. 4.8, Chapter 4). From Fig. 5.3 and Fig. A3 (Appendix), at the age of 90 days, the peak intensity of albite, anorthoclase, nepheline, sodalite, and muscovite in the XRD patterns mostly increased with increase in molarity of NaOH solution from 8 M to 14 M followed by a decrease at 16 M NaOH solution in 3% NaCl admixed GPC mixes. When comparing these variations in the peak intensity of the geopolymeric compounds with compressive strength at the age of 90 days, there was increase in compressive strength of 3% NaCl admixed GPC mixes with increase in concentration of NaOH solution from 8 M to 16 M (Fig. 4.8).

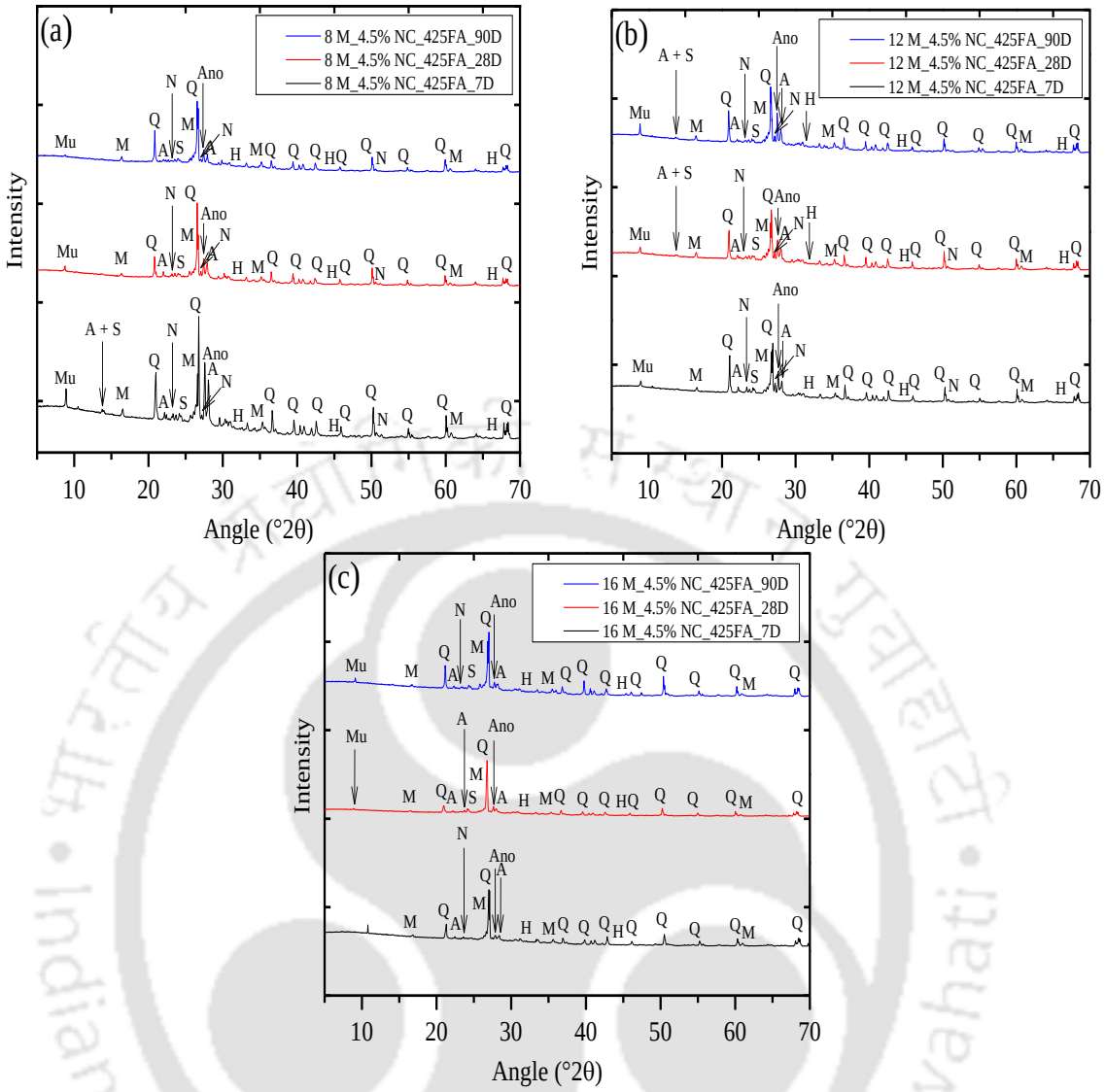

(GPC made with fly ash passing through 300 μm sieve, fly ash content of 425 kg/m^3, alkaline solution content of 210 kg/m^3, and SS/SH ratio of 1.75)

Fig. 5.4: XRD patterns of GPC mixes at different ages: a) NaOH solution of 8 M, b) NaOH solution of 12 M, and c) NaOH solution of 16 M for admixed NaCl concentration of 4.5%

From Fig. 5.4 and Fig. A4 (Appendix), the peak intensity of albite, anorthoclase, nepheline, sodalite, and muscovite in the XRD patterns mostly increased with increase in molarity of NaOH solution from 8 M to 14 M in 4.5% NaCl admixed GPC mixes at all ages i.e., 7, 28 and 90 days. However, between NaOH solutions of 14 M and 16 M, the peak intensity of these compounds were mostly higher at NaOH solution of 14 M as compared to NaOH solution of 16 M at the age of 28 days and 90 days with opposite variation between NaOH solutions of 14 M and 16 M at the age of 7 days. Overall, these observations indicate mostly consistent variation in the formation of geopolymer gels as indicated by the peak intensity of the compounds in the XRD patterns with the variations in the compressive strength where the compressive strength of 4.5% NaCl admixed GPC mixes increased with increase in molarity

of NaOH solution from 8 M to 14 M followed by a decrease at NaOH solution of 16 M at the age of 7, 28 and 90 days (Fig. 4.8, Chapter 4).

From Fig. 5.1 - 5.4, and Fig. A1 - A4 (Appendix), it is inferred that the peak intensity of the compounds related to geopolymer gels in the XRD patterns were mostly higher in control GPC mixes as compared to NaCl admixed GPC mixes irrespective of molarity of NaOH solution, concentration of admixed NaCl, and age. This is consistent with the variation in compressive strength between control and NaCl admixed GPC mixes as observed from the compressive strength results shown in Fig. 4.8 (Chapter 4). Further, the variations in the peak intensity of albite, anorthoclase, nepheline, sodalite, and muscovite in the XRD patterns with increase in admixed NaCl concentration as observed from Fig. 5.2 - 5.4, and Fig. A2 - A4 (Appendix) are in line with the variations in the compressive strength of GPC mixes (Fig. 4.8, Chapter 4). From Fig. 5.1 - 5.4, and Fig. A1 - A4 (Appendix), the peak intensity of the compounds related to geopolymer gels in the XRD patterns mostly increased with age from 7 to 28 days for control as well as NaCl admixed GPC mixes irrespective of molarity of NaOH solution thereby indicating more formation of geopolymer gels at the age of 28 days. This is corroborated with the results of compressive strength where there was increase in compressive strength of GPC mixes with increase in age from 7 to 28 days (Fig. 4.8). From Fig. 5.1 - 5.4, and Fig. A1 - A4 (Appendix), the peak intensity of the compounds related to geopolymer gels in the XRD patterns mostly decreased with increase in age from 28 to 90 days in control as well as NaCl admixed GPC mixes for NaOH solution molarity of 8 M to 14 M. This is substantiated with the variations in compressive strength of GPC, as in case of molarity of NaOH solution from 8 M to 14 M, the compressive strength mostly decreased with increase in age from 28 to 90 days for control as well as chloride admixed GPC mixes (Fig. 4.8 (a-d)). However, at NaOH solution of 16 M, although the compressive strength increased with increase in age from 28 to 90 days (Fig. 4.8 (e)), there was unsystematic variation in the peak intensity of the compounds related to geopolymer gels with increase in age from 28 to 90 days for control and chloride admixed GPC mixes (Fig. 5.1 - 5.4, and Fig. A1 - A4 (Appendix)). From Fig. 5.2 - 5.4, and Fig. A2 - A4 (Appendix), mostly there was unsystematic variation in the peak intensity of halite in the XRD patterns with molarity of NaOH solution, admixed NaCl concentration, and age.

As already stated in Chapter 3, the FTIR-Attenuated Total Reflectance (ATR) analysis was carried out on the GPC mixes to identify the functional groups associated with different compounds in the mixes. Typical plots of obtained FTIR spectra of GPC mixes admixed with

NaCl concentrations of 0%, 1.5%, and 4.5% are shown in Fig. 5.5 to Fig. 5.7 for different molarity of NaOH solution i.e., 8 M, 10 M, 12 M, 14 M and 16 M, and different ages i.e., 7 days, 28 days and 90 days. The remaining plots of FTIR spectra are presented in Appendix (Fig. A5). In Fig. 5.5 to Fig. 5.7, the peak in the range of 770 cm^{-1} - 778 cm^{-1} indicates the tetrahedral bending vibration of Si–O–Si bond corresponding to quartz in the GPC mixes [96]. From Fig. 5.5 - Fig. 5.7, and Fig. A5 (Appendix), the peak in the range of 997 cm^{-1} to 1010 cm^{-1} corresponds to the asymmetric stretching vibration of Si–O–Si(Al) bond, which shows the presence of sodium aluminosilicate hydrate (N-A-S-H) gel in the GPC mixes for different molarity of NaOH solution, and concentration of admixed NaCl [90]. This corroborates the results of XRD analysis where the compounds related to sodium aluminosilicate hydrate (N-A-S-H) gel i.e., albite, anorthoclase, and nepheline were identified in the XRD patterns of GPC mixes (discussed above). When compared with the FTIR spectra of raw fly ash (Fig. 3.1(c), Chapter 3), the observed peak corresponding to Si–O–Si(Al) bond at 1052 cm^{-1} in raw fly ash shifted to lower wavenumbers (997 cm^{-1} to 1010 cm^{-1}) in GPC mixes thereby indicating the formation of geopolymer gels in control and chloride admixed GPC mixes as a result of geopolymerization process. From Fig. 5.5 to Fig. 5.7, and Fig. A5 (Appendix), there was no significant shift in the wavenumber corresponding to the peak indicating the asymmetric stretching vibration of Si–O–Si(Al) bond with change in molarity of NaOH solution, admixed NaCl concentration and age. This indicates that the results of FTIR spectra corresponding to the peak indicating the asymmetric stretching vibration of Si–O–Si(Al) bond did not show significant variation related to presence of geopolymer gels with change in molarity of NaOH solution, admixed NaCl concentration, and age.

From Fig. 5.5 to Fig. 5.7, and Fig. A5 (Appendix), the peak in the range of 1364 cm^{-1} to 1532 cm^{-1} corresponds to the stretching vibration of carbonate group (CO_3^{2-}) in GPC mixes [97,98]. Further, in the FTIR spectra (Fig. 5.5 to Fig. 5.7 and Fig. A5 (Appendix)), the peak in the range of 1641 - 1715 cm^{-1}, and the band in the range of 3386 - 3749 cm^{-1} are associated with the bending vibration of H–O–H group, and stretching vibration of –OH group respectively, which shows the presence of adsorbed water molecules in the geopolymer gels in GPC mixes [43,99].

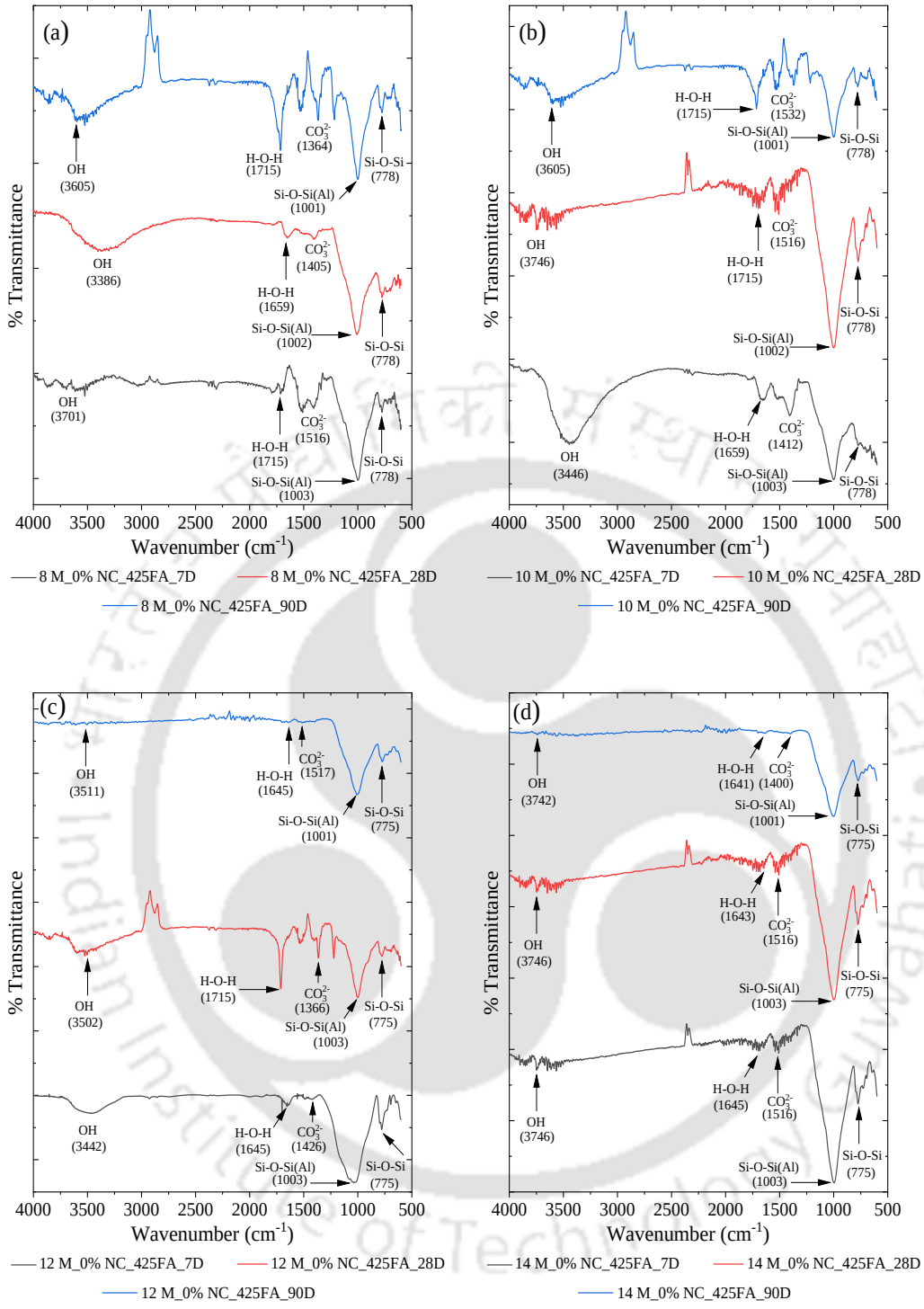

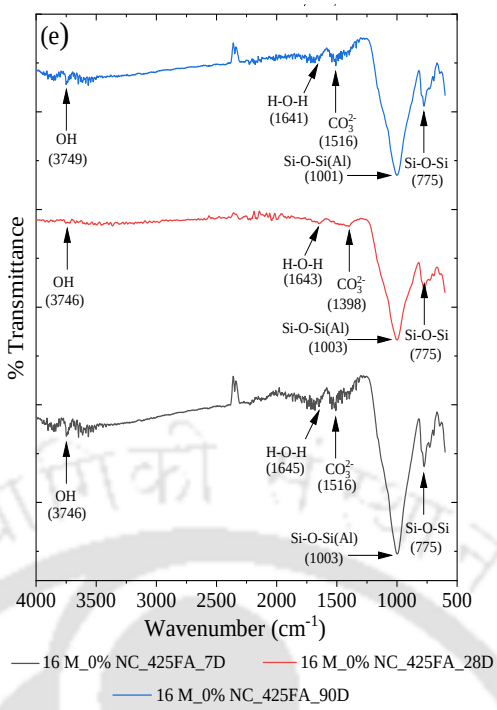

(GPC made with fly ash passing through 300 μm sieve, fly ash content of 425 kg/m^3, alkaline solution content of 210 kg/m^3, and SS/SH ratio of 1.75)

Fig. 5.5: FTIR spectra of control GPC mixes at different ages: a) NaOH solution of 8 M, b) NaOH solution of 10 M, c) NaOH solution of 12 M, d) NaOH solution of 14 M, and e) NaOH solution of 16 M

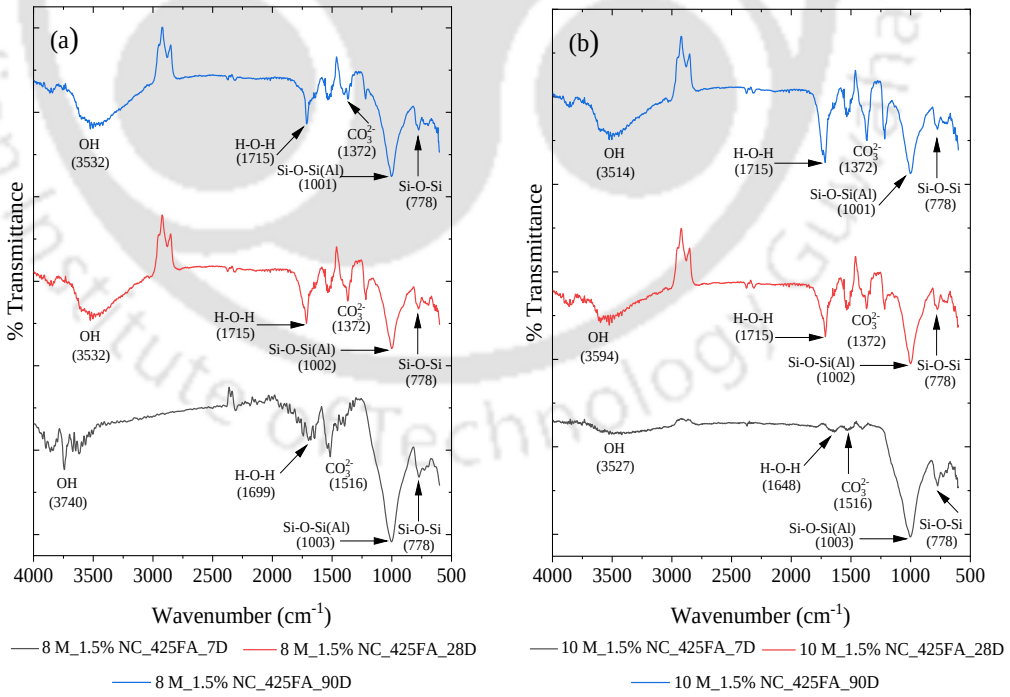

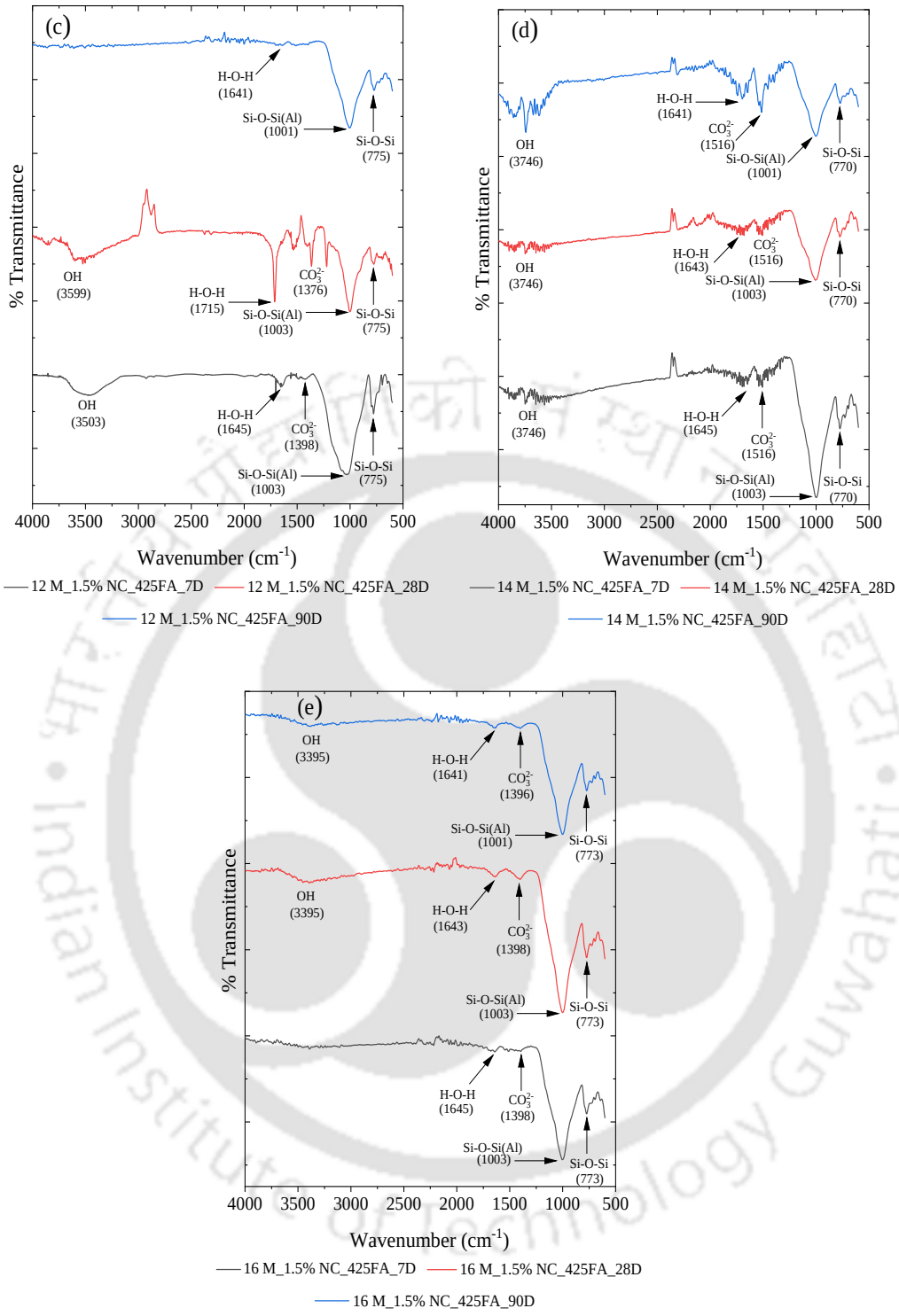

(GPC made with fly ash passing through 300 μm sieve, fly ash content of 425 kg/m^3, alkaline solution content of 210 kg/m^3, and SS/SH ratio of 1.75)

Fig. 5.6: FTIR spectra of GPC mixes at different ages: a) NaOH solution of 8 M, b) NaOH solution of 10 M, c) NaOH solution of 12 M, d) NaOH solution of 14 M, and e) NaOH solution of 16 M for admixed NaCl concentration of 1.5%

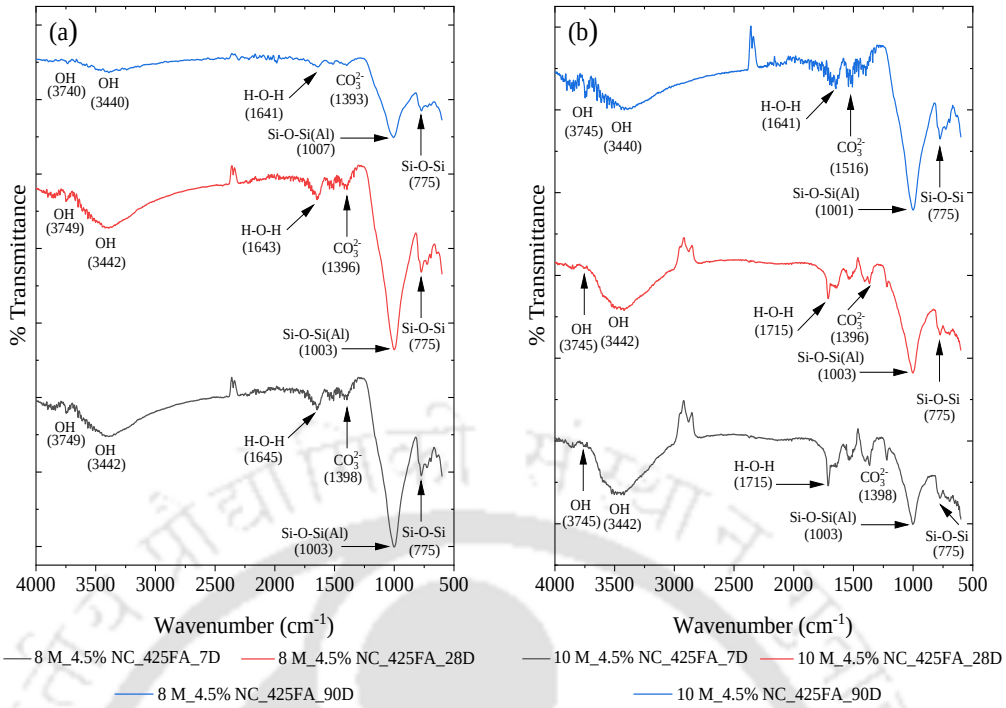

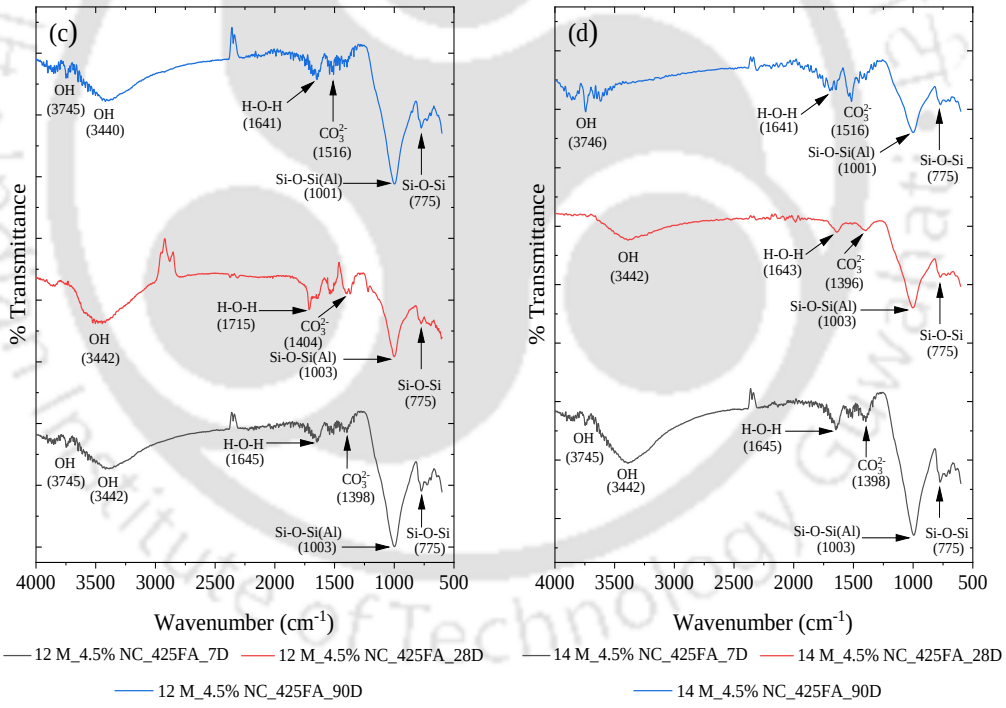

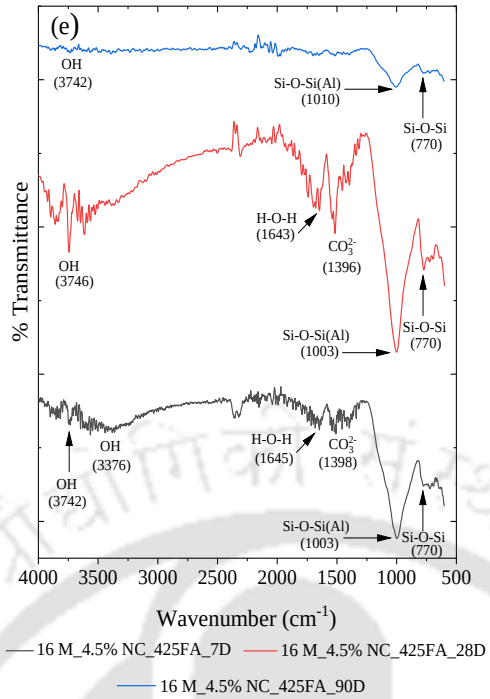

(GPC made with fly ash passing through 300 μm sieve, fly ash content of 425 kg/m^3, alkaline solution content of 210 kg/m^3, and SS/SH ratio of 1.75)

Fig. 5.7: FTIR spectra of GPC mixes at different ages: a) NaOH solution of 8 M, b) NaOH solution of 10 M, c) NaOH solution of 12 M, d) NaOH solution of 14 M, and e) NaOH solution of 16 M for admixed NaCl concentration of 4.5%

The typical FESEM images of GPC mixes are shown in Fig. 5.8 for different molarity of NaOH solution, different concentrations of admixed NaCl, and age. The remaining FESEM images are shown in Appendix (Fig. A6 to Fig. A17).

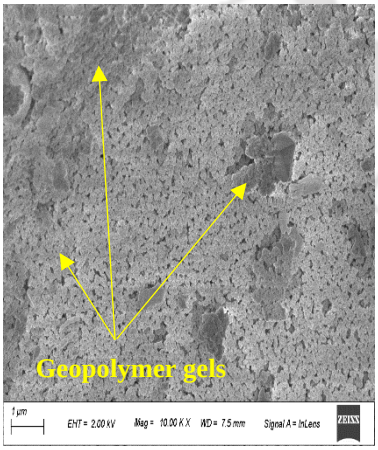

(a) 12 M/0%NC/425FA/90D

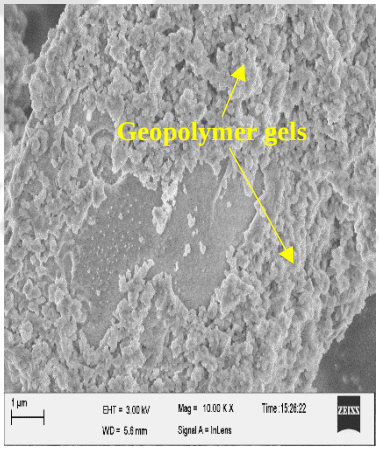

(b) 8 M/1.5%NC/425FA/90D

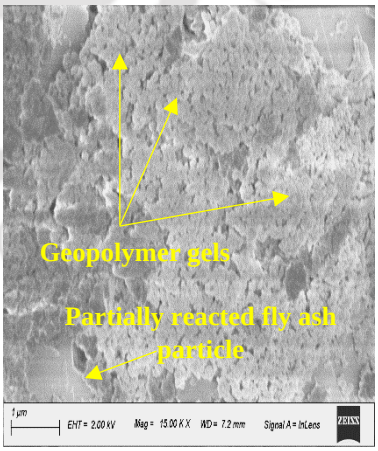

(c) 10 M/1.5%NC/425FA/90D

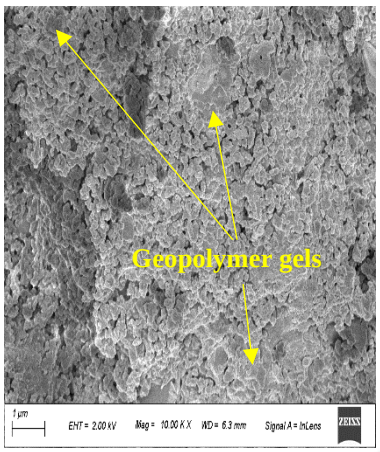

(d) 12 M/1.5%NC/425FA/90D

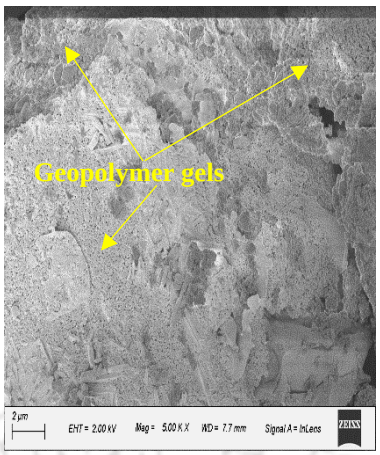

(e) 10 M/1.5%NC/425FA/7D

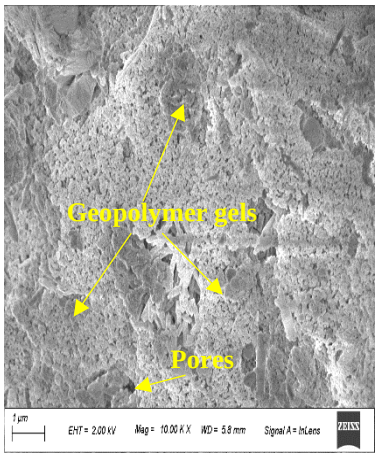

(f) 10 M/1.5%NC/425FA/28D

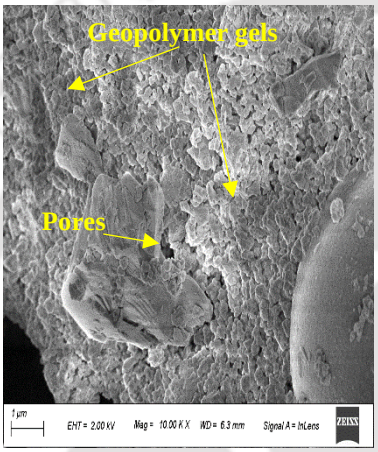

(g) 12 M/3%NC/425FA/90D

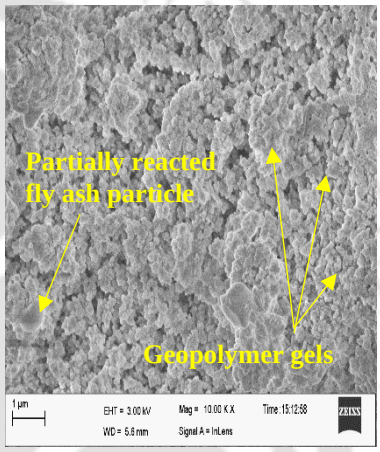

(h) 12 M/4.5%NC/425FA/90D

(GPC made with fly ash passing through 300 µm sieve, fly ash content of 425 kg/m^3, alkaline solution content of 210 kg/m^3, and SS/SH ratio of 1.75)

Fig. 5.8: FESEM images of GPC for different molarity of NaOH solution, different concentrations of admixed NaCl and age

From Fig. 5.8 (b, c, d), it is inferred that the GPC mixes made with higher molarity of NaOH solution showed comparatively more formation of geopolymer gels thereby resulting in compact microstructure in GPC mixes. This is substantiated with the results of XRD analysis wherein the peak intensity of albite, anorthoclase, nepheline, sodalite, and muscovite mostly increased with increase in molarity of NaOH solution (Fig. 5.2 (a, b)). While comparing the morphology between control and NaCl admixed GPC mixes (Fig. 5.8 (a, d, g, h)), it is inferred that there was formation of comparatively denser microstructure in control GPC mixes as compared to NaCl admixed GPC mixes, which is in line with the results of XRD analysis where the control GPC mixes mostly showed higher peak intensity of geopolymeric compounds as compared to NaCl admixed GPC mixes (Fig. 5.1 (b), Fig. 5.2 (b), Fig. 5.3 (b) and Fig. 5.4 (b)). The FESEM images shown in Fig. 5.8 (e, f) indicate more formation of

geopolymer gels in GPC mixes at the age of 28 days as compared to that at the age of 7 days. Further, noticeable difference was not observed in the FESEM images of GPC mixes between the age of 28 days and 90 days (Fig. 5.8 (c, f)), although the peak intensity of the compounds related to geopolymer gels in the XRD patterns (Fig. A2, Appendix) and the compressive strength of GPC mixes (Fig. 4.8 (b)) were mostly higher at the age of 28 days than that at the age of 90 days. In addition, the presence of partially reacted fly ash particles (Fig. 5.8 (c, h)) and some pores (Fig. 5.8 (f, g)) were observed in the FESEM images of GPC mixes.

5.2.2 Effect of alkaline solution content on microstructure of GPC

The obtained XRD patterns of GPC mixes made from alkaline solution contents of 190 kg/m^3 and 210 kg/m^3 are shown in Fig. 5.9 to Fig. 5.12 for the age of 7 and 28 days. From Fig. 5.9 to Fig. 5.12, the peak intensity of albite, anorthoclase, nepheline, sodalite, and muscovite in XRD patterns mostly increased with increase in alkaline solution content at both ages for control and 3% NaCl admixed GPC mixes, which shows more formation of geopolymer gels in GPC mixes at higher alkaline solution content. This is consistent with the variation in compressive strength of GPC mixes as the compressive strength was mostly higher at higher alkaline solution content as compared to lower alkaline solution content (Fig. 4.9 and Fig. 4.10).

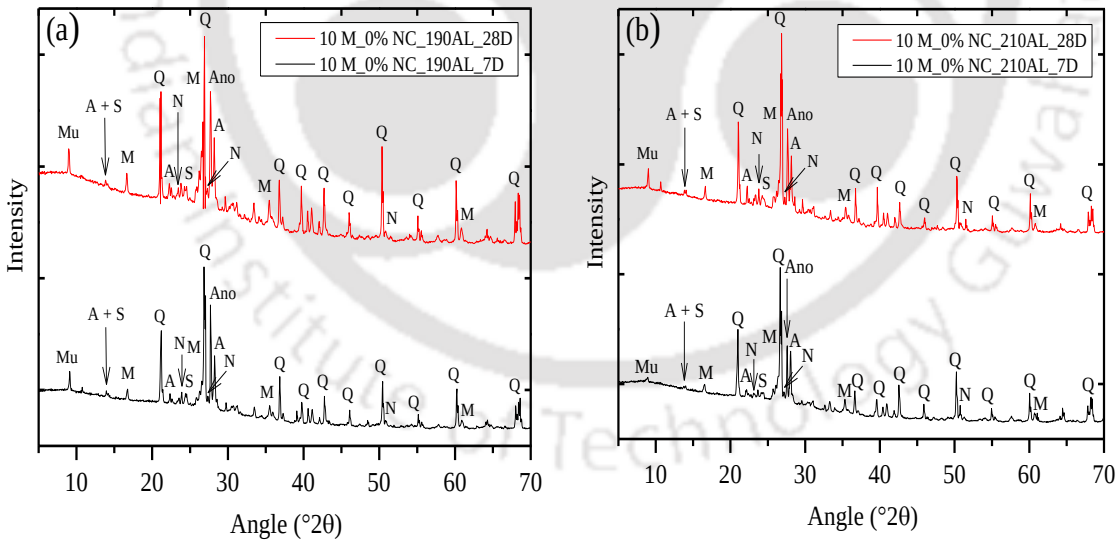

(GPC made with fly ash passing through 150 μm sieve, fly ash content of 425 kg/m^3, and SS/SH ratio of 1.75)

Fig. 5.9: XRD patterns of control GPC mixes made with NaOH solution of 10 M for alkaline solution content of a) 190 kg/m^3, and b) 210 kg/m^3, at the age of 7 and 28 days

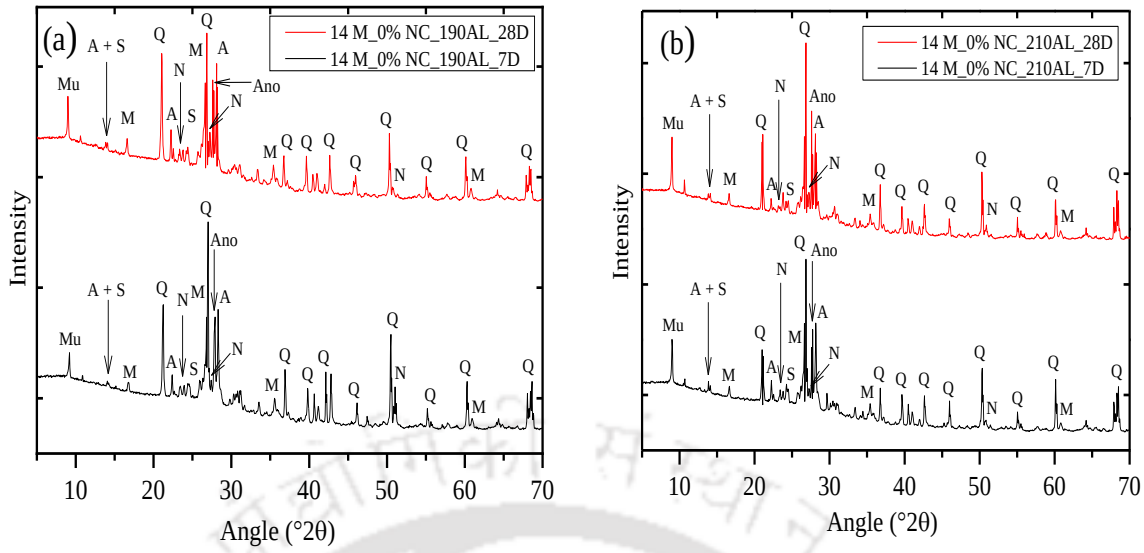

(GPC made with fly ash passing through 150 μm sieve, fly ash content of 425 kg/m^3, and SS/SH ratio of 1.75)

Fig. 5.10: XRD patterns of control GPC mixes made with NaOH solution of 14 M for alkaline solution content of a) 190 kg/m^3, and b) 210 kg/m^3, at the age of 7 and 28 days

Further, in few cases i.e., in case of 3% NaCl admixed GPC mixes at 14 M NaOH solution, the peak intensity of albite, anorthoclase, nepheline, sodalite, and muscovite in XRD patterns (Fig. 5.12) were lower at higher alkaline solution content, which is also supported by the variation in compressive strength of GPC mixes (Fig. 4.9 and Fig. 4.10) i.e., the compressive strength was lower at higher alkaline solution content and the reason for this variation in compressive strength was already stated in Section 4.3.2 (Chapter 4). From Fig. 5.9 to Fig. 5.12, in the XRD patterns, the peak intensity of the compounds related to geopolymer gels increased with increase in molarity of NaOH solution from 10 M to 14 M in control and 3% NaCl admixed GPC mixes for both alkaline solution contents and both ages. This is substantiated with the variation in compressive strength as the formation of more amount of geopolymer gels with increase in molarity of NaOH solution led to higher compressive strength of GPC mixes as evident from Fig. 4.9 and Fig. 4.10 (Chapter 4).

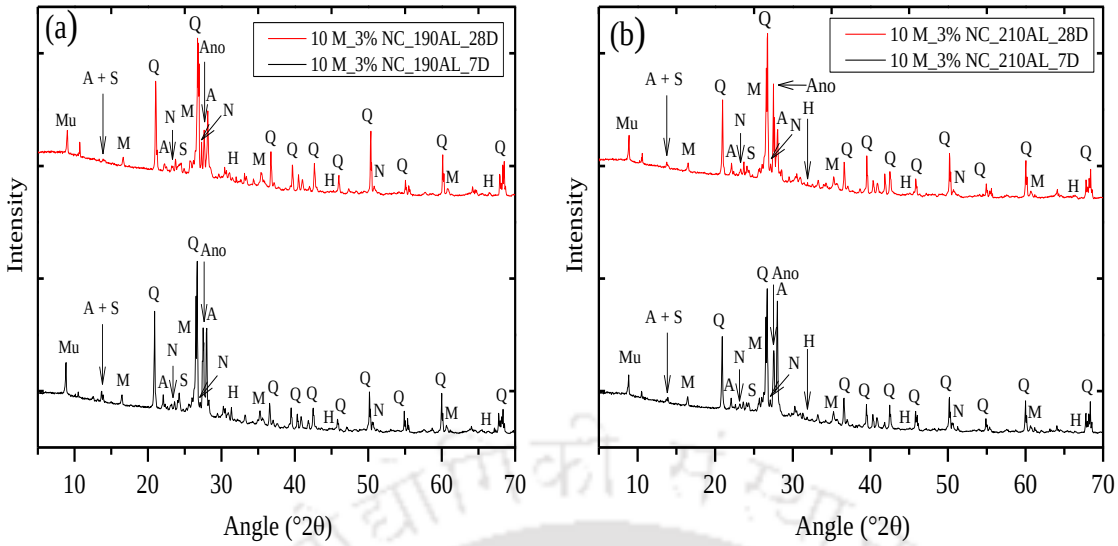

(GPC made with fly ash passing through 150 μm sieve, fly ash content of 425 kg/m^3, and SS/SH ratio of 1.75)

Fig. 5.11: XRD patterns of 3% NaCl admixed GPC mixes made with NaOH solution of 10 M for alkaline solution content of a) 190 kg/m^3, and b) 210 kg/m^3, at the age of 7 and 28 days

From Fig. 5.9 to Fig. 5.12, the peak intensity of the geopolymeric compounds were higher in control GPC mixes as compared to 3% NaCl admixed GPC mixes. This indicates alteration in the extent of geopolymerization reaction in the presence of chloride ions, which is in line with the variation in compressive strength of GPC mixes (Fig. 4.9 and Fig. 4.10). The peak intensity of albite, anorthoclase, nepheline, sodalite, and muscovite increased with increase in age from 7 to 28 days irrespective of alkaline solution content and molarity of NaOH solution for control and 3% NaCl admixed GPC mixes as evident from Fig. 5.9 to Fig. 5.12. This shows more formation of geopolymer gels in GPC mixes with increase in age that resulted in higher compressive strength at the age of 28 days when compared with that at the age of 7 days (Fig. 4.9 and Fig. 4.10). There was no systematic variation in the peak intensity of halite in the XRD patterns with molarity of NaOH solution (Fig. 5.11 and Fig. 5.12) in NaCl admixed GPC mixes. Further, the peak intensity of halite was lower in the GPC mixes made with higher alkaline solution content than that made with lower alkaline solution content (Fig. 5.11 and Fig. 5.12). It may be noted that comparatively more amount of NaCl was added in GPC mixes made with higher alkaline solution content during preparation where NaCl was admixed in GPC mixes as percentage by mass of geopolymer solids that includes the solids of both NaOH and Na_2SiO_3 solutions. Thus, lower peak intensity of halite in GPC mixes made with higher alkaline solution content may be possibly due to alteration in the crystallinity of sodium chloride during early age in the GPC mixes. Further, there was unsystematic variation in the peak intensity of halite with increase in age from 7 to 28 days in GPC mixes.

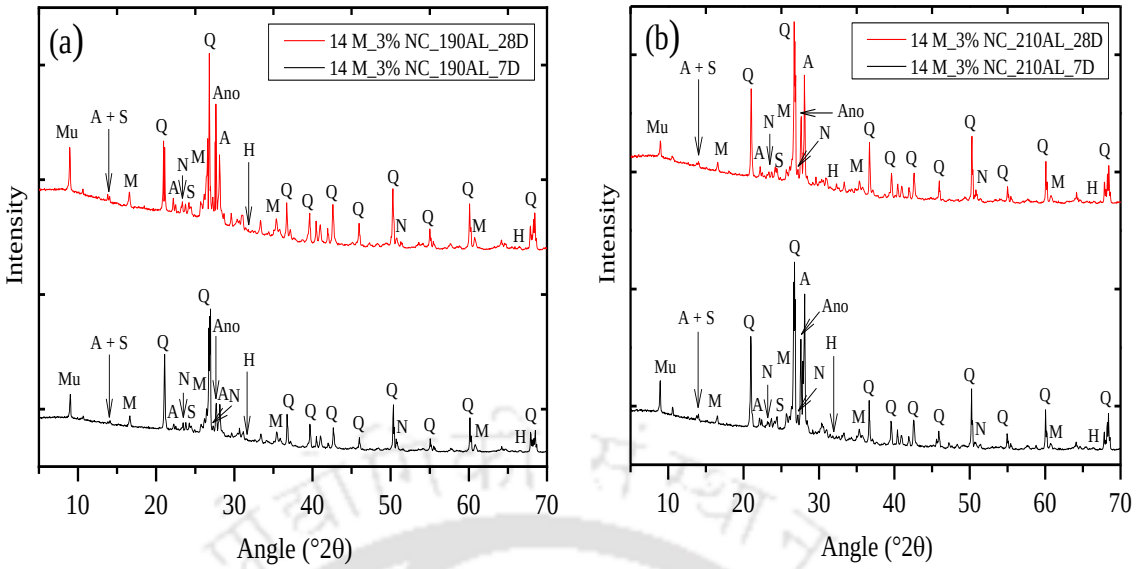

(GPC made with fly ash passing through 150 μm sieve, fly ash content of 425 kg/m^3, and SS/SH ratio of 1.75)

Fig. 5.12: XRD patterns of 3% NaCl admixed GPC mixes made with NaOH solution of 14 M for alkaline solution content of a) 190 kg/m^3, and b) 210 kg/m^3, at the age of 7 and 28 days

The obtained FTIR spectra of GPC made from alkaline solution contents of 190 kg/m^3 and 210 kg/m^3 are shown in Fig. 5.13 to Fig. 5.16. In the FTIR spectra shown in Fig. 5.13 to Fig. 5.16, the peak in the range of 770 cm^{-1} -775 cm^{-1} shows the presence of quartz in all GPC mixes. In the FTIR spectra (Fig. 5.13 to Fig. 5.16), the peak in the range of 988 cm^{-1} to 999 cm^{-1} is associated with the asymmetric stretching vibration of Si–O–Si(Al) bond that indicates the presence of geopolymer gels in control and chloride admixed GPC mixes made with different alkaline solution contents, and molarity of NaOH solution for the age of 7 days and 28 days. From Fig. 5.13 to Fig. 5.16, it is inferred that the peak corresponding to Si–O–Si(Al) bond mostly shifted to lower wavenumbers in GPC mixes made with higher alkaline solution content (210 kg/m^3) when compared with lower alkaline solution content (190 kg/m^3), which shows comparatively higher extent of geopolymerization reaction in GPC mixes at higher alkaline solution content. This is validated with the results of XRD analysis where the peak intensity of the compounds related to geopolymer gels were mostly higher in the GPC mixes made with higher alkaline solution content than lower alkaline solution content (Fig. 5.9 to Fig. 5.12).

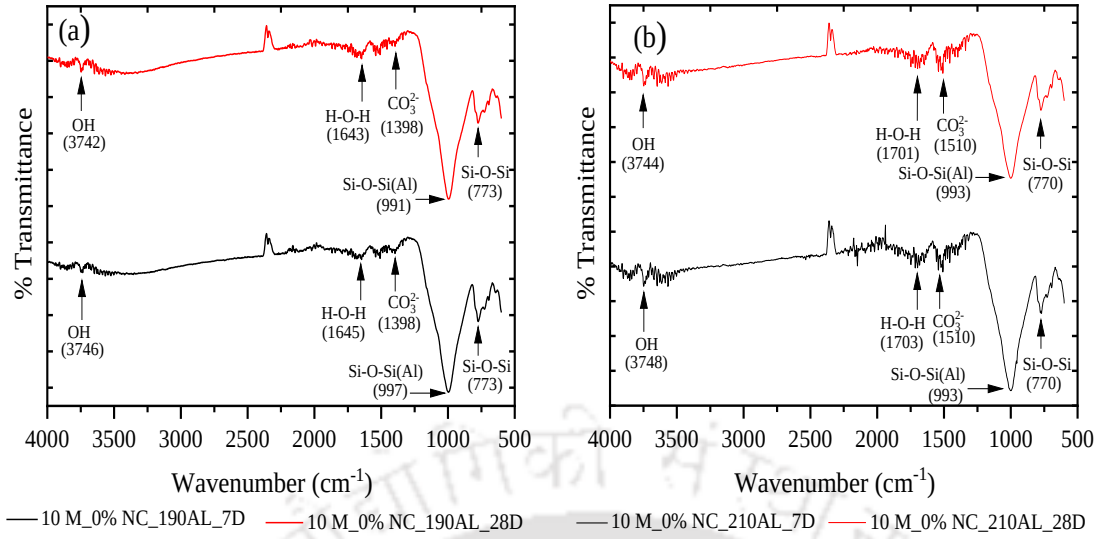

(GPC made with fly ash passing through 150 μm sieve, fly ash content of 425 kg/m^3, and SS/SH ratio of 1.75)

Fig. 5.13: FTIR spectra of control GPC mixes made with NaOH solution of 10 M for alkaline solution content of a) 190 kg/m^3, and b) 210 kg/m^3, at the age of 7 and 28 days

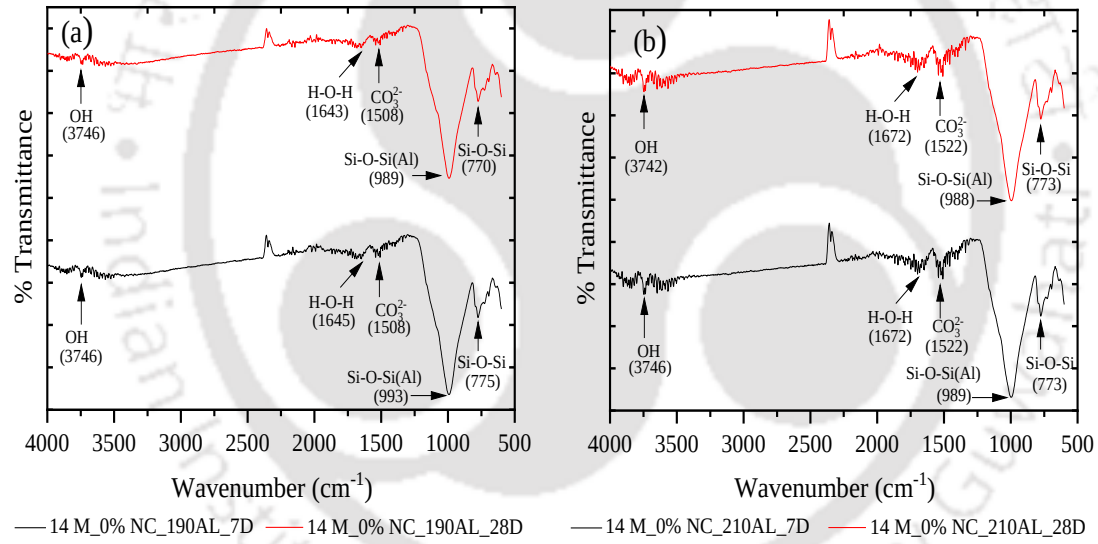

(GPC made with fly ash passing through 150 μm sieve, fly ash content of 425 kg/m^3, and SS/SH ratio of 1.75)

Fig. 5.14: FTIR spectra of control GPC mixes made with NaOH solution of 14 M for alkaline solution content of a) 190 kg/m^3, and b) 210 kg/m^3, at the age of 7 and 28 days

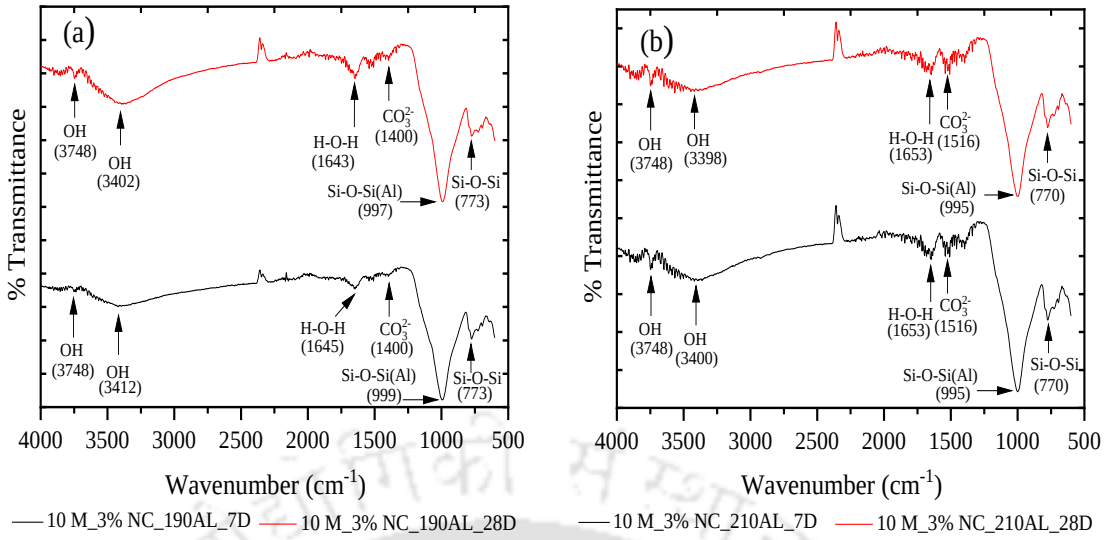

(GPC made with fly ash passing through 150 μm sieve, fly ash content of 425 kg/m^3, and SS/SH ratio of 1.75)

Fig. 5.15: FTIR spectra of 3% NaCl admixed GPC mixes made with NaOH solution of 10 M for alkaline solution content of a) 190 kg/m^3, and b) 210 kg/m^3, at the age of 7 and 28 days

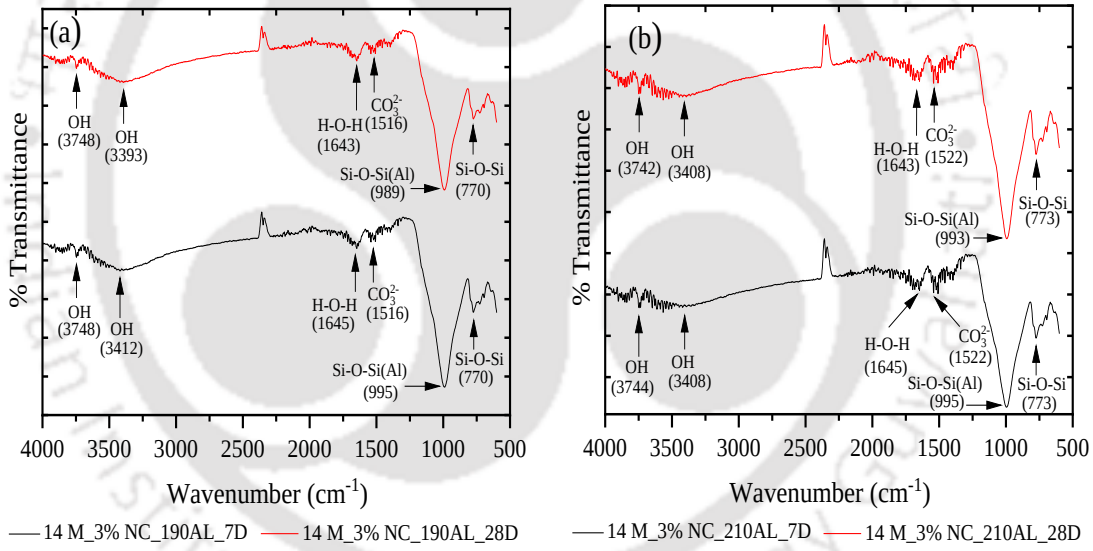

(GPC made with fly ash passing through 150 μm sieve, fly ash content of 425 kg/m^3, and SS/SH ratio of 1.75)

Fig. 5.16: FTIR spectra of 3% NaCl admixed GPC mixes made with NaOH solution of 14 M for alkaline solution content of a) 190 kg/m^3, and b) 210 kg/m^3, at the age of 7 and 28 days

The peak corresponding to Si–O–Si(Al) bond (Fig. 5.13 to Fig. 5.16) shifted to lower wavenumbers for higher molarity of NaOH solution (14 M), control mix (0% NaCl), and the age of 28 days when compared with lower molarity of NaOH solution (10 M), 3% NaCl admixed mix, and age of 7 days respectively thereby indicating the occurrence of geopolymerization reaction to a higher degree in GPC mixes at higher molarity of NaOH solution, 0% NaCl, and at comparatively later age [59]. This is supported by the XRD analysis where the peak intensity of geopolymeric compounds in XRD patterns (Fig. 5.9 to Fig. 5.12)

were higher in GPC made with higher molarity of NaOH solution, control GPC mix, and at the age of 28 days. From Fig. 5.13 to Fig. 5.16, the peak in the range of 1398 cm^{-1} to 1522 cm^{-1}, the band in the range of 3393 cm^{-1} to 3748 cm^{-1}, and the peak in the range of 1643 cm^{-1} to1703 cm^{-1} correspond to the stretching vibration of carbonate group, stretching vibration of –OH group, and bending vibration of H–O–H group respectively irrespective of alkaline solution content, molarity of NaOH solution, concentration of NaCl, and age.

Typical FESEM images of GPC for alkaline solution contents of 190 kg/m^3 and 210 kg/m^3 are shown in Fig. 5.17. The remaining FESEM images are provided in Appendix (Fig. A18).

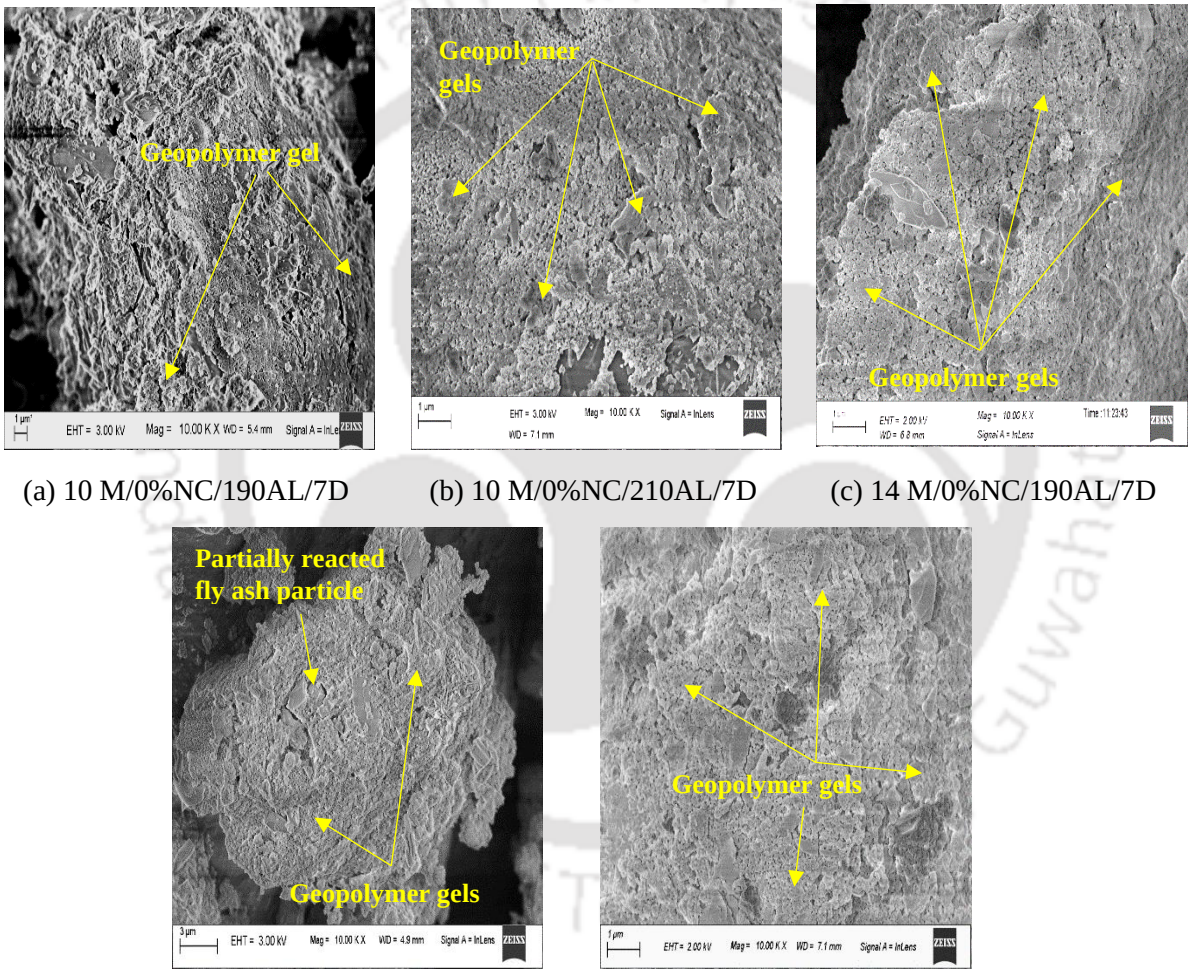

(a) 10 M/0%NC/190AL/7D (b) 10 M/0%NC/210AL/7D (c) 14 M/0%NC/190AL/7D

(d) 10 M/3%NC/210AL/7D (e) 14 M/0%NC/190AL/28D

(GPC made with fly ash passing through 150 µm sieve, fly ash content of 425 kg/m^3, and SS/SH ratio of 1.75)

Fig. 5.17: FESEM images of GPC mixes for different alkaline solution contents and molarity of NaOH solution

From Fig. 5.17 (a, b), it is observed that the GPC mix made with higher alkaline solution content showed denser microstructure with more formation of geopolymer gels as compared to that made with lower alkaline solution content. This is supported by the XRD analysis where

the GPC mix made with higher alkaline solution content showed higher peak intensity of the compounds related to geopolymer gels as compared to lower alkaline solution content (Fig. 5.9). Further, the GPC mix made with higher molarity of NaOH solution, and control mix showed compact microstructure with more amount of geopolymer gels as compared to that made with lower molarity of NaOH solution (Fig. 5.17 (a, c)), and 3% NaCl admixed GPC mix (Fig. 5.17 (b, d)), which is in line with the variations in the peak intensity of the geopolymeric compounds indicated by the XRD patterns (Fig. 5.9 (a), Fig. 5.10 (a), Fig. 5.9 (b), and Fig. 5.11 (b)). The FESEM images shown in Fig. 5.17 (c, e) indicate more formation of geopolymer gels at the age of 28 days as compared to that at the age of 7 days thereby indicating higher extent of geopolymerization reaction at the age of 28 days in GPC mixes. This is corroborated with the XRD analysis where the peak intensity of albite, anorthoclase, nepheline, sodalite, and muscovite were higher at the age of 28 days as compared to that at the age of 7 days (Fig. 5.10 (a)). In addition, the FESEM image showed the presence of partially reacted fly ash particles in the GPC mix at the age of 7 days (Fig. 5 17 (d)).

5.2.3 Effect of SS/SH ratio on microstructure of GPC

The obtained XRD patterns of GPC mixes made from alkaline solution (SS/SH) ratios of 1.5 and 1.75 are shown in Fig. 5.18 to Fig. 5.21.

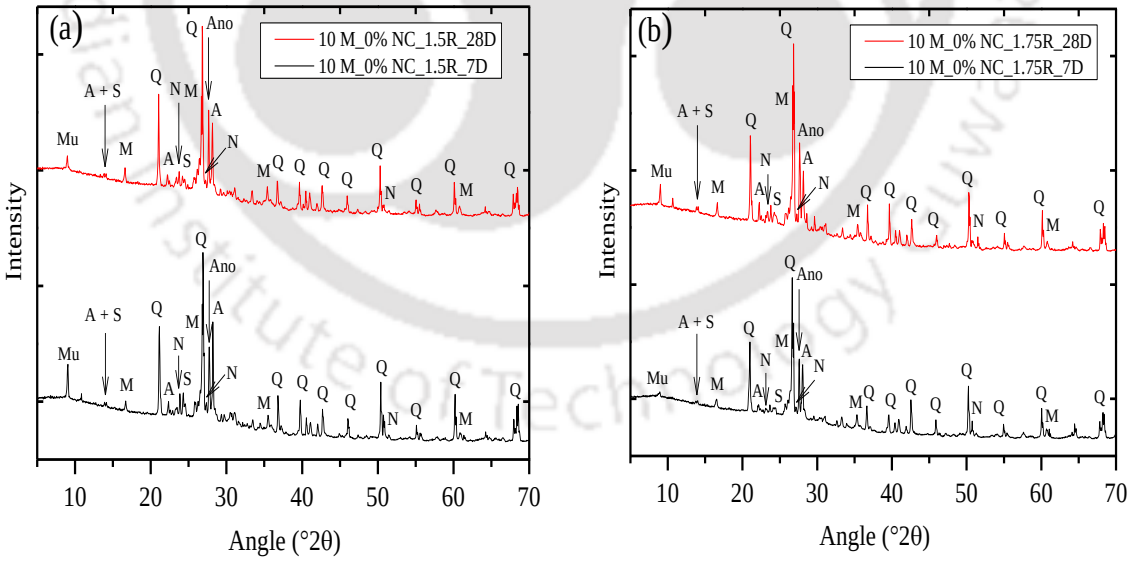

(GPC made with fly ash passing through 150 μm sieve, fly ash content of 425 kg/m^3, and alkaline solution content of 210 kg/m^3)

Fig. 5.18: XRD patterns of control GPC mixes made with NaOH solution of 10 M for SS/SH ratio of a) 1.5, and b) 1.75, at the age of 7 and 28 days

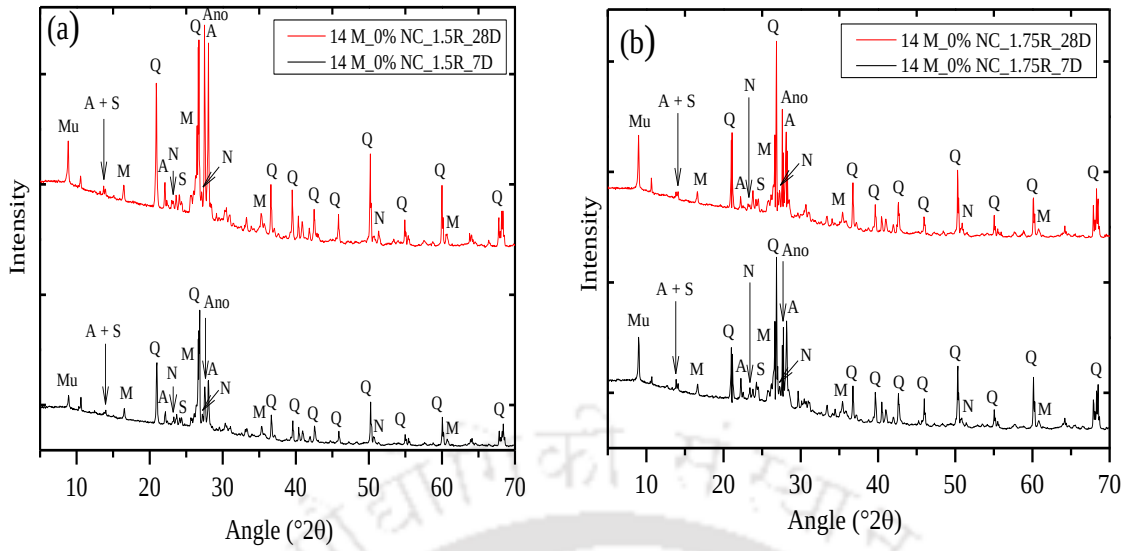

(GPC made with fly ash passing through 150 μm sieve, fly ash content of 425 kg/m³, and alkaline solution content of 210 kg/m³)

Fig. 5.19: XRD patterns of control GPC mixes made with NaOH solution of 14 M for SS/SH ratio of a) 1.5, and b) 1.75, at the age of 7 and 28 days

From Fig. 5.18 to Fig. 5.21, it is observed that the peak intensity of albite, anorthoclase, nepheline, sodalite, and muscovite were mostly higher in GPC mixes made with higher SS/SH ratio (1.75) as compared to that made with lower SS/SH ratio (1.5), which signifies comparatively more formation of geopolymer gels at higher SS/SH ratio. This is in line with the variations in compressive strength of GPC with SS/SH ratio (Fig. 4.11 and Fig. 4.12) i.e., the compressive strength of GPC was mostly higher at higher SS/SH ratio than that at lower SS/SH ratio.

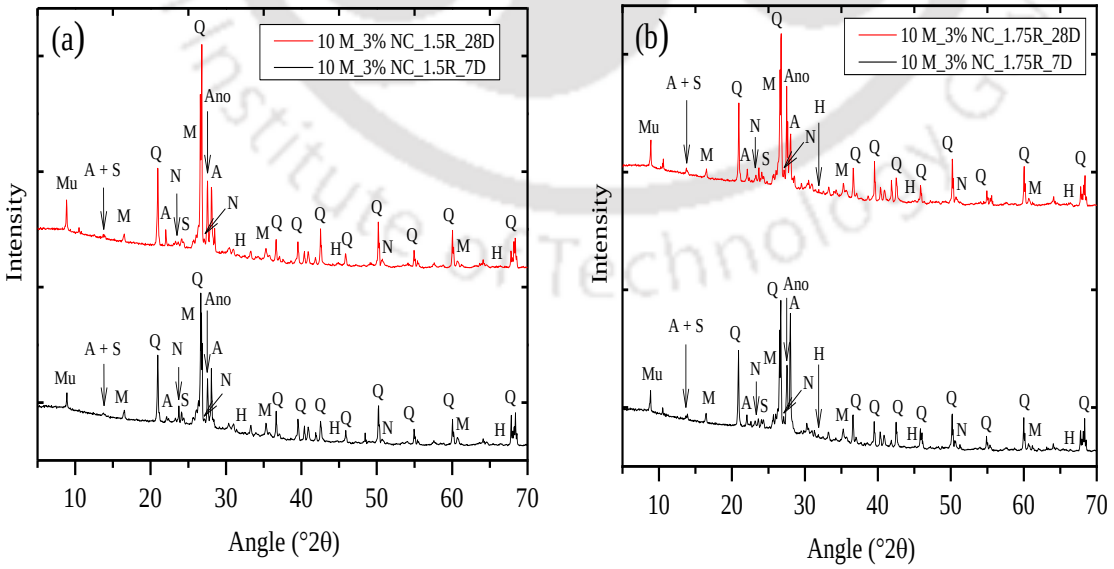

(GPC made with fly ash passing through 150 μm sieve, fly ash content of 425 kg/m³, and alkaline solution content of 210 kg/m³)

Fig. 5.20: XRD patterns of 3% NaCl admixed GPC mixes made with NaOH solution of 10 M for SS/SH ratio of a) 1.5, and b) 1.75, at the age of 7 and 28 days

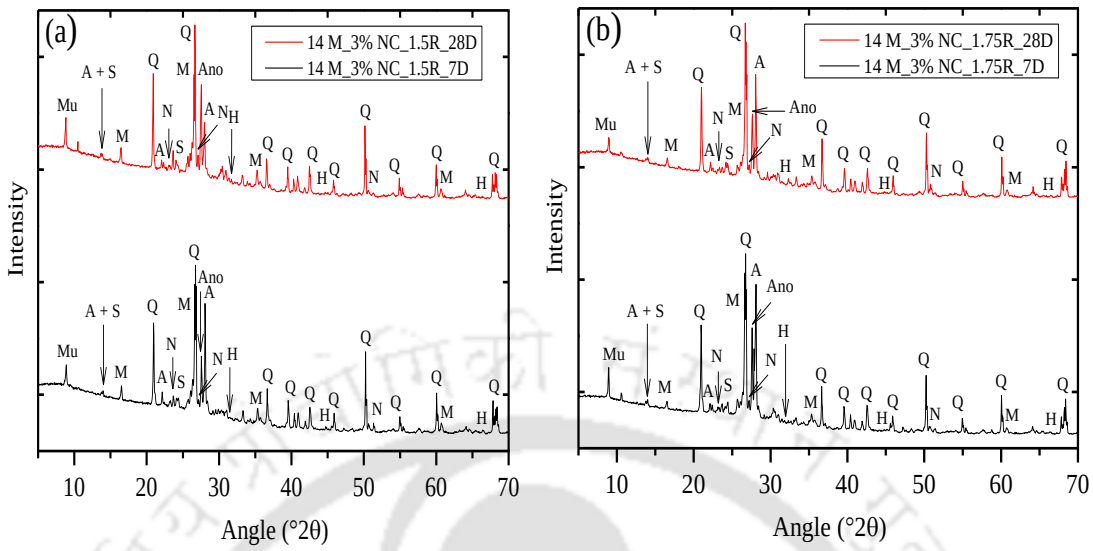

(GPC made with fly ash passing through 150 μm sieve, fly ash content of 425 kg/m^3, and alkaline solution content of 210 kg/m^3)

Fig. 5.21: XRD patterns of 3% NaCl admixed GPC mixes made with NaOH solution of 14 M for SS/SH ratio of a) 1.5, and b) 1.75, at the age of 7 and 28 days

The lower compressive strength at higher SS/SH ratio in few cases i.e., in case of GPC mixes made with 3% NaCl and 14 M NaOH solution (Fig. 4.11 and Fig. 4.12) is also supported by lower peak intensity of the compounds related to geopolymer gels in GPC mixes at higher SS/SH ratio as observed from Fig. 5.21. From Fig. 5.18 to Fig. 5.21, it is noted that the peak intensity of albite, anorthoclase, nepheline, sodalite, and muscovite in the XRD patterns were higher at higher molarity of NaOH solution (14 M), and at the age of 28 days as compared to that at lower molarity of NaOH solution (10 M) and at the age of 7 days respectively. This shows more formation of geopolymer gels at higher molarity of NaOH solution, and at comparatively later age, which substantiates the variation in compressive strength of GPC with molarity of NaOH solution, and age (Fig. 4.11 and Fig. 4.12). The presence of NaCl in GPC mixes altered the extent of geopolymerization process thereby showing lower peak intensity of albite, anorthoclase, nepheline, sodalite, and muscovite as compared to control GPC mixes (Fig. 5.18 to Fig. 5.21), which is supported by the variation in compressive strength between control mix and 3% NaCl admixed GPC mix (Fig. 4.11 and Fig. 4.12). From Fig. 5.20 and Fig. 5.21, it is inferred that mostly there was unsystematic variation in peak intensity of halite with molarity of NaOH solution in NaCl admixed GPC mixes. Further, the peak intensity of halite was higher at lower alkaline solution ratio, and at the age of 7 days than that at higher alkaline

solution ratio and at the age of 28 days respectively, which shows comparatively more crystallization of sodium chloride at lower SS/SH ratio in GPC mixes during early age.

The FTIR spectra of GPC mixes made with alkaline solution (SS/SH) ratios 1.5 and 1.75 are presented in Fig. 5.22 to Fig. 5.25.

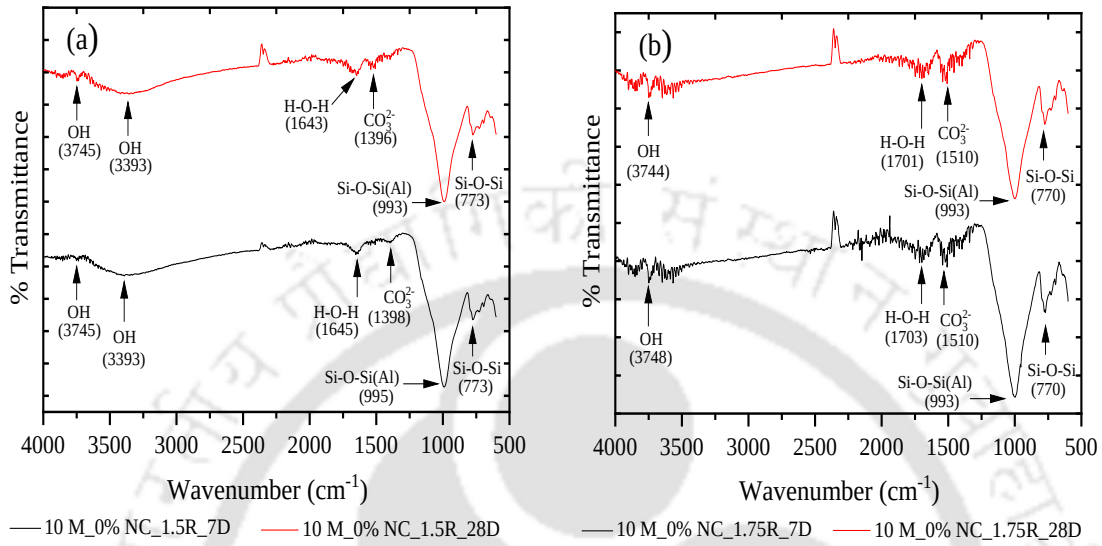

(GPC made with fly ash passing through 150 μm sieve, fly ash content of 425 kg/m³, and alkaline solution content of 210 kg/m³)

Fig. 5.22: FTIR spectra of control GPC mixes made with NaOH solution of 10 M for SS/SH ratio of a) 1.5, and b) 1.75, at the age of 7 and 28 days

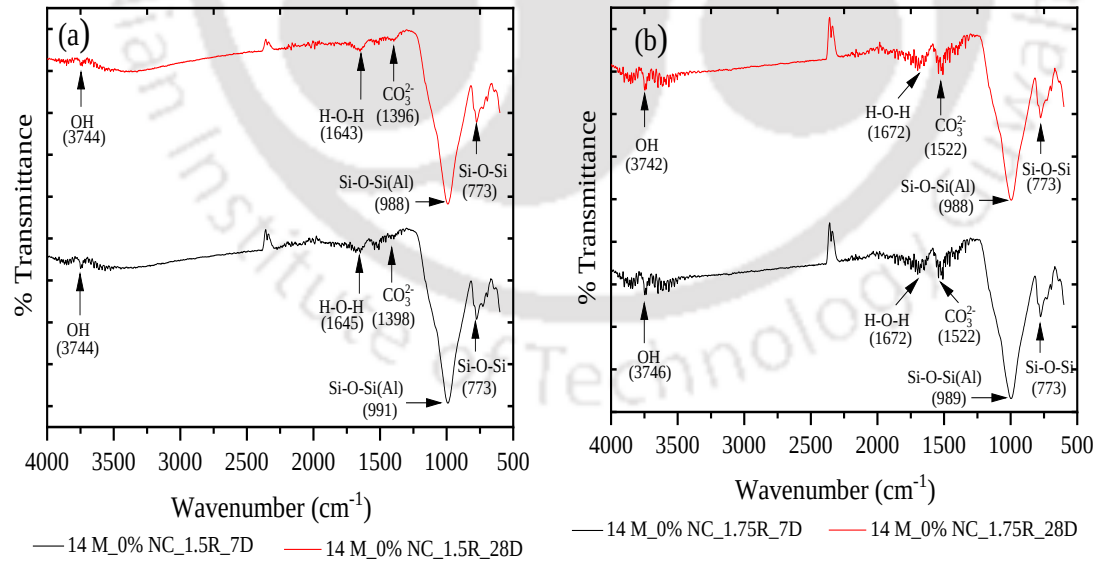

(GPC made with fly ash passing through 150 μm sieve, fly ash content of 425 kg/m³, and alkaline solution content of 210 kg/m³)

Fig. 5.23: FTIR spectra of control GPC mixes made with NaOH solution of 14 M for SS/SH ratio of a) 1.5, and b) 1.75, at the age of 7 and 28 days

In the FTIR spectra, the peak in the range of 770 cm^{-1} - 773 cm^{-1} and that in the range of 1381 cm^{-1} - 1522 cm^{-1} correspond to the presence of quartz, and stretching vibration of carbonate group respectively (Fig. 5.22 to Fig. 5.25). The peak associated with asymmetric stretching vibration of Si–O–Si(Al) bond observed in the range of 988 cm^{-1} to 997 cm^{-1} (Fig. 5.22 to Fig. 5.25) shows the presence of geopolymer gels in GPC mixes made with different SS/SH ratios (1.5 and 1.75). From the FTIR spectra, the peak associated with Si–O–Si(Al) bond mostly shifted to lower wavenumbers at higher SS/SH ratio when compared with lower SS/SH ratio of GPC mixes, which indicates higher extent of geopolymerization reaction at higher SS/SH ratio. This is also substantiated by mostly higher peak intensity of albite, anorthoclase, nepheline, sodalite, and muscovite in the XRD patterns at higher SS/SH ratio than that at lower SS/SH ratio (Fig. 5.18 to Fig. 5.21).

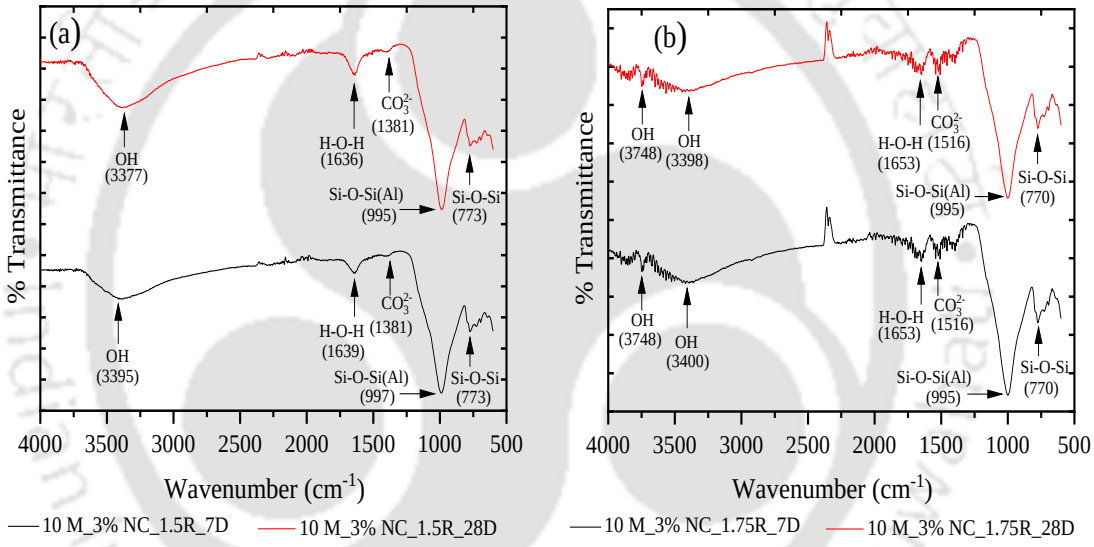

(GPC made with fly ash passing through 150 μm sieve, fly ash content of 425 kg/m^3, and alkaline solution content of 210 kg/m^3)

Fig. 5.24: FTIR spectra of 3% NaCl admixed GPC mixes made with NaOH solution of 10 M for SS/SH ratio of a) 1.5, and b) 1.75, at the age of 7 and 28 days

Further, with respect to lower molarity of NaOH solution (10 M), and 3% NaCl admixed GPC mix, the peak corresponding to asymmetric stretching vibration of Si–O–Si(Al) bond shifted to lower wavenumbers for higher molarity of NaOH solution (14 M) and control mix (Fig. 5.22 to Fig. 5.25) respectively for both alkaline solution ratios thereby indicating greater extent of geopolymerization process at higher molarity of NaOH solution, and in control GPC mix [59]. While analyzing the effect of age, it is inferred from Fig. 5.22 to Fig. 5.25 that the peak corresponding to asymmetric stretching vibration of Si–O–Si(Al) bond shifted to lower wavenumbers at the age of 28 days when compared with that at the age of 7 days. These

variations in the wavenumbers associated with the peak indicating the asymmetric stretching vibration of Si–O–Si(Al) bond with change in molarity of NaOH solution (10 M and 14 M), admixed NaCl concentration (0% and 3%) and age (7 and 28 days) are supported by the variations in the peak intensity of albite, anorthoclase, nepheline, sodalite, and muscovite in the XRD patterns (Fig. 5.18 to Fig. 5.21). In the FTIR spectra shown in Fig. 5.22 to Fig. 5.25, the band in the range of 3377 cm^{-1} to 3748 cm^{-1}, and the peak in the range of 1636 cm^{-1} to 1703 cm^{-1} are associated with stretching vibration of –OH group, and bending vibration of H–O–H group respectively for different SS/SH ratios, molarity of NaOH solution and age.

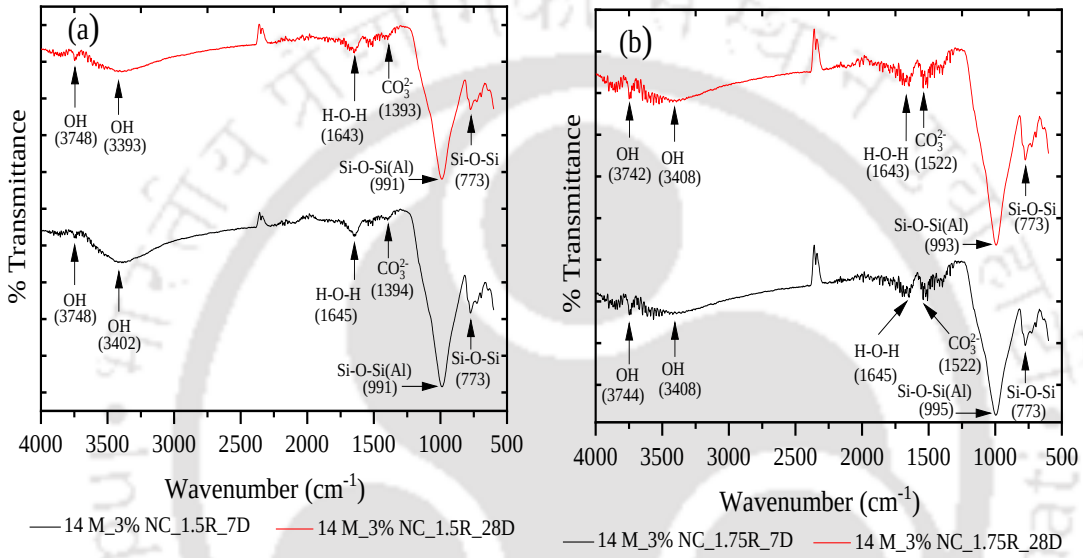

(GPC made with fly ash passing through 150 μm sieve, fly ash content of 425 kg/m^3, and alkaline solution content of 210 kg/m^3)

Fig. 5.25: FTIR spectra of 3% NaCl admixed GPC mixes made with NaOH solution of 14 M for SS/SH ratio of a) 1.5, and b) 1.75, at the age of 7 and 28 days

Typical FESEM images of GPC mixes for alkaline solution (SS/SH) ratios of 1.5 and 1.75 are shown in Fig. 5.26. The remaining FESEM images are provided in Appendix (Fig. A19). From Fig. 5.26 (a, b), it is inferred that the GPC mix made with higher SS/SH ratio showed compact microstructure with comparatively more formation of geopolymer gels than lower SS/SH ratio. This is corroborated with the XRD results as the GPC mix made with higher SS/SH ratio showed higher peak intensity of albite, anorthoclase, nepheline, sodalite, and muscovite than that made with lower SS/SH ratio (Fig. 5.19). Further, the presence of partially reacted fly ash particles was observed in the GPC mix as noted from Fig. 5.26 (a).

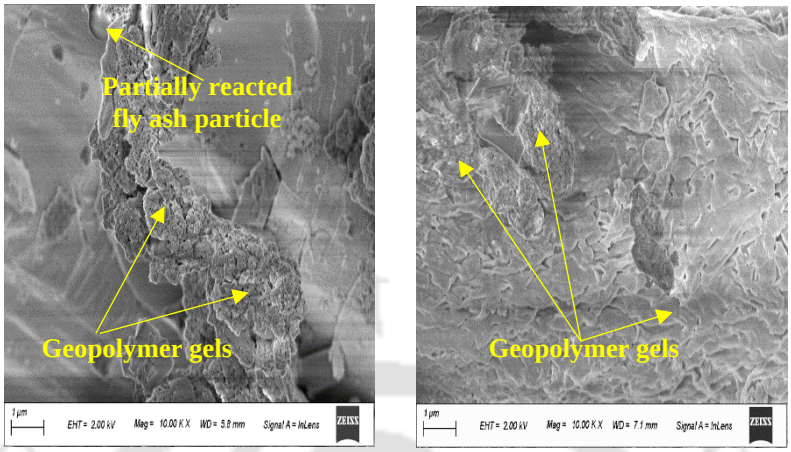

(a) 1.5R/14 M/0%NC/28D (b) 1.75R/14 M/0%NC/28D

(GPC made with fly ash passing through 150 μm sieve, fly ash content of 425 kg/m^3, and alkaline solution content of 210 kg/m^3)

Fig. 5.26: FESEM images of control GPC mixes made with NaOH solution of 14 M for SS/SH ratio of a) 1.5, and b) 1.75, at the age of 28 days

5.2.4 Effect of particle size of fly ash on microstructure of GPC

The obtained XRD patterns of GPC mixes made with fly ash passing through 150 μm sieve, and 300 μm sieve are shown in Fig. 5.27 to 5.30 for fly ash content of 425 kg/m^3. From Fig. 5.27 to Fig. 5.30, it is noted that the GPC mixes made with comparatively larger fly ash particles i.e., fly ash passing through 300 μm sieve mostly showed higher peak intensity of the compounds related to N-A-S-H gel in the XRD patterns as compared to that made with smaller fly ash particles i.e., fly ash passing through 150 μm sieve. This shows comparatively more formation of geopolymer gels in GPC mixes made with larger fly ash particles than smaller fly ash particles at comparatively lower fly ash content of 425 kg/m^3, which contributed toward higher compressive strength of GPC mixes made with larger fly ash particles than smaller fly ash particles (Fig. 4.13 and Fig. 4.14).

From Fig. 5.27 to Fig. 5.30, the peak intensity of the compounds related to geopolymer gels were mostly higher at higher molarity of NaOH solution (14 M), in control mix (0% NaCl), and at the age of 28 days as compared to lower molarity of NaOH solution (10 M), 3% NaCl admixed mix, and age of 7 days respectively for both sizes of fly ash particles. These variations in the peak intensity of the geopolymeric compounds with molarity of NaOH solution, NaCl concentration, and age are consistent with the variations in the compressive strength of GPC mixes (Fig. 4.13 and Fig. 4.14).

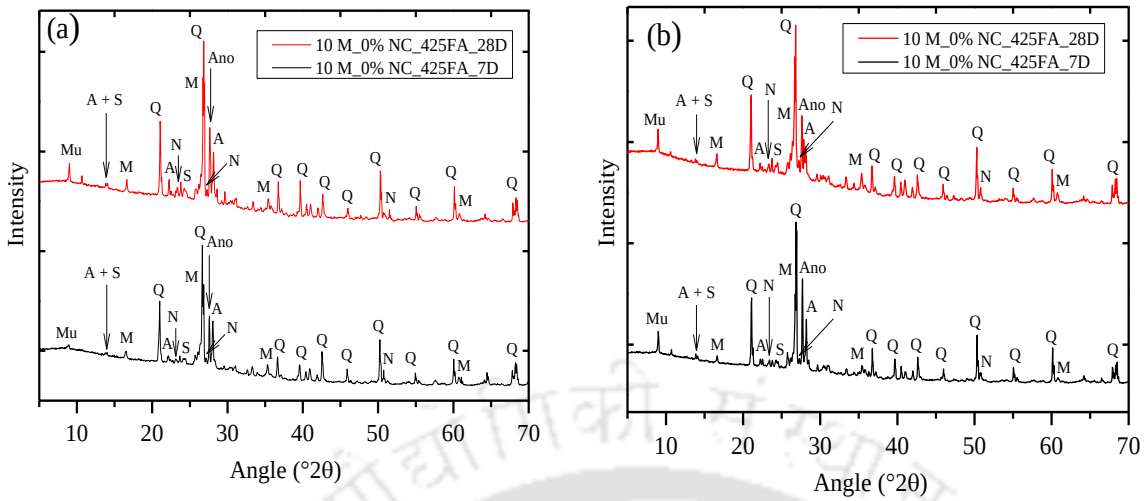

(GPC made with fly ash content of 425 kg/m^3, alkaline solution content of 210 kg/m^3, and SS/SH ratio of 1.75)

Fig. 5.27: XRD patterns of control GPC mixes made with NaOH solution of 10 M for fly ash passing through a) 150 µm sieve, and b) 300 µm sieve, at the age of 7 and 28 days

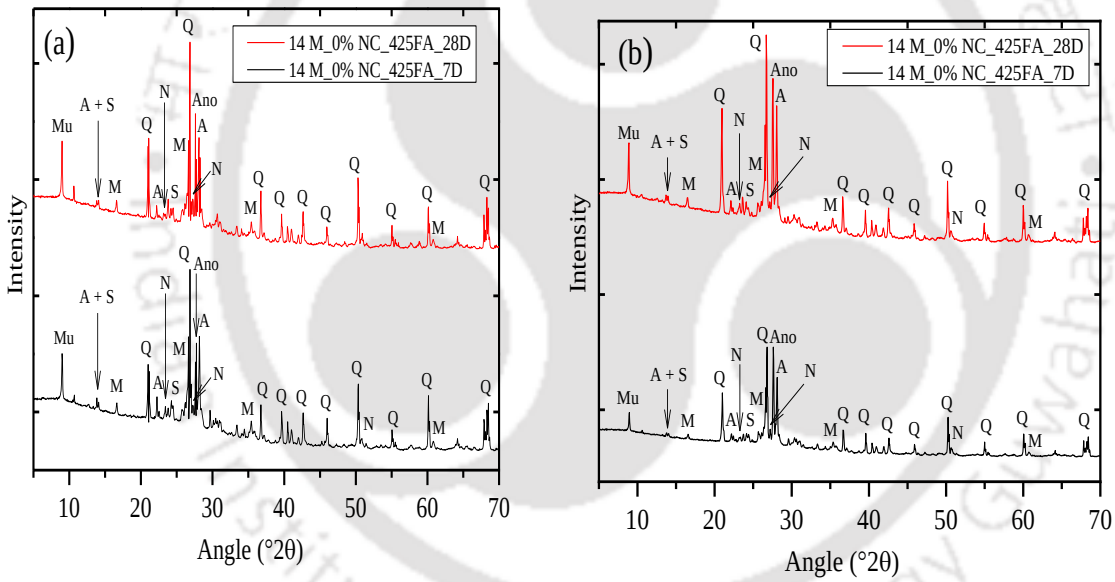

(GPC made with fly ash content of 425 kg/m^3, alkaline solution content of 210 kg/m^3, and SS/SH ratio of 1.75)

Fig. 5.28: XRD patterns of control GPC mixes made with NaOH solution of 14 M for fly ash passing through a) 150 µm sieve, and b) 300 µm sieve, at the age of 7 and 28 days

From Fig. 5.29 and Fig. 5.30, it is inferred that the peak intensity of halite was mostly higher at the age of 7 days than that at the age of 28 days in NaCl admixed GPC mixes. Further, as observed from Fig. 5.29 and Fig. 5.30, the variation in the peak intensity of halite in the XRD patterns was mostly unsystematic with molarity of NaOH solution. From Fig. 5.29 and Fig. 5.30, it is inferred that the peak intensity of halite in the XRD patterns was mostly higher in the GPC mixes made with larger fly ash particles (fly ash passing through 300 µm sieve) than that made with smaller fly ash particles (fly ash passing through 150 µm sieve). However, it

may be noted that the compressive strength of GPC was higher for fly ash passing through 300 µm sieve than that passing through 150 µm sieve (Fig. 4.13 and Fig. 4.14). Thus, although there was comparatively more crystallization of sodium chloride in GPC made with larger fly ash particles as indicated by the peak intensity of halite, the combined effect of pore filling with unreacted/partially reacted larger fly ash particles, and geopolymerization reaction contributed toward higher compressive strength of GPC made with larger fly ash particles (already discussed in Section 4.3.4) over the effect of higher crystallization of sodium chloride.

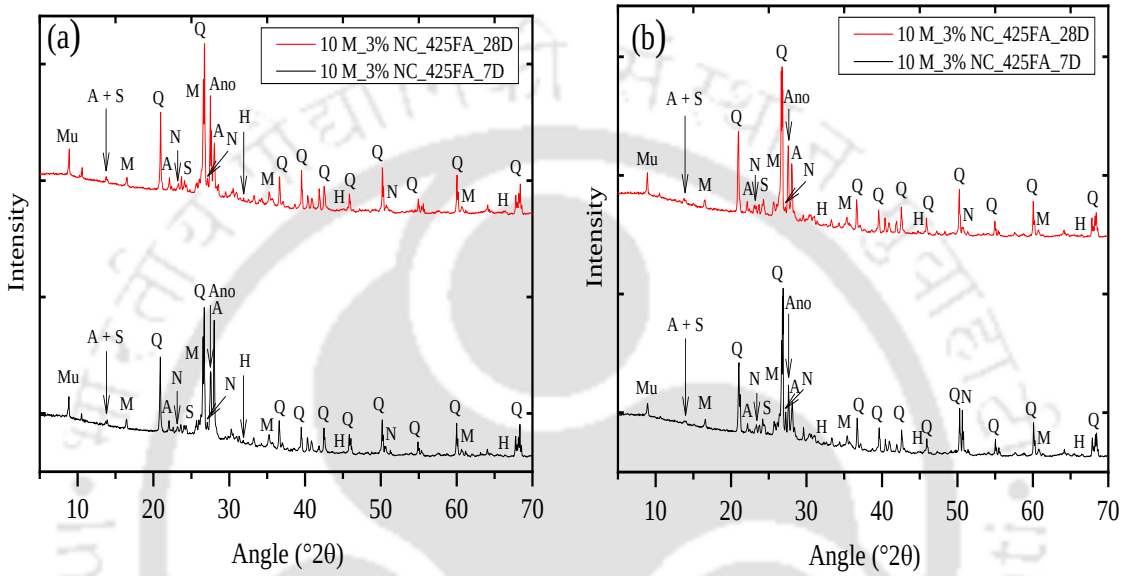

(GPC made with fly ash content of 425 kg/m^3, alkaline solution content of 210 kg/m^3, and SS/SH ratio of 1.75)

Fig. 5.29: XRD patterns of 3% NaCl admixed GPC mixes made with NaOH solution of 10 M for fly ash passing through a) 150 µm sieve, and b) 300 µm sieve, at the age of 7 and 28 days

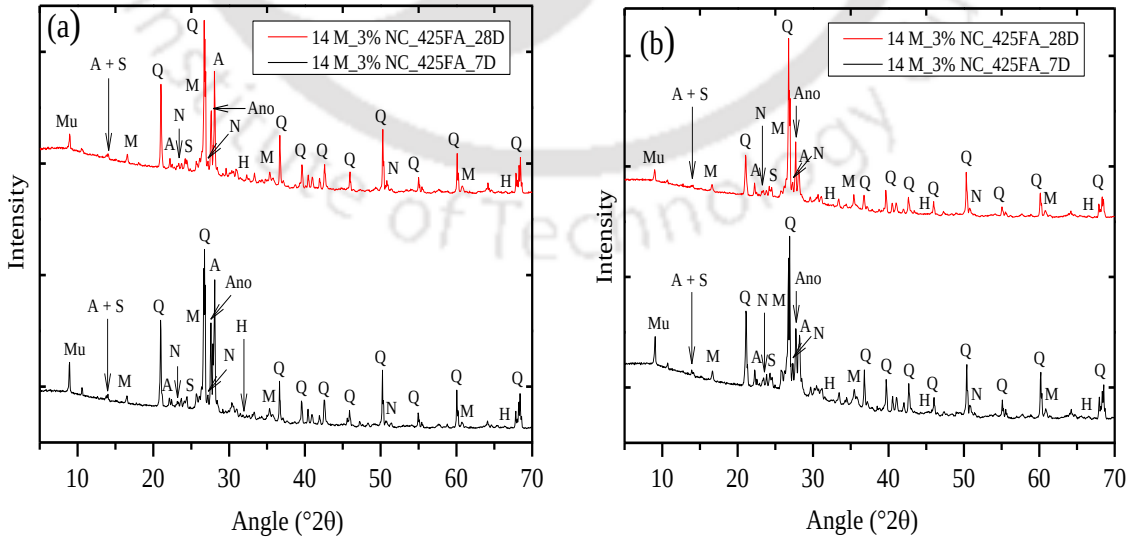

(GPC made with fly ash content of 425 kg/m^3, alkaline solution content of 210 kg/m^3, and SS/SH ratio of 1.75)

Fig. 5.30: XRD patterns of 3% NaCl admixed GPC mixes made with NaOH solution of 14 M for fly ash passing through a) 150 µm sieve, and b) 300 µm sieve, at the age of 7 and 28 days

For fly ash content of 425 kg/m^3, the obtained FTIR spectra of GPC mixes made with fly ash passing through 150 µm sieve, and 300 µm sieve are shown in Fig. 5.31 to Fig. 5.34. From Fig. 5.31 to Fig. 5.34, the peak in the range of 770 cm^{-1} to 778 cm^{-1} and that in the range of 1398 cm^{-1} to 1522 cm^{-1} are associated with the presence of quartz, and stretching vibration of carbonate group respectively in both control and chloride admixed GPC mixes. From Fig. 5.31 to Fig. 5.34, the band identified in the range of 3398 cm^{-1} - 3748 cm^{-1}, and peak in the range of 1643 cm^{-1} - 1715 cm^{-1} are related to –OH group stretching vibration, and H–O–H group bending vibration respectively. In Fig. 5.31 to Fig. 5.34, the peak associated with the asymmetric stretching vibration of Si–O–Si(Al) bond that indicates the presence of geopolymer gels in GPC mixes shifted to higher wavenumbers (997 cm^{-1} to 1003 cm^{-1}) for GPC mixes made with larger fly ash particles (passing through 300 µm sieve) when compared with that (988 cm^{-1} to 995 cm^{-1}) made with smaller fly ash particles (passing through 150 µm sieve), although the peak intensity of the compounds related to geopolymer gels were mostly higher in GPC made with larger fly ash particles than that made with smaller fly ash particles (Fig. 5.27 to Fig. 5.30).

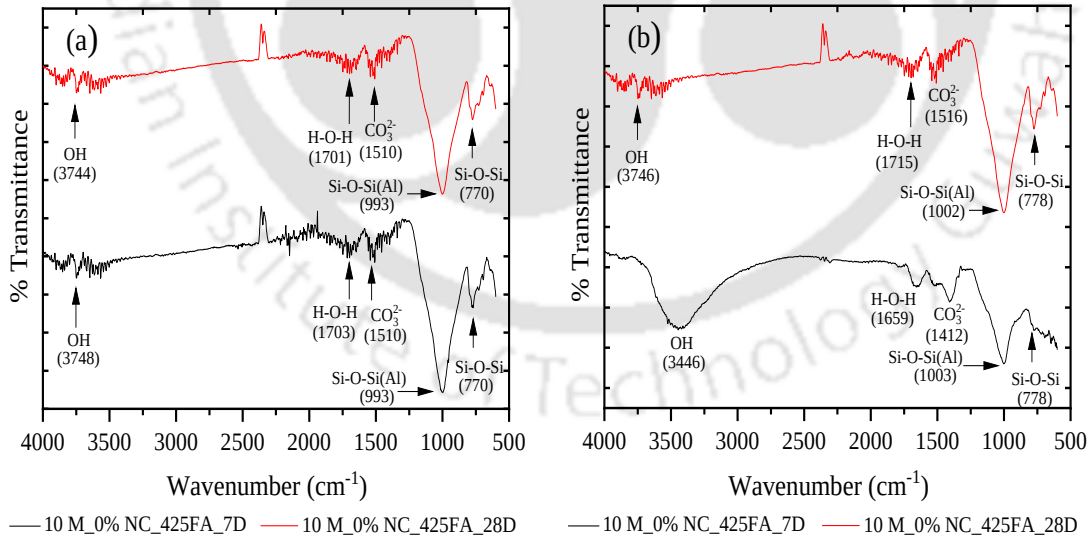

(GPC made with fly ash content of 425 kg/m^3, alkaline solution content of 210 kg/m^3, and SS/SH ratio of 1.75)

Fig. 5.31: FTIR spectra of control GPC mixes made with NaOH solution of 10 M for fly ash passing through a) 150 µm sieve, and b) 300 µm sieve, at the age of 7 and 28 days

In Fig. 5.31 to Fig. 5.34, the peak related to asymmetric stretching vibration of Si–O–Si(Al) bond that shows the presence of geopolymer gels mostly shifted to lower wavenumbers in case

of GPC made with NaOH solution of 14 M, control GPC mix (0% NaCl), and at the age of 28 days when compared with GPC made with NaOH solution of 10 M, 3% NaCl admixed GPC, and at the age of 7 days for both sizes of fly ash particles. This signifies comparatively higher extent of geopolymerization reaction for higher molarity of NaOH solution [59], control mix and at the age of 28 days, which is consistent with the variations in the peak intensity of geopolymeric compounds with these parameters in the XRD patterns (Fig. 5.27 to Fig. 5.30).

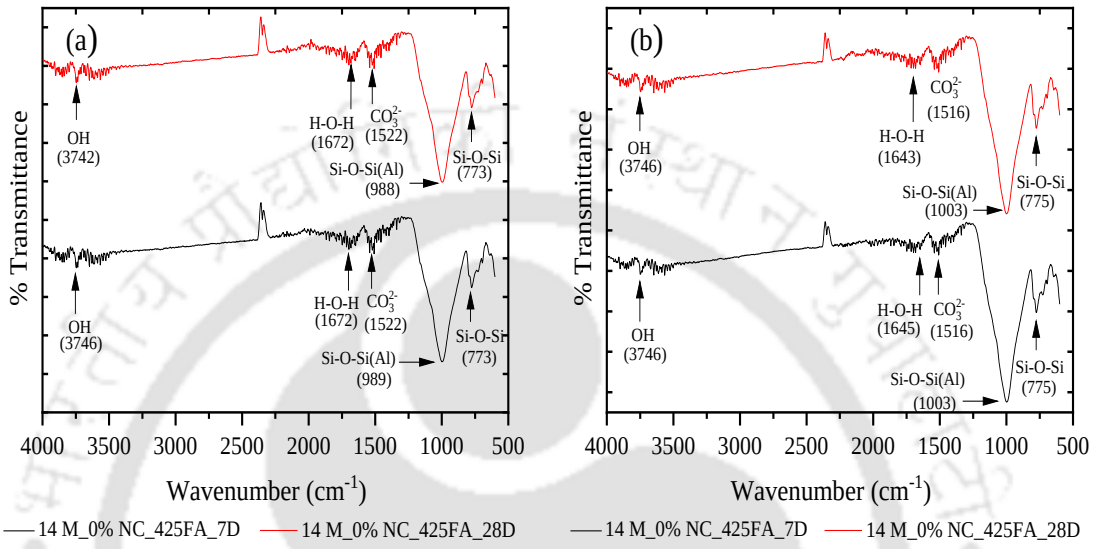

(GPC made with fly ash content of 425 kg/m^3, alkaline solution content of 210 kg/m^3, and SS/SH ratio of 1.75)

Fig. 5.32: FTIR spectra of control GPC mixes made with NaOH solution of 14 M for fly ash passing through a) 150 µm sieve, and b) 300 µm sieve, at the age of 7 and 28 days

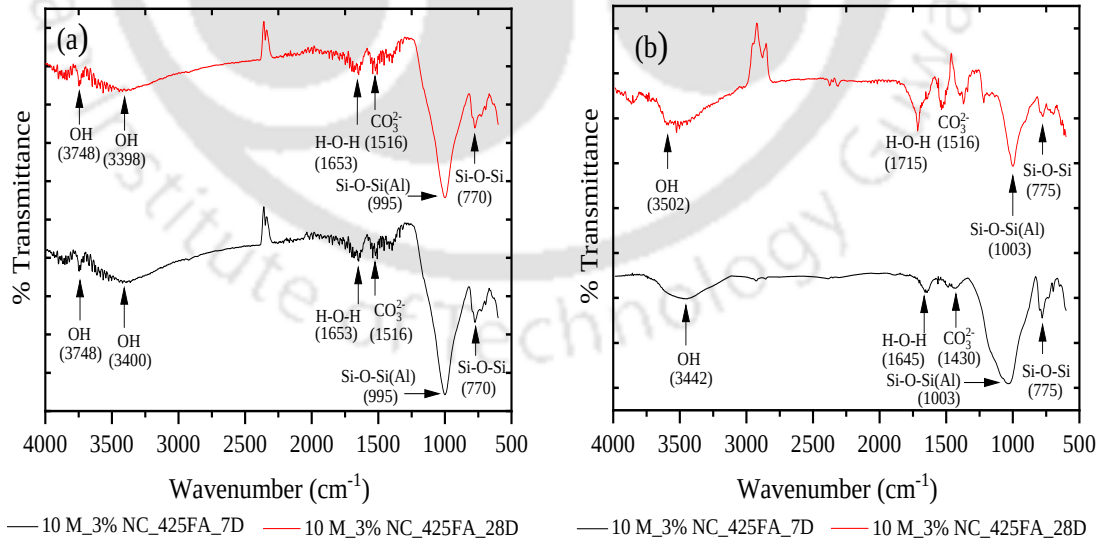

(GPC made with fly ash content of 425 kg/m^3, alkaline solution content of 210 kg/m^3, and SS/SH ratio of 1.75)

Fig. 5.33: FTIR spectra of 3% NaCl admixed GPC mixes made with NaOH solution of 10 M for fly ash passing through a) 150 µm sieve, and b) 300 µm sieve, at the age of 7 and 28 days

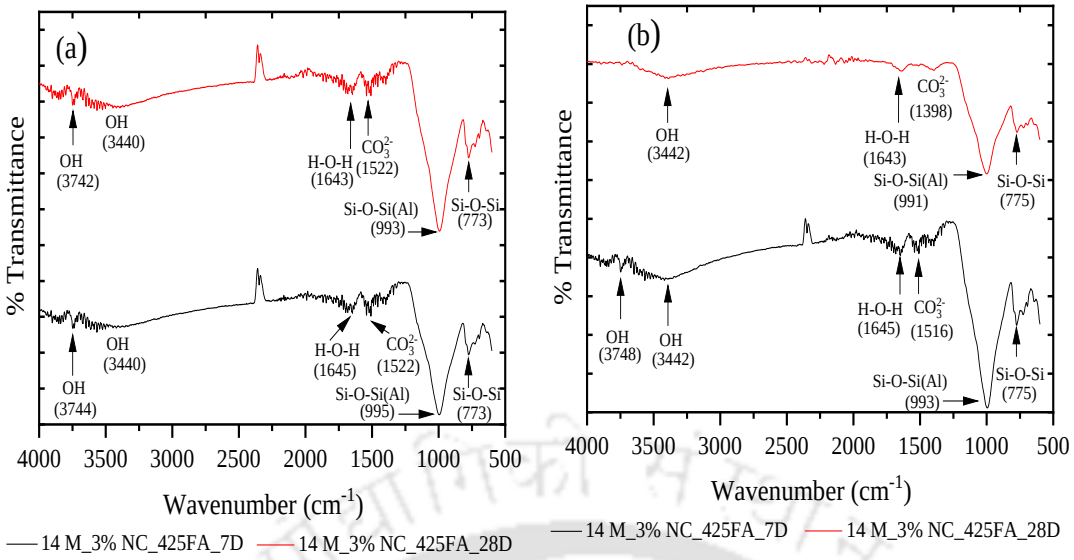

(GPC made with fly ash content of 425 kg/m^3, alkaline solution content of 210 kg/m^3, and SS/SH ratio of 1.75)

Fig. 5.34: FTIR spectra of 3% NaCl admixed GPC mixes made with NaOH solution of 14 M for fly ash passing through a) 150 µm sieve, and b) 300 µm sieve, at the age of 7 and 28 days

Typical FESEM images of GPC mixes made with fly ash passing through 150 µm sieve, and 300 µm sieve are shown in Fig. 5.35 for fly ash content of 425 kg/m^3. The remaining FESEM images are shown in Appendix A.

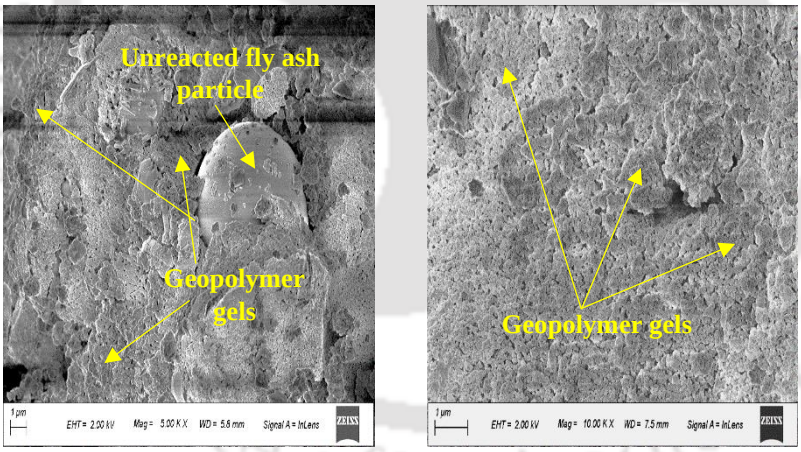

(a) 14 M/3%NC/150 µm/7D (b) 14 M/3%NC/300 µm /7D

(GPC made with fly ash content of 425 kg/m^3, alkaline solution content of 210 kg/m^3, and SS/SH ratio of 1.75)

Fig. 5.35: FESEM images of 3% NaCl admixed GPC mixes made with NaOH solution of 14 M for fly ash passing through a) 150 µm sieve, and b) 300 µm sieve, at the age of 7 days

The FESEM micrographs shown in Fig. 5.35 indicate comparatively more formation of geopolymer gels in GPC made with larger fly ash particles (passing through 300 µm sieve) leading to denser microstructure than that made with smaller fly ash particles (passing through 150 µm sieve). This is supported by mostly higher peak intensity of the geopolymeric compounds in the XRD patterns of GPC made with larger fly ash particles than that made with

smaller fly ash particles (Fig. 5.30 (a, b)). In addition, the FESEM image showed the presence of unreacted fly ash particle in the GPC mix during the early age of 7 days (5.35 (a)).

For fly ash content of 450 kg/m^3, the obtained XRD patterns of GPC mixes made with fly ash passing through 150 µm sieve, and 300 µm sieve are shown in Fig. 5.36 to Fig. 5.43 for different molarity of NaOH solution (10 M and 14 M), admixed concentrations of NaCl (0%, 1.5%, 3% and 4.5%), and age (7, 28, and 90 days).

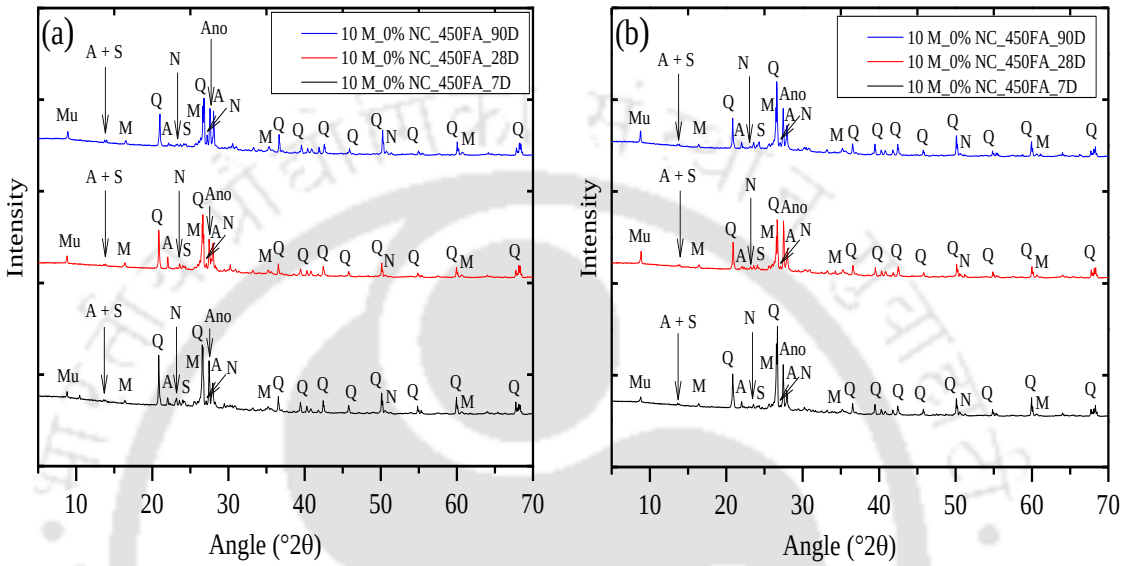

(GPC made with fly ash content of 450 kg/m^3, alkaline solution content of 210 kg/m^3, and SS/SH ratio of 1.75)

Fig. 5.36: XRD patterns of control GPC mixes made with NaOH solution of 10 M for fly ash passing through a) 150 µm sieve, and b) 300 µm sieve, at the age of 7, 28, and 90 days

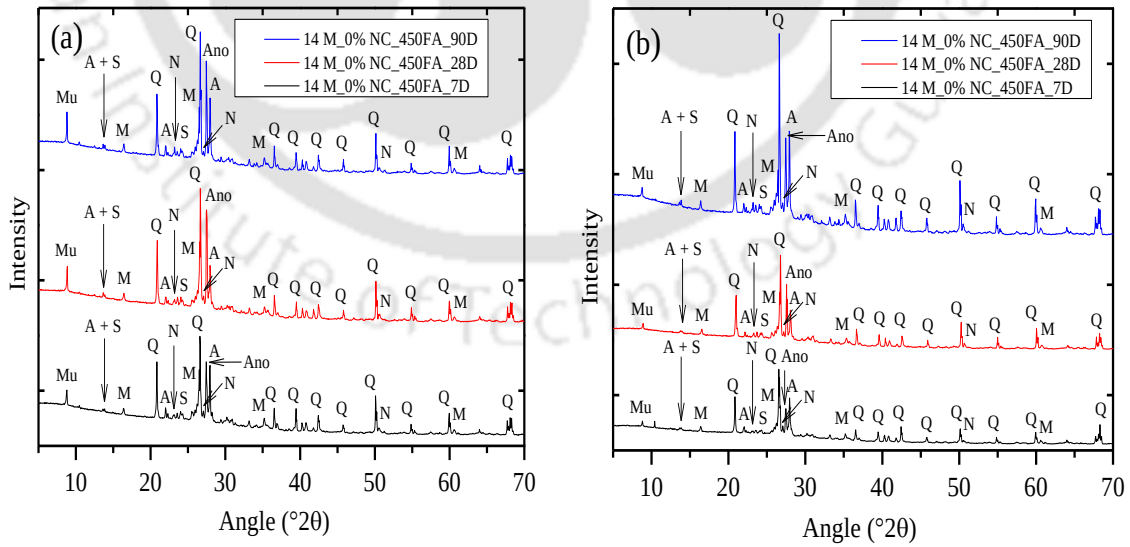

(GPC made with fly ash content of 450 kg/m^3, alkaline solution content of 210 kg/m^3, and SS/SH ratio of 1.75)

Fig. 5.37: XRD patterns of control GPC mixes made with NaOH solution of 14 M for fly ash passing through a) 150 µm sieve, and b) 300 µm sieve, at the age of 7, 28, and 90 days

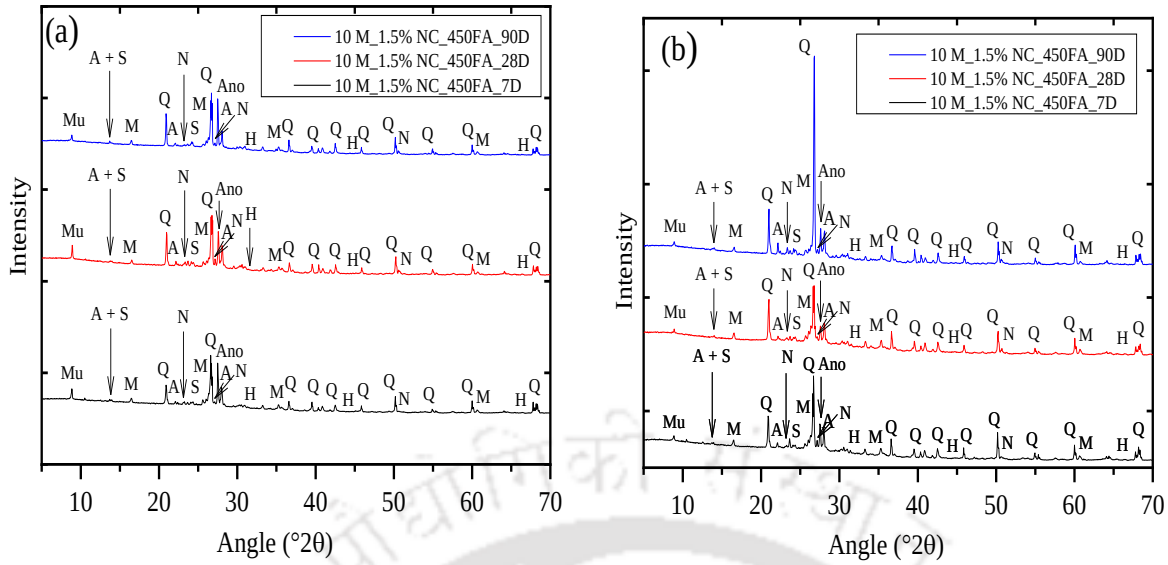

(GPC made with fly ash content of 450 kg/m^3, alkaline solution content of 210 kg/m^3, and SS/SH ratio of 1.75)

Fig. 5.38: XRD patterns of 1.5% NaCl admixed GPC mixes made with NaOH solution of 10 M for fly ash passing through a) 150 µm sieve, and b) 300 µm sieve, at the age of 7, 28, and 90 days

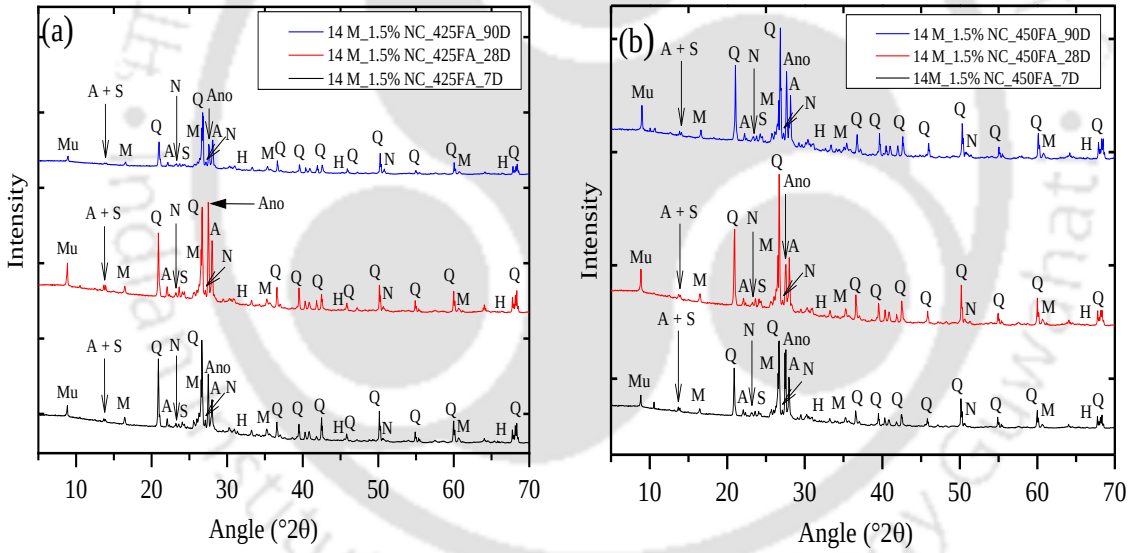

(GPC made with fly ash content of 450 kg/m^3, alkaline solution content of 210 kg/m^3, and SS/SH ratio of 1.75)

Fig. 5.39: XRD patterns of 1.5% NaCl admixed GPC mixes made with NaOH solution of 14 M for fly ash passing through a) 150 µm sieve, and b) 300 µm sieve, at the age of 7, 28, and 90 days

From Fig. 5.36 to Fig. 5.43, it is observed that the peak intensity of the compounds related to geopolymer gels in the XRD patterns were mostly higher in GPC mixes made with smaller fly ash particles (fly ash passing through 150 µm sieve) than that made with larger fly ash particles (fly ash passing through 300 µm sieve) for NaOH solution of 10 M and for some cases in case of NaOH solution of 14 M at all ages thereby indicating more formation of geopolymer gels in case of smaller fly ash particles, which is in line with the variations in compressive strength

of GPC mixes with particle size of fly ash (i.e., higher compressive strength in case of smaller fly ash particles as compared to larger fly ash particles) at fly ash content of 450 kg/m^3 (Fig. 4.15 to Fig. 4.17). As indicated by obtained compressive strength results i.e., lower compressive strength in majority of the cases in NaCl admixed GPC mixes at 14 M NaOH solution in case of smaller fly ash particles as compared to larger fly ash particles (Fig. 4.15 to Fig. 4.17) is consistent with the variations in the peak intensity of the geopolymeric compounds in the XRD patterns with particle size of fly ash (Fig. 5.39, Fig. 5.41 and Fig. 5.43). The reason for these variations in compressive strength of GPC with particle size of fly ash at fly ash content of 450 kg/m^3 was already stated in Section 4.3.4 (Chapter 4). From Fig. 5.36 to Fig. 5.43, the GPC mixes made with higher molarity of NaOH solution (14 M) mostly showed higher peak intensity of geopolymeric compounds as compared to that made with lower molarity of NaOH solution (10 M) for different concentrations of admixed NaCl, particle size of fly ash, and age. This is corroborated with the variations in the compressive strength of GPC with molarity of NaOH solution as evident from Fig. 4.15 to Fig. 4.17.

From Fig. 5.36 to Fig. 5.43, the peak intensity of albite, anorthoclase, nepheline, sodalite, and muscovite were mostly higher in control GPC mixes (0% NaCl) as compared to that admixed with 4.5% NaCl for both sizes of fly ash particles. However, there was mostly unsystematic variation in the peak intensity of these compounds between control GPC mix and 1.5% NaCl admixed GPC mix, and that between control GPC mix and 3% NaCl admixed GPC mix. It may be noted that the compressive strength of control GPC mix was mostly higher as compared to GPC mixes admixed with different concentrations of NaCl (Fig. 4.15 to Fig. 4.17). With admixed NaCl concentration, it is observed that the peak intensity of the compounds related to geopolymer gels in the XRD patterns mostly decreased with increase in concentration of NaCl from 1.5% to 3%, and that from 3% to 4.5%, which is consistent with the variations in compressive strength of GPC mixes with NaCl concentration (Fig. 4.15 to Fig. 4.17). Further, mostly the increase in compressive strength of GPC mixes from 7 to 28 days and that from 28 days to 90 days (as observed from Fig. 4.15 to Fig. 4.17) is substantiated with the variations in the peak intensity of the geopolymeric compounds in the XRD patterns shown in Fig. 5.36 to Fig. 5.43, where the peak intensity of the geopolymeric compounds mostly increased with increase in age. There was unsystematic variation in the peak intensity of halite in the XRD patterns of GPC mixes with particle size of fly ash, molarity of NaOH solution and age as observed from Fig. 5.38 to Fig. 5.43. With admixed NaCl concentration, it is inferred that the peak intensity of halite in the XRD patterns was mostly lower at NaCl concentration of 3% as

compared to 1.5%, however, it was mostly higher at NaCl concentration of 4.5% when compared with 3% (Fig. 5.38 to Fig. 5.43). These variations in the peak intensity of halite with admixed concentration of sodium chloride may be ascribed to the effect of alteration in its degree of crystallinity in the microstructure of GPC mixes.

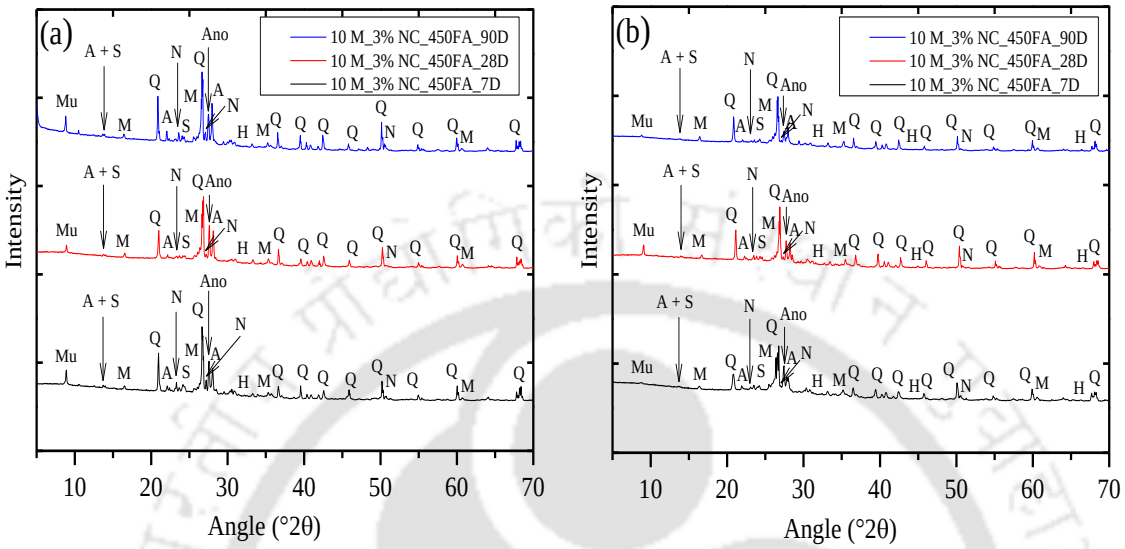

(GPC made with fly ash content of 450 kg/m^3, alkaline solution content of 210 kg/m^3, and SS/SH ratio of 1.75)

Fig. 5.40: XRD patterns of 3% NaCl admixed GPC mixes made with NaOH solution of 10 M for fly ash passing through a) 150 µm sieve, and b) 300 µm sieve, at the age of 7, 28, and 90 days

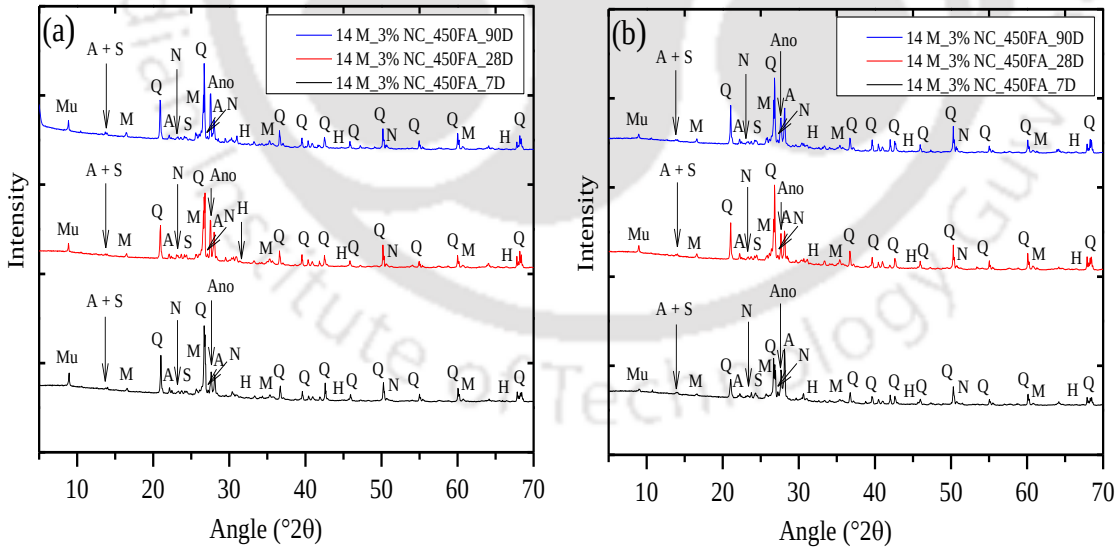

(GPC made with fly ash content of 450 kg/m^3, alkaline solution content of 210 kg/m^3, and SS/SH ratio of 1.75)

Fig. 5.41: XRD patterns of 3% NaCl admixed GPC mixes made with NaOH solution of 14 M for fly ash passing through a) 150 µm sieve, and b) 300 µm sieve, at the age of 7, 28, and 90 days

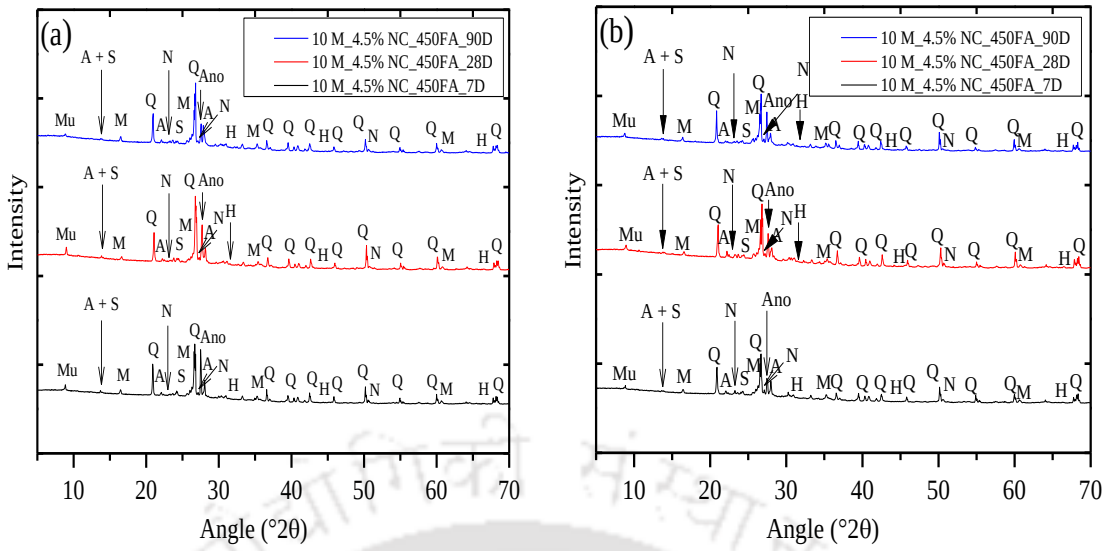

(GPC made with fly ash content of 450 kg/m^3, alkaline solution content of 210 kg/m^3, and SS/SH ratio of 1.75)

Fig. 5.42: XRD patterns of 4.5% NaCl admixed GPC mixes made with NaOH solution of 10 M for fly ash passing through a) 150 µm sieve, and b) 300 µm sieve, at the age of 7, 28, and 90 days

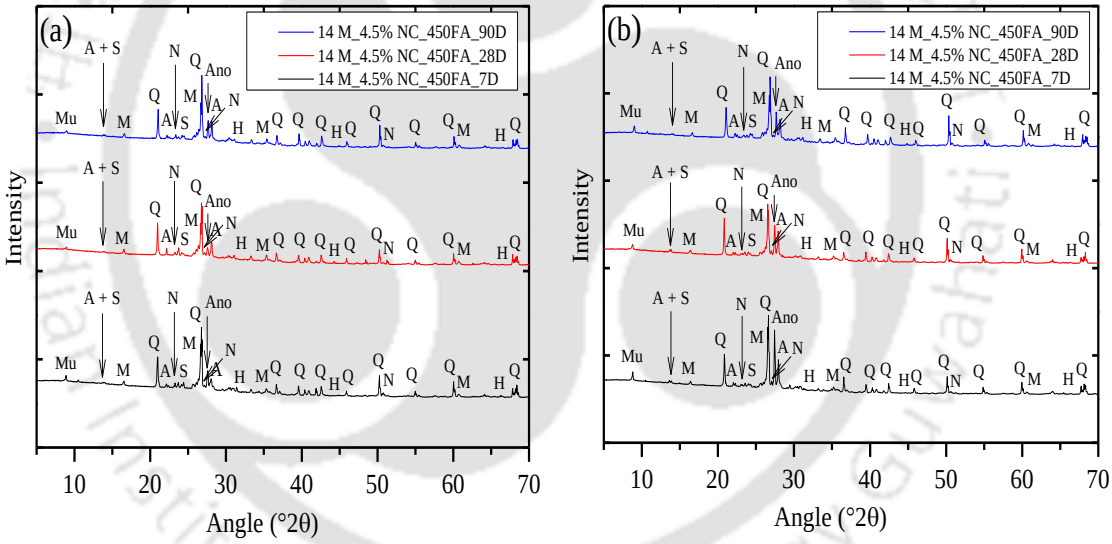

(GPC made with fly ash content of 450 kg/m^3, alkaline solution content of 210 kg/m^3, and SS/SH ratio of 1.75)

Fig. 5.43: XRD patterns of 4.5% NaCl admixed GPC mixes made with NaOH solution of 14 M for fly ash passing through a) 150 µm sieve, and b) 300 µm sieve, at the age of 7, 28, and 90 days

The obtained FTIR spectra of GPC mixes made with fly ash passing through 150 µm sieve, and 300 µm sieve are shown in Fig. 5.44 to Fig. 5.51 for different molarity of NaOH solution (10 M and 14 M), admixed concentrations of NaCl (0%, 1.5%, 3% and 4.5%) and age (7, 28 and 90 days) for fly ash content of 450 kg/m^3. In the FTIR spectra shown in Fig. 5.44 to Fig. 5.51, the peak corresponding to asymmetric stretching vibration of Si–O–Si(Al) bond, which shows the presence of geopolymer gels in GPC mixes shifted to lower wavenumbers in case

of fly ash passing through 150 µm sieve (993 cm^{-1} to 1007 cm^{-1}) when compared with that passing through 300 µm sieve (997 cm^{-1} to 1016 cm^{-1}) for all cases in case of NaOH solution of 10 M and for some cases in case of NaOH solution of 14 M at all ages. This indicates comparatively higher extent of geopolymerization process in GPC mixes made with smaller fly ash particles than that made with larger fly ash particles, which is in line with the variations in the peak intensity of the compounds related to geopolymer gels in XRD patterns i.e., higher peak intensity of the compounds related to geopolymer gels in case of smaller fly ash particles as compared to larger fly ash particles, at fly ash content of 450 kg/m^3 (Fig. 5.36-5.38, Fig. 5.40, and Fig. 5.42). In case of NaCl (1.5%, 3% and 4.5%) admixed GPC mixes at NaOH solution of 14 M, the peak associated with asymmetric stretching vibration of Si–O–Si(Al) bond in FTIR spectra shifted to lower wavenumbers in GPC mixes made with larger fly ash particles (997 cm^{-1} to 1003 cm^{-1}) as compared to that made with smaller fly ash particles (1001 cm^{-1} to 1005 cm^{-1}) thereby indicating comparatively higher extent of geopolymerization process in GPC mixes made with larger fly ash particles than that made with smaller fly ash particles at higher molarity of NaOH solution in the presence of NaCl. This is corroborated with the variations in the peak intensity of the geopolymeric compounds in the XRD patterns with particle size of fly ash in NaCl admixed GPC mixes at NaOH solution of 14 M (Fig. 5.39, Fig. 5.41 and Fig. 5.43). Further, in the FTIR spectra shown in Fig. 5.44 to Fig. 5.51, the peak associated with asymmetric stretching vibration of Si–O–Si(Al) bond shifted to lower wavenumbers for NaOH solution of 14 M (991 cm^{-1} to 1005 cm^{-1}) when compared with NaOH solution of 10 M (997 cm^{-1} to 1016 cm^{-1}) irrespective of particle size of fly ash, NaCl concentration, and age, which is substantiated with the variations in the peak intensity of compounds related to N-A-S-H gel in the XRD patterns with molarity of NaOH solution (Fig. 5.36 to Fig. 5.43).

Between control (0% NaCl), and NaCl admixed (1.5%, 3% and 4.5%) GPC mixes, the peak related to asymmetric stretching vibration of Si–O–Si(Al) bond shifted to lower wavenumbers in case of control GPC mix (993 cm^{-1} to 1003 cm^{-1}) as compared to NaCl admixed GPC mixes (997 cm^{-1} to 1016 cm^{-1}) irrespective of particle size of fly ash, molarity of NaOH solution and age (Fig. 5.44 to Fig. 5.51). Further, the peak related to asymmetric stretching vibration of Si–O–Si(Al) bond in the FTIR spectra shifted to lower wavenumbers (although the difference was less) with decrease in concentration of admixed NaCl from 4.5% (1001 cm^{-1} to 1016 cm^{-1}) to 3% (999 cm^{-1} to 1015 cm^{-1}), and that from 3% (999 cm^{-1} to 1015 cm^{-1}) to 1.5% (997 cm^{-1} to 1005 cm^{-1}). This is consistent with the results of XRD analysis where the peak intensity of

the compounds related to N-A-S-H gel mostly increased with decrease in concentration of admixed NaCl (Fig. 5.38 to Fig. 5.43). Similarly, in the FTIR spectra (Fig. 5.44 to Fig.5.51), the peak related to asymmetric stretching vibration of Si–O–Si(Al) bond shifted to lower wavenumbers with increase in age from 7 (999 cm^{-1} to 1013 cm^{-1}) to 28 days (997 cm^{-1} to 1009 cm^{-1}), and that from 28 (997 cm^{-1} to 1009 cm^{-1}) to 90 days (993 cm^{-1} to 1005 cm^{-1}) for different concentrations of admixed NaCl, particle size of fly ash, and molarity of NaOH solution. In the FTIR spectra shown in Fig. 5.44 to Fig.5.51, the peak in the range of 770 cm^{-1} to 775 cm^{-1}, 1393 cm^{-1} to 1522 cm^{-1} and 1641 cm^{-1} to 1694 cm^{-1}, and the band in the range of 3390 cm^{-1} to 3748 cm^{-1} are associated with the presence of quartz, stretching vibration of carbonate group, bending vibration of H–O–H group, and stretching vibration of –OH group respectively.

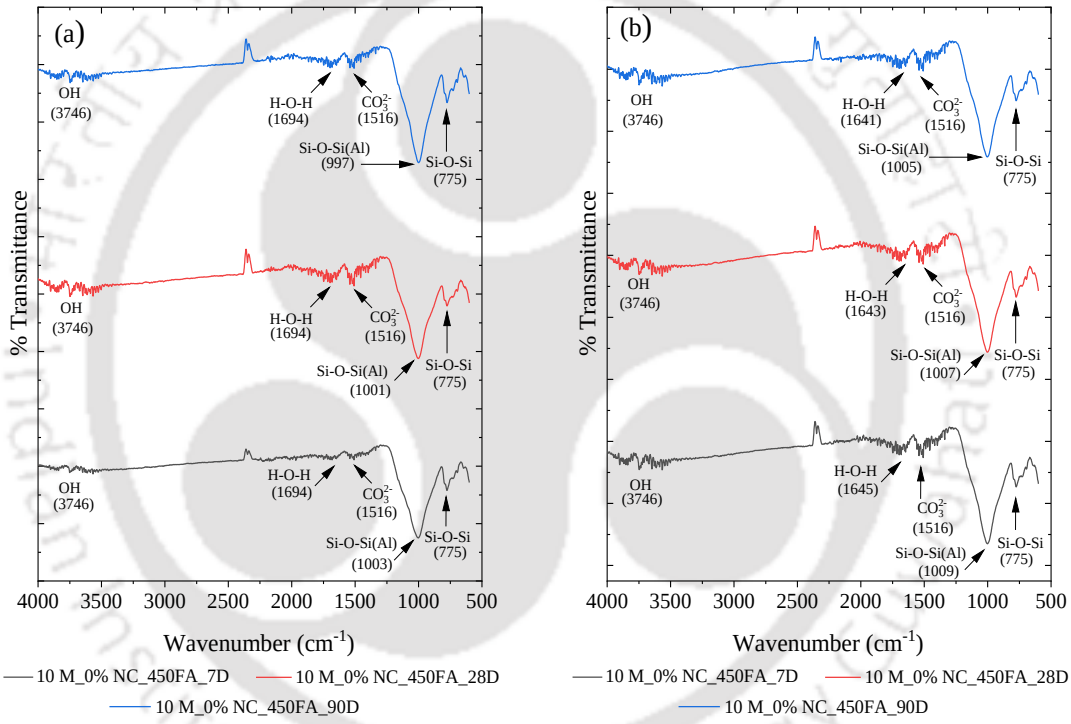

(GPC made with fly ash content of 450 kg/m^3, alkaline solution content of 210 kg/m^3, and SS/SH ratio of 1.75)

Fig. 5.44: FTIR spectra of control GPC mixes made with NaOH solution of 10 M for fly ash passing through a) 150 µm sieve, and b) 300 µm sieve, at the age of 7, 28, and 90 days

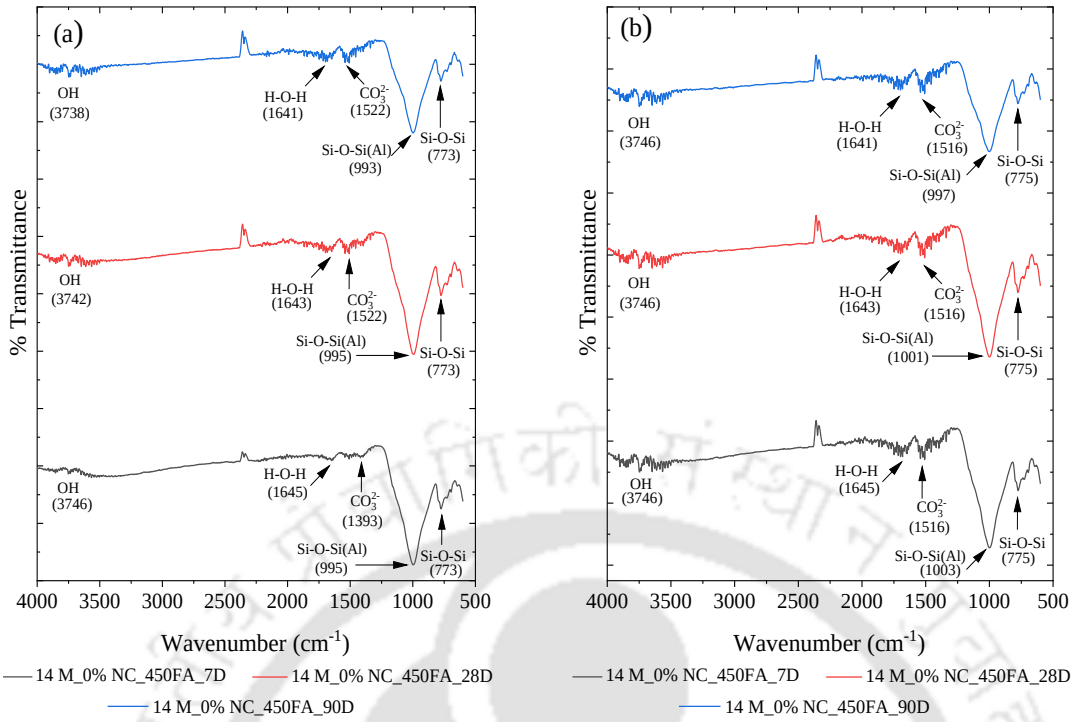

(GPC made with fly ash content of 450 kg/m^3, alkaline solution content of 210 kg/m^3, and SS/SH ratio of 1.75)

Fig. 5.45: FTIR spectra of control GPC mixes made with NaOH solution of 14 M for fly ash passing through a) 150 µm sieve, and b) 300 µm sieve, at the age of 7, 28, and 90 days

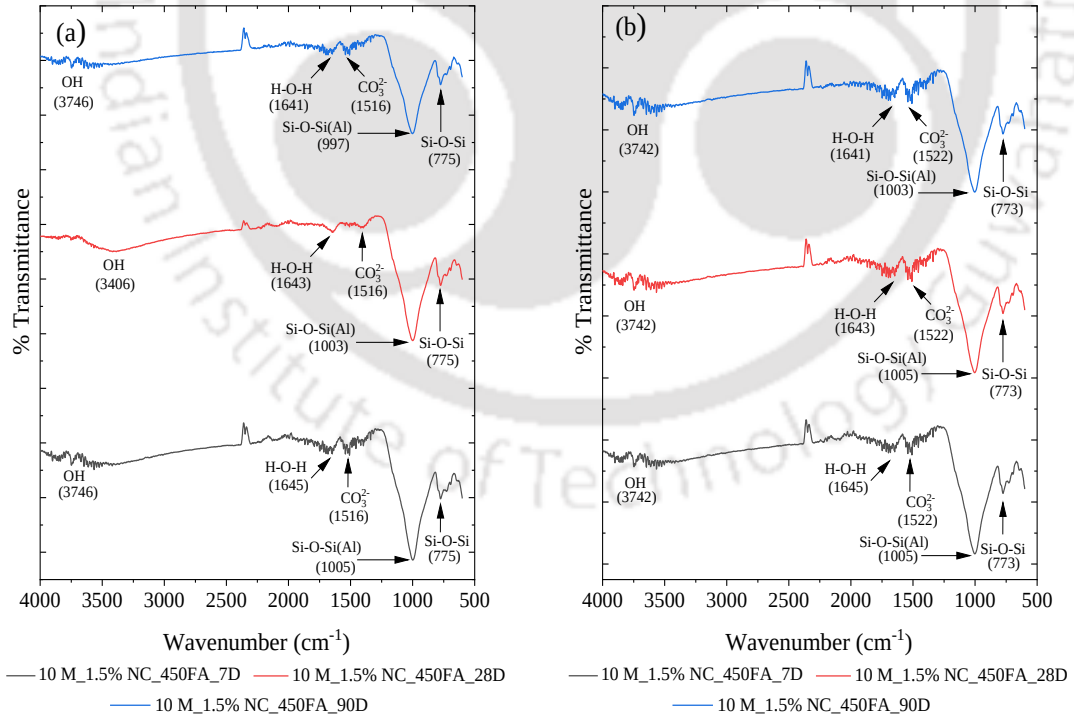

(GPC made with fly ash content of 450 kg/m^3, alkaline solution content of 210 kg/m^3, and SS/SH ratio of 1.75)

Fig. 5.46: FTIR spectra of 1.5% NaCl admixed GPC mixes made with NaOH solution of 10 M for fly ash passing through a) 150 µm sieve, and b) 300 µm sieve, at the age of 7, 28, and 90 days

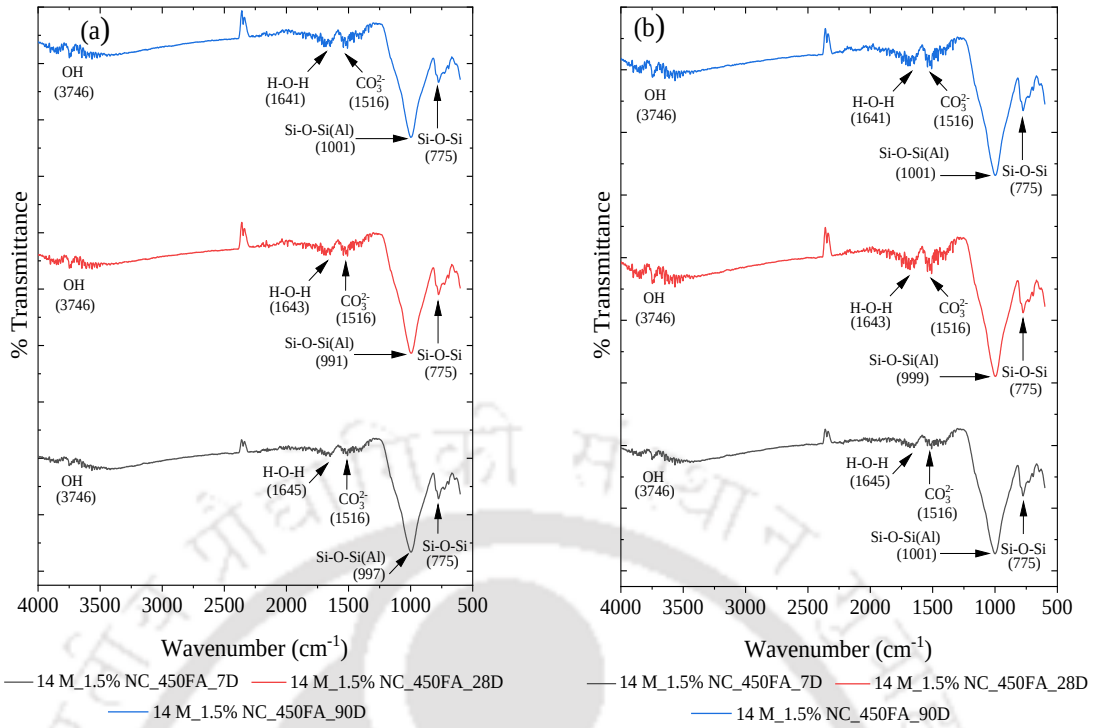

(GPC made with fly ash content of 450 kg/m^3, alkaline solution content of 210 kg/m^3, and SS/SH ratio of 1.75)

Fig. 5.47: FTIR spectra of 1.5% NaCl admixed GPC mixes made with NaOH solution of 14 M for fly ash passing through a) 150 µm sieve, and b) 300 µm sieve, at the age of 7, 28, and 90 days

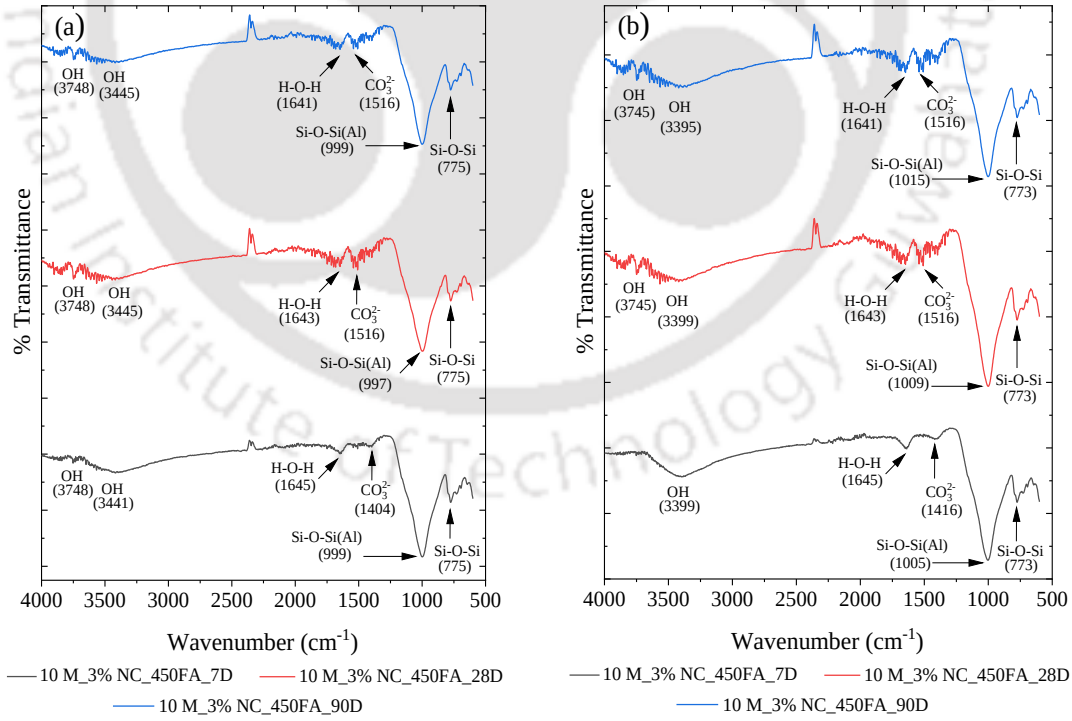

(GPC made with fly ash content of 450 kg/m^3, alkaline solution content of 210 kg/m^3, and SS/SH ratio of 1.75)

Fig. 5.48: FTIR spectra of 3% NaCl admixed GPC mixes made with NaOH solution of 10 M for fly ash passing through a) 150 µm sieve, and b) 300 µm sieve, at the age of 7, 28, and 90 days

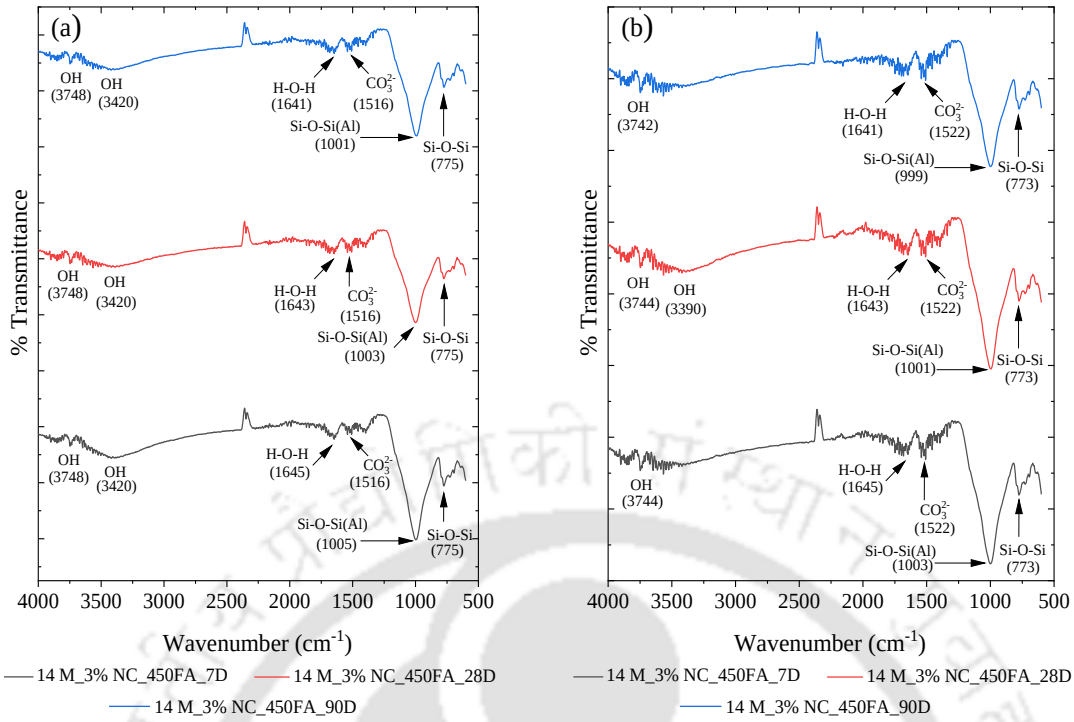

(GPC made with fly ash content of 450 kg/m^3, alkaline solution content of 210 kg/m^3, and SS/SH ratio of 1.75)

Fig. 5.49: FTIR spectra of 3% NaCl admixed GPC mixes made with NaOH solution of 14 M for fly ash passing through a) 150 µm sieve, and b) 300 µm sieve, at the age of 7, 28, and 90 days

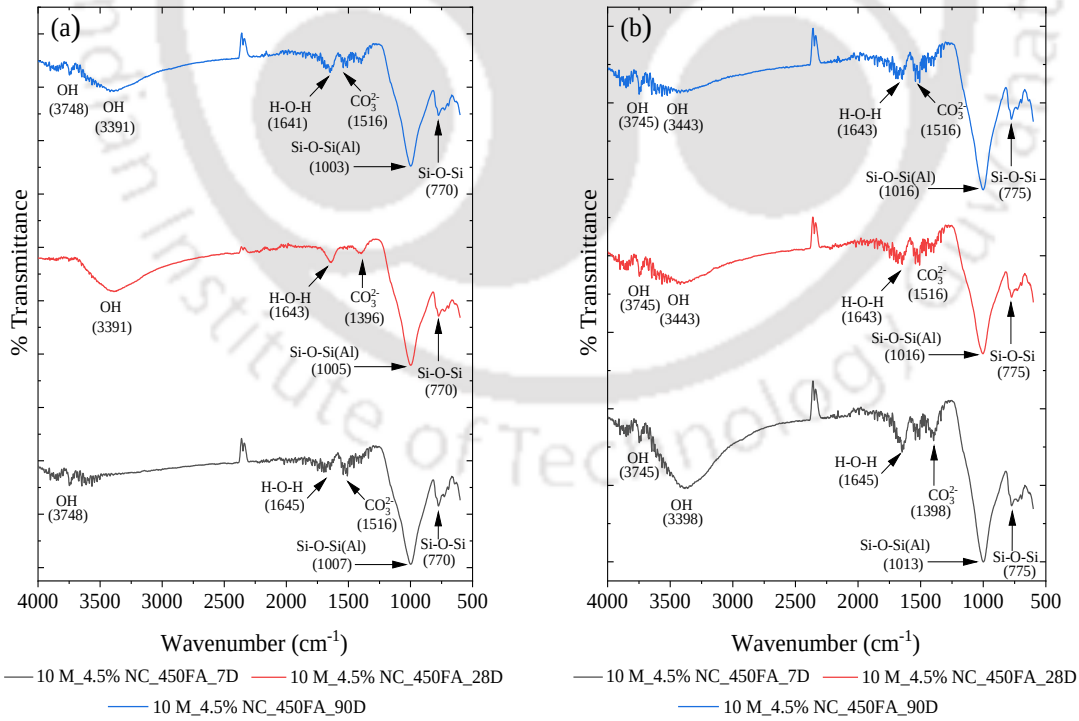

(GPC made with fly ash content of 450 kg/m^3, alkaline solution content of 210 kg/m^3, and SS/SH ratio of 1.75)

Fig. 5.50: FTIR spectra of 4.5% NaCl admixed GPC mixes made with NaOH solution of 10 M for fly ash passing through a) 150 µm sieve, and b) 300 µm sieve, at the age of 7, 28, and 90 days

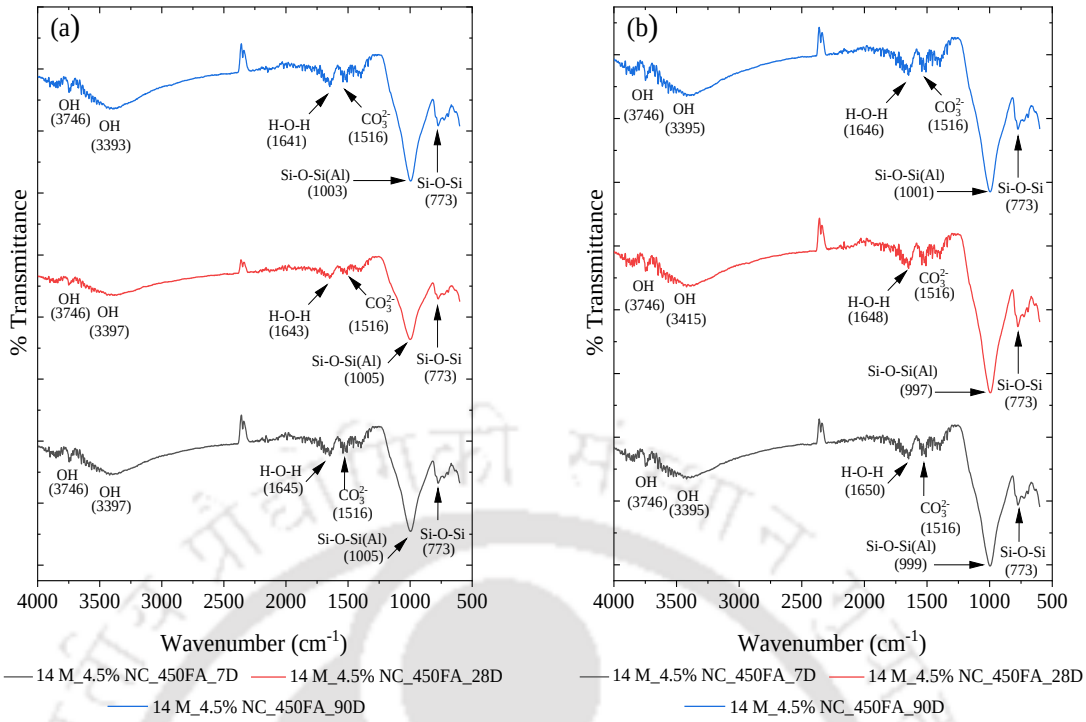

(GPC made with fly ash content of 450 kg/m^3, alkaline solution content of 210 kg/m^3, and SS/SH ratio of 1.75)

Fig. 5.51: FTIR spectra of 4.5% NaCl admixed GPC mixes made with NaOH solution of 14 M for fly ash passing through a) 150 µm sieve, and b) 300 µm sieve, at the age of 7, 28, and 90 days

For fly ash content of 450 kg/m^3, typical FESEM images of GPC mixes made with fly ash passing through 150 µm sieve, and 300 µm sieve are shown in Fig. 5.52. The remaining FESEM images are presented in Appendix (Fig. A20 to A22). From Fig. 5.52 (a, b) it is observed that the control GPC mix made with smaller fly ash particles (passing through 150 µm sieve) showed more formation of geopolymer gels and denser microstructure as compared to that made with larger fly ash particles (passing through 300 µm sieve). This is substantiated by the results of XRD analysis where the peak intensity of compounds related to geopolymer gels were mostly higher in control GPC mix made with smaller fly ash particles than that made with larger fly ash particles (Fig. 5.36). From Fig. 5.52 (b, c), the FESEM images indicated more formation of geopolymer gels and a compact microstructure in GPC mix made with NaOH solution of 14 M as compared to that made with NaOH solution of 10 M, which is in line with the variation in the peak intensity of geopolymeric compounds (Fig. 5.36 (b) and Fig. 5.37 (b)) i.e., the peak intensity of geopolymeric compounds were mostly higher in GPC mix made with NaOH solution of 14 M than that made with NaOH solution of 10 M. The FESEM images indicated comparatively less denser microstructure in NaCl admixed GPC mixes as compared to control (0% NaCl) GPC mix (Fig. 5.52 (c, d, f)). This indicates that the presence

of NaCl resulted in a less homogeneous microstructure that led to lower compressive strength of GPC mixes (Fig. 4.15 to Fig. 4.17). It may be noted that the peak intensity of geopolymeric compounds were mostly lower in 4.5% NaCl admixed GPC mix than control GPC mix (Fig. 5.37 (b) and Fig. 5.43 (b)). However, there was mostly unsystematic variation in the peak intensity of geopolymeric compounds between control GPC mix and 3% NaCl admixed GPC mix (Fig. 5.37 (b) and Fig. 5.41 (b)). The FESEM images (Fig. 5.52 (e, f)) showed more formation of geopolymer gels with homogenous microstructure with increase in age from 7 to 28 days, which is supported by the variations in the peak intensity of the compounds related to N-A-S-H gel (Fig. 5.43 (b)) as well as by the variations in the compressive strength of GPC mixes with increase in age (Fig. 4.15 to Fig. 4.17).

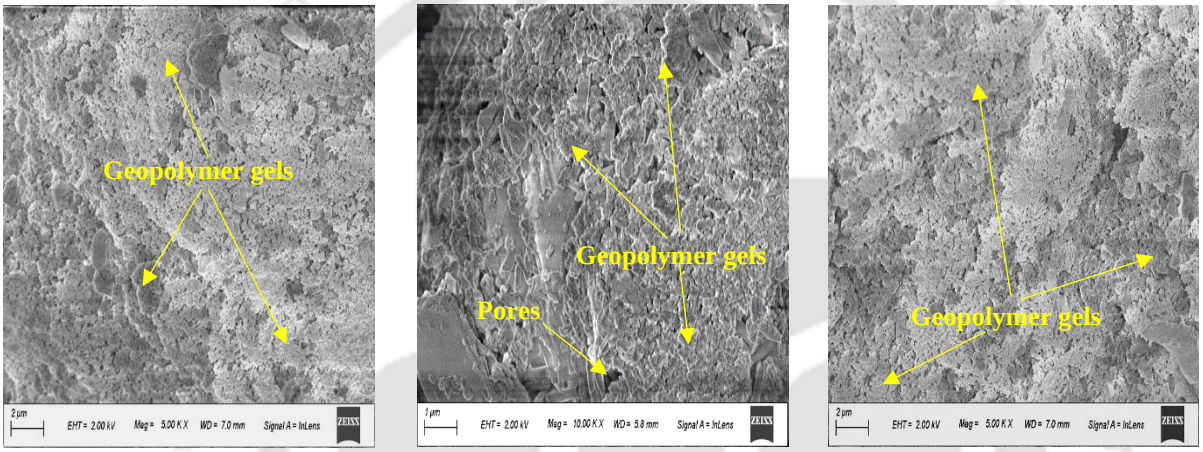

(a) 10 M/0%NC/150 µm/28D (b) 10 M/0%NC/300 µm/28D (c) 14 M/0%NC/300 µm/28D

(d) 14 M/3%NC/300 µm/28D (e) 14 M/4.5%NC/300 µm/7D (f) 14 M/4.5%NC/300 µm/28D

(GPC made with fly ash content of 450 kg/m^3, alkaline solution content of 210 kg/m^3, and SS/SH ratio of 1.75)

Fig. 5.52: FESEM images of GPC mixes made with fly ash of different particle size, molarity of NaOH solution, and admixed NaCl

5.2.5 Effect of fly ash content on microstructure of GPC

For fly ash passing through 150 μm sieve, the obtained XRD patterns of GPC mixes made with fly ash content of 425 kg/m^3, and 450 kg/m^3 are shown in Fig. 5.53 to 5.56. From Fig. 5.53 and Fig. 5.54, it is inferred that the peak intensity of the compounds related to geopolymer gels were mostly lower in control GPC mixes (0% NaCl) made with higher fly ash content (450 kg/m^3) than that made with lower fly ash content (425 kg/m^3) for both molarity of NaOH solution (10 M and 14 M) and age (7 and 28 days). However, mostly opposite variation in peak intensity of the compounds related to geopolymer gels with fly ash content was observed in 3% NaCl admixed GPC mixes (Fig. 5.55 and Fig. 5.56). These variations in peak intensity of the compounds related to geopolymer gels with fly ash content in control and chloride admixed GPC mixes are consistent with the variations in the compressive strength of GPC mixes with fly ash content for fly ash passing through 150 μm sieve (Fig. 4.18 and Fig. 4.19). The reasons for these variations in compressive strength of GPC with fly ash content for fly ash passing through 150 μm sieve are already mentioned in Section 4.3.5 (Chapter 4). From Fig. 5.53 to 5.56, with molarity of NaOH solution, the peak intensity of geopolymeric compounds in the XRD patterns were mostly higher at higher molarity of NaOH solution (14 M) than lower molarity of NaOH solution (10 M) in all cases except in case of 3% NaCl admixed GPC mix for fly ash content of 450 kg/m^3. This indicates mostly higher formation of geopolymer gels at higher molarity of NaOH solution, which is consistent with the variation in compressive strength of GPC mixes with molarity of NaOH solution (Fig. 4.18 and Fig. 4.19). Further, from Fig. 5.53 to Fig. 5.56, the peak intensity of the compounds related to N-A-S-H gel were mostly higher in control mixes as compared to NaCl admixed GPC mixes, and at the age of 28 days than that at the age of 7 days for both fly ash contents. In NaCl admixed GPC mixes, the peak intensity of halite in the XRD patterns (Fig. 5.55 and Fig. 5.56) was higher in GPC mixes made with fly ash content of 450 kg/m^3 than that made with fly ash content of 425 kg/m^3. This may be ascribed to the addition of more amount of NaCl in GPC mixes made with higher fly ash content during preparation where NaCl was added in GPC mixes as percentage by mass of geopolymer solids that includes fly ash. However, the compressive strength of NaCl admixed GPC mixes was higher in case of higher fly ash content than that made with lower fly ash content (Fig. 4.18 and Fig. 4.19). Therefore, although there was comparatively more crystallization of sodium chloride in GPC mixes made with higher fly ash content as indicated by the peak intensity of halite in the XRD patterns, the inhibiting effect of NaCl on geopolymerization process in GPC mix made with higher fly ash content to a relatively lower

extent led to comparatively more compressive strength in case of higher fly ash content (already discussed in Section 4.3.5) than lower fly ash content over the effect of crystallization of sodium chloride. There was mostly unsystematic variation in the peak intensity of halite in the XRD patterns with molarity of NaOH solution. Further, the peak intensity of halite was mostly lower at the age of 28 days as compared to that at the age of 7 days (Fig. 5.55 and Fig. 5.56).

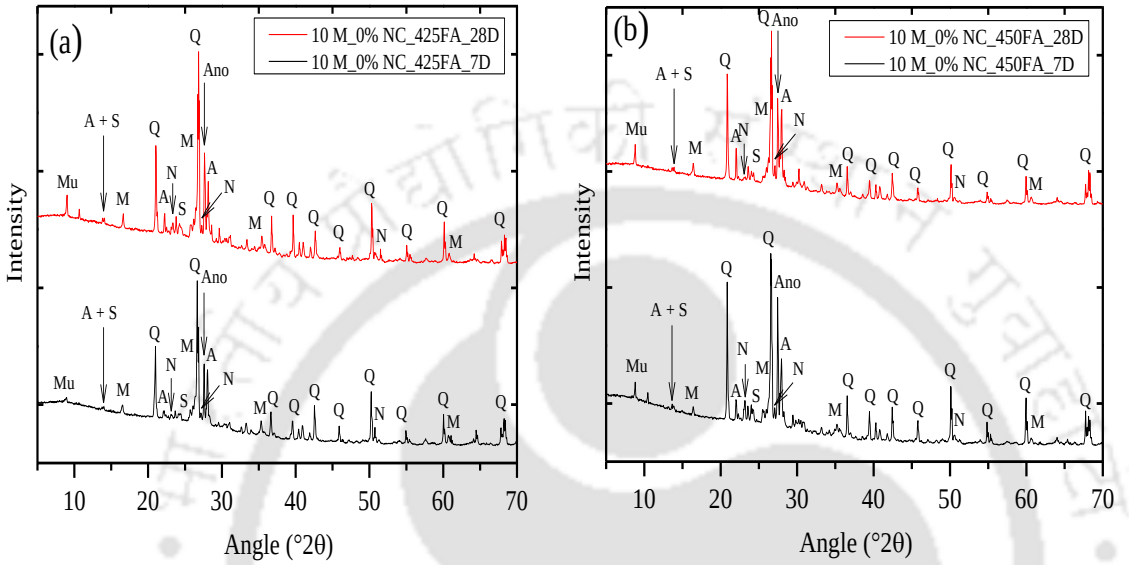

(GPC made with fly ash passing through 150 μm sieve, alkaline solution content of 210 kg/m³ and SS/SH ratio of 1.75)

Fig. 5.53: XRD patterns of control GPC mixes made with NaOH solution of 10 M for fly ash content of a) 425 kg/m^3, and b) 450 kg/m^3, at the age of 7 and 28 days

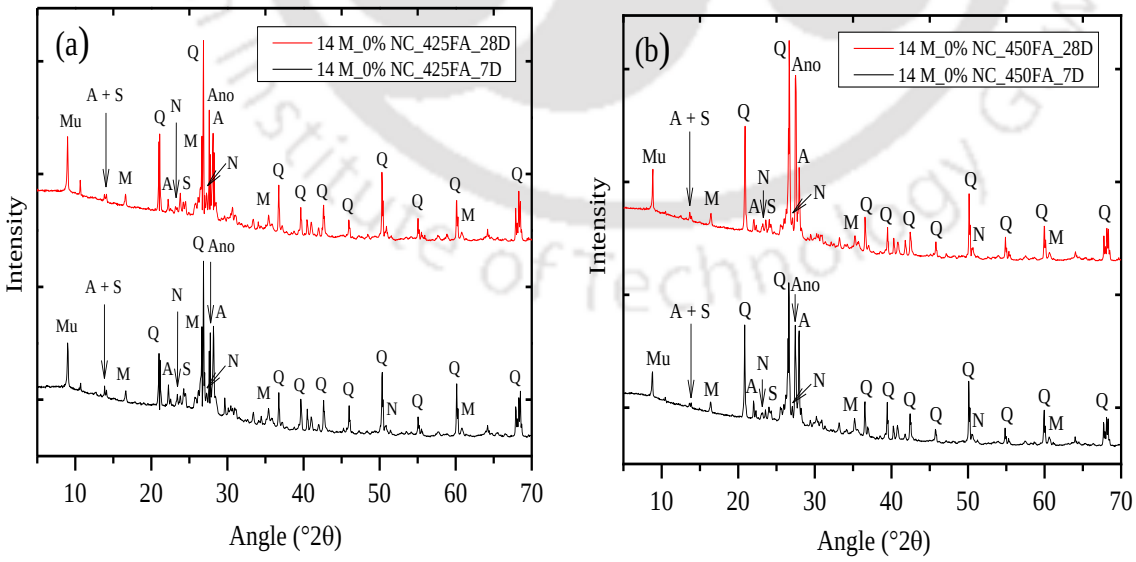

(GPC made with fly ash passing through 150 μm sieve, alkaline solution content of 210 kg/m³ and SS/SH ratio of 1.75)

Fig. 5.54: XRD patterns of control GPC mixes made with NaOH solution of 14 M for fly ash content of a) 425 kg/m^3, and b) 450 kg/m^3, at the age of 7 and 28 days

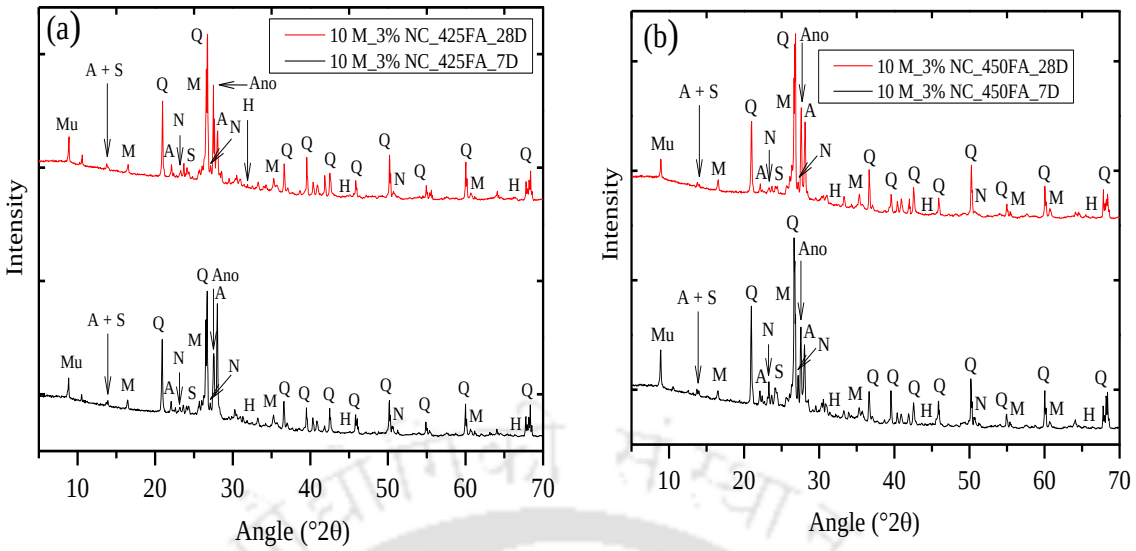

(GPC made with fly ash passing through 150 μm sieve, alkaline solution content of 210 kg/m^3 and SS/SH ratio of 1.75)

Fig. 5.55: XRD patterns of 3% NaCl admixed GPC mixes made with NaOH solution of 10 M for fly ash content of a) 425 kg/m^3, and b) 450 kg/m^3, at the age of 7 and 28 days

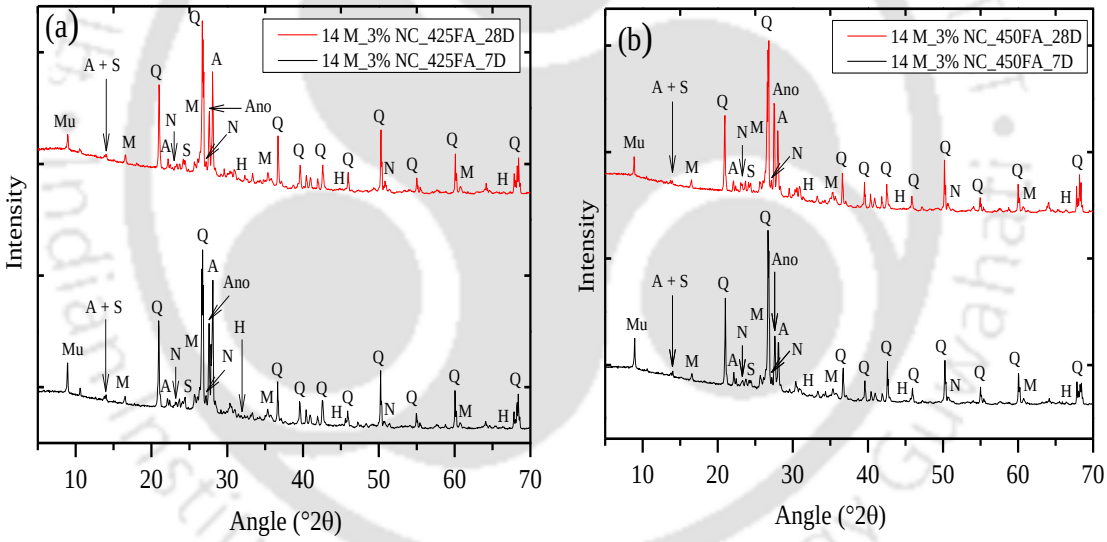

(GPC made with fly ash passing through 150 μm sieve, alkaline solution content of 210 kg/m^3 and SS/SH ratio of 1.75)

Fig. 5.56: XRD patterns of 3% NaCl admixed GPC mixes made with NaOH solution of 14 M for fly ash content of a) 425 kg/m^3, and b) 450 kg/m^3, at the age of 7 and 28 days

The obtained FTIR spectra of GPC mixes made with fly ash content of 425 kg/m^3, and 450 kg/m^3 for fly ash passing through 150 μm sieve are shown in Fig. 5.57 to 5.60. In the FTIR spectra shown in Fig. 5.57 to Fig. 5.60, the peak associated with asymmetric stretching vibration of Si–O–Si(Al) bond, indicating the presence of geopolymer gels in GPC mixes, shifted to lower wavenumbers in case of fly ash content of 425 kg/m^3 (988 cm^{-1} to 993 cm^{-1}) as compared to fly ash content of 450 kg/m^3 (995 cm^{-1} to 1003 cm^{-1}) for control mixes.

Similarly, in NaCl admixed GPC mixes, the peak related to asymmetric stretching vibration of Si–O–Si(Al) bond shifted to lower wavenumbers for fly ash content of 425 kg/m^3 (993 cm^{-1} to 995 cm^{-1}) when compared with fly ash content of 450 kg/m^3 (997 cm^{-1} to 1005 cm^{-1}) for both molarity of NaOH solution, and both ages. It may be noted that the peak intensity of the geopolymeric compounds in the XRD patterns were mostly higher in case of lower fly ash content (425 kg/m^3) than higher fly ash content (450 kg/m^3) for control GPC mixes (Fig. 5.53 and Fig. 5.54) whereas, in case of 3% NaCl admixed GPC mixes, mostly opposite variation was observed in the peak intensity of the geopolymeric compounds with fly ash content (Fig. 5.55 to Fig. 5.56). Thus, although the variation in the peak intensity of the geopolymeric compounds with fly ash content in the XRD patterns was not consistent with the variation in the wavenumber corresponding to the peak related to asymmetric stretching vibration of Si–O–Si(Al) bond in case of NaCl admixed GPC mixes, the shift in the peak associated with asymmetric stretching vibration of Si–O–Si(Al) bond to comparatively higher wavenumber in case of higher fly ash content as compared to lower fly ash content indicates higher extent of changes in the geopolymerization process in the GPC mixes made with higher fly ash content. In Fig. 5.57 to Fig. 5.60, the peak related to asymmetric stretching vibration of Si–O–Si(Al) bond shifted to lower wavenumbers with increase in age from 7 (989 cm^{-1} to 1005 cm^{-1}) to 28 days (988 cm^{-1} to 1003 cm^{-1}), with increase in molarity of NaOH solution from 10 M (993 cm^{-1} to 1003 cm^{-1}) to 14 M (988 cm^{-1} to 1001 cm^{-1}), and in control GPC mixes (988 cm^{-1} to 1003 cm^{-1}) as compared to 3% NaCl admixed GPC mixes (993 cm^{-1} to 1005 cm^{-1}) for both fly ash contents. This indicates continuation as well as higher extent of geopolymerization reaction with age, at higher molarity of NaOH solution, and in control in GPC mixes as compared to chloride admixed GPC mixes. These variations in the wavenumbers corresponding to the peak related to asymmetric stretching vibration of Si–O–Si(Al) bond are substantiated with the variations in the peak intensity of the compounds related to geopolymer gels in the XRD patterns with age, molarity of NaOH solution, and due to the effect of presence of NaCl in the GPC mixes (Fig. 5.53, to Fig. 5.56). From Fig. 5.57 to Fig. 5.60, the peak in the range of 770 cm^{-1} to 775 cm^{-1}, and that in the range of 1393 cm^{-1} to 1522 cm^{-1} in the FTIR spectra indicate the presence of quartz, and stretching vibration of carbonate group respectively. Further, the bending vibration of H–O–H group, and stretching vibration of –OH group are indicated by the peak in the range of 1643 cm^{-1} to 1703 cm^{-1}, and the band in the range of 3398 cm^{-1} to 3748 cm^{-1} in the FTIR spectra respectively.

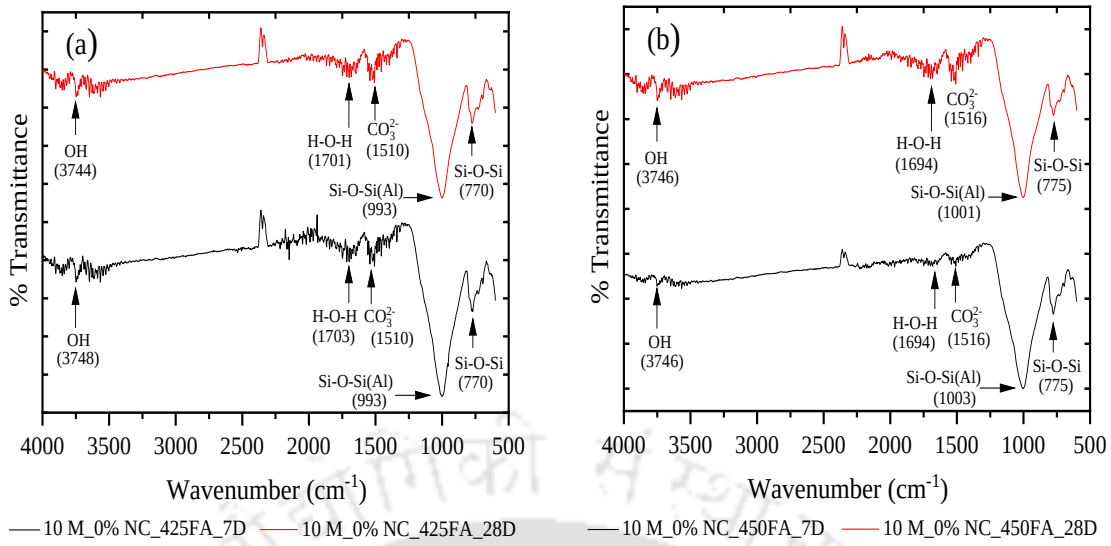

(GPC made with fly ash passing through 150 μm sieve, alkaline solution content of 210 kg/m^3 and SS/SH ratio of 1.75)

Fig. 5.57: FTIR spectra of control GPC mixes made with NaOH solution of 10 M for fly ash content of a) 425 kg/m^3, and b) 450 kg/m^3, at the age of 7 and 28 days

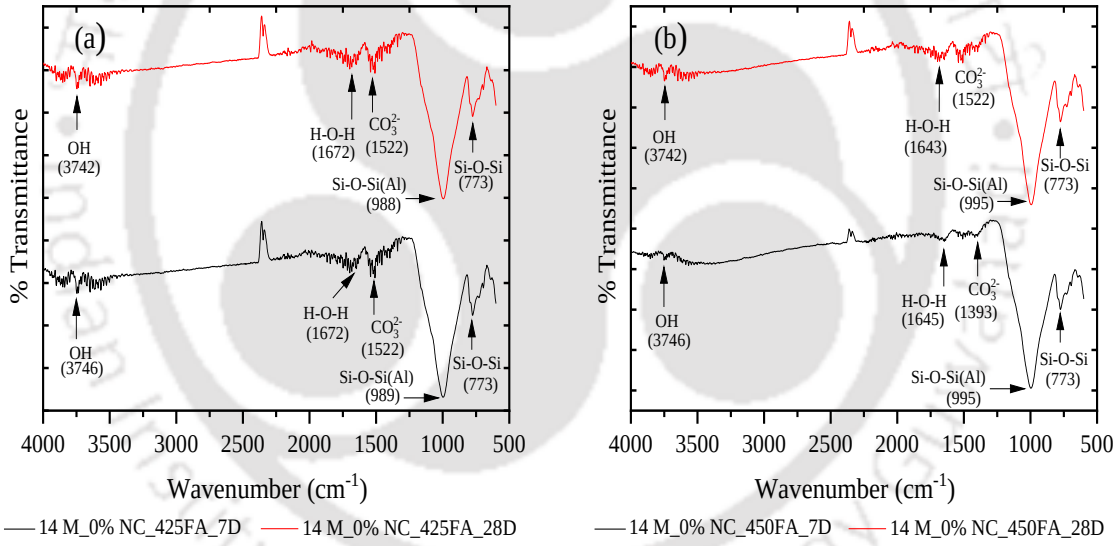

(GPC made with fly ash passing through 150 μm sieve, alkaline solution content of 210 kg/m^3 and SS/SH ratio of 1.75)

Fig. 5.58: FTIR spectra of control GPC mixes made with NaOH solution of 14 M for fly ash content of a) 425 kg/m^3, and b) 450 kg/m^3, at the age of 7 and 28 days

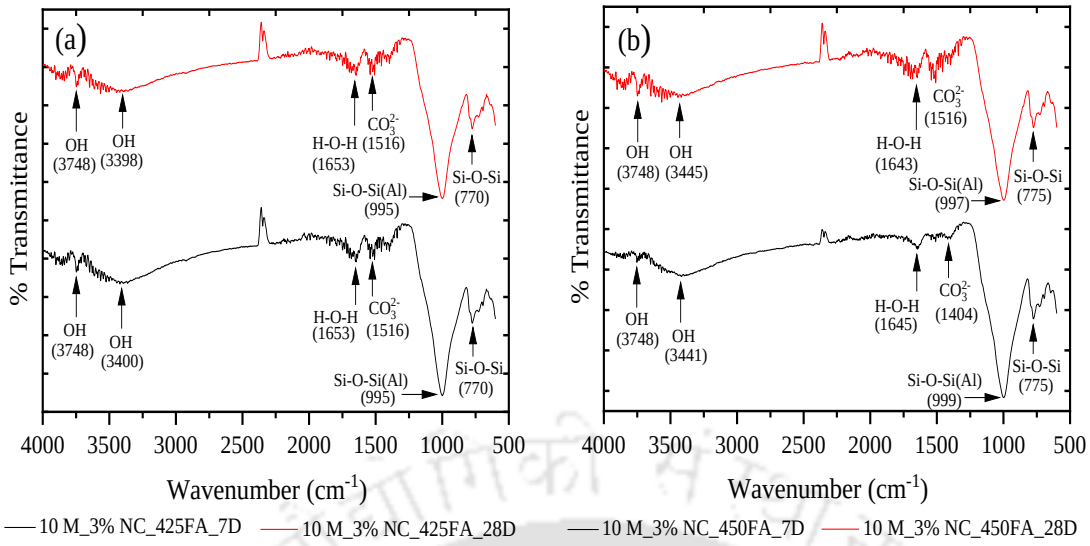

(GPC made with fly ash passing through 150 μm sieve, alkaline solution content of 210 kg/m³ and SS/SH ratio of 1.75)

Fig. 5.59: FTIR spectra of 3% NaCl admixed GPC mixes made with NaOH solution of 10 M for fly ash content of a) 425 kg/m^3, and b) 450 kg/m^3, at the age of 7 and 28 days

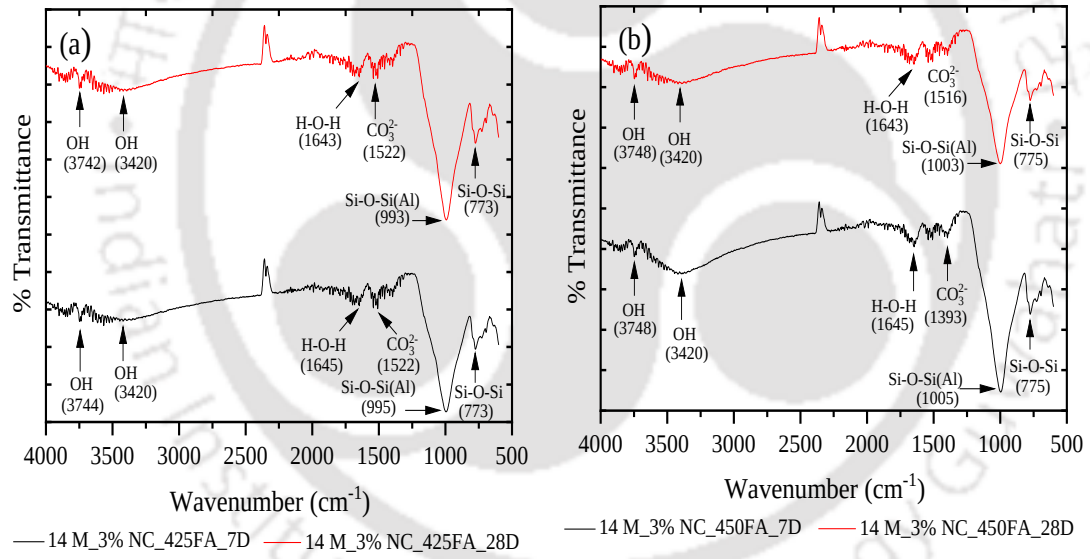

(GPC made with fly ash passing through 150 μm sieve, alkaline solution content of 210 kg/m³ and SS/SH ratio of 1.75)

Fig. 5.60: FTIR spectra of 3% NaCl admixed GPC mixes made with NaOH solution of 14 M for fly ash content of a) 425 kg/m^3, and b) 450 kg/m^3, at the age of 7 and 28 days

For fly ash passing through 150 μm sieve, the typical FESEM images of GPC mixes made with fly ash content of 425 kg/m^3, and 450 kg/m^3 are shown in Fig. 5.61. The remaining FESEM images are shown in Appendix A. From Fig. 5.61 (a, b), it is noted that the control GPC mix made with fly ash content of 425 kg/m^3 showed more compact microstructure as compared to that made with fly ash content of 450 kg/m^3. However, the GPC mix made with fly ash content of 450 kg/m^3 showed comparatively denser microstructure than that made with fly ash content

of 425 kg/m^3 in the presence of NaCl (Fig. 5.61 (c, d)). These observations are in line with the variations in the peak intensity of the compounds related to N-A-S-H gel in the GPC mixes as observed from the XRD results (Fig. 5.53 and Fig. 5.55).

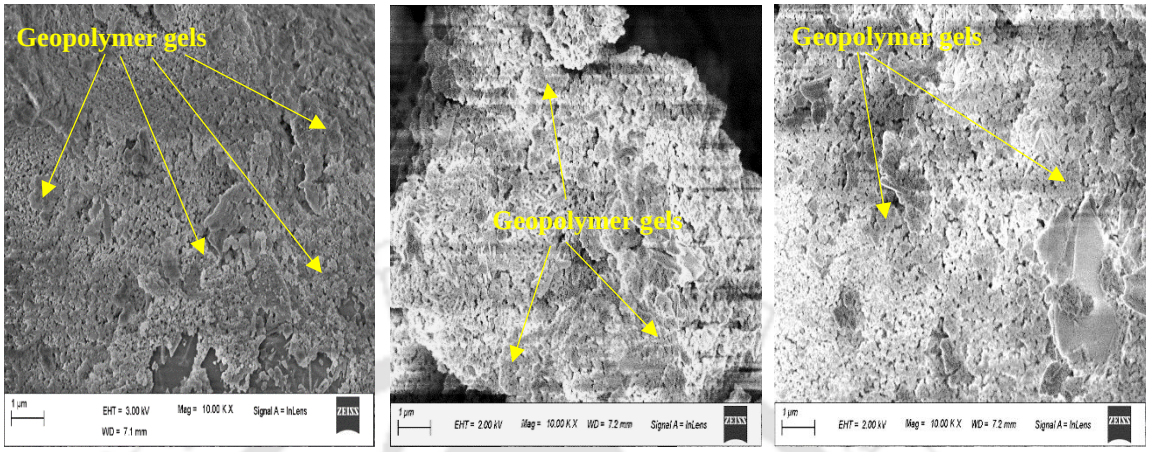

(a) 10 M/0%NC/425FA/7D (b) 10 M/0%NC/450FA/7D (c) 10 M/3%NC/425FA/28D

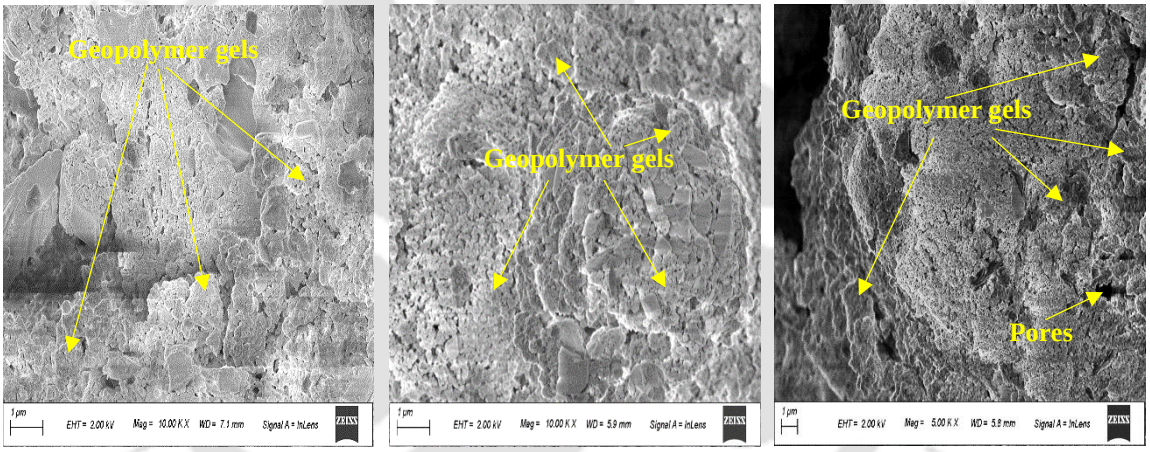

(d) 10 M/3%NC/450FA/28D (e) 14 M/0%NC/450FA/7D (f) 10 M/0%NC/425FA/28D

(GPC made with fly ash passing through 150 μm sieve, alkaline solution content of 210 kg/m^3 and SS/SH ratio of 1.75)

Fig. 5.61: FESEM images of GPC made with fly ash contents of 425 kg/m^3 and 450 kg/m^3

There is formation of more amount of geopolymer gels in GPC mix at NaOH solution of 14 M as compared to that made with NaOH solution of 10 M as observed from the FESEM micrographs shown in Fig. 5.61 (b, e). The FESEM micrographs (Fig. 5.61 (c, f)) indicated formation of less amount of geopolymer gels as well as less homogeneous microstructure in 3% NaCl admixed GPC mix as compared to control GPC mix that led to lower compressive strength of NaCl admixed GPC mix than control GPC mix (Fig. 4.19).

For fly ash passing through 300 μm sieve, the obtained XRD patterns of GPC mixes made with fly ash content of 425 kg/m^3, and 450 kg/m^3 are shown in Fig. 5.62 to Fig. 5.69 for NaOH solution molarity of 10 M and 14 M, admixed NaCl concentrations of 0%, 1.5%, 3% and 4.5%, and at the age of 7, 28 and 90 days.

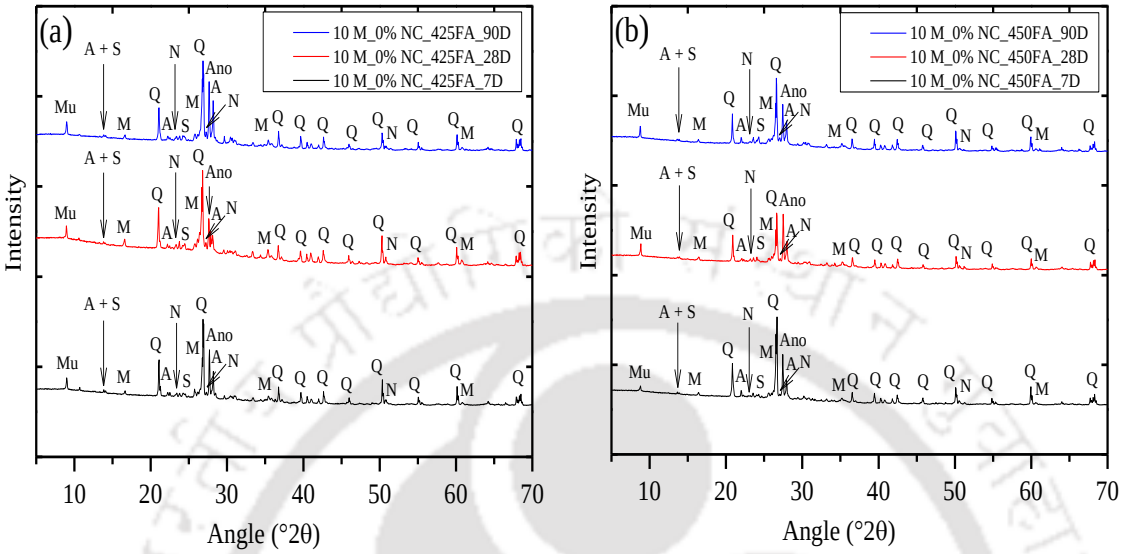

(GPC made with fly ash passing through 300 μm sieve, alkaline solution content of 210 kg/m^3 and SS/SH ratio of 1.75)

Fig. 5.62: XRD patterns of control GPC mixes made with NaOH solution of 10 M for fly ash content of a) 425 kg/m^3, and b) 450 kg/m^3, at the age of 7, 28, and 90 days

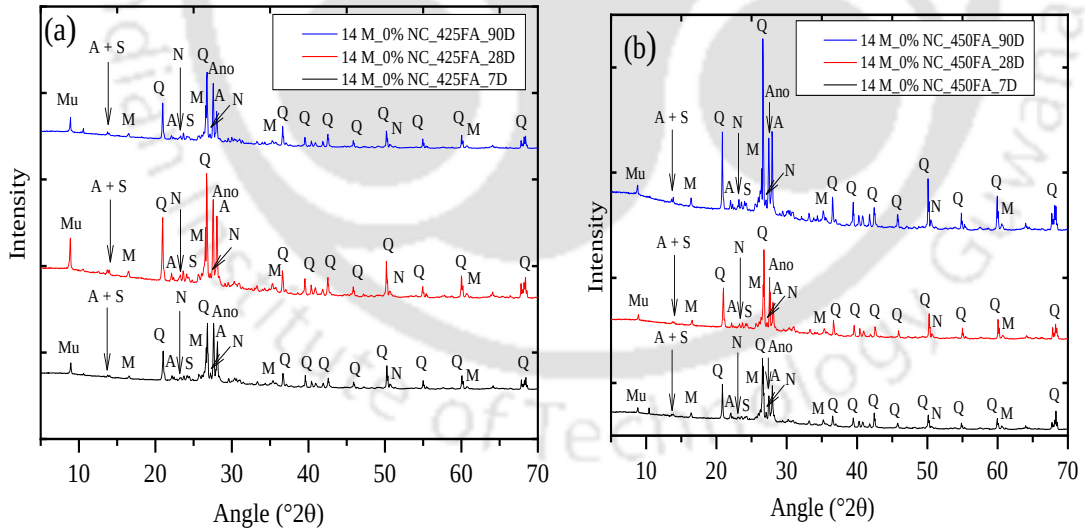

(GPC made with fly ash passing through 300 μm sieve, alkaline solution content of 210 kg/m^3 and SS/SH ratio of 1.75)

Fig. 5.63: XRD patterns of control GPC mixes made with NaOH solution of 14 M for fly ash content of a) 425 kg/m^3, and b) 450 kg/m^3, at the age of 7, 28, and 90 days

From Fig. 5.62 to Fig. 5.69, the GPC mixes made with fly ash content of 450 kg/m^3 mostly showed lower peak intensity of albite, anorthoclase, nepheline, sodalite, and muscovite in the XRD patterns as compared to that made with fly ash content of 425 kg/m^3 for fly ash passing

through 300 μm sieve irrespective of molarity of NaOH solution, admixed NaCl concentration and age. This shows lower extent of geopolymerization process in the GPC mixes made with higher fly ash content that led to lower compressive strength as compared to the GPC mixes made with lower fly ash content (Fig. 4.20 to Fig. 4.22). The reason for this variation in compressive strength with fly ash content is already stated in Section 4.3.5 (Chapter 4).

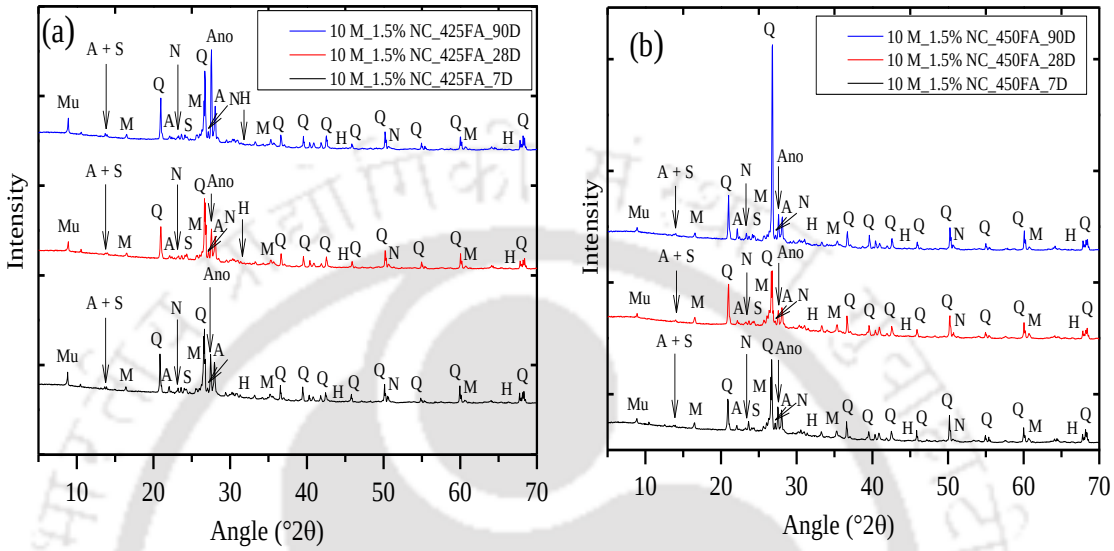

(GPC made with fly ash passing through 300 μm sieve, alkaline solution content of 210 kg/m^3 and SS/SH ratio of 1.75)

Fig. 5.64: XRD patterns of 1.5% NaCl admixed GPC mixes made with NaOH solution of 10 M for fly ash content of a) 425 kg/m^3, and b) 450 kg/m^3, at the age of 7, 28, and 90 days

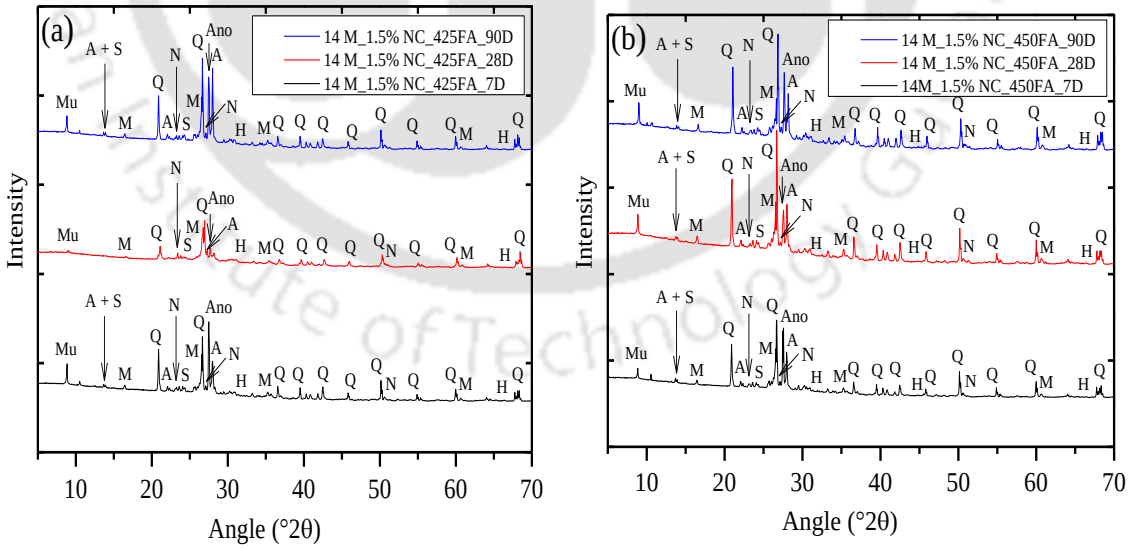

(GPC made with fly ash passing through 300 μm sieve, alkaline solution content of 210 kg/m^3 and SS/SH ratio of 1.75)

Fig. 5.65: XRD patterns of 1.5% NaCl admixed GPC mixes made with NaOH solution of 14 M for fly ash content of a) 425 kg/m^3, and b) 450 kg/m^3, at the age of 7, 28, and 90 days

As observed from Fig. 5.62 to Fig. 5.69, the peak intensity of the geopolymeric compounds were mostly higher in the GPC mixes at higher molarity of NaOH solution (14 M) than that at lower molarity of NaOH solution (10 M). Further, control GPC mixes (0% NaCl) mostly showed higher peak intensity of the geopolymeric compounds in the XRD patterns as compared to NaCl admixed GPC mixes irrespective of fly ash content, molarity of NaOH solution and age. In addition, the peak intensity of the compounds related to geopolymer gels mostly decreased with increase in admixed NaCl concentration from 1.5% to 3% and that from 3% to 4.5%. These variations in the peak intensity of the geopolymeric compounds in the XRD patterns with molarity of NaOH solution, between control and NaCl admixed GPC mixes, and with increase in NaCl concentration are consistent with the obtained compressive strength of GPC mixes (Fig. 4.20 to Fig. 4.22).

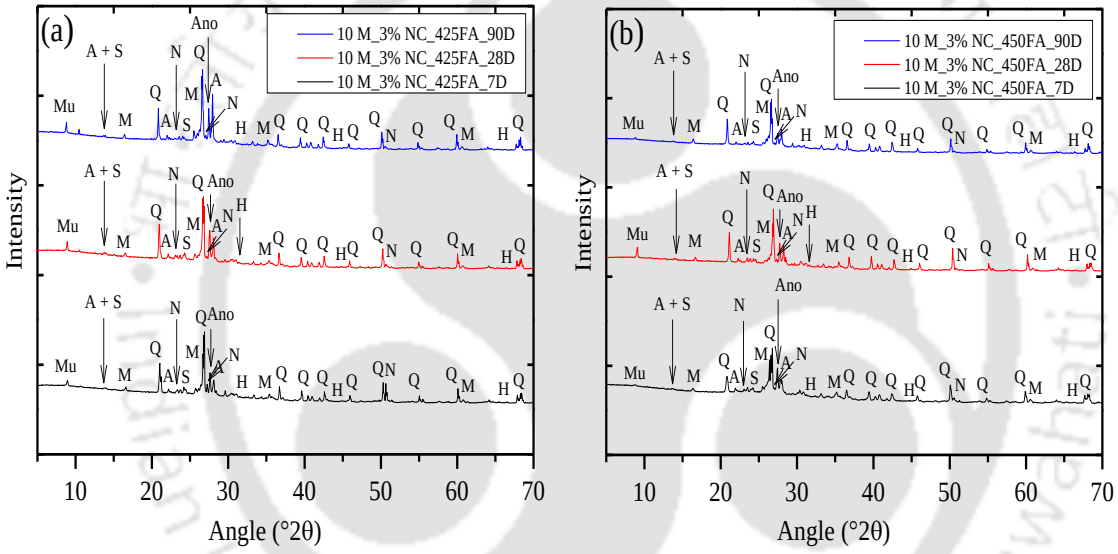

(GPC made with fly ash passing through 300 μm sieve, alkaline solution content of 210 kg/m^3 and SS/SH ratio of 1.75)

Fig. 5.66: XRD patterns of 3% NaCl admixed GPC mixes made with NaOH solution of 10 M for fly ash content of a) 425 kg/m^3, and b) 450 kg/m^3, at the age of 7, 28, and 90 days

From Fig. 5.62 and Fig. 5.63, the peak intensity of albite, anorthoclase, nepheline, sodalite, and muscovite in the XRD patterns increased with increase in age from 7 to 28 days in control GPC mixes for both fly ash contents and molarity of NaOH solution. This indicates continuation of geopolymerization process with age. This is corroborated with increase in compressive strength of GPC mixes with increase in age from 7 to 28 days (Fig. 4.20 and Fig. 4.21). The peak intensity of albite, anorthoclase, nepheline, sodalite, and muscovite in the XRD patterns increased with increase in age from 28 to 90 days in control GPC mixes for fly ash content of 450 kg/m^3 whereas opposite variation in the peak intensity of these compounds with increase in age from 28 to 90 days was observed for fly ash content of 425 kg/m^3. These

variations in the peak intensity of albite, anorthoclase, nepheline, sodalite, and muscovite in the XRD patterns of control GPC mixes with increase in age from 28 to 90 days for different fly ash contents are in line with the variations in compressive strength of GPC with increase in age from 28 to 90 days (Fig. 4.21 and Fig. 4.22). The reason for lower compressive strength at the age of 90 days in control GPC mixes made with lower fly ash content is already mentioned in Section 4.3.5 (Chapter 4).

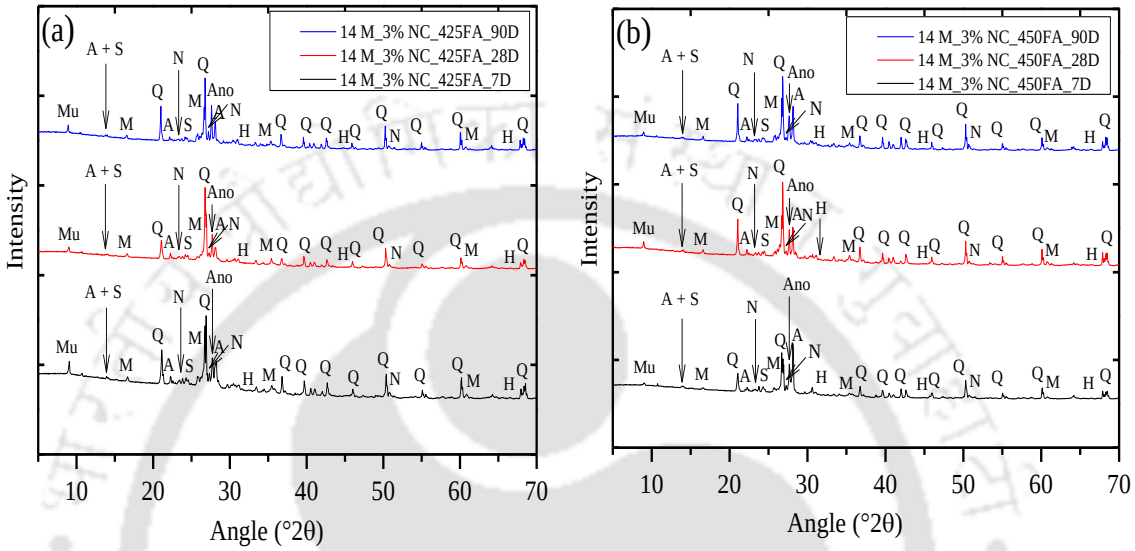

(GPC made with fly ash passing through 300 μm sieve, alkaline solution content of 210 kg/m^3 and SS/SH ratio of 1.75)

Fig. 5.67: XRD patterns of 3% NaCl admixed GPC mixes made with NaOH solution of 14 M for fly ash content of a) 425 kg/m^3, and b) 450 kg/m^3, at the age of 7, 28, and 90 days

From Fig. 5.64 to Fig. 5.69, the peak intensity of albite, anorthoclase, nepheline, sodalite, and muscovite in the XRD patterns mostly increased with increase in age from 7 to 28 days in NaCl admixed GPC mixes for fly ash content of 425 kg/m^3 whereas there was unsystematic variation in the peak intensity of these compounds with increase in age from 7 to 28 days for fly ash content of 450 kg/m^3. It may be noted that the compressive strength of NaCl admixed GPC mixes mostly increased with increase in age from 7 to 28 days for lower fly ash content, however, mostly opposite variation in compressiev strength with increase in age from 7 to 28 days was observed for higher fly ash content (Fig. 4.20 and Fig. 4.21). Further, the reason for lower compressive strength at the age of 28 days in the NaCl admixed GPC mixes for higher fly ash content is already stated in Section 4.3.5 (Chapter 4). From Fig. 5.64 to Fig. 5.69, the peak intensity of the compounds related to geopolymer gels in NaCl admixed GPC mixes were mostly lower at the age of 90 days as compared to that at the age of 28 days for fly ash content of 450 kg/m^3, which is substantiated by the results of compressive strength where the compressive strength of NaCl admixed GPC mixes was mostly lower at the age of 90 days

than that at the age of 28 days (Fig. 4.21 and Fig. 4.22). At fly ash content of 425 kg/m^3, there was mostly unsystematic variation in the peak intensity of albite, anorthoclase, nepheline, sodalite, and muscovite in the XRD patterns of NaCl admixed GPC mixes with increase in age from 28 to 90 days (Fig.5.64 to Fig. 5.69). It may be noted that the variation in compressive strength of NaCl admixed GPC mixes was not systematic with increase in age from 28 to 90 days at fly ash content of 425 kg/m^3 (Fig. 4.21 and Fig. 4.22).

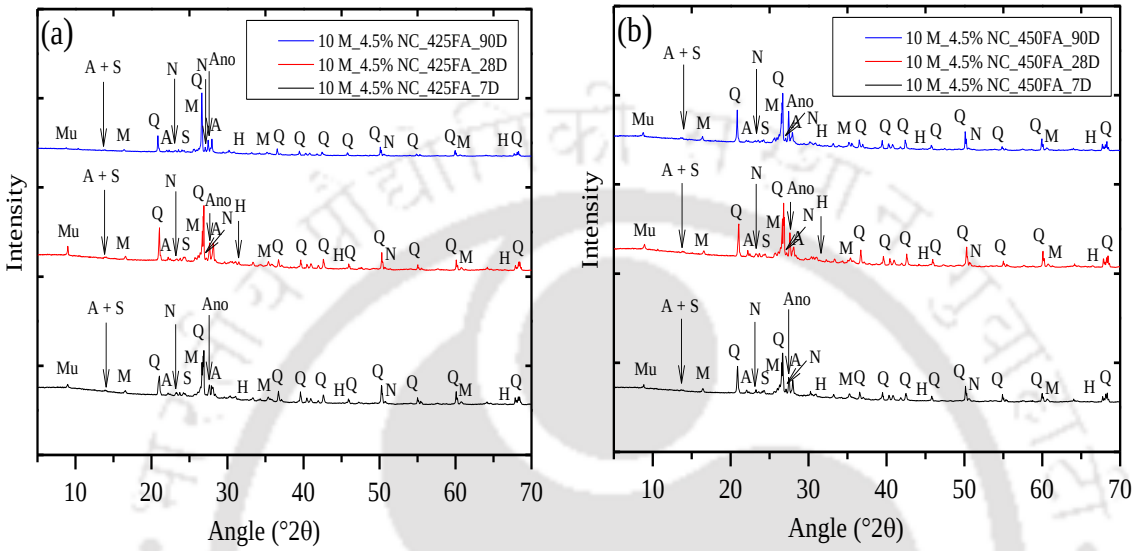

(GPC made with fly ash passing through 300 μm sieve, alkaline solution content of 210 kg/m^3 and SS/SH ratio of 1.75)

Fig. 5.68: XRD patterns of 4.5% NaCl admixed GPC mixes made with NaOH solution of 10 M for fly ash content of a) 425 kg/m^3, and b) 450 kg/m^3, at the age of 7, 28, and 90 days

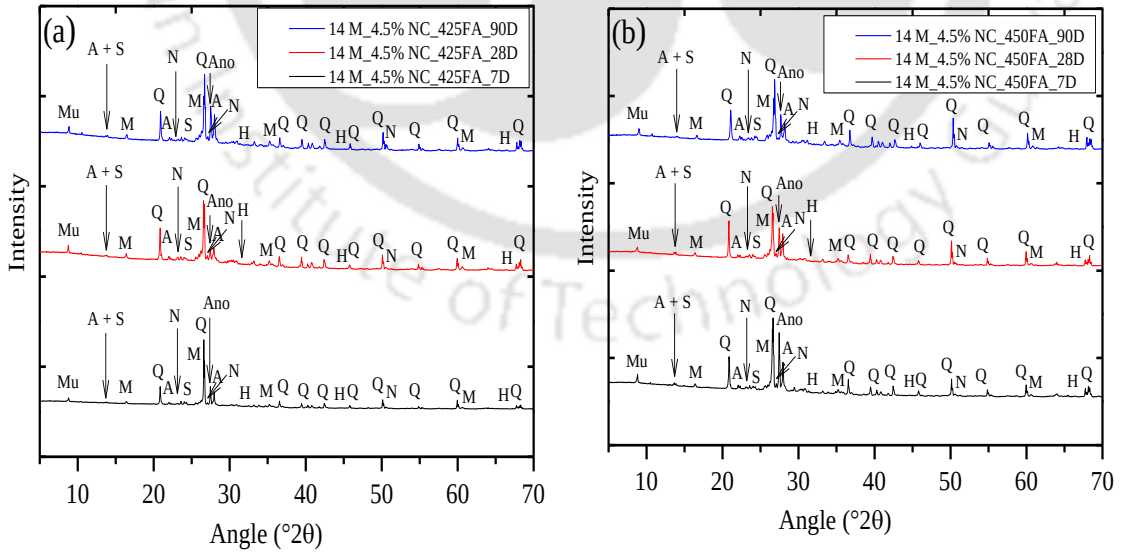

(GPC made with fly ash passing through 300 μm sieve, alkaline solution content of 210 kg/m^3 and SS/SH ratio of 1.75)

Fig. 5.69: XRD patterns of 4.5% NaCl admixed GPC mixes made with NaOH solution of 14 M for fly ash content of a) 425 kg/m^3, and b) 450 kg/m^3, at the age of 7, 28, and 90 days

From Fig. 5.64 to Fig. 5.69, the variation in peak intensity of halite in the XRD patterns was not systematic with increase in admixed NaCl concentration, which may be ascribed to the alteration in its degree of crystallinity in the microstructure of GPC as a result of variations in the extent of interaction of chloride ions with the aluminosilicate gels in the GPC mixes. Further, there was no systematic variation in the peak intensity of halite with increase in age from 7 to 28 days and that from 28 to 90 days as observed from the XRD patterns (Fig. 5.64 to Fig. 5.69). The peak intensity of halite in the NaCl admixed GPC mixes was mostly higher at fly ash content of 450 kg/m^3 as compared to that at fly ash content of 425 kg/m^3 (Fig. 5.64 to Fig. 5.69), which may be due to addition of more NaCl content in GPC mixes made with higher fly ash content than that made with lower fly ash content during preparation where NaCl was added in GPC mixes as percentage by mass of geopolymer solids, which include fly ash. It may be noted that the compressive strength was mostly lower at higher fly ash content as compared to that at lower fly ash content (Fig. 4.20 to Fig. 4.22). Thus, in addition to the effect of insufficient amount of alkaline solution for higher fly ash content that resulted in lower dissolution of alumina and silica from fly ash thereby leading to lower extent of geopolymerization process in the GPC mixes made with higher fly ash content, the comparatively more crystallization of sodium chloride in GPC mixes made with higher fly ash content as indicated by the peak intensity of halite in the XRD patterns also led to lower compressive strength at higher fly ash content. From Fig. 5.64 to Fig. 5.69, the peak intensity of halite in the XRD patterns was mostly higher at NaOH solution of 10 M as compared to that at NaOH solution of 14 M. Thus, higher extent of crystallization of sodium chloride in NaCl admixed GPC mixes at lower molarity of NaOH solution contributed toward lower compressive strength of GPC mixes (Fig. 4.20 to Fig.4.22).

For fly ash passing through 300 μm sieve, the FTIR spectra of GPC mixes made with fly ash content of 425 kg/m^3, and 450 kg/m^3 are shown in Fig. 5.70 to Fig. 5.77. From Fig. 5.70 to Fig. 5.77, the peak in the range of 770 cm^{-1} to 778 cm^{-1}, 1372 cm^{-1} to 1532 cm^{-1}, and 1641 cm^{-1} to 1715 cm^{-1}, and the band in the range of 3390 cm^{-1} to 3748 cm^{-1} are related to the presence of quartz, stretching vibration of carbonate group, bending vibration of H–O–H group, and stretching vibration of –OH group respectively irrespective of fly ash content, molarity of NaOH solution, admixed NaCl concentration and age. From Fig. 5.70 to Fig. 5.77, the peak corresponding to asymmetric stretching vibration of Si–O–Si(Al) bond, which is associated with the presence of geopolymer gels in GPC mixes mostly shifted to lower wavenumbers in case of fly ash content of 425 kg/m^3 (997 cm^{-1} to 1003 cm^{-1}) as compared to fly ash content of

450 kg/m^3 (997 cm^{-1} to 1016 cm^{-1}) irrespective of molarity of NaOH solution, admixed NaCl concentration and age for fly ash passing through 300 μm sieve. This shows comparatively higher extent of geopolymerization process in GPC mixes made with lower fly ash content as compared to that made with higher fly ash content, which is substantiated with the variations in the peak intensity of the compounds related to N-A-S-H gel in XRD patterns where the peak intensity of the compounds related to N-A-S-H gel were mostly higher at lower fly ash content than that at higher fly ash content (Fig. 5.62 to Fig. 5.69). From Fig. 5.70 to Fig. 5.77, the peak associated with asymmetric stretching vibration of Si–O–Si(Al) bond in the FTIR spectra shifted to lower wavenumbers in case of NaOH solution of 14 M (997 cm^{-1} to 1003 cm^{-1}) as compared to NaOH solution of 10 M (1001 cm^{-1} to 1016 cm^{-1}) regardless of fly ash content, admixed NaCl concentration, and age, which indicates higher extent of geopolymerization process in GPC mixes made with NaOH solution of higher molarity than NaOH solution of lower molarity [59]. This variation is supported by the results of XRD analysis where the peak intensity of geopolymeric compounds in the XRD patterns were mostly higher at higher molarity (14 M) of NaOH solution than that at lower molarity (10 M) of NaOH solution (Fig. 5.62 to Fig. 5.69).

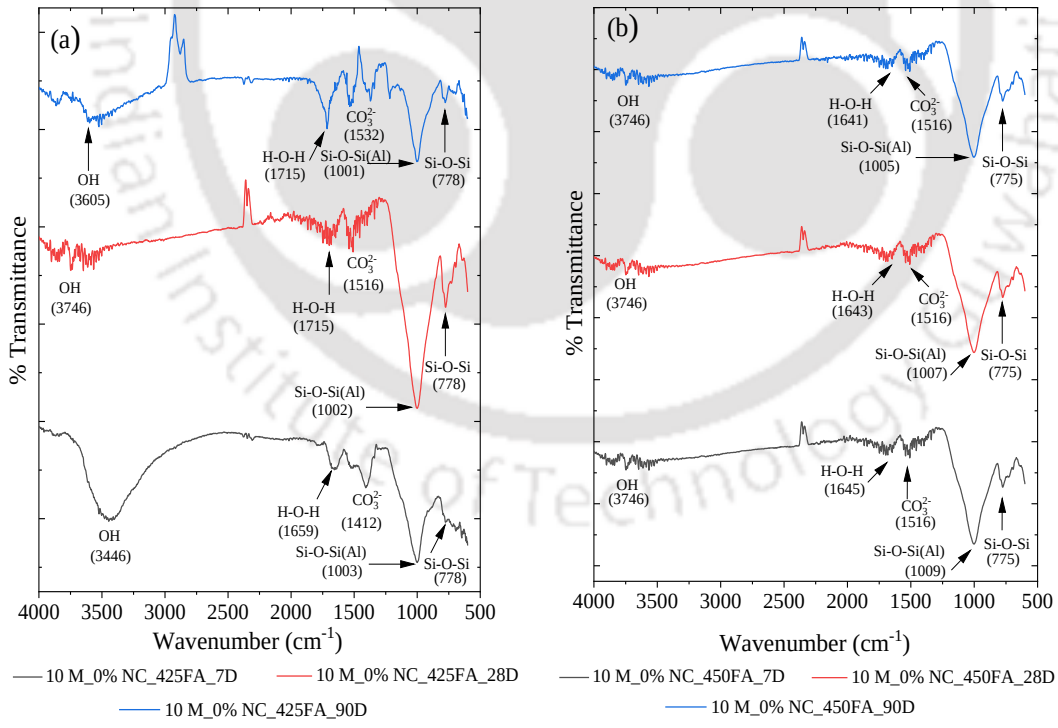

(GPC made with fly ash passing through 300 μm sieve, alkaline solution content of 210 kg/m^3 and SS/SH ratio of 1.75)

Fig. 5.70: FTIR spectra of control GPC mixes made with NaOH solution of 10 M for fly ash content of a) 425 kg/m^3, and b) 450 kg/m^3, at the age of 7, 28, and 90 days

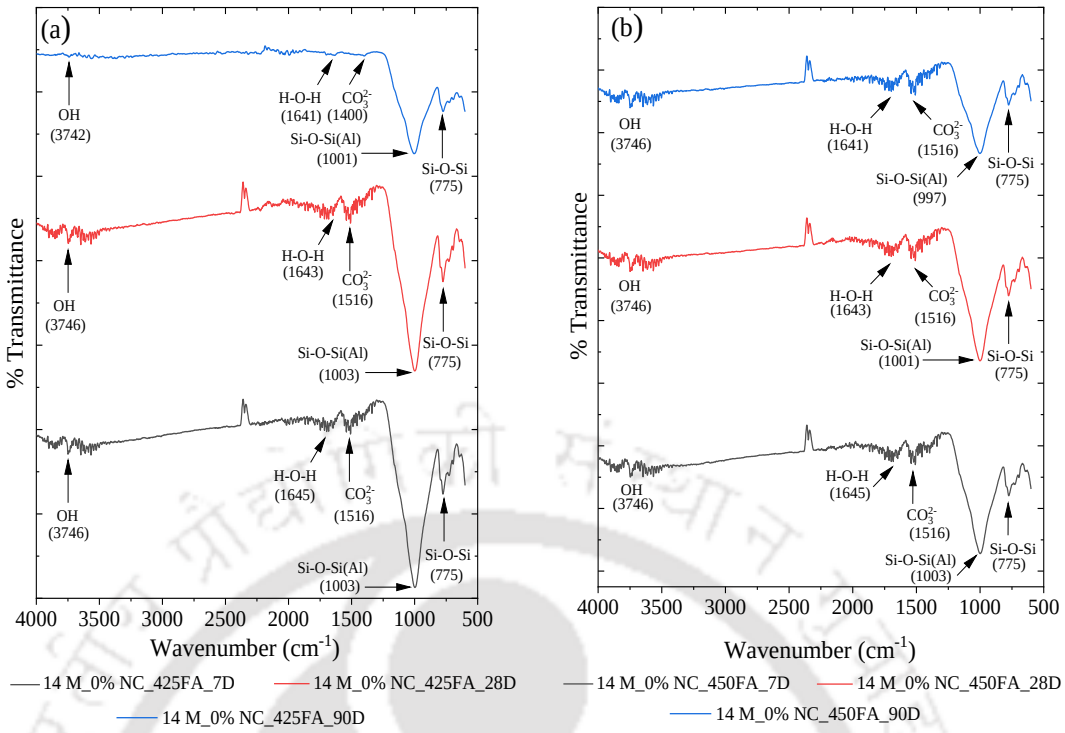

(GPC made with fly ash passing through 300 μm sieve, alkaline solution content of 210 kg/m^3 and SS/SH ratio of 1.75)

Fig. 5.71: FTIR spectra of control GPC mixes made with NaOH solution of 14 M for fly ash content of a) 425 kg/m^3, and b) 450 kg/m^3, at the age of 7, 28, and 90 days

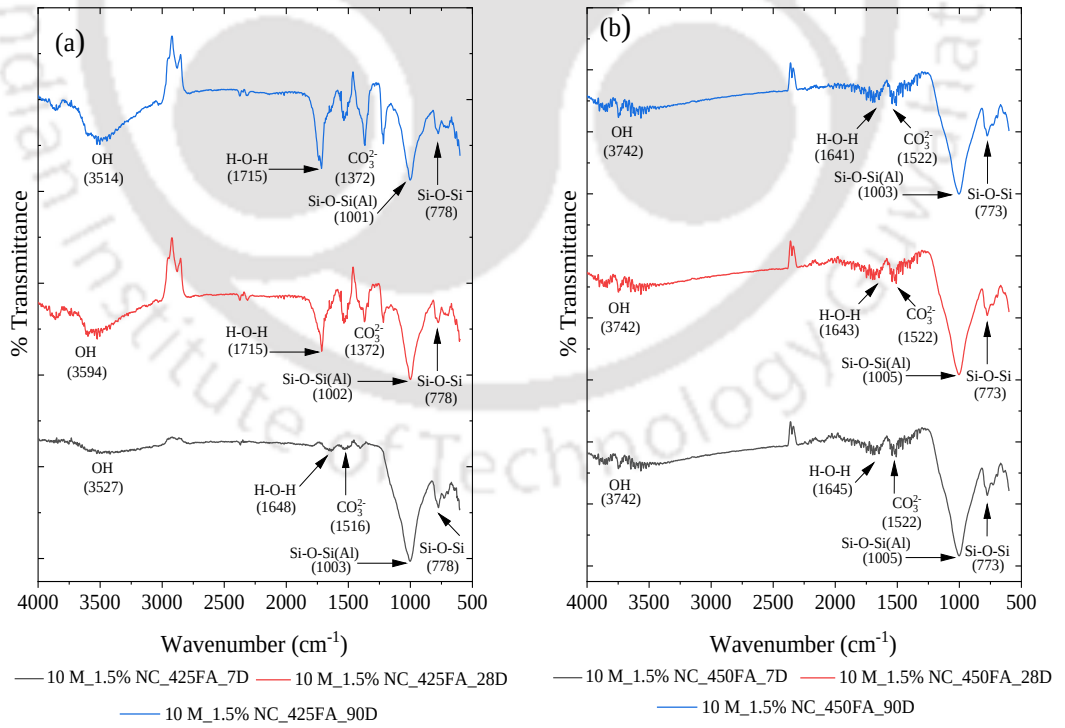

(GPC made with fly ash passing through 300 μm sieve, alkaline solution content of 210 kg/m^3 and SS/SH ratio of 1.75)

Fig. 5.72: FTIR spectra of 1.5% NaCl admixed GPC mixes made with NaOH solution of 10 M for fly ash content of a) 425 kg/m^3, and b) 450 kg/m^3, at the age of 7, 28, and 90 days

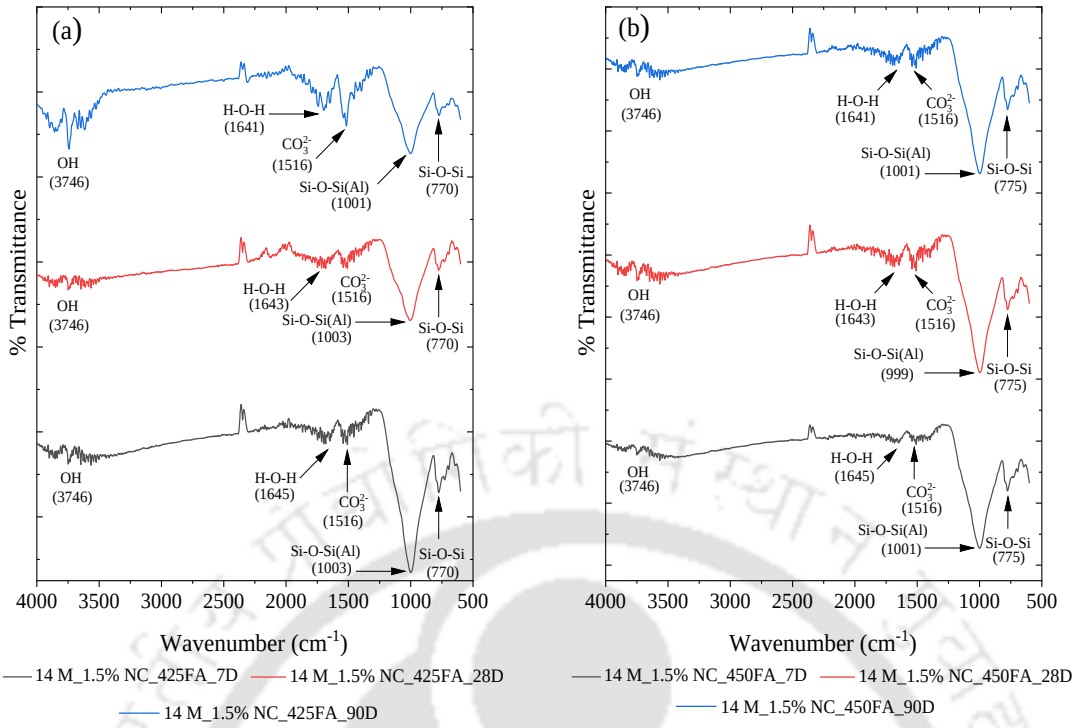

(GPC made with fly ash passing through 300 μm sieve, alkaline solution content of 210 kg/m^3 and SS/SH ratio of 1.75)

Fig. 5.73: FTIR spectra of 1.5% NaCl admixed GPC mixes made with NaOH solution of 14 M for fly ash content of a) 425 kg/m^3, and b) 450 kg/m^3, at the age of 7, 28, and 90 days

From Fig. 5.70 Fig. 5.77, the peak corresponding to asymmetric stretching vibration of Si–O–Si(Al) bond in the FTIR spectra mostly shifted to lower wavenumbers in case of control GPC mix (997 cm^{-1} to 1009 cm^{-1}) when compared with NaCl admixed GPC mixes (997 cm^{-1} to 1016 cm^{-1}) regardless of fly ash content, molarity of NaOH solution and age. Further, the peak associated with asymmetric stretching vibration of Si–O–Si(Al) bond mostly shifted to lower wavenumbers with decrease in NaCl concentration i.e., from 997 cm^{-1} – 1015 cm^{-1} at NaCl concentration of 3% to 999 cm^{-1} – 1005 cm^{-1} at NaCl concentration of 1.5%, and from 997 cm^{-1} – 1016 cm^{-1} at NaCl concentration of 4.5% to 997 cm^{-1} – 1015 cm^{-1} at NaCl concentration of 3%, although the variation was very less. This indicates mostly lower extent of geopolymerization process in NaCl admixed GPC mixes when compared with control mix and with increase in admixed NaCl concentration. These observations are in line with the variations in compressive strength (Fig. 4.20 to Fig. 4.22), and in the peak intensity of geopolymeric compounds in the XRD patterns of control and NaCl admixed GPC mixes (Fig 5.62 to Fig. 5.69).

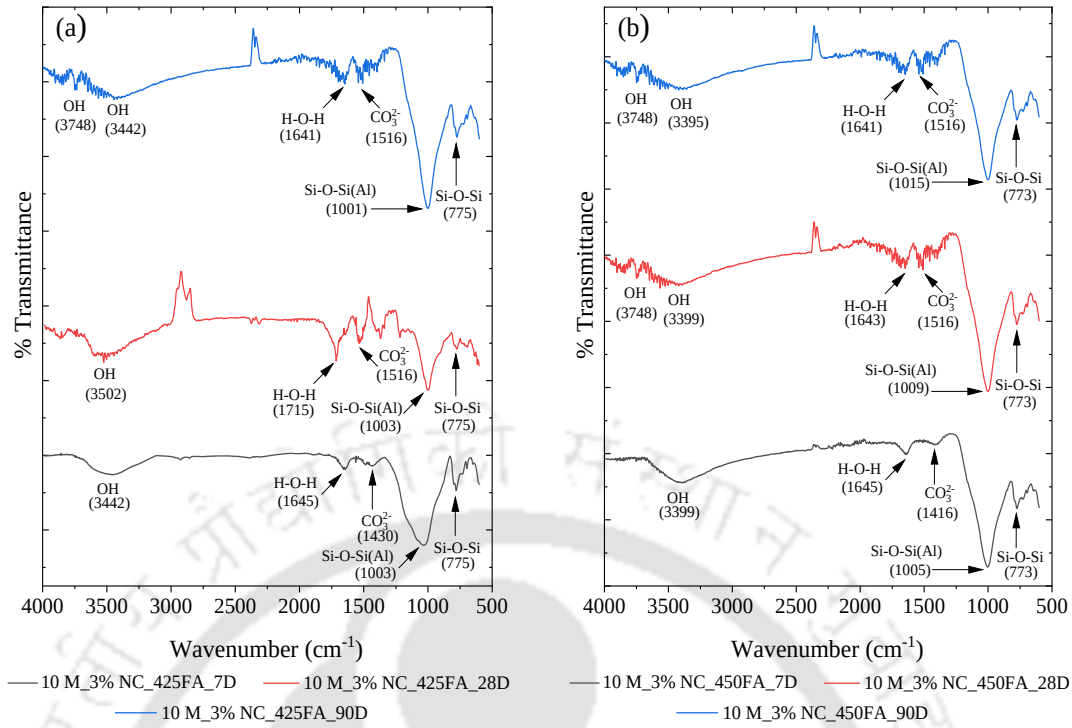

(GPC made with fly ash passing through 300 μm sieve, alkaline solution content of 210 kg/m^3 and SS/SH ratio of 1.75)

Fig. 5.74: FTIR spectra of 3% NaCl admixed GPC mixes made with NaOH solution of 10 M for fly ash content of a) 425 kg/m^3, and b) 450 kg/m^3, at the age of 7, 28, and 90 days

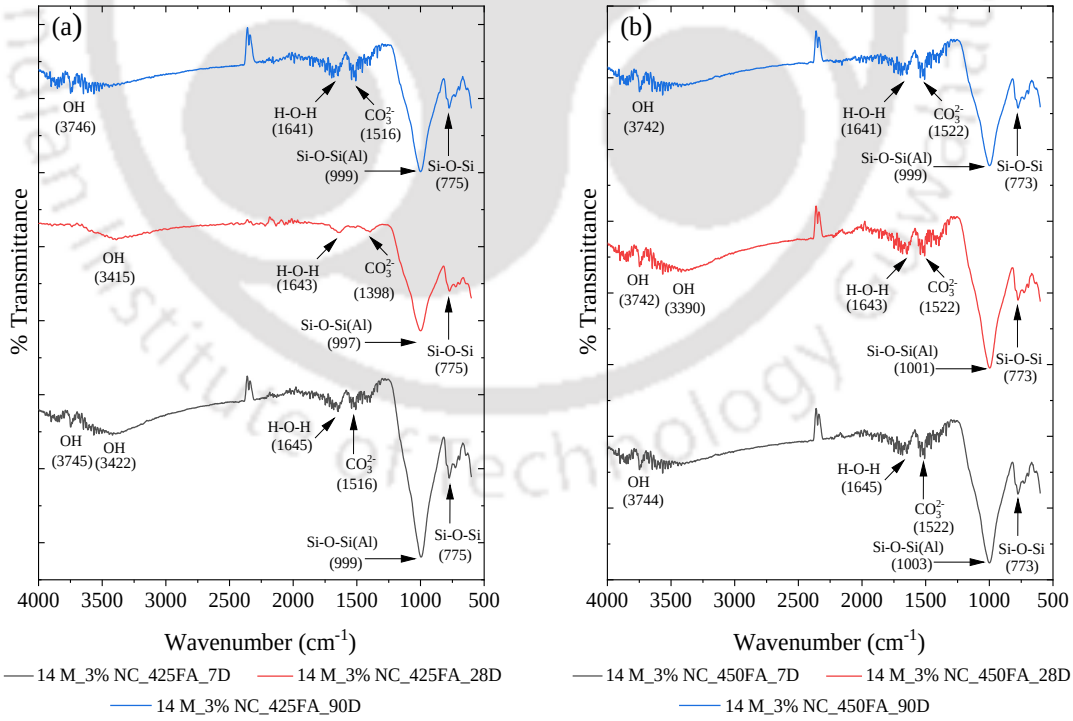

(GPC made with fly ash passing through 300 μm sieve, alkaline solution content of 210 kg/m^3 and SS/SH ratio of 1.75)

Fig. 5.75: FTIR spectra of 3% NaCl admixed GPC mixes made with NaOH solution of 14 M for fly ash content of a) 425 kg/m^3, and b) 450 kg/m^3, at the age of 7, 28, and 90 days

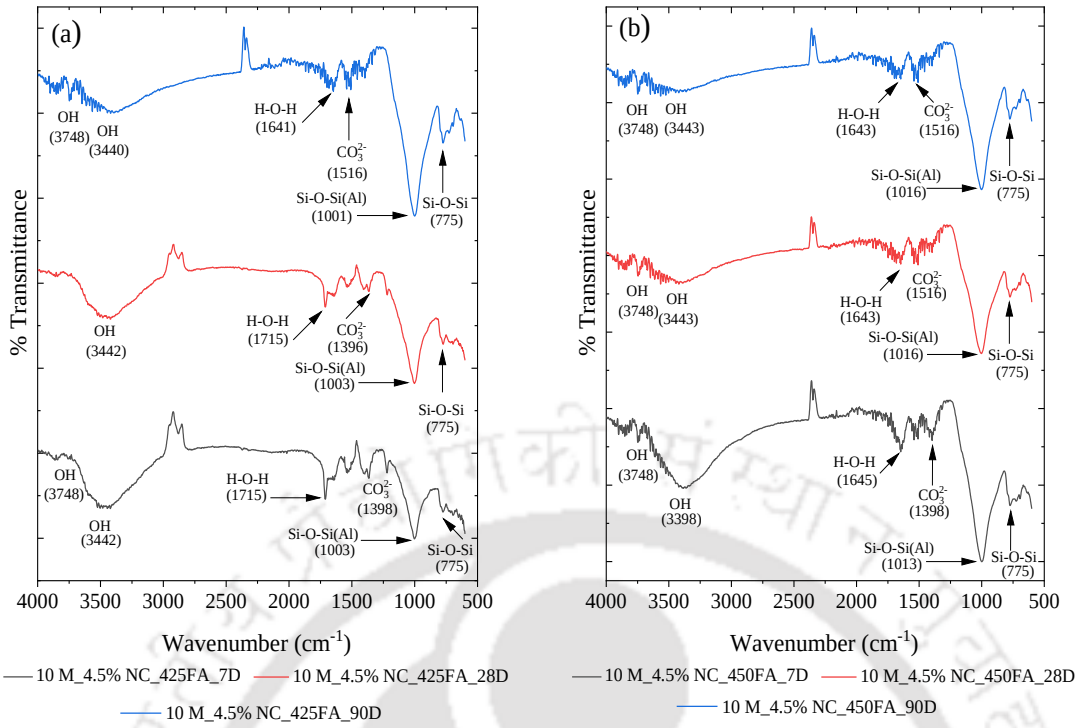

(GPC made with fly ash passing through 300 μm sieve, alkaline solution content of 210 kg/m^3 and SS/SH ratio of 1.75)

Fig. 5.76: FTIR spectra of 4.5% NaCl admixed GPC mixes made with NaOH solution of 10 M for fly ash content of a) 425 kg/m^3, and b) 450 kg/m^3, at the age of 7, 28, and 90 days

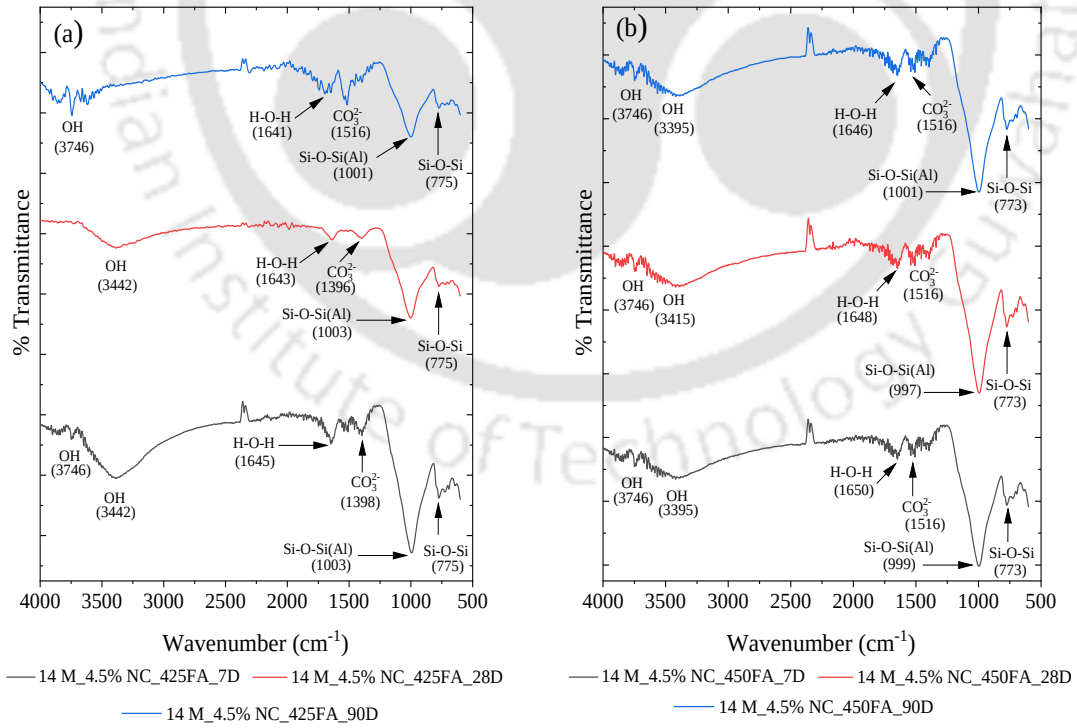

(GPC made with fly ash passing through 300 μm sieve, alkaline solution content of 210 kg/m^3 and SS/SH ratio of 1.75)

Fig. 5.77: FTIR spectra of 4.5% NaCl admixed GPC mixes made with NaOH solution of 14 M for fly ash content of a) 425 kg/m^3, and b) 450 kg/m^3, at the age of 7, 28, and 90 days

In the FTIR spectra shown in Fig. 5.70 and Fig. 5.71 for control GPC mixes, the peak associated with asymmetric stretching vibration of Si–O–Si(Al) bond shifted to lower wavenumbers with increase in age from 7 to 28 days i.e., 1003 cm^{-1} at 7 days to 1002 cm^{-1} – 1003 cm^{-1} at 28 days (less variation) for fly ash content of 425 kg/m^3, and 1003 cm^{-1} – 1009 cm^{-1} at 7 days to 1001 cm^{-1} – 1007 cm^{-1} at 28 days for fly ash content of 450 kg/m^3. This indicates continuation of geopolymerization reaction with increase in age from 7 to 28 days, which is substantiated with the variations in the peak intensity of geopolymeric compounds in the XRD patterns with increase in age in control GPC mixes (Fig. 5.62 and Fig. 5.63). Similarly, the peak related to asymmetric stretching vibration of Si–O–Si(Al) bond shifted to lower wavenumbers with increase in age from 28 to 90 days i.e., 1002 cm^{-1} – 1003 cm^{-1} at 28 days to 1001 cm^{-1} at 90 days (less variation) for fly ash content of 425 kg/m^3, and 1001 cm^{-1} – 1007 cm^{-1} at 28 days to 997 cm^{-1} – 1005 cm^{-1} at 90 days for fly ash content of 450 kg/m^3. It may be noted that the peak intensity of the compounds related to N-A-S-H gel in control GPC mixes increased with increase in age from 28 days to 90 days for fly ash content of 450 kg/m^3 whereas there was opposite variation in the peak intensity of geopolymeric compounds for fly ash content of 425 kg/m^3 (Fig. 5.62 and Fig. 5.63). This indicates inconsistent variation in the peak intensity of the geopolymeric compounds in the XRD patterns with increase in age from 28 to 90 days with the variation (although less) in the wavenumber corresponding to the peak related to asymmetric stretching vibration of Si–O–Si(Al) bond for fly ash content of 425 kg/m^3. Although there is inconsistent variation, the shift in the peak associated with asymmetric stretching vibration of Si–O–Si(Al) bond to comparatively lower wavenumber at 90 days as compared to 28 days (although less variation) in case of lower fly ash content indicates alteration in the geopolymerization process to certain extent in the GPC mixes made with lower fly ash content.

In the FTIR spectra shown in Fig. 5.72 to Fig. 5.77 for NaCl admixed GPC mixes, the peak corresponding to asymmetric stretching vibration of Si–O–Si(Al) bond, although the variation was less, mostly shifted to lower wavenumbers with increase in age from 7 (999 cm^{-1} to 1003 cm^{-1}) to 28 days (997 cm^{-1} to 1003 cm^{-1}) at fly ash content of 425 kg/m^3 irrespective of NaCl concentration and molarity of NaOH solution, which is supported by the results of XRD analysis where there was mostly increase in the peak intensity of the geopolymeric compounds in the XRD patterns with increase in age from 7 to 28 days (Fig. 5.64 to Fig. 5.69). At fly ash content of 450 kg/m^3, there was unsystematic variation in the wavenumber of the peak related to asymmetric stretching vibration of Si–O–Si(Al) bond with increase in age from 7 (999 cm^{-}

^{1} to 1013 cm^{-1}) to 28 days (997 cm^{-1} to 1016 cm^{-1}) in NaCl admixed GPC mixes, which is in line with the unsystematic variation in the peak intensity of the compounds related to N-A-S-H gel in the XRD patterns with increase in age from 7 to 28 days at fly ash content of 450 kg/m^3 (Fig. 5.64 to Fig. 5.69). In the FTIR spectra shown in Fig. 5.72 to Fig. 5.77, there was unsystematic variation in the wavenumber corresponding to the peak associated with asymmetric stretching vibration of Si–O–Si(Al) bond with increase in age from 28 (997 cm^{-1} to 1003 cm^{-1}) to 90 days (999 cm^{-1} to 1001 cm^{-1}) in NaCl admixed GPC mixes for fly ash content of 425 kg/m^3. It may be noted that mostly there was unsystematic variation in the peak intensity of albite, anorthoclase, nepheline, sodalite, and muscovite in the XRD patterns (Fig. 5.64 to Fig. 5.69), and that in the compressive strength of NaCl admixed GPC mixes with increase in age from 28 to 90 days for fly ash content of 425 kg/m^3 (Fig. 4.21 and Fig. 4.22). For fly ash content of 450 kg/m^3, the peak corresponding to asymmetric stretching vibration of Si–O–Si(Al) bond mostly shifted to higher wavenumbers (although the variation was less) with increase in age from 28 days (997 cm^{-1} to 1016 cm^{-1}) to 90 days (999 cm^{-1} to 1016 cm^{-1}) in NaCl admixed GPC mixes. This indicates comparatively lower extent of geopolymerization reaction at later age (90 days) in NaCl admixed GPC mixes made with higher fly ash content, which is substantiated with mostly lower compressive strength (Fig. 4.21 and Fig. 4.22), and lower peak intensity of geopolymeric compounds in the XRD patterns (Fig. 5.64 to Fig. 5.69) of NaCl admixed GPC mixes for fly ash content of 450 kg/m^3 at the age of 90 days than that at the age of 28 days.

The typical FESEM images of GPC mixes made with fly ash content of 425 kg/m^3, and 450 kg/m^3 for fly ash passing through 300 μm sieve are shown in Fig. 5.78. The remaining FESEM images are shown in Appendix A. The FESEM micrographs shown in Fig. 5.78 (a, b) indicated comparatively less formation of geopolymer gels at fly ash content of 450 kg/m^3 than that at fly ash content of 425 kg/m^3. This is supported by mostly lower peak intensity of geopolymeric compounds in the XRD patterns of GPC mixes made with fly ash content of 450 kg/m^3 as compared to fly ash content of 425 kg/m^3 (Fig. 5.63). The formation of more amount of geopolymer gels as well as denser microstructure were observed in the FESEM image of GPC made with higher molarity of NaOH solution as compared to that made with lower molarity of NaOH solution (Fig. 5.78 (c, d)), which is substantiated by higher peak intensity of the compounds related to geopolymer gels in the XRD patterns at higher molarity of NaOH solution than lower molarity of NaOH solution (Fig. 5.62 and Fig. 5.63).

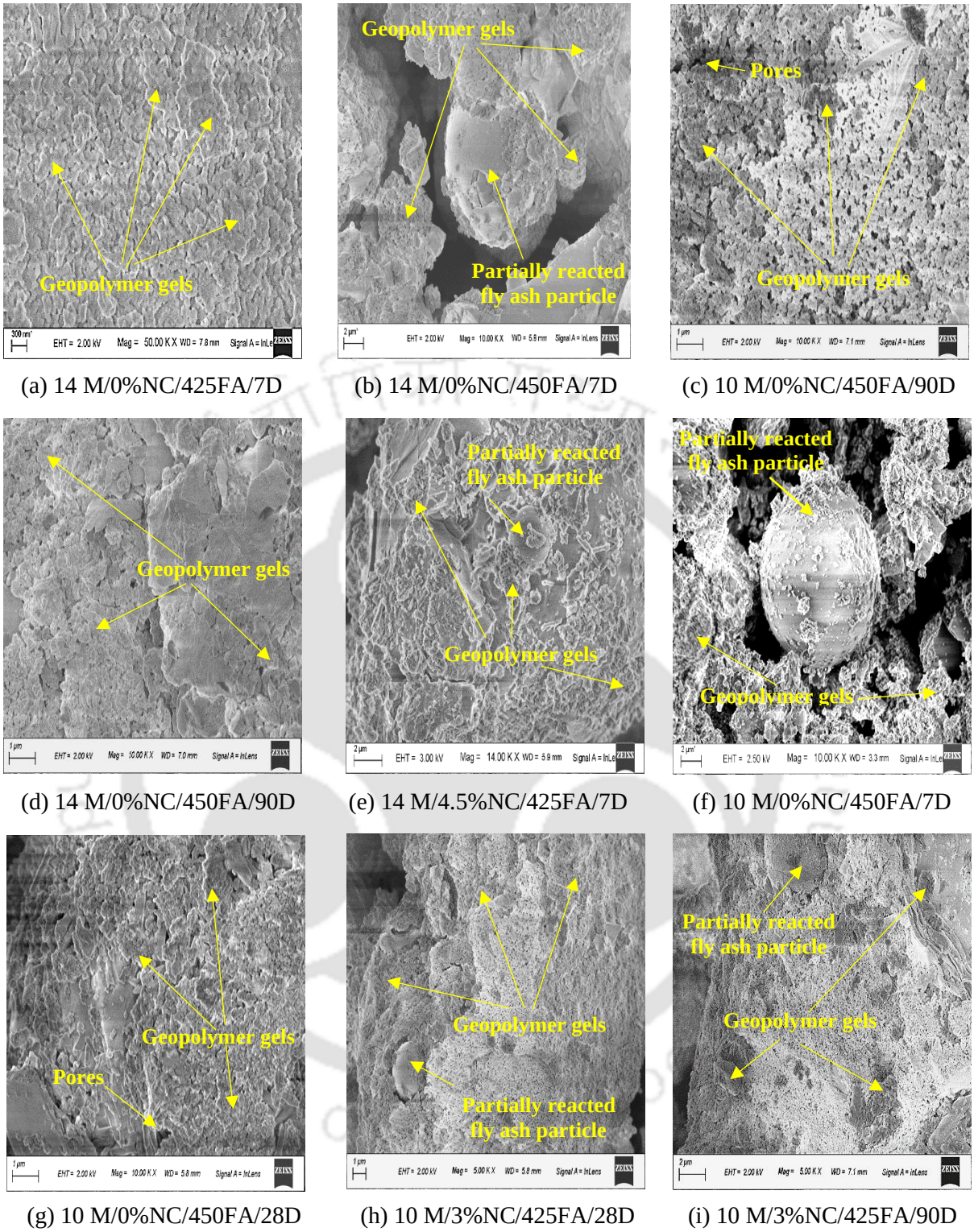

(a) 14 M/0%NC/425FA/7D (b) 14 M/0%NC/450FA/7D (c) 10 M/0%NC/450FA/90D

(d) 14 M/0%NC/450FA/90D (e) 14 M/4.5%NC/425FA/7D (f) 10 M/0%NC/450FA/7D

(g) 10 M/0%NC/450FA/28D (h) 10 M/3%NC/425FA/28D (i) 10 M/3%NC/425FA/90D

(GPC made with fly ash passing through 300 μm sieve, alkaline solution content of 210 kg/m^3 and SS/SH ratio of 1.75)

Fig. 5.78: FESEM images of GPC made with fly ash contents of 425 kg/m^3 and 450 kg/m^3, at different ages

The FESEM images shown in from Fig. 5.78 (a, e) indicated formation of more amount of geopolymer gels in control GPC mix as compared to that in NaCl admixed GPC mix. The same variation was observed in the peak intensity of the compounds related to N-A-S-H gel in XRD patterns between control GPC mix and NaCl admixed GPC mix (Fig. 5.63 and Fig. 5.69). In the FESEM images shown in Fig. 5.78 (f, g), the formation of more amount of geopolymer gels was observed at the age of 28 days as compared to that at the age of 7 days in control GPC mixes, which indicates continuation of geopolymerization process with increase in age from 7 to 28 days. In the FESEM images shown in Fig. 5.78 (h, i), there was no noticeable difference in the microstructure of NaCl admixed GPC mixes with increase in age from 28 to 90 days. These variations in the microstructure of GPC mixes with age as observed from the FESEM images are in line with the variations in the peak intensity of the compounds related to geopolymer gels in the XRD patterns of GPC mixes (Fig. 5.62 and Fig. 5.66).

5.3 Summary

The results of XRD analysis indicated formation of more amount of geopolymer gels in geopolymer concrete (GPC) at higher molarity of NaOH solution as the peak intensity of albite, anorthoclase, and nepheline in the XRD patterns mostly increased with increase in molarity of NaOH solution from 8 M to 16 M in control as well as 1.5% NaCl admixed GPC mixes at the age of 7, 28 and 90 days. In GPC mixes admixed with higher concentration of NaCl i.e., 3% and 4.5%, the peak intensity of these compounds in the XRD patterns mostly increased with increase in molarity of NaOH solution from 8 M to 14 M followed by a decrease at 16 M NaOH solution. These variations in the peak intensity of the geopolymeric compounds are substantiated by the variations in the compressive strength of GPC with molarity of NaOH solution in control and NaCl admixed mixes. Further, from XRD analysis, the variations in the peak intensity of the compounds related to geopolymer gels are mostly supported by the variations in compressive strength of GPC with alkaline solution content, SS/SH ratio, particle size of fly ash, fly ash content, and age. Irrespective of molarity of NaOH solution, alkaline solution content, SS/SH ratio, particle size of fly ash, and fly ash content, the NaCl admixed GPC mixes mostly showed lower peak intensity of albite, anorthoclase, nepheline, sodalite, and muscovite in the XRD patterns when compared with control GPC mixes at different ages. In addition, the peak intensity of these compounds mostly decreased with increase in admixed NaCl concentration in GPC mixes.

The variations in the wavenumber associated with the peak corresponding to asymmetric stretching vibration of Si–O–Si(Al) bond in the FTIR spectra that shows the presence of

geopolymer gels in GPC mixes are corroborated with the variations in the peak intensity of the compounds related to geopolymer gels in XRD patterns with molarity of NaOH solution, alkaline solution content, SS/SH ratio, particle size of fly ash, fly ash content, admixed NaCl concentration and age. There was formation of comparatively denser microstructure at higher molarity of NaOH solution, and in control GPC mixes as observed from FESEM images when compared with lower molarity of NaOH solution, and NaCl admixed GPC mixes, which is in line with higher peak intensity of albite, anorthoclase, nepheline, sodalite, and muscovite in the XRD patterns at higher molarity of NaOH solution and in control GPC mixes. Further, the variations in the formation of microstructure in GPC as observed from the FESEM images with alkaline solution content, SS/SH ratio, particle size of fly ash, fly ash content, and age are consistent with the variations in the peak intensity of the geopolymeric compounds in the XRD patterns of GPC mixes.

Chapter 6

Corrosion Behaviour of Rebar and Microstructure of Chloride Admixed Fly ash based Geopolymer Concrete

6.1 General

In this chapter, the results obtained from the study on corrosion behaviour of steel reinforcement in chloride-rich fly ash based geopolymer concrete (GPC) are presented and the effects of different mix parameters on variations in corrosion potential and corrosion current density of steel reinforcement are discussed. The influence of mix parameters on free, total, and bound chloride contents at rebar level at the age of 600 days are analyzed and discussed. Further, the changes in microstructure of geopolymer concrete near rebar level at the age of 600 days are analyzed and discussed from the obtained results of X-ray diffraction (XRD), Fourier transform infrared (FTIR) spectroscopy and Field emission scanning electron microscope (FESEM) analyses.

6.2 Corrosion potential and corrosion current density of rebar in fly ash based geopolymer concrete

The influence of different mix parameters namely molarity of NaOH solution, alkaline solution content, SS/SH ratio, particle size of fly ash and fly ash content on variations in corrosion potential and corrosion current density of steel reinforcement in NaCl admixed fly ash based geopolymer concrete (GPC) are analyzed and discussed. As already stated in Chapter 3, the tests for corrosion potential and corrosion current density were conducted on the prismatic reinforced GPC specimens at different ages. It may be noted that the prismatic specimens were kept under ambient laboratory condition.

6.2.1 Influence of molarity of NaOH solution on corrosion potential and corrosion current density

The corrosion potential values of steel reinforcement in fly ash based GPC made with different molarity of NaOH solution such as 8 M, 10 M, 12 M, 14 M and 16 M are shown in Fig. 6.1 for admixed with NaCl concentrations 0%, 1.5%, 3%, and 4.5%, and different ages i.e., 60 days, 180 days, 360 days and 600 days from the day of casting. Each value of corrosion potential shown in these figures is the average value of three replicate prismatic specimens. From Fig. 6.1, it is observed that the corrosion potential values of steel bar embedded in control GPC specimens (i.e., admixed without NaCl) were less negative than -270 mV (SCE) for all molarity of NaOH solution and at all ages. This indicates lower probability of occurrence of steel

reinforcement corrosion in control GPC mixes as per ASTM C876 [100]. According to ASTM C876 [100], the potential values of steel reinforcement more negative than -270 mV (SCE) correspond to greater than 90% probability of occurrence of steel reinforcement corrosion.

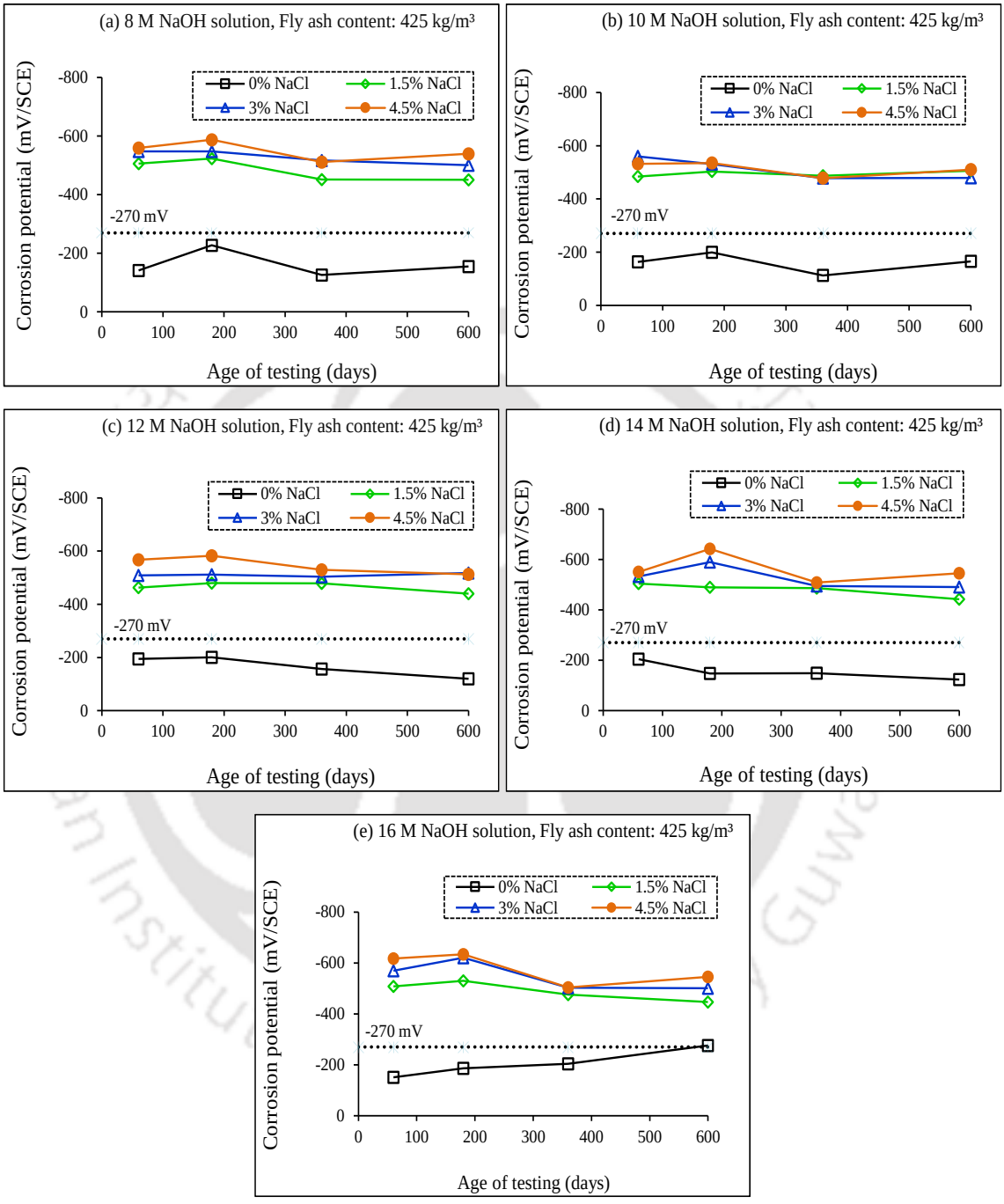

(GPC made with fly ash passing through 300 μm sieve, fly ash content of 425 kg/m³, alkaline solution content of 210 kg/m³, and SS/SH ratio of 1.75)

Fig. 6.1: Corrosion potential of steel reinforcement in geopolymer concrete (GPC) admixed with different concentrations of NaCl: a) NaOH solution of 8 M, b) NaOH solution of 10 M, c) NaOH solution of 12 M, d) NaOH solution of 14 M, and e) NaOH solution of 16 M

From Fig. 6.1, it is observed that the corrosion potential values of rebar were more negative than -270 mV (SCE) in NaCl (1.5%, 3% and 4.5%) admixed GPC specimens for all molarity of NaOH solution and all ages. Thus, there is greater probability of occurrence of steel reinforcement corrosion in chloride admixed fly ash based GPC mixes. This may be attributed to the presence of chloride ions near rebar level that might have altered the passivity of steel bar. While analyzing the effect of molarity of NaOH solution on corrosion potential of steel reinforcement in geopolymer concrete (Fig. 6.1), it is observed that mostly there is unsystematic variation in corrosion potential of steel reinforcement with increase in molarity of NaOH solution in both control, and chloride admixed GPC mixes irrespective of age. This may be ascribed to the significant effect of variations in the availability of oxygen and moisture content in the vicinity of steel reinforcement with change in molarity of NaOH solution in the GPC mixes. From Fig. 6.1, it is inferred that the corrosion potential of steel reinforcement mostly became more negative with increase in concentration of admixed NaCl for all molarity of NaOH solution at all ages. This indicates comparatively greater probability of occurrence of corrosion in the presence of more amount of chloride ions near rebar level in the GPC mixes. From Fig. 6.1, it is observed that there was mostly insignificant variation in corrosion potential with increase in age, however, the potential values became slightly less negative during later age. These variations in corrosion potential with increase in age may be due to the dominant effect of alterations in the amount of oxygen near steel reinforcement with age over the influence of chloride ions.

The corrosion current density values of steel reinforcement in fly ash based GPC made with different molarity of NaOH solution (8 M, 10 M, 12 M, 14 M and 16 M) are shown in Fig. 6.2 for different concentrations of admixed NaCl (0%, 1.5%, 3%, and 4.5%), and different ages (60 days, 180 days, 360 days and 600 days). Each value of corrosion current density shown in these figures is the average value of three replicate prismatic specimens. From Fig. 6.2, it is inferred that mostly there was higher corrosion current density at higher molarity of NaOH solution than that at lower molarity of NaOH solution in control GPC mixes for different ages. However, in GPC mixes admixed with 1.5% NaCl, there was mostly unsystematic variation in corrosion current density with molarity of NaOH solution. In case of GPC mixes admixed with 3% NaCl, the corrosion current density was mostly higher at higher molarity of NaOH solution as compared to that at lower molarity of NaOH solution. This may be ascribed to the effect of increase in conductivity of concrete at higher molarity of NaOH solution in the presence of chloride ions in the GPC mixes.

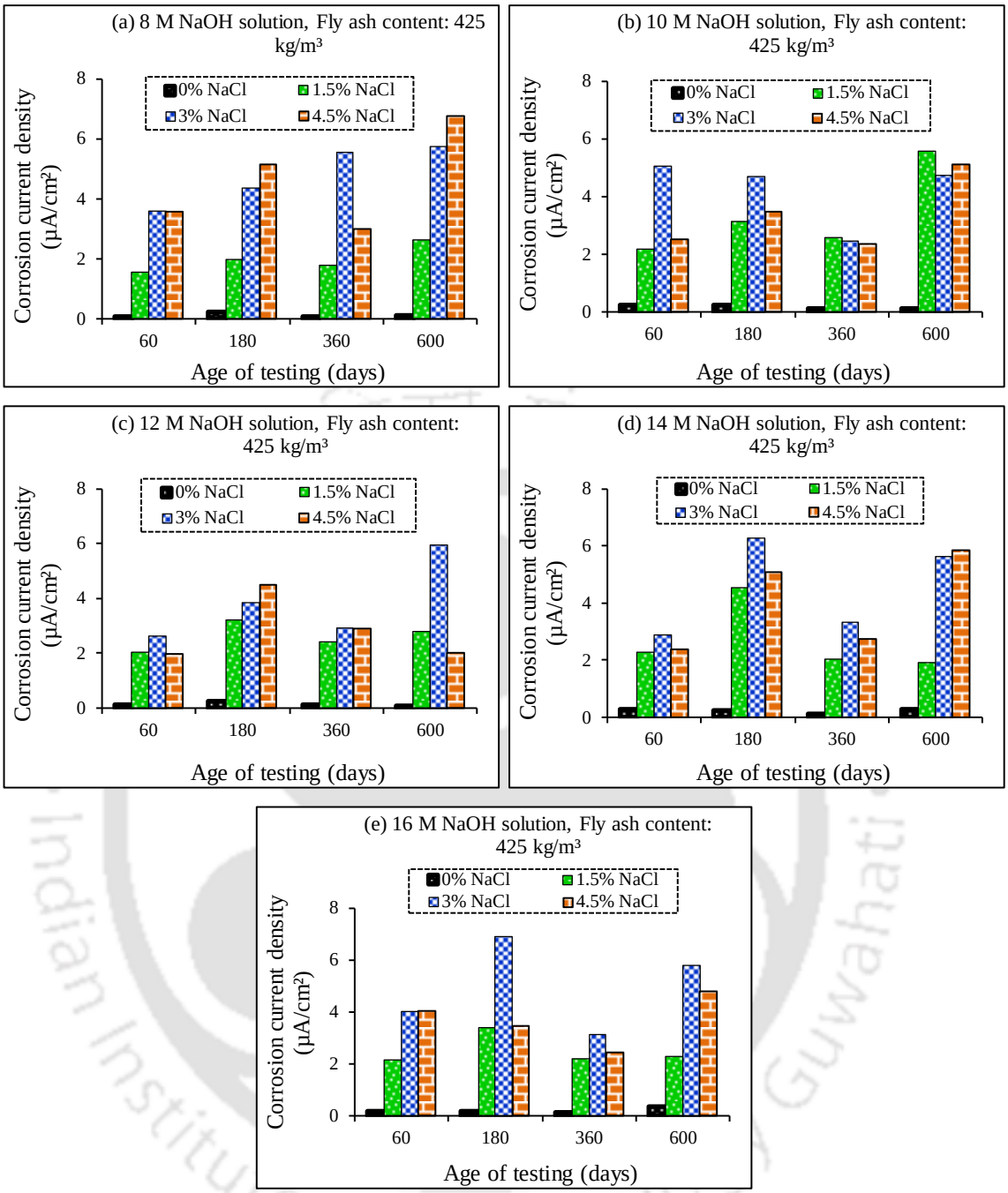

(GPC made with fly ash passing through 300 µm sieve, fly ash content of 425 kg/m³, alkaline solution content of 210 kg/m³, and SS/SH ratio of 1.75)

Fig. 6.2: Corrosion current density of steel reinforcement in geopolymer concrete (GPC) admixed with different concentrations of NaCl: a) NaOH solution of 8 M, b) NaOH solution of 10 M, c) NaOH solution of 12 M, d) NaOH solution of 14 M, and e) NaOH solution of 16 M

However, at 4.5% NaCl concentration, the GPC mixes made with lower molarity of NaOH solution mostly exhibited higher corrosion current density as compared to that made with higher molarity of NaOH solution. The effect of alterations in the electrolytic pore solution of GPC at lower molarity of NaOH solution in the presence of higher amount of chloride ions led

to comparatively higher corrosion current density at lower molarity of NaOH solution. From Fig. 6.2, it is noted that the corrosion current density of steel reinforcement was significantly lower in control GPC mixes (without admixed NaCl) as compared to NaCl admixed GPC mixes for all molarity of NaOH solution and ages. Further, the corrosion current density of steel reinforcement in GPC mixes increased with increase in concentration of admixed NaCl till 3%, which is attributed to the effect of increase in conductivity of GPC in the presence of higher amount of chloride ions. However, the corrosion current density mostly decreased at NaCl concentration of 4.5% as compared to that at 3% for all molarity of NaOH solution. The mostly lower corrosion current density at higher NaCl concentration i.e., 4.5% may be ascribed to the dominant effect of insufficient amount of oxygen and alterations in the availability of moisture content near steel reinforcement over the effect of presence of higher amount of chloride ions in the GPC mixes. From Fig. 6.2, it is inferred that mostly there is unsystematic variation in corrosion current density of steel reinforcement with increase in age for all molarity of NaOH solution and admixed NaCl concentrations. This may be due to the variations in the conductivity of GPC with age due to alterations in the electrolytic pore solution of concrete surrounding the rebar in GPC.

6.2.2 Influence of alkaline solution content on corrosion potential and corrosion current density

The obtained corrosion potential values of steel reinforcement in fly ash based GPC made with different alkaline solution contents i.e., 190 kg/m^3 and 210 kg/m^3 are shown in Fig. 6.3, and Fig. 6.4 for NaOH solution molarity of 10 M and 14 M respectively. Similarly, the obtained corrosion current density of steel reinforcement in GPC mixes made with different alkaline solution contents are shown in Fig. 6.5, and Fig. 6.6 for NaOH solution molarity of 10 M and 14 M respectively. From Fig. 6.3 to Fig. 6.6, it is noted that the corrosion potential values were more negative than -270 mV (SCE), and corrosion current density values were significantly higher in chloride admixed (3% NaCl) GPC mixes as compared to control (without admixed NaCl) GPC mixes for both alkaline solution contents (190 kg/m^3 and 210 kg/m^3) and molarity of NaOH solution (10 M and 14 M). This indicates greater extent of rebar corrosion in NaCl admixed GPC mixes.

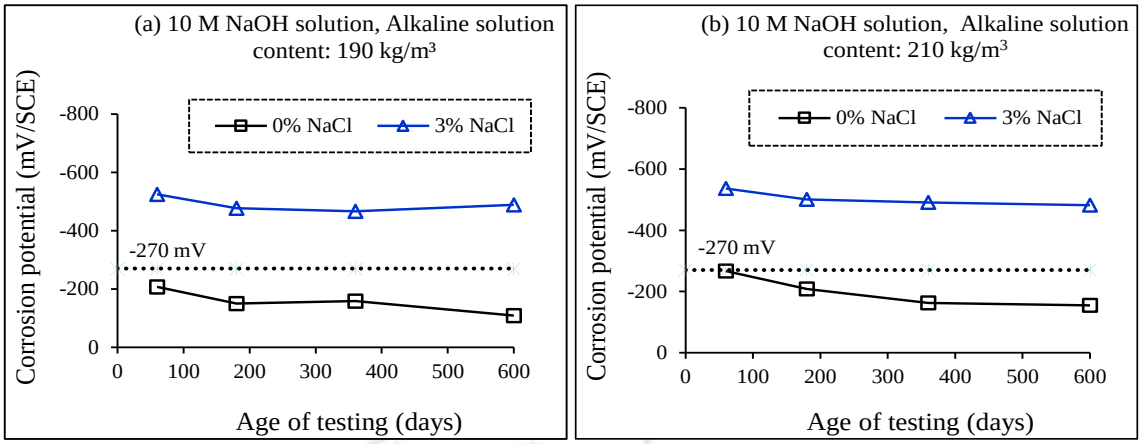

(GPC made with fly ash passing through 150 μm sieve, fly ash content of 425 kg/m³, and SS/SH ratio of 1.75)

Fig. 6.3: Corrosion potential of steel reinforcement in geopolymer concrete (GPC) made with 10 M NaOH solution: a) alkaline solution content of 190 kg/m^3, and b) alkaline solution content of 210 kg/m^3

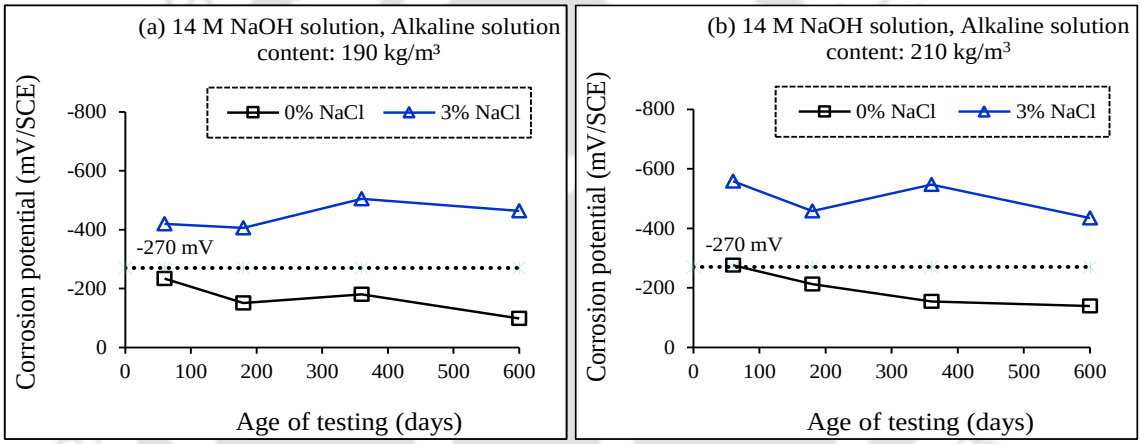

(GPC made with fly ash passing through 150 μm sieve, fly ash content of 425 kg/m³, and SS/SH ratio of 1.75)

Fig. 6.4: Corrosion potential of steel reinforcement in geopolymer concrete (GPC) made with 14 M NaOH solution: a) alkaline solution content of 190 kg/m^3, and b) alkaline solution content of 210 kg/m^3

While analysing the effect of alkaline solution content, it is inferred that the corrosion potential of steel reinforcement mostly became more negative and corrosion current density of steel reinforcement mostly increased with increase in alkaline solution content in control as well chloride admixed GPC mixes for different ages (Fig. 6.3 to Fig. 6.6). The lower extent of corrosion in GPC mixes made with lower alkaline solution content in the presence of chloride ions may be attributed to the changes in the electrolytic pore solution surrounding the steel reinforcement as a result of variations in the formation of aluminosilicate gel (N-A-S-H) in the GPC mixes.

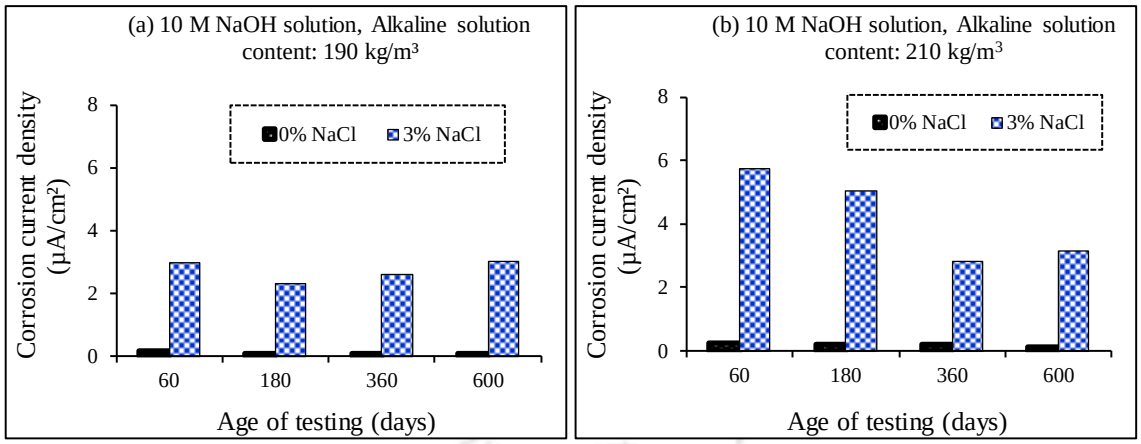

(GPC made with fly ash passing through 150 µm sieve, fly ash content of 425 kg/m³, and SS/SH ratio of 1.75)

Fig. 6.5: Corrosion current density of steel reinforcement in geopolymer concrete (GPC) made with 10 M NaOH solution: a) alkaline solution content of 190 kg/m^3, and b) alkaline solution content of 210 kg/m^3

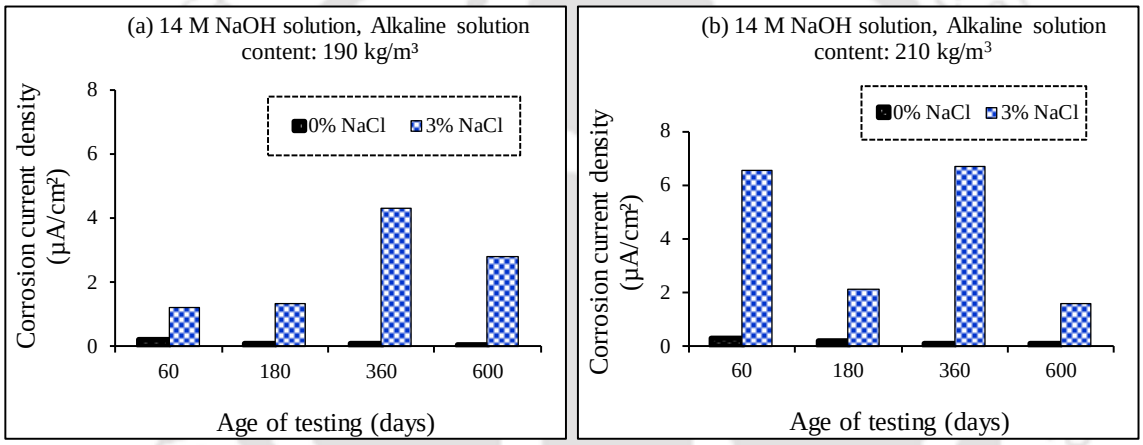

(GPC made with fly ash passing through 150 µm sieve, fly ash content of 425 kg/m³, and SS/SH ratio of 1.75)

Fig. 6.6: Corrosion current density of steel reinforcement in geopolymer concrete (GPC) made with 14 M NaOH solution: a) alkaline solution content of 190 kg/m^3, and b) alkaline solution content of 210 kg/m^3

From Fig. 6.3 to Fig. 6.6, it is inferred that, in case of control GPC mixes, the corrosion potential was mostly more negative at higher molarity of NaOH solution (14 M) than that at lower molarity of NaOH solution (10 M) whereas the corrosion current density was mostly higher at lower molarity of NaOH solution as compared to that at higher molarity of NaOH solution. These variations in the corrosion parameters of steel reinforcement with change in molarity of NaOH solution in the GPC mixes in the absence of chloride ions may be ascribed to the variations in the electrolytic pore solution of GPC surrounding the steel reinforcement. In the presence of chloride ions (3% NaCl), the corrosion potential became mostly more negative and the corrosion current density mostly increased at lower molarity of NaOH solution (10 M) as compared to that at higher molarity of NaOH solution (14 M) at different ages as evident from Fig. 6.3 to Fig. 6.6. This is ascribed to the presence of more amount of

chloride ions near rebar at lower molarity of NaOH solution that affected the passivity of steel reinforcement. The presence of more amount of chloride ions near steel reinforcement at lower molarity of NaOH solution may be ascribed to the formation of comparatively less denser microstructure as a result of formation of lower amount of aluminosilicate gel (N-A-S-H) in the GPC mixes. Further, from Fig. 6.3 and Fig. 6.4, it is noted that there was no significant variation in corrosion potential with increase in age although the corrosion potential became slightly less negative during late age. However, mostly there was no systematic variation in corrosion current density of steel reinforcement with increase in age for both alkaline solution contents and molarity of NaOH solution in the GPC mixes in the presence of chloride ions as evident from Fig. 6.5 and Fig.6.6. This may be attributed to the effect of change in the passivity of steel reinforcement with age as a result of combined effect of chloride ions, and variations in the availability of oxygen and moisture in the vicinity of rebar in GPC mixes.

6.2.3 Influence of SS/SH ratio on corrosion potential and corrosion current density

The corrosion potential of steel reinforcement in fly ash based GPC made with different SS/SH ratios (ratio of sodium silicate solution to sodium hydroxide solution) i.e., 1.5 and 1.75 are illustrated in Fig. 6.7, and Fig. 6.8 for NaOH solution molarity of 10 M and 14 M respectively. Similarly, the corrosion current density of rebar in GPC mixes made with different SS/SH ratios are displayed in Fig. 6.9, and Fig. 6.10. From Fig. 6.7 to Fig. 6.10, it is inferred that the GPC mixes admixed with 3% NaCl showed potential values more negative than -270 mV (SCE), and resulted in significantly higher corrosion current density as compared to control GPC mixes (without admixed NaCl), indicating higher corrosion activity in GPC mixes in the presence of chloride ions. From Fig. 6.7 to Fig. 6.10, it can be observed that, in case of control GPC mixes, the corrosion potential was mostly more negative and corrosion current density was higher at higher SS/SH ratio than that at lower SS/SH ratio. In case of chloride admixed GPC mixes (3% NaCl), there was unsystematic variation in corrosion potential of steel reinforcement with SS/SH ratio over different ages (Fig. 6.7 and 6.8). This is ascribed to the effect of alterations in the extent of oxygen diffusion near rebar level.

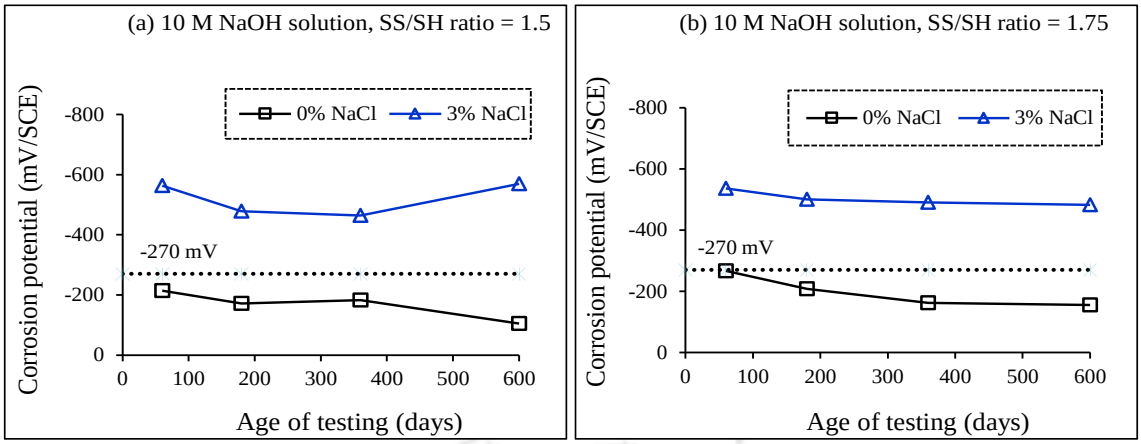

(GPC made with fly ash passing through 150 μm sieve, fly ash content of 425 kg/m^3, and alkaline solution content of 210 kg/m^3)

Fig. 6.7: Corrosion potential of rebar in geopolymer concrete (GPC) made with 10 M NaOH solution: a) SS/SH ratio of 1.5, and b) SS/SH ratio of 1.75

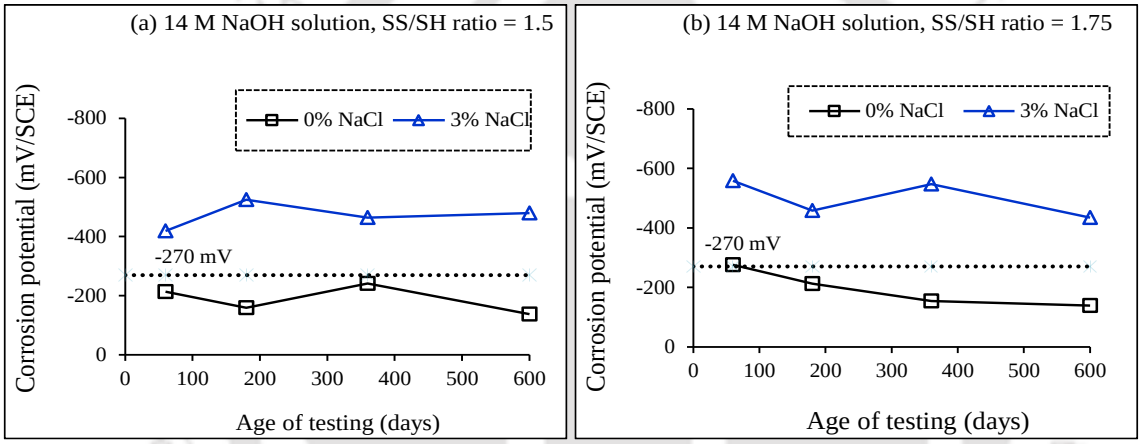

(GPC made with fly ash passing through 150 μm sieve, fly ash content of 425 kg/m^3, and alkaline solution content of 210 kg/m^3)

Fig. 6.8: Corrosion potential of rebar in geopolymer concrete (GPC) made with 14 M NaOH solution: a) SS/SH ratio of 1.5, and b) SS/SH ratio of 1.75

From Fig. 6.9 and 6.10, the corrosion current density was higher in the GPC mixes made with higher SS/SH ratio (1.75) as compared to that made with lower SS/SH ratio (1.5) in the presence of chloride ions for both molarity of NaOH solution and at all ages. The higher corrosion current density of steel reinforcement at higher SS/SH ratio may be ascribed to the effect of decrease in the alkalinity as a result of lower concentration of $(OH)^-$ ions due to lower amount of NaOH solution in the alkaline solution at higher SS/SH ratio.

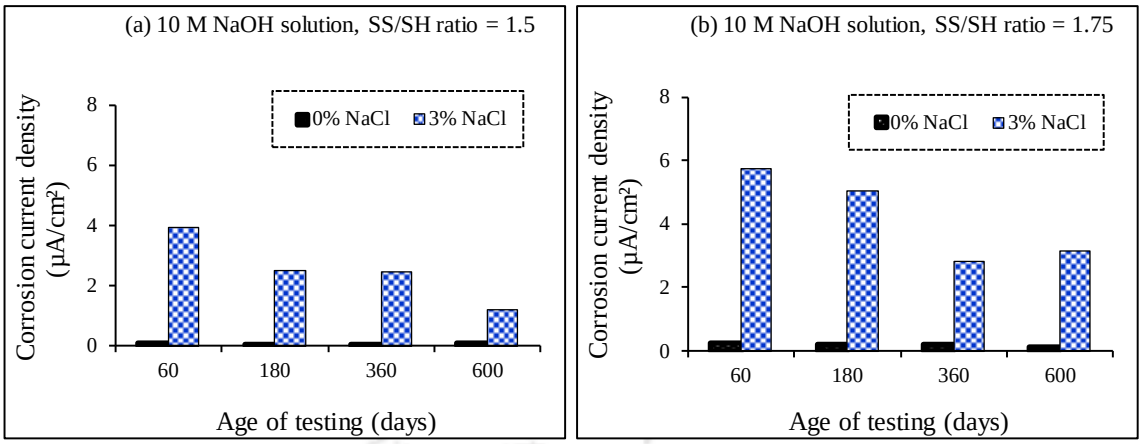

(GPC made with fly ash passing through 150 µm sieve, fly ash content of 425 kg/m^3, and alkaline solution content of 210 kg/m^3)

Fig. 6.9: Corrosion current density of rebar in geopolymer concrete (GPC) made with 10 M NaOH solution: a) SS/SH ratio of 1.5, and b) SS/SH ratio of 1.75

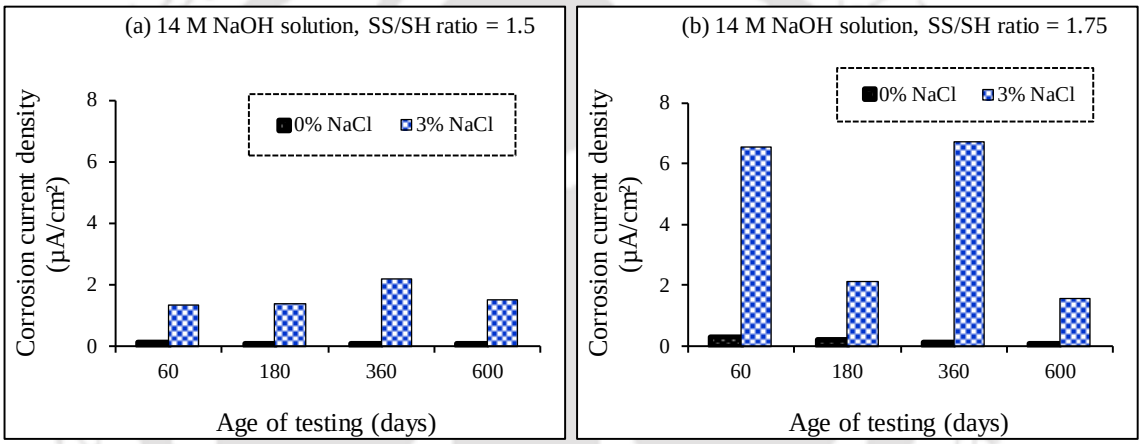

(GPC made with fly ash passing through 150 µm sieve, fly ash content of 425 kg/m^3, and alkaline solution content of 210 kg/m^3)

Fig. 6.10: Corrosion current density of rebar in geopolymer concrete (GPC) made with 14 M NaOH solution: a) SS/SH ratio of 1.5, and b) SS/SH ratio of 1.75

From Fig. 6.7 to Fig. 6.10, it is observed that, with change in molarity of NaOH solution, there was unsystematic variation in corrosion potential of steel reinforcement, and the corrosion current density was mostly higher at higher molarity of NaOH solution than lower molarity of NaOH solution in control GPC mixes. In 3% NaCl admixed GPC mixes, there was unsystematic variation in corrosion potential of steel reinforcement with molarity of NaOH solution, however, the corrosion current density was mostly lower at higher molarity of NaOH solution (14 M) than that at lower molarity of NaOH solution (10 M) for both SS/SH ratios. The lower corrosion current density at higher molarity of NaOH solution may be ascribed to the effect of higher resistivity due to formation of denser microstructure as a result of formation of more amount of N-A-S-H gel at higher molarity of NaOH solution in the GPC mixes. From

Fig. 6.7 and 6.8, it is inferred that there is less variation in corrosion potential with increase in age, however, the corrosion potential mostly became less negative during later age both in control and chloride admixed GPC mixes. Further, there was insignificant difference in corrosion density with increase in age for control GPC mixes although the corrosion current density mostly decreased with increase in age. In 3% NaCl admixed GPC mixes, the corrosion current density mostly decreased with increase in age for NaOH solution of 10 M (Fig. 6.9), which may be attributed to the effect of improved passivity of steel reinforcement during later ages. However, for NaOH solution of 14 M, mostly there was unsystematic variation in corrosion current density of steel reinforcement with increase in age although the corrosion current density was mostly lower at the age of 600 days as compared to earlier ages (Fig. 6.10) thereby indicating improved passivity of rebar at later age.

6.2.4 Influence of particle size of fly ash on corrosion potential and corrosion current density

6.2.4.1 GPC made with fly ash content of 425 kg/m^3

For fly ash content of 425 kg/m^3, the corrosion potential of steel reinforcement in fly ash based GPC mixes made with fly ash passing through 150 μm sieve, and 300 μm sieve are shown in 6.11 and Fig. 6.12 for NaOH solution molarity of 10 M and 14 M respectively. Similarly, the corrosion current density of rebar in GPC mixes made with fly ash particles of different sizes are illustrated in Fig. 6.13, and Fig. 6.14. From Fig. 6.11 and Fig. 6.12, it is observed that the corrosion potential values of steel bar embedded in control GPC specimens (without admixed NaCl) were less negative than -270 mV (SCE) for both sizes of fly ash particles at all ages. This indicated lower probability of occurrence of steel reinforcement corrosion in control GPC mixes as per ASTM C876 [100]. However, the corrosion potential values of steel reinforcement were more negative than -270 mV (SCE) in chloride admixed (3% NaCl) GPC mixes as evident from Fig. 6.11 and Fig. 6.12, thereby indicating greater probability of occurrence of corrosion activity in the presence of chloride ions. Further, the corrosion current density values were significantly higher in 3% NaCl admixed GPC mixes as compared to control GPC mixes as evident from Fig. 6.13 and Fig. 6.14. In case of control GPC mixes, the corrosion potential was mostly more negative in case of smaller size fly ash particles (passing through 150 μm sieve) than larger size fly ash particles (passing through 300 μm sieve), however, the corrosion current density was mostly higher in GPC mixes made with larger fly ash particles as compared to that made with smaller fly ash particles (Fig. 6.13 and Fig. 6.14). These variations in corrosion parameters in the absence of chloride ions with change in particle

size of fly ash is ascribed to combined effect of changes in the electrolytic pore solution as well as changes in the availability of oxygen in the vicinity of rebar in GPC.

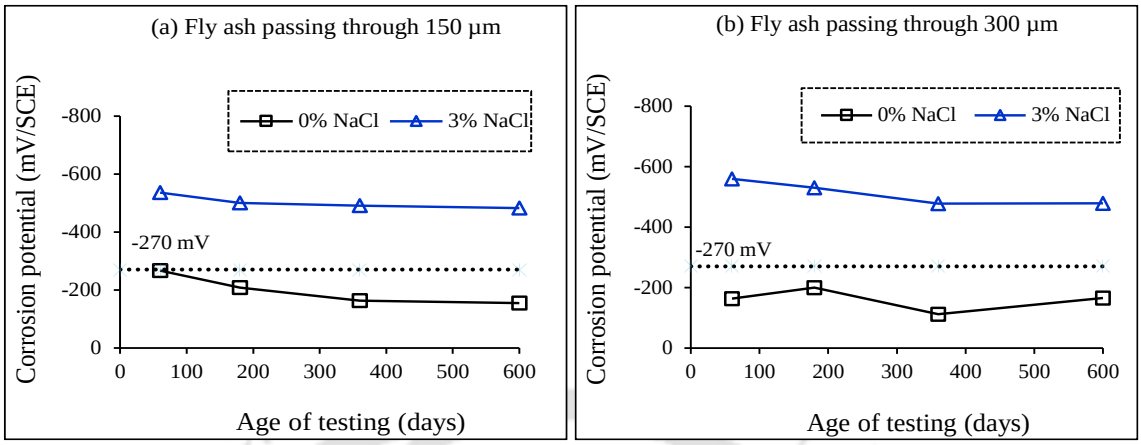

(GPC made with fly ash content of 425 kg/m^3, alkaline solution content of 210 kg/m^3, and SS/SH ratio of 1.75)

Fig. 6.11: Corrosion potential of rebar in GPC made with 10 M NaOH solution: a) fly ash passing through 150 µm, and b) fly ash passing through 300 µm

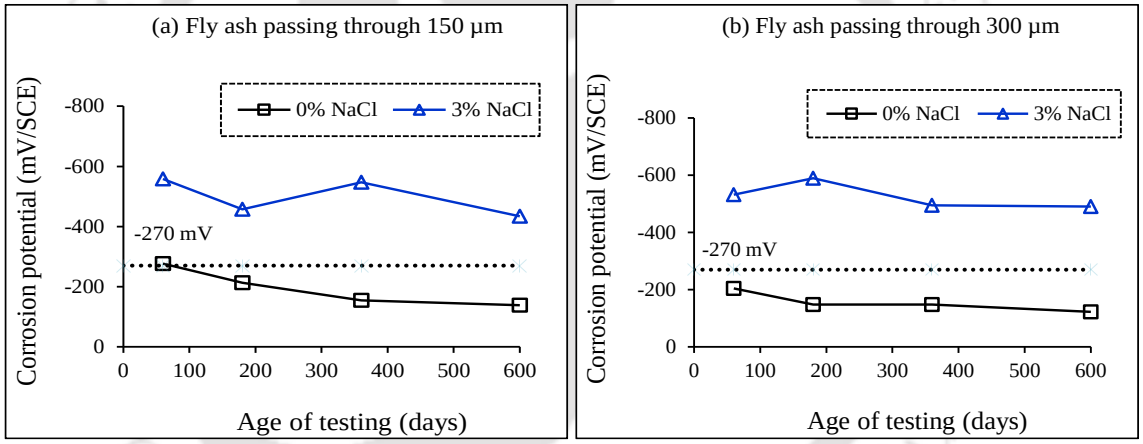

(GPC made with fly ash content of 425 kg/m^3, alkaline solution content of 210 kg/m^3, and SS/SH ratio of 1.75)

Fig. 6.12: Corrosion potential of rebar in GPC made with 14 M NaOH solution: a) fly ash passing through 150 µm, and b) fly ash passing through 300 µm

From Fig. 6.11 and Fig. 6.12, it is inferred that there was no systematic variation in corrosion potential of steel reinforcement with particle size of fly ash in chloride admixed GPC mixes over different ages. However, the corrosion current density was mostly lower in GPC mixes made with larger fly ash particles (passing through 300 µm sieve) than that made with smaller fly ash particles (passing through 150 µm sieve) at different ages (Fig. 6.13 and Fig. 6.14). The lower corrosion current density in GPC made with larger fly ash particles may be due to the effect of higher resistivity as a result of denser microstructure in the GPC mixes made with larger fly ash particles at fly ash content of 425 kg/m^3.

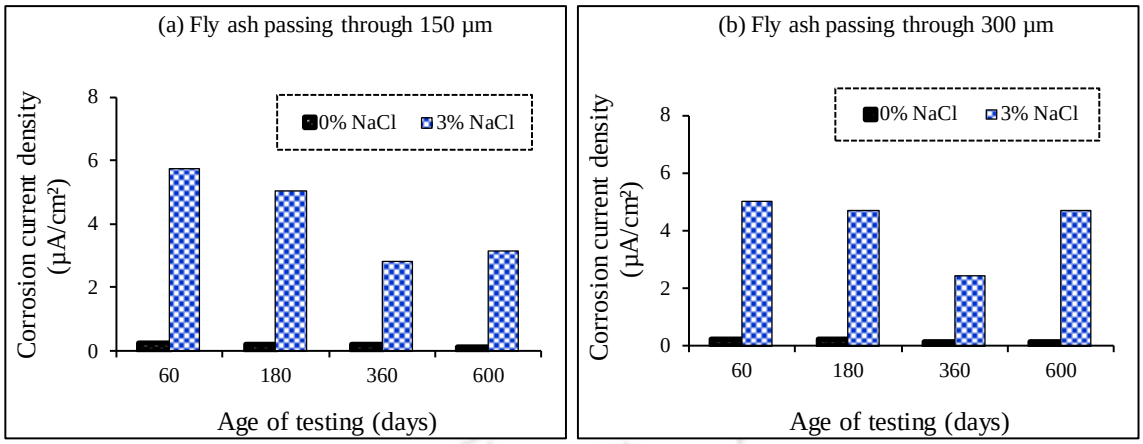

(GPC made with fly ash content of 425 kg/m³, alkaline solution content of 210 kg/m³, and SS/SH ratio of 1.75)

Fig. 6.13: Corrosion current density of rebar in GPC made with 10 M NaOH solution: a) fly ash passing through 150 µm, and b) fly ash passing through 300 µm

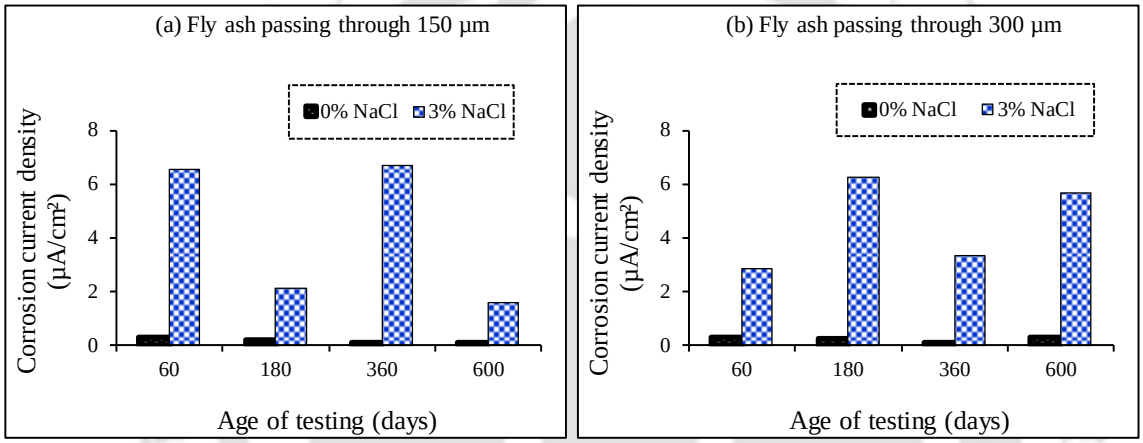

(GPC made with fly ash content of 425 kg/m³, alkaline solution content of 210 kg/m³, and SS/SH ratio of 1.75)

Fig. 6.14: Corrosion current density of rebar in GPC made with 14 M NaOH solution: a) fly ash passing through 150 µm, and b) fly ash passing through 300 µm

In case of control GPC mixes, there was unsystematic variation in corrosion potential as well as in corrosion current density with change in molarity of NaOH solution from 10 M to 14 M (Fig. 6.11 to Fig. 6.14). In case of chloride admixed GPC mixes, the corrosion potential was mostly more negative as well as the corrosion current density was mostly higher in case of NaOH solution of 14 M as compared to NaOH solution of 10 M. The mostly higher corrosion activity in the GPC mixes made with higher molarity of NaOH solution may be ascribed to the dominant effect of alterations in the concentrations of chloride and hydroxyl ions in the electrolytic pore solution near the steel reinforcement over the effect of formation of denser microstructure at higher molarity of NaOH solution. While analyzing the variation in corrosion potential with age, it is observed that there is less variation in corrosion potential of steel reinforcement with increase in age, however, the corrosion potential mostly became less negative during later age as compared to early age both in control and chloride admixed GPC

mixes. Further, in case of control GPC mixes, the corrosion current density mostly decreased with increase in age. In chloride admixed (3% NaCl) GPC mixes, mostly there was unsystematic variation in corrosion current density with increase in age as evident from Fig. 6.13 and Fig. 6.14. This may be ascribed to the effect of changes in conductivity of concrete as a result of variations in the availability of chloride ions near rebar level in GPC mixes with increase in age.

6.2.4.2 GPC made with fly ash content of 450 kg/m^3

The corrosion potential of rebar at different concentrations of admixed NaCl in fly ash based GPC mixes made with fly ash passing through 150 µm sieve, and 300 µm sieve are shown in Fig. 6.15 and Fig. 6.16 for NaOH solution molarity of 10 M and 14 M respectively for fly ash content of 450 kg/m^3. Similarly, the corrosion current density of rebar in GPC mixes made with fly ash particles of different sizes at different concentrations of admixed NaCl are shown in Fig. 6.17, and Fig. 6.18.

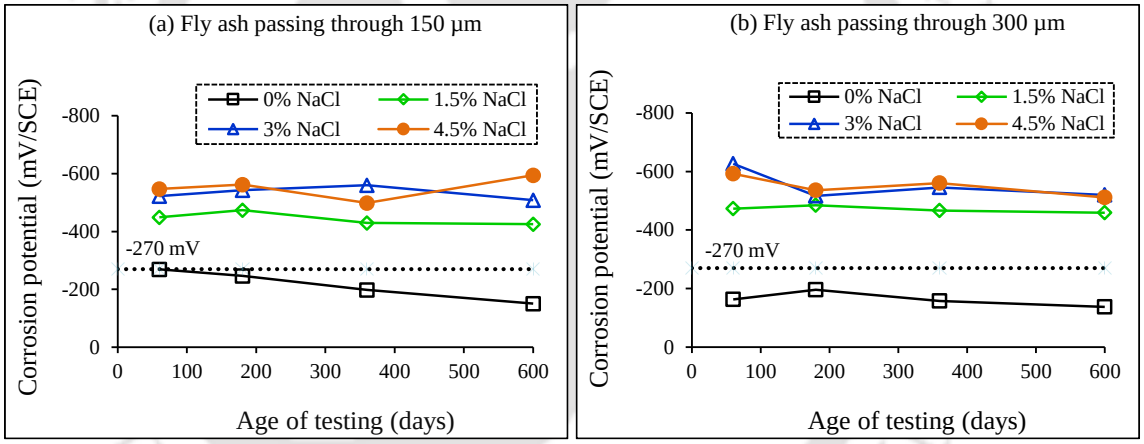

(GPC made with fly ash content of 450 kg/m^3, alkaline solution content of 210 kg/m^3, and SS/SH ratio of 1.75)

Fig. 6.15: Corrosion potential of rebar in GPC made with 10 M NaOH solution and admixed with different concentrations of NaCl: a) fly ash passing through 150 µm, and b) fly ash passing through 300 µm

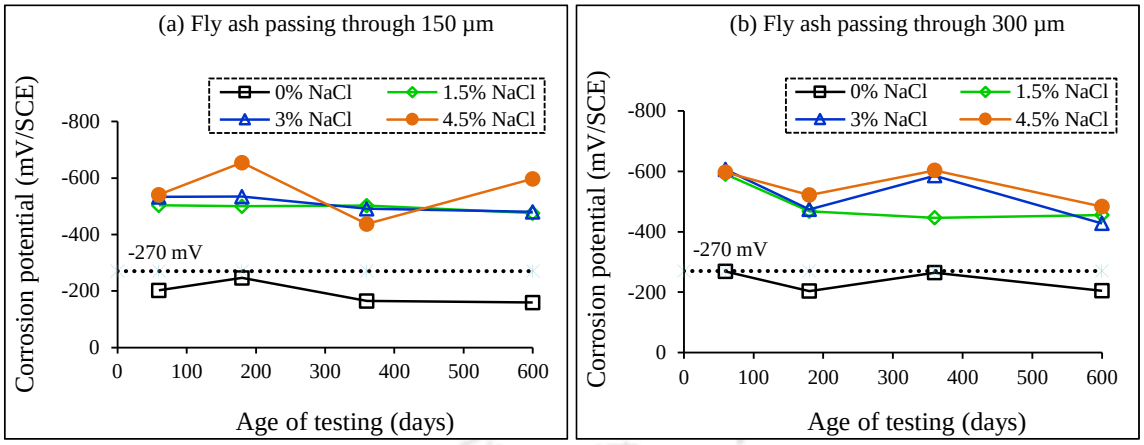

(GPC made with fly ash content of 450 kg/m^3, alkaline solution content of 210 kg/m^3, and SS/SH ratio of 1.75)

Fig. 6.16: Corrosion potential of rebar in GPC made with 14 M NaOH solution and admixed with different concentrations of NaCl: a) fly ash passing through 150 µm, and b) fly ash passing through 300 µm

From Fig. 6.15 and Fig. 6.16, it is observed that the corrosion potential values were less negative than -270 mV (SCE) in control GPC specimens (without admixed NaCl) whereas in chloride admixed GPC mixes, the corrosion potential values were more negative than -270 mV (SCE) at all ages. Further, the chloride admixed GPC mixes exhibited significantly higher corrosion current density as compared to control GPC mixes (Fig. 6.17 and Fig. 6.18), thereby indicating higher extent of corrosion of rebar in the presence of chloride ions. From Fig. 6.15 and Fig. 6.16, the corrosion potential mostly became more negative with increase in admixed NaCl concentration as evident from Fig. 6.15 and Fig. 6.16.

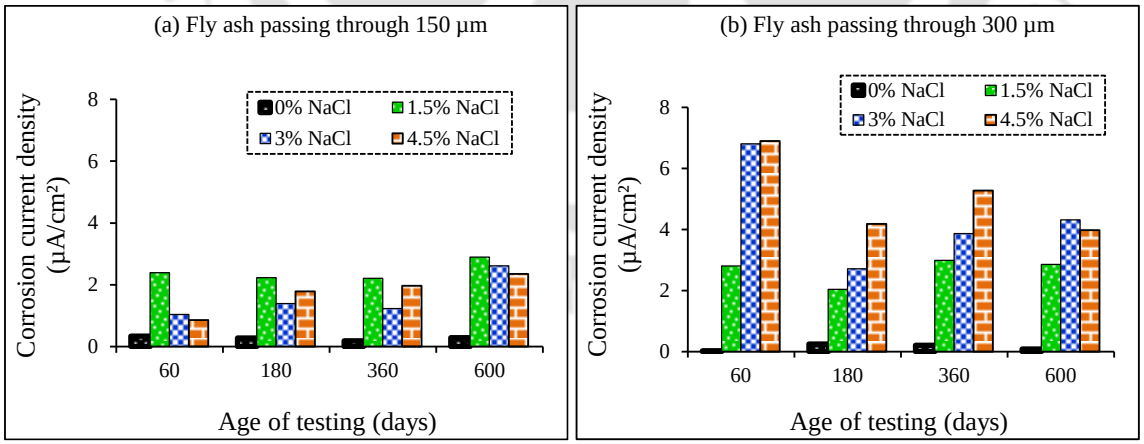

(GPC made with fly ash content of 450 kg/m^3, alkaline solution content of 210 kg/m^3, and SS/SH ratio of 1.75)

Fig. 6.17: Corrosion current density of rebar in GPC made with 10 M NaOH solution and admixed with different concentrations of NaCl: a) fly ash passing through 150 µm, and b) fly ash passing through 300 µm

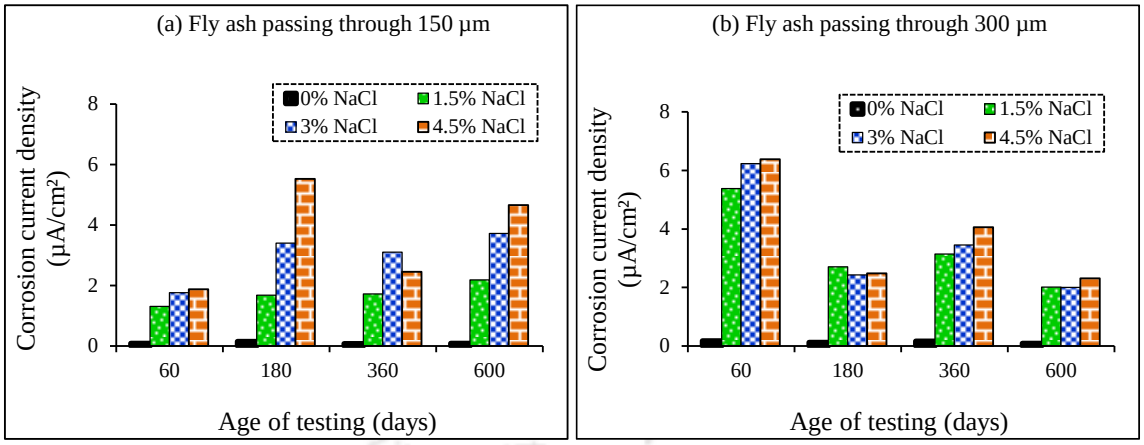

(GPC made with fly ash content of 450 kg/m^3, alkaline solution content of 210 kg/m^3, and SS/SH ratio of 1.75)

Fig. 6.18: Corrosion current density of rebar in GPC made with 14 M NaOH solution and admixed with different concentrations of NaCl: a) fly ash passing through 150 µm, and b) fly ash passing through 300 µm

From Fig. 6.17 and Fig. 6.18, the corrosion current density of steel reinforcement mostly increased with increase in admixed NaCl concentration from 1.5% to 4.5% except in case of GPC mixes made with NaOH solution of 10 M and fly ash passing through 150 µm sieve where the GPC mixes admixed with NaCl concentration of 1.5% showed higher corrosion current density as compared to higher NaCl concentrations (3% and 4.5%). The higher corrosion current density at higher concentration of admixed NaCl is ascribed to the dominant effect of increased conductivity in the presence of higher amount of chloride ions in the GPC mixes. However, in case of GPC mixes made with smaller fly ash particles and NaOH solution of 10 M, the lower corrosion current density at higher concentration of NaCl i.e., 3% and 4.5% as compared to that at lower concentration of NaCl i.e., 1.5% may be ascribed to the combined effect of alterations in the concentrations of chloride and hydroxyl ions in the electrolytic pore solution, and the variations in oxygen and moisture content near rebar level in the GPC mixes. While analyzing the effect of particle size of fly ash, it is inferred that, in control GPC mixes, the corrosion potential was mostly more negative in case of smaller fly particles as compared to larger fly ash particles, however, there was unsystematic variation in corrosion current density of rebar with particle size of fly ash. In case of chloride admixed GPC mixes, for different ages, overall mostly there was unsystematic variation in corrosion potential of steel reinforcement with particle size of fly ash (Fig. 6.15 and Fig. 6.16). However, the corrosion current density of steel reinforcement was mostly lower in GPC mixes made with smaller fly ash particles as compared to that made with larger fly ash particles in the presence of chloride ions (Fig. 6.17 and Fig. 6.18). The lower corrosion current density of steel reinforcement in GPC mixes made with smaller fly ash particles may be ascribed to the effect of improved

passivation of steel reinforcement as a result of increased resistivity of GPC mixes made with smaller fly ash particles due to higher extent of geopolymerization reaction leading to formation of denser microstructure.

While analyzing the effect of molarity of NaOH solution, it is noted that, in case of control GPC mixes, the corrosion potential was mostly more negative at higher molarity of NaOH solution (14 M) whereas the corrosion current density was mostly higher at lower molarity of NaOH solution (10 M) for both sizes of fly ash particles (Fig. 6.15 to Fig. 6.18). The changes in the extent of diffusion of oxygen near steel reinforcement as well as alterations in the resistivity of GPC mixes contributed toward these variations in corrosion parameters with molarity of NaOH solution in control GPC mixes. From Fig. 6.15 to Fig. 6.18, in chloride admixed GPC mixes, overall the variations in corrosion potential as well as corrosion current density of steel reinforcement for different ages were unsystematic with molarity of NaOH solution for both sizes of fly ash particles. This may be ascribed to the alterations in the conductivity of GPC mixes with change in molarity of NaOH solution as a result of changes in the concentrations of chloride ions in the electrolytic pore solution in the vicinity of rebar over different ages. From Fig. 6.15 to Fig. 6.18, it is inferred that mostly there is unsystematic variation in corrosion potential and corrosion current density of steel reinforcement with age in control as well as chloride admixed GPC mixes. However, the corrosion current density mostly reduced at the later age of 600 days in GPC mixes made with NaOH solution of 14 M at all concentrations of admixed NaCl, and in GPC mix made with NaOH solution of 10 M at NaCl concentration of 4.5% for fly ash passing through 300 μm sieve. The lower corrosion current density at later age is ascribed to the effect of reduced conductivity as result of presence of lower concentration of chloride ions in the electrolytic pore solution of GPC at later age.

6.2.5 Influence of fly ash content on corrosion potential and corrosion current density

6.2.5.1 GPC made with fly ash passing through 150 μm sieve

For fly ash passing through 150 μm sieve, the corrosion potential of steel reinforcement in GPC mixes made with fly content of 425 kg/m^3, and 450 kg/m^3 are illustrated in Fig. 6.19 and Fig. 6.20 for NaOH solution molarity of 10 M and 14 M respectively. Similarly, the corrosion current density of steel reinforcement in GPC mixes made with different fly ash contents are displayed in Fig. 6.21, and Fig. 6.22.

From Fig. 6.19 and Fig. 6.20, it is noted that, for both fly ash contents, the corrosion potential values were more negative than -270 mV (SCE) in chloride admixed (3% NaCl) GPC mixes as compared to control GPC mixes (less negative -270 mV (SCE)). Similarly, the NaCl

admixed GPC mixes exhibited substantially higher corrosion current density as compared to control GPC mixes (Fig. 6.21 and Fig. 6.22), which is due to the influence of chloride ions resulting in higher extent of corrosion.

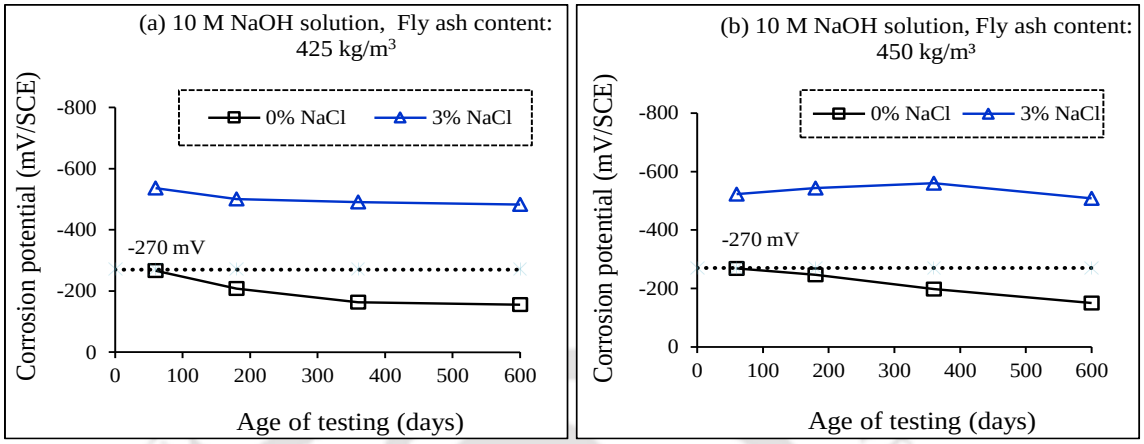

(GPC made with fly ash passing through 150 µm sieve, alkaline solution content of 210 kg/m^3, and SS/SH ratio of 1.75)

Fig. 6.19: Corrosion potential of rebar in GPC made with 10 M NaOH solution: a) fly ash content of 425 kg/m^3, and b) fly ash content of 450 kg/m^3

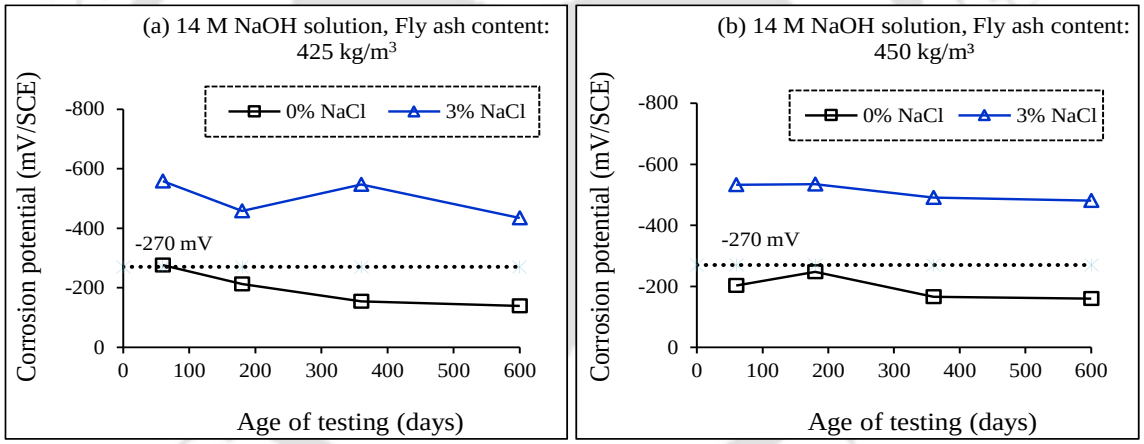

(GPC made with fly ash passing through 150 µm sieve, alkaline solution content of 210 kg/m^3, and SS/SH ratio of 1.75)

Fig. 6.20: Corrosion potential of rebar in GPC made with 14 M NaOH solution: a) fly ash content of 425 kg/m^3, and b) fly ash content of 450 kg/m^3

From Fig. 6.19 to Fig. 6.22, it is inferred that, in case of control mixes, the corrosion potential was mostly more negative in GPC mixes made with higher fly ash content (450 kg/m^3) as compared to lower fly ash content (425 kg/m^3) whereas mostly opposite variation was observed in corrosion current density with fly ash content. These variations in corrosion parameters with change in fly ash content may be ascribed to the effect of changes in the resistivity of GPC mixes due to variations in the extent of geopolymerization reaction with change in fly ash

content as well as alterations in the availability of oxygen and moisture in the vicinity of steel reinforcement in GPC mixes.

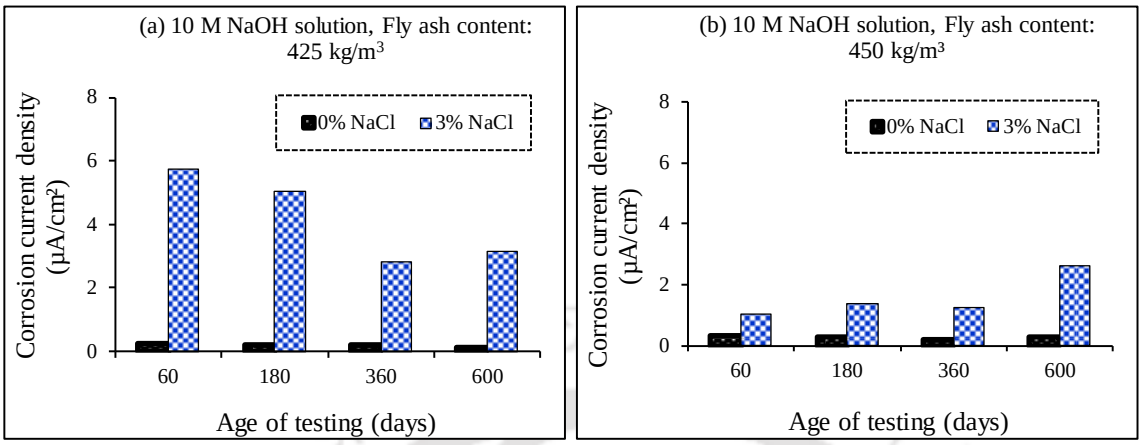

(GPC made with fly ash passing through 150 µm sieve, alkaline solution content of 210 kg/m³, and SS/SH ratio of 1.75)

Fig. 6.21: Corrosion current density of rebar in GPC made with 10 M NaOH solution: a) fly ash content of 425 kg/m^3, and b) fly ash content of 450 kg/m^3

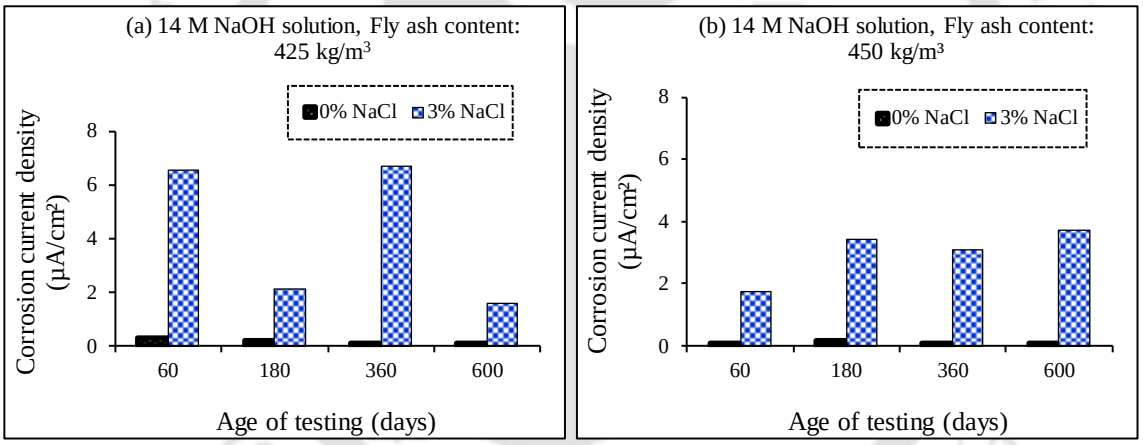

(GPC made with fly ash passing through 150 µm sieve, alkaline solution content of 210 kg/m³, and SS/SH ratio of 1.75)

Fig. 6.22: Corrosion current density of rebar in GPC made with 14 M NaOH solution: a) fly ash content of 425 kg/m^3, and b) fly ash content of 450 kg/m^3

In the presence of chloride ions, the GPC mixes made with higher fly ash content mostly exhibited more negative corrosion potential as compared to that made with lower fly ash content at different ages. However, the corrosion current density was mostly higher at lower fly ash content than that at higher fly ash content. The mostly more negative corrosion potential in GPC mixes made with higher fly ash content in the presence of chloride ions is ascribed to the dominant effect of alterations in the diffusion of oxygen and variations in the moisture content near steel reinforcement. The mostly higher corrosion current density of steel

reinforcement in GPC mixes made with lower fly ash content may be due to the effect of lower resistivity of GPC at lower fly ash content.

With change in molarity of NaOH solution from 10 M to 14 M, the variation in corrosion potential was unsystematic whereas the corrosion current density was mostly higher at lower molarity of NaOH solution than that at higher molarity of NaOH solution in control GPC mixes at different ages as observed from Fig. 6.19 to Fig. 6.22. In the presence of NaCl (3%), at different ages, the corrosion potential was mostly more negative in case of GPC mixes made with lower molarity of NaOH solution (10 M) as compared to higher molarity of NaOH solution (14 M) whereas mostly opposite variation was observed in corrosion current density with molarity of NaOH solution. The more negative corrosion potential and lower corrosion current density in case of GPC mixes made with lower molarity of NaOH solution may be attributed to substantial effect of variations in the availability of oxygen as well as moisture content near rebar over the effect of chloride ions as comparatively less denser microstructure might have formed at lower molarity of NaOH solution.

With increase in age, the corrosion potential became mostly less negative in control GPC mixes whereas, there was insignificant difference in corrosion potential with age in NaCl admixed GPC mixes as observed from Fig. 6.19 and Fig. 6.20. In case of control GPC mixes, the corrosion current density, although significantly lower, mostly decreased with increase in age (Fig. 6.21 and Fig. 6.22), which may be due to the effect of enhanced resistivity of GPC with age. In case of chloride (3% NaCl) admixed GPC mixes, there was unsystematic variation in corrosion current density of steel reinforcement with age (Fig. 6.21 and Fig. 6.22). This is ascribed to the alterations in the conductivity of GPC with age as a result of changes in the availability of chloride ions in the electrolytic pore solution.

6.2.5.2 GPC made with fly ash passing through 300 µm sieve

For fly ash passing through 300 µm sieve, the corrosion potential of reinforcing steel at different concentrations of admixed NaCl in GPC mixes made with fly content of 425 kg/m^3, and 450 kg/m^3 are depicted in Fig. 6.23 and Fig. 6.24 for NaOH solution molarity of 10 M and 14 M respectively. Similarly, the corrosion current density of reinforcing steel in GPC mixes made with different fly ash contents are illustrated in Fig. 6.25, and Fig. 6.26.

From Fig. 6.23 and Fig. 6.24, it is observed that the corrosion potential values of reinforcing steel embedded in control GPC specimens (without admixed NaCl) were less negative than -270 mV (SCE) for both fly ash contents at all ages. However, in chloride admixed GPC mixes,

the corrosion potential values were more negative than -270 mV (SCE). Similarly, the corrosion current density of reinforcing steel was significantly higher in NaCl admixed GPC mixes as compared to control GPC mixes as evident from Fig. 6.25, and Fig. 6.26.

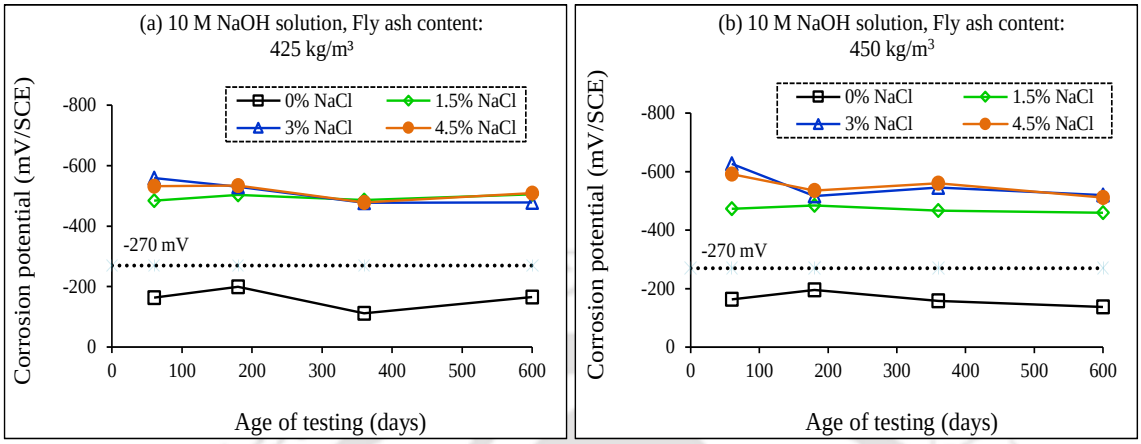

(GPC made with fly ash passing through 300 µm sieve, alkaline solution content of 210 kg/m³, and SS/SH ratio of 1.75)

Fig. 6.23: Corrosion potential of rebar in GPC made with 10 M NaOH solution and admixed with different concentrations of NaCl: a) fly ash content of 425 kg/m^3, and b) fly ash content of 450 kg/m^3

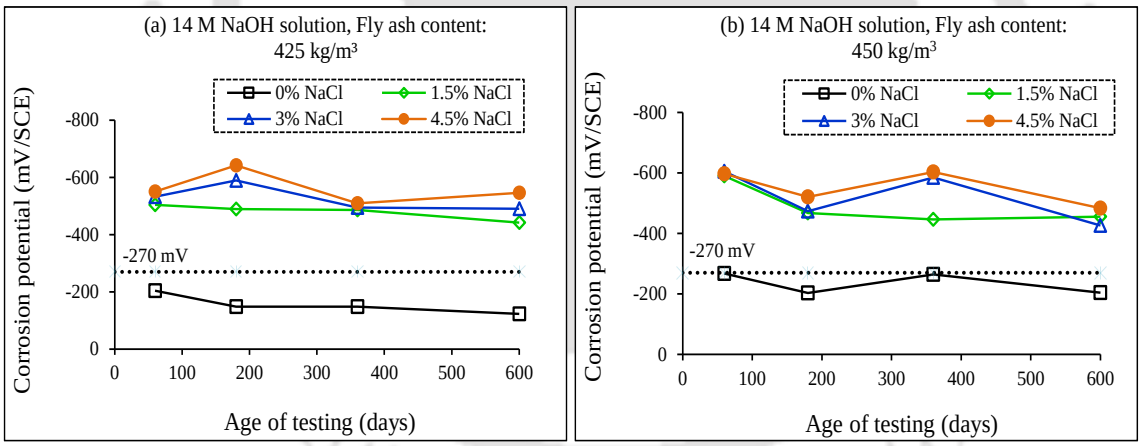

(GPC made with fly ash passing through 300 µm sieve, alkaline solution content of 210 kg/m³, and SS/SH ratio of 1.75)

Fig. 6.24: Corrosion potential of rebar in GPC made with 14 M NaOH solution and admixed with different concentrations of NaCl: a) fly ash content of 425 kg/m^3, and b) fly ash content of 450 kg/m^3

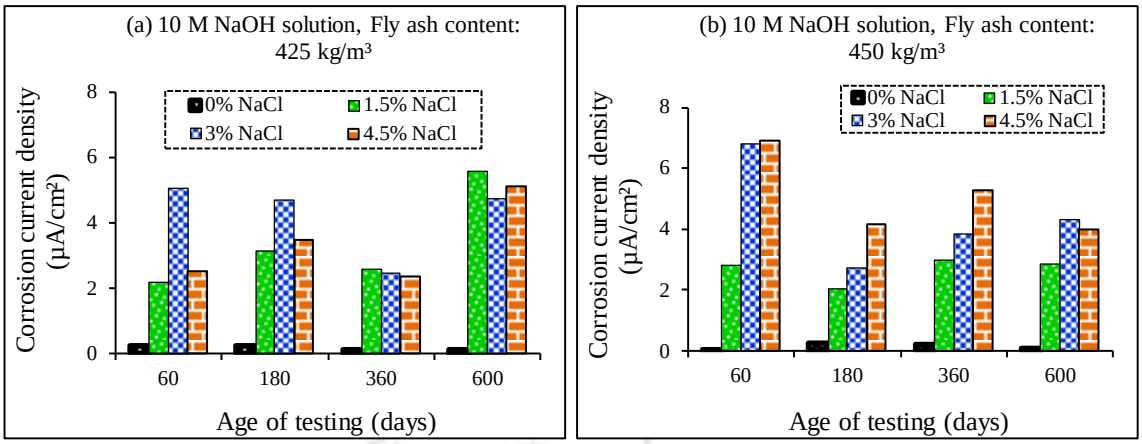

(GPC made with fly ash passing through 300 µm sieve, alkaline solution content of 210 kg/m^3, and SS/SH ratio of 1.75)

Fig. 6.25: Corrosion current density of rebar in GPC made with 10 M NaOH solution and admixed with different concentrations of NaCl: a) fly ash content of 425 kg/m^3, and b) fly ash content of 450 kg/m^3

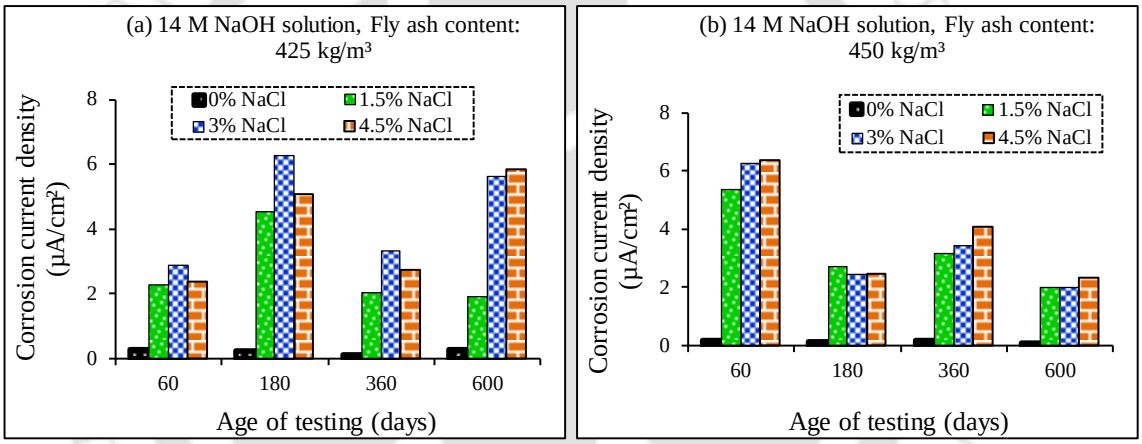

(GPC made with fly ash passing through 300 µm sieve, alkaline solution content of 210 kg/m^3, and SS/SH ratio of 1.75)

Fig. 6.26: Corrosion current density of rebar in GPC made with 14 M NaOH solution and admixed with different concentrations of NaCl: a) fly ash content of 425 kg/m^3, and b) fly ash content of 450 kg/m^3

From Fig. 6.23 and Fig. 6.24, it is observed that the corrosion potential of rebar became mostly more negative with increase in admixed NaCl concentration thereby indicating higher probability of occurrence of steel reinforcement corrosion in the presence of higher amount of chloride ions. From Fig. 6.25 and Fig. 6.26, it is inferred that the corrosion current density of steel reinforcement mostly increased with increase in admixed NaCl concentration at different ages in GPC mixes made with fly ash content of 450 kg/m^3. However, at fly ash content of 425 kg/m^3, there was mostly unsystematic variation in corrosion current density of steel reinforcement with increase in admixed NaCl concentration. At fly ash content of 450 kg/m^3, the increase in corrosion current density with increase in NaCl concentration is ascribed to the

effect of lower resistivity in the presence of higher amount of chloride ions. At fly ash content of 425 kg/m^3, the unsystematic variation in corrosion current density with increase in admixed NaCl concentration may be due to the substantial effect of variations in the chloride and hydroxyl ion concentrations in the pore solution near rebar as a result of alterations in the microstructure of GPC at comparatively lower fly ash content. In addition, the effect of alterations in oxygen and moisture content near rebar level might have also contributed toward the unsystematic variation in corrosion current density of rebar over the effect of chloride ions in the GPC mixes.

While analyzing the effect of fly ash content, it is inferred that, in control GPC mixes, the corrosion potential was mostly more negative at fly ash content of 450 kg/m^3 (Fig. 6.23 and Fig. 6.24) whereas the corrosion current density was mostly higher at fly ash content of 425 kg/m^3 (Fig. 6.25 and Fig. 6.26) at different ages. The opposite variation between corrosion potential and corrosion current density with change in fly ash content in GPC mixes in the absence of chloride ions may be ascribed to the variations in the availability of oxygen and moisture content near steel reinforcement at different ages. From Fig. 6.23 to Fig. 6.26, in NaCl admixed GPC mixes, at different ages, there was mostly unsystematic variation in corrosion potential of steel reinforcement with fly ash content, however, at different ages, overall the GPC mixes made with higher fly ash content mostly exhibited higher corrosion current density as compared to that made with lower fly ash content. The higher corrosion current density in the GPC mixes made with higher fly ash content may be ascribed to the availability of more amount of chloride ions near rebar level in GPC.

From Fig. 6.23 to Fig. 6.26, it is inferred that the corrosion potential was mostly more negative as well as corrosion current density was mostly higher in control GPC mixes made with higher molarity of NaOH solution (14 M) when compared with that made with lower molarity of NaOH solution (10 M) at different ages. This indicates dominant effect of alterations in the availability of oxygen and moisture near steel reinforcement over the effect of formation of denser microstructure at higher molarity of NaOH solution in the GPC mixes in the absence of chloride ions that led to above variations in the corrosion parameters. In chloride admixed GPC mixes (Fig. 6.23 to Fig. 6.26), there was mostly unsystematic variation in corrosion potential as well as in corrosion current density of steel reinforcement with molarity of NaOH solution at different ages. The unsystematic variation in the extent of corrosion with molarity of NaOH solution may be ascribed to the alterations in the conductivity of electrolytic pore solution as a result of variations in chloride and hydroxyl ion concentrations in the pore solution near steel

reinforcement although comparatively denser microstructure might have formed in GPC at higher molarity of NaOH solution than lower molarity of NaOH solution. From Fig. 6.23 to Fig. 6.26, it is inferred that mostly there was unsystematic variation in corrosion potential as well as in corrosion current density of steel reinforcement with age in both control and chloride admixed GPC mixes. The dominant effect of variations in the availability of oxygen and moisture near rebar level with age might have contributed toward the unsystematic variations in the extent of corrosion with age in the GPC mixes. Further, the alterations in the amount of chloride ions near rebar level with age might have affected the passivity of rebar in chloride admixed GPC mixes.

6.3 Chloride content at rebar level of fly ash based geopolymer concrete

The results of free and total chloride contents of powder samples collected from near the rebar level of NaCl admixed prismatic GPC specimens at the age of 600 days are discussed in subsequent sections. In addition, the variations in bound chloride content (calculated as the difference of total and free chloride content) with mix parameters are also discussed.

6.3.1 Effect of molarity of NaOH solution on chloride content near rebar level of GPC

The obtained free, total, and bound chloride content at rebar level of prismatic reinforced GPC specimens at the age of 600 days are shown in Fig. 6.27 for different molarity of NaOH solution such as 8 M, 10 M, 12 M, 14 M and 16 M, and different concentrations of admixed NaCl such as 1.5%, 3% and 4.5%. From Fig. 6.27, it is observed that the total chloride content is slightly higher than free chloride content in the GPC mixes for different molarity of NaOH solution and different concentrations of admixed NaCl. This indicates lower extent of chloride binding in fly ash based geopolymer concrete mixes that led to higher free chloride content in pore solution near rebar level. As stated earlier in Chapter 4, the chloride binding is ascribed to the physical adsorption of chloride ions on the sodium aluminosilicate hydrate gel in the GPC mixes. In few cases, the total chloride content was equal to free chloride content. Thus, the bound chloride content was shown as 0% for those cases in Fig. 6.27.

From Fig. 6.27, it is inferred that the free chloride content near steel reinforcement at the age of 600 days increased with increase in admixed NaCl concentration for all molarity of NaOH solution. This may be ascribed to the presence of more amount of chloride ions near rebar level at higher concentration of admixed NaCl. This observation is in line with the obtained corrosion parameters as the corrosion potential became mostly more negative and corrosion current density mostly increased with increase in admixed NaCl concentration, at the age of 600 days (Fig. 6.1 and Fig. 6.2). Further, the total chloride content increased with increase in

admixed NaCl concentration as observed from Fig. 6.27. From Fig. 6.27, the bound chloride content varied unsystematically with increase in admixed NaCl concentration (Fig. 6.27). This may be ascribed to effect of variations in the extent of physical adsorption of chloride ions with aluminosilicate gels at later age with increase in NaCl concentration.

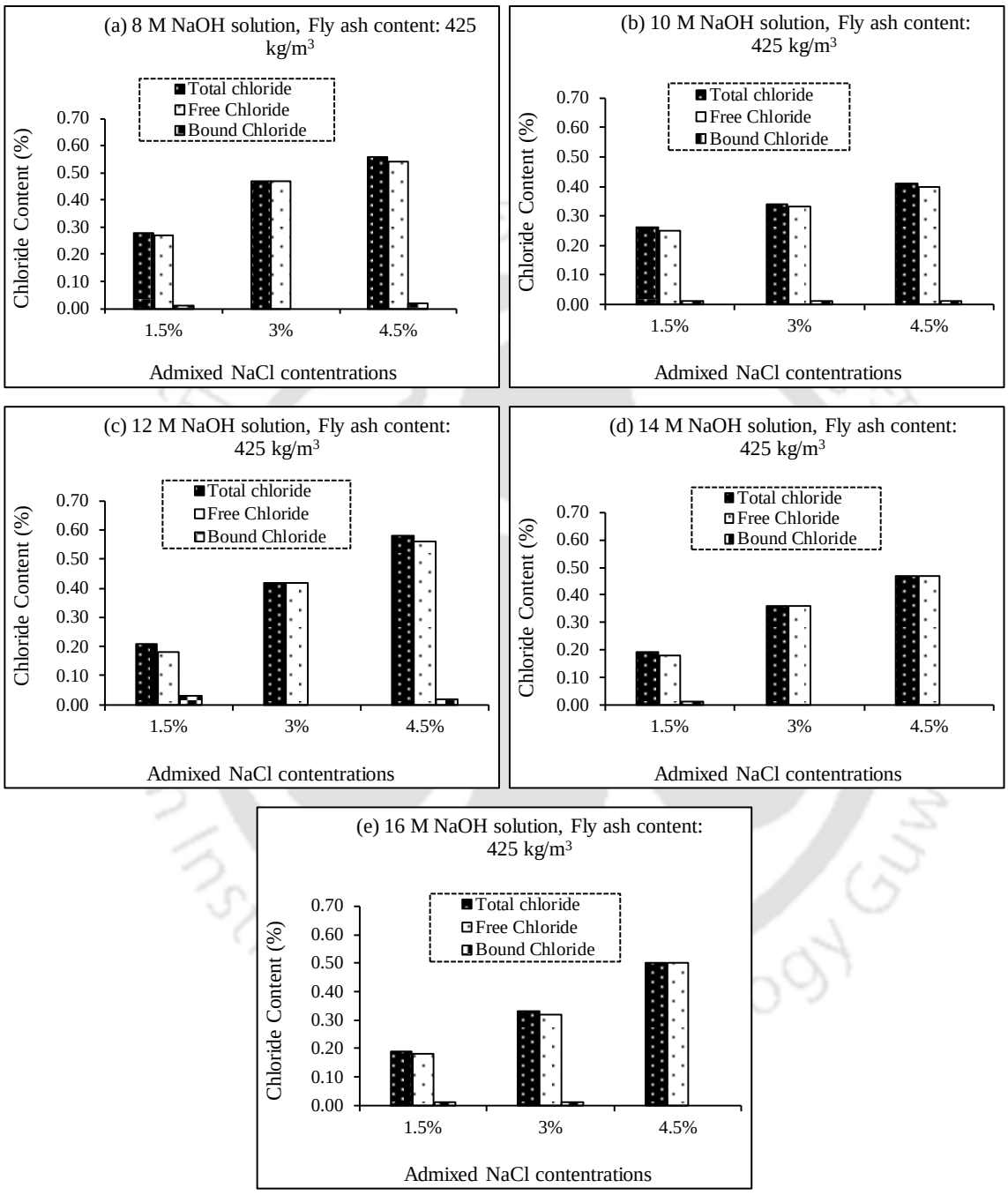

(GPC made with fly ash passing through 300 μm sieve, fly ash content of 425 kg/m^3, alkaline solution content of 210 kg/m^3, and SS/SH ratio of 1.75)

Fig. 6.27: Free, total, and bound chloride content at rebar level of prismatic reinforced GPC specimens at the age of 600 days for different concentrations of admixed NaCl: a) NaOH solution of 8 M, b) NaOH solution of 10 M, c) NaOH solution of 12 M, d) NaOH solution of 14 M, and e) NaOH solution of 16 M

From Fig. 6.27, it inferred that the free chloride content near rebar level at the age of 600 days was mostly lower at higher molarity of NaOH solution as compared to that at lower molarity of NaOH solution. This may be ascribed to the effect of availability of lower amount of chloride ions near rebar level possibly as a result of denser microstructure due to formation of more amount of aluminosilicate gels at higher molarity of NaOH solution. While comparing with the variations in corrosion parameters at the age of 600 days, it is observed that the corrosion potential was mostly less negative at lower molarity of NaOH solution whereas there was mostly unsystematic variation in corrosion current density of steel reinforcement with increase in molarity of NaOH solution (Fig. 6.1 and Fig. 6.2). Thus, the inconsistent variation between corrosion parameters and free chloride content is attributed to the dominant effect of alterations in oxygen and moisture content near rebar level at later age in GPC mixes. The total chloride content mostly increased with increase in molarity of NaOH solution as observed from Fig. 6.27. Further, there was unsystematic variation in bound chloride content with molarity of NaOH solution at the age of 600 days. Although, there may be formation of more amount of binding gels at higher molarity of NaOH solution, the unsystematic variation in bound chloride content with molarity of NaOH solution may be attributed to the alteration in the adsorption of chloride ions on binding gels at later age.

6.3.2 Effect of alkaline solution content on chloride content near rebar level of GPC

The free, total, and bound chloride content at rebar level of prismatic reinforced GPC specimens at the age of 600 days are illustrated in Fig. 6.28 for different alkaline solution contents i.e., 190 kg/m^3 and 210 kg/m^3. From Fig. 6.28 (a), it is observed that the free chloride content near rebar level of GPC mixes at the age of 600 days was higher at lower alkaline solution content (190 kg/m^3) than that at higher alkaline solution content (210 kg/m^3) for both molarity of NaOH solution (10 M and 14 M). This is ascribed to the fact that the variations in the concentrations of different ionic species in the pore solution might have led to availability of higher amount of chloride ions in the pore solution near rebar level in the GPC mixes made with lower amount of alkaline solution. It may be noted that the corrosion potential was more negative at lower alkaline solution content and there was unsystematic variation in corrosion current density with alkaline solution content at the age of 600 days (Fig. 6.3 to Fig. 6.6). Although, the free chloride content was higher at lower alkaline solution content, the unsystematic variation in the extent of corrosion as indicated by the corrosion current density may be ascribed to the variations in the conductivity of GPC as a result of alterations in moisture content near rebar level. From Fig. 6.28 (b), the total chloride content was higher in

GPC mixes made with lower alkaline solution content as compared to higher alkaline solution content. Further, the bound chloride content was also higher at lower alkaline solution content than higher alkaline solution content (Fig. 6.28 (c)), which may be ascribed to the effect of release of physically adsorbed chloride ions from aluminosilicate gels to a comparatively lower extent at lower alkaline solution content.

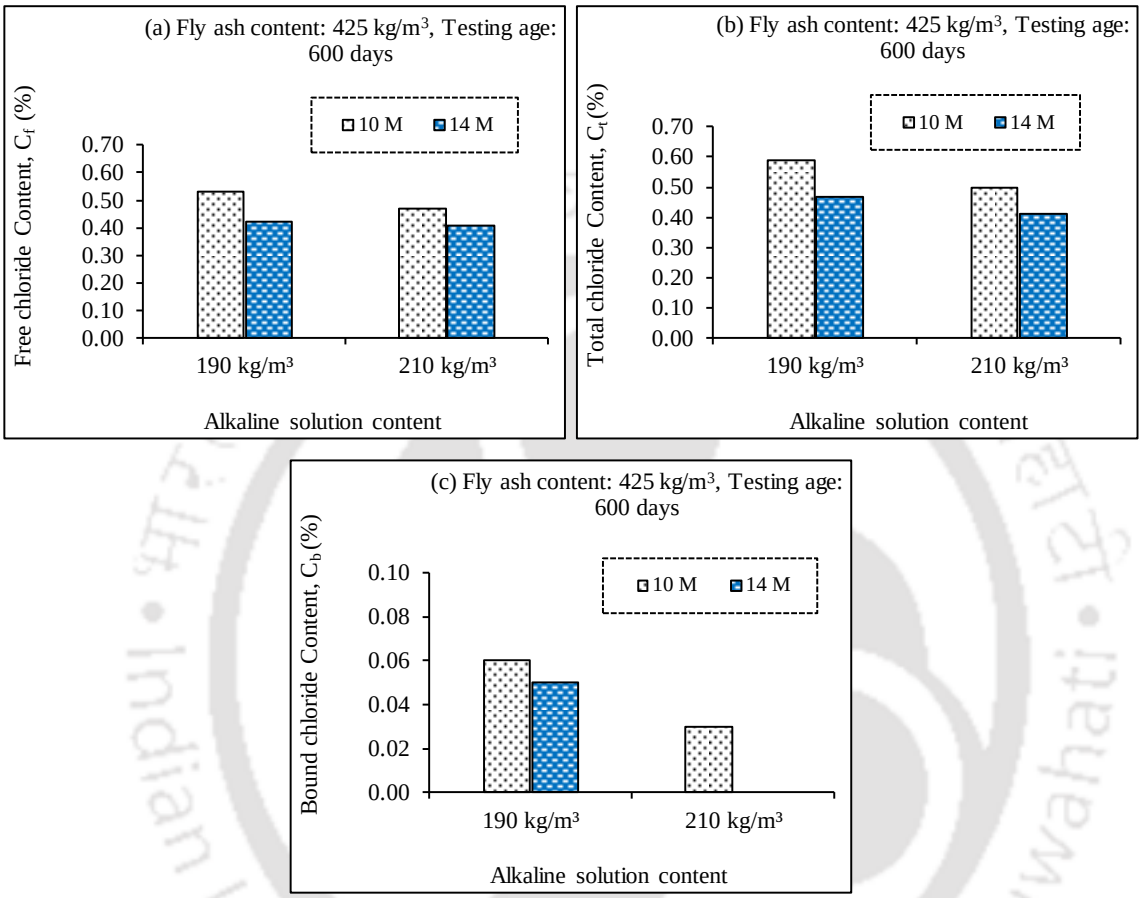

(GPC made with fly ash passing through 150 μm sieve, fly ash content of 425 kg/m³, and SS/SH ratio of 1.75)

Fig. 6.28: Chloride content at rebar level of prismatic reinforced GPC specimens admixed with 3% NaCl for alkaline solution content of 190 kg/m^3 and 210 kg/m^3: a) Free chloride content, b) Total chloride content, and c) Bound chloride content at the age of 600 days

From Fig. 6.28 (a), the free chloride content near rebar level at the age of 600 days was higher at lower molarity of NaOH solution (10 M) as compared to higher molarity of NaOH solution (14 M). This resulted in more negative corrosion potential and higher corrosion current density at the age of 600 days in GPC mixes made with lower molarity of NaOH solution as compared to that made with higher molarity of NaOH solution as observed from Fig. 6.3 to Fig. 6.6. The total chloride content was also higher at lower molarity of NaOH solution as compared to higher molarity of NaOH solution as observed from Fig. 6.28 (b). From Fig. 6.28 (c), it is inferred that the bound chloride content was higher in GPC mixes made with lower molarity of NaOH solution than that made with higher molarity of NaOH solution. This indicates

comparatively higher extent of physical binding of chloride ions with binding gels at lower molarity of NaOH solution at later age although the free chloride content was higher at lower molarity of NaOH solution.

6.3.3 Effect of SS/SH ratio on chloride content near rebar level of GPC

Fig. 6.29 illustrates the free, total, and bound chloride content of prismatic reinforced GPC specimens near steel reinforcement at the age of 600 days for different values of SS/SH ratio (ratio of sodium silicate solution to sodium hydroxide solution) i.e., 1.5 and 1.75.

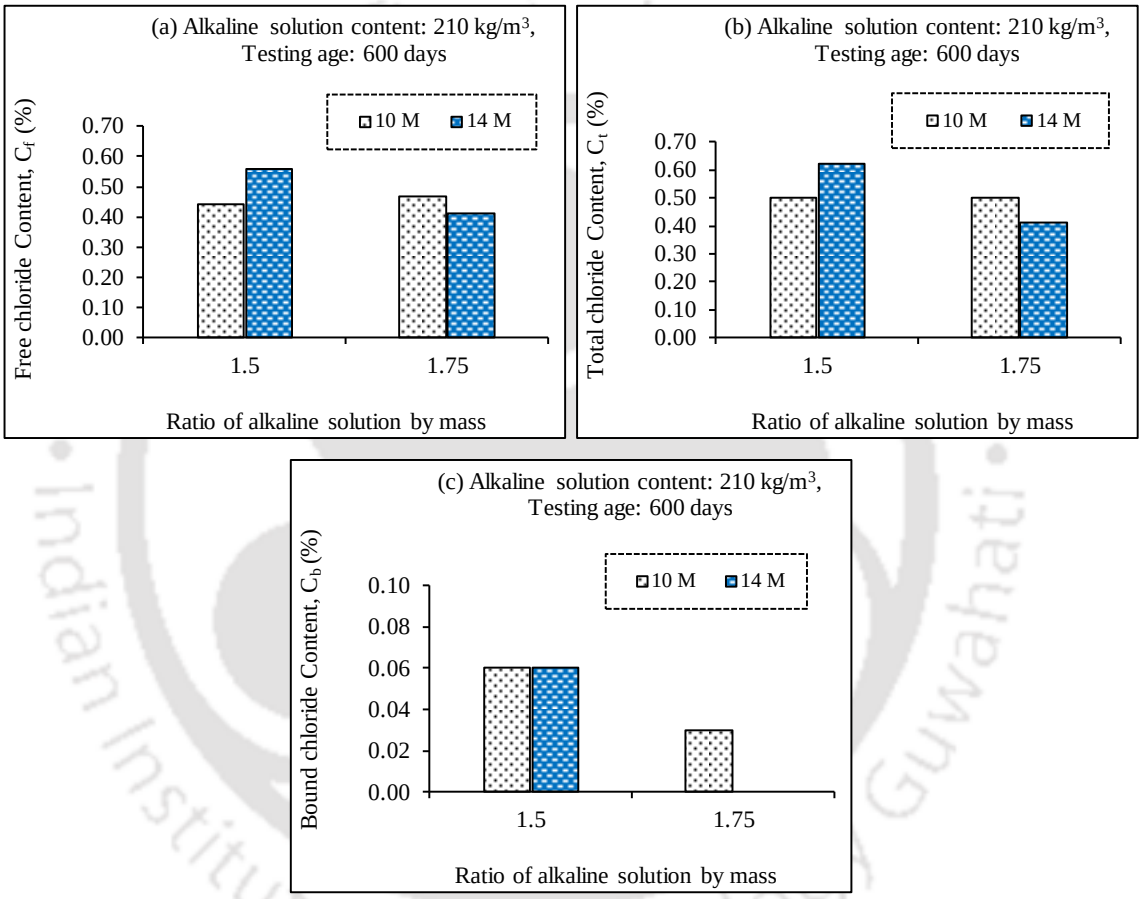

(GPC made with fly ash passing through 150 μm sieve, fly ash content of 425 kg/m^3, and alkaline solution content of 210 kg/m^3)

Fig. 6.29: Chloride content at rebar level of prismatic reinforced GPC specimens admixed with 3% NaCl for SS/SH ratio of 1.5 and 1.75: a) Free chloride content, b) Total chloride content, and c) Bound chloride content at the age of 600 days

From Fig. 6.29, it is noted that the free chloride content near rebar level obtained at the age of 600 days was more at higher SS/SH ratio for NaOH solution of 10 M whereas opposite variation in free chloride content with SS/SH ratio was observed at NaOH solution of 14 M. It may be noted that the corrosion potential at the age of 600 days was more negative at SS/SH ratio of 1.5 whereas the corrosion current density was higher at SS/SH ratio of 1.75 for both

molarity of NaOH solution i.e., 10 M and 14 M (Fig. 6.7 to Fig. 6.10). This indicates consistent variation in the effect of chloride ions on the extent of corrosion as indicated by corrosion current density with change in SS/SH ratio for NaOH solution of 10 M whereas inconsistent variation for NaOH solution of 14 M at the age of 600 days. The inconsistent variation in the effect of chloride ions on the extent of corrosion at NaOH solution of 14 M may be attributed to the dominant effect of variations in the conductivity of concrete as a result of variations in moisture content, and changes in oxygen content near steel reinforcement at later age. From Fig. 6.29 (b), the total chloride content was mostly higher at lower SS/SH ratio as compared to that at higher SS/SH ratio. Further, the bound chloride content was higher at lower SS/SH ratio as compared to higher SS/SH ratio as observed from Fig. 6.29 (c), which indicates comparatively higher extent of adsorption of chloride ions with N-A-S-H gel at lower SS/SH ratio in GPC mixes at later age. From Fig. 6.29 (a), the free chloride content near rebar level at the age of 600 days was higher at higher molarity of NaOH solution (14 M) for SS/SH ratio of 1.5 whereas there was opposite variation in free chloride content with molarity of NaOH solution for SS/SH ratio of 1.75. It may be noted that the corrosion potential of steel reinforcement was more negative at NaOH solution of 10 M as compared to NaOH solution of 14 M at the age of 600 days for both SS/SH ratios (Fig. 6.7 and Fig. 6.8). However, the corrosion current density was higher at lower molarity of NaOH solution as compared to higher molarity of NaOH solution at SS/SH ratio of 1.5 whereas opposite variation in corrosion current density with molarity of NaOH solution was observed at SS/SH ratio of 1.75 (Fig. 6.9 and Fig. 6.10). These variations in corrosion current density with molarity of NaOH solution indicate inconsistent effect of chloride ions on corrosion activity of rebar for different SS/SH ratios at later age in GPC mixes. The variation in total chloride content with molarity of NaOH solution was same as that in case of free chloride content as observed from Fig. 6.29 (b). From Fig. 6.29 (c), there was no difference in bound chloride content with molarity of NaOH solution at SS/SH ratio of 1.5 whereas it was higher in GPC mix made with lower molarity of NaOH solution (10 M) as compared to that made with higher molarity of NaOH solution (14 M) at SS/SH ratio of 1.75. It may be noted that no chloride binding was observed in GPC mix made with NaOH solution of 14 M at SS/SH ratio of 1.75 as there was no difference between total and free chloride content. Although the free chloride content was higher at lower molarity of NaOH solution, the dominant effect of higher SS/SH ratio over the effect of lower molarity of NaOH solution might have resulted in higher extent of physical binding of chloride ions with N-A-S-H gel at later age.

6.3.4 Effect of particle size of fly ash on chloride content near rebar level of GPC

6.3.4.1 GPC prepared with fly ash content of 425 kg/m^3

Fig. 6.30 shows the free, total, and bound chloride content near rebar level of prismatic reinforced GPC specimens at the age of 600 days for fly ash passing through 150 μm sieve, and 300 μm sieve at fly ash content of 425 kg/m^3.

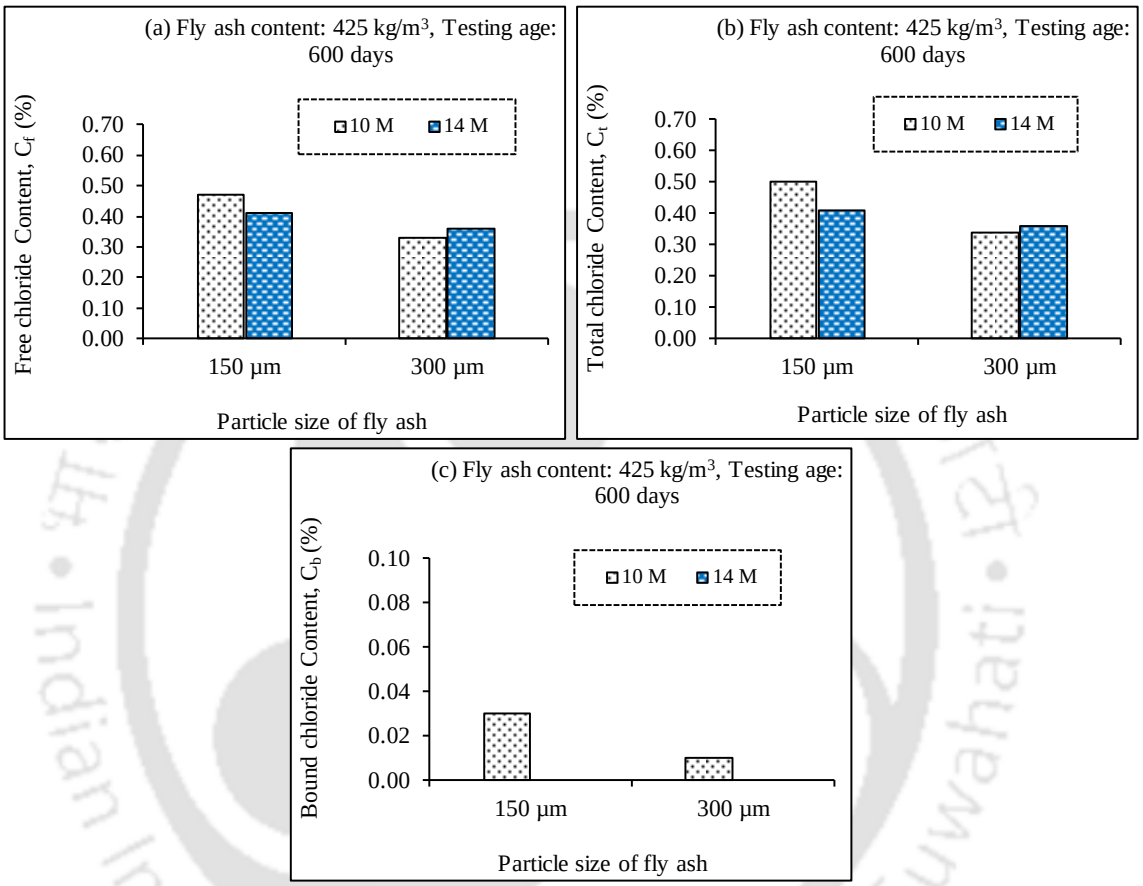

(GPC made with fly ash content of 425 kg/m^3, alkaline solution content of 210 kg/m^3, and SS/SH ratio of 1.75)

Fig. 6.30: Chloride content at rebar level of prismatic reinforced GPC specimens admixed with 3% NaCl for fly ash passing through 150 μm sieve, and 300 μm sieve: a) Free chloride content, b) Total chloride content, and c) Bound chloride content at the age of 600 days

From Fig. 6.30 (a), the free chloride content near rebar level measured at the age of 600 days was higher in the GPC mixes made with smaller fly ash particles (passing through 150 μm sieve) than that made with larger fly ash particles (passing through 300 μm sieve) for both molarity of NaOH solution. However, the corrosion current density was lower in GPC mixes made with smaller fly ash particles as compared to that made with larger fly ash particles, at the age of 600 days (Fig. 6.13 and Fig. 6.14). Thus, lower corrosion current density in the GPC mixes made with smaller fly ash particles even though the chloride content was higher may be ascribed to the significant effect of variations in the availability of oxygen and moisture in the

vicinity of rebar. From Fig. 6.30 (b), the total chloride content was higher in the GPC mixes prepared with smaller fly ash particles as compared to that prepared with larger fly ash particles for both molarity of NaOH solution. Further, from Fig. 6.30 (c), no chloride binding was observed at the age of 600 days in GPC made with NaOH solution of 14 M for both sizes of fly ash particles as there was no difference between total and free chloride content. At NaOH solution of 10 M, the GPC mix made with smaller fly ash particles showed higher bound chloride content than that made with larger fly ash particles (Fig. 6.30 (c)) thereby indicating comparatively more extent of binding of chloride ions with aluminosilicate gels in GPC made with smaller fly ash particles. From Fig. 6.30 (a), the free chloride content near rebar level was higher at lower molarity of NaOH solution (10 M) for fly ash passing through 150 μm sieve whereas it was higher at higher molarity of NaOH solution (14 M) for fly ash passing through 300 μm sieve. These variations in free chloride content near steel reinforcement in prismatic specimens with molarity of NaOH solution for fly ash particles of different sizes are consistent with the variations in corrosion potential and corrosion current density of steel reinforcement at the age of 600 days as observed from Fig. 6.11 to Fig. 6.14. The variation in total chloride content (Fig. 6.30 (b)) with molarity of NaOH solution was same as that in case of free chloride content. Further, chloride binding was observed only in case of GPC mixes made with lower molarity of NaOH solution when compared with higher molarity of NaOH solution for both sizes of fly ash particles as observed from Fig. 6.30 (c). The absence of chloride binding as indicated by 0% bound chloride content in GPC mixes made with higher molarity of NaOH solution at lower fly ash content may be ascribed to the release of physically bound chloride ions from aluminosilicate gels to a comparatively higher extent.

6.3.4.2 GPC prepared with fly ash content of 450 kg/m^3

For fly ash content of 450 kg/m^3, the free, total, and bound chloride content near steel reinforcement in prismatic specimens at the age of 600 days are shown in Fig. 6.31 for GPC made with fly ash passing through 150 μm sieve, and 300 μm sieve. From Fig. 6.31 (a, b), it is inferred that, at the age of 600 days, both free and total chloride content increased with increase in concentration of admixed NaCl. While comparing the variations in corrosion parameters, the corrosion potential was mostly more negative at higher concentration of admixed NaCl as compared to lower concentration of NaCl whereas there was no systematic variation in corrosion current density with concentration of admixed NaCl at the age of 600 days (Fig. 6.15 to Fig. 6.18). Therefore, above variations in corrosion parameters, although the free chloride content was higher at higher concentration of admixed NaCl, indicates

inconsistent effect of chloride ions on corrosion activity of rebar in GPC at later age. This shows that the passivity of steel reinforcement was not altered even in the presence of higher amount of chloride ions in some cases, which may be ascribed to the effect of improved resistivity of GPC at later age. From Fig. 6.31 (c), chloride binding was not observed in majority of the cases, however, the bound chloride content mostly increased with increase in admixed NaCl concentration in remaining cases. This indicates comparatively higher extent of physical binding of chloride ions with geopolymer gels in the presence of more amount of NaCl.

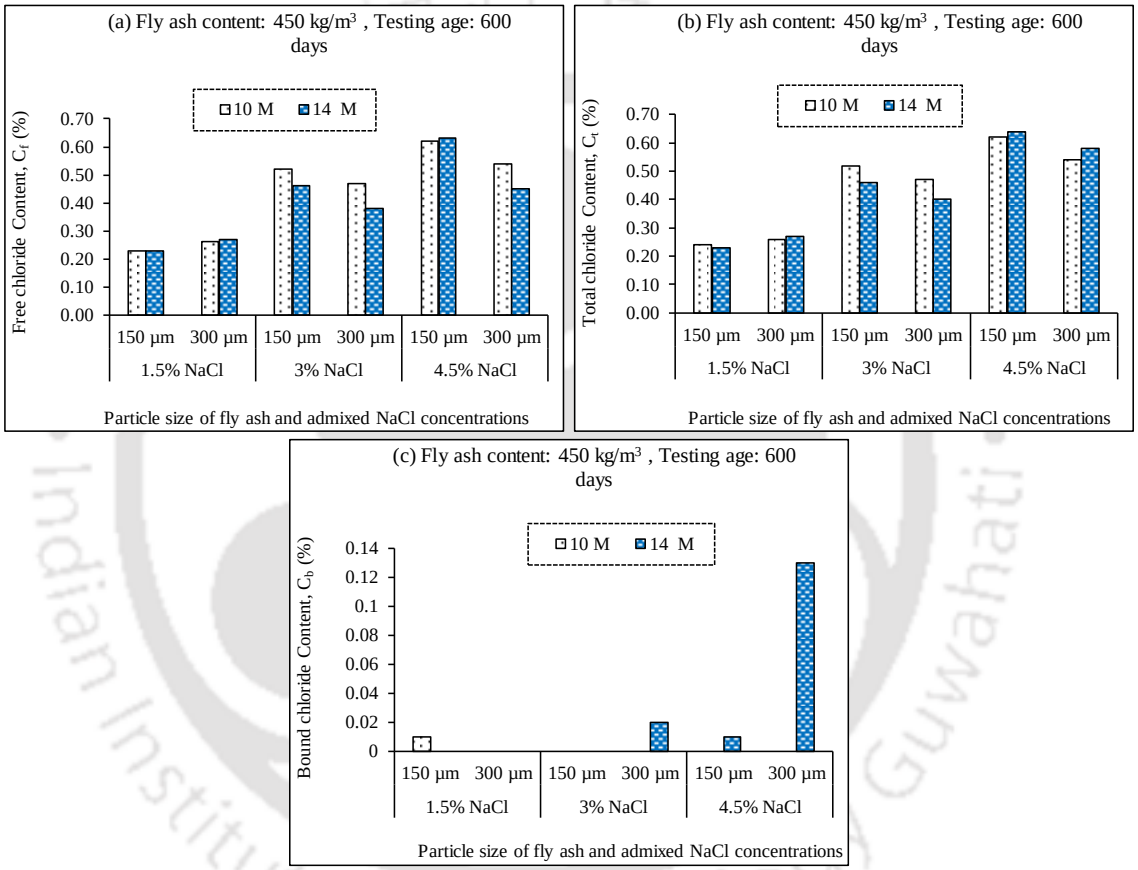

(GPC made with fly ash content of 450 kg/m^3, alkaline solution content of 210 kg/m^3, and SS/SH ratio of 1.75)

Fig. 6.31: Chloride content at rebar level of prismatic reinforced GPC specimens admixed with different concentrations of NaCl for fly ash passing through 150 µm sieve, and 300 µm sieve: a) Free chloride content, b) Total chloride content, and c) Bound chloride content at the age of 600 days

From Fig. 6.31 (a, b), the free and total chloride content near rebar level at the age of 600 days were mostly higher in GPC mixes made with smaller fly ash particles (passing through 150 µm sieve) as compared to that made with larger fly ash particles (passing through 300 µm sieve). The higher free chloride content near rebar level resulted in mostly more negative corrosion potential and higher corrosion current density of steel reinforcement at the age of

600 days in GPC mixes made with smaller fly ash particles as observed from Fig. 6.15 to Fig. 6.18. From Fig. 6.31 (c), the bound chloride content was mostly higher in GPC mixes made with larger fly ash particles as compared to that made with smaller fly ash particles, which led to presence of lower amount of free chloride ions in GPC mixes made with larger fly ash particles. From Fig. 6.31 (a), the free chloride content near steel reinforcement at the age of 600 days was mostly higher at lower molarity of NaOH solution as compared to higher molarity of NaOH solution. This may be ascribed to the availability of more amount of chloride ions near rebar level at lower molarity of NaOH solution due to formation of less denser microstructure. The presence of higher amount of chloride ions near steel reinforcement led to mostly more negative corrosion potential and higher corrosion current density at the age of 600 days in GPC mixes made with lower molarity of NaOH solution as observed from Fig. 6.15 to Fig. 6.18. From Fig. 6.31 (b), mostly there was unsystematic variation in total chloride content at the age of 600 days with molarity of NaOH solution. The bound chloride content was mostly higher at higher molarity of NaOH solution than that at lower molarity of NaOH solution as observed from Fig. 6.31 (c). This may be attributed to the effect of higher extent of physical binding of chloride ions with N-A-S-H gel at later age in GPC mixes made with higher molarity of NaOH solution at higher fly ash content.

6.3.5 Effect of fly ash content on chloride content near rebar level of GPC

6.3.5.1 GPC prepared with fly ash passing through 150 µm sieve

Fig. 6.32 illustrates the free, total, and bound chloride content near steel reinforcement in prismatic reinforced GPC specimens at the age of 600 days for different fly ash contents namely 425 kg/m^3 and 450 kg/m^3 for fly ash passing through 150 µm sieve.

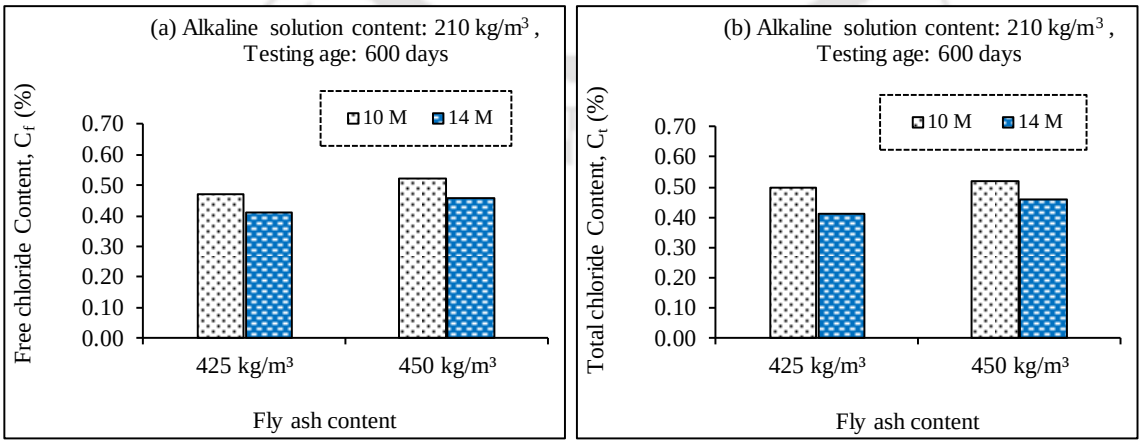

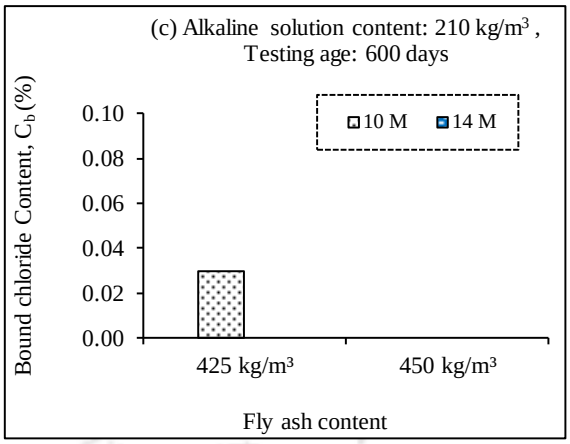

(GPC made with fly ash passing through 150 μm sieve, alkaline solution content of 210 kg/m^3 and SS/SH ratio of 1.75)

Fig. 6.32: Chloride content at rebar level of prismatic reinforced GPC specimens admixed with 3% NaCl for fly ash contents of 425 kg/m^3 and 450 kg/m^3: a) Free chloride content, b) Total chloride content, and c) Bound chloride content at the age of 600 days

From Fig. 6.32 (a), the free chloride content near steel reinforcement at the age of 600 days was higher in the GPC mixes made with higher fly ash content than that made with lower fly ash content. While comparing with the variations in corrosion parameters at the age of 600 days, the corrosion potential was more negative at higher fly ash content (450 kg/m^3) as compared to lower fly ash content (425 kg/m^3) and the corrosion current density was higher at lower fly ash content for NaOH solution of 10 M whereas it was higher at higher fly ash content for NaOH solution of 14 M (Fig. 6.19 to Fig. 6.22). These variations in corrosion parameters with fly ash content when compared with that in free chloride content indicate comparatively higher effect of chloride ions on the extent of corrosion of rebar in the GPC mixes made with higher fly ash content. From Fig. 6.32 (b), there was higher total chloride content near rebar level in the GPC mixes made with higher fly ash content as compared to that made with lower fly ash content. From Fig. 6.32 (c), chloride binding was observed only in the GPC mix made with lower fly ash content when compared with that made with higher fly ash content. From Fig 6.32 (a), the free chloride content near rebar at the age of 600 days was higher in the GPC mixes made with lower molarity (10 M) of NaOH solution as compared to that made with higher molarity (14 M) of NaOH solution, which indicates presence of more amount of chloride ions in the electrolytic pore solution of GPC made with lower molarity of NaOH solution. It may be noted that, at the age of 600 days, the corrosion potential of rebar was more negative at lower molarity of NaOH solution than higher molarity of NaOH solution and the corrosion current density was higher at higher molarity of NaOH solution for fly ash content of 450 kg/m^3 whereas it was higher at lower molarity of NaOH solution for fly ash content 425

kg/m^3 (Fig. 6.19 to Fig. 6.22). The comparison of the variations between corrosion parameters and free chloride content at the age of 600 days with molarity of NaOH solution signifies mostly consistent effect of chloride ions on rebar corrosion i.e., mostly higher extent of reinforcing steel corrosion at lower molarity of NaOH solution due to dominant effect of presence of higher amount of chloride ions. The total chloride content near rebar level was higher in the GPC mixes made with lower molarity of NaOH solution than that made with higher molarity of NaOH as evident from Fig. 6.32 (b). Further, chloride binding was observed only in the GPC mix made with lower molarity of NaOH solution at fly ash content of 425 kg/m^3 as observed from Fig. 6.32 (c).

6.3.5.2 GPC prepared with fly ash passing through 300 µm sieve

For fly ash passing through 300 µm sieve, the free, total, and bound chloride content near rebar in prismatic specimens at the age of 600 days are shown in Fig. 6.33 for GPC mixes made with fly ash contents of 425 kg/m^3 and 450 kg/m^3.

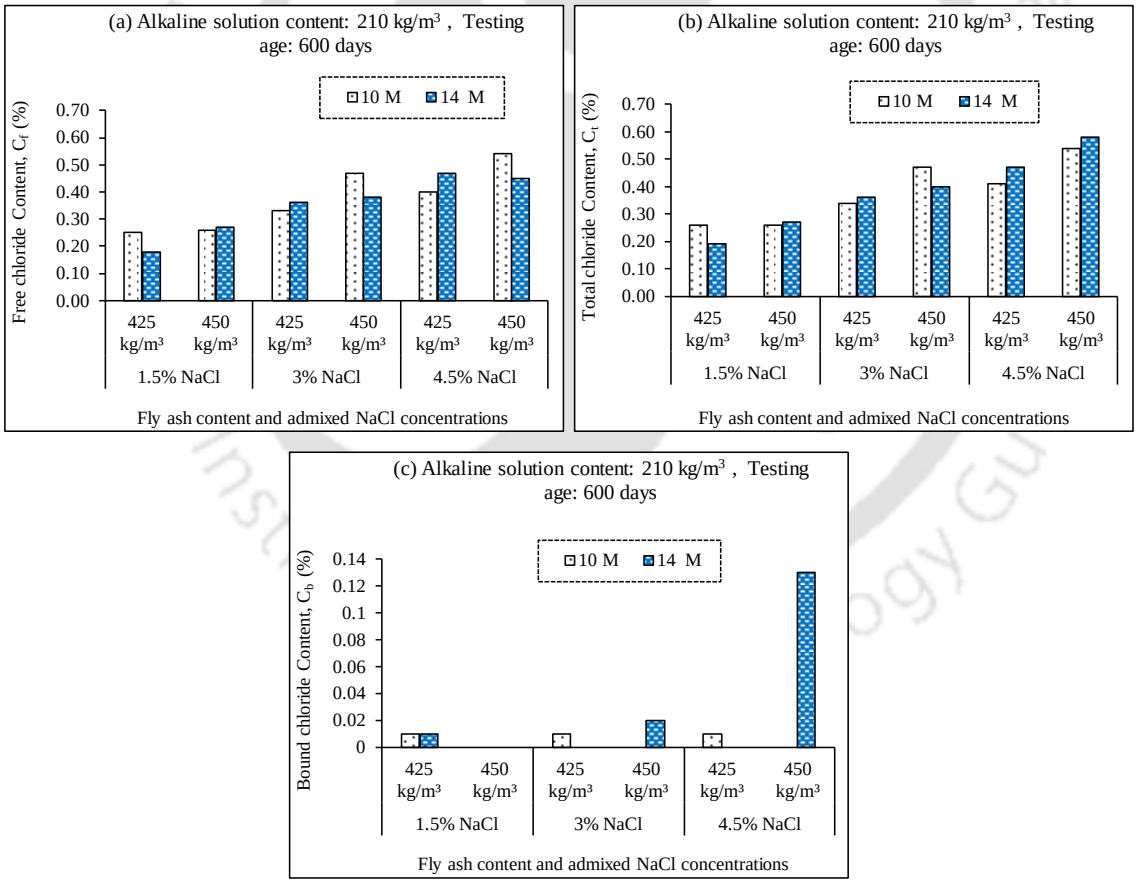

(GPC made with fly ash passing through 300 µm sieve, alkaline solution content of 210 kg/m^3 and SS/SH ratio of 1.75)

Fig. 6.33: Chloride content at rebar level of prismatic reinforced GPC specimens admixed with different concentrations of NaCl for fly ash contents of 425 kg/m^3 and 450 kg/m^3: a) Free chloride content, b) Total chloride content, and c) Bound chloride content at the age of 600 days

From Fig. 6.33 (a), at the age of 600 days, the free chloride content near rebar level was mostly higher in the GPC mixes made with higher fly ash content (450 kg/m^3) as compared to that made with lower fly ash content (425 kg/m^3). At the age of 600 days (Fig. 6.23 to Fig. 6.26), the variation in corrosion potential was unsystematic with fly ash content, however, the corrosion current density was mostly lower at higher fly ash content than that at lower fly ash content irrespective of molarity of NaOH solution and admixed NaCl concentration. The lower extent of corrosion in GPC mixes made with higher fly ash content at later age, even though the chloride content was higher, may be due to the effect of improved passivation of steel reinforcement as a result of enhanced resistivity exhibited by the geopolymeric structure at later age in the GPC made with higher fly ash content and larger fly ash particles. From Fig. 6.33 (b), the GPC mixes made with higher fly ash content showed more total chloride content as compared to that made with lower fly ash content. Further, from Fig. 6.33 (c), chloride binding was not observed in some cases, whereas in remaining cases, mostly there was unsystematic variation in bound chloride content with fly ash content thereby indicating alteration in the extent of physical adsorption of chloride ions with N-A-S-H gel.

From Fig. 6.33 (a), there was unsystematic variation in free chloride content near steel reinforcement in GPC mixes at the age of 600 days with molarity of NaOH solution irrespective of fly ash content and admixed NaCl concentration, which may be attributed to the dominant effect of alterations in chloride ion concentration in the electrolytic pore solution of GPC near rebar level. From Fig. 6.23 to Fig. 6.26, at the age of 600 days, the corrosion potential was mostly less negative and the corrosion current density was mostly lower at higher molarity of NaOH solution (14 M) as compared to that at lower molarity of NaOH solution (10 M). This indicates that, although there was unsystematic variation in free chloride content with molarity of NaOH solution, the lower extent of corrosion in the GPC mixes made with higher molarity of NaOH solution may be attributed to the increased resistivity of geopolymer concrete made with higher molarity of NaOH solution that improved the passivity of steel reinforcement at later age. From Fig. 6.33 (b), the total chloride content was mostly higher at higher molarity of NaOH solution, however, there was unsystematic variation in bound chloride content with molarity of NaOH solution at the age of 600 days as observed from Fig. 6.33 (c). The free and total chloride content near steel reinforcement at the age of 600 days increased with increase in admixed NaCl concentration in GPC mixes as observed from Fig. 6.33 (a, b). It may be noted that, at the age of 600 days, there was no systematic variation in corrosion potential and corrosion current density with increase in NaCl concentration from 1.5% to 3% (Fig. 6.23 to Fig. 6.26). However, the corrosion potential became mostly more

negative and corrosion current density mostly increased with increase in NaCl concentration from 3% to 4.5%. Thus, the presence of more amount of chloride ions near rebar level resulted in higher extent of corrosion activity of steel reinforcement in GPC mixes admixed with relatively higher concentration of NaCl. Further, although chloride binding was not observed in some cases, there was mostly increase in bound chloride content with increase in admixed NaCl concentration as observed from Fig. 6.33 (c).

6.4 Microstructure analysis of fly ash based geopolymer concrete near rebar level in prismatic specimens

As stated earlier in Chapter 3, the microstructure of geopolymer concrete near rebar level was analysed by conducting X-ray diffraction (XRD), Field emission scanning electron microscope (FESEM) and Fourier transform infrared spectroscopy - Attenuated total reflectance (FTIR-ATR) analyses on powder samples collected from near the rebar level of prismatic GPC specimens at the age of 600 days.

6.4.1 XRD analysis

The obtained XRD patterns of GPC near steel reinforcement at the age of 600 days are shown in Fig. 6.34 for different molarity of NaOH solution (8 M, 10 M, 12 M, 14 M and 16 M) and different concentrations of admixed NaCl (0%, 1.5%, 3% and 4.5%). From Fig. 6.34, the peaks related to albite, anorthoclase, nepheline, sodalite and muscovite were observed in control (without NaCl) as well as NaCl admixed GPC mixes at the age of 600 days [90]. Further, the XRD patterns also indicate the presence of quartz and mullite in the GPC mixes. Less intense peaks of halite were observed in the XRD patterns of chloride admixed mixes, which is due to the crystallization of NaCl in the GPC mixes.

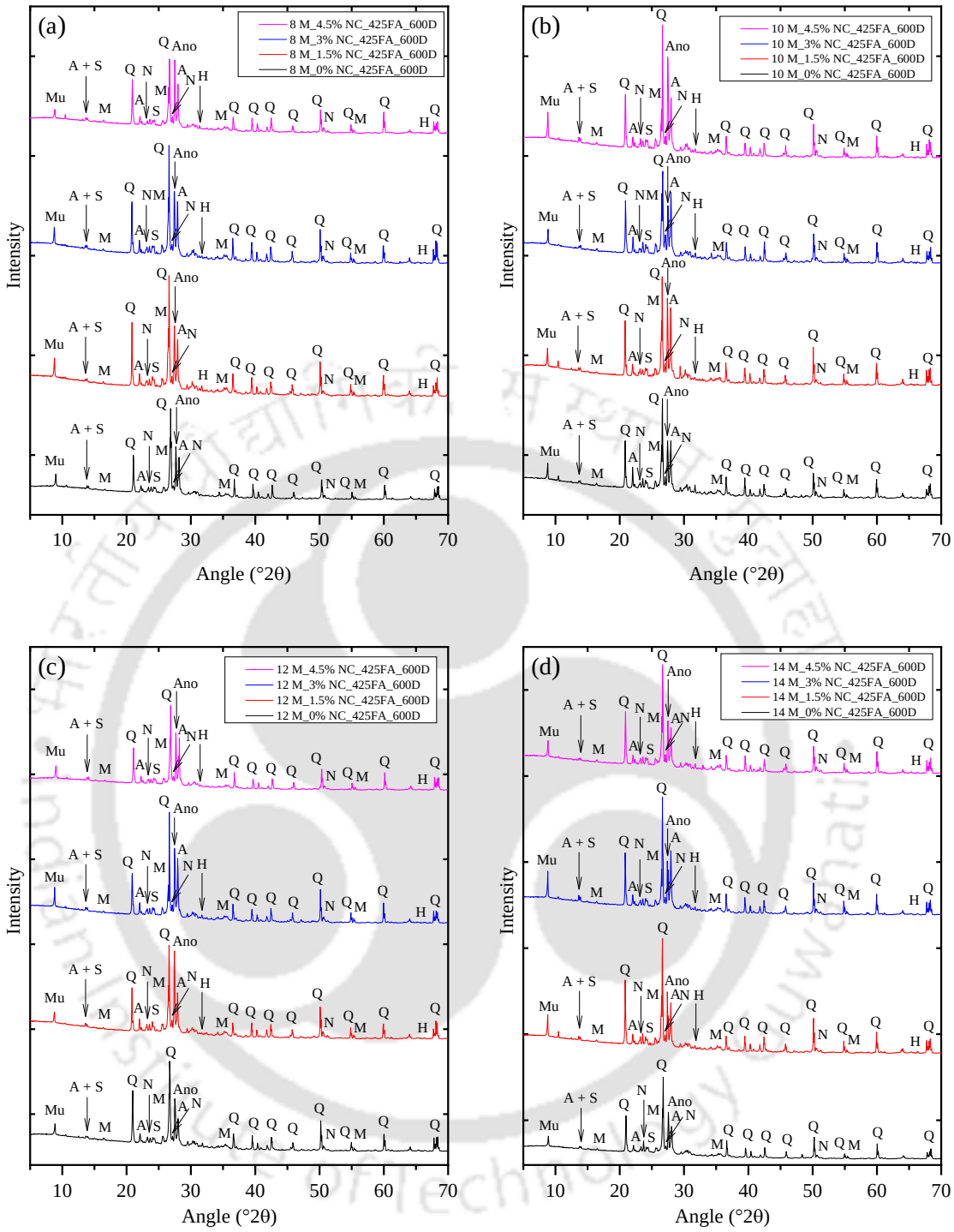

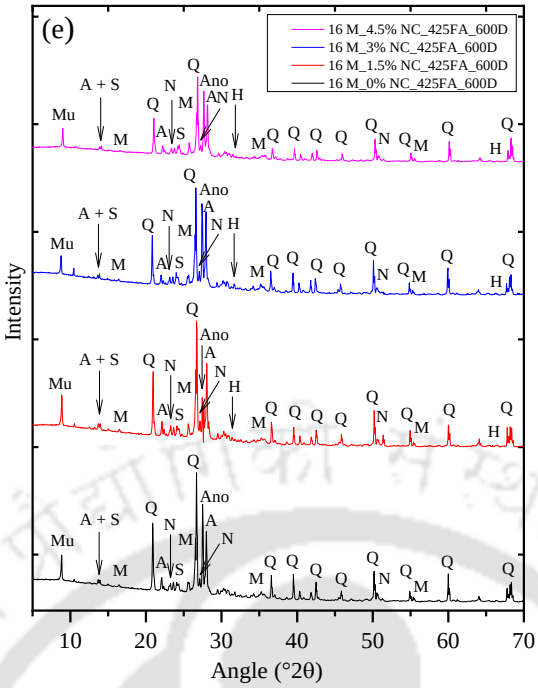

(GPC made with fly ash passing through 300 μm sieve, fly ash content of 425 kg/m^3, alkaline solution content of 210 kg/m^3, and SS/SH ratio of 1.75)

Fig. 6.34: XRD patterns of GPC near steel reinforcement in prismatic specimens at the age of 600 days for different molarity of NaOH solution and different concentrations of admixed sodium chloride

From the XRD patterns (Fig. 6.34), it is observed that the GPC mixes made with higher molarity of NaOH solution mostly showed higher peak intensity of albite, anorthoclase and nepheline at the age of 600 days for different concentrations of admixed NaCl. This indicates formation of more amount of geopolymer gels leading to denser microstructure in the GPC mixes made with higher molarity of NaOH solution, which resulted in availability of lower amount of chloride ions near rebar level at the age of 600 days. It may be noted that, as discussed earlier in Section 6.3.1, the free chloride content near steel reinforcement in the prismatic specimens at the age of 600 days was mostly lower in GPC mixes made with higher molarity of NaOH solution (Fig. 6.27). Further, the peak intensity of muscovite and sodalite mostly increased with increase in molarity of NaOH solution in NaCl admixed GPC mixes as observed from Fig. 6.34. In control GPC mixes, mostly there was unsystematic variation in peak intensity of albite, anorthoclase, nepheline, muscovite, and sodalite with molarity of NaOH solution as observed from the XRD patterns shown in Fig. 6.34. With increase in concentration of admixed NaCl, mostly there was decrease in the peak intensity of albite, anorthoclase, nepheline, muscovite, and sodalite in the XRD patterns of GPC mixes as observed from Fig. 6.34. which indicates formation of lower amount of geopolymer gels that

led to comparatively less denser microstructure in the GPC mixes admixed with higher concentration of NaCl. This led to more free chloride content near rebar level (Fig. 6.27) thereby resulting in higher extent of corrosion activity of steel reinforcement (Fig. 6.1 and Fig. 6.2) in the GPC mixes admixed with higher concentration of sodium chloride. Between control and chloride admixed GPC mixes, mostly there was unsystematic variation in the peak intensity of albite, anorthoclase and nepheline between control mix and that admixed with 1.5% NaCl as observed from Fig. 6.34. However, the peak intensity of these compounds related to N-A-S-H gel were mostly lower in GPC mixes admixed with higher concentration of NaCl i.e., 3% and 4.5% as compared to that in control GPC mixes. This indicates lower extent of formation of geopolymer gels in GPC mixes in the presence of higher amount of sodium chloride. From Fig. 6.34, mostly there was unsystematic variation in the peak intensity of halite with admixed NaCl concentration and molarity of NaOH solution. This may be ascribed to the effect of alterations in the extent of crystallization of sodium chloride in GPC mixes owing to the effect of variations in the microstructure of GPC with change in molarity of NaOH solution. The obtained XRD patterns of GPC near rebar level in prismatic specimens at the age of 600 days are illustrated in Fig. 6.35 for alkaline solution contents of 190 kg/m^3 and 210 kg/m^3. From Fig. 6.35, the peak intensity of albite, anorthoclase and nepheline in XRD patterns of GPC near rebar level were mostly higher in the mixes made with lower alkaline solution content as compared to that made with higher alkaline solution content in both control and 3% NaCl admixed GPC mixes. The higher amount of aluminosilicate gels at lower alkaline solution content in 3% NaCl admixed GPC mixes led to comparatively higher extent of physical binding of chloride ions as the bound chloride content was higher at lower alkaline solution content than that at higher alkaline solution content (Fig. 6.28(c)). The peak intensity of muscovite, and sodalite in the XRD patterns were mostly higher at lower alkaline solution content than that at higher alkaline solution content.

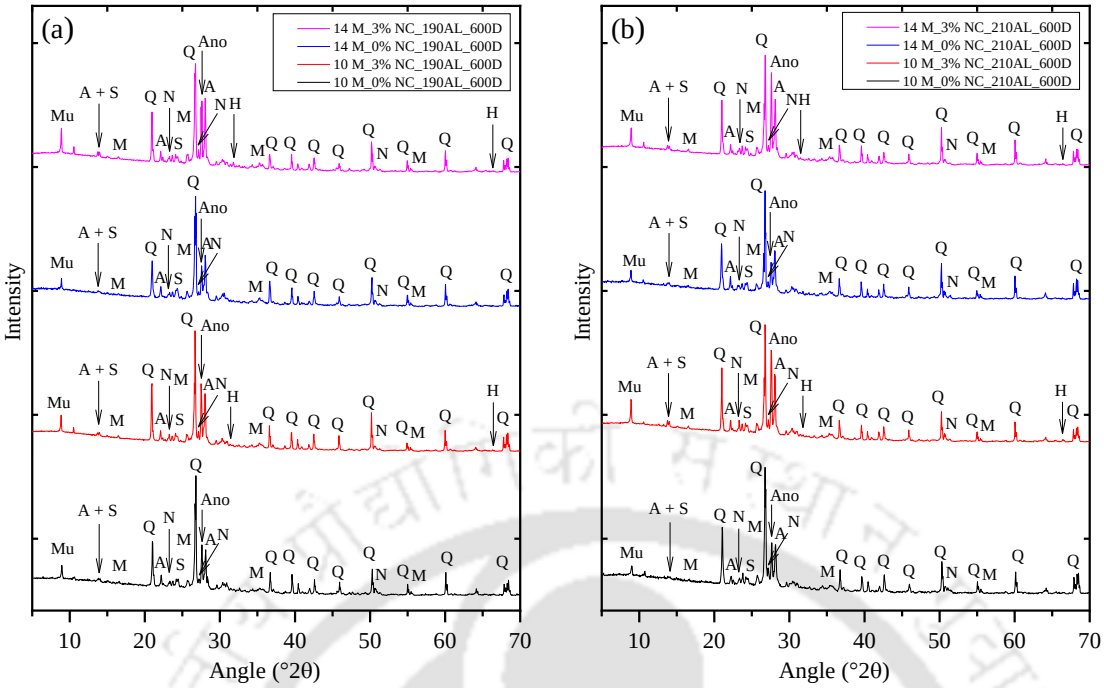

(GPC made with fly ash passing through 150 μm sieve, fly ash content of 425 kg/m^3, and SS/SH ratio of 1.75)

Fig. 6.35: XRD patterns of GPC near steel reinforcement in prismatic specimens at the age of 600 days for alkaline solution content of a) 190 kg/m^3, and b) 210 kg/m^3

From Fig. 6.35, the peak intensity of albite, anorthoclase, nepheline, muscovite, and sodalite in the XRD patterns were higher at higher molarity of NaOH solution (14 M) as compared to lower molarity of NaOH solution (10 M) for both control and 3% NaCl admixed GPC mixes, thereby indicating formation of compact microstructure in GPC made with higher molarity of NaOH solution. The formation of denser microstructure led to lower amount of chloride ions near rebar level as free chloride content was lower at higher molarity of NaOH solution than that at lower molarity of NaOH solution in 3% NaCl admixed GPC mixes (Fig.6.28 (a)). The lower free chloride content resulted in lower corrosion activity of rebar at the age of 600 days in GPC made with higher molarity of NaOH solution (Fig. 6.3 to Fig. 6.6). Further, the peak intensity of albite, anorthoclase, nepheline, muscovite, and sodalite in the XRD patterns were lower in 3% NaCl admixed GPC mixes as compared to control GPC mixes thereby indicating formation of lower amount of geopolymer gels and less compact microstructure in NaCl admixed GPC mixes. Although, less intense peaks of halite were observed in the XRD patterns of NaCl admixed GPC mixes (Fig. 6.35), the peak intensity of halite was comparatively higher in GPC mixes made with higher alkaline solution content than lower alkaline solution content. Similarly, the GPC mixes made with higher molarity of NaOH solution mostly showed higher peak intensity of halite as compared to lower molarity of NaOH solution. The higher peak

intensity of halite in GPC mixes made with higher alkaline solution content as well as higher molarity of NaOH solution may be ascribed to addition of more amount of sodium chloride in GPC mixes during preparation. It may be noted that the NaCl was added in GPC mixes as percentage by mass of geopolymer solids, which includes the solids present in both NaOH and Na_2SiO_3 solutions.

The XRD patterns of GPC near steel reinforcement in prismatic specimens at the age of 600 days are shown in Fig. 6.36 for SS/SH ratios of 1.5 and 1.75.

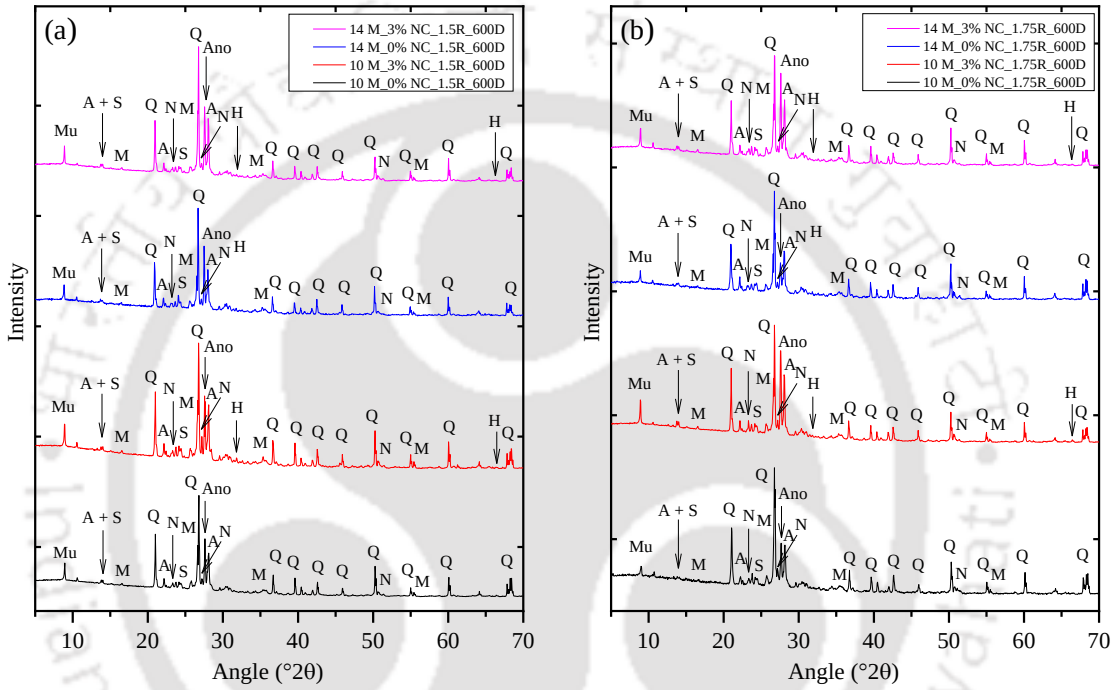

(GPC made with fly ash passing through 150 μm sieve, fly ash content of 425 kg/m^3, and alkaline solution content of 210 kg/m^3)

Fig. 6.36: XRD patterns of GPC near steel reinforcement in prismatic specimens at the age of 600 days for SS/SH ratio of a) 1.5, and b) 1.75

From Fig. 6.36, at the age of 600 days, the peak intensity of albite, anorthoclase, nepheline, muscovite, and sodalite in the XRD patterns were lower in the GPC mixes made with higher SS/SH ratio (1.75) as compared to lower SS/SH ratio (1.5) for control as well as 3% NaCl admixed GPC mixes. This indicates more amount of geopolymer gels in the GPC mixes made with lower SS/SH ratio, which led to higher extent of physical binding of chloride ions with geopolymer gels in NaCl admixed GPC mixes. It may be noted that the bound chloride content was higher in GPC mixes at lower SS/SH ratio as compared to that at higher SS/SH ratio (Fig. 6.29 (c)). From Fig. 6.36, the GPC mixes made with lower molarity of NaOH solution (10 M) showed higher peak intensity of albite, anorthoclase, nepheline, muscovite, and sodalite at

SS/SH ratio of 1.5 whereas the opposite variation was observed at SS/SH ratio of 1.75 i.e., the peak intensity of albite, anorthoclase, nepheline, muscovite, and sodalite were higher at higher molarity of NaOH solution (14 M) for SS/SH ratio of 1.75 in control as well as 3% NaCl admixed GPC mixes. The formation of microstructure of GPC as indicated by above variations in peak intensity of the compounds related to geopolymer gels with molarity of NaOH solution at different SS/SH ratios indicate consistent variation in the availability of chloride ions near rebar level. This is because the free chloride content at the age of 600 days was lower at lower molarity of NaOH solution for SS/SH ratio of 1.5 whereas it was lower at higher molarity of NaOH solution for SS/SH ratio of 1.75 (Fig. 6.29 (a)). The control GPC mixes showed higher peak intensity of the compounds related to geopolymer gels as compared to 3% NaCl admixed GPC mixes irrespective of SS/SH ratio and molarity of NaOH solution as evident from the XRD patterns shown in Fig. 6.36. Further, the XRD patterns of chloride admixed GPC mixes showed presence of halite in the GPC mixes. The peak intensity of halite was mostly higher at higher SS/SH ratio, and higher molarity of NaOH solution as observed from the XRD patterns shown in Fig. 6.36, which indicates comparatively more crystallization of sodium chloride in GPC mixes at higher SS/SH ratio, and higher molarity of NaOH solution.

Fig. 6.37 illustrates the XRD patterns of GPC near steel reinforcement in prismatic specimens at the age of 600 days for fly ash passing through 150 μm sieve, and 300 μm sieve at fly ash content of 425 kg/m^3. From Fig. 6.37, the peak intensity of albite, anorthoclase, nepheline, muscovite, and sodalite were higher in the XRD patterns of GPC mixes made with larger fly ash particles (passing through 300 μm sieve) as compared to smaller fly ash particles (passing through 150 μm sieve) in control as well as 3% NaCl admixed GPC mixes. This indicates presence of comparatively more amount of geopolymer gels in the GPC mixes made with larger fly ash particles that led to denser microstructure and resulted in availability of lower amount of chloride ions near rebar level. It may be noted that, as discussed earlier, the free chloride near rebar level at the age of 600 days was lower in the GPC mixes made with larger fly ash particles as compared to smaller fly ash particles (Fig. 6.30 (a)). With molarity of NaOH solution, the peak intensity of albite, anorthoclase, nepheline, muscovite, and sodalite were higher in the GPC mixes made with higher molarity of NaOH solution (14 M) for fly ash passing through 150 μm sieve whereas the opposite variation in peak intensity of above compounds with molarity of NaOH solution was observed for fly ash passing through 300 μm sieve in chloride admixed GPC mixes (Fig. 6.37). The variations in the microstructure of GPC at the age of 600 days as indicated by the peak intensity of the compounds related to

geopolymer gels in the GPC mixes with molarity of NaOH solution led to the availability of chloride ions near rebar level, which was dependent on the molarity of NaOH solution as well as particle size of fly ash. It may be noted that, the variations in free chloride content (Fig. 6.30 (a)) with molarity of NaOH solution for fly ash of different particle sizes are in line with the variations in the microstructure of GPC as indicated by the peak intensity of albite, anorthoclase, nepheline, muscovite, and sodalite in the XRD patterns of NaCl admixed GPC mixes.

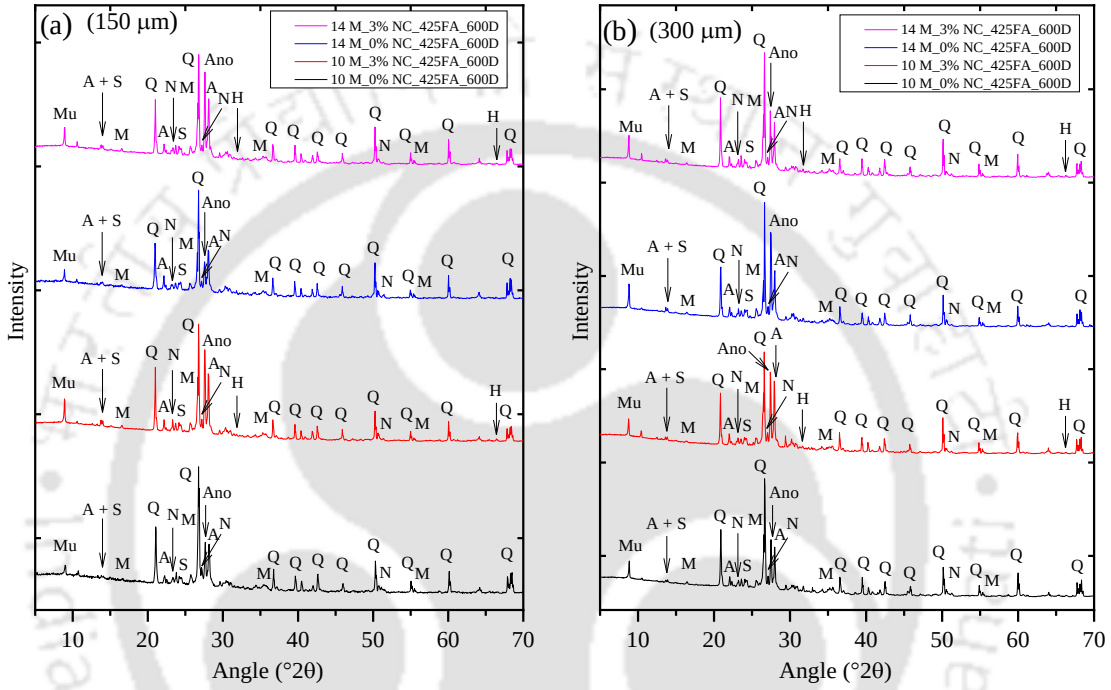

(GPC made with fly ash content of 425 kg/m^3, alkaline solution content of 210 kg/m^3, and SS/SH ratio of 1.75)

Fig. 6.37: XRD patterns of GPC near steel reinforcement in prismatic specimens at the age of 600 days for fly ash passing through a) 150 µm sieve, and b) 300 µm sieve

In control GPC mixes, the peak intensity of albite, anorthoclase, nepheline, muscovite, and sodalite were mostly higher at higher molarity of NaOH solution than lower molarity of NaOH solution thereby indicating formation of more amount of geopolymer gels in GPC mixes made with higher molarity of NaOH solution. Further, the peak intensity of above compounds in the XRD patterns were mostly higher in control GPC mixes as compared to NaCl admixed GPC mixes irrespective of particle size of fly ash, and NaOH solution molarity as observed from Fig. 6.37. The presence of halite in chloride admixed GPC mixes was evident from the XRD patterns shown in Fig. 6.37. Further, the peak intensity of halite was higher in GPC mixes at higher molarity of NaOH solution, and in case of larger fly ash particles as compared to lower molarity of NaOH solution, and smaller fly ash particles as inferred from the XRD patterns shown in Fig. 6.37.

Fig. 6.38 and Fig. 6.39 show the XRD patterns of GPC near rebar level in prismatic specimens at the age of 600 days for fly ash passing through 150 μm sieve, and 300 μm sieve at fly ash content of 450 kg/m^3. From Fig. 6.38 and Fig. 6.39, in control GPC mixes, the peak intensity of albite, anorthoclase, nepheline, muscovite, and sodalite in the XRD patterns were mostly higher in the mixes made with larger fly ash particles (passing through 300 μm sieve) as compared to that made with smaller fly ash particles (passing through 150 μm sieve) irrespective of molarity of NaOH solution thereby indicating presence of more amount of geopolymer gels in GPC mixes made with larger fly ash particles. In NaCl admixed GPC mixes, mostly there was unsystematic variation in peak intensity of muscovite and sodalite with particle size of fly ash. Further, the peak intensity of albite, anorthoclase, and nepheline were mostly higher in the mixes made with larger fly ash particles as compared to smaller fly ash particles for different concentrations of NaCl as observed from Fig. 6.38 and Fig. 6.39. This indicates presence of more amount of N-A-S-H gel in GPC mixes made with larger fly ash particles that led to formation of denser microstructure, and resulted in lower free chloride content near rebar level (Fig. 6.31 (a)) and more chloride binding with geopolymer gels leading to higher bound chloride content at the age of 600 days (Fig. 6.31 (c)).

From Fig. 6.38 and Fig. 6.39, there was unsystematic variation in peak intensity of albite, anorthoclase, nepheline, muscovite, and sodalite with molarity of NaOH solution in control GPC mixes for both sizes of fly ash particles. In NaCl admixed GPC mixes, the peak intensity of albite, anorthoclase, nepheline, muscovite, and sodalite in XRD patterns were mostly higher at higher molarity of NaOH solution as compared to lower molarity of NaOH solution for both sizes of fly ash particles thereby indicating comparatively more formation of geopolymer gels, which led to denser microstructure at higher molarity of NaOH solution. This resulted in lower free chloride content near steel reinforcement as observed from Fig. 6.31 (a)). The formation of more amount of geopolymer gels at higher molarity of NaOH solution as indicated by the XRD patterns resulted in comparatively more extent of physical binding of chloride ions with geopolymer gels that led to more bound chloride content as observed from Fig. 6.31 (c)).

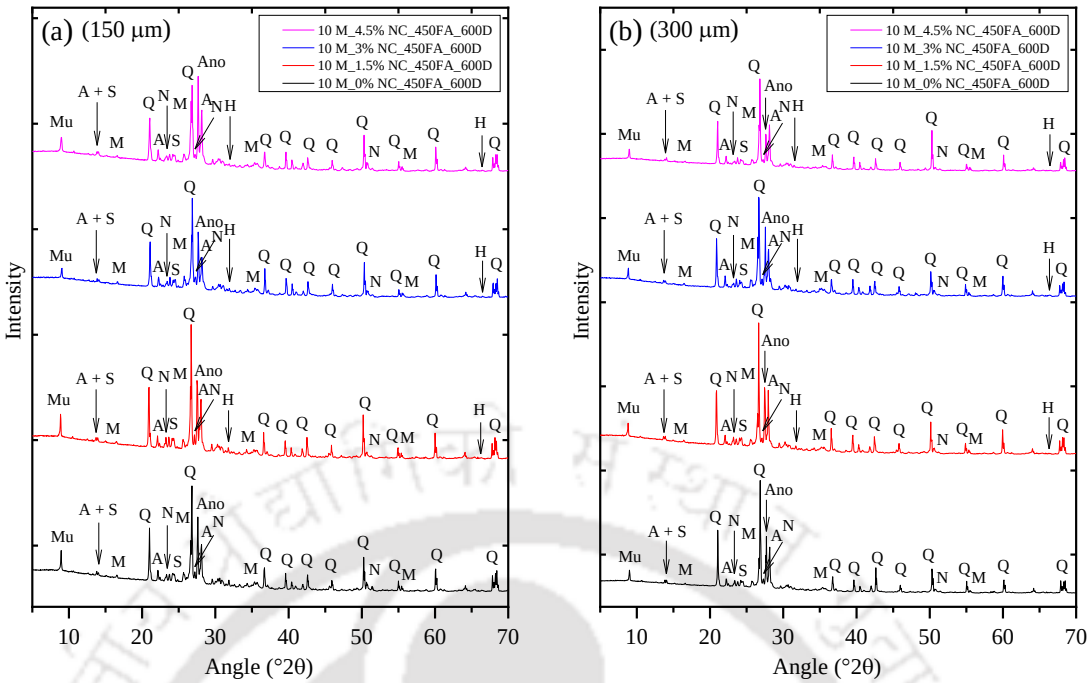

(GPC made with fly ash content of 450 kg/m^3, alkaline solution content of 210 kg/m^3, and SS/SH ratio of 1.75)

Fig. 6.38: XRD patterns of GPC near steel reinforcement in prismatic specimens at the age of 600 days for fly ash passing through a) 150 µm sieve, and b) 300 µm sieve for NaOH solution of 10 M

From Fig. 6.38 and Fig. 6.39, the peak intensity of albite, anorthoclase, nepheline, muscovite, and sodalite were lower in NaCl admixed GPC mixes as compared to control GPC mixes. This indicates less formation of geopolymer gels in GPC mixes in the presence of NaCl. Further, the peak intensity of above compounds in XRD patterns mostly decreased with increase in admixed NaCl concentration in GPC mixes. This indicates formation of comparatively less amount of geopolymer gels at higher concentration of admixed NaCl that led to availability of more chloride content near steel reinforcement in prismatic specimens as the free chloride content was higher at higher concentration of admixed NaCl (Fig. 6.31 (a)). From Fig. 6.38 and Fig. 6.39, mostly there was unsystematic variation in the peak intensity of halite with particle size of fly ash, molarity of NaOH solution and admixed NaCl concentration.

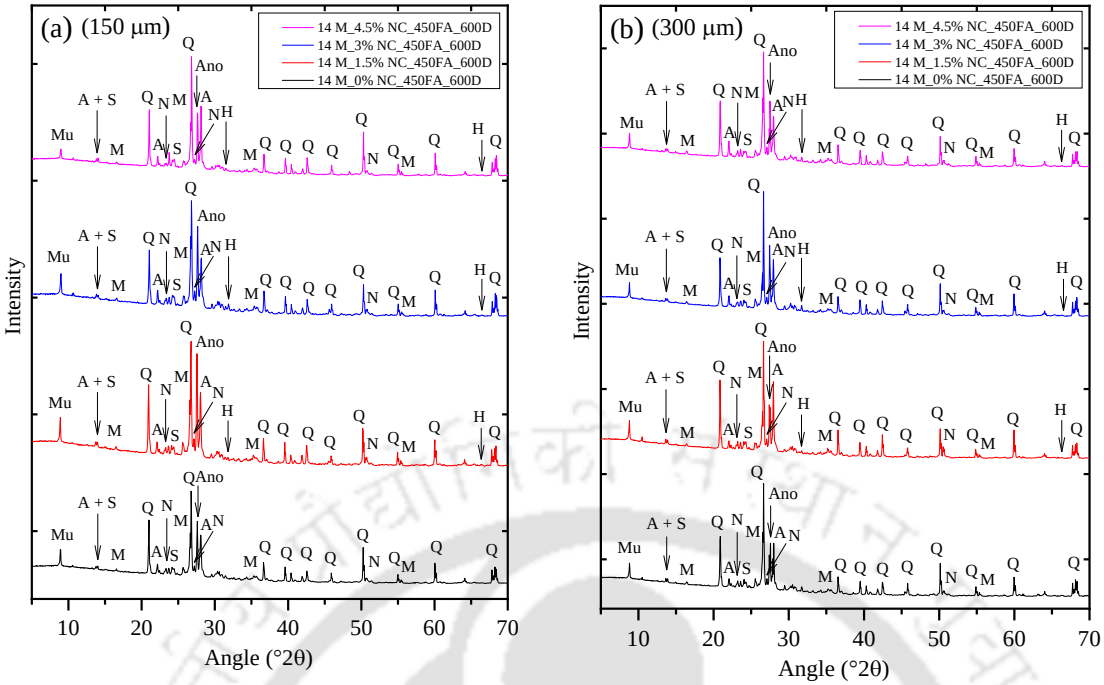

(GPC made with fly ash content of 450 kg/m^3, alkaline solution content of 210 kg/m^3, and SS/SH ratio of 1.75)

Fig. 6.39: XRD patterns of GPC near steel reinforcement in prismatic specimens at the age of 600 days for fly ash passing through a) 150 µm sieve, and b) 300 µm sieve for NaOH solution of 14 M

The obtained XRD patterns of GPC near steel reinforcement in prismatic specimens at the age of 600 days are shown in Fig. 6.40 for fly ash contents of 425 kg/m^3 and 450 kg/m^3 for GPC mixes made with fly ash passing through 150 µm sieve. From Fig. 6.40, the peak intensity of albite, anorthoclase, nepheline, muscovite, and sodalite in the XRD patterns were higher at higher fly ash content (450 kg/m^3) as compared to lower fly ash content (425 kg/m^3) in control as well as 3% NaCl admixed GPC mixes irrespective of molarity of NaOH solution. This indicates more formation of geopolymer gels in GPC mixes made with higher fly ash content. It may be noted that the free chloride content near steel reinforcement in GPC specimens at the age of 600 days was higher in GPC mixes made with higher fly ash content as compared to lower fly ash content (Fig. 6.32 (a)). Although, there was more formation of geopolymer gels in GPC mixes made with higher fly ash content as indicated by the peak intensity of associated compounds in the XRD patterns, the higher free chloride content near steel reinforcement may possibly be due to the effect of release of physically adsorbed chloride ions from geopolymer gels to a comparatively higher extent in GPC mixes made with higher fly ash content.

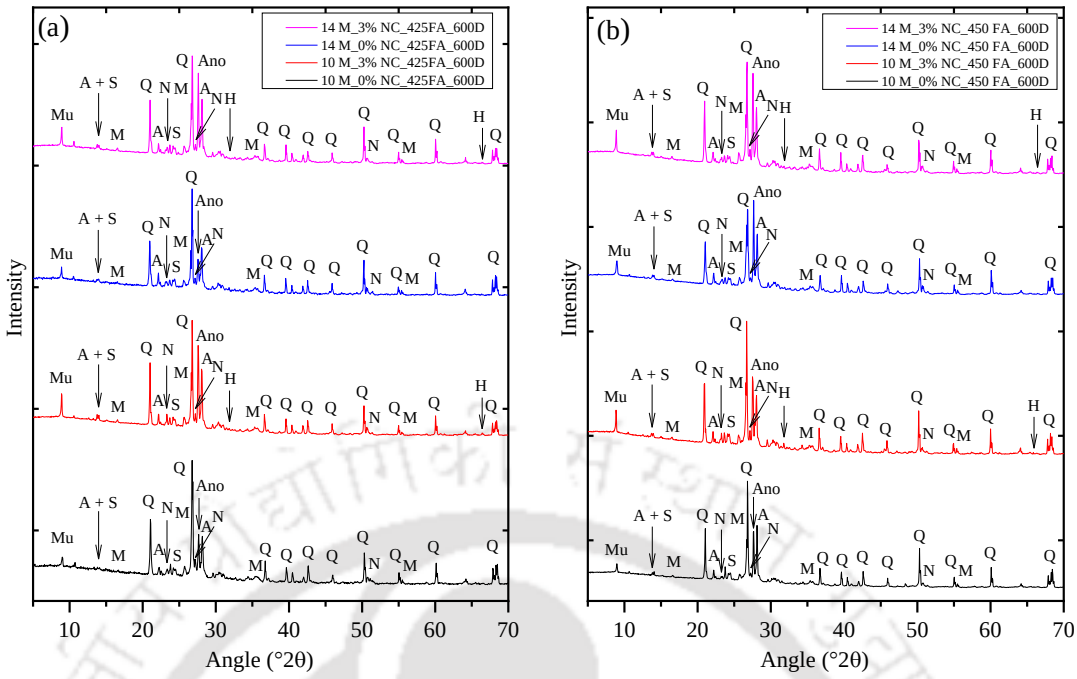

(GPC made with fly ash passing through 150 μm sieve, alkaline solution content of 210 kg/m^3 and SS/SH ratio of 1.75)

Fig. 6.40: XRD patterns of GPC near steel reinforcement in prismatic specimens at the age of 600 days for fly ash content of a) 425 kg/m^3, and b) 450 kg/m^3

The peak intensity of the compounds related to geopolymer gels were higher in control GPC mixes as compared to 3% NaCl admixed GPC mixes near rebar level in prismatic specimens as evident from the XRD patterns shown in Fig. 6.40. Further, the peak intensity of albite, anorthoclase, nepheline, muscovite, and sodalite in the XRD patterns were higher at higher molarity of NaOH solution (14 M) as compared to lower molarity of NaOH solution (10 M) in control GPC mixes for both fly ash contents as observed from Fig. 6.40, thereby indicating more formation of geopolymer gels at higher molarity of NaOH solution. In 3% NaCl admixed GPC mixes, the peak intensity of the compounds related to geopolymer gels in XRD patterns were higher at higher molarity of NaOH solution for fly ash content of 425 kg/m^3, whereas there was opposite variation in peak intensity of the compounds related to geopolymer gels with molarity of NaOH solution for fly ash content of 450 kg/m^3. This indicates that the dominant effect of presence of chloride ions might have altered the formation of geopolymer gels at higher molarity of NaOH solution for fly ash content of 450 kg/m^3 as indicated by the peak intensity of the compounds related to geopolymer gels in the XRD patterns. As already discussed earlier, the free chloride content near rebar level in prismatic specimens at the age of 600 days was higher in the GPC mixes made with lower molarity of NaOH solution than higher molarity of NaOH solution for both fly ash contents (Fig. 6.32 (a)). Thus, higher free

chloride content near steel reinforcement in GPC mixes made with lower molarity of NaOH solution, even though there was more amount of geopolymer gels as indicated from the XRD patterns for higher fly ash content, may be attributed to the dominant effect of release of physically bound chloride ions from geopolymer gels to a greater extent at lower molarity of NaOH solution than higher molarity of NaOH solution. The XRD patterns shown in Fig. 6.40 indicate unsystematic variation in the peak intensity of halite with fly ash content and molarity of NaOH solution of GPC mixes.

The XRD patterns of GPC near steel reinforcement in prismatic specimens at the age of 600 days for fly ash contents of 425 kg/m^3 and 450 kg/m^3 are shown in Fig. 6.41 and Fig. 6.42 for NaOH solution of 10 M and 14 M respectively for GPC mixes made with fly ash passing through 300 µm sieve. From Fig. 6.41 and Fig. 6.42, the peak intensity of albite, anorthoclase, nepheline, muscovite, and sodalite in the XRD patterns were mostly higher at higher fly ash content (450 kg/m^3) than lower fly ash content (425 kg/m^3) in control GPC mixes near steel reinforcement in prismatic specimens. However, in NaCl admixed GPC mixes, the peak intensity of albite, anorthoclase, nepheline, muscovite, and sodalite in XRD patterns were mostly higher at lower fly ash content as compared to that at higher fly ash content for larger fly ash particles (passing through 300 µm sieve). This indicates that the particle size of fly ash might have influenced the extent of formation of geopolymer gels in GPC mixes in the presence of NaCl as opposite variation in peak intensity of the compounds related to geopolymer gels in XRD patterns with fly ash content was observed in GPC mixes made with smaller fly ash particles (passing through 150 µm sieve, Fig. 6.40). The formation of comparatively more amount of geopolymer gels at lower fly ash content in NaCl admixed GPC mixes as indicated by the XRD patterns might have led to lower amount of chloride ions as the free chloride content near steel reinforcement in the prismatic specimens at the age of 600 days was mostly lower at lower fly ash content as compared to higher fly ash content (Fig. 6.33 (a)). From Fig. 6.41 and Fig. 6.42, in control mixes, the peak intensity of compounds related to geopolymer gels in XRD patterns were higher at lower molarity of NaOH solution (10 M) than higher molarity of NaOH solution (14 M) at fly ash content of 450 kg/m^3, however, at fly ash content of 425 kg/m^3, mostly opposite variation was observed in peak intensity of the compounds related to geopolymer gels with molarity of NaOH solution. In NaCl admixed mixes, the peak intensity of compounds related to geopolymer gels were mostly higher at higher molarity of NaOH solution (14 M) than lower molarity of NaOH solution (10 M) for both fly ash contents. Although, there was more formation of geopolymer gels at higher

molarity of NaOH solution in NaCl admixed GPC mixes as indicated by the XRD patterns, as discussed earlier, there was unsystematic variation in free chloride content near rebar level with molarity of NaOH solution at the age of 600 days (Fig. 6.33 (a)). This may be ascribed to the dominant effect of variations in the extent of interaction of chloride ions with the geopolymer gels that led to alterations in chloride ion concentration in the pore solution of GPC.

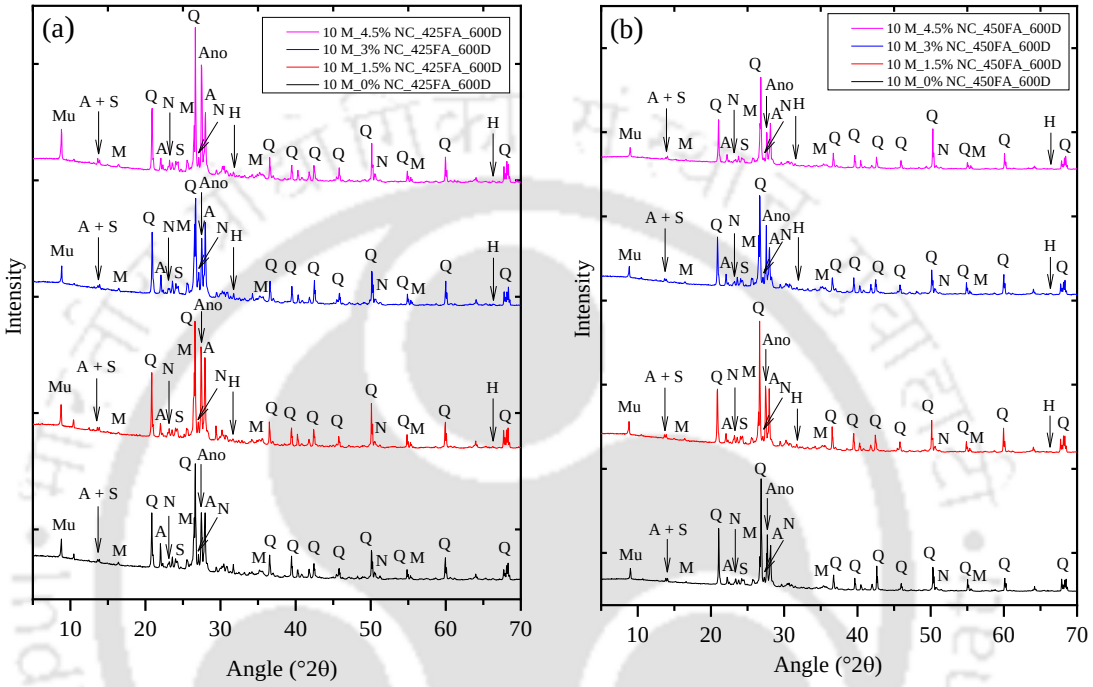

(GPC made with fly ash passing through 300 μm sieve, alkaline solution content of 210 kg/m^3 and SS/SH ratio of 1.75)

Fig. 6.41: XRD patterns of GPC near steel reinforcement in prismatic specimens at the age of 600 days for fly ash content of a) 425 kg/m^3, and b) 450 kg/m^3 for NaOH solution of 10 M

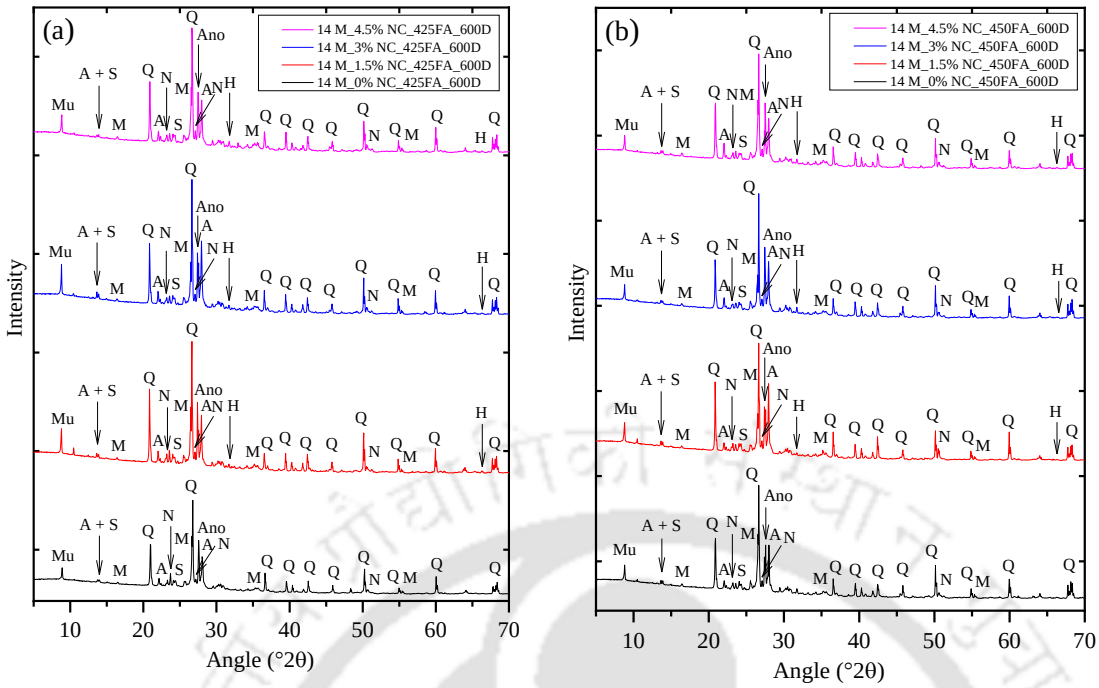

(GPC made with fly ash passing through 300 μm sieve, alkaline solution content of 210 kg/m^3 and SS/SH ratio of 1.75)

Fig. 6.42: XRD patterns of GPC near steel reinforcement in prismatic specimens at the age of 600 days for fly ash content of a) 425 kg/m^3, and b) 450 kg/m^3 for NaOH solution of 14 M

The XRD patterns shown in Fig. 6.41 and Fig. 6.42 indicated more formation of geopolymer gels in control GPC mixes as compared to NaCl admixed GPC mixes, as the peak intensity of albite, anorthoclase, nepheline, muscovite, and sodalite were mostly higher in control mixes than NaCl admixed mixes. Further, there was unsystematic variation in peak intensity of the compounds related to geopolymer gels in XRD patterns between NaCl concentrations of 1.5% and 3%, however, the peak intensity of the compounds related to the geopolymer gels were mostly lower at NaCl concentration of 4.5% as compared to 3% as observed from Fig. 6.41 and 6.42. This indicates mostly lower formation of geopolymer gels in GPC mixes admixed with comparatively higher concentration of NaCl that led to formation of less denser microstructure and resulted in comparatively higher free chloride content near steel reinforcement at the age of 600 days in prismatic specimens admixed with comparatively higher concentration of NaCl (Fig. 6.33 (a)). The XRD patterns shown in Fig. 6.41 and Fig. 6.42 indicated mostly unsystematic variation in the peak intensity of halite with molarity of NaOH solution and fly ash content. However, the peak intensity of halite was mostly higher at higher concentration of admixed NaCl as compared to lower concentration of admixed NaCl in the GPC mixes as observed from the XRD patterns shown in Fig. 6.41 and Fig. 6.42.

6.4.2 FTIR-Attenuated Total Reflectance (ATR) analysis

The obtained FTIR spectra of GPC near rebar level in prismatic specimens at the age of 600 days are shown in Fig. 6.43 for different molarity of NaOH solution i.e., 8 M, 10 M, 12 M, 14 M and 16 M and different concentrations of admixed NaCl i.e., 1.5%, 3% and 4.5%. In the FTIR spectra, the peak in the range of 773 cm^{-1} - 777 cm^{-1} indicates the tetrahedral bending vibration of Si–O–Si bond corresponding to quartz in the GPC mixes [96]. From Fig. 6.43, the peak ranging from 995 cm^{-1} to 1003 cm^{-1} irrespective of molarity of NaOH solution and admixed NaCl concentration is attributed to the asymmetric stretching vibration of Si–O–Si(Al) bond, which indicates the presence of geopolymer gels (N-A-S-H) in the GPC mixes [90]. When compared with the FTIR spectra of raw fly ash (Fig. 3.1(c), Chapter 3), the observed peak corresponding to Si–O–Si(Al) bond at 1052 cm^{-1} in raw fly ash shifted to lower wavenumbers in GPC mixes thereby indicating the formation of geopolymer gels in the GPC mixes as a result of geopolymerization process.

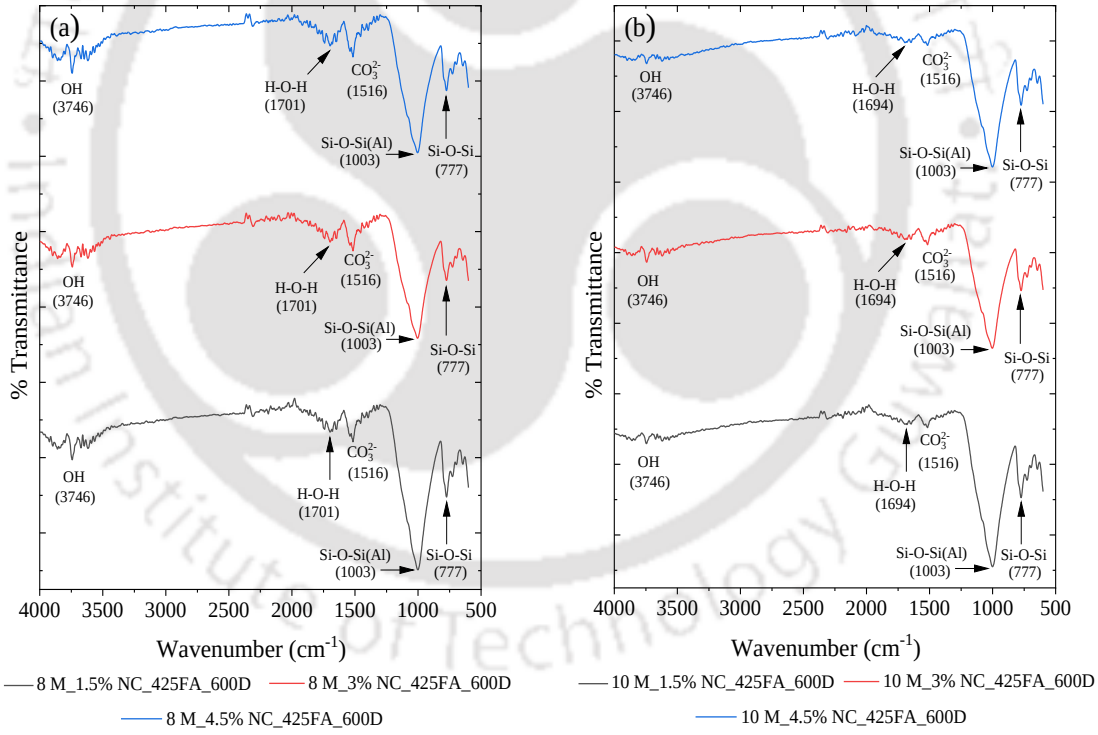

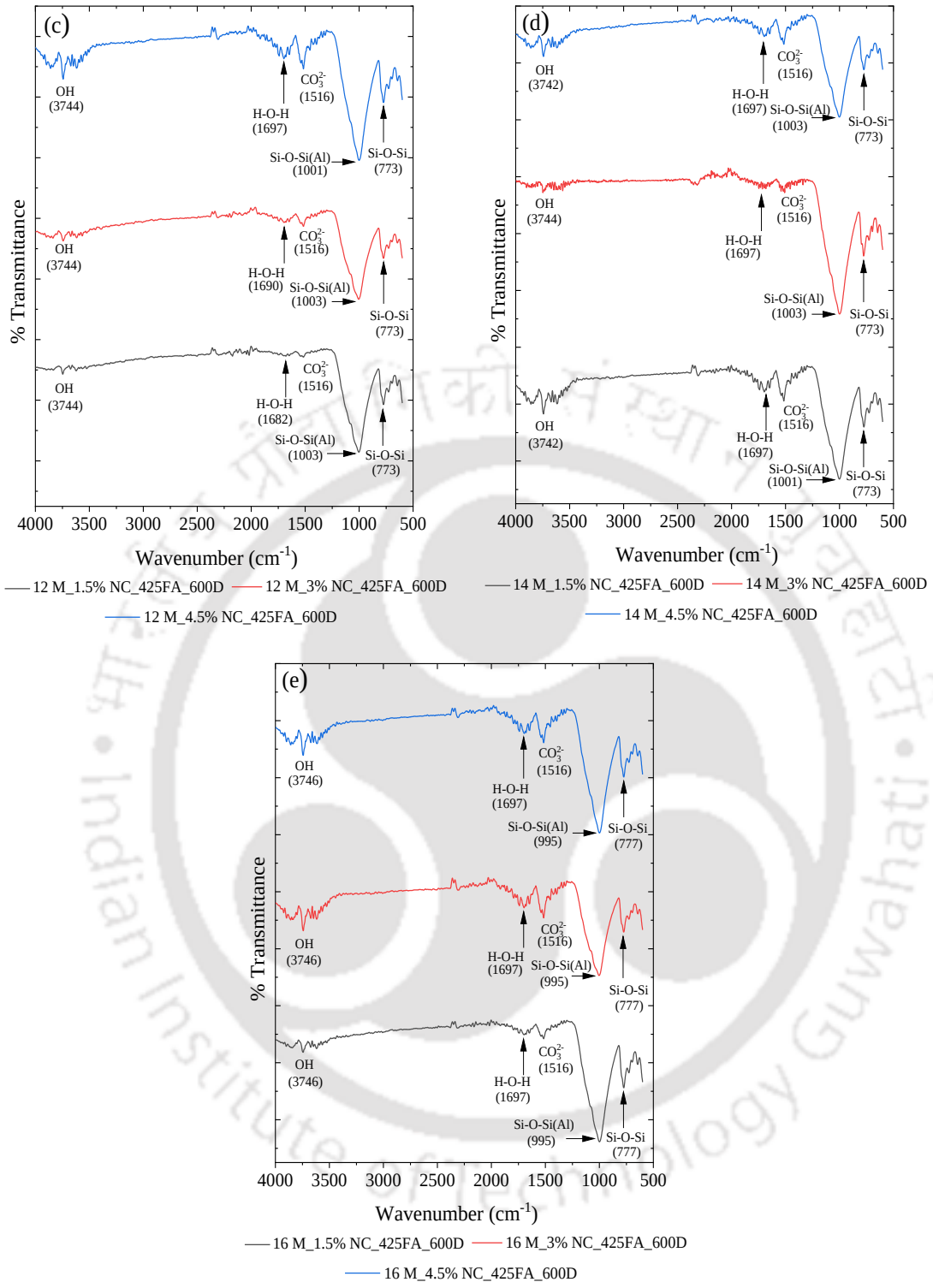

(GPC made with fly ash passing through 300 μm sieve, fly ash content of 425 kg/m^3, alkaline solution content of 210 kg/m^3, and SS/SH ratio of 1.75)

Fig. 6.43: FTIR spectra of GPC near rebar in prismatic specimens at the age of 600 days: a) 8 M NaOH solution, b) 10 M NaOH solution, c) 12 M NaOH solution, d) 14 M NaOH solution, and e) 16 M NaOH solution, for different concentrations of admixed sodium chloride

Although, there was a narrow range of wavenumbers, the peak corresponding to asymmetric stretching vibration of Si–O–Si(Al) bond in GPC mixes shifted to lower wavenumbers particularly at higher molarity of NaOH solution i.e., 14 M and 16 M, which indicates comparatively higher extent of geopolymerization process at higher molarity of NaOH solution [59]. This is in line with the results of XRD analysis (Fig. 6.34), where the peak intensity of the compounds related to sodium aluminosilicate hydrate gel were mostly higher at higher molarity of NaOH solution. From Fig. 6.43, mostly there was unsystematic variation in the wavenumbers corresponding to the peak indicating the asymmetric stretching vibration of Si–O–Si(Al) bond with admixed NaCl concentration in the GPC mixes. In Fig. 6.43, the band in the region of 1516 cm^{-1} is related to the stretching vibration of carbonate group (CO_3^{2-}) in GPC mixes [97,98]. The band located in the range of 1682 - 1701 cm^{-1}, and the peak located in the range of 3742 - 3746 cm^{-1} in the FTIR spectra in Fig. 6.43 correspond to the bending vibration of H–O–H group, and stretching vibration of –OH group respectively indicating the presence of adsorbed water molecules in the geopolymer gels in GPC mixes [43,99].

The FTIR spectra of 3% NaCl admixed GPC near steel reinforcement in prismatic specimens at the age of 600 days are illustrated in Fig. 6.44 for alkaline solution contents of 190 kg/m^3 and 210 kg/m^3.

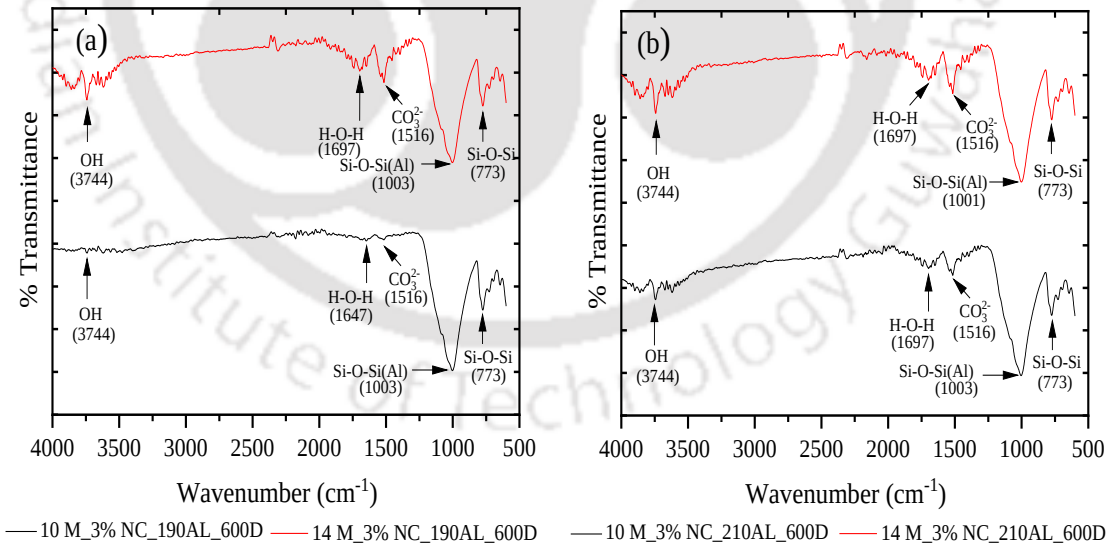

(GPC made with fly ash passing through 150 μm sieve, fly ash content of 425 kg/m^3, and SS/SH ratio of 1.75)

Fig. 6.44: FTIR spectra of GPC near rebar in prismatic specimens at the age of 600 days for alkaline solution content of a) 190 kg/m^3, and b) 210 kg/m^3

From Fig. 6.44, the peak at 773 cm^{-1} in the FTIR spectra indicated the presence of quartz in the GPC mixes [96]. In the FTIR spectra, the peak in the range of 1001 cm^{-1} to 1003 cm^{-1} is

associated with the asymmetric stretching vibration of Si–O–Si(Al) bond that indicates the formation of geopolymer gels in GPC mixes. The observed peak corresponding to asymmetric stretching vibration of Si–O–Si(Al) bond in GPC mixes shifted to lower wavenumbers when compared with that of raw fly ash in the FTIR spectra shown in Fig. 3.1(c). Further, the asymmetric stretching vibration of Si–O–Si(Al) bond in GPC mixes did not alter with alkaline solution content, and molarity of NaOH solution as observed from the corresponding wavenumbers in the FTIR spectra shown in Fig. 6.44. In the FTIR spectra, the band at 1516 cm^{-1} indicates the stretching vibration of carbonate group in the GPC mixes. Further, the band in the range of 1647 cm^{-1} to 1697 cm^{-1}, and the peak at 3744 cm^{-1} in the FTIR spectra of GPC mixes are associated with the bending vibration of H–O–H group, and stretching vibration of –OH group respectively.

Fig. 6.45 illustrates the FTIR spectra of 3% NaCl admixed GPC near rebar level in prismatic specimens at the age of 600 days for SS/SH ratios of 1.5 and 1.75. In the FTIR spectra, the peak corresponding to asymmetric stretching vibration of Si–O–Si(Al) bond appearing in the range of 1001 cm^{-1} to 1003 cm^{-1} indicates the presence of geopolymer gels in GPC mixes. The wavenumber of the peak corresponding to asymmetric stretching vibration of Si–O–Si(Al) bond did not alter with change in SS/SH ratio as observed from Fig. 6.45. However, it shifted to comparatively lower wavenumbers with increase in molarity of NaOH solution from 10 M to 14 M for both SS/SH ratios as evident from Fig. 6.45. The peak in the range of 773 cm^{-1} to 777 cm^{-1}, and the band in the range of 1510 cm^{-1} to 1516 cm^{-1} are associated with quartz, and stretching vibration of carbonate group respectively. Similarly, the peak located in the range of 3744 cm^{-1} - 3746 cm^{-1}, and the band in the range 1697 cm^{-1} - 1701 cm^{-1} are related to the stretching vibration of –OH group, and bending vibration of H–O–H group respectively. This indicates the presence of adsorbed water in geopolymeric products in GPC mixes.

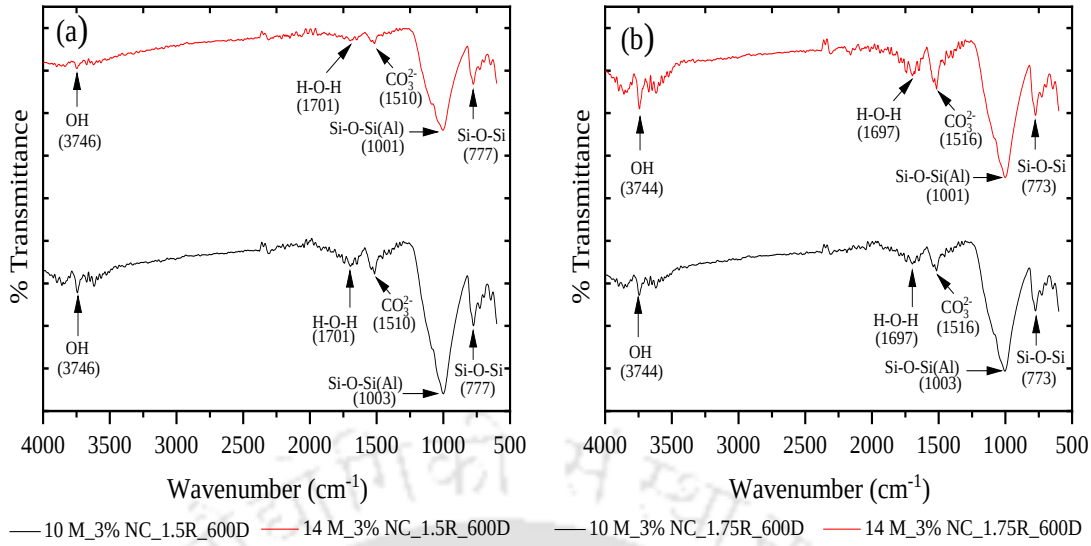

(GPC made with fly ash passing through 150 μm sieve, fly ash content of 425 kg/m^3, and alkaline solution content of 210 kg/m^3)

Fig. 6.45: FTIR spectra of GPC near rebar in prismatic specimens at the age of 600 days for a) SS/SH ratio of 1.5, and b) SS/SH ratio of 1.75

Fig. 6.46 shows the FTIR spectra of GPC near steel reinforcement in prismatic specimens at the age of 600 days for fly ash passing through 150 μm sieve, and 300 μm sieve at fly ash content of 425 kg/m^3. In Fig. 6.46, for both sizes of fly ash particles, the peak corresponding to the asymmetric stretching vibration of Si–O–Si(Al) bond in GPC mixes shifted to lower wavenumbers (in the range of 1001 cm^{-1} to 1003 cm^{-1}) when compared with that of raw fly ash (1052 cm^{-1} in FTIR spectra shown in Fig. 3.1(c)). Further, the asymmetric stretching vibration of Si–O–Si(Al) bond in GPC mixes did not vary with particle size of fly ash, and molarity of NaOH solution as observed from the wavenumbers in the FTIR spectra shown in Fig. 6.46. In the FTIR spectra, the band in the range of 773 cm^{-1} to 777 cm^{-1}, at 1516 cm^{-1}, and from 1694 cm^{-1} to 1697 cm^{-1}, and the peak in the range of 3744 cm^{-1} to 3746 cm^{-1} are associated with quartz, stretching vibration of carbonate group, bending vibration of H–O–H group, and stretching vibration of –OH group respectively.

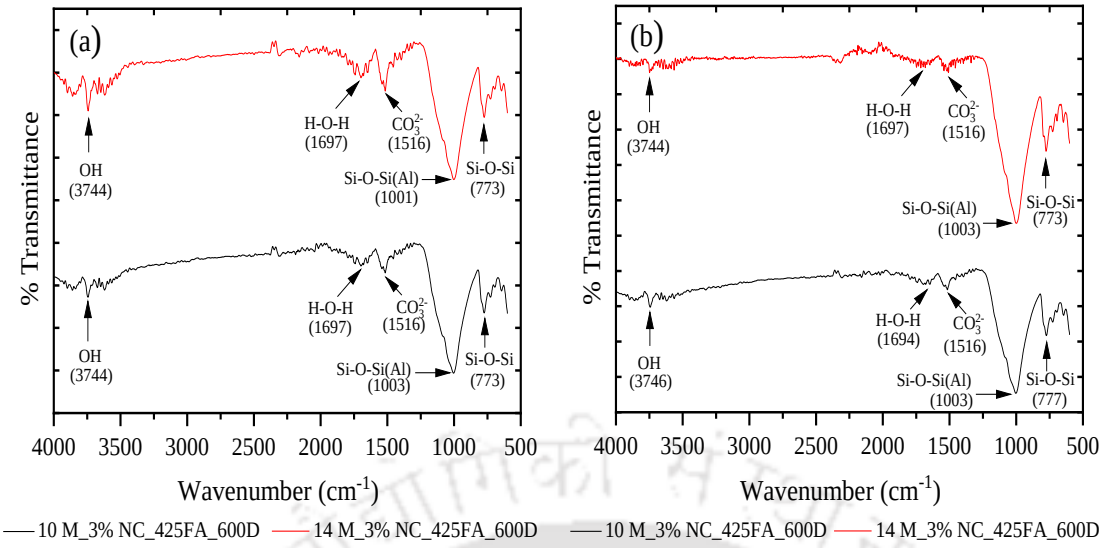

(GPC made with fly ash content of 425 kg/m^3, alkaline solution content of 210 kg/m^3, and SS/SH ratio of 1.75)

Fig. 6.46: FTIR spectra of GPC near rebar in prismatic specimens at the age of 600 days for fly ash passing through a) 150 µm sieve, and b) 300 µm sieve

The FTIR spectra of GPC near rebar level in prismatic specimens at the age of 600 days for fly ash passing through 150 µm sieve, and 300 µm sieve are shown in Fig. 6.47 and 6.48 for fly ash content of 450 kg/m^3. In the FTIR spectra shown in Fig. 6.47 and Fig. 6.48, the wavenumber of the peak corresponding to asymmetric stretching vibration of Si–O–Si(Al) bond did not vary significantly with particle size of fly ash, molarity of NaOH solution and admixed NaCl concentration in GPC mixes as the peak appeared in a narrow range i.e., from 1001 cm^{-1} to 1003 cm^{-1}. The peak corresponding to asymmetric stretching vibration of Si–O–Si(Al) bond, although there was a narrow range, shifted to lower wavenumber for fly ash passing through 300 µm sieve as compared to that passing through 150 µm sieve for 14 M NaOH solution. This indicates comparatively higher extent of geopolymerization reaction in case of GPC made with larger fly ash particles, which is in line with the results of XRD analysis (Fig. 6.38 and Fig. 6.39), where the peak intensity of albite, anorthoclase, and nepheline were mostly higher in case of GPC made with larger fly ash particles than smaller fly ash particles. In the FTIR spectra shown in Fig. 6.47 and Fig. 6.48, the band in the range of 774 cm^{-1} - 780 cm^{-1}, 1510 cm^{-1} - 1516 cm^{-1}, and 1688 cm^{-1} - 1703 cm^{-1}, and the peak in the range of 3742 cm^{-1} - 3746 cm^{-1} are related to quartz, stretching vibration of carbonate group, bending vibration of H–O–H group, and stretching vibration of –OH group respectively irrespective of particle size of fly ash, molarity of NaOH solution and admixed NaCl concentration in GPC mixes.

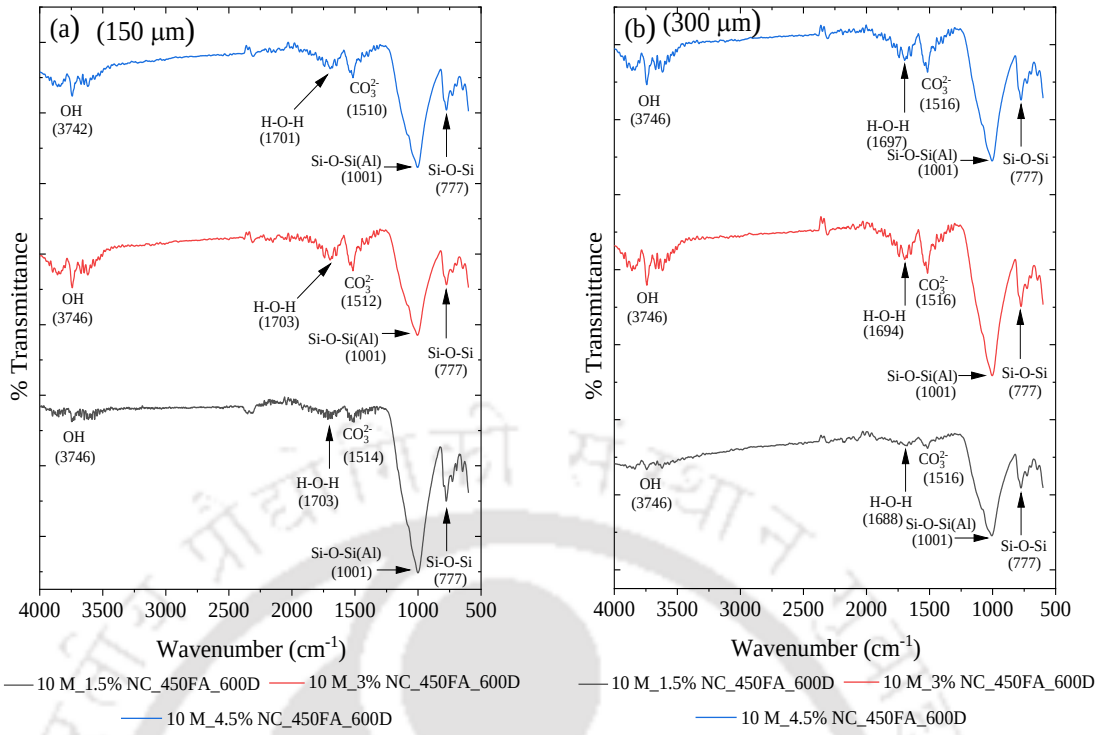

(GPC made with fly ash content of 450 kg/m^3, alkaline solution content of 210 kg/m^3, and SS/SH ratio of 1.75)

Fig. 6.47: FTIR spectra of GPC near rebar level in prismatic specimens at the age of 600 days for fly ash passing through a) 150 µm sieve, and b) 300 µm sieve for NaOH solution of 10 M

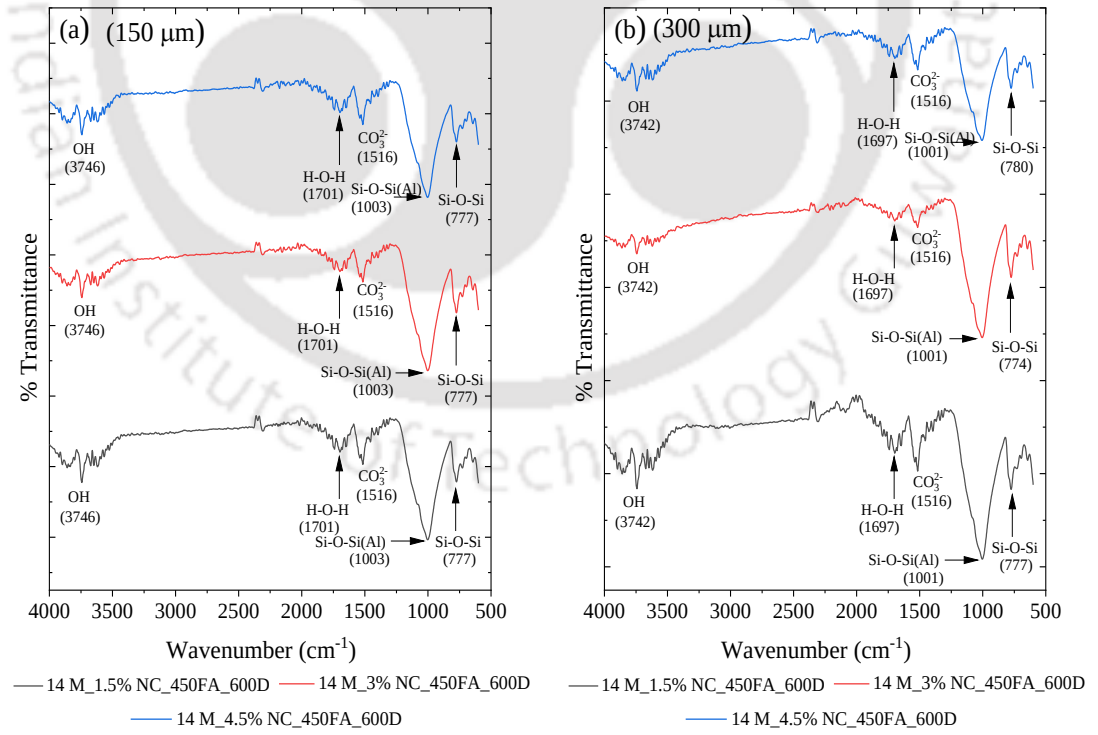

(GPC made with fly ash content of 450 kg/m^3, alkaline solution content of 210 kg/m^3, and SS/SH ratio of 1.75)

Fig. 6.48: FTIR spectra of GPC near rebar level in prismatic specimens at the age of 600 days for fly ash passing through a) 150 µm sieve, and b) 300 µm sieve for NaOH solution of 14 M

For fly ash passing through 150 µm sieve, the FTIR spectra of GPC near rebar level in prismatic specimens at the age of 600 days for fly ash contents of 425 kg/m^3 and 450 kg/m^3 are shown in Fig. 6.49.

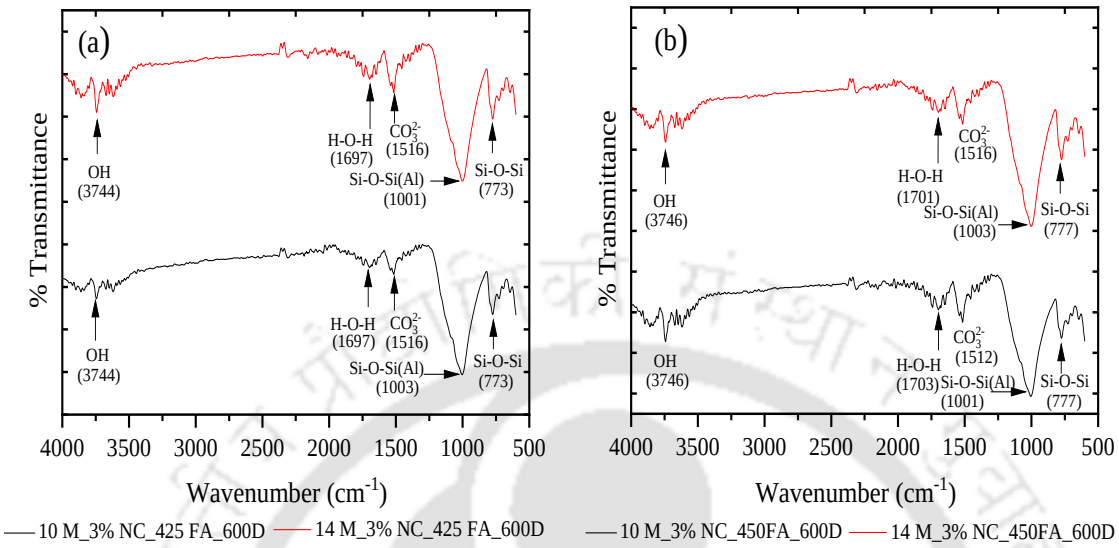

(GPC made with fly ash passing through 150 µm sieve, alkaline solution content of 210 kg/m^3 and SS/SH ratio of 1.75)

Fig. 6.49: FTIR spectra of GPC near rebar level in prismatic specimens at the age of 600 days for fly ash content of a) 425 kg/m^3, and b) 450 kg/m^3

In Fig. 6.49, the band in the range of 773 cm^{-1} to 777 cm^{-1}, 1512 cm^{-1} to 1516 cm^{-1}, and 1697 cm^{-1} to 1703 cm^{-1}, and the peak in the range of 3744 cm^{-1} to 3746 cm^{-1} correspond to quartz, stretching vibration of carbonate group, bending vibration of H–O–H group, and stretching vibration of –OH group respectively for both fly ash contents and molarity of NaOH solution. In the FTIR spectra shown in Fig. 6.49, there was unsystematic variation in the wavenumber corresponding to the peak indicating the asymmetric stretching vibration of Si–O–Si(Al) bond with fly ash content. However, although there was a narrow range, the peak corresponding to asymmetric stretching vibration of Si–O–Si(Al) bond shifted to lower wavenumbers at higher molarity of NaOH solution (14 M) when compared with lower molarity of NaOH solution (10 M) for fly ash content of 425 kg/m^3 whereas there was opposite variation in the wavenumber corresponding to the peak indicating the asymmetric stretching vibration of Si–O–Si(Al) bond with molarity of NaOH solution for fly ash content of 450 kg/m^3. These variations in the wavenumbers corresponding to the peak indicating the asymmetric stretching vibration of Si–O–Si(Al) bond with molarity of NaOH solution are in line with the variations in the peak intensity of the compounds related to sodium aluminosilicate hydrate gel with molarity of NaOH solution as observed from the XRD patterns shown in Fig. 6.40.

For fly ash passing through 300 µm sieve, the obtained FTIR spectra of GPC near rebar level in prismatic specimens at the age of 600 days for fly ash contents of 425 kg/m^3 and 450 kg/m^3 are shown in Fig. 6.50 and Fig. 6.51 for NaOH solution of 10 M and 14 M respectively. In the FTIR spectra shown in Fig. 6.50 and Fig. 6.51, the peak corresponding to asymmetric stretching vibration of Si–O–Si(Al) bond appeared in a narrow range of wavenumber i.e., from 1001 cm^{-1} to 1003 cm^{-1}. The peak corresponding to asymmetric stretching vibration of Si–O–Si(Al) bond mostly shifted to lower wavenumbers at higher fly ash content (450 kg/m^3) when compared with lower fly ash content (425 kg/m^3) as observed from Fig. 6.50 and 6.51. From Fig. 6.50 and Fig. 6.51, the peak corresponding to asymmetric stretching vibration of Si–O–Si(Al) bond did not vary with the molarity of NaOH solution and admixed NaCl concentration for both fly ash contents.

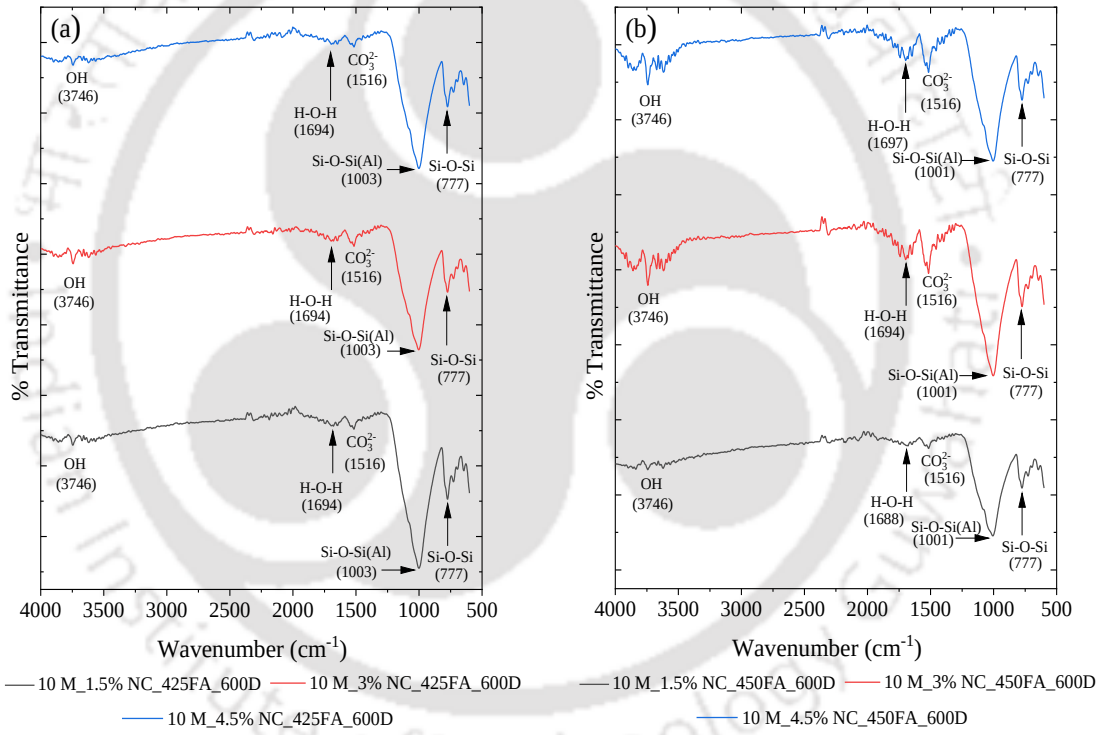

(GPC made with fly ash passing through 300 µm sieve, alkaline solution content of 210 kg/m^3 and SS/SH ratio of 1.75)

Fig. 6.50: FTIR spectra of GPC near rebar level in prismatic specimens at the age of 600 days for fly ash content of a) 425 kg/m^3, and b) 450 kg/m^3 for NaOH solution of 10 M

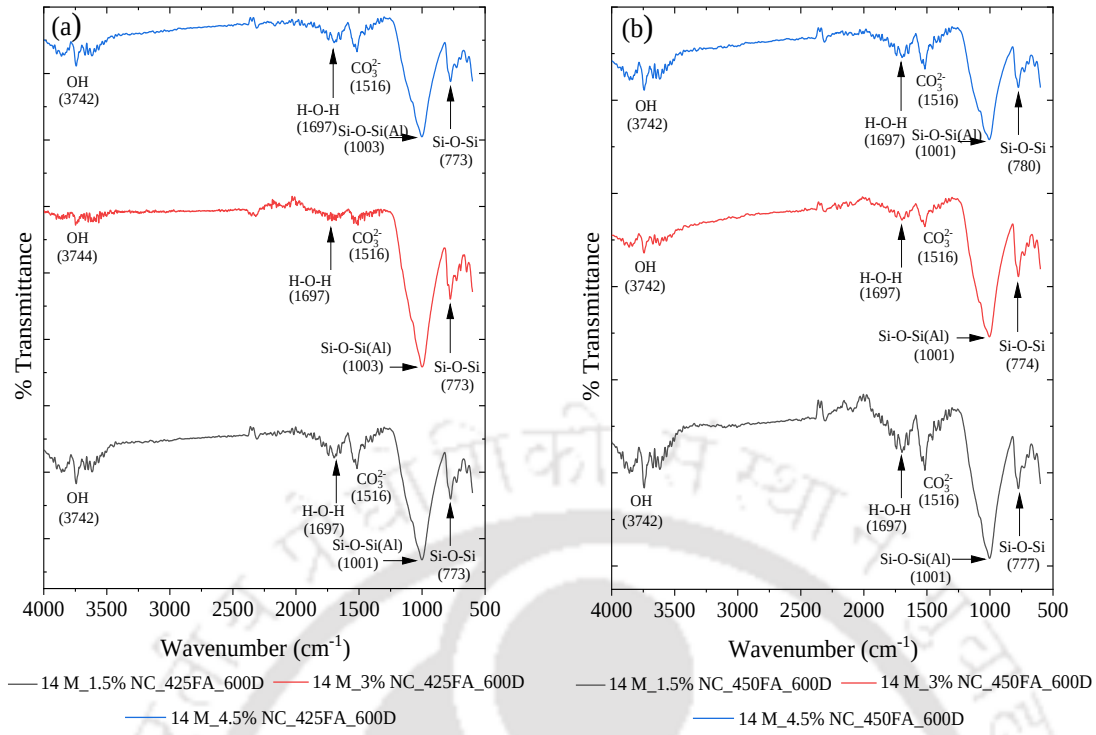

(GPC made with fly ash passing through 300 μm sieve, alkaline solution content of 210 kg/m^3 and SS/SH ratio of 1.75)

Fig. 6.51: FTIR spectra of GPC near rebar level in prismatic specimens at the age of 600 days for fly ash content of a) 425 kg/m^3, and b) 450 kg/m^3 for NaOH solution of 14 M

The band related to quartz, stretching vibration of carbonate group, and bending vibration of H–O–H group, and the peak related to stretching vibration of –OH group are located in the range of 773 cm^{-1} to 780 cm^{-1}, at 1516 cm^{-1}, 1688 cm^{-1} to 1697 cm^{-1}, and 3742 cm^{-1} to 3746 cm^{-1} respectively as observed from the FTIR spectra shown in Fig. 6.50 and Fig. 6.51.

6.4.3 Field Emission Scanning Electron Microscope (FESEM) analysis

The typical FESEM images of GPC near steel reinforcement in prismatic specimens at the age of 600 days are shown in Fig. 6.52 for different molarity of NaOH solution (8 M, 10 M, 12 M, 14 M and 16 M) and in Fig. 6.53 for different concentrations of admixed NaCl (1.5%, 3% and 4.5%). The remaining FESEM images are presented in Appendix section (Fig. B1). From the FESEM images shown in Fig. 6.52, the microstructure of GPC comprised mainly of geopolymer gels and few pores. From the FESEM images shown Fig. 6.52 and Fig. 6.53, the presence of unreacted/partially reacted fly ash particles was not observed in GPC mixes at the age of 600 days, which indicates continued dissolution of alumina and silica from fly ash in the geopolymerization reaction with age. From Fig. 6.52, it is inferred that there was comparatively more formation of geopolymer gels in GPC mixes made with higher molarity of NaOH solution that resulted in denser microstructure. This is in line with the results of XRD

analysis (Fig. 6.34 (a, b, c, d)), where the peak intensity of the compounds related to sodium aluminosilicate hydrate gel were mostly higher in the GPC mixes made with higher molarity of NaOH solution.

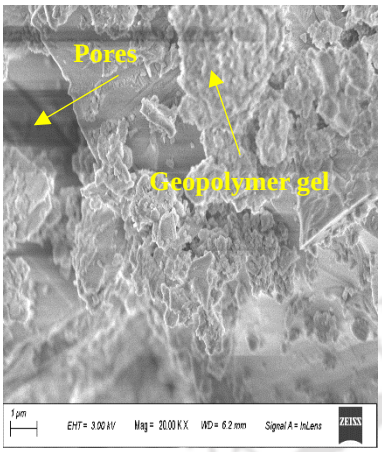

(a) 425FA/8 M/3NC/600D

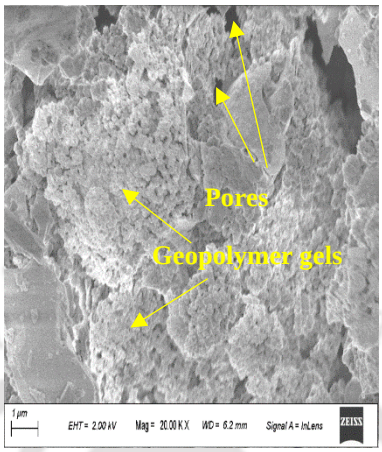

(b) 425FA/10 M/3NC/600D

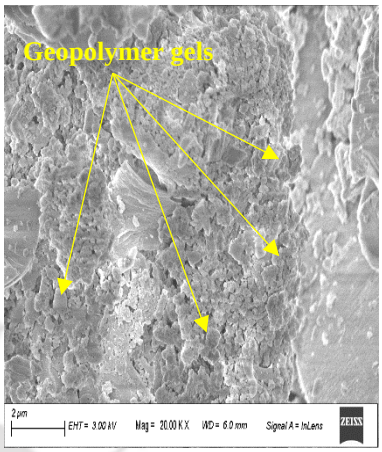

(c) 425FA/12 M/3NC/600D

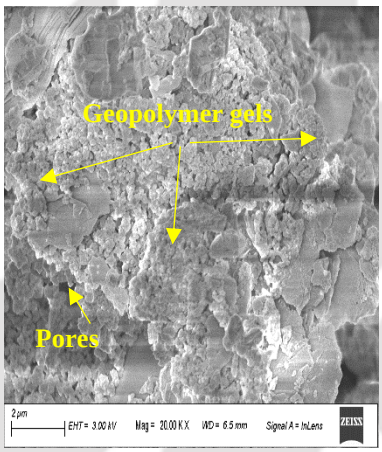

(d) 425FA/14 M/3NC/600D

(GPC made with fly ash passing through 300 μm sieve, fly ash content of 425 kg/m^3, alkaline solution content of 210 kg/m^3, and SS/SH ratio of 1.75)

Fig. 6.52: FESEM images of GPC near steel reinforcement in prismatic specimens at the age of 600 days for different molarity of NaOH solution

The FESEM images shown in Fig. 6.53 indicate comparatively less denser and non-uniform microstructure in the GPC mixes admixed with higher concentration of sodium chloride. This is supported by the results of XRD analysis (Fig. 6.34 (b), discussed earlier) where the peak intensity of albite, anorthoclase, and nepheline in the XRD patterns were mostly lower in the GPC mixes admixed with higher concentration of sodium chloride. Further, there was presence of comparatively more pores in the microstructure of GPC mixes admixed with higher concentration of sodium chloride as observed from Fig. 6.53. In addition, the formation of microcracks was observed in the FESEM image of GPC mix admixed with higher concentration of NaCl (Fig. 6.53 (c)). This may be ascribed to the effect of crystallization of

sodium chloride in the pores of GPC mixes that might have exerted swelling pressure leading to expansion and formation of microcracks in the GPC mixes.

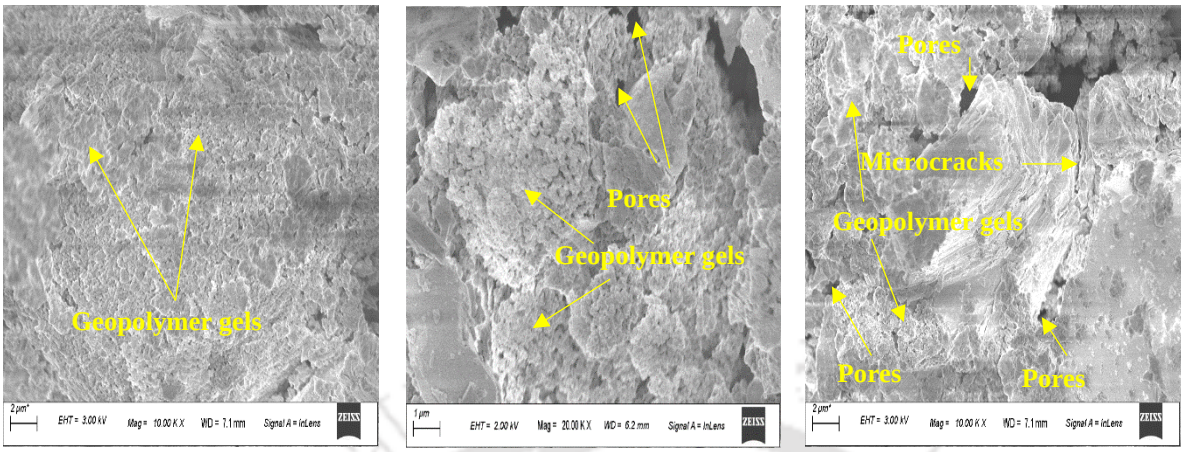

(a) 425FA/10 M/1.5NC/600D (b) 425FA/10 M/3NC/600D (c) 425FA/10 M/4.5NC/600D

(GPC made with fly ash passing through 300 μm sieve, fly ash content of 425 kg/m^3, alkaline solution content of 210 kg/m^3, and SS/SH ratio of 1.75)

Fig. 6.53: FESEM images of GPC near steel reinforcement in prismatic specimens at the age of 600 days for different concentrations of admixed sodium chloride

Typical FESEM images of NaCl admixed GPC near steel reinforcement in prismatic specimens at the age of 600 days are shown in Fig. 6.54 for alkaline solution contents of 190 kg/m^3 and 210 kg/m^3, and NaOH solution of 10 M and 14 M. The remaining FESEM image is presented in Appendix section (Fig. B2). From FESEM images shown in Fig. 6.54 (a, b), comparatively denser microstructure was observed in GPC mix made with lower alkaline solution content (190 kg/m^3) as compared to higher alkaline solution content (210 kg/m^3) at later age. This is substantiated by the results of XRD analysis (Fig. 6.35), where the GPC mix made with lower alkaline solution content mostly showed higher peak intensity of the compounds related to geopolymer gels as compared to that made with higher alkaline solution content. With molarity of NaOH solution, the FESEM images shown in Fig. 6.54 (b, c) indicated formation of comparatively more compact microstructure in GPC mix made with higher molarity of NaOH solution (14 M) as compared to lower molarity of NaOH solution (10 M). This is supported by the XRD analysis (Fig. 6.35 (b)), where the peak intensity of the compounds i.e., nepheline, albite, and anorthoclase in the XRD patterns were higher at higher molarity of NaOH solution than lower molarity of NaOH solution.

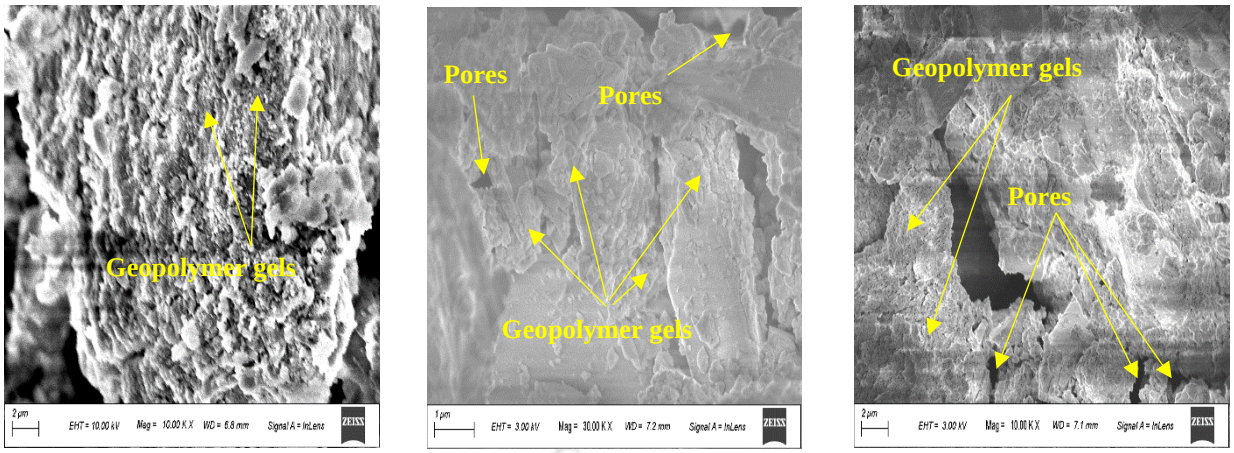

(a) 190AL/14 M/3NC/600D (b) 210AL/14 M/3NC/600D (c) 210AL/10 M/3NC/600D

(GPC made with fly ash passing through 150 μm sieve, fly ash content of 425 kg/m^3, and SS/SH ratio of 1.75)

Fig. 6.54: FESEM images of GPC near steel reinforcement in prismatic specimens at the age of 600 days: a) alkaline solution content of 190 kg/m^3 for NaOH solution of 14 M, b) alkaline solution content of 210 kg/m^3 for NaOH solution of 14 M, and c) alkaline solution content of 210 kg/m^3 for NaOH solution of 10 M

Fig. 6.55 illustrates typical FESEM images of NaCl admixed GPC near steel reinforcement in prismatic specimens at the age of 600 days for SS/SH ratios of 1.5 and 1.75. The remaining FESEM image is presented in Appendix section (Fig. B2). From Fig. 6.55 (a, b), it is inferred that there was no significant difference in the microstructure of GPC mixes with SS/SH ratio. However, there was formation of comparatively compact microstructure in GPC mix made with lower SS/SH ratio (1.5) than higher SS/SH ratio (1.75), which is consistent with the variations in the peak intensity of the compounds related to geopolymer gels in the XRD patterns (Fig. 6.36) with change in SS/SH ratio. Further, the FESEM images shown in Fig. 6.55 (b, c) indicate formation of less denser microstructure with presence of pores in GPC mix made with lower molarity of NaOH solution than that made with higher molarity of NaOH solution at SS/SH ratio of 1.75.

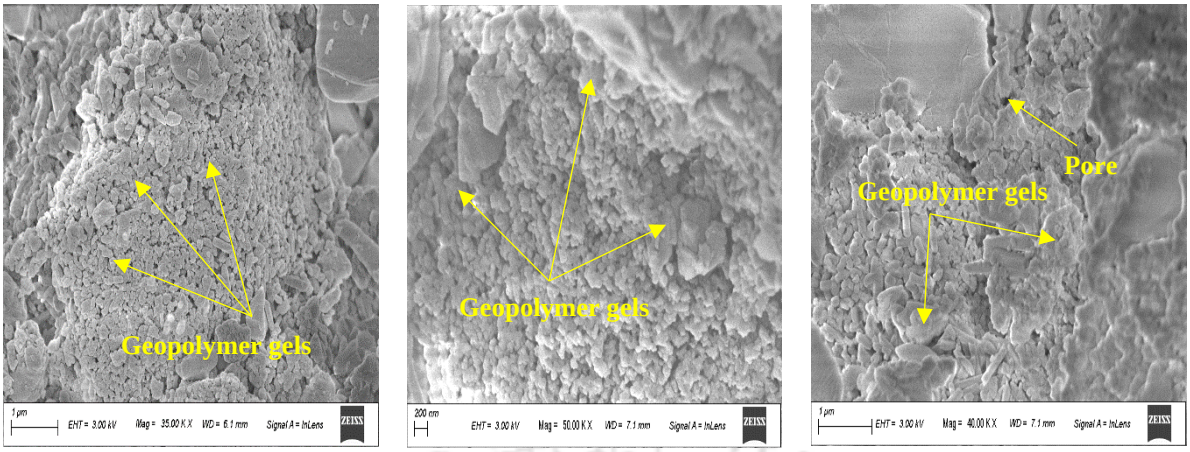

(a) 1.5R/14 M/3NC/600D (b) 1.75R/14 M/3NC/600D (c) 1.75R/10 M/3NC/600D

(GPC made with fly ash passing through 150 μm sieve, fly ash content of 425 kg/m^3, and alkaline solution content of 210 kg/m^3)

Fig. 6.55: FESEM images of GPC near steel reinforcement in prismatic specimens at the age of 600 days: a) SS/SH ratio of 1.5 for NaOH solution of 14 M, b) SS/SH ratio of 1.75 for NaOH solution of 14 M, and c) SS/SH ratio of 1.75 for NaOH solution of 10 M

Typical FESEM images of NaCl admixed GPC near steel reinforcement in prismatic specimens at the age of 600 days are illustrated in Fig. 6.56 for fly ash passing through 150 μm sieve, and 300 μm sieve for fly ash content of 425 kg/m^3. From the FESEM images shown in Fig. 6.56 (a, b), the GPC mix made with larger fly ash particles indicated comparatively more formation of geopolymer gels leading to denser microstructure with less pores as compared to that made with smaller fly ash particles. This is corroborated with the results of XRD analysis (Fig. 6.37) where the GPC mix made with larger fly ash particles showed higher peak intensity of albite, anorthoclase, and nepheline in the XRD patterns. Further, the GPC mix made with NaOH solution of 14 M showed compact microstructure as compared to that made with NaOH solution of 10 M as observed from Fig. 6.56 (a, c).

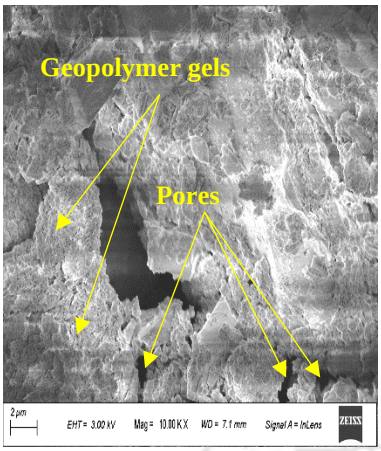

(a) 425FA/10 M/3NC/150 µm/ 600D

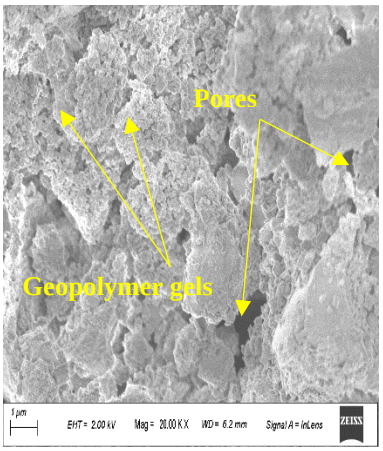

(b) 425FA/10 M/3NC/300 µm/ 600D

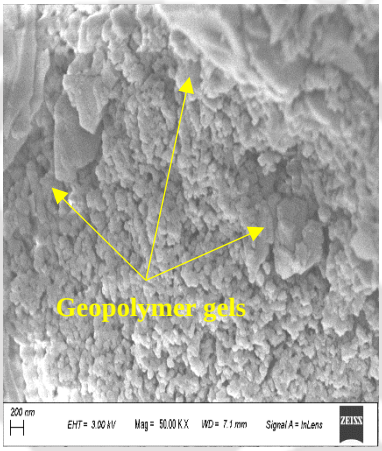

(c) 425FA/14 M/3NC/150 µm/ 600D

(GPC made with fly ash content of 425 kg/m^3, alkaline solution content of 210 kg/m^3, and SS/SH ratio of 1.75)

Fig. 6.56: FESEM images of GPC near steel reinforcement in prismatic specimens at the age of 600 days: a) fly ash passing through 150 µm sieve for NaOH solution of 10 M, b) fly ash passing through 300 µm sieve for NaOH solution of 10 M, and c) fly ash passing through 150 µm sieve for NaOH solution of 14 M

For fly ash content of 450 kg/m^3, typical FESEM images of GPC near rebar in prismatic specimens at the age of 600 days are shown in Fig. 6.57, Fig. 6.58 and Fig. 6.59 for fly ash passing through 150 µm sieve, and 300 µm sieve for different concentrations of admixed NaCl, and molarity of NaOH solution. The remaining FESEM image is presented in Appendix section (Fig. B3). Similar to fly ash content of 425 kg/m^3 (as discussed above, Fig. 6.56), the FESEM images shown in Fig. 6.57, for fly ash content of 450 kg/m^3, indicated compact microstructure with formation of more amount of geopolymer gels in the GPC mix made with larger fly ash particles (passing through 300 µm sieve) than that made with smaller fly ash particles (150 µm sieve). This is consistent with the variations in the peak intensity of albite, anorthoclase, and nepheline in the XRD patterns (Fig. 6.39) with particle size of fly ash in GPC mixes.

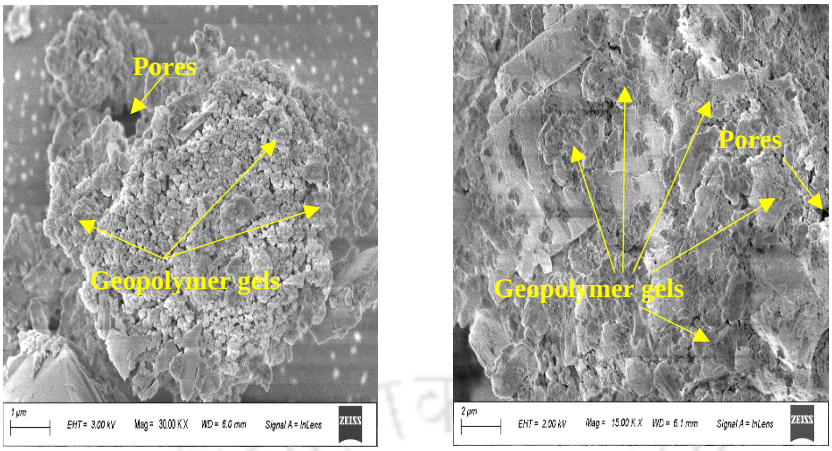

(a) 450FA/14 M/3NC/150 µm/600D (b) 450FA/14 M/3NC/300 µm/600D

(GPC made with fly ash content of 450 kg/m^3, alkaline solution content of 210 kg/m^3, and SS/SH ratio of 1.75)

Fig. 6.57: FESEM images of GPC near steel reinforcement in prismatic specimens at the age of 600 days: a) fly ash passing through 150 µm sieve, and b) fly ash passing through 300 µm sieve for NaOH solution of 14 M

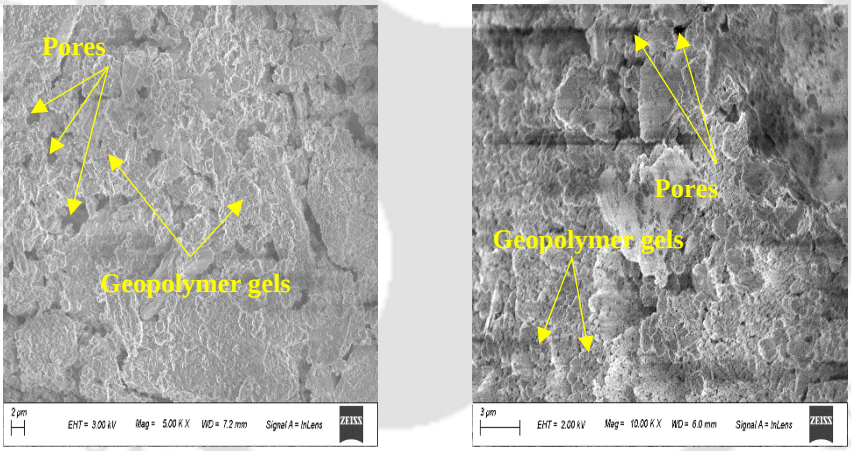

(a) 10 M/4.5NC/150 µm/600D (b) 14 M/4.5NC/150 µm/600D

(GPC made with fly ash content of 450 kg/m^3, alkaline solution content of 210 kg/m^3, and SS/SH ratio of 1.75)

Fig. 6.58: FESEM images of GPC near steel reinforcement in prismatic specimens at the age of 600 days: a) NaOH solution of 10 M, and b) NaOH solution of 14 M for fly ash passing through 150 µm sieve

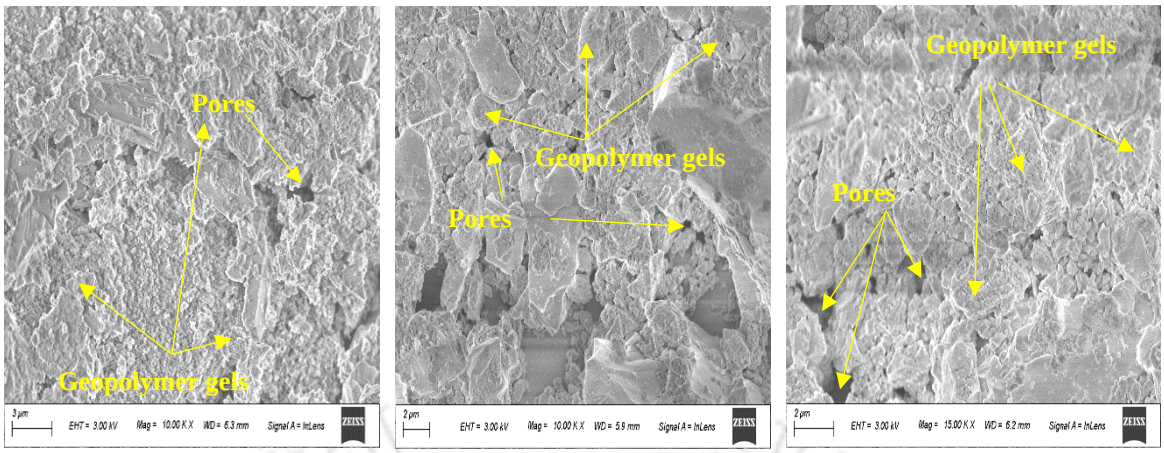

(a) 10 M/1.5NC/300 µm/600D (b) 10 M/3NC/300 µm/600D (c) 10 M/4.5NC/300 µm/600D

(GPC made with fly ash content of 450 kg/m^3, alkaline solution content of 210 kg/m^3, and SS/SH ratio of 1.75)

Fig. 6.59: FESEM images of GPC near steel reinforcement in prismatic specimens at the age of 600 days: a) NaCl concentration of 1.5%, and b) NaCl concentration of 3%, and c) NaCl concentration of 4.5% for fly ash passing through 300 µm sieve

From the FESEM images shown in Fig. 6.58, formation of relatively denser microstructure was observed in the GPC mix made with higher molarity of NaOH solution as compared to that made with lower molarity of NaOH solution. Further, comparatively less homogeneous microstructure with presence of more pores was observed in the GPC mixes admixed with higher concentrations of NaCl i.e., 3% and 4.5% as compared to that admixed with NaCl concentration of 1.5% as observed from the FESEM images shown in Fig. 6.59. These variations in the formation of microstructure with molarity of NaOH solution and admixed NaCl concentration as observed from the FESEM images are consistent with the variations in the peak intensity of the compounds related to geopolymer gels in the XRD patterns shown in Fig. 6.38 (a), Fig. 6.39 (a), and 6.38 (b).

For fly ash passing through 150 µm sieve, typical FESEM images of NaCl admixed GPC near steel reinforcement in prismatic specimens at the age of 600 days are shown in Fig. 6.60 for fly ash content of 425 kg/m^3 and 450 kg/m^3. The FESEM images shown in Fig. 6.60 (a, b) indicate relatively more formation of sodium aluminosilicate hydrate gels in GPC mix made with higher fly ash content (450 kg/m^3) than that made with lower fly ash content (425 kg/m^3). It may be noted that, as discussed earlier, the GPC mix made with higher fly ash content showed higher peak intensity of the phases related to aluminosilicate gels i.e., albite, anorthoclase, and nepheline in the XRD patterns as compared to that made with lower fly ash content (Fig. 6.40). Further, comparatively more formation of geopolymer gels was observed

in the GPC mix made with higher molarity of NaOH solution (14 M) as compared to that made with lower molarity of NaOH solution as inferred from Fig. 6.60 (a, c).

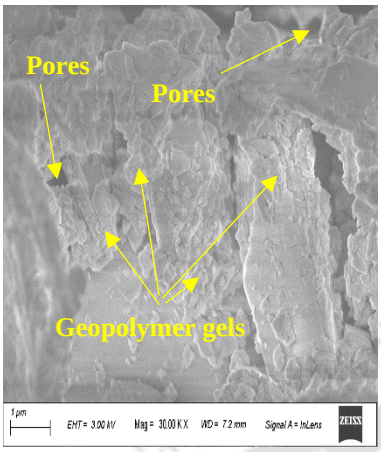

(a) 425FA/14 M/3NC/150 µm/600D

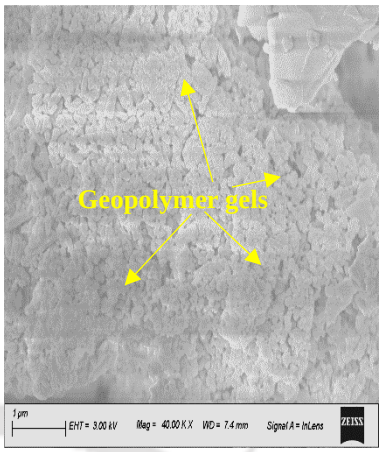

(b) 450FA/14 M/3NC/150 µm/600D

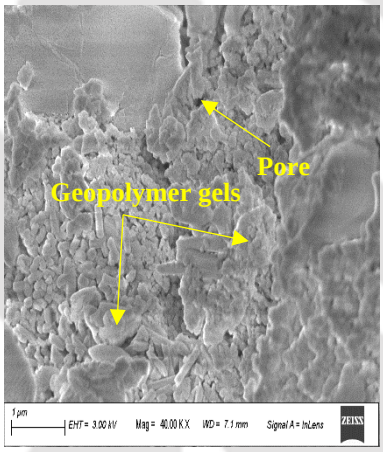

(c) 425FA/10 M/3NC/150 µm/ 600D

(GPC made with fly ash passing through 150 µm sieve, alkaline solution content of 210 kg/m^3 and SS/SH ratio of 1.75)

Fig. 6.60: FESEM images of GPC near rebar level in prismatic specimens at the age of 600 days: a) fly ash content of 425 kg/m^3 for NaOH solution of 14 M, b) fly ash content of 450 kg/m^3 for NaOH solution of 14 M, and c) fly ash content of 425 kg/m^3 for NaOH solution of 10 M

Typical FESEM images of GPC near steel reinforcement in prismatic specimens at the age of 600 days are shown in Fig. 6.61, Fig. 6.62 and Fig. 6.63 for fly ash content of 425 kg/m^3 and 450 kg/m^3 at different concentrations of admixed NaCl, and molarity of NaOH solution for GPC mixes made with fly ash passing through 300 µm sieve. From Fig. 6.61, it is inferred that there was more formation of geopolymer gels with relatively homogeneous microstructure in GPC mix made with lower fly ash content (425 kg/m^3) as compared to that made with higher fly ash content (450 kg/m^3) for larger fly ash particles. Further, the GPC mix made with higher

molarity of NaOH solution (14 M) showed comparatively more formation of geopolymer gels than that made with lower molarity of NaOH solution (10 M) where less denser microstructure with presence of more pores was observed at lower molarity of NaOH solution as evident from the FESEM images shown in Fig. 6.62. These variations in the microstructure of GPC with fly ash content and molarity of NaOH solution as indicated by the FESEM images are in line with the results of XRD analysis with respect to the variations in the peak intensity of the phases related to geopolymer gels (Fig. 6.41 and 6.42 (b)).

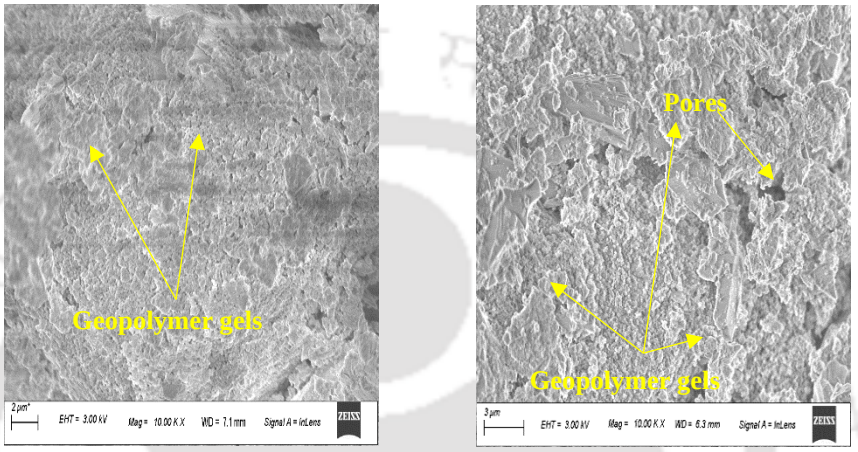

(a) 425FA/10 M/1.5NC/300 µm/600D (b) 450FA/10 M/1.5NC/300 µm/600D

(GPC made with fly ash passing through 300 µm sieve, alkaline solution content of 210 kg/m^3 and SS/SH ratio of 1.75)

Fig. 6.61: FESEM images of GPC near rebar level in prismatic specimens at the age of 600 days: a) fly ash content of 425 kg/m^3, and b) fly ash content of 450 kg/m^3 for NaOH solution of 10 M

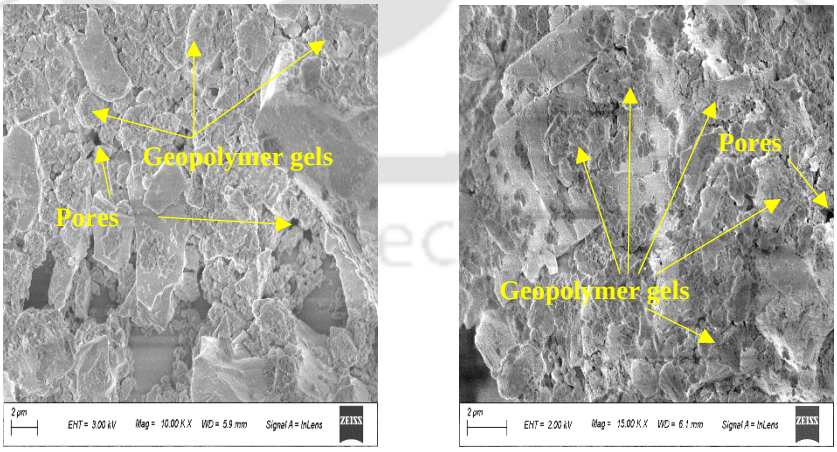

(a) 450FA/10 M/3NC/300 µm/600D (b) 450FA/14 M/3NC/300 µm/600D

(GPC made with fly ash passing through 300 µm sieve, alkaline solution content of 210 kg/m^3 and SS/SH ratio of 1.75)

Fig. 6.62: FESEM images of GPC near rebar level in prismatic specimens at the age of 600 days: a) NaOH solution of 10 M, and b) NaOH solution of 14 M for fly ash content of 450 kg/m^3

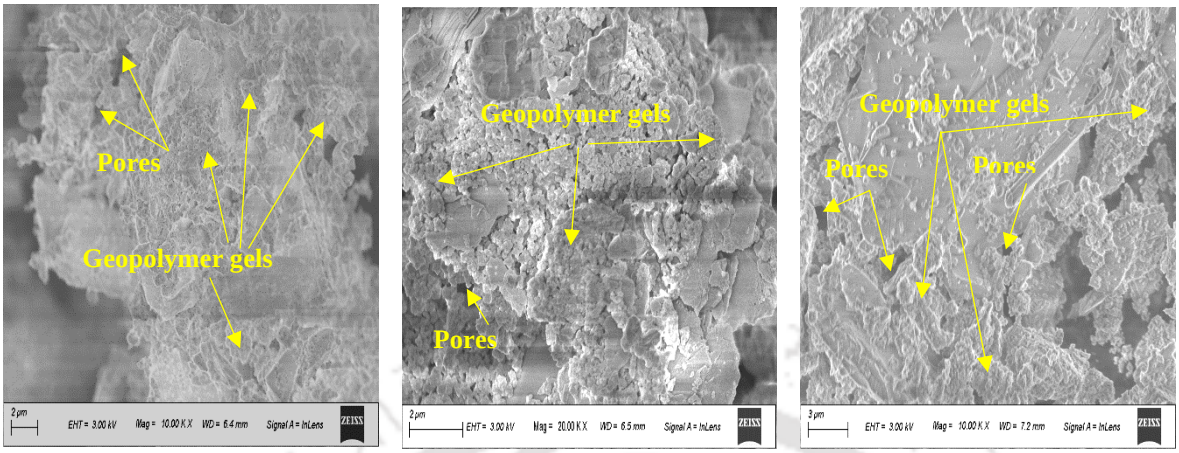

(a) 425FA/14 M/1.5NC/600D (b) 425FA/14 M/3NC/600D (c) 425FA/14 M/4.5NC/600D

(GPC made with fly ash passing through 300 μm sieve, alkaline solution content of 210 kg/m^3 and SS/SH ratio of 1.75)

Fig. 6.63: FESEM images of GPC near rebar level in prismatic specimens at the age of 600 days: a) NaCl concentration of 1.5%, and b) NaCl concentration of 3%, and c) NaCl concentration of 4.5% for fly ash content of 425 kg/m^3

From the FESEM images shown in Fig. 6.63, there was no significant difference in the microstructure of GPC mixes between admixed NaCl concentrations of 1.5% and 3%, however, there was comparatively less formation of geopolymer gels at NaCl concentration of 4.5%. These variations in the microstructure of GPC as observed from the FESEM images with admixed NaCl concentration are supported by the results of XRD analysis where unsystematic variation in the peak intensity of the phases related to geopolymer gels in XRD patterns was observed between NaCl concentrations of 1.5% and 3%. However, the peak intensity of the phases related to the geopolymer gels were mostly lower at NaCl concentration of 4.5% than NaCl concentration of 3% (Fig. 6.42 (a)).

6.5 Summary

The results from corrosion behaviour of rebar in prismatic GPC specimens indicated that the presence of chloride ions increased the probability of occurrence of corrosion, and corrosion current density of rebar when compared with control GPC mixes. Further, the extent of corrosion of rebar increased with increase in NaCl concentration in GPC mixes. At different ages, the variations in corrosion potential and corrosion current density of rebar in GPC were mostly unsystematic with increase in molarity of NaOH solution from 8 M to 16 M, however, there was increase in extent of corrosion with increase in alkaline solution content and SS/SH

ratio in the presence of chloride ions in GPC mixes. The obtained results of corrosion study indicated that the fly ash content influenced the corrosion activity of steel reinforcement in the presence of chloride ions in GPC mixes with change in particle size of fly ash. Similarly, the particle size of fly ash influenced the extent of chloride induced rebar corrosion in GPC mixes with a change in fly ash content. There was insignificant variation in corrosion potential of rebar in GPC with increase in age. Similarly, the variation in corrosion current density with age was mostly unsystematic. The effect of change in passivity of steel reinforcement in GPC with age due to combined effect of chloride ions, and the variations in oxygen and moisture content near steel reinforcement led to these variations in corrosion parameters with increase in age.

At the later age of 600 days, the free chloride content near rebar in prismatic GPC specimens increased with increase in admixed NaCl concentration that led to more negative corrosion potential, and higher corrosion current density at higher concentration of NaCl. The total chloride and bound chloride content of GPC near rebar level also increased with increase in NaCl concentration. When compared with higher molarity of NaOH solution, the GPC made with lower molarity of NaOH solution showed higher free chloride content near rebar level at the age of 600 days, which resulted in more negative corrosion potential and higher corrosion current density at lower molarity of NaOH solution than higher molarity of NaOH solution. However, the bound chloride content was mostly higher at lower molarity of NaOH solution when compared with higher molarity of NaOH solution. Higher amount of free chloride, total chloride and bound chloride were observed at lower alkaline solution content as compared to higher alkaline solution content. With change in SS/SH ratio, there was consistent variation in the effect of chloride ions on corrosion activity of rebar in GPC at later age for NaOH solution of 10 M whereas there was inconsistent variation at NaOH solution of 14 M. The bound chloride content was higher in GPC made with larger fly ash particles as compared to smaller fly ash particles at higher fly ash content whereas opposite variation in bound chloride content with particle size of fly ash was observed at lower fly ash content. At higher fly ash content, there was comparatively higher effect of chloride ions on the extent of corrosion of steel reinforcement in GPC in case of smaller fly ash particles. However, in case of larger fly ash particles, the lower corrosion current density in GPC made with higher fly ash content at the later age of 600 days, although the free chloride content was higher, is attributed to the improvement in passivity of steel reinforcement due to higher resistivity exhibited by the geopolymeric structure at later age.

The higher peak intensity of albite, anorthoclase and nepheline in the XRD patterns of GPC near rebar level in the prismatic specimens at the age of 600 days observed at higher molarity of NaOH solution indicated more formation of geopolymer gels that resulted in denser microstructure. This led to lower free chloride content near rebar level thereby resulting in lower corrosion activity of rebar at later age in GPC made with higher molarity of NaOH solution than lower molarity of NaOH solution. The formation of more amount of geopolymer gels in GPC mixes at lower alkaline solution content, and lower SS/SH ratio as indicated by higher peak intensity of the compounds related to geopolymer gels in XRD patterns led to comparatively higher extent of physical binding of chloride ions with geopolymer gels as bound chloride content was higher at lower alkaline solution content, and lower SS/SH ratio than higher alkaline solution content, and higher SS/SH ratio. In case of larger fly ash particles, the formation of more amount of geopolymer gels in GPC as indicated by higher peak intensity of the compounds related to geopolymer gels in XRD patterns resulted in denser microstructure that led to lower free chloride content near rebar level at the later age of 600 days when compared with smaller fly ash particles. The XRD results indicated that in chloride admixed GPC, the extent of formation of geopolymer gels with change in fly ash content was influenced by the particle size of fly ash. At the later age of 600 days, the XRD patterns of GPC near rebar level showed lower peak intensity of albite, anorthoclase, nepheline, muscovite, and sodalite in NaCl admixed mixes when compared with control mix. Further, there was mostly decrease in peak intensity of these compounds with increase in NaCl concentration. In the FTIR spectra of GPC near steel reinforcement, the variation in the wavenumber associated with the peak corresponding to asymmetric stretching vibration of Si–O–Si(Al) bond was not significant with change in molarity of NaOH solution, alkaline solution content, SS/SH ratio, particle size of fly ash, fly ash content, and NaCl concentration. From FESEM images of GPC near steel reinforcement in prismatic specimens at later age, the variations in the formation of microstructure with above mix parameters are corroborated with the variations in the peak intensity of the compounds related to geopolymer gels in XRD patterns of GPC mixes.

Chapter 7

Conclusions and Suggestions for Future Work

7.1 General

In this chapter, the conclusions obtained from the present research work are presented. The conclusions obtained on the influence of molarity of NaOH solution, alkaline solution content, SS/SH ratio, particle size of fly ash, fly ash content and admixed sodium chloride (NaCl) on variations in consistency, compressive strength, and free, total and bound chloride contents of fly ash based geopolymer concrete (GPC) are presented. Further, the conclusions on microstructural changes in GPC at different ages with above mix parameters are presented. In addition, the conclusions obtained from the influence of mix parameters on variations in corrosion behaviour of rebar in fly ash based GPC in the presence of internal chloride are presented in this chapter. The conclusions on the effect of mix parameters on free, total, and bound chloride contents near rebar level in GPC specimens at later age of 600 days are presented. Thereafter, the conclusions drawn on the variations in microstructure of GPC near steel reinforcement at later age are presented. Further, the significance of research outcome obtained from the present research work, and the suggestions for future work are also presented in this chapter.

7.2 Conclusions from influence of mix parameters on consistency and compressive strength of fly ash based geopolymer concrete

1) Irrespective of fly ash content, the dominant effect of lower particle mobility in case of larger fly ash particles over the effect of more specific surface area in case of smaller fly ash particles resulted in reduced consistency of GPC mix made with larger fly ash particles as compared to that made with smaller fly ash particles. Further, the consistency of GPC decreased with increase in fly ash content irrespective of particle size of fly ash.

2) Regardless of molarity of NaOH solution, alkaline solution content, SS/SH ratio, particle size of fly ash, and fly ash content, the presence of sodium chloride in GPC mixes resulted in improved particle mobility that led to higher consistency as compared to control GPC mix (without admixed NaCl). Further, there was increase in consistency of GPC mixes with increase in concentration of admixed NaCl.

3) The increase in molarity of NaOH solution from 8 M to 16 M resulted an increase in compressive strength of control, and 1.5% NaCl admixed GPC mixes. In case of GPC mixes admixed with higher concentration of NaCl i.e., 3% and 4.5%, although the compressive strength increased with molarity of NaOH solution from 8 M to 14 M, at NaOH solution of 16 M, there was decrease in compressive strength, which may be attributed to the hindering effect of higher concentration of NaCl in the geopolymerization process in GPC mixes.

4) The increase in particle size of fly ash showed improvement in compressive strength of GPC at comparatively lower fly ash content, however, mostly opposite variation in compressive strength with particle size of fly ash was observed at higher fly ash content.

5) In the presence of NaCl, the GPC mixes made with lower fly ash content exhibited lower compressive strength as compared to that made with higher fly ash content for smaller fly ash particles (passing through 150 µm sieve) whereas the opposite variation in compressive strength with fly ash content was observed for larger fly ash particles (passing through 300 µm sieve). This shows that the particle size of fly ash significantly influenced the variation in compressive strength of GPC for different fly ash contents in the presence of NaCl.

6) The compressive strength of GPC mix was mostly lower in the presence of NaCl as compared to control GPC mix. Further, the compressive strength mostly decreased with increase in concentration of admixed NaCl with comparatively more reduction at higher concentration of admixed NaCl. This is ascribed to the effect of alteration in the extent of geopolymerization process as well as crystallization of sodium chloride in the pores of GPC mixes.

7) The compressive strength of GPC mostly increased with increase in age from 7 to 28 days in control as well as in NaCl admixed GPC mixes irrespective of molarity of NaOH solution, alkaline solution content, SS/SH ratio, particle size of fly ash, and fly ash content. However, the compressive strength of GPC mostly decreased with increase in age from 28 to 90 days, which may due to the effect of formation of shrinkage cracks due to loss of moisture to a comparatively higher extent from GPC mixes at later age with the presence of NaCl affecting the geopolymerization process in NaCl admixed GPC mixes.

7.3 Conclusions from influence of mix parameters on chloride content of fly ash based geopolymer concrete

1) The GPC made with higher molarity of NaOH solution showed lower free chloride content than lower molarity of NaOH solution in case of smaller fly ash particles. The formation of

comparatively denser microstructure at higher molarity of NaOH solution as indicated by higher compressive strength resulted in lower availability of chloride ions in the pore solution of GPC. However, in case of GPC made with larger fly ash particles, mostly there was unsystematic variation in free chloride content with molarity of NaOH solution. This shows that the particle size of fly ash affected the availability of chloride ions in the pore solution due to alteration in the microstructure of GPC with change in molarity of NaOH solution.

2) There was decrease in free chloride content with increase in alkaline solution content for both molarity of NaOH solution i.e., 10 M and 14M. The higher compressive strength at higher alkaline solution content indicating formation of denser microstructure resulted in lower amount of chloride ions in the pore solution thereby showing lower free chloride content in GPC made with higher alkaline solution content for NaOH solution of 10 M, whereas at NaOH solution of 14 M, the denser microstructure as indicated by higher compressive strength at lower alkaline solution content did not affect the variation in chloride concentration in the pore solution significantly thus resulting in comparatively more free chloride concentration at lower alkaline solution content.

3) The GPC mixes made with larger fly ash particles (passing through 300 µm sieve) mostly exhibited higher free chloride content as compared to that made with smaller fly ash particles (passing through 150 µm sieve) for both fly ash contents i.e., 425 kg/m^3 and 450 kg/m^3. Similarly, the free chloride content was mostly higher in GPC mixes made with higher fly ash content (450 kg/m^3) than that made with lower fly ash content (425 kg/m^3) for both sizes of fly ash particles.

4) With age, mostly there was increase in free chloride content of GPC with increase in age from 7 to 28 days whereas the free chloride content mostly decreased with age from 28 days to 90 days regardless of molarity of NaOH solution, alkaline solution content, SS/SH ratio, particle size of fly ash, fly ash content, and admixed NaCl dosage.

5) There was lower chloride binding in fly ash based geopolymer concrete as indicated by lower bound chloride content. The GPC mixes made with lower molarity of NaOH solution mostly exhibited higher chloride binding as compared to that made with higher molarity of NaOH solution.

6) The bound chloride content was mostly higher in GPC mixes made with larger fly ash particles (passing through 300 µm sieve) as compared to that made with smaller fly ash particles (passing through 150 µm sieve) for both fly ash contents. The formation of more

amount of geopolymer gels in GPC mixes made with larger fly ash particles as indicated by higher compressive strength resulted in comparatively more extent of physical adsorption of chloride ions on aluminosilicate gels that led to higher bound chloride content.

7) In case of smaller fly ash particles, the bound chloride content was mostly higher in GPC made with higher fly ash content (450 kg/m^3) than that made with lower fly ash content (425 kg/m^3) at higher molarity of NaOH solution (14 M). However, in case of larger fly ash particles, the GPC made with lower fly ash content mostly showed higher bound chloride content than that made with higher fly ash content at higher molarity of NaOH solution. These variations in bound chloride content are in line with the extent of formation of geopolymer gels as indicated by the obtained compressive strength of GPC made with these mix parameters.

8) At lower molarity of NaOH solution (10 M), the GPC made with lower fly ash content mostly exhibited higher bound chloride content as compared to that made with higher fly ash content in case of smaller fly ash particles whereas opposite variation in bound chloride content with fly ash content was observed in case of larger fly ash particles. This indicates inconsistent variation in bound chloride content with the formation of microstructure as indicated by the obtained compressive strength of GPC made with different fly ash contents at lower molarity of NaOH solution.

7.4 Conclusions from influence of mix parameters and admixed chloride on microstructure of fly ash based geopolymer concrete

1) The peak intensity of albite, anorthoclase, and nepheline in the XRD patterns mostly increased with increase in molarity of NaOH solution from 8 M to 16 M in control and 1.5% NaCl admixed GPC mixes at the age of 7, 28 and 90 days thereby indicating formation of more amount of geopolymer gels in GPC mixes at higher molarity of NaOH solution. In case of 3% and 4.5% NaCl admixed GPC mixes, the peak intensity of these compounds in the XRD patterns mostly increased with increase in molarity of NaOH solution from 8 M to 14 M followed by a decrease at 16 M NaOH solution. These variations in the peak intensity of above geopolymeric compounds in the XRD patterns are in line with the obtained variations in the compressive strength with molarity of NaOH solution in control and NaCl admixed GPC mixes.

2) In the presence of NaCl, the GPC mixes mostly showed lower peak intensity of albite, anorthoclase, nepheline, sodalite, and muscovite in the XRD patterns as compared to control GPC mixes irrespective of molarity of NaOH solution, alkaline solution content, SS/SH ratio,

particle size of fly ash, and fly ash content for different ages, which is consistent with the obtained variations in compressive strength of GPC mixes with these mix parameters. Further, the peak intensity of the compounds related to geopolymer gels in XRD patterns mostly decreased with increase in admixed NaCl concentration in GPC mixes regardless of molarity of NaOH solution, particle size, and amount of fly ash.

3) The variations in peak intensity of the compounds related to geopolymer gels in the XRD patterns are mostly in line with the obtained variations in compressive strength of GPC mixes with alkaline solution content, SS/SH ratio, particle size of fly ash, and fly ash content.

4) The increases in peak intensity of geopolymeric compounds in XRD patterns with age from 7 to 28 days, and the decrease in peak intensity of these compounds with age from 28 to 90 days are substantiated by the obtained variations in the compressive strength of GPC with age in control as well as NaCl admixed GPC mixes.

5) The variations in the wavenumber associated with the peak corresponding to asymmetric stretching vibration of Si–O–Si(Al) bond in the FTIR spectra that indicates the presence of geopolymer gels in GPC mixes are substantiated with the variations in the peak intensity of the compounds related to geopolymer gels in XRD patterns with change in molarity of NaOH solution, alkaline solution content, SS/SH ratio, particle size of fly ash, and fly ash content in control as well as NaCl admixed GPC mixes.

6) There is also consistent variation in the wavenumber associated with the peak corresponding to asymmetric stretching vibration of Si–O–Si(Al) bond in the FTIR spectra with that in the peak intensity of the compounds related to geopolymer gels in XRD patterns of GPC mixes with increase in admixed NaCl concentration, and age.

7) The FESEM images indicated formation of comparatively denser microstructure at higher molarity of NaOH solution, and in control GPC mixes as compared to lower molarity of NaOH solution, and NaCl admixed GPC mixes, which is substantiated by the higher peak intensity of albite, anorthoclase, nepheline, sodalite, and muscovite in the XRD patterns as well as by higher compressive strength at higher molarity of NaOH solution and in control GPC mixes.

8) As observed from FESEM analysis, the GPC mix made with higher alkaline solution content, and that made with higher SS/SH ratio showed denser microstructure with formation of more amount of geopolymer gels than that made with lower alkaline solution content, and lower SS/SH ratio respectively, which are supported by the results of XRD analysis where

higher peak intensity of the compounds related to geopolymer gels in XRD patterns were observed in case of higher alkaline solution content, and higher SS/SH ratio.

9) The variations in the formation of microstructure in GPC mixes as indicated by the FESEM images with change in particle size of fly ash, fly ash content, and age are in line with the variations in the peak intensity of the compounds related to geopolymer gels in the XRD patterns of GPC mixes.

7.5 Conclusions from corrosion behaviour of rebar in fly ash based geopolymer concrete

1) The corrosion activity of rebar in GPC mixes in the presence of chloride ions mostly increased with increase in alkaline solution content and SS/SH ratio at different ages.

2) There was mostly unsystematic variation in corrosion potential of rebar with particle size of fly ash in GPC mixes in the presence of chloride ions for both fly ash contents over different ages. However, the GPC mixes made with larger fly ash particles mostly exhibited lower corrosion current density than that made with smaller fly ash particles at fly ash content of 425 kg/m^3, whereas opposite variation in corrosion current density with particle size of fly ash was observed at fly ash content of 450 kg/m^3. The lower corrosion current density of rebar for different particle size of fly ash is attributed to the improved passivation of steel reinforcement due to increased resistivity of GPC mixes with change in fly ash content. This indicates that the fly ash content influenced the corrosion activity of rebar in the presence of chloride ions in GPC mixes made with fly ash particles of different sizes.

3) The GPC mixes made with higher fly ash content mostly showed more negative corrosion potential than that made with lower fly ash content for both sizes of fly ash particles over different ages. However, the corrosion current density was mostly higher at lower fly ash content than that at higher fly ash content for smaller fly ash particles (passing through 150 µm sieve), whereas opposite variation in corrosion current density with fly ash content was observed for larger fly ash particles (passing through 300 µm sieve). This signifies that the particle size of fly ash affected the extent of corrosion of rebar in NaCl admixed GPC mixes with a change in fly ash content.

7.6 Conclusions from chloride content near rebar level in fly ash based geopolymer concrete

1) The GPC mixes made with lower molarity of NaOH solution showed higher free chloride content near steel reinforcement in the prismatic specimens when compared with higher molarity of NaOH solution at the age of 600 days irrespective of alkaline solution content,

SS/SH ratio, particle size of fly ash, and fly ash content. The higher amount of chloride ions near rebar level led to mostly more negative corrosion potential and higher corrosion current density in GPC at lower molarity of NaOH solution as compared to higher molarity of NaOH solution.

2) Mostly higher bound chloride content was observed at lower molarity of NaOH solution as compared to higher molarity of NaOH solution.

3) The free chloride, total chloride and bound chloride content near rebar level in prismatic GPC specimens were higher at lower alkaline solution content as compared to that at higher alkaline solution content. Although, the free chloride content was higher at lower alkaline solution content, the unsystematic variation in corrosion current density with alkaline solution content at the age of 600 days indicates that the passivity of steel reinforcement was not altered even in the presence of higher amount of chloride ions at lower alkaline solution content, which is attributed to the effect of improved resistivity of geopolymer concrete at later age.

4) The higher free chloride content near rebar level at the age of 600 days was observed at higher SS/SH ratio for NaOH solution of 10 M whereas opposite variation in free chloride content with SS/SH ratio was observed at NaOH solution of 14 M. Thus, with change in SS/SH ratio, there was consistent variation in the effect of chloride ions on the extent of corrosion at the age of 600 days as indicated by corrosion current density for NaOH solution of 10 M whereas inconsistent variation was observed for NaOH solution of 14 M. Further, the total chloride and bound chloride content near rebar level at later age were higher at lower SS/SH ratio than that at higher SS/SH ratio.

5) The free chloride and total chloride content near steel reinforcement in the prismatic specimens were higher in case of GPC mixes made with smaller fly ash particles as compared to that made with larger fly ash particles irrespective of fly ash content. However, the GPC made with larger fly ash particles showed higher bound chloride content than that made with smaller fly ash particles for higher fly ash content whereas the bound chloride content was mostly higher in GPC mixes made with smaller fly ash particles than that made with larger fly ash particles for lower fly ash content.

6) The GPC mixes made with higher fly ash content showed higher free chloride content near steel reinforcement in the prismatic specimens at the age of 600 days when compared with that made with lower fly ash content irrespective of particle size of fly ash.

7) When compared with the corrosion parameters at the age of 600 days, there was comparatively higher effect of chloride ions on the extent of corrosion of rebar in GPC at higher fly ash content in case of smaller fly ash particles. However, in case of larger fly ash particles, although the free chloride content was higher, the lower corrosion current density in GPC made with higher fly ash content at the later age of 600 days is ascribed to the effect of improved passivation of rebar due to higher resistivity exhibited by the geopolymeric structure during later age in the GPC made with higher fly ash content.

7.7 Conclusions from variations in microstructure near rebar level in fly ash based geopolymer concrete

1) From the XRD patterns of GPC near steel reinforcement in the prismatic specimens at the age of 600 days, the peak intensity of albite, anorthoclase and nepheline were mostly higher at higher molarity of NaOH solution than that at lower molarity of NaOH solution, which indicates formation of more amount of geopolymer gels that led to denser microstructure at higher molarity of NaOH solution. This resulted in lower free chloride content near rebar level at the age of 600 days, which led to lower corrosion activity of steel reinforcement in GPC made with higher molarity of NaOH solution.

2) The peak intensity of albite, anorthoclase, nepheline, muscovite, and sodalite in the XRD patterns of GPC near rebar level at the age of 600 days were lower in NaCl admixed GPC mixes as compared to control GPC mixes. Further, the peak intensity of above compounds mostly decreased with increase in NaCl concentration. This indicates less formation of geopolymer gels in the presence of NaCl that led to less denser microstructure in the presence of NaCl, which resulted in more free chloride content near rebar level at higher concentration of NaCl thereby resulting in higher extent of corrosion of rebar in the presence of chloride ions.

3) The peak intensity of the compounds related to geopolymer gels in XRD patterns of GPC near rebar level at the age of 600 days were mostly higher at lower alkaline solution content, and lower SS/SH ratio as compared to that at higher alkaline solution content, and higher SS/SH ratio respectively. This indicates more amount of geopolymer gels in GPC mixes at lower alkaline solution content, and lower SS/SH ratio that resulted in comparatively higher extent of physical binding of chloride ions with geopolymer gels as higher bound chloride content was observed in GPC mixes at lower alkaline solution content, and lower SS/SH ratio as compared to higher alkaline solution content, and higher SS/SH ratio respectively.

4) The GPC made with larger fly ash particles showed higher peak intensity of the compounds related to geopolymer gels in the XRD patterns as compared to smaller fly ash particles irrespective fly ash content. This indicated comparatively more amount of geopolymer gels in GPC mixes made with larger fly ash particles, which resulted in denser microstructure that led to availability of lower amount of chloride ions near steel reinforcement. It is to be noted that the free chloride content near steel reinforcement at the later age of 600 days was lower in GPC made with larger fly ash particles than that made with smaller fly ash particles.

5) The variation in the peak intensity of albite, anorthoclase, nepheline, muscovite, and sodalite in the XRD patterns near rebar level with fly ash content was opposite between fly ash particles of different sizes. This shows that the particle size of fly ash influenced the extent of formation of geopolymer gels in GPC mixes in the presence of NaCl with change in fly ash content.

6) In the FTIR spectra of GPC near rebar level at the later age, the wavenumber associated with the peak corresponding to asymmetric stretching vibration of Si–O–Si(Al) bond did not vary significantly with change in molarity of NaOH solution, alkaline solution content, SS/SH ratio, particle size and amount of fly ash content, and admixed NaCl concentration.

7) From FESEM images of GPC near steel reinforcement at the later age, formation of comparatively denser microstructure was observed at higher molarity of NaOH solution than lower molarity of NaOH solution, which is supported by the results of XRD analysis where the peak intensity of the phases related to geopolymer gels were higher at higher molarity of NaOH solution.

8) From the FESEM images, the variations in the formation of microstructure of GPC near rebar level at the later age with alkaline solution content, SS/SH ratio, particle size of fly ash, fly ash content, and admixed NaCl concentration are substantiated by the variations in the formation of the phases related to geopolymer gels as indicated by their peak intensity in the XRD patterns.

7.8 Significance of research outcome from present study

In the context of sustainability, the attention of researchers and construction industry is currently focused on searching alternative binders for Portland cement, which are associated with lesser energy consumption and low CO_2 emission. In order to reduce the problems associated with higher energy consumption, higher CO_2 emission, and disposal of industrial wastes, these waste materials are now used in the production of useful products such as geopolymer binder, which is now widely considered as the suitable replacement for Portland

cement binders. In the present research work, the effect of different mix parameters on workability, compressive strength, microstructure variation, and corrosion of rebar in fly ash based geopolymer concrete in the presence of internal chloride has been evaluated. The research outcome obtained from the present work provided important information about the influence of molarity of NaOH solution, alkaline solution content, mass ratio of sodium silicate solution to sodium hydroxide solution (SS/SH ratio), particle size of fly ash, and fly ash content on variations in consistency, compressive strength and microstructure at different ages, chloride content and corrosion of rebar in fly ash based geopolymer concrete (GPC). For example, the obtained results of present study showed that there was improvement in consistency as well compressive strength of GPC with increase in alkaline solution content. However, there was opposite variation between consistency and compressive strength of GPC with increase in SS/SH ratio. Similarly, the GPC made with larger fly ash particles and that made with higher fly ash content showed higher consistency when compared with the mixes made with smaller fly ash particles and lower fly ash content. Further, opposite variation in compressive strength with change in particle size of fly ash was observed between lower and higher fly ash contents. Thus, the obtained variations in constancy, and compressive strength with mix parameters furnishes useful information about the appropriate level of the mix parameters related to alkaline activator and fly ash to be selected for the production of geopolymer concrete that will exhibit adequate consistency and compressive strength.

The correlations between variations in free chloride and bound chloride content with the extent of formation of geopolymer gels as indicated by the obtained compressive strength of GPC at different ages provided important insights about the changes in availability of chloride ions in the pore solution of GPC as well in the extent of physical binding of chloride ions with geopolymer gels in the GPC mixes made with different mix parameters. It may be noted that lower extent of chloride binding was observed in the fly ash based GPC mixes. The obtained outcome from the corrosion study indicated that corrosion behaviour of rebar at different ages in fly ash based geopolymer concrete in the presence of chloride ions was influenced by alkaline solution content, SS/SH ratio, particle size of fly ash, and fly ash content. Although, there was unsystematic variation in corrosion parameters of rebar in GPC with change in molarity of NaOH solution at different ages, however, at the later age, lower free chloride content near steel reinforcement in the prismatic specimens at higher molarity of NaOH solution led to lower corrosion activity of rebar at later age as compared to lower molarity of NaOH solution. Thus, the obtained correlations between free chloride content, and corrosion

behaviour of rebar as indicated by corrosion parameters at the later age with change in mix parameters is essential to understand the changes in the availability of chloride ions in the pore solution of GPC near steel reinforcement, which will affect the extent of corrosion of rebar with age. Further, the extent of chloride binding in GPC near rebar level as indicated by bound chloride content signify the variations in the physical binding of chloride ions with geopolymer gels at later age with change in mix parameters of GPC mixes. The variations in the formation of microstructure of GPC at different ages and that near rebar level as indicated by the results of XRD, FTIR and FESEM analyses mostly showed consistent variation with compressive strength, chloride content and chloride induced corrosion of steel reinforcement in fly ash based geopolymer concrete, which is significant from the viewpoint of understanding the behaviour of fly ash based geopolymer concrete through mechanical and durability properties while taking into account the effect of wide range of mix parameters related to alkaline activator and fly ash.

7.9 Suggestions for future research work

The suggestions for future research work are as follows:

- The present research work can be extended to study the influence of molarity of NaOH solution, alkaline solution content, alkaline solution ratio (SS/SH ratio), particle size of fly ash and fly ash content on microstructure and chloride induced corrosion of steel reinforcement in fly ash based geopolymer concrete exposed to external chloride environment.

- The present research work can be extended to carry out chloride diffusion study in fly ash based geopolymer concrete.

- The present study can be extended to evaluate the efficiency of different corrosion inhibitors against chloride induced rebar corrosion in fly ash based geopolymer concrete exposed chloride environment.

REFERENCES

[1] A. R. Sakulich, "Reinforced geopolymer composites for enhanced material greenness and durability," Sustainable Cities and Society, vol. 1, no. 4, pp. 195-210, 2011.

[2] M. C. G. Juenger, F. Winnefeld, J. L. Provis, and J. H. Ideker, "Advances in alternative cementitious binders," Cement and Concrete Research, vol. 41, no. 12, pp. 1232-1243, 2011.

[3] W. K. Part, M. Ramli, and C. B. Cheah, "An overview on the influence of various factors on the properties of geopolymer concrete derived from industrial by-products," Construction and Building Materials, vol. 77, pp. 370-395, 2015.

[4] K. A. Komnitsas, "Potential of geopolymer technology towards green buildings and sustainable cities," Procedia engineering, vol. 21, pp. 1023-1032, 2011.

[5] E. M. Gartner and D. E. MacPhee, "A physico-chemical basis for novel cementitious binders," Cement and Concrete Research, vol. 41, no. 7, pp. 736-749, 2011.

[6] P. Pavithra, M. Srinivasula Reddy, P. Dinakar, B. Hanumantha Rao, B. K. Satpathy, and A. N. Mohanty, "A mix design procedure for geopolymer concrete with fly ash," Journal of Cleaner Production, vol. 133, pp. 117-125, 2016.

[7] M. Babaee and A. Castel, "Chloride-induced corrosion of reinforcement in low-calcium fly ash-based geopolymer concrete," Cement and Concrete Research, vol. 88, pp. 96-107, 2016.

[8] B. Suhendro, "Toward green concrete for better sustainable environment," Procedia engineering, vol. 95, pp. 305-320, 2014.

[9] A. A. Aliabdo, A. E. M. Abd Elmoaty, and H. A. Salem, "Effect of water addition, plasticizer and alkaline solution constitution on fly ash based geopolymer concrete performance," Construction and Building Materials, vol. 121, pp. 694-703, 2016.

[10] B. Singh, G. Ishwarya, M. Gupta, and S. K. Bhattacharyya, "Geopolymer concrete: A review of some recent developments," Construction and Building Materials, vol. 85, pp. 78-90, 2015.

[11] P. Duxson, J. L. Provis, G. C. Lukey, and J. S. J. van Deventer, "The role of inorganic polymer technology in the development of 'green concrete,'" Cement and Concrete Research, vol. 37, no. 12, pp. 1590-1597, 2007.

[12] M. Torres-Carrasco and F. Puertas, "Waste glass in the geopolymer preparation. mechanical and microstructural characterisation," Journal of Cleaner Production, vol. 90, pp. 397-408, 2015.

[13] A. B. Malkawi, M. F. Nuruddin, A. Fauzi, H. Almattarneh, and B. S. Mohammed, "Effects of alkaline solution on properties of the HCFA geopolymer mortars," Procedia engineering, vol. 148, pp. 710-717, 2016.

[14] J. Davidovits and S. Cordi, "Synthesis of new high temperature geo-polymers for reinforced plastics / composites," SPE PACTEC 79, pp. 151-154, 1979.

[15] J. Davidovits, "Geopolymers and geopolymeric materials," Journal of Thermal Analysis, vol. 35, no. 2, pp. 429-441, 1989.

[16] Z. Li, S. Zhang, Y. Zuo, W. Chen, and G. Ye, "Chemical deformation of metakaolin based geopolymer," Cement and Concrete Research, vol. 120, pp. 108-118, 2019.

[17] C. A. Rees, J. L. Provis, G. C. Lukey, and J. S. J. van Deventer, "The mechanism of geopolymer gel formation investigated through seeded nucleation," Colloids and Surfaces A: Physicochemical and Engineering Aspects, vol. 318, pp. 97-105, 2008.

[18] Y. J. Zhang, H. H. Li, Y. C. Wang, and D. L. Xu, "Geopolymer microstructure and hydration mechanism of alkali-activated fly ash-based geopolymer," Advanced Materials Research, vol. 374, pp. 1481-1484, 2012.

[19] P. Zhang, Z. Gao, J. Wang, J. Guo, S. Hu, and Y. Ling, "Properties of fresh and hardened fly ash/slag based geopolymer concrete: A review," Journal of Cleaner Production, vol. 270, p. 122389, 2020.

[20] J. Davidovits, "Geopolymers," Journal of Thermal Analysis, vol. 37, no. 8, pp. 1633-1656, 1991.

[21] C. Shi, A. F. Jiménez, and A. Palomo, "New cements for the 21st century: The pursuit of an alternative to Portland cement," Cement and Concrete Research, vol. 41, no. 7, pp. 750-763, 2011.

[22] A. A. Aliabdo, A. Elmoaty, M. A. Elmoaty, and H. A. Salem, "Effect of cement addition, solution resting time and curing characteristics on fly ash based geopolymer concrete performance," Construction and Building Materials, vol. 123, pp. 581-593, 2016.

[23] K. T. Nguyen, N. Ahn, T. A. Le, and K. Lee, "Theoretical and experimental study on mechanical properties and flexural strength of fly ash-geopolymer concrete," Construction and Building Materials, vol. 106, pp. 65-77, 2016.

[24] K. Kupwade-Patil and E. N. Allouche, "Examination of chloride-induced corrosion in reinforced geopolymer concretes," ASCE Journal of Materials in Civil Engineering, vol. 25, no. 10, pp. 1465-1476, 2013.

[25] C. Gunasekara, D. Law, S. Bhuiyan, S. Setunge, and L. Ward, "Chloride induced corrosion in different fly ash based geopolymer concretes," Construction and Building Materials, vol. 200, pp. 502-513, 2019.

[26] M. Soutsos, A. P. Boyle, R. Vinai, A. Hadjierakleous, and S. J. Barnett, "Factors influencing the compressive strength of fly ash based geopolymers," Construction and Building Materials, vol. 110, pp. 355-368, 2016.

[27] M. Olivia and H. Nikraz, "Properties of fly ash geopolymer concrete designed by Taguchi method," Materials and Design, vol. 36, pp. 191-198, 2012.

[28] M. N. S. Hadi, M. Al-Azzawi, and T. Yu, "Effects of fly ash characteristics and alkaline activator components on compressive strength of fly ash-based geopolymer mortar," Construction and Building Materials, vol. 175, pp. 41-54, 2018.

[29] X. Y. Zhuang et al., "Fly ash-based geopolymer: Clean production, properties and applications," Journal of Cleaner Production, vol. 125, pp. 253-267, 2016.

[30] ASTM C618-23, "Standard Specification for Coal Ash and Raw or Calcined Natural Pozzolan for Use in Concrete," ASTM International, West Conshohocken, PA, 2023.

[31] A. M. Neville and J. J. Brooks, "Concrete Technology'', Fourth Indian reprint, New Delhi: Pearson Education Limited, 2004.

[32] A. Hassan, M. Arif, and M. Shariq, "Use of geopolymer concrete for a cleaner and sustainable environment - A review of mechanical properties and microstructure," Journal of Cleaner Production, vol. 223, pp. 704-728, 2019.

[33] P. K. Mehta and P. J. M. Monteiro, "Concrete: microstructure, properties, and materials," 3rd Edition, New Delhi: Tata McGraw Hill Education Private Limited, 2006.

[34] A. M. Neville and J. J. Brooks, "Concrete Technology'', 17th Edition, New Delhi: Pearson Education Limited, 2013.

[35] A. Noushini, A. Castel, J. Aldred, and A. Rawal, "Chloride diffusion resistance and chloride binding capacity of fly ash-based geopolymer concrete," Cement and Concrete Composites, vol. 105, p. 103290, 2019.

[36] F. Tittarelli, A. Mobili, C. Giosuè, A. Belli, and T. Bellezze, "Corrosion behaviour of bare and galvanized steel in geopolymer and Ordinary Portland Cement based mortars with the same strength class exposed to chlorides," Corrosion Science, vol. 134, pp. 64-77, 2018.

[37] P. S. Mangat and O. O. Ojedokun, "Free and bound chloride relationships affecting reinforcement cover in alkali activated concrete," Cement and Concrete Composites, vol. 112, p. 103692, 2020.

[38] J. Zhang, C. Shi, and Z. Zhang, "Chloride binding of alkali-activated slag/fly ash cements," Construction and Building Materials, vol. 226, pp. 21-31, 2019.

[39] C. Fu, H. Ye, K. Zhu, D. Fang, and J. Zhou, "Alkali cation effects on chloride binding of alkali-activated fly ash and metakaolin geopolymers," Cement and Concrete Composites, vol. 114, p. 103721, 2020.

[40] M. T. Junaid, O. Kayali, A. Khennane, and J. Black, "A mix design procedure for low calcium alkali activated fly ash-based concretes," Construction and Building Materials, vol. 79, pp. 301-310, 2015.

[41] C. D. Atiş, E. B. Görür, O. Karahan, C. Bilim, S. Ilkentapar, and E. Luga, "Very high strength (120 MPa) class F fly ash geopolymer mortar activated at different NaOH amount, heat curing temperature and heat curing duration," Construction and Building Materials, vol. 96, pp. 673-678, 2015.

[42] A. Mehta and R. Siddique, "Strength, permeability and micro-structural characteristics of low-calcium fly ash based geopolymers," Construction and Building Materials, vol. 141, pp. 325-334, 2017.

[43] J. G. Jang, "Effect of fly ash characteristics on delayed high-strength development of geopolymers," Construction and Building Materials, vol. 102, pp. 260-269, 2016.

[44] P. Chindaprasirt, T. Chareerat, and V. Sirivivatnanon, "Workability and strength of coarse high calcium fly ash geopolymer," Cement and Concrete Composites, vol. 29, no. 3, pp. 224-229, 2007.

[45] M. Kaur, J. Singh, and M. Kaur, "Synthesis of fly ash based geopolymer mortar considering different concentrations and combinations of alkaline activator solution," Ceramics International, vol. 44, no. 2, pp. 1534-1537, 2018.

[46] U. Rattanasak and P. Chindaprasirt, "Influence of NaOH solution on the synthesis of fly ash geopolymer," Minerals Engineering, *vol.* 22, no. 12, pp. 1073-1078, 2009.

[47] P. Topark-Ngarm, P. Chindaprasirt, and V. Sata, "Setting time, strength, and bond of high-calcium fly ash geopolymer concrete," ASCE Journal of Materials in Civil Engineering, vol. 27, no. 7, pp. 04014198-1-7, 2015.

[48] G. Görhan and G. Kürklü, "The influence of the NaOH solution on the properties of the fly ash-based geopolymer mortar cured at different temperatures," Composites Part B: Engineering, vol. 58, pp. 371-377, 2014.

[49] B. Joseph and G. Mathew, "Influence of aggregate content on the behavior of fly ash based geopolymer concrete," Scientia Iranica, vol. 19, no. 5, pp. 1188-1194, 2012.

[50] H. Abdulrahman, R. Muhamad, P. Visintin, and A. Azim Shukri, "Mechanical properties and bond stress-slip behaviour of fly ash geopolymer concrete," Construction and Building Materials, vol. 327, p. 126909, 2022.

[51] P. S. Deb, P. Nath, and P. K. Sarker, "The effects of ground granulated blast-furnace slag blending with fly ash and activator content on the workability and strength properties of geopolymer concrete cured at ambient temperature," Materials and Design, vol. 62, pp. 32-39, 2014.

[52] S. Saha and C. Rajasekaran, "Enhancement of the properties of fly ash based geopolymer paste by incorporating ground granulated blast furnace slag," Construction and Building Materials, vol. 146, pp. 615-620, 2017.

[53] H. K. Shehab, A. S. Eisa, and A. M. Wahba, "Mechanical properties of fly ash based geopolymer concrete with full and partial cement replacement," Construction and Building Materials, vol. 126, pp. 560-565, 2016.

[54] P. Chindaprasirt, T. Chareerat, S. Hatanaka, and T. Cao, "High-strength geopolymer using fine high-calcium fly ash," ASCE Journal of Materials in Civil Engineering, vol. 23, no. 3, pp. 264-270, 2011.

[55] E. J. Guades, "Experimental investigation of the compressive and tensile strengths of geopolymer mortar: The effect of sand/fly ash (S/FA) ratio," Construction and Building Materials, vol. 127, pp. 484-493, 2016.

[56] W. Lokuge, A. Wilson, C. Gunasekara, D. W. Law, and S. Setunge, "Design of fly ash geopolymer concrete mix proportions using Multivariate Adaptive Regression Spline model," Construction and Building Materials, vol. 166, pp. 472-481, 2018.

[57] A. Mehta and R. Siddique, "Properties of low-calcium fly ash based geopolymer concrete incorporating OPC as partial replacement of fly ash," Construction and Building Materials, vol. 150, pp. 792-807, 2017.

[58] G. Nagalia, Y. Park, A. Abolmaali, and P. Aswath, "Compressive strength and microstructural properties of fly ash-based geopolymer concrete," ASCE Journal of Materials in Civil Engineering, vol. 28, no. 12, pp. 04016144-1-11, 2016.

[59] P. Chindaprasirt, C. Jaturapitakkul, W. Chalee, and U. Rattanasak, "Comparative study on the characteristics of fly ash and bottom ash geopolymers," Waste Management, vol. 29, no. 2, pp. 539-543, 2009.

[60] G. S. Ryu, Y. B. Lee, K. T. Koh, and Y. S. Chung, "The mechanical properties of fly ash-based geopolymer concrete with alkaline activators," Construction and Building Materials, vol. 47, pp. 409-418, 2013.

[61] S. Hanjitsuwan, S. Hunpratub, P. Thongbai, S. Maensiri, and V. Sata, "Effects of NaOH concentrations on physical and electrical properties of high calcium fly ash geopolymer paste," Cement and Concrete Composites, vol. 45, pp. 9-14, 2014.

[62] T. Xie and T. Ozbakkaloglu, "Behavior of low-calcium fly and bottom ash-based geopolymer concrete cured at ambient temperature," Ceramics International, vol. 41, no. 4, pp. 5945-5958, 2015.

[63] P. Sajan, T. Jiang, C. Lau, G. Tan, and K. Ng, "Combined effect of curing temperature, curing period and alkaline concentration on the mechanical properties of fly ash-based geopolymer," Cleaner Materials, vol. 1, p. 100002, 2021.

[64] Parveen, D. Singhal, M. T. Junaid, B. B. Jindal, and A. Mehta, "Mechanical and microstructural properties of fly ash based geopolymer concrete incorporating alccofine at ambient curing," Construction and Building Materials, vol. 180, pp. 298-307, 2018.

[65] A. G. de S. Azevedo and K. Strecker, "Brazilian fly ash based inorganic polymers production using different alkali activator solutions," Ceramics International, vol. 43, no. 12, pp. 9012-9018, 2017.

[66] S. K. Nath and S. Kumar, "Role of particle fineness on engineering properties and microstructure of fly ash derived geopolymer," Construction and Building Materials, vol. 233, p. 117294, 2020.

[67] S. Kumar, F. Kristály, and G. Mucsi, "Geopolymerisation behaviour of size fractioned fly ash," Advanced Powder Technology, vol. 26, no. 1, pp. 24-30, 2015.

[68] A. M. Mustafa Al Bakri, H. Kamarudin, M. Bnhussain, A. R. Rafiza, and Y. Zarina, "Effect of Na_2SiO_3/NaOH ratios and NaOH molarities on compressive strength of fly-ash-based geopolymer," ACI Materials Journal, vol. 109, no. 5, pp. 503-508, 2012.

[69] N. A. Farhan, M. N. Sheikh, and M. N. S. Hadi, "Investigation of engineering properties of normal and high strength fly ash based geopolymer and alkali-activated slag concrete compared to ordinary Portland cement concrete," Construction and Building Materials, vol. 196, pp. 26-42, 2019.

[70] S. J. Chithambaram, S. Kumar, and M. M. Prasad, "Thermo-mechanical characteristics of geopolymer mortar," Construction and Building Materials, vol. 213, pp. 100-108, 2019.

[71] H. E. Elyamany, A. Elmoaty, M. A. Elmoaty, and A. M. Elshaboury, "Setting time and 7-day strength of geopolymer mortar with various binders," Construction and Building Materials, vol. 187, pp. 974-983, 2018.

[72] T. Phoo-Ngernkham, A. Maegawa, N. Mishima, S. Hatanaka, and P. Chindaprasirt, "Effects of sodium hydroxide and sodium silicate solutions on compressive and shear bond strengths of FA-GBFS geopolymer," Construction and Building Materials, vol. 91, pp. 1-8, 2015.

[73] P. Nath and P. K. Sarker, "Effect of GGBFS on setting , workability and early strength properties of fly ash geopolymer concrete cured in ambient condition," Construction and Building Materials, vol. 66, pp. 163-171, 2014.

[74] C. Gunasekara, D. W. Law, and S. Setunge, "Long term permeation properties of different fly ash geopolymer concretes," Construction and Building Materials, vol. 124, pp. 352-362, 2016.

[75] P. Nuaklong, V. Sata, and P. Chindaprasirt, "Influence of recycled aggregate on fly ash geopolymer concrete properties," Journal of Cleaner Production, vol. 112, pp. 2300-2307, 2016.

[76] D. V. Reddy, J.-B. Edouard, and K. Sobhan, "Durability of fly ash-based geopolymer structural concrete in the marine environment," ASCE Journal of Materials in Civil Engineering, vol. 25, no. 6, pp. 781-787, 2013.

[77] P. Chindaprasirt and W. Chalee, "Effect of sodium hydroxide concentration on chloride penetration and steel corrosion of fly ash-based geopolymer concrete under marine site," Construction and Building Materials, vol. 63, pp. 303-310, 2014.

[78] K. Pasupathy, M. Berndt, J. Sanjayan, P. Rajeev, and D. S. Cheema, "Durability of low-calcium fly ash based geopolymer concrete culvert in a saline environment," Cement and Concrete Research, vol. 100, pp. 297-310, 2017.

[79] K. Pasupathy, D. Singh, and J. Sanjayan, "Durability performance of fly ash-based geopolymer concrete buried in saline environment for 10 years," Construction and Building Materials, vol. 281, p. 122596, 2021.

[80] A. Ojha and P. Aggarwal, "Durability performance of low calcium fly ash-based geopolymer concrete," Structures, vol. 54, pp. 956-963, 2023.

[81] D. Adak and S. Mandal, "Strength and durability performance of fly ash-based process-modified geopolymer concrete," ASCE Journal of Materials in Civil Engineering, vol. 31, no. 9, pp. 04019174-1-8, 2019.

[82] IS: 2386 (Part-1): 1963 (Reaffirmed 2021), "Methods of Test for Aggregate for Concrete Part 1 Particle Size and Shape," Bureau of Indian Standards, New Delhi, 2021.

[83] IS: 383: 2016 (Reaffirmed 2021), "Coarse and Fine Aggregate for Concrete - Specification," Bureau of Indian Standards, New Delhi, 2021.

[84] IS: 2386 (Part-3): 1963 (Reaffirmed 2021), "Methods of Test for Aggregate for Concrete Part 3 Specific Gravity, Density, Voids, Absorption and Bulking," Bureau of Indian Standards, New Delhi, 2021.

[85] IS: 1199 (Part-2): 2018, "Fresh Concrete-Methods of Sampling, Testing and Analysis-Determination of Consistency of Fresh Concrete," Bureau of Indian Standards, New Delhi, 2018.

[86] IS: 516 (Part 1/Sec 1): 2021, "Hardened Concrete - Methods of Tests," Bureau of Indian Standards, New Delhi, 2021.

[87] B. Pradhan, "Corrosion behavior of steel reinforcement in concrete exposed to composite chloride-sulfate environment," Construction and Building Materials, vol. 72, pp. 398-410, 2014.

[88] O. S. B. Al-Amoudi and M. Maslehuddin, "The effect of chloride and sulfate ions on reinforcement corrosion," Cement and Concrete Research, vol. 23, no. 1, pp. 139-146, 1993.

[89] M. T. Ghafoor, Q. S. Khan, A. U. Qazi, M. N. Sheikh, and M. N. S. Hadi, "Influence of alkaline activators on the mechanical properties of fly ash based geopolymer concrete cured at ambient temperature," Construction and Building Materials, vol. 273, p. 121752, 2021.

[90] J. K. Prusty and B. Pradhan, "Evaluation of durability and microstructure evolution of chloride added fly ash and fly ash-GGBS based geopolymer concrete," Construction and Building Materials, vol. 401, p. 132925, 2023.

[91] J. Wongpa, K. Kiattikomol, C. Jaturapitakkul, and P. Chindaprasirt, "Compressive strength, modulus of elasticity, and water permeability of inorganic polymer concrete," Materials and Design, vol. 31, no. 10, pp. 4748-4754, 2010.

[92] S. Samantasinghar and S. P. Singh, "Effect of synthesis parameters on compressive strength of fly ash-slag blended geopolymer," Construction and Building Materials, vol. 170, pp. 225-234, 2018.

[93] N. K. Lee, H. R. Khalid, and H. K. Lee, "Synthesis of mesoporous geopolymers containing zeolite phases by a hydrothermal treatment," Microporous Mesoporous Mater., vol. 229, pp. 22-30, 2016.

[94] I. Ismail, S. A. Bernal, J. L. Provis, R. S. Nicolas, D. G. Brice, A. R. Kilcullen, S. Hamdan, J. S. J. van Deventer, "Influence of fly ash on the water and chloride permeability of alkali-activated slag mortars and concretes," Construction and Building Materials, vol. 48, pp. 1187-1201, 2013.

[95] N. K. Lee and H. K. Lee, "Influence of the slag content on the chloride and sulfuric acid resistances of alkali-activated fly ash/slag paste," Cement and Concrete Composites, vol. 72, pp. 168-179, 2016.

[96] L. N. Tchadjie, J. N. Y. Djobo, N. Ranjbar, H. K. Tchakoute, B. B. D. Kenne, A. Elimbi, D. Njopwouo, "Potential of using granite waste as raw material for geopolymer synthesis," Ceramics International, vol. 42, no. 2, pp. 3046-3055, 2016.

[97] B. Yuan, Q. L. Yu, and H. J. H. Brouwers, "Reaction kinetics, reaction products and compressive strength of ternary activators activated slag designed by Taguchi method," Materials and Design, vol. 86, pp. 878-886, 2015.

[98] N. Ranjbar, M. Mehrali, M. R. Maheri, and M. Mehrali, "Hot-pressed geopolymer," Cement and Concrete Research, vol. 100, pp. 14-22, 2017.

[99] X. Guo, H. Shi, and W. A. Dick, "Compressive strength and microstructural characteristics of class C fly ash geopolymer," Cement and Concrete Composites, vol. 32, no. 2, pp. 142-147, 2010.

[100] ASTM: C 876-15, "Standard Test Method for Corrosion Potential of Uncoated Reinforcing Steel in Concrete," ASTM International, West Conshohocken, PA, 2015.

Appendix A

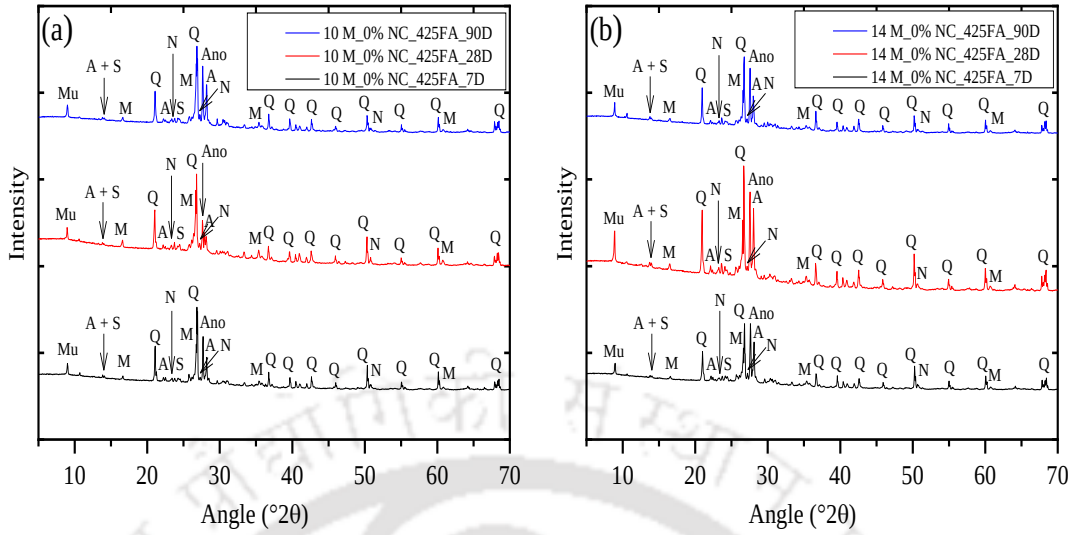

(GPC made with fly ash passing through 300 μm sieve, fly ash content of 425 kg/m^3, alkaline solution content of 210 kg/m^3, and SS/SH ratio of 1.75)

Fig. A1: XRD patterns of control GPC mixes at different ages: a) NaOH solution of 10 M, and b) NaOH solution of 14 M

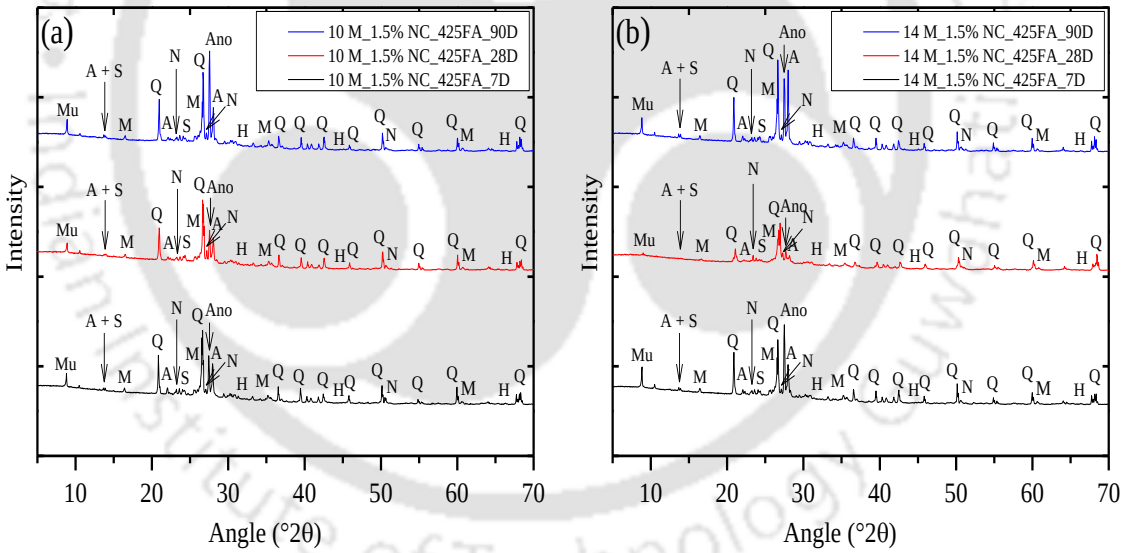

(GPC made with fly ash passing through 300 μm sieve, fly ash content of 425 kg/m^3, alkaline solution content of 210 kg/m^3, and SS/SH ratio of 1.75)

Fig. A2: XRD patterns of GPC mixes at different ages: a) NaOH solution of 10 M, and b) NaOH solution of 14 M for admixed NaCl concentration of 1.5%

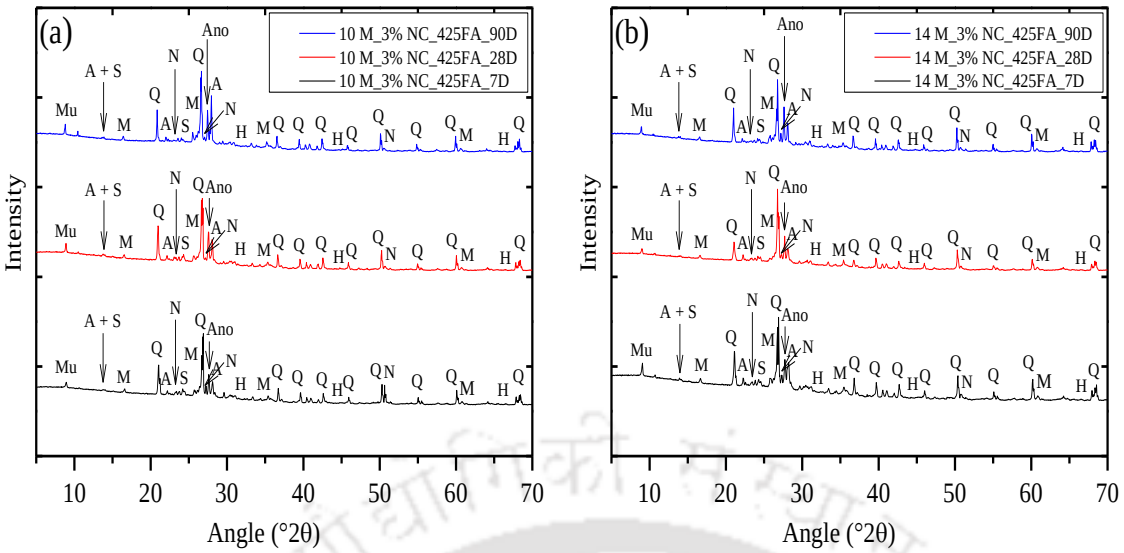

(GPC made with fly ash passing through 300 μm sieve, fly ash content of 425 kg/m^3, alkaline solution content of 210 kg/m^3, and SS/SH ratio of 1.75)

Fig. A3: XRD patterns of GPC mixes at different ages: a) NaOH solution of 10 M, and b) NaOH solution of 14 M for admixed NaCl concentration of 3%

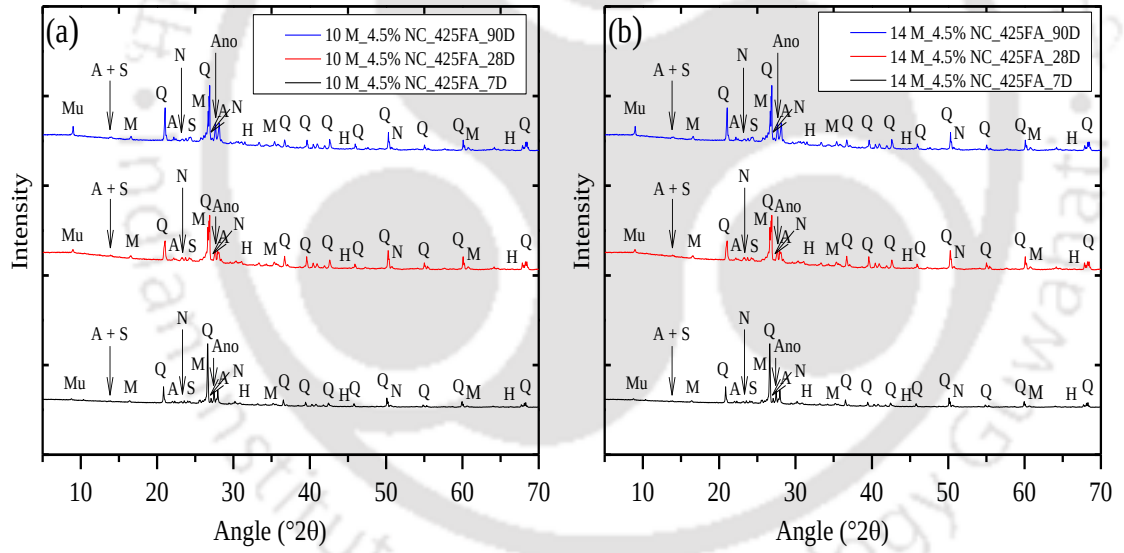

(GPC made with fly ash passing through 300 μm sieve, fly ash content of 425 kg/m^3, alkaline solution content of 210 kg/m^3, and SS/SH ratio of 1.75)

Fig. A4: XRD patterns of GPC mixes at different ages: a) NaOH solution of 10 M, and b) NaOH solution of 14 M for admixed NaCl concentration of 4.5%

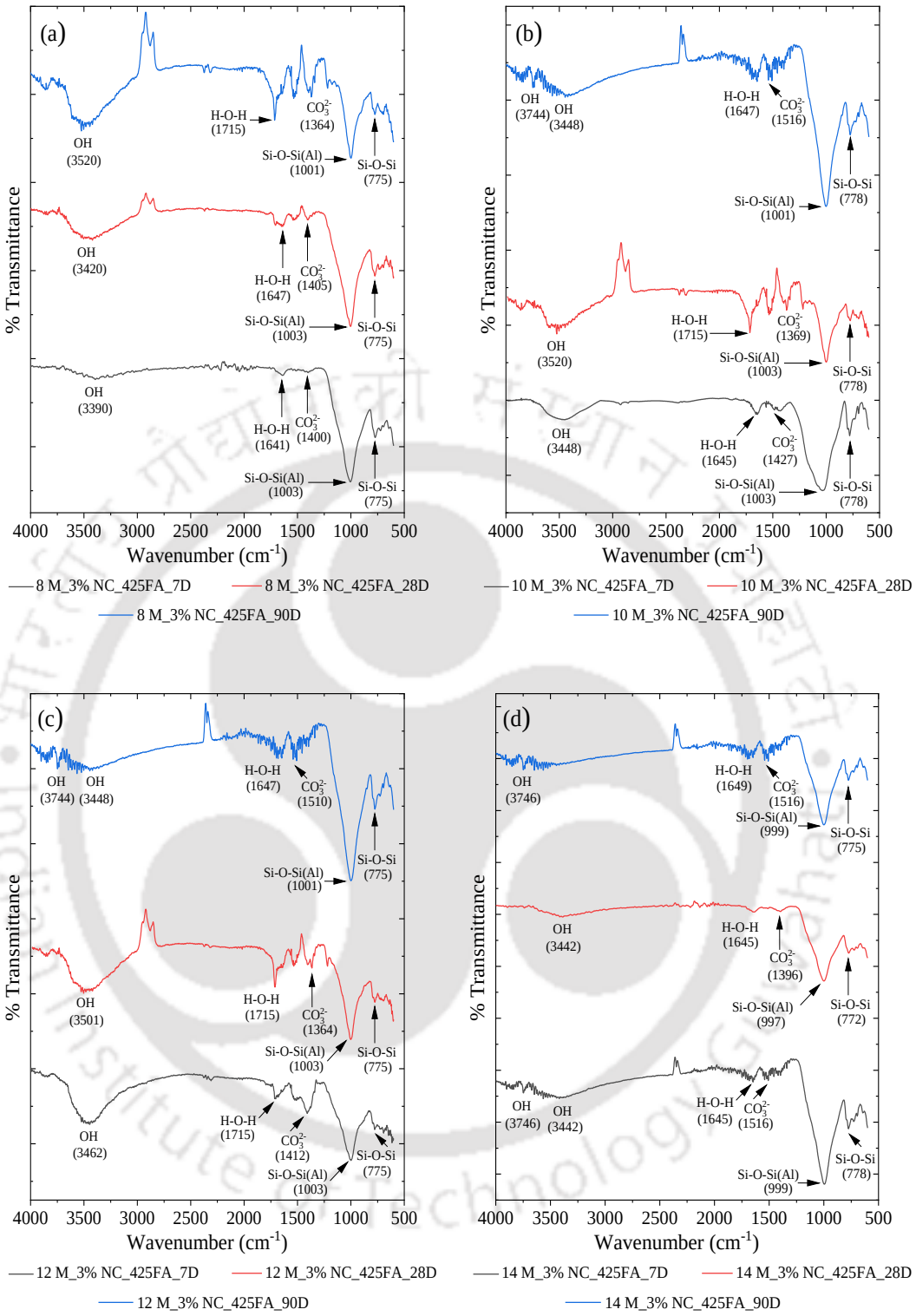

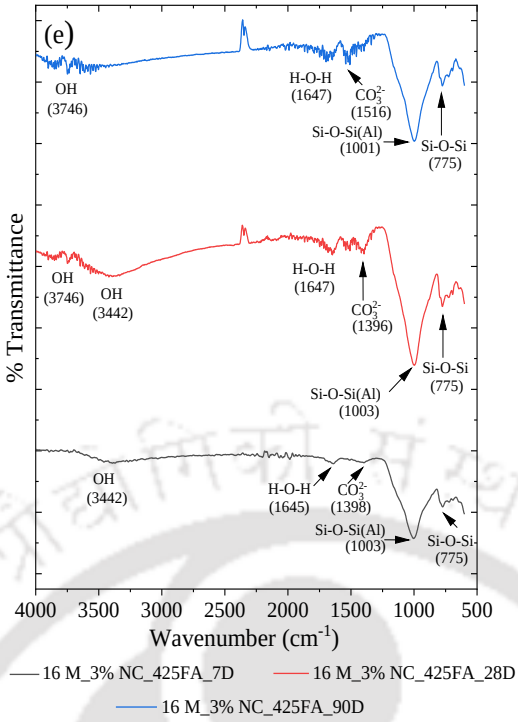

(GPC made with fly ash passing through 300 μm sieve, fly ash content of 425 kg/m^3, alkaline solution content of 210 kg/m^3, and SS/SH ratio of 1.75)

Fig. A5: FTIR spectra of GPC mixes at different ages: a) NaOH solution of 8 M, b) NaOH solution of 10 M, c) NaOH solution of 12 M, d) NaOH solution of 14 M, and e) NaOH solution of 16 M for admixed NaCl concentration of 3%

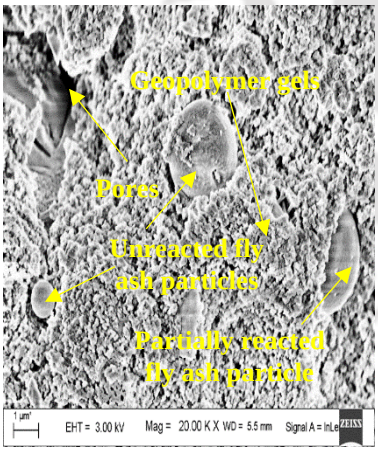

(a) 8 M/0%NC/425FA/7D

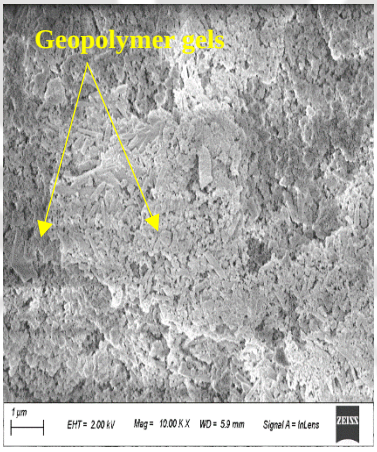

(b) 10 M/0%NC/425FA/7D

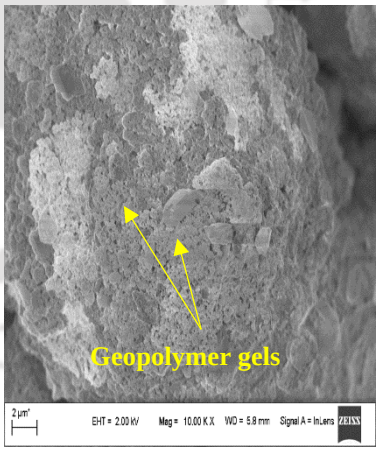

(c) 12 M/0%NC/425FA/7D

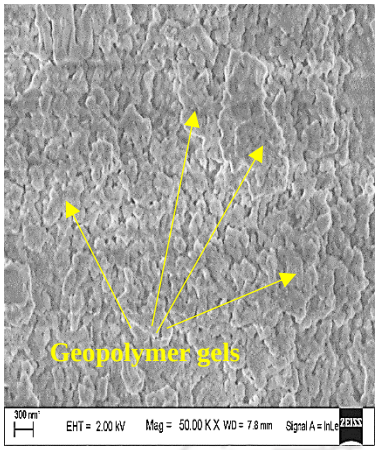

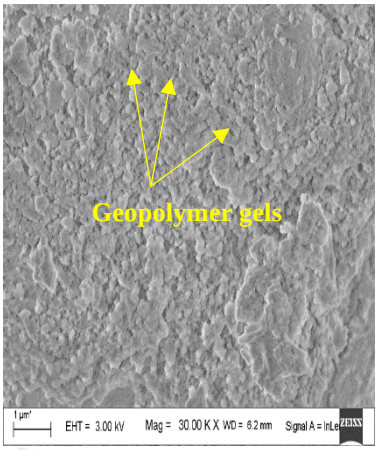

(d) 14 M/0%NC/425FA/7D (e) 16 M/0%NC/425FA/7D

(GPC made with fly ash passing through 300 μm sieve, fly ash content of 425 kg/m^3, alkaline solution content of 210 kg/m^3, and SS/SH ratio of 1.75)

Fig. A6: FESEM images of control GPC for different molarity of NaOH solution at the age of 7 days

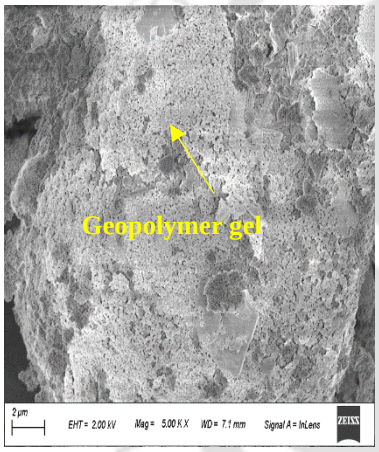

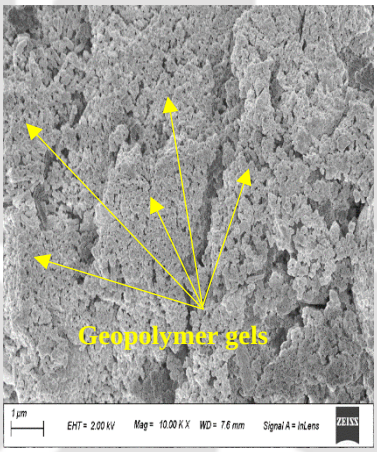

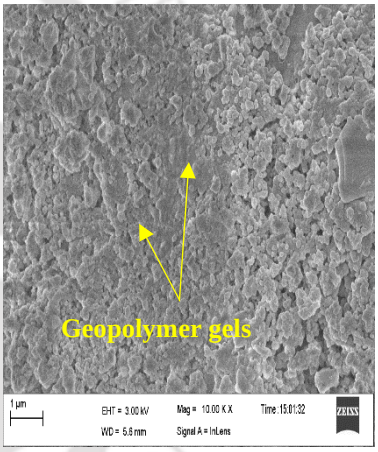

(a) 8 M/0%NC/425FA/28D (b) 10 M/0%NC/425FA/28D (c) 12 M/0%NC/425FA/28D

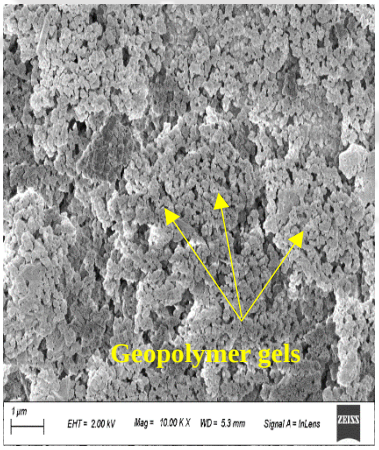

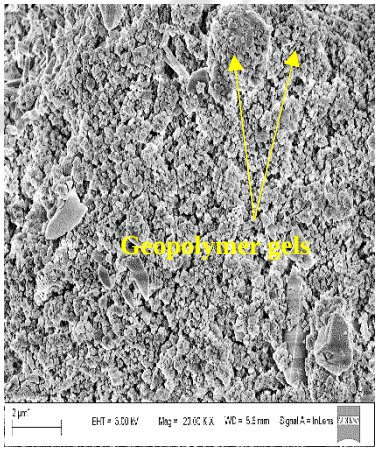

(d) 14 M/0%NC/425FA/28D (e) 16 M/0%NC/425FA/28D

(GPC made with fly ash passing through 300 μm sieve, fly ash content of 425 kg/m^3, alkaline solution content of 210 kg/m^3, and SS/SH ratio of 1.75)

Fig. A7: FESEM images of control GPC for different molarity of NaOH solution at the age of 28 days

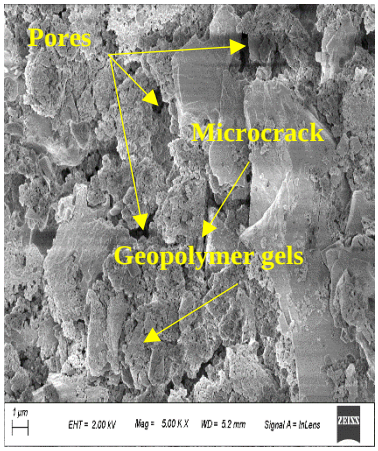

(a) 8 M/0%NC/425FA/90D

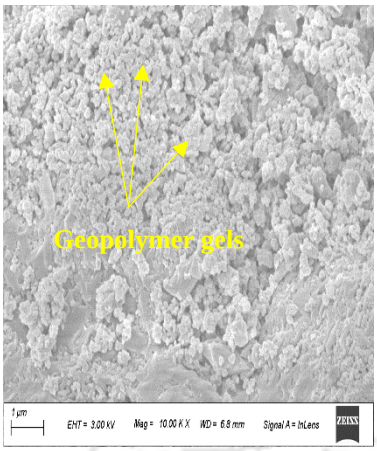

(b) 10 M/0%NC/425FA/90D

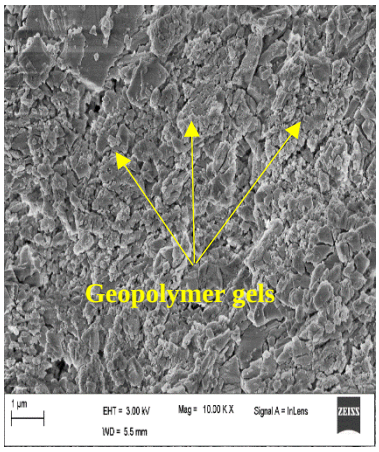

(c) 14 M/0%NC/425FA/90D

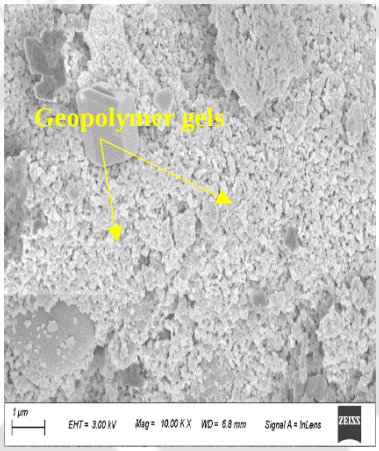

(d) 16 M/0%NC/425FA/90D

(GPC made with fly ash passing through 300 μm sieve, fly ash content of 425 kg/m^3, alkaline solution content of 210 kg/m^3, and SS/SH ratio of 1.75)

Fig. A8: FESEM images of control GPC for different molarity of NaOH solution at the age of 90 days

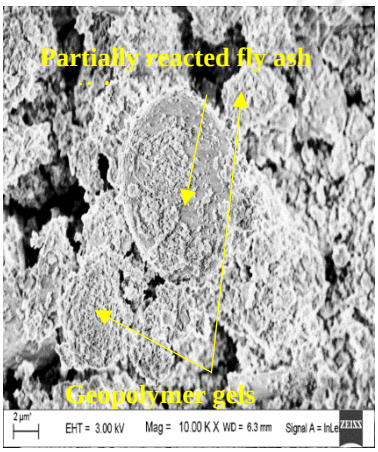

(a) 8 M/1.5%NC/425FA/7D

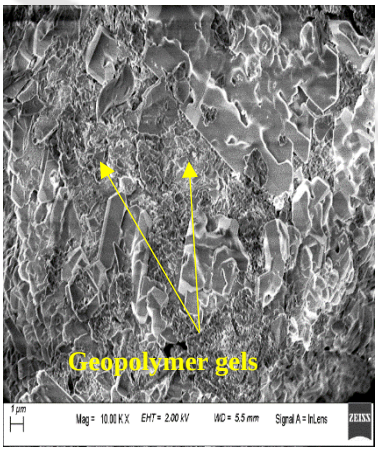

(b) 12 M/1.5%NC/425FA/7D

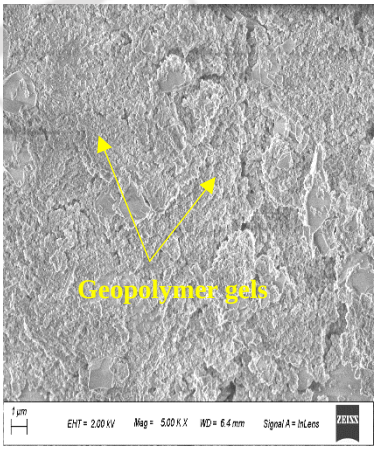

(c) 14 M/1.5%NC/425FA/7D

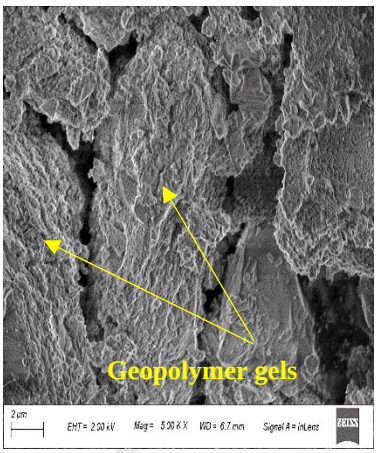

(d) 16 M/1.5%NC/425FA/7D

(GPC made with fly ash passing through 300 μm sieve, fly ash content of 425 kg/m^3, alkaline solution content of 210 kg/m^3, and SS/SH ratio of 1.75)

Fig. A9: FESEM images of GPC for different molarity of NaOH solution, admixed NaCl concentrations of 1.5% at the age of 7 days

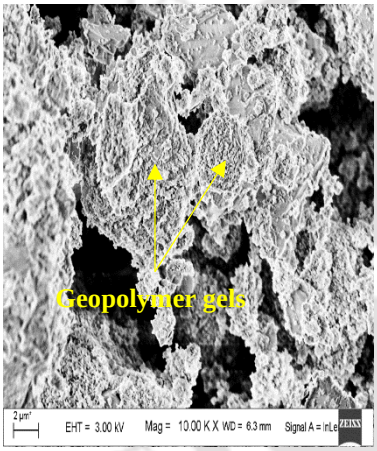

(a) 8 M/1.5%NC/425FA/28D

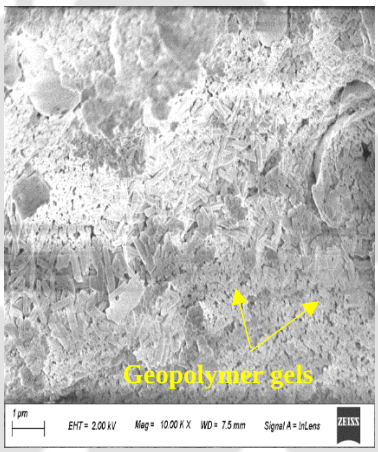

(b) 12 M/1.5%NC/425FA/28D

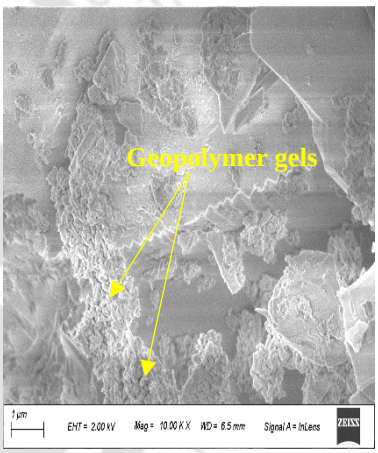

(c) 14 M/1.5%NC/425FA/28D

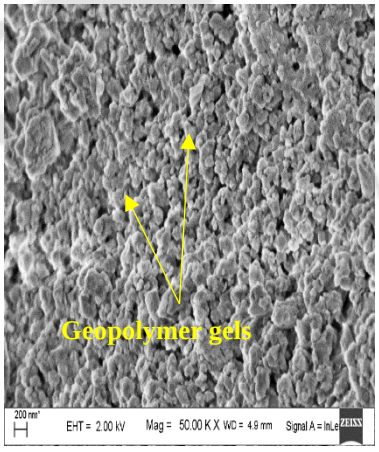

(d) 16 M/1.5%NC/425FA/28D

(GPC made with fly ash passing through 300 μm sieve, fly ash content of 425 kg/m^3, alkaline solution content of 210 kg/m^3, and SS/SH ratio of 1.75)

Fig. A10: FESEM images of GPC for different molarity of NaOH solution, admixed NaCl concentrations of 1.5% at the age of 28 days

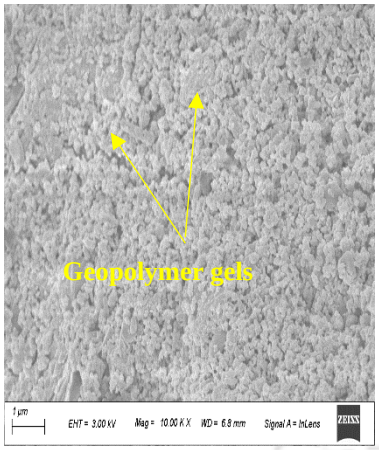

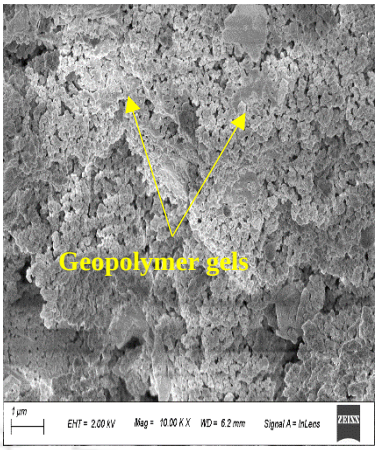

(a) 14 M/1.5%NC/425FA/90D (b) 16 M/1.5%NC/425FA/90D

(GPC made with fly ash passing through 300 μm sieve, fly ash content of 425 kg/m^3, alkaline solution content of 210 kg/m^3, and SS/SH ratio of 1.75)

Fig. A11: FESEM images of GPC for different molarity of NaOH solution, admixed NaCl concentrations of 1.5% at the age of 90 days

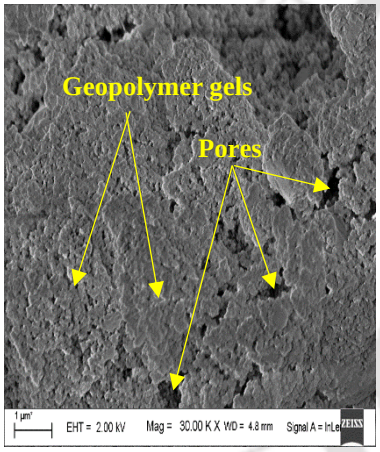

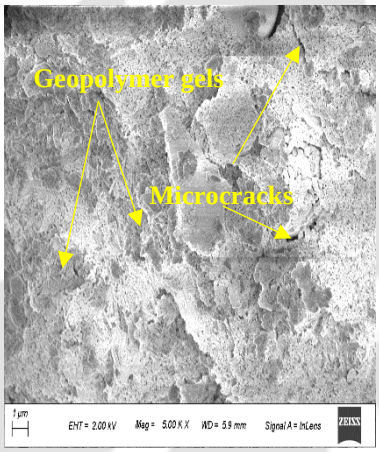

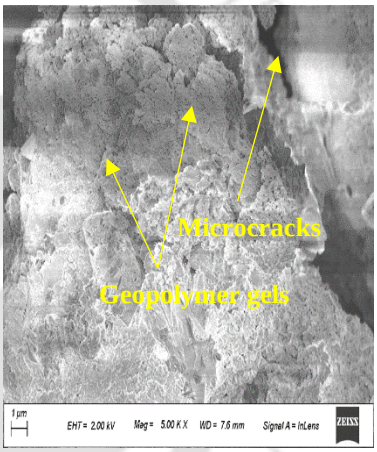

(a) 8 M/3%NC/425FA/7D (b) 10 M/3%NC/425FA/7D (c) 12 M/3%NC/425FA/7D

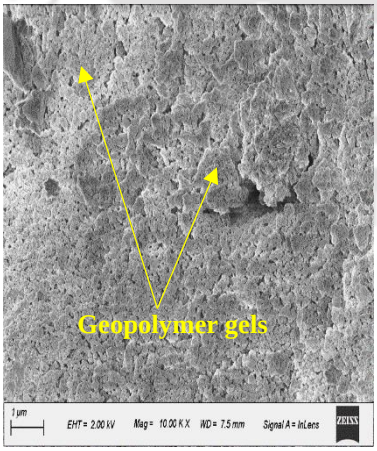

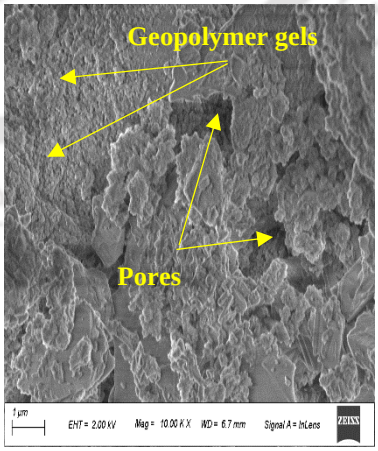

(d) 14 M/3%NC/425FA/7D (e) 16 M/3%NC/425FA/7D

(GPC made with fly ash passing through 300 μm sieve, fly ash content of 425 kg/m^3, alkaline solution content of 210 kg/m^3, and SS/SH ratio of 1.75)

Fig. A12: FESEM images of GPC for different molarity of NaOH solution, admixed NaCl concentrations of 3% at the age of 7 days

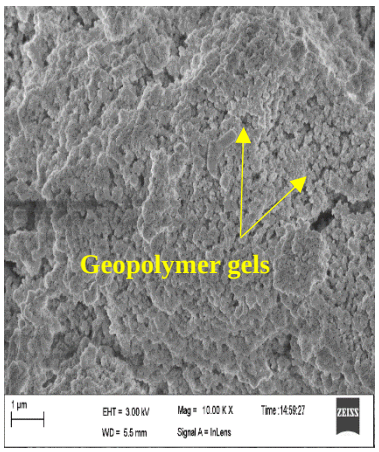

(a) 8 M/3%NC/425FA/28D

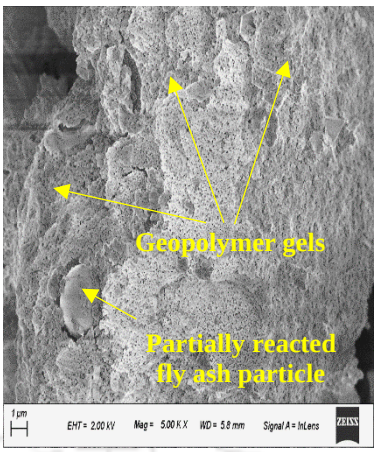

(b) 10 M/3%NC/425FA/28D

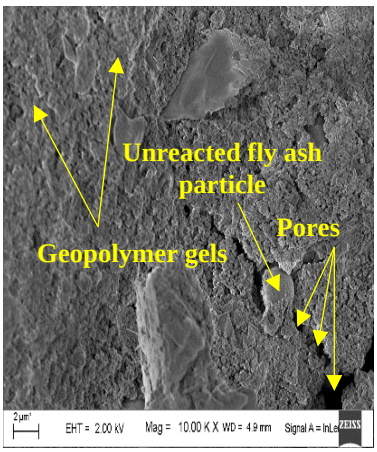

(c) 12 M/3%NC/425FA/28D

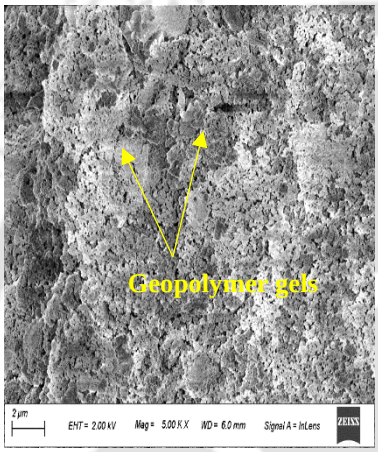

(d) 14 M/3%NC/425FA/28D

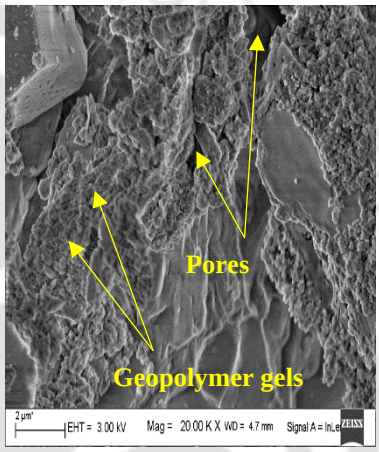

(e) 16 M/3%NC/425FA/28D

(GPC made with fly ash passing through 300 μm sieve, fly ash content of 425 kg/m^3, alkaline solution content of 210 kg/m^3, and SS/SH ratio of 1.75)

Fig. A13: FESEM images of GPC for different molarity of NaOH solution, admixed NaCl concentrations of 3% at the age of 28 days

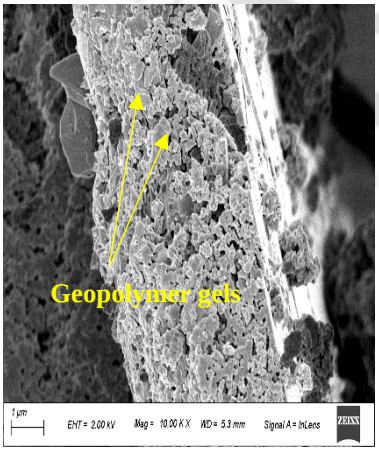

(a) 8 M/3%NC/425FA/90D

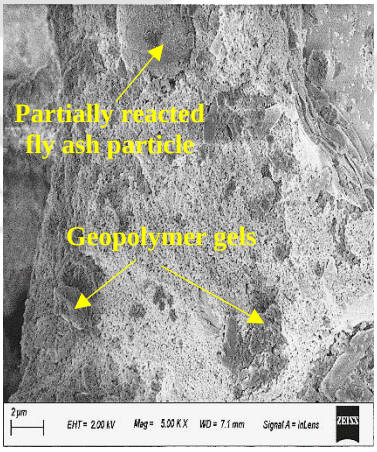

(b) 10 M/3%NC/425FA/90D

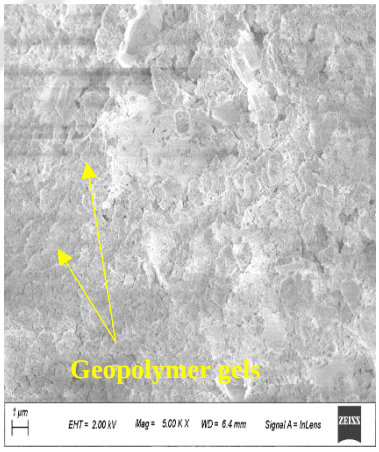

(c) 14 M/3%NC/425FA/90D

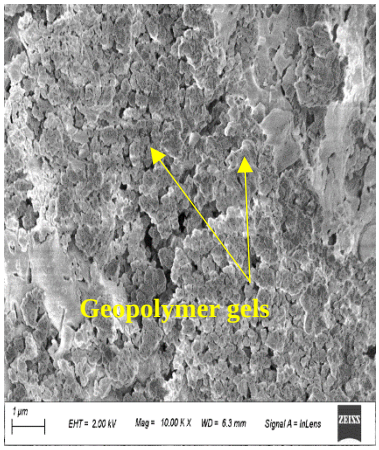

(d) 16 M/3%NC/425FA/90D

(GPC made with fly ash passing through 300 μm sieve, fly ash content of 425 kg/m^3, alkaline solution content of 210 kg/m^3, and SS/SH ratio of 1.75)

Fig. A14: FESEM images of GPC for different molarity of NaOH solution, admixed NaCl concentrations of 3% at the age of 90 days

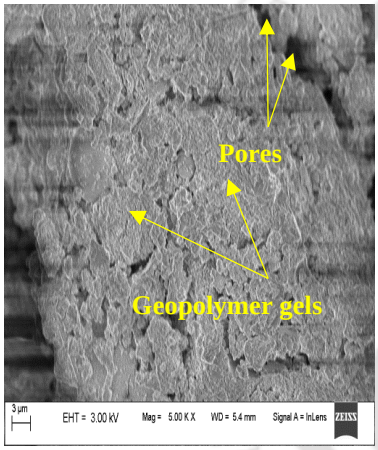

(a) 8 M/4.5%NC/425FA/7D

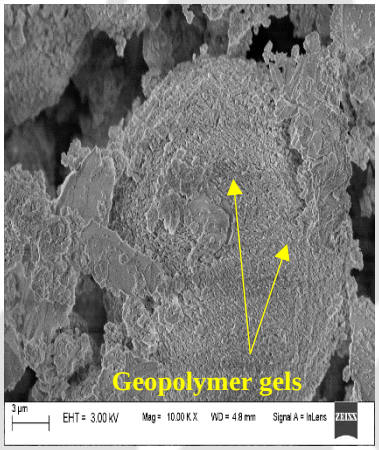

(b) 10 M/4.5%NC/425FA/7D

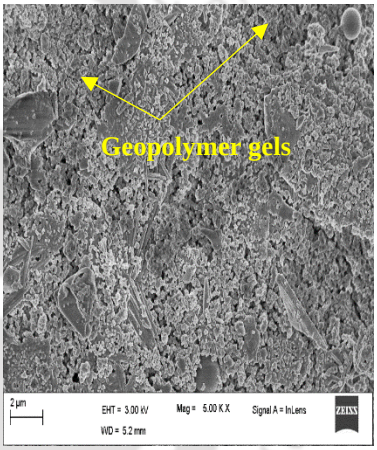

(c) 12 M/4.5%NC/425FA/7D

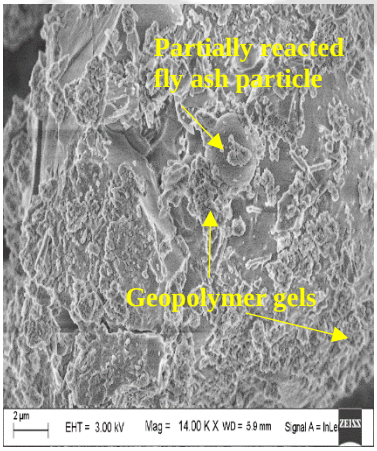

(d) 14 M/4.5%NC/425FA/7D

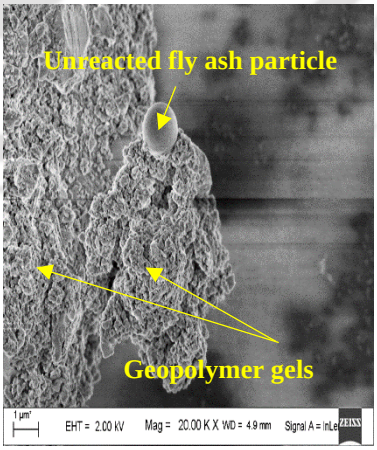

(e) 16 M/4.5%NC/425FA/7D

(GPC made with fly ash passing through 300 μm sieve, fly ash content of 425 kg/m^3, alkaline solution content of 210 kg/m^3, and SS/SH ratio of 1.75)

Fig. A15: FESEM images of GPC for different molarity of NaOH solution, admixed NaCl concentrations of 4.5% at the age of 7 days

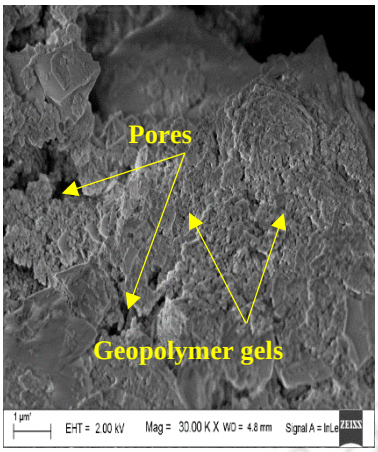

(a) 8 M/4.5%NC/425FA/28D

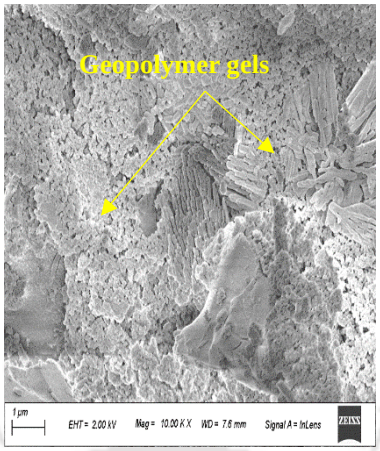

(b) 10 M/4.5%NC/425FA/28D

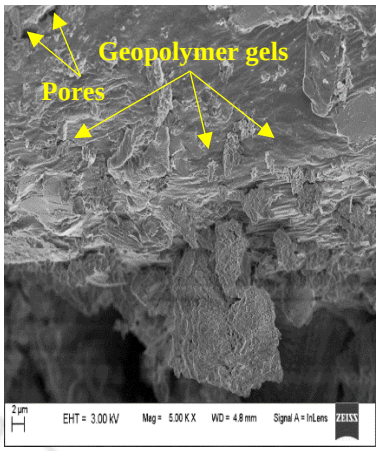

(c) 12 M/4.5%NC/425FA/28D

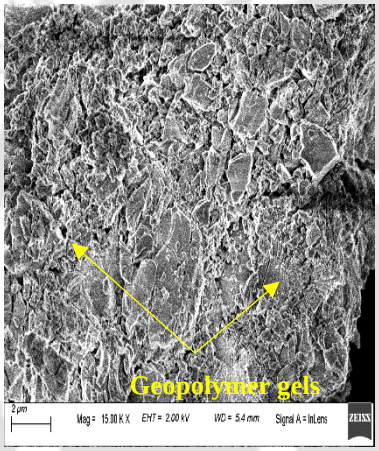

(d) 14 M/4.5%NC/425FA/28D

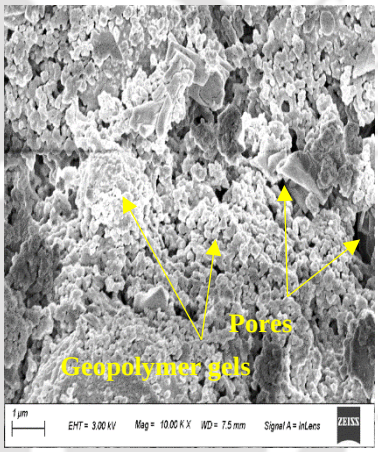

(e) 16 M/4.5%NC/425FA/28D

(GPC made with fly ash passing through 300 µm sieve, fly ash content of 425 kg/m^3, alkaline solution content of 210 kg/m^3, and SS/SH ratio of 1.75)

Fig. A16: FESEM images of GPC for different molarity of NaOH solution, admixed NaCl concentrations of 4.5% at the age of 28 days

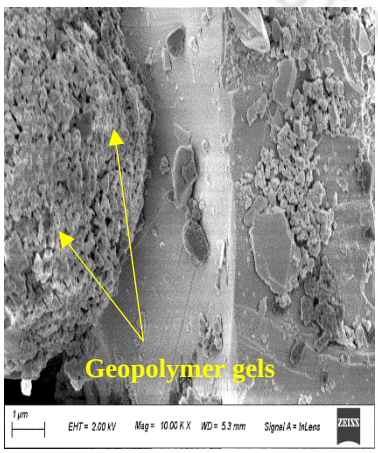

(a) 8 M/4.5%NC/425FA/90D

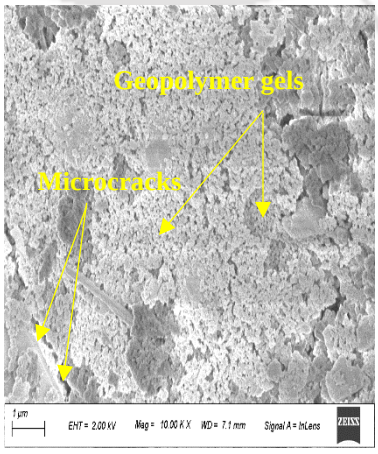

(b) 10 M/4.5%NC/425FA/90D

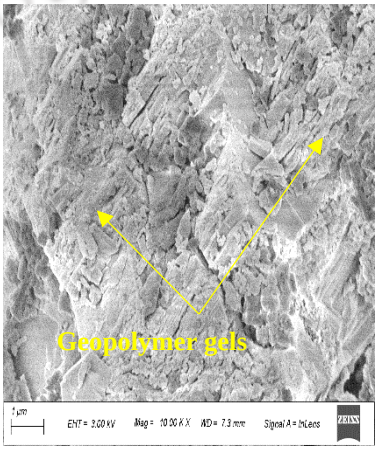

(c) 14 M/4.5%NC/425FA/90D

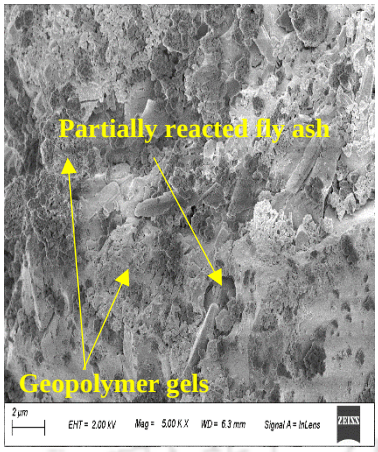

(d) 16 M/4.5%NC/425FA/90D

(GPC made with fly ash passing through 300 μm sieve, fly ash content of 425 kg/m^3, alkaline solution content of 210 kg/m^3, and SS/SH ratio of 1.75)

Fig. A17: FESEM images of GPC for different molarity of NaOH solution, admixed NaCl concentrations of 4.5% at the age of 90 days

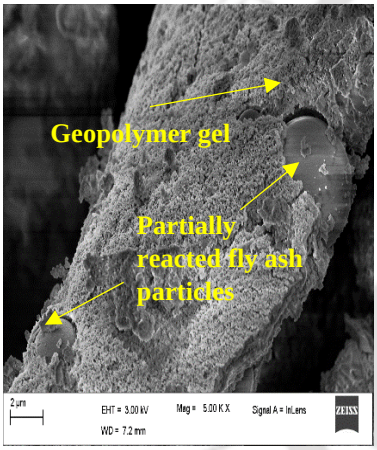

(a) 10 M/0%NC/190AL/28D

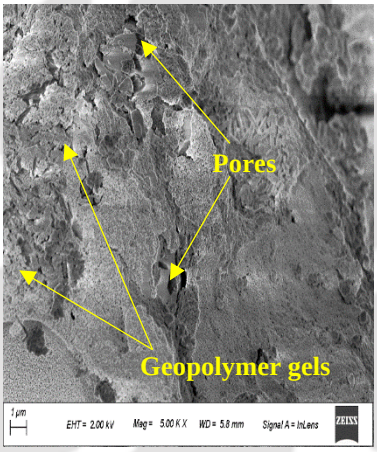

(b) 10 M/3%NC/190AL/7D

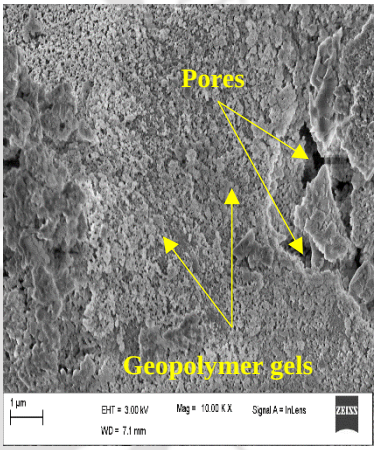

(c) 10 M/3%NC/190AL/28D

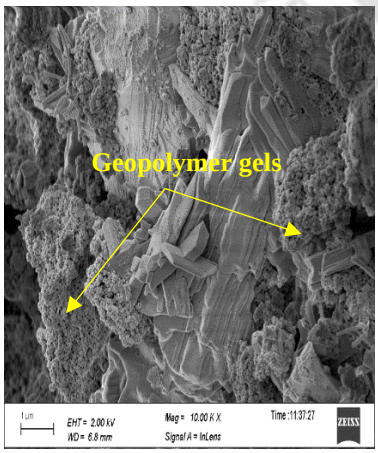

(d) 14 M/3%NC/190AL/7D

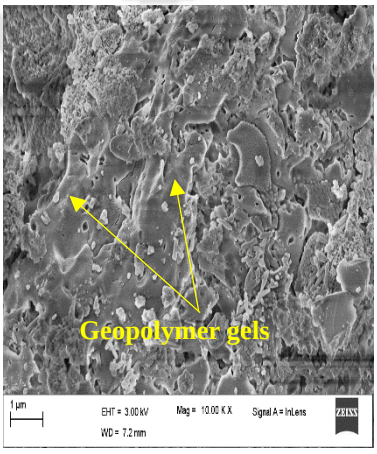

(e) 14 M/3%NC/190AL/28D

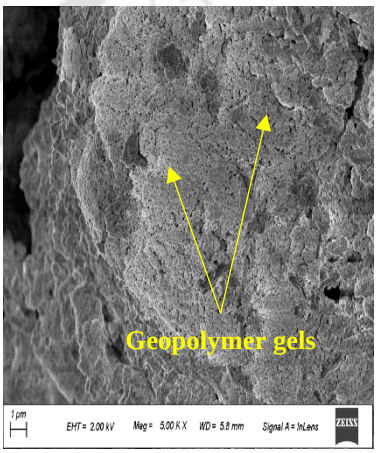

(f) 10 M/0%NC/210AL/28D

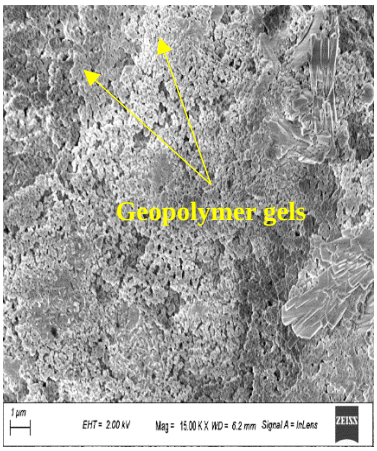

(g) 14 M/0%NC/210AL/7D

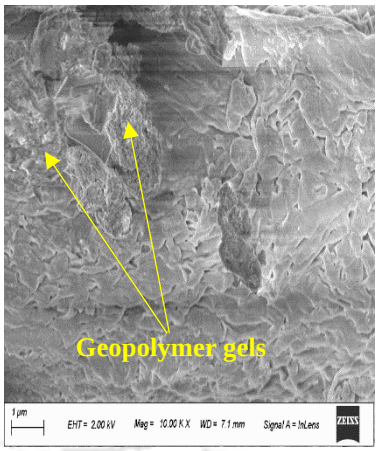

(h) 14 M/0%NC/210AL/28D

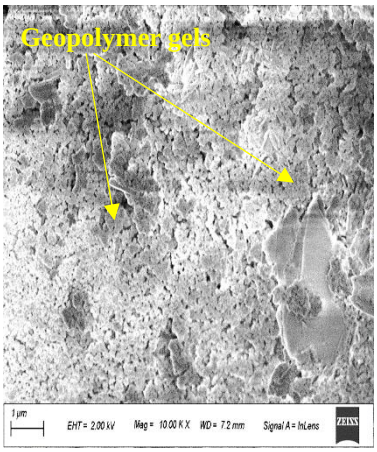

(i) 10 M/3%NC/210AL/28D

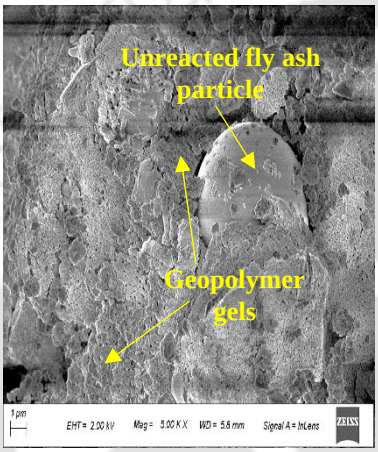

(j) 14 M/3%NC/210AL/7D

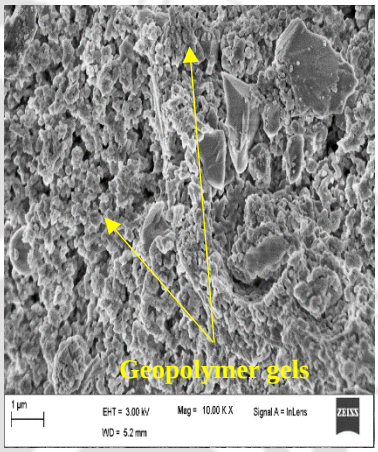

(k) 14 M/3%NC/210AL/28D

(GPC made with fly ash passing through 150 μm sieve, fly ash content of 425 kg/m^3, and SS/SH ratio of 1.75)

Fig. A18: FESEM images of GPC mixes for different alkaline solution contents and molarity of NaOH solution

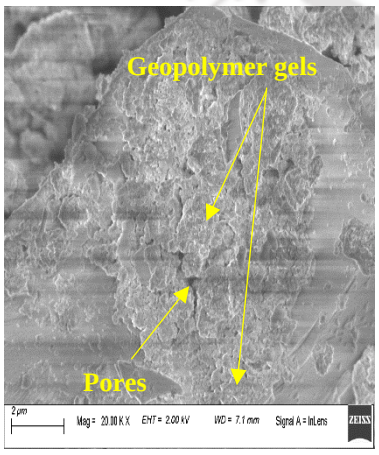

(a) 1.5R/10 M/0%NC/7D

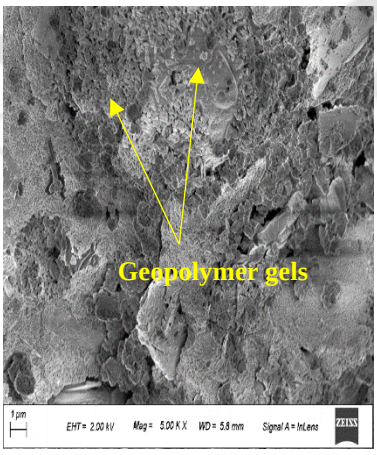

(b) 1.5R /14 M/0%NC/7D

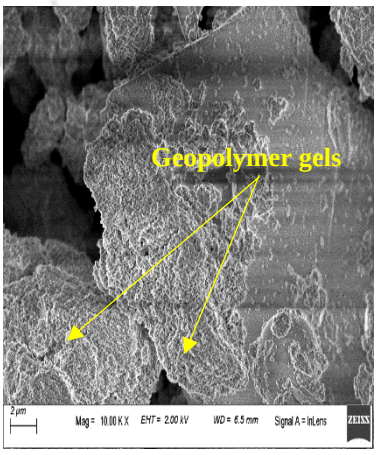

(c) 1.5R /10 M/3%NC/7D

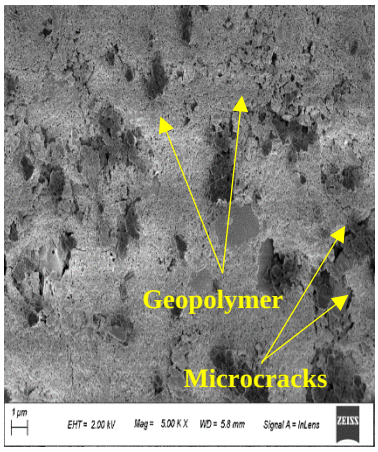

(d) 1.5R /14 M/3%NC/7D

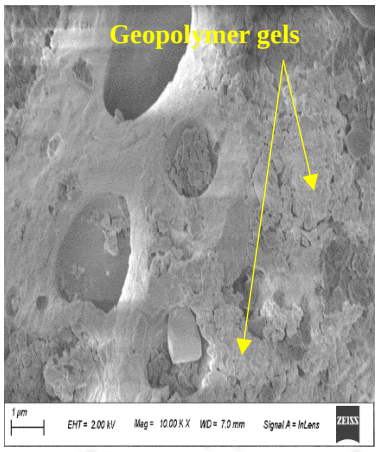

(e) 1.5R /10 M/0%NC/28D

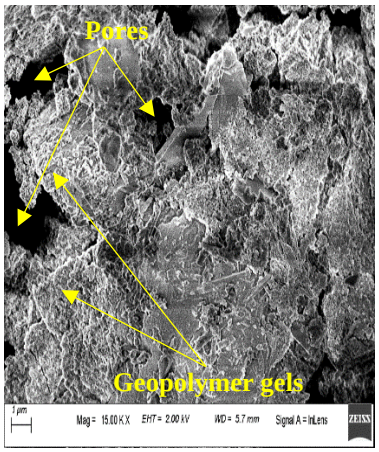

(f) 1.5R /10 M/3%NC/28D

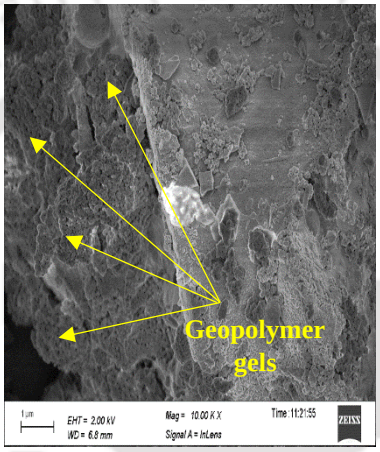

(g) 14 M/3%NC/1.5R /28D

(GPC made with fly ash passing through 150 µm sieve, fly ash content of 425 kg/m^3, and alkaline solution content of 210 kg/m^3)

Fig. A19: FESEM images of GPC mixes for different ratio of alkaline solution and molarity of NaOH solution

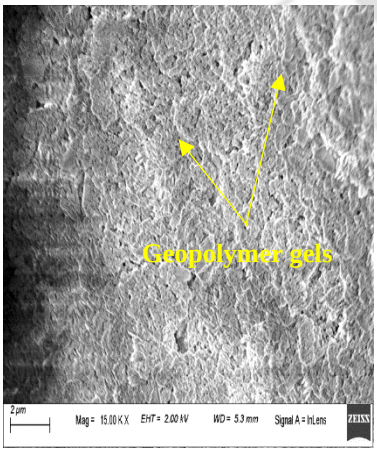

(a) 10 M/1.5%NC/150 µm/7D

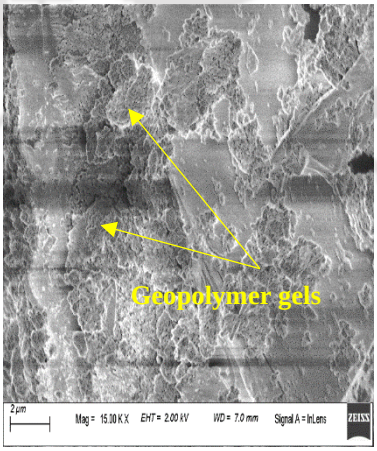

(b) 10 M/3%NC/150 µm/7D

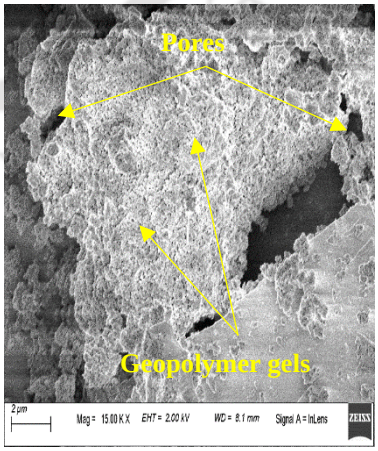

(c) 10 M/4.5%NC/150µm/7D

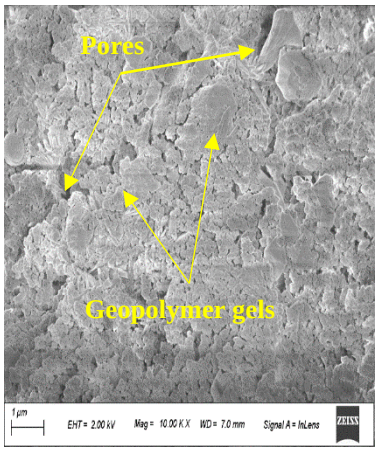

(d) 14 M/1.5%NC/150 µm/7D

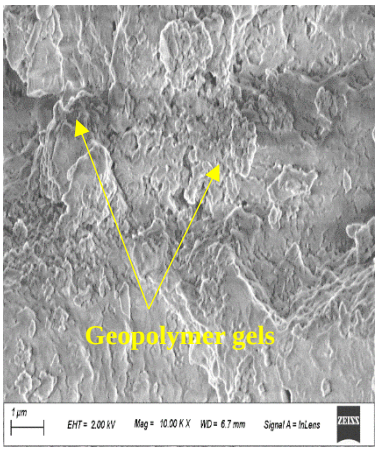

(e) 14 M/3%NC/150 µm/7D

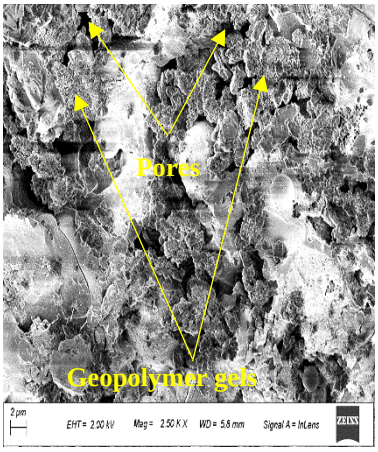

(f) 14 M/4.5%NC/150µm/7D

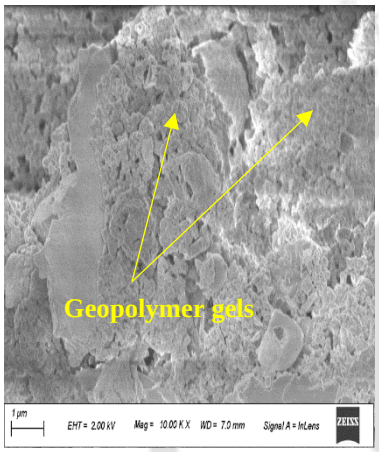

(g) 10 M/1.5%NC/300 µm/7D

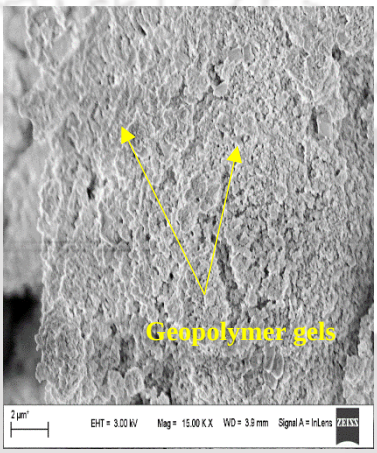

(h) 10 M/3%NC/300 µm/7D

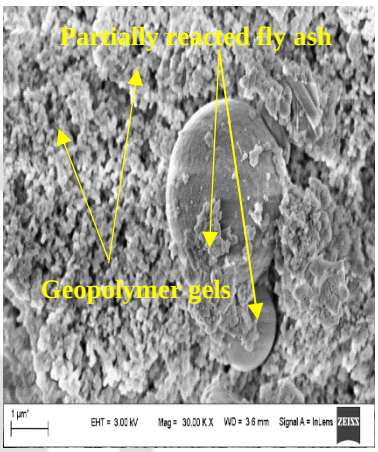

(i) 10 M/4.5%NC/300µm/7D

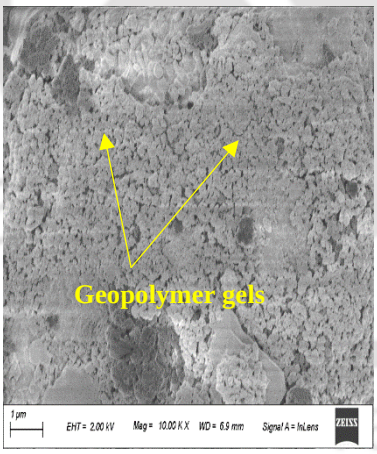

(j) 14 M/1.5%NC/300 µm/7D

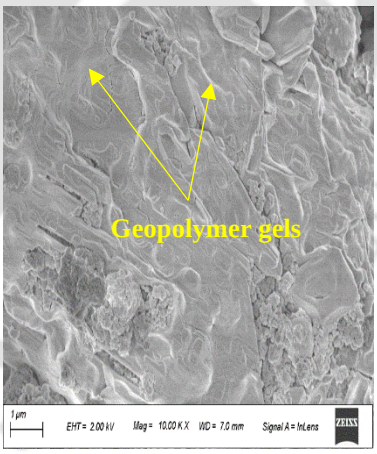

(k) 14 M/3%NC/300 µm/7D

(GPC made with fly ash content of 450 kg/m^3, alkaline solution content of 210 kg/m^3, and SS/SH ratio of 1.75)

Fig. A20: FESEM images of GPC mixes for different particle size of fly ash, molarity of NaOH solution, admixed NaCl concentration at the age of 7 days

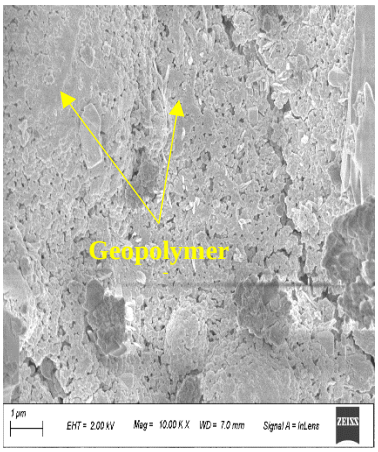

(a) 14 M/0%NC/150 µm/28D

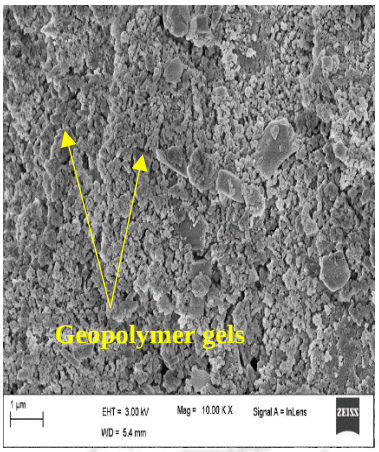

(b) 10 M/1.5%NC/150 µm/28D

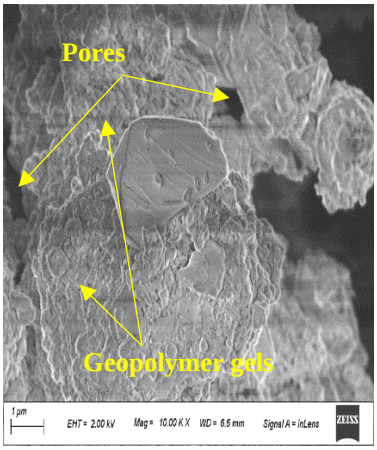

(c) 10 M/4.5%NC/150µm/28D

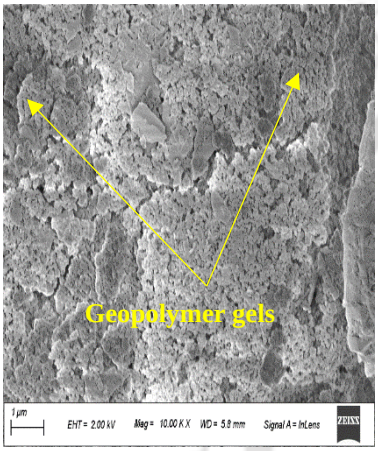

(d) 14 M/1.5%NC/150 µm/28D

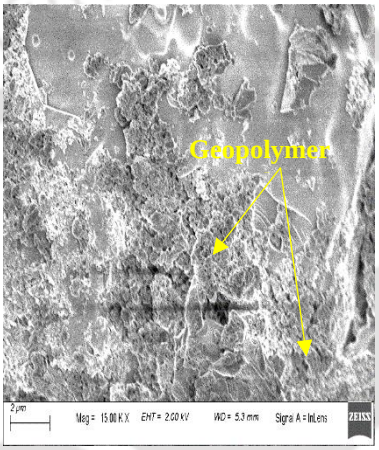

(e) 14 M/3%NC/150µm/28D

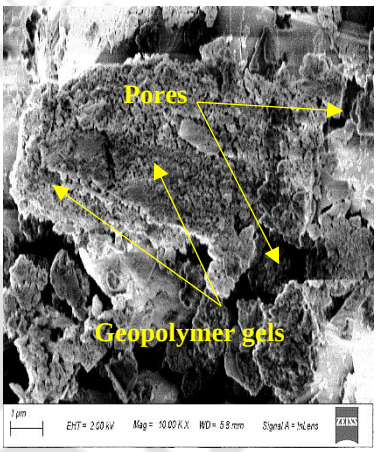

(f) 14 M/4.5%NC/150µm/28D

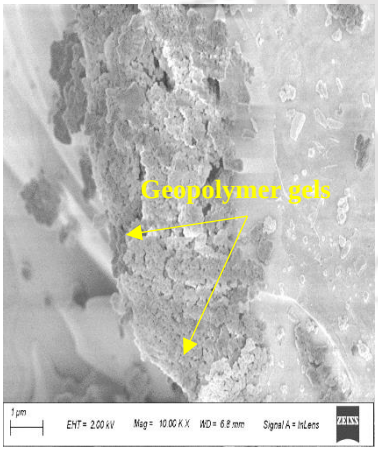

(g) 10 M/1.5%NC/300 µm/28D

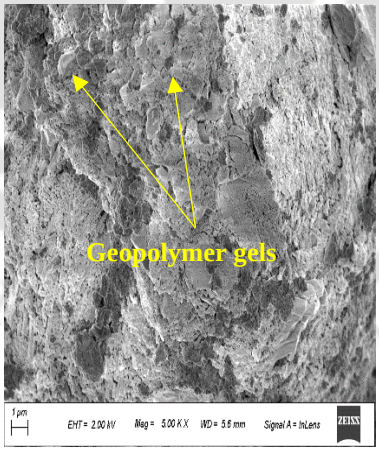

(h) 10 M/3%NC/300 µm/28D

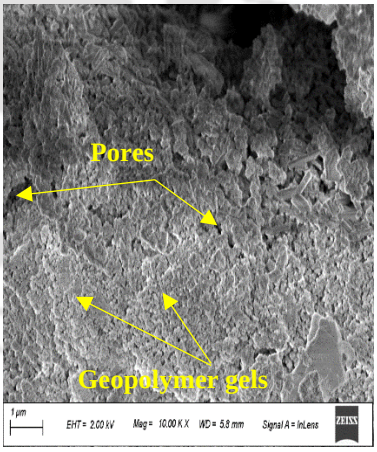

(i) 10 M/4.5%NC/300µm/28D

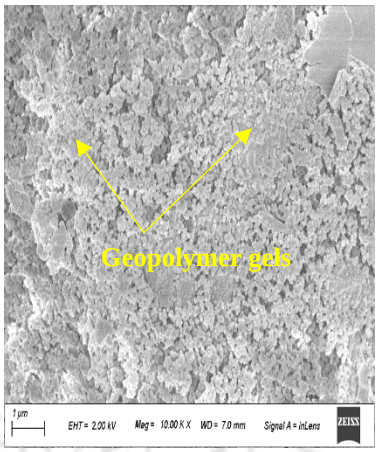

(j) 14 M/1.5%NC/300 µm/28D

(GPC made with fly ash content of 450 kg/m^3, alkaline solution content of 210 kg/m^3, and SS/SH ratio of 1.75)

Fig. A21: FESEM images of GPC mixes for different particle size of fly ash, molarity of NaOH solution, admixed NaCl concentration at the age of 28 days

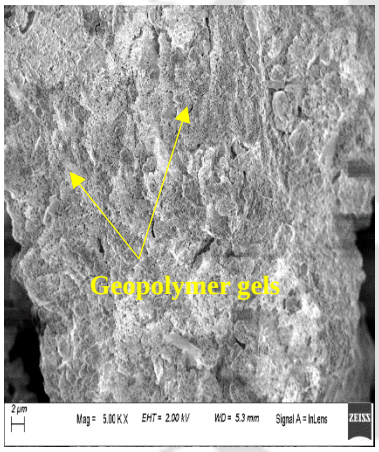

(a) 10 M/0%NC/150 µm/90D

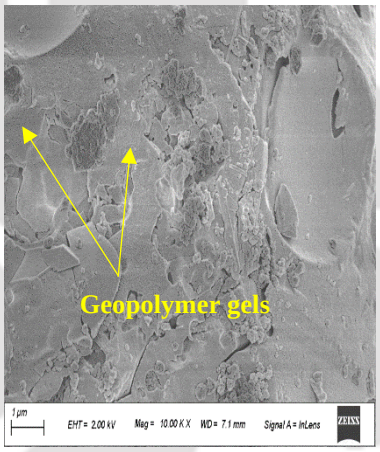

(b) 10 M/1.5%NC/150 µm/90D

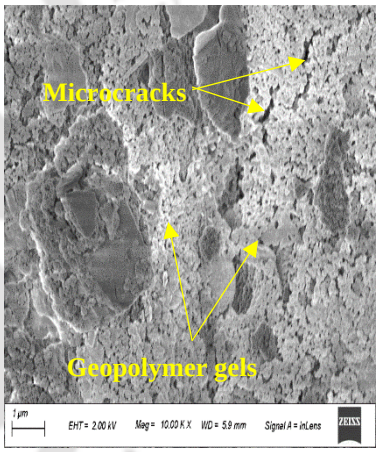

(c) 10 M/3%NC/150µm/90D

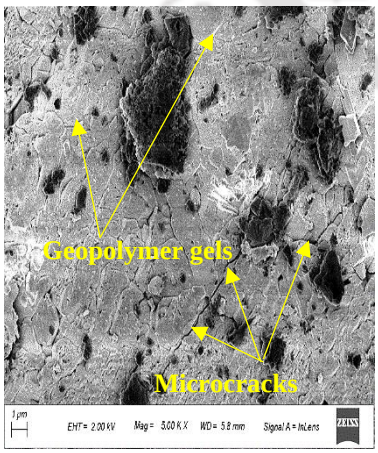

(d) 10 M/4.5%NC/150 µm/90D

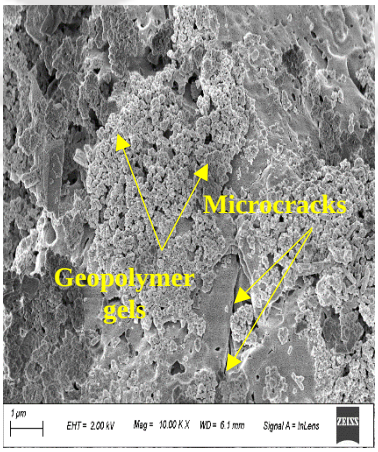

(e) 14 M/0%NC/150µm/90D

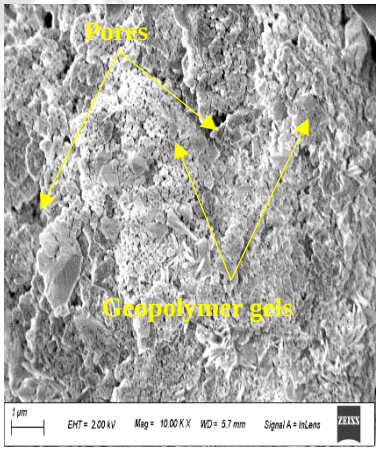

(f) 14 M/1.5%NC/150µm/90D

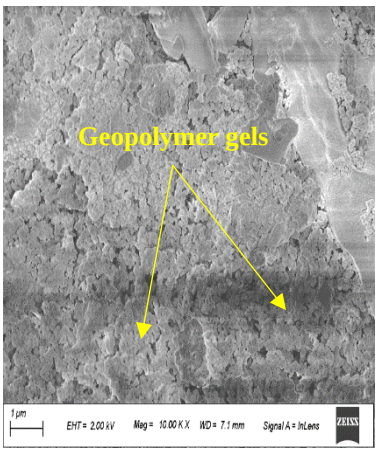

(g) 14 M/3%NC/150µm/90D

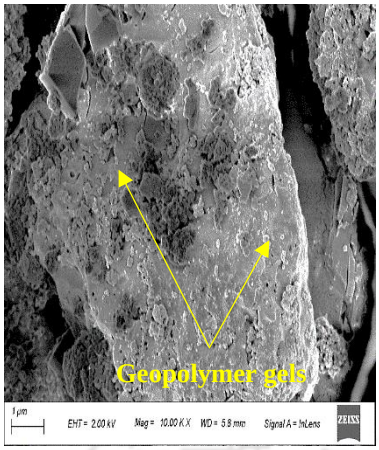

(h) 14 M/4.5%NC/150µm/90D

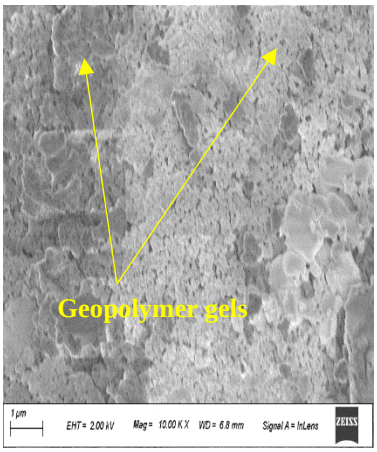

(i) 10 M/1.5%NC/300 µm/90D

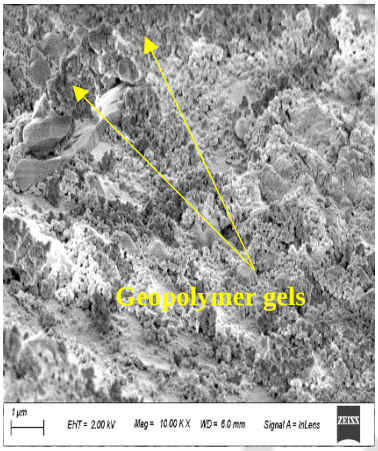

(j) 10 M/3%NC/300µm/90D

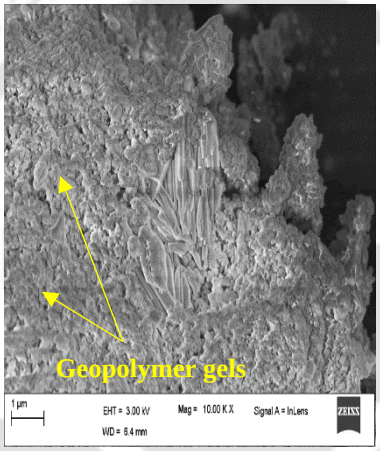

(k) 10 M/4.5%NC/300µm/90D

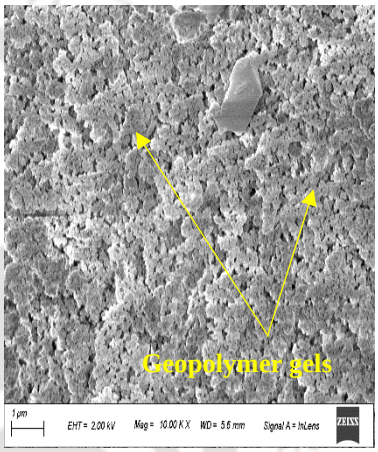

(l) 14 M/1.5%NC/300 µm/90D

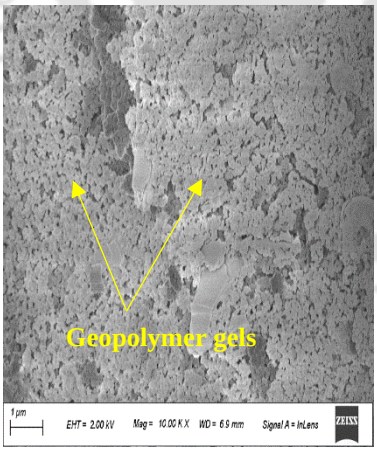

(m) 10 M/3%NC/300µm/90D

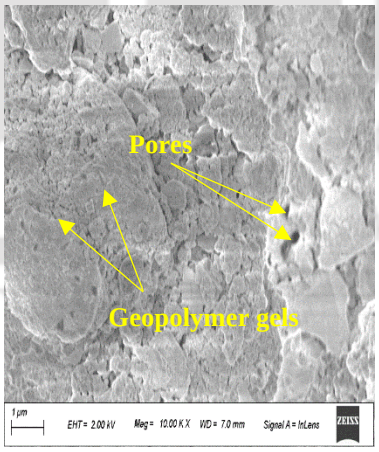

(n) 10 M/4.5%NC/300µm/90D

(GPC made with fly ash content of 450 kg/m^3, alkaline solution content of 210 kg/m^3, and SS/SH ratio of 1.75)

Fig. A22: FESEM images of GPC mixes for different particle size of fly ash, molarity of NaOH solution, admixed NaCl concentration at the age of 90 days

Appendix B

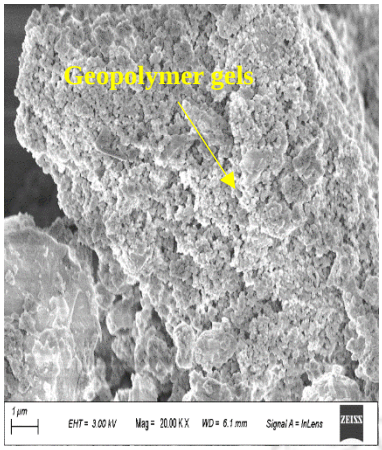

(a) 8 M/1.5NC/425FA/600D

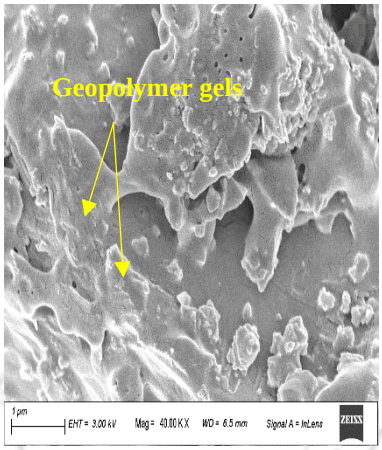

(b) 8 M/4.5NC/425FA/600D

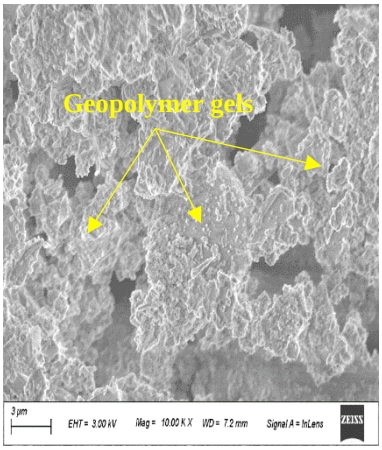

(c) 12 M/1.5NC/425FA/600D

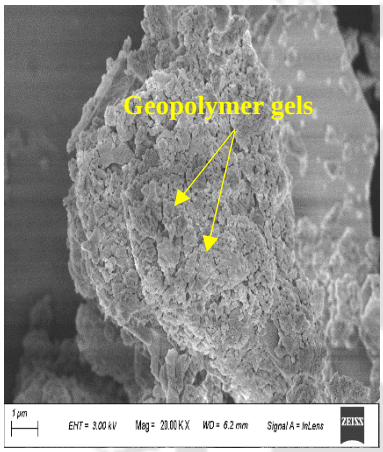

(d) 12 M/4.5NC/425FA/600D

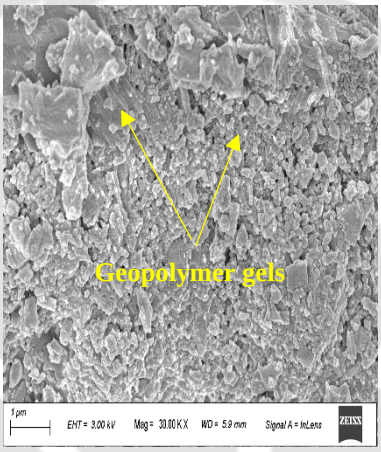

(e) 16 M/1.5NC/425FA/600D

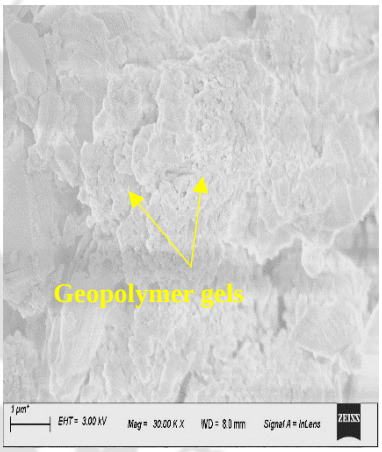

(f) 16 M/3NC/425FA/600D

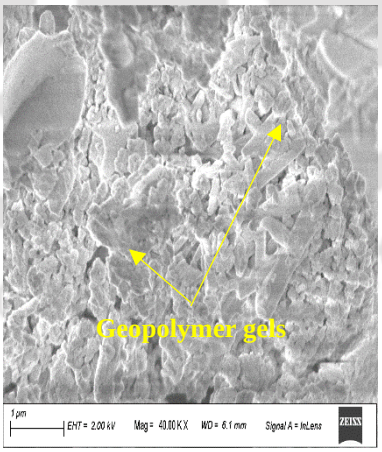

(g) 425FA/16 M/4.5NC/600D

(GPC made with fly ash passing through 300 μm sieve, fly ash content of 425 kg/m^3, alkaline solution content of 210 kg/m^3, and SS/SH ratio of 1.75)

Fig. B1: FESEM images of GPC near steel reinforcement in prismatic specimens made with different molarity of NaOH solution at the age of 600 days for different admixed NaCl concentrations

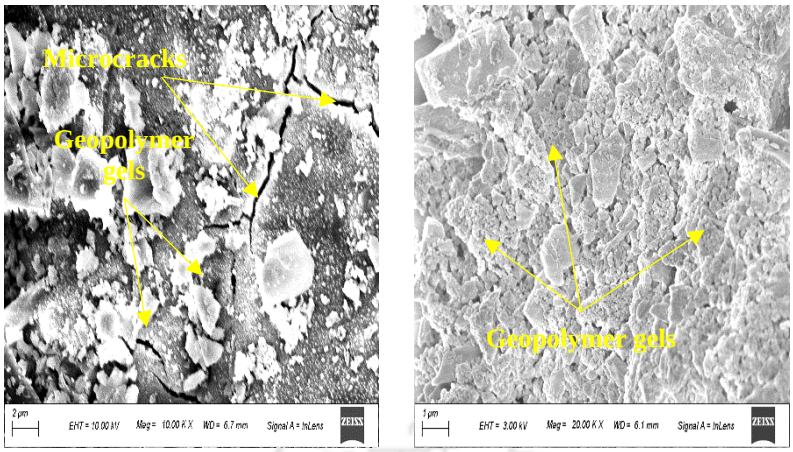

(a) 190AL/14 M/3NC/600D (b) 1.5R/10 M/3NC/600D

(GPC made with fly ash passing through 150 μm sieve, and fly ash content of 425 kg/m^3)

Fig. B2: FESEM images of GPC near steel reinforcement in prismatic specimens at the age of 600 days: a) alkaline solution content of 190 kg/m^3 for NaOH solution of 10 M, and b) alkaline solution ratio of 1.5 for NaOH solution of 10 M

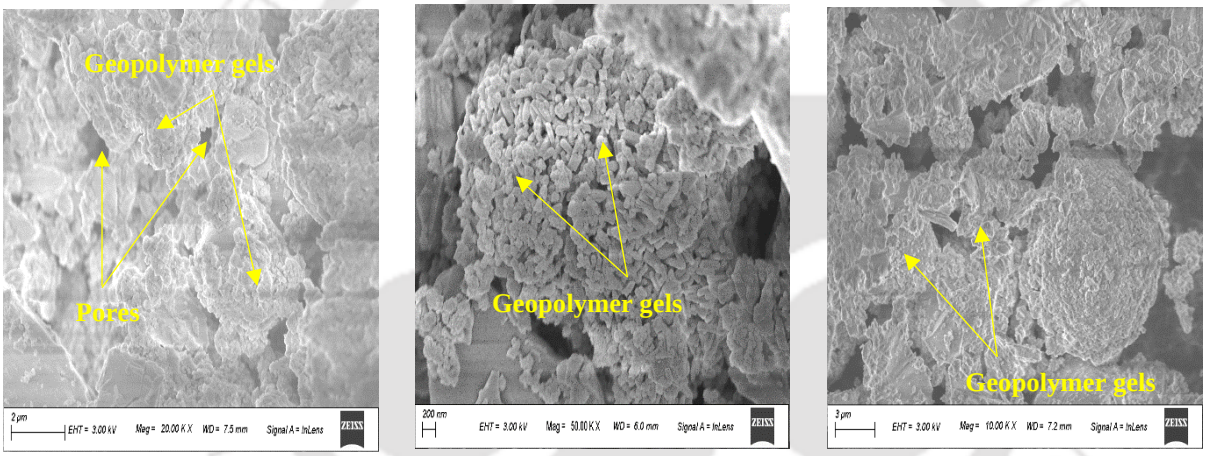

(a) 10 M/1.5NC/150 μm/600D (b) 10 M/3NC/150 μm/600D (c) 14 M/1.5NC/150 μm/600D

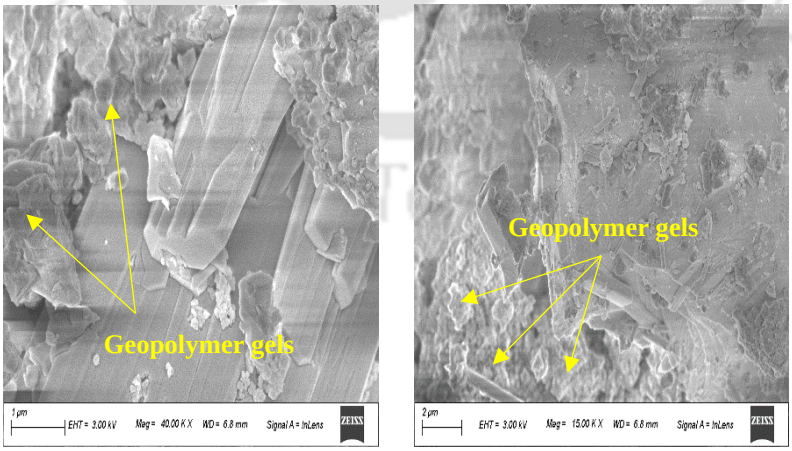

(d) 14 M/1.5NC/300 μm/600D (e) 14 M/4.5NC/300 μm/600D

(GPC made with fly ash content of 450 kg/m^3, alkaline solution content of 210 kg/m^3, and SS/SH ratio of 1.75)

Fig. B3: FESEM images of GPC near steel reinforcement in prismatic specimens at the age of 600 days for different particle size of fly ash, and molarity of NaOH solution

List of Publications

Journals:

[1] S. Mani and B. Pradhan, "A study on compressive strength and corrosion behavior of reinforcing steel in chloride contaminated fly ash based geopolymer concrete", *Journal of Structural Engineering (India),* Vol. 44, pp. 214-219, 2017.

[2] S. Mani and B. Pradhan, "Investigation on effect of fly ash content on strength and microstructure of geopolymer concrete in chloride-rich environment", *Materials Today: Proceedings*, Vol. 32, pp. 865-870, 2020.

Conferences/Book Chapter:

[1] S. Mani and B. Pradhan, "A study on compressive strength and corrosion behavior of reinforcing steel in chloride contaminated fly ash based geopolymer concrete", *Tenth Structural Engineering Convention (SEC-2016),* CSIR-SERC, Chennai, Tamil Nadu, India, December 21-23, 2016.

[2] S. Mani and B. Pradhan, "Effect of alkaline solution content on strength and chloride induced corrosion of steel in geopolymer concrete made from fly ash", *Proceedings of SECON'19,* Lecture Notes in Civil Engineering, Vol. 46, pp. 123-137, 2020.

[3] S. Mani and B. Pradhan, "Influence of fly ash content on strength and microstructure of fly ash based geopolymer concrete subjected to chloride-rich environment", *3rd International Conference on Innovative Technologies for Clean and Sustainable Development (ITCSD-2020),* NITTTR Chandigarh, Chandigarh, India, February 19-21, 2020.